Modeling kidney diseases using Urine-derived renal progenitor cells and their therapeutic potential

Inaugural-Dissertation

Zur Erlangung des Doktorgrades
der mathematisch-naturwissenschaftliche Fakultät
der Heinrich-Heine-Universität Düsseldorf

vorgelegt von

Chantelle Thimm

aus Köln,

Düsseldorf, August 2025

Aus dem Institut für Stammzellforschung und Regenerative Medizin
der Heinrich-Heine-Universität Düsseldorf

Gedruckt mit der Genehmigung der Mathematisch-Naturwissenschaftlichen Fakultät der
Heinrich-Heine-Universität Düsseldorf

Berichterstatter:

1. Prof. Dr. James Adjaye

2. Prof. Dr.Constantin Czekelius

3. Prof. Dr. Bernhard Schermer

Tag der mündlichen Prüfung: 20.05.2026

Die vorliegende Arbeit ist eine kumulative Dissertation
gemäß § 6 (3) der Promotionsordnung der
Mathematisch-Naturwissenschaftlichen Fakultät
der Heinrich-Heine-Universität Düsseldorf vom 15.08.2018
zur Verleihung des Grades „Doctor rerum naturalium"

Acknowledgement

I would like to take this opportunity to thank all those who have supported me in the preparation of this dissertation.

First and foremost, I would like to thank Prof. Dr. James Adjaye for his dedicated supervision. His helpful suggestions and patience as well as his active support have contributed significantly to the success of this thesis. He gave me the opportunity to carry out this work and to learn from his expert advice and suggestions.

I would also like to thank Prof. Dr. Constantin Czekelius for his willingness to supervise my dissertation.

I thank Dr. Lars Erichsen, who, through his selfless willingness to proofread my work, is largely responsible for the grammatical correctness and correct spelling, but who has also decisively advanced this work through his scientific expertise. Through his support over the past years, he shared not only successes but also failures, strengthening my back and always having an open ear. Thank you so much!

A big thank you belongs to my family and friends, who have always supported and motivated me, even without a scientific background. Without them, I would not have been able to complete this work and muster the necessary perseverance. Thank you for accompanying me on this journey.

The most important thank you goes to my friend Etienne Bojer, who managed to calm me down even in moments of occasional panic attacks and always reassured me that everything would be fine. Thank you for supporting and motivating me when my head had long since given up. Your words of encouragement and your pretending to understand my technical monologues gave me the self-confidence I needed for this work.

I would also like to thank the members of the ISRM laboratory for their support during my time as a doctoral student and for the scientific exchange. Thank you, Silke Wehrmeyer, Marina Jovanovic, Rosanne Mack, Alessia Lofrano, Sejla Pulo, Tama Amin, Nele Liedtke, Dr. Claus Cordes, Dr. Wasco Wruck and Dr. Nina Graffmann.

My special thanks also go to all the cooperation partners of Heinrich-Heine University for the consumables, which have decisively advanced this work.

Table of contents

ACKNOWLEDGEMENT **1**

TABLE OF CONTENTS **3**

TABLE OF FIGURES **6**

LIST OF ABBREVIATIONS **7**

SUMMARY **10**

ZUSAMMENFASSUNG **14**

STRUCTURE OF THIS THESIS **19**

1 INTRODUCTION **22**

1.1 FUNDAMENTALS OF RENAL ANATOMY AND FUNCTION 22

1.2 DEVELOPMENT OF THE NEPHRON 24

1.3 GLOMERULUS OF THE KIDNEY 25

1.4 RENIN-ANGIOTENSIN-ALDOSTERONE SYSTEM 27

1.4.1 Angiotensin II receptor antagonists *29*

1.5 KIDNEY DISEASES 31

1.5.1 Acute kidney injury *31*

1.5.2 Chronic kidney disease *33*

1.6 APOLIPOPROTEIN L1-MEDIATED KIDNEY DISEASE 35

1.6.1 Mechanisms of Interferon-γ and the JAK/STAT pathway *37*

1.7 DISEASE THAT LEADS TO A MAGNESIUM DEFICIENCY 39

1.7.1 Bartter syndrome *40*

1.8 AGING 43

1.9 INDUCED PLURIPOTENT STEM CELL 44

1.10 IMMORTALIZATION OF CELL LINES 45

1.10.1 Immortalization with human telomerase *45*

1.10.2 Immortalization with SV40 ..... *46*

2 AIM OF THIS WORK **48**

3 PUBLICATIONS **51**

3.1 DERIVATION OF THE IMMORTALIZED CELL LINE UM51-PREPODO-HTERT AND ITS RESPONSIVENESS TO ANGIOTENSIN II AND ACTIVATION OF THE RAAS PATHWAY 51

3.2 Modelling APOL1-mediated kidney inflammation and fibrosis using a partially reprogrammed urine derived SIX2-positive renal progenitor cell line 71
3.3 Activation of the Renin-Angiotensin System Disrupts the Cytoskeletal Architecture of Human Urine-Derived Podocytes 108
3.4 Unveiling Angiotensin II and Losartan-Induced Gene Regulatory Networks Using Human Urine-Derived Podocytes 136
3.5 Secreted Cytokines within the Urine of AKI Patients Modulate TP53 and SIRT1 Levels in a Human Podocyte Cell Model 155
3.6 Urine-Based Detection of Biomarkers Indicative of Chronic Kidney Disease in a Patient Cohort from Ghana…. 174
3.7 Untangling the Uncertain Role of Overactivation of the Renin–Angiotensin–Aldosterone System with the Aging Process Based on Sodium Wasting Human Models 193
3.8 Generation of a Bartter syndrome type 3 patient-derived induced pluripotent stem cell line ISRM-BS3-UM18-iPSC (HHUUKDi014-A) 213
3.9 Evidence for conserved gene expression and biological processes operative in human podocytes and adult brain..... 222
3.10 Urinary proteins from Sickle Cell patients induce inflammation and kidney injury via the TGFB-p53 axis in a podocyte cell culture model. 277
3.11 Human Urine-derived SIX2-positive renal progenitor cells improve kidney injury in an IRI mouse model 323

4 DISCUSSION 349

4.1 Generation and characterization of immortalized podocytes derived from human urine 350
4.2 Reduction of ANGII-induced cytoskeletal changes in human podocytes by angiotensin receptor blockade 353
4.3 Secreted urinary cytokines in AKI and CKD patients as diagnostic and prognostic tools for kidney diseases 354
4.4 JAK1/JAK2-Inhibition reduces IFN–r–induced APOL1 expression and fibrotic markers in human podocytes 357
4.5 Understanding the effects of RAAS overactivation in the aging process using sodium-wasting models 359
4.6 Urine-derived renal progenitor cells as a therapeutic approach in an IRI mouse model 362

5 CONCLUSION 364

6 REFERENCES 366

7 APPENDIX 385

7.1 POSTER PRESENTATIONS 385

8 DECLARATION OF INDEPENDENCE 386

Table of Figures

Figure 1: Kidney anatomy 24

Figure 2: Renin-angiotensin-aldosterone system.....31

Figure 3: Chronic kidney disease criteria 35

Figure 4: Interferon-γ signaling pathway. 39

Figure 5: Bartter syndrome.....42

Figure 6: Therapeutic potential of urine-derived renal progenitor cells (UdRPCs).....365

List of Abbreviations

%	Percent
ACE	Angiotensin-converting enzyme
ACEI	Angiotensin-converting enzyme inhibitor
ACTN4	Alpha-actinin4
ADH	Antidiuretic hormone
ADIPO	Adiponectin
AGER	Advanced Glycosylation End-Product Specific Receptor
AGTR1	Angiotensin II receptor type 1
AGTR2	Angiotensin II receptor type 2
AKI	Acute kidney injury
ANG II	Angiotensin II
ANGPT2	Angiopoietin 2
APOL1	Apolipoprotein A1
ARB	Angiotensin II receptor blocker
ATP	Adenosintriphosphat
BS	Bartter syndrome
BSND	Barttin CLCNK Type Accessory Subunit Beta
c-Myc	MYC Proto-Oncogene
Ca^{2+}	Calciumion
CASR	Calcium Sensing Receptor
CD	Cluster of differentiation
CD2AP	CD2 Associated Protein
CFD	Complement Factor D
CGA classification Assign	Identify cause of CKD (C), Assign GFR category (G), albuminuria category (A)
Cited1	Cbp/P300 Interacting Transactivator with Glu/Asp Rich Carboxy-Terminal Domain 1
CKD	Chronic kidney disease
CLC-Ka	Chloride Voltage-Gated Channel Ka
CLCNKB	Chloride Voltage-Gated Channel Kb
CLU	Clusterin
CXCL1	C-X-C Motif Chemokine Ligand 1
DNA	Desoxyribonukleinsäure
E2F-1	E2F Transcription Factor 1
EGF	Epidermal Growth Factor
eGFR	Epidermal Growth Factor Receptor
Et al.	Et alia
Eya1	EYA Transcriptional Coactivator and Phosphatase 1
FSGS	Focal segmental glomerulosclerosis
GBM	Glomerular basement membrane
GFR	Glomerular filtrationrate
GH1	Growth Hormone 1
GS	Gitelmansyndrome
H3K4 methylation	Trimethylation of lysine 4 on histone H3 protein subunit
HDAC	Histone Deacetylase
hESC	Human embryonic stem cell
Hox11/TLX1	T-cell leukemia homeobox protein 1
hTERT	human telomerase reverse transcriptase

ICAM1	Intercellular adhesion molecule 1
IGFBP	Insulin Like Growth Factor Binding Protein
IL	Interleukin
iPSC	Induced pluripotent stem cell
ISN	International Society of Nephrology
JGA	Juxtaglomerular apparatus
K^+	Potassium ion
KCNJ1	Potassium Inwardly Rectifying Channel Subfamily J Member 1
KDIGO	Kidney Disease: Improving Global Outcomes
KI67/MK67	Marker of Proliferation Ki-67
KLF4	KLF transcription factor 4
KLK4	Kallikrein Related Peptidase 4
LMX1B	LIM Homeobox Transcription Factor 1 Beta
MET	Mesenchymal-epithelial transition
Mg	Magnesium
MME	Membrane Metalloendopeptidase
MMP9	Matrix Metallopeptidase 9
MN	Mesonephros
mRNA	Messenger ribonucleic acid
NADPH	Nicotinamide adenine dinucleotide phosphate
NGAL	Lipocalin 2
NO	Nitric oxide
NOX4	Nicotinamide-Adenine-Dinucleotide-Phosphate oxidase 4
NPHS1	Nephrin
NPHS2	Podocin
NSAID	Non-steroidal anti-inflammatory drugs
OCT4	Octamer-Binding Protein 4
Osr1	Odd-Skipped Related Transcription Factor 1
PAX2	Paired Box 2
PCNA	Proliferating Cell Nuclear Antigen
PCR	Polymerase chain reaction
PhD	Doctor of Philosophy
PKC	Proteinkinase C
PRC	Polycomb repressor complexes
RAAS	Renin-angiotensin-aldosterone system
RB1	Retinoblastoma genes
RDA	Recommended Daily Allowances
RETN	Resistin
RNA	Ribonucleic acid
ROS	Reactive oxygen species
Sall1	Spalt Like Transcription Factor 1
sCr	Serum creatinine
SIM-1	Single-minded homolog 1
SIRT1	Sirtuine 1
SIX1/2	SIX Homeobox 1/2
SLC12A1	Solute Carrier Family 12 Member 1
SOX2	SRY-Box Transcription Factor 2
SSEA3/4	Stage-specific embryonic antigen 3/4
SSP1	Secreted Phosphoprotein 1

SV40	Simian vacuolating virus 40
SV40 LT	Simian vacuolating virus 40 large T antigen
SYNPO	Synaptopodin
t-PA	Tissue Plasminogen Activator
TAL	Thick ascending limb
TERC/hTR	Telomerase RNA component
TET1	Tet Methylcytosine Dioxygenase 1
TIMP-2	TIMP Metallopeptidase Inhibitor 2
TRA-1-60/81	T-cell receptor alpha locus 1-60/81 epitope
UdRPC	Urine-derived renal progenitor cell
UO	Urine output
VEGF/ VEGFA	Vascular Endothelial Growth Factor A
WD	Wolffian duct
WT1	Wilms tumor protein 1
ZO-1	Zonula Occludens-1

Summary

The most common kidney diseases include chronic and acute kidney failure, degenerative kidney diseases, various kidney inflammations, kidney stones, renal cell carcinoma, and genetic kidney diseases such as autosomal-dominant polycystic kidney disease or rare inherited disorders like Bartter syndrome. Globally, chronic kidney disease (CKD) affects approximately 10% of the population, making it one of the most significant health burdens. Kidney stones are also widespread, with varying prevalence across different regions. Renal cell carcinoma, one of the most common types of kidney cancer, accounts for about 2–3% of all cancers worldwide. Rare inherited kidney diseases, such as Bartter syndrome, a disorder of kidney tubule function, are extremely rare, with an estimated prevalence of less than 1 in 1,000,000 individuals.

However, since the human body is a complex and multifaceted system, kidney diseases are closely linked to other organs, such as the heart or brain. It is known that a damaged and non-functioning kidney stops the elimination of waste products from the blood and therefore an enormous amount of fluid collects in the blood vessels, causing high blood pressure. The harmony and balance of the system and the cooperation of the organs is essential. In the past, disease modelling of the kidney has been challenging due to the challenge of obtaining cells derived from the kidney. Although relatively few kidney cells are shed under healthy- compared to dysfunctional conditions, we were able to isolate, cultivate and expand urine cells from healthy donors with a non-invasive method. These cells were identified as multipotent urinary stem cells, with a broad differentiation potential. We named these cells urine-derived nephron progenitor cells (UdRPCs) who can be differentiated into renal cell types such as glomerular podocytes and can be used for iPSC reprogramming.

Since kidney diseases are often caused by damage to the glomerulus or tubule, the use of UdRPCs has a wide potential for *in vitro* studies. UdRPCs can be immortalized and reprogrammed into induced pluripotent stem cells. In this study, immortalization was performed using human telomerase (hTERT) and partial programming by the Yamanaka factors (UM30-OSN). The use of these cell lines provides a long-term and far-reaching platform for investigating kidney-associated diseases.

In addition, the cell lines produced were able to differentiate into a highly specialized cell type, named podocytes. Podocytes play a role in blood filtration in the glomeruli of the kidney. The restriction or malfunction of podocytes is associated with numerous renal diseases, therefore, the study and application of this cell type as a disease model is highly important. Worldwide,

approximately 9.4 million deaths annually are attributable to elevated blood pressure. Hypertension is mainly regulated by the renin-angiotensin-aldosterone system (RAAS), with its main mediator angiotensin II (ANG II). Elevated ANG II levels lead to a pro-fibrotic, inflammatory, and hypertrophic environment, inducing apoptosis in podocytes. Prolonged activation of the RAAS is crucial for the pathogenesis of podocyte injury and causes proteinuria. To counteract podocyte damage, drugs that modulate the RAAS pathway such as losartan are administered to patients with high blood pressure. In the following studies, the UdRPCs-derived podocytes show activation of RAAS by being responsive to ANG II stimulation. The research data reveals an ANG II-dependent down regulation of the podocyte specific markers Nephrin (*NPHS1*) and Synaptopodin *(SYNPO*) leading to changes in the cytoskeleton. Adding a precise concentration of losartan counteracts the ANG II-induced changes. These changes lead to increased expression of specific-podocyte-markers that rescue the podocyte cytoskeleton, as shown by quantitative real-time PCR and Western blot analysis. In addition, the disruption of the podocyte cytoskeleton, which is detected by immunofluorescence-based detection of phalloidin, is prevented by losartan. This knowledge is important for further nephrotoxicity studies as well to understand the molecular pathway in many kidney diseases.

Diseases such as acute kidney injury or even chronic kidney disease can also be investigated using UdRPCs. In the two studies presented here, the secretome of the urine of an AKI patient cohort was analyzed. In addition, the effect of patient and healthy urine on human podocytes was investigated. Based on the results, we identified ADIPOQ, EGF, and SERPIN3A as potential early biomarkers that could detect acute kidney injury (AKI) as early as 24 hours after surgery. Besides that, genes were upregulated 72 hours after surgery, among them are CXCL1, VEGF, and RENIN.

Another study carried out by our lab was a study of CKD patients from Ghana that revealed decreased secretion of EGFR and VEGF in CKD progression. EGFR and VEGF may act in maintaining microvascular integrity and promoting endothelial and tubular cell survival and repair. Early detection of such cytokines could enable timely interventions to prevent filtration barrier breakdown, potentially yielding significant patient benefits. Moreover, cytokine-based tests are non-invasive, cost-effective, and easily conducted using urine samples and flow-cell detection devices, presenting a promising alternative for AKI and CKD monitoring.

Apolipoprotein L1 (APOL1) is a key genetic risk factor for CKD in individuals of African ancestry. Understanding this association is critical for risk stratification, early detection, and the development of targeted therapies in the future. To demonstrate the utility of the partially reprogrammed cell line UM30-OSN as a model for APOL1-associated kidney disease, we investigated the effects of interferon-γ (IFN-γ) on UM30-OSN-derived podocytes and evaluated the potential of the JAK1/JAK2 inhibitor baricitinib to mitigate IFN-γ-induced cellular responses.
Stimulation with IFN-γ resulted in enhanced STAT1 phosphorylation, increased APOL1 expression, upregulation of pro-inflammatory and fibrotic markers such as IL-6, TGF-β, vimentin, and fibronectin, as well as morphological changes indicative of cellular stress. Pretreatment with baricitinib effectively inhibited STAT1 phosphorylation, reduced the expression of pro-inflammatory and fibrosis-associated genes, and preserved podocyte morphology.

Furthermore, I carried out another study with UdRPCs from individuals with sodium-wasting conditions, named Bartter syndrome. Regarding the previous studies, Bartter syndrome has an interesting angle, by looking at hypertension and aging-related processes. The RAAS involves several systematic processes to regulate blood pressure caused by electrolyte imbalance. Salt intake is a critical factor influencing hypertension and plays a significant role in determining sensitivity to hypertensive responses.
To study the etiology of Bartter syndrome at the molecular level an induced pluripotent stem cell line (iPSC) of an 18-year-old Bartter syndrome type 3 (BS3) patient within a homozygous whole gene deletion of CLCNKB genotype was generated and characterized.

Research is the key to a better future, for each individual and society. Science investigates the smallest building blocks of life, molecules such as DNA, RNA, proteins, lipids and carbohydrates and their interactions in biological systems. This field of research is central to understanding the foundations of life and developing solutions for medical, biotechnological and ecological challenges. For this reason, in vitro studies aim to create therapeutic options, considering both ethical and legal guidelines. Previously published studies have shown that the use of UdRPCs, already used for urological tissue regeneration, bone regeneration or used in the treatment of acute to chronic kidney injuries.
In these previous studies, few experiments were conducted to explain the mechanism that describes the positive effect of transplanted urinary stem cells on the regeneration of injured

kidneys. The present study should provide a starting point to further investigate the mechanism. Accordingly, healthy human UdRPCs from a female individual aged 31 years were unilaterally transplanted under the renal capsule of mice kidneys subjected to ischaemia-reperfusion injury (IRI). Analyses of the blood serum of the transplanted mice showed that the secretome of the animals is altered in a time-dependent manner by the transplantation. UdRPCs reduce fibrosis and inflammation in a mouse model of kidney injury. They downregulated the expression of profibrotic and inflammatory markers and modulated the systemic secretome by releasing factors like IL-10, VEGF, and HGF. Complete kidney function was not restored within 21 days due to limitations imposed by ethics to conform with the R^3 principle-Reduce,Refine,Replace. The results highlight UdRPCs as a promising, non-invasive therapy for kidney repair.

This thesis underlines the significant potential of urine-derived renal progenitor cells for modelling not only kidney diseases such as acute kidney injury, chronic kidney disease, APOL1-mediated disease, Bartter syndrome, High blood pressure, or sickle cell disease but also similarities between kidney and brain and emphasizes the need for further investigation to validate their therapeutic use in the future.

Zusammenfassung

Die häufigsten Nierenerkrankungen umfassen chronisches und akutes Nierenversagen, degenerative Nierenerkrankungen, verschiedene Nierenentzündungen, Nierensteine, Nierenzellkarzinom sowie genetische Nierenerkrankungen wie die autosomal-dominante polyzystische Nierenerkrankung oder seltene erbliche Erkrankungen wie das Bartter-Syndrom. Weltweit betrifft chronische Nierenerkrankung (CKD) etwa 10 % der Bevölkerung, was sie zu einer der bedeutendsten Gesundheitsbelastungen macht. Nierensteine sind ebenfalls weit verbreitet, mit unterschiedlicher Prävalenz in verschiedenen Regionen. Das Nierenzellkarzinom, eine der häufigsten Krebsarten der Niere, macht etwa 2–3 % aller Krebserkrankungen weltweit aus. Seltene erbliche Nierenerkrankungen wie das Bartter-Syndrom, eine Störung der Nierenröhrenfunktion, sind äußerst selten, mit einer geschätzten Prävalenz von weniger als 1 von 1.000.000 Individuen.

Da der menschliche Körper jedoch ein komplexes und weit verzweigtes System ist, stehen Erkrankungen in enger Verbindung mit anderen Organen wie dem Herzen oder dem Gehirn. Es ist bekannt, dass eine geschädigte und nicht funktionierende Niere die Ausscheidung von Abfallstoffen aus dem Blut stoppt. Dadurch sammelt sich eine enorme Menge Flüssigkeit in den Blutgefäßen an, was zu Bluthochdruck oder noch höheren Werten führt. Die Harmonie und das Gleichgewicht des Systems sowie die Zusammenarbeit der Organe sind essenziell.

In der Vergangenheit war die Modellierung von Nierenerkrankungen äußerst schwierig, da es eine große Herausforderung darstellte, aus der Niere gewonnene Zellen zu erhalten. Obwohl unter gesunden Bedingungen relativ wenige Nierenzellen im Vergleich zu dysfunktionalen Zuständen ausgeschieden werden, konnten wir Zellen aus dem Urin gesunder Spender mit einer nicht-invasiven Methode isolieren, kultivieren und vermehren. Multipotente Stammzellen aus dem Urin besitzen ein breites Differenzierungspotenzial; sie können in renale Zelltypen wie glomeruläre Podozyten differenziert und auch für die Reprogrammierung zu induzierten pluripotenten Stammzellen (iPSCs) genutzt werden. Da Nierenerkrankungen häufig durch Schäden an Glomerulus oder Tubuli verursacht werden, bietet diese Methode ein breites Potenzial für In-vitro-Studien.

Die sogenannten aus Urin gewonnenen nephronalen Vorläuferzellen (UdRPCs) können auf verschiedene Weise immortalisiert und in induzierte pluripotente Stammzellen reprogrammiert

werden. In diesem Fall wurde die Immortalisierung mithilfe von humaner Telomerase (hTERT) und einer teilweisen Programmierung der Yamanaka-Faktoren durchgeführt. Die Verwendung dieser Zelllinien bietet eine langfristige und weitreichende Plattform zur Untersuchung nierenassoziierter Erkrankungen.

Entsprechend wurden die erzeugten Zelllinien unter anderem in einen hochspezialisierten Zelltyp, die Podozyten, differenziert. Podozyten spielen eine Rolle im Blutfiltrationsprozess in den Glomeruli der Niere. Einschränkungen oder Fehlfunktionen der Podozyten stehen mit zahlreichen Nierenerkrankungen in Verbindung, weshalb die Untersuchung und Anwendung dieses Zelltyps als Krankheitsmodell von großer Bedeutung ist. Weltweit sind jährlich etwa 9,4 Millionen Todesfälle auf Bluthochdruck zurückzuführen. Bluthochdruck wird hauptsächlich durch das Renin-Angiotensin-Aldosteron-System (RAAS) reguliert, dessen Hauptmediator Angiotensin II (ANG II) ist. Erhöhte ANG-II-Werte führen zu einem pro-fibrotischen, -inflammatorischen und -hypertrophischen Milieu und induzieren Apoptose in Podozyten. Eine verlängerte Aktivierung des RAAS ist entscheidend für die Pathogenese von Podozytenschäden und verursacht Proteinurie. Um Podozytenschäden entgegenzuwirken, werden Medikamente verabreicht, die den RAAS-Weg modulieren, wie beispielsweise Losartan.

In den vorliegenden Studien zeigen die aus UdRPCs differenzierten Podozyten eine Aktivierung des RAAS durch ihre Reaktion auf ANG-II-Stimulation. Die Forschungsdaten belegen eine ANG-II-abhängige Herunterregulierung der podozytenspezifischen Marker Nephrin (NPHS1) und Synaptopodin (SYNPO), was zu einer Veränderung des Zytoskeletts führt. Die Zugabe einer präzisen Konzentration von Losartan verhindert die ANG-II-abhängige Veränderung des Zytoskeletts. Dies führte zu einer erhöhten Expression spezifischer Podozytenmarker, die das Podozyten-Zytoskelett rettete, wie durch quantitative Echtzeit-PCR und Western-Blot-Analysen gezeigt wurde. Darüber hinaus konnte die Zytoskelettstörung der Podozyten, die durch immunfluoreszenzbasierte Phalloidin-Detektion sichtbar gemacht wurde, durch Losartan verhindert werden. Dieses Wissen ist sowohl für weitere Nephrotoxizitätsstudien als auch für das Verständnis molekularer Mechanismen vieler Nierenerkrankungen von Bedeutung.

Erkrankungen wie akute Nierenschädigung (AKI) oder sogar chronische Nierenerkrankung (CKD) können ebenfalls mithilfe von UdRPCs untersucht werden. In den beiden vorgestellten Studien wurde das Sekretom des Urins einer AKI-Patientenkohorte analysiert und die Wirkung

von Patienten- und gesundem Urin auf humane Podozyten untersucht. Heute kann man schlussfolgern, dass biologische Prozesse geschlechts- und altersabhängige Variationen aufweisen können. Basierend auf den Ergebnissen konnten wir ADIPOQ, EGF und SERPIN3A als potenzielle frühe Biomarker identifizieren, die eine akute Nierenschädigung bereits 24 Stunden nach einer Operation nachweisen können. Zusätzlich wurden Gene identifiziert, die 72 Stunden nach der Operation hochreguliert waren, darunter CXCL1, VEGF und RENIN.

Parallel dazu zeigte eine Studie an CKD-Patienten aus Ghana eine verminderte Sekretion von EGFR und VEGF im Verlauf der CKD-Progression. Dies deutet darauf hin, dass EGFR und VEGF als Initiatoren bei AKI wirken und während der CKD-Progression abnehmen könnten. Eine frühzeitige Erkennung solcher Zytokine könnte rechtzeitige Interventionen ermöglichen, um einen Zusammenbruch der Filtrationsbarriere zu verhindern, was potenziell erhebliche Vorteile für Patienten bringen könnte. Darüber hinaus sind zytokinbasierte Tests nicht-invasiv, kostengünstig und können leicht mit Urinproben und Flusszell-Detektionsgeräten durchgeführt werden, was eine vielversprechende Alternative für das Monitoring von AKI und CKD darstellt.

APOL1 ist ein entscheidender genetischer Risikofaktor für CKD bei Menschen mit afrikanischer Abstammung. Das Verständnis dieses Zusammenhangs hilft bei der Risikostratifizierung, Früherkennung und in Zukunft möglicherweise bei gezielter Therapie. Um die Nützlichkeit der partiell reprogrammierten Zelllinie, UM30-OSN als Modell für APOL1-vermittelte Nierenerkrankungen zu demonstrieren, haben wir die Auswirkungen von Interferon-γ (IFN-γ) auf UM30-OSN-Podozyten untersucht und das Potenzial des JAK1/JAK2-Inhibitors Baricitinib zur Abschwächung IFN-γ-induzierter zellulärer Reaktionen bewertet. Die IFN-γ-Stimulation führte zu einer erhöhten Phosphorylierung von STAT1, einer Aktivierung von APOL1, einer Hochregulierung von proinflammatorischen und fibrotischen Markern wie IL-6, TGF-β, Vimentin und Fibronectin sowie zu morphologischen Veränderungen, die auf Zellstress hinweisen. Die Vorbehandlung mit Baricitinib hemmte wirksam die STAT1-Phosphorylierung, verringerte die Expression von pro-inflammatorischen und Fibrose-assoziierten Genen und bewahrte die Morphologie der Podozyten.

In einer weiteren Studie wurden UdRPCs von Individuen mit Natriumverlustsyndromen, wie dem Bartter-Syndrom, analysiert. Im Hinblick auf die vorherigen Studien bietet das Bartter-Syndrom einen interessanten Ansatz, da es Bluthochdruck und altersbedingte Prozesse untersucht. Das RAAS umfasst mehrere systemische Prozesse zur Regulierung des

Blutdrucks, die durch Elektrolytungleichgewichte verursacht werden. Der Salzkonsum ist ein kritischer Faktor, der die Empfindlichkeit gegenüber hypertensiven Reaktionen beeinflusst.

Zur Untersuchung der Ätiologie des Bartter-Syndroms auf molekularer Ebene wurde eine induzierte pluripotente Stammzelllinie (iPSC) eines 18-jährigen Patienten mit Bartter-Syndrom Typ 3 (BS3) und einer homozygoten Deletion des gesamten Gens CLCNKB generiert und charakterisiert.

Forschung ist der Schlüssel zu einer besseren Zukunft – für jede Einzelperson und für die Gesellschaft als Ganzes**.** Die Wissenschaft untersucht die kleinsten Bausteine des Lebens – Moleküle wie DNA, RNA, Proteine, Lipide und Kohlenhydrate – und deren Wechselwirkungen in biologischen Systemen. Dieses Forschungsfeld ist zentral für das Verständnis der Grundlagen des Lebens und für die Entwicklung von Lösungen für medizinische, biotechnologische und ökologische Herausforderungen.

Aus diesem Grund zielen In-vitro-Studien darauf ab, therapeutische Optionen zu schaffen, wobei sowohl ethische als auch gesetzliche Richtlinien berücksichtigt werden. Bereits veröffentlichte Studien haben gezeigt, dass UdRPCs in der urologischen Geweberegeneration, der Knochenregeneration oder in der Behandlung von akuten bis chronischen Nierenschäden eingesetzt werden können.

Dementsprechend wurden gesunde menschliche UdRPCs eines weiblichen Individuums im Alter von 31 Jahren einseitig unter die Nierenkapsel von Mäusen transplantiert, die einer Ischämie-Reperfusionsverletzung (IRI) ausgesetzt waren. Analysen des Blutserums der transplantierten Mäuse zeigten, dass das Sekretom der Tiere durch die Transplantation zeitabhängig verändert wird. UdRPCs reduzieren Fibrose und Entzündung in einem Mausmodell für Nierenverletzungen. Sie verringerten die Expression von profibrotischen und entzündlichen Markern und modulierten das systemische Sekretom durch Freisetzung von Faktoren wie IL-10, VEGF und HGF. Die vollständige Nierenfunktion konnte nicht innerhalb von 21 Tagen wiederhergestellt werden, da die Einhaltung des R^3-Prinzips (Verringern, Verfeinern, Ersetzen) ethische Einschränkungen mit sich brachte. Die Ergebnisse zeigen, dass UdRPCs eine vielversprechende, nicht-invasive Therapie für die Nierenreparatur darstellen.
Diese Arbeit unterstreicht das bedeutende Potenzial von aus Urin gewonnenen Nierenvorläuferzellen für die Modellierung nicht nur von Nierenerkrankungen wie akuter

Nierenschädigung, chronischer Nierenerkrankung, APOL1-vermittelter Erkrankung, Bartter syndrom, Bluthochdruck oder Sichelzellkrankheit, sondern auch von Ähnlichkeiten zwischen Niere und Gehirn und betont die Notwendigkeit weiterer Untersuchungen, um ihren therapeutischen Einsatz in Zukunft zu validieren.

Structure of this Thesis

This thesis compiles ten publications, which address the potential use of urine and urine-derived renal progenitor cells in kidney diseases and further the use of their therapeutic potential. The publications are presented in chronological order:

1. Erichsen L, Thimm C, Bohndorf M, Rahman S, Wruck W, Adjaye J (2022). **Activation of the Re Activation of the Renin–Angiotensin System Disrupts the Cytoskeletal Architecture of Human Urine-Derived Podocytes**. *Cells;* https://doi.org/10.3390/cells11071095 (original research).

2. Erichsen L, Kloss L, Thimm C, Bohndorf M, Schichel K, Wruck W, Adjaye J (2023). **Derivation of the Immortalized Cell Line UM51-PrePodo-hTERT and Its Responsiveness to Angiotensin II and Activation of the RAAS Pathway**. *Cells*; https:// doi.org/10.3390/cells12030342 (original research).

3. Wruck W[#], Thimm C[#], Adjaye J (2025). **Evidence for conserved gene expression and biological processes operative in human podocytes and adult brain.** *BioRxiv;* https://doi.org/10.1101/2025.03.17.643629 (original research).

4. Thimm C, Zhong C, Wruck W, Grillo A, Mack R, Bohndorf M, Graffmann N, Tang A, D'Ambriosio V, Wan E, Siew K, Evans R, Walsh S, Adjaye J (2025). **Generation of a Bartter syndrome type 3 patient-derived induced pluripotent stem cell line ISRM-BS3-UM18-iPSC (HHUUKDi014-A).** *Stem Cell Research*; https://doi.org/10.1016/j.scr.2025.103760 (original research).

5. Kordes C, Spitzhorn LS, Bohndorf M, Ncube A, Thimm C, Erichsen L, Wruck W, Adjaye J (2025). **Human urine-derived SIX2-positive renal progenitor cells improve kidney injury in an ischemia reperfusion injury mouse model.** *BioRxiv*; https://doi.org/10.1101/2025.07.02.662781 (original research).

6. Thimm C, Mack R, Aruna-Adjei O, Wruck W, Adjaye J (2025). **Modelling APOL1-mediated kidney inflammation and fibrosis usinga partially reprogrammed urine derived SIX2-positive renal progenitor cell line.** *BioRxiv;* https://doi.org/10.1101/2025.07.28.667124 (original research).

7. Erichsen L, Thimm C, Wruck W, Kaierle D, Schless, Huthmann L, Dimski T, Kindgen-Milles D, Brandenburger T, Adjaye J (2023). **Secreted Cytokines within the Urine of AKI Patients Modulate TP53 and SIRT1 Levels in a Human Podocyte Cell Model.** *International Journal of Molecular Sciences;* https:// doi.org/10.3390/ijms24098228 (original research).

8. Thimm C, Adjaye J (2024). **Untangling the Uncertain Role of Overactivation of the Renin–Angiotensin–Aldosterone System with the Aging Process Based on Sodium Wasting Human Models**. *International Journal of Molecular Sciences; https:// doi.org/10.3390/ijms25179332* (original review).

9. Thimm C, Erichsen L, Wruck W, Adjaye J (2023). **Unveiling Angiotensin II and Losartan-Induced Gene Regulatory Networks Using Human Urine-Derived Podocytes.** *International Journal of Molecular Sciences;* https://doi.org/10.3390/ ijms241310551 (original research).

10. Wruck W[#], Pranty A[#], Thimm C[#], Loerch C, Mack R, Boima V, Adjaye J (2025). **Urinary proteins from Sickle Cell patients induce inflammation and kidney injury via the TGFβ-p53 axis in a podocyte cell culture model**. *BioRxiv*; https://doi.org/10.1101/2025.08.08.669286 (original research).

11. Wruck W, Boima V, Erichsen L, Thimm C, Koranteng T, Kwakyi E, Antwi S, Adu D, Adjaye J (2022). **Urine-Based Detection of Biomarkers Indicative of Chronic Kidney Disease in a Patient Cohort from Ghana.** *Journal of Personalized Medicine;* https://doi.org/10.3390/ jpm13010038 (original research).

A general synopsis outlines the anatomy and function of the kidney, beginning with nephron development and the glomerulus. It further addresses the Renin-Angiotensin-Aldosterone System, common kidney diseases such as acute kidney disease and chronic kidney disease, Apolipoprotein 1-mediated disease and magnesium-related disorders. Subsequent sections explore the effects of aging, the role of induced pluripotent stem cells, and approaches to cell line immortalization. The included publications provide deeper insight into the interconnection of these topics, offering background information and methodological details. This is followed by a discussion, with a final summary concluding the key findings.

1 Introduction

1.1 Fundamentals of renal anatomy and function

The kidneys are organs that fulfill many important functions to maintain normal bodily functions. The kidneys' main function is to filter the urine, removing urinary components such as urea, uric acid, salts, water, creatine, and toxins. Thereby controlling the homeostasis of electrolytes such as phosphate, potassium, calcium, and potassium. They also control blood pressure and regulate the acid-base balance, such as the synthesis site of calcitriol hormones, erythropoietin, and renin[1].

The kidneys are in the retroperitoneal space on both sides of the spine and have a bean-shaped form. They each weigh between 55 and 261 grams. A kidney is usually 5 cm wide, 90 to 130 cm long, and 2.5 to 3 cm thick. All these parameters depend on gender, ethic, racial diversity and the lateral position of the kidney[2–5].

The kidneys develop from the intermediate mesoderm and are controlled by the renal arteries. From the outside, the kidney is surrounded by a stretchable connective tissue envelope, the so-called *capsula fibrosa renis*. Each kidney consists of renal lobes, which are divided into the *medulla renalis* and the *cortex renalis* (A). The *medulla* is pyramid-shaped, with the renal calyces of the entire pyramid forming the renal pelvis, renal pelvis. The *cortex* is approximately one cm thick strip above and between the pyramids (Figure 1A).

To create a highly specialized and uniform network of arterioles that supply the glomeruli, the kidneys organize their blood vessels through a series of branching divisions. Upon entering the kidney, the renal artery undergoes multiple levels of branching. The renal artery first splits into segmental arteries, each serving a specific region of the kidney. Segmental Arteries, the interlobar arteries, these segmental arteries further branch into interlobar arteries, which run along the renal columns toward the junction between the cortex and medulla.

A nephron, the smallest functional unit of the kidney, consists of a glomerulus. There are approximately 1.3 million nephrons in a kidney (Figure 1B). These consist of the glomerulus and the tubule system[6]. The glomerulus is composed of a capillary vascular plexus that includes an inflow (*vas afferens*) and an outflow (*vas efferens*) vessel surrounded by the Bowman's capsule. Small tubes that run through the inner part of the kidney, known as renal tubules, play a critical role in filtering and regulating the flow of various chemical substances between the blood and the urine. These tubules are integral components of the nephron and

are responsible for the reabsorption of essential molecules and the secretion of waste products. After the initial filtration of blood in the glomeruli, the filtrate enters the tubules, where several processes occur. Through these processes through the proximal convolted tubule, loop of Henle, distal convoluted tubule and the collecting ducts, the renal tubules maintain homeostasis by balancing electrolytes, water, and pH levels, while ensuring the removal of metabolic wastes. Their function is critical to overall kidney health and the body's ability to regulate blood composition.

The surface of the glomerular capillaries has size- and charge-selective characteristics and therefore serves as a filtration barrier for the blood passing through the glomerulus. The glomerular excretion of blood plasma into the urinary cavity of Bowman's capsule leads to the formation of approximately 200 liters of primary urine per day. This process of glomerular excretion of blood plasma prevents the following three-part filtration unit from containing important blood components such as macromolecular proteins and blood cells. The fenestrated endothelium of the capillary bulb, the glomerular basement membrane, and a highly specialized cell type, the podocyte, form the tripartite filtration unit[1].

The secondary urine is formed by resorption and secretion processes in the tubule system. The filtered fluid reaches the mitochondria-rich proximal tubule, which opens into the Henle loop. There the filtered low-molecular substances such as glucose and smaller proteins are reabsorbed. This is where freely filterable glucose is completely reabsorbed through active transport processes. The collecting ducts transport the secondary urine into the renal pelvis. From there, it reaches the bladder, where the urine is moved forwards by peristaltic contraction waves (2 - 6 /min) and is finally released via the *urethra*[1].

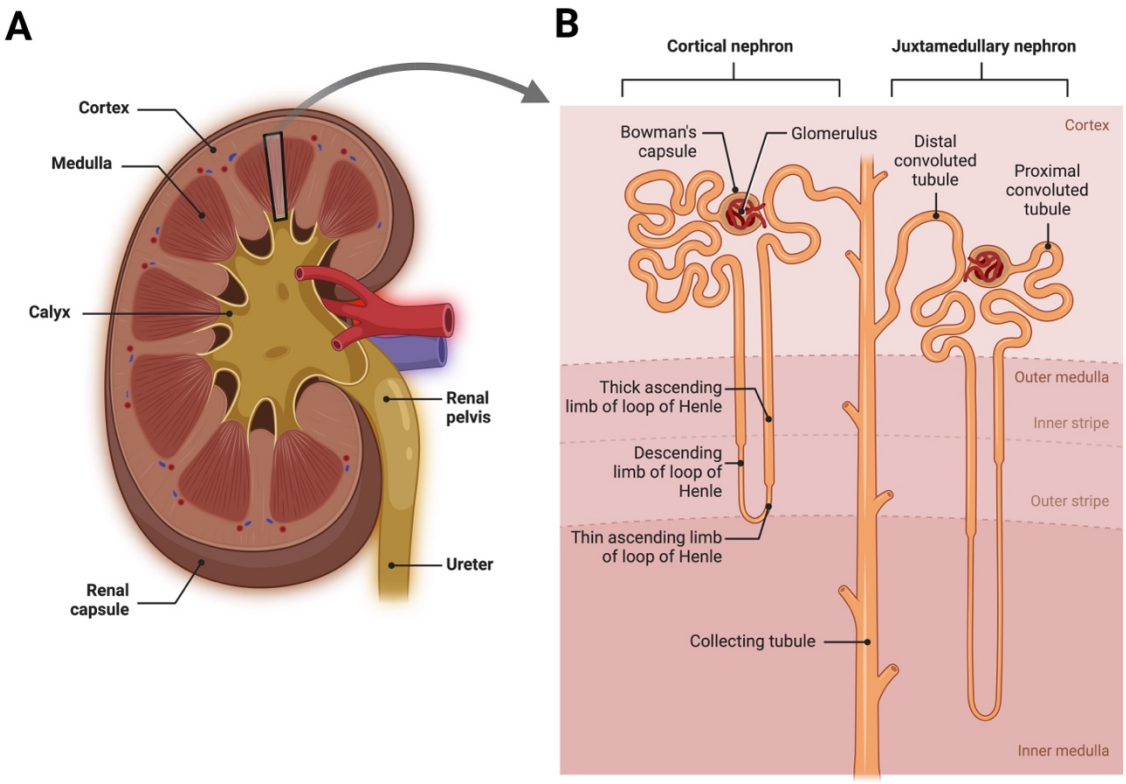


Figure 1: Kidney anatomy
The kidney is a paired bean-shaped endocrine organ that is responsible for the filtration, reabsorption, and concentration of urine, as well as for the production of renin and erythropoietin. From the outside, the kidney is surrounded by a stretchable connective tissue envelope, capsula fibrosa renis. Each kidney consists of renal lobes, which are divided into the medulla renalis and the cortex renalis (A). The medulla is pyramid-shaped, with the renal calyces of the entire pyramid forming the renal pelvis, renal pelvis. The cortex is approximately one cm thick strip above and between the pyramids (A). The kidney tissue consists of small filter units, the nephrons (B). The nephron is the smallest unit of the kidney and consists of the renal corpuscle and the renal tubular system. Whereby the renal corpuscle contains the glomerulus and a collection of capillaries enclosed by Bowman's capsule. The renal tubule can be subdivided from proximal to distal. The straight section between the two, together with the loop of Henle, is known as the intermediate tubule. The distal tubule opens into the collecting tubule from the uterine bud. The figure was created and edited with the BioRender Template "Kidney Anatomy"[7].

1.2 Development of the nephron

The functional unit of the kidney is the nephron, which develops from the progenitor stem cells induced by Wnt signaling [8]. The development of the mammalian kidney resembles relics of evolution. Initially, embryos have two transitional kidneys, the pro- and mesonephron, from which the adult kidney of the metanephros eventually develops after a spatial and temporal sequence[9].

The first stages of kidney development are part of the reproductive system in that the kidney begins with the sprouting of the ureteral bud from the ductus pronephricus. Primitive kidney

development is initiated by the expression of Pax-2 and Sim-1 in the intermediate mesoderm. As the ureteric bud grows into the metanephrogenic mesenchyme, it begins with branching morphogenesis. Isolated mesenchymal cells aggregate at the newly formed branches and begin a transformation from mesenchyme to epithelium, while other mesenchymal cells form the interstitial stroma. Both tissue types are descendants of the interstitial mesoderm of a narrow cell population that lies between the paraxial and lateral plate mesoderm and specializes during gastrulation. Development takes place sequentially in the metanephric blastema. The onset starts when the epithelial forms the ureteric bud at its extreme caudal end. The nephron progenitor cells express various signaling factors that play an important role during kidney development. These factors are: Eya1, Cited1, Hox11, Osr1, Pax2, Sall1, Six1, Six2 and WT1[10–16]. The deletion of each of these factors leads to defective kidney development in the mammalian kidney.

Subsequently, the ureteric bud invades the predetermined renal mesenchyme, begins to branch, and initiates nephrogenesis. The nephron develops through the mesenchymal-epithelial transition (MET) and morphogenesis, which is activated via the non-canonical WNT signalling pathway via WNT4. The migration of endothelial cells into the developing glomerulus is essential for the attachment of a functional nephron. The development of a second kidney is triggered by the caudal elongation of the epithelial Wolffian duct (WD), which leads to the formation of the mesonephros (MN). In aquatic vertebrates, the MN serves as the main excretory organ, whereas in reptiles, birds and mammals it is only a transient organ. Although the MN is only transiently present during kidney formation in mammals, it is crucial for the development of other organs derived from the urogenital system such as gonads, adrenal glands and also for hematopoiesis[17]. The WD finally forms the ureteric bud, which induces nephron formation in the neighboring metanephric mesenchyme by induced signals. When the mesenchyme receives signals from the ureteric bud, it can undergo two independent fates. One is the pathway of self-renewal to maintain the progenitor pool and the other is the initiation of MET, leading to the formation of the segmented nephron[14].

1.3 Glomerulus of the kidney

The nephrons of mammals have at least 16 different highly specialized epithelial cell types. The interaction of epithelial cells, endothelial cells, immune cells, and interstitial cell types is essential for kidney function and, above all, for maintaining the internal environment[18,19]. the

system is divided into distal and proximal systems. There are also spatial differences between the medulla and cortex. There are further differences in the interstitial sodium and urea concentrations, which are essential for water homeostasis. The hypoxic conditions present can only be survived by specialized epithelial and immune cells[20]. The glomerulus, the filtering unit of the kidney, is a specialized bundle of capillaries uniquely located between two resistance vessels.

Blood from the glomerular capillaries is collected in the efferent arterioles, which in turn divide to form the second capillary bed, the peritubular capillaries. This second capillary system has a low hydrostatic pressure and is responsible for returning the reabsorbed fluid and electrolytes to the circulation.

These capillaries are each located within Bowman's capsule and are the only capillary beds in the body that are not surrounded by interstitial tissue. Therefore, a unique support structure is required. The proximal component layer of the glomerular filter itself is a fenestrated endothelium characterized by the presence of individual fenestrae in the order of 70-100 nm in diameter. These cells envelop the luminal aspect of the capillary and enable filtration. The second layer of the filter, the glomerular basement membrane (GBM), is a complex meshwork of extracellular proteins, including collagen type IV, laminins, fibronectins, and proteoglycans. The distal layer of the glomerular filter consists of the visceral epithelial cells, named podocytes.

These highly differentiated and specialized cells adhere to the outer surface of the glomerular capillaries and extend into the urethra of Bowman's capsule. They contributing to the formation of the filtration slit diaphragm and serve as a support to maintain the integrity of the free-standing capillary loops. They have a large cell body from which numerous foot processes taper around the glomerular capillaries. Neighboring podocytes thus form lamellipodia-like foot processes, between which an interdigital unique cell-cell contact is formed. At the same time, the podocytes ensure the size selectivity of glomerular filtration: the slit diaphragm. These foot processes are separated from each other by 30 - 40 nm wide filtration slits and covered by a thin, electron-dense membrane, the slit diaphragm[21]. The podocyte slit membrane expresses several characteristic molecules like the "tight junction"-associated molecule zonula occludens-1 (ZO-1) at the cytoplasmic side of slit membranes, which is co-localized with P-cadherin, α-, β- and γ-catenin[22,23]. In addition to P-cadherin, there are three other transmembrane molecules with large extracellular domains in the zipper-like structure of the slit diaphragm. These are the cadherin-like molecule FAT, the protein Neph-1 and Nephrin (NPHS1)[24–26].

Near to the extracellular proteins of the slit membrane is the hairpin-like transmembrane protein NPHS2 with two cytoplasmic ends, which is expressed within the glomerulus only in podocytes[27]. The CD2-associated protein (CD2AP) is localized in the cytoplasm within the podocyte foot processes on the side of the slit membrane and anchors NPHS1 and NPHS2 to the F-actin of the cells[28]. An interaction between Podocin (NPHS2) and NPHS1, Neph1, and CD2AP has already been demonstrated[29,30]. This highly conserved complex, through which podocytes are connected to cell-cell contacts, controls podocyte function and maintains an internal support network[21,28].

The morphology of podocytes, which form the filtration slits with their primary and secondary foot processes, can only be maintained by a mature internal support network.

Actin forms the basis of the cytoskeleton in the secondary foot processes of the podocyte, while the cytoskeleton of the cell body and the primary processes are based on microtubules and intermediate filaments[31]. The secondary foot processes have a cytoskeleton based on microfilaments. This contractile apparatus consists mainly of F-actin, Myosin-II, Alpha-actinin-4 (ACTN4), talin, and vinculin. ACTN4 is one of four highly homologous alpha-actinin proteins that form "head-to-tail" homodimers, which are ubiquitously expressed[32]. In non-muscular cells, ACTN4 is involved in the organization of the cortical cytoskeleton and localizes to stress fibers and focal contacts, where it interacts with several cytoskeletal and membrane-associated molecules. Other proteins such as synaptopodin (SYNPO) and podocalyxin-like protein (PODXL) are key maker of differentiated podocytes[33–35].

A third cell type, the mesangial cells, also contributes to the integrity of the glomerular tuft and the dynamics of filtration. Taken together, this elegant structure enables the formation of the primary glomerular filtrate, which enters a space delimited by the visceral and parietal epithelial cells before being altered during transport through the tubule.

1.4 Renin-angiotensin-aldosterone system

Glomerular diseases are subject to a slow and asymptomatic progression over many years. This leads to serious health problems such as hypertension, nephrotic syndrome, acute kidney disease, chronic kidney disease or kidney failure. Kidney failure can lead in some cases to confusion and death if not treated immediately[36].

The renin-angiotensin-aldosterone system (RAAS) is a bioenzymatic cascade that influences the systemic and localized physiological processes. One major systemic role of RAAS is blood

pressure regulation, primarily achieved by increasing peripheral vascular resistance, enhancing cardiac contractility, promoting water and sodium reabsorption, and stimulating aldosterone secretion. Additionally, RAAS facilitates catecholamine release from sympathetic nerve terminals, thus contributing further to blood pressure control[1].

The RAAS activation is typically triggered by a reduction in renal perfusion, blood pressure, or sodium levels, which are detected by specialized sensors in the kidneys. According to Guyton and Hall, “the juxtaglomerular cells of the kidney release renin in response to decreased arterial pressure or sympathetic nervous system stimulation”[37]. This release marks the first step in a cascade that significantly impacts cardiovascular and renal function. Renin, an enzyme secreted into the bloodstream, catalyzes the conversion of angiotensinogen, a liver-derived protein, into angiotensin I. This relatively inactive precursor is subsequently converted into angiotensin II (ANG II) by angiotensin-converting enzyme (ACE), primarily in the lungs. The ANG II sequence—Asp-Arg-Val-Tyr-Ile-His-Pro-Phe—is conserved across many mammalian species like humans, horses, and pigs. Notably, ANG II can also be synthesized independently of renin through alternate pathways involving tissue plasminogen activators (t-PA), cathepsin G, tonin[38,39], and the enzyme chymase, which cleaves angiotensin I directly into ANG II, accounting for about 40% of the renal ANG II production[40].

Angiotensin II, an octapeptide, plays a pivotal role in the RAAS pathway, acting as a potent vasoconstrictor and promoting the release of aldosterone from the adrenal cortex. As Hall and Guyton note, “Angiotensin II directly increases blood pressure by constricting blood vessels and indirectly through stimulating aldosterone secretion”[1]. Aldosterone enhances sodium and water reabsorption in the distal nephron, leading to an increase in blood volume and pressure. Additionally, angiotensin II stimulates antidiuretic hormone (ADH) secretion from the posterior pituitary, which further promotes water reabsorption in the kidneys. Collectively, these mechanisms work to restore hemodynamic stability. However, this adaptive response can have detrimental effects if chronically activated.

Prolonged RAAS activation, often seen in conditions such as hypertension, heart failure, and chronic kidney disease, leads to pathological consequences. Angiotensin II not only perpetuates high blood pressure but also promotes cardiac remodeling and fibrosis, as described by Schmieder et al.[41], who highlight that “sustained RAAS activation accelerates organ damage through pro-inflammatory and pro-fibrotic pathways.” In the kidney, elevated intraglomerular pressure due to angiotensin II-mediated efferent arteriole constriction contributes to podocyte injury and proteinuria.

ANG II interacts with two primary receptor subtypes: AT1 (AGTR1) and AT2 (AGTR2). Beyond the systemic RAAS effects, localized RAAS is present in various organs[42], including the kidney, where ANG II concentrations can reach up to 1000 times higher than in the general circulation[39,43]. Both AGTR1 and AGTR2 receptors in the kidney play essential roles in regulating renal hemodynamics, tubular function, cellular growth, and matrix production (Figure 2)[43].

So far, physiological and pathological effects have been reported to be mainly mediated via AGTR1 receptors. Within the kidney, AGTR1 receptors are found in glomerular mesangial cells, proximal and distal tubular epithelial cells, medullary interstitial cells, and renal vasculature[38,43,44]. Renal AGTR1 activation induces vasoconstriction, sodium reabsorption, protein synthesis, and cellular growth, all of which are key to angiotensin II-mediated responses (Figure 2)[43,45]. AGTR2 receptors are critical in fetal development, where they are highly expressed; however, their expression declines after birth and remains limited in adult tissues such as the brain, heart, and reproductive organs[46–48].

In adult humans, AGTR2 receptors are found in the vasculature, glomeruli, juxtaglomerular apparatus, renal tubules, afferent arterioles, and the renal capsule[43]. Although their precise function is not fully understood, AGTR2 receptors are believed to play roles in regulating renal hemodynamics and tubular functions, may promote vasodilation and kidney function (Figure 2)[49].

Pharmacological interventions, including ACE inhibitors, angiotensin receptor blockers (ARBs), and aldosterone antagonists, have proven effective in mitigating these effects. By interrupting the RAAS pathway, these agents reduce blood pressure, decrease proteinuria, and slow the progression of kidney and cardiovascular disease. As targeting the RAAS is a cornerstone in the management of cardiovascular and renal pathologies. In summary (Figure 2), the RAAS is vital for maintaining blood pressure and fluid balance during acute stress, but its chronic overactivation can lead to significant harm. Understanding the interplay between its physiological and pathological roles underscores the importance of targeted therapies in mitigating its long-term effects.

1.4.1 Angiotensin II receptor antagonists

Persistent activation of the RAAS is a key factor in the pathogenesis of podocyte injury, leading to proteinuria, a primary indicator of filtration barrier failure. Proteinuria, often resulting from podocyte injury, significantly predicts disease progression and renal outcomes in glomerular

diseases[50,51]. ANG II, a major effector of RAAS, triggers the downregulation of ACTN4 and reduces focal adhesion expression in podocytes. This leads to F-actin restructuring and redistribution of ZO-1 in cultured podocytes, destabilizing the actin cytoskeleton[52].

With prolonged RAAS activation, ANG II promotes a shift in podocyte phenotype from stable to migratory, resulting in increased actin cytoskeletal turnover. This shift can eventually deplete podocytes, contributing to focal segmental glomerulosclerosis[53]. Clinical studies support the benefits of RAAS blockade in reducing proteinuria, whether through ACE inhibitors or AGTR1 antagonists[51,54]. Angiotensin II receptor blockers (ARBs) generally have fewer side effects than other antihypertensive medications, including dizziness or light-headedness, headache, and fatigue.

The 1990s saw the development of losartan, the first orally active, nonpeptide ARB. Since then, other ARBs—such as valsartan, eprosartan, and olmesartan—have been synthesized[55]. Unlike ACE inhibitors, ARBs prevent ANG II from binding to AGTR1 without affecting bradykinin and substance P degradation. However, AGTR1 inhibition interrupts negative feedback, leading to increased renin secretion and ANG II synthesis. Consequently, elevated ANG II may activate AGTR2 or other receptors, modulating effects on the kidney and other tissues[45,56,57].

Losartan is widely used to treat glomerular diseases linked to podocyte damage, such as focal segmental glomerulosclerosis. However, its precise signaling mechanisms in these contexts remain partially speculative[58].

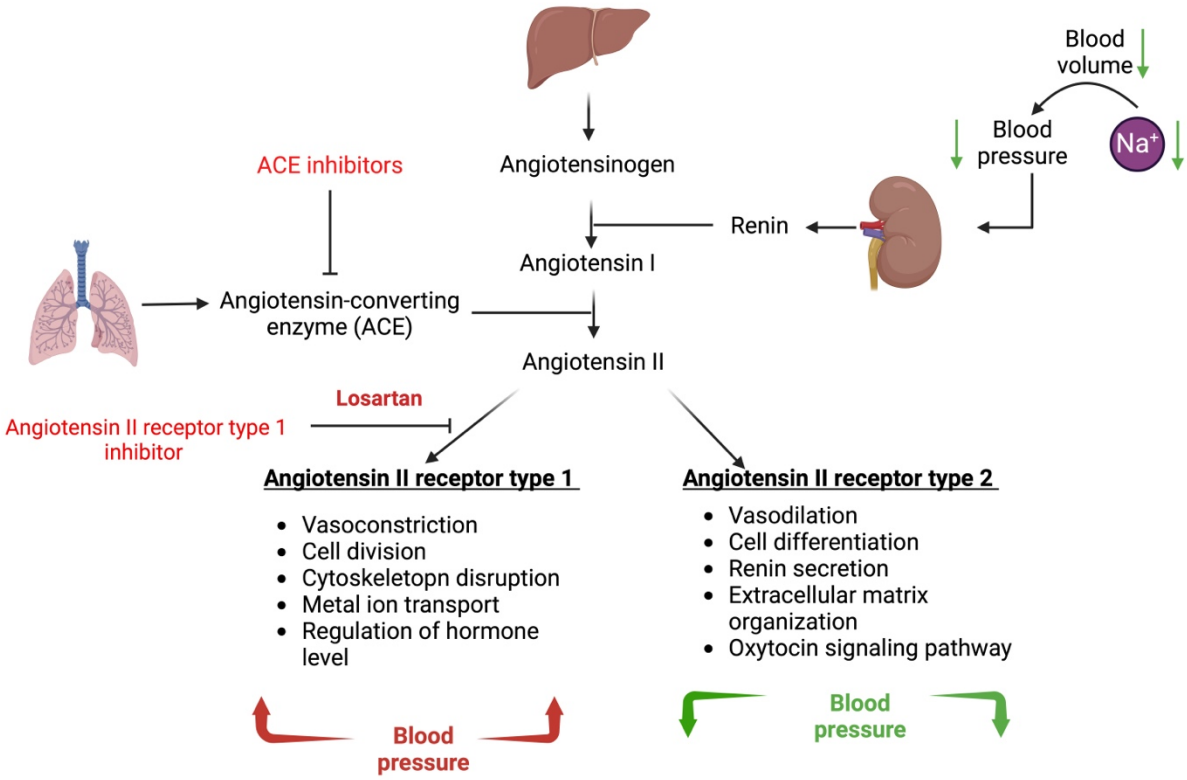


Figure 2: Renin-angiotensin-aldosterone system
The renin-angiotensin-aldosterone system (RAAS) is crucial for regulating fluid balance, electrolytes, and blood pressure. Renin, an enzyme primarily produced by the juxtaglomerular cells of the kidney, is secreted when renal blood flow drops below 70 mmHg. Renin's role is to convert angiotensinogen into angiotensin I, which is then transformed into angiotensin II (ANG II) by the angiotensin-converting enzyme (ACE), mainly produced in the endothelial cells of the lungs. Angiotensin II acts through angiotensin receptors, type 1 and 2 (AGTR1/2), to influence various processes such as regulating renal hemodynamics, tubular function, cellular growth, and matrix production. By binding to AGTR1, ANG II causes vasoconstriction, cell division, cytoskeleton disruption, metal ion transport and regulates the hormone level. By binding to AGTR2, it causes vasodilation, cell differentiation, renin secretion, extracellular matrix organization, and oxytocin signalling pathway. Clinical studies support the benefits of RAAS blockade in reducing high blood pressure, whether through ACE inhibitors or AGTR1 antagonists, e.g. losartan. Created and edited the biorender template *„Renin-Angiotensin System“,*https://BioRender.com.

1.5 Kidney diseases

1.5.1 Acute kidney injury

Acute kidney injury (AKI) is a kidney disease with a poor clinical outcome. According to the International Society of Nephrology (ISN), around 13 million people worldwide suffer AKI every year, with around 85% of cases occurring in low- and middle-income countries[59]. The mortality rate is high, with an estimated 1.7 million deaths annually. The ISN describes AKI as “a global health crisis that disproportionately affects the most vulnerable in society”[59]. It is associated

with increased morbidity and mortality up to 50% even in patients requiring dialysis, and is also linked to prolonged hospitalization[60–64].
It is characterized by an abrupt (within hours or weeks) deterioration in kidney function, which can be caused by reduced renal perfusion (prerenal failure), direct structural damage to the nephrons (intrarenal) or drainage disorders (postrenal)[65].

According to studies, even minor injuries or impairment of kidney function can lead to serious consequences, such as changes in serum creatinine (sCr) and/or urine output (UO)[66]. Based on this, the diagnosis is made according to the kidney disease Improving Global Outcome (KDIGO) criteria[67]. This measures both the creatinine increase and the reduced urine excretion. The reference value is an increase in serum creatinine of ≥0.3 mg/dL (26.5 µmol/L) within 48 h or an increase in serum creatinine of ≥1.5 times or new reduction in urine volume to <0.5 mL/kgKG/h over 6 h.

Intrinsic acute kidney injury is a serious kidney disease, refers to a form of acute kidney injury resulting from direct damage to the kidney tissue itself[66]. This distinguishes it from prerenal AKI (caused by insufficient blood flow to the kidneys) or postrenal AKI (caused by obstruction of the urinary tract). Intrinsic AKI is a significant subset of AKI cases, particularly in hospitalized or critically ill patients[66].
The pre- and postrenal AKI is the result of extrarenal disease leading to a reduced glomerular filtration rate (GFR).
However, in persistent conditions, cellular damage can also develop and progress to intrinsic renal disease[66]. At the same time, the risk of chronic kidney disease (CKD) increases. After AKI, renal function continues to deteriorate in some patients. In a proinflammatory and profibrotic environment, the proximal tubules undergo maladaptive repair. In the transition from AKI to CKD, impaired recovery from AKI leads to a reduction in tubular and glomerular filtration and thus to CKD. Pre-existing CKD is also one of the most important risk factors for AKI, with an increased risk of more than tenfold[68].
Other risk factors for AKI include patient-related factors such as advanced age, pre-existing chronic organ failure (especially kidney, heart, or liver failure), cancer, or autoimmune diseases, as well as the etiology of AKI[59,69–71].

At the cellular level aberrant expression of proteins such as NGAL, which is known as a typical marker for tubular damage, are associated with AKI[72]. Nowadays NGAL has been proposed

as an AKI biomarker, as it has already been highly expressed in patients who progressed rapidly to end-stage renal failure[73].

In addition, other cellular and molecular targets play an essential role in the pathogenesis of AKI. Among them is p21 induction in AKI, which can be induced by p53-dependent and p53-independent mechanisms[74,75]. In this context, in AKI p53 has been reported to induce the DNA damage response mediated by ATR/Chk2[76,77] or p53 can trigger tubular cell death in AKI[74,78].

AKI in humans is acknowledged to be multifactorial and is associated with other major risk factors including advanced age, sepsis, diabetes, cardiovascular diseases, and the use of nephrotoxic agents[79]. These interrelated factors often exacerbate kidney damage and complicate recovery, underscoring the need for a comprehensive approach to prevention and management. This requires new therapeutic approaches targeting molecular pathways[80].

1.5.2 Chronic kidney disease

Chronic kidney disease, which describes the change in the level of pathological functionality or structure of the kidney over at least three months, is a widespread disease worldwide. It leads to a progressive, usually irreversible decline in excretory and incretory kidney function and can consequently lead to terminal kidney failure. By 2022, more than 10% of the global population will be affected, i.e. more than 800 million people[81]. CKD is one of the most common causes of death worldwide[82,83]

The early stages are usually asymptomatic over time and symptoms arise when the final stages are reached. In 2019, a standardized nomenclature was developed by the National Kidney Foundation Kidney Disease Outcomes Quality Initiative[84] and the international guideline group Kidney Disease Improving Global Outcomes (KIDIGO)[85].

The classification of CKD is based on estimated glomerular filtration rate (eGFR) and albuminuria (Figure 3). The glomerular filtration rate (GFR) is a key measure of kidney function. It estimates how much blood is filtered by the glomeruli in the kidneys per minute, reflecting the kidneys' ability to remove waste, toxins, and excess fluids from the blood[86]. GFR is essential in diagnosing, staging, and managing kidney diseases, particularly ´CKD. Normal GFR in healthy adults is approximately 90–120 mL/min/1.73 m²[86].

Albuminuria refers to the presence of albumin, a type of protein, in the urine. It is a key indicator of kidney damage or dysfunction and is often associated with CKD and other systemic conditions such as diabetes and hypertension[87]. Normal albumin excretion is less than 30 mg/day or 30 mg/g creatinine[87].

Based on the GFR, kidney disease can be categorized into five stages of severity (G1 - G5). Stage 1 describes an eGFR of more than 90 mL/min per 1.73 m^2 for more than three months. Normal renal function is usually present. An eGFR in the range between 60 - 89 mL/min per 1.73 m^2 is associated with reduced renal impairment. Patients with stage 3a -3b have moderate functional impairment, with an eGFR of 45 - 59 mL/min per 1.73 m^2. An eGFR of 15 - 29 and < 15 is referred to as stage 4-5, where there is severe functional impairment or even chronic kidney failure.

Classifications in view of albuminuria are additionally combined with the creatinine value and are divided into three stages (A1 - A3). In stage 1, the albuminuria is < 30 mg/day with a creatinine rate of < 3 mg/mmol. The values are normal to slightly elevated.

Albuminuria values of 30 to 300 mg/day with a creatinine rate of 3 to 30 mg/mmol classify patients in stage 2. Patients in stage 3 have values of >300 mg/day albuminuria and >30 mg/mmol creatinine rate. The classification according to GFR and albuminuria is summarized together with the underlying disease in the CGA classification. C stands for ‘cause’, G for the GFR category (G1 - G5), and A for the albuminuria category (A1 - A3).

KDIGO: Prognosis of CKD by GFR and albuminuria categories				Persistent albuminuria categories Description and range		
				A1	**A2**	**A3**
				Normal to mildly increased	Moderately increased	Severely increased
				<30 mg/g <3 mg/mmol	30–300 mg/g 3–30 mg/mmol	>300 mg/g >30 mg/mmol
GFR categories (ml/min/1.73 m²) Description and range	**G1**	Normal or high	≥90			
	G2	Mildly decreased	60–89			
	G3a	Mildly to moderately decreased	45–59			
	G3b	Moderately to severely decreased	30–44			
	G4	Severely decreased	15–29			
	G5	Kidney failure	<15			

Figure 3: Chronic kidney disease criteria
The chronic kidney disease (CKD) has been standardized and developed by the National Kidney Foundation Kidney Disease Outcomes Quality Initiative[84]and the international guideline group Kidney Disease Improving Global Outcomes (KIDIGO)[85]. Classification as CKD is assessed based on the estimated glomerular filtration rate (eGFR) and albuminuria. The GFR is divided into G1 - G5 and the albuminuria into A1 - A3. Boxes marked in green indicate a low risk, which does not lead to CKD due to any other kidney diseases. Yellow indicates a moderate risk of CKD, whereas orange indicates an increased risk. Red boxes describe a very high risk. The figure was adopted from Stevens et al.[88].

In addition to the etiology of CKD, several molecular mechanisms are involved, including oxidative stress and inflammation , which contribute to the progression of renal injury and the development of end-stage renal disease[89]. Studies have described several uraemic toxins that are associated with increased oxidative stress in CKD and the associated deterioration in renal function[89]. These include indoxyl sulphate, which accumulates in the serum of CKD patients. This mainly activates nicotinamide adenine dinucleotide phosphate oxidases such as NOX4. Resulting in the cellular production of superoxides. In addition, indoxyl sulphate increases the production of growth factor-beta1, tissue inhibitor of metalloproteinase-1, proalpha1(I) collagen and free radicals in vascular smooth muscle and vascular endothelium[90,91]. Inflammation also plays an important role. Interleukins are among the first immune responses and inflammatory effects[92]. Interleukins are currently used as a diagnostic indicator for all diseases. For CKD, the focus is on IL-6[93]. IL-1[94] and IL-20[92,95,96]. In addition, there are biomarkers associated with CKD that are both gender-specific and independent. The gender-specific markers are IL10 and MME for male and CLU, RETN, AGER, EGFR and VEGFA for female[97]. The gender-independent cytokine markers were APOA1, ANGPT2, C5, CFD, GH1, ICAM1, IGFBP2, IL8, KLK4, MMP9 and SPP1[97].
Targeting genes that are aberrantly expressed in CKD are important for early detection and possible therapeutics[98].

1.6 Apolipoprotein L1-mediated kidney disease

Apolipoprotein L1 (APOL1), encoded a protein that plays a central role in the innate immune response, in particularly in the killing of *Trypanosoma parasites*[99]. APOL1 is a member of the apolipoprotein L gene family and is primarily expressed in podocytes, endothelial cells, and various immune cell types[100,101].
APOL1 has received particular attention in recent years due to the discovery of two genetic variants - G1 and G2. The APOL1 risk variants G1 comprises two missense mutations (rs73885319 and rs60910145) and G2 (6 bp deletion, rs71785313) are widespread in sub-Saharan Africa as they provide evolutionary protection against sleeping sickness

(*Trypanosoma brucei rhodesiense*)[102–104].However, they also increase the risk of certain kidney diseases when two risk variants are present, including G1/G1, G1/G2 or G2/G2. Individual risk variants G1 or G2 are present in over 40-50% of the population in West Africa, particularly in Nigeria and Ghana[105,106].

Homozygous or combined carriers of G1/G1, G2/G2 or G1/G2, which approximately 13-15% of the West African population carry[107], have a significant 10-30 times higher risk of developing diseases such as focal segmental glomerulosclerosis (FSGS)[108], HIV-associated nephropathy (HIVAN)[106] or CKD[109].

In comparison, the genetic variant G0/G0, which does not carry the risk-associated mutations is predominantly found in the European population. These strong differences in genotypes contribute significantly to ethnic disparities observed in the epidemiology of CKD[102,103,109,110].

Besides the epidemiological associations, the molecular mechanisms by which APOL1 risk variants lead to kidney damage is not yet fully understood. However, studies suggest that toxic effects on podocytes, resulting in foot process effacement and detachment, inflammatory reactions, cellular stress and disruption of mitochondrial function play a role[111–118].

Renal fibrosis is a defining feature of chronic kidney disease (CKD) and serves as a hallmark of disease progression, regardless of the underlying cause[119]. Fibrogenesis is initiated in response to chronic kidney damage; following renal injury, profibrotic factors are produced by injured tubular epithelial cells and infiltrating inflammatory cells that stimulate signaling events leading to extracellular matrix (ECM) production[120–123]. APOL1 risk variants are linked to accelerated fibrosis in the kidneys, contributing to the progression of kidney disease[108,124,125]. This has been shown in mouse models[113,126,127]. In a transgenic mouse model expressing the podocyte-specific APOL1-G2 risk variant (G2APOL1), these variants induced activation of STING and NLRP3 inflammasome pathway, triggered pronounced renal fibrosis, increased albuminuria and impaired renal function[127].

Given the high prevalence of risk variants in populations of African descent and the severity of associated kidney disease, there is growing interest in incorporating APOL1 genotyping into clinical practice, particularly in the context of kidney transplantation. Emerging evidence suggests that donor APOL1 genotype may influence allograft survival, leading to an ongoing debate about the role of genetic screening in donor selection and transplant outcomes[118,128–131]. Understanding the pathophysiological links between APOL1 variants and CKD is therefore crucial for the development of new therapeutic strategies. This aimed at reducing disease risk in genetically predisposed individuals. Future research needs to further elucidate the cellular and molecular

pathways underlying APOL1-associated kidney damage to develop precision medicine approaches and reduce the global burden of kidney disease.

1.6.1 Mechanisms of Interferon-γ and the JAK/STAT pathway

Janus kinase 1 (JAK1) is a central member of the Janus kinase (JAK) family, which plays a key role in the signal transduction of numerous cytokines and growth factors via the JAK-STAT signaling pathway. This pathway is essential for regulating immune responses, inflammation, cell proliferation, and apoptosis[132]. In the context of CKD, JAK1-mediated signaling has emerged as a significant contributor to inflammation and fibrosis, two core mechanisms driving CKD progression[133].

Activation of the JAK-STAT pathway is initiated by the binding of interferon-γ (IFN-γ) to its receptor complex, composed of IFNGR1 and IFNGR2, which leads to receptor dimerization and subsequent transphosphorylation of the associated kinases JAK1 and JAK2[134]. As a result, the signal transducers STAT1, STAT2, and STAT3 are recruited and phosphorylated. These phosphorylated STATs dimerize, translocate into the nucleus, and bind to specific DNA sequences such as GAS or ISRE elements, thereby activating transcription of target genes including IRF-1, STAT1/2, and APOL1 (Figure 4)[100,118,132,135,136].

Persistent activation of this pathway promotes tubulointerstitial inflammation, fibrosis, glomerulosclerosis, and leads to the loss of functional nephrons. Particularly relevant in this context is the APOL1 gene, whose risk variants induce toxic gain-of-function activity, especially in podocytes, resulting in cellular injury[114,118,137–139]. Numerous studies have shown that APOL1 expression is upregulated by pro-inflammatory cytokines such as IFN-γ and TNF-α, a process mediated directly through the JAK-STAT signaling cascade[112,114,136,140–144]. This makes targeted modulation of this pathway a promising therapeutic approach.

Preclinical studies have demonstrated that JAK1 blockade can attenuate the inflammatory response and reduce renal fibrosis. In this context, baricitinib, an oral and selective JAK1/2 inhibitor, has emerged as a promising candidate. Baricitinib specifically inhibits JAK1 and JAK2, leading to downstream suppression of inflammatory gene transcription, reduction of tissue damage, and decreased APOL1 expression in kidney cells. In experimental models, baricitinib has been shown to reduce APOL1-induced cytotoxicity and alleviate podocyte injury[112,118,136,145]. A Phase 2 trail of baricitinib in patients with protenuria APOL1-associated

FSGS or APOL1-associated HTN-CKD without diabetes where dialy treated with and without baricitinib[146]. This study demonstrated the antiproteinuric efficacy and safety of baricitinib in patients with APOL1-associated FSGS and APOL1-associated HTN-CKD[146].

Baricitinib is already approved for several inflammatory and autoimmune diseases, including rheumatoid arthritis[147], atopic dermatitis[148], and alopecia areata[149]. Its potential use is also being explored in chronic kidney diseases, particularly those with inflammatory or immune-mediated components, such as diabetic nephropathy. In an ongoing Phase II clinical trial involving type 2 diabetes with proteinuric kidney disease, baricitinib significantly reduced proteinuria over 24 weeks[149]. Also in a Phase III clincial trail for lupus nephritis, baricitinib showed a significant improve in disease activity[150].

Overall, baricitinib represents a promising therapeutic option, particularly for patients with a genetically determined high-risk profile, such as those with APOL1-associated nephropathies. The potential to slow disease progression through targeted JAK inhibition would represent a significant advancement in the treatment of this vulnerable patient population.

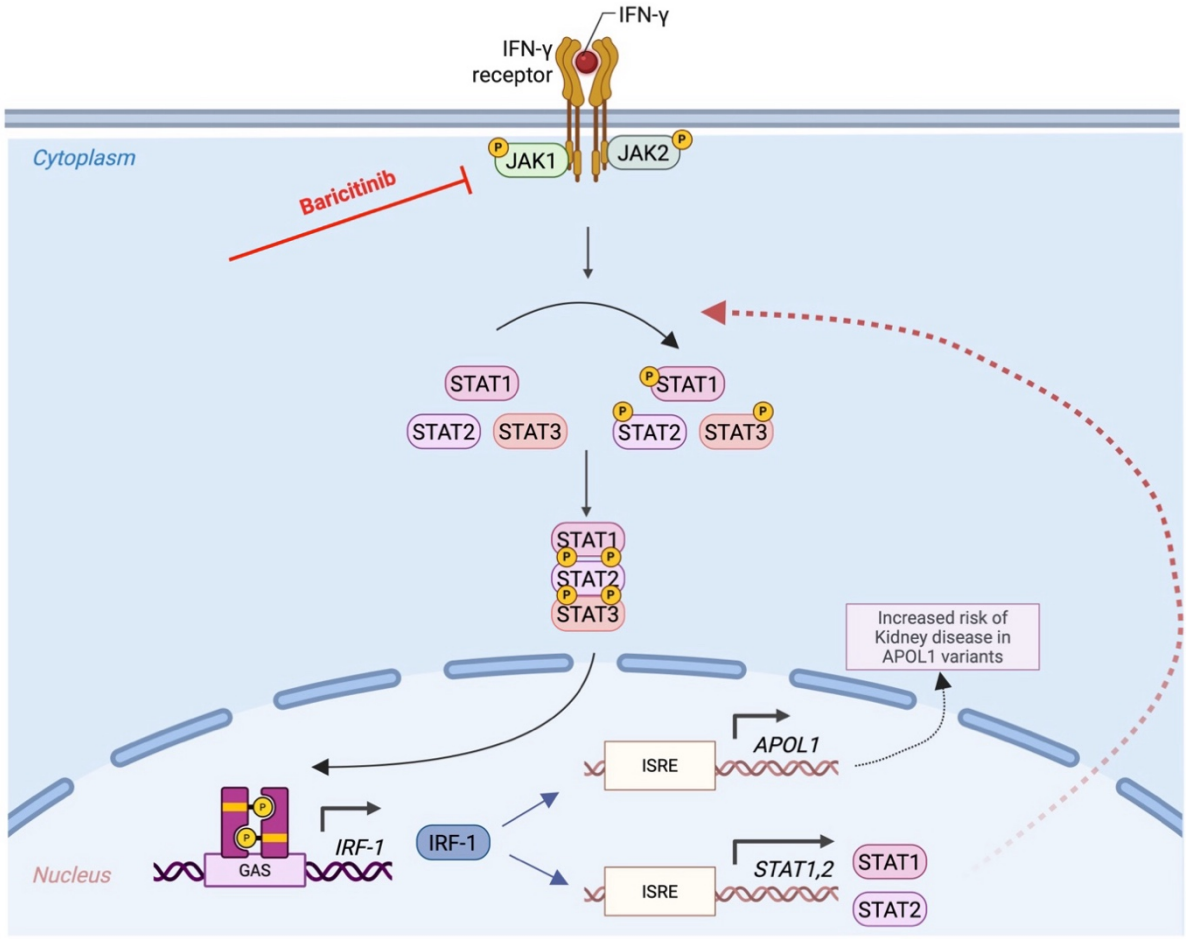


Figure 4: Interferon-γ signaling pathway.
Interferon-γ binds to its heterodimeric receptor, composed of interferon gamma receptor 1 (IFNGR1) and interferon gamma receptor 2 (IFNGR2), inducing receptor dimerisation. This leads to the activation of the associated Janus kinases JAK1 and JAK2 via transphosphorylation. Subsequently, the signal transducers STAT1, STAT2, and STAT3 are recruited and phosphorylated. The phosphorylated STATs form dimers and translocate to the nucleus, where they bind to specific DNA elements such as gamma interferon activation site (GAS) or IFN-stimulated response element (ISRE) sequences, thereby promoting the transcription of target genes including Interferon Regulatory Factor 1 (IRF-1), STAT1/2, and Apolipoprotein L1 (APOL1). Baricitinib inhibits this upstream signaling by selectively blocking JAK1 and JAK2 activity, thereby suppressing STAT activation and downstream gene expression. Created in https://BioRender.com[169]

1.7 Disease that leads to a magnesium deficiency

Magnesium is an element from the alkaline earth group. It is an easily metabolizable light metal, which is a vital mineral for humans, animals, and plants. Humans cannot produce magnesium themselves and must ingest it with food to ensure that the body is adequately supplied.

Magnesium is an important electrolyte for protein synthesis, the stability of nucleic acids, oxidative phosphorylation, intracellular anionic ligands, especially ATP, and neuromuscular

excitability[151,152]. most magnesium within the body is found in bones, muscle cells, and soft tissues. Only Less than 1% of the organism's total magnesium is found in the blood[153]. The body contains of approximately 24 g of magnesium[153], whereby the recommended dietary allowance (RDA) for magnesium varies by age and sex, with adult men requiring 400–420 mg/day and adult women 310–320 mg/day to support essential physiological functions, including muscle and nerve function, bone health, and energy production[154].

The magnesium content of the body is controlled by intestinal absorption and renal excretion. Approximately 80% of the free serum magnesium is filtered in the glomeruli, with 95% being reabsorbed along the nephron. Whereas 15-20% is reabsorbed in the proximal tubules, approximately 70% in the loop of Henle, and 5-10% in the distal tubule.

Magnesium deficiency, also known as hypomagnesemia, describes a serum magnesium concentration >2.6 mg/dl. Hypomagnesaemia is often asymptomatic. However, it is accompanied by several symptoms including abdominal pain, nausea, lethargy, weakness, increased neuromuscular excitability, e.g. muscle cramps, and cardiac manifestations. In addition, magnesium deficiency can lead to hypokalemia due to increased sodium excretion in the loop of Henle and the collecting duct[155].

Magnesium deficiency is symptomatic for several diseases, including Gitelman syndrome (GS)[156] and Bartter's syndrome (BS)[157]. Furthermore, many therapies have been reported to cause an increased loss of magnesium[158]. Subsequently, only the BS will be discussed further in this dissertation.

1.7.1 Bartter syndrome

In 1962, Dr. Frederic Bartter and colleagues first described Bartter syndrome (BS), an autosomal-recessive inherited disorder (Figure 5A)[157].

They identified this condition after observing a group of patients who presented with specific clinical features, including Hypokalemia, Growth retardation, metabolic alkalosis, normal to low blood pressure and increased renin and aldosterone levels. Bartter and his colleagues found that these symptoms were caused by an inherited defect in the kidney’s ability to reabsorb salt, specifically in the thick ascending limb (TAL) of the loop of Henle.

Nowadays Bartter syndrome describes a plethora of subtypes, each associated with mutations in specific genes that affect ion channels or transporters involved in electrolyte reabsorption within the TAL. These genetic differences contribute to variability in severity and symptom

presentation. The Bartter syndrome typically manifests in the early years, often within the first year of life[159]. Multidisciplinary management involving nephrologists, dietitians, and primary care physicians is essential for addressing the complex care needs of affected individuals. Regular monitoring and tailored treatment strategies are vital to mitigating complications associated with electrolyte imbalances.

Treatment usually focuses on electrolyte supplementation, potassium-sparing diuretics, and in some cases, non-steroidal anti-inflammatory drugs (NSAIDs) to help reduce kidney prostaglandin production and slow down electrolyte losses[157,160].

BS is a polygenic disease caused by homozygous or mixed heterozygous mutations in one of the following genes: *SLC12A1, KCNJ1, CLCNKB, BSND* or *CASR* (Figure 5B*).*

The five different subtypes of Bartter syndrome illustrate the diverse genetic and phenotypic expressions of the disorder, which are expressed in the tubular epithelial cells of the TAL.

Type I BS is characterized by loss-of-function mutations within the *SLC12A1* gene. It presents in the infancy or early childhood and is the most common form of the BS. The *SLC12A1* codes for the apical sodium-potassium-chloride co-transporter NKCC2. Type II of BS is caused by loss-of-function mutations in the *KCNJ1* gene. It codes for the apical inwardly rectifying potassium channel ROMK. BS type III, also known as classic Bartter syndrome, is caused by mutations in the *CLCNKB* gene, which codes for the basolateral chloride channel- ClC-Kb.

Distinct variants of chloride channels are present in most organs but *CLCNKB* affected here is found exclusively in the kidney, so the clinical manifestation of a mutation in this channel is only seen in the kidney[161].

Bartter syndrome with sensorineural hearing loss (hyperprostaglandin E syndrome), or BS type IVa, is caused by loss-of-function mutations in the *BSND* gene, which encodes Barttin, a β-subunit for ClC-Ka and ClC-Kb. Parallel to BS type IVa, simultaneous mutations in CIC-Ka and CIC-Kb are present in type IVb. Bartter syndrome type V with hypocalcemia is also known as autosomal dominant hypoparathyroidism. This is characterized by gain-of-function mutations in the Ca^{2+}-sensing receptor-*CASR*, which codes for the basolateral calcium receptor CASR.

Bartter syndrome is an inherited disorder of the renal tubules caused by impaired salt reabsorption. It leads to several electrolyte abnormalities including low potassium and chloride, salt wasting, hypokalemia, and metabolic alkalosis[162,163].

Previously BS patients were classified based on age, the presence of hypercalciuria, polyhydramnios or growth retardation, and severity. Based on differences in the metabolism

of divalent cations, BS can be distinguished by laboratory measurements which include urinary Ca^{2+-} excretion, Ca^{2+}/Creatinine, and serum Mg[161].

Due to the rare nature of the syndrome, there is only limited clinical information on treatment. Therapeutically, BS patients urgently need sufficient fluid and electrolyte replacement. For newborns, it is important to control the risk of pre-renal failure due to imbalances in fluid homeostasis. The classic pharmacological therapy for BS patients include the administration of potassium chloride, prostaglandin inhibitors (indomethacin), and aldosterone antagonists (spironolactone)[164,165].

The symptoms of BS patients are initially treated with the help of potassium supplementation. Also, potassium-sparing diuretics such as spironolactone, eplerenone, or amiloride are often prescribed. According to the literature, these diuretics lead to reduced aldosterone levels, which subsequently increases serum potassium and hence counteracting metabolic alkalosis. In cases of persistent hypokalemia and or other side-effects of medications, potassium-sparing diuretics, renin-angiotensin system blockers, or NSAIDs are also prescribed. Combinations of these medications are also recommended in certain cases[160,166,167].

Angiotensin-converting enzyme inhibitors (ACE inhibitors) are used to correct low K+ levels or to counteract proteinuria[167,168].

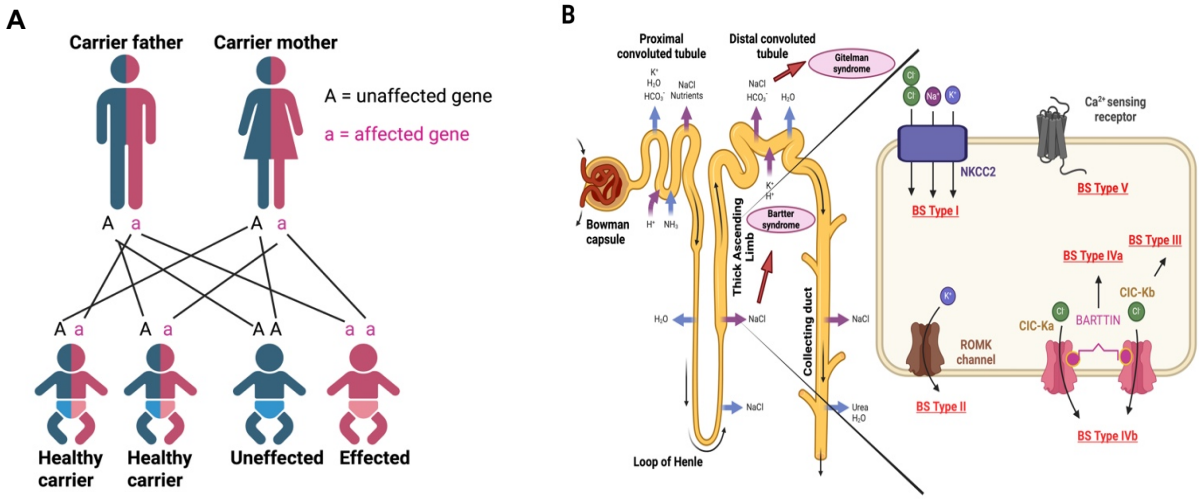


Figure 5: Bartter syndrome
Bartter syndrome is a relatively rare renal salt wasting syndrome caused by an autosomal recessive inherited defect in tubular transport proteins SLC12A1, KCNJ1, CLCNKB, BSND or CASR (A and B). BS Type I is characterized by loss-of-function mutations within the SLC12A1 gene. Type II is caused by loss-of-function mutations in the KCNJ1 gene. BS Type III caused by mutations in the CLCNKB gene, which codes for the basolateral chloride channel-ClC-Kb. The Type IV is divided into Type IVa and IVb. BS type IVa is caused by loss-of-function mutations in the BSND gene, where type IVb has, simultaneous mutations in CIC-Ka and CIC-Kb. The last Type of BS This is characterized by gain-of-function mutations in the Ca^{2+}-sensing receptor-CASR, which codes for the basolateral

calcium receptor CASR. The Figure was adopted and added by the Licensee MDPI, Basel, Switzerland. Created in https://BioRender.com[169].

1.8 Aging

The aging process is a complex biological and social process that is influenced by a variety of factors. Biologically, aging is characterised by the gradual deterioration of cell function, which is associated with loss of homeostasis and increased susceptibility to disease[170]. Aging research has identified several key mechanisms that drive the ageing process, the so-called Hallmarks of Aging[170]. These twelve hallmarks include genomic instability, telomere attrition, epigenetic changes, loss of proteostasis, impaired macroautophagy, impaired nutrient recognition, mitochondrial dysfunction, cellular senescence, stem cell exhaustion, altered intercellular communication, chronic inflammation and dysbiosis[170–172]. Telomeres, the protective caps at the ends of chromosomes, play a central role: their shortening during cell division limits the ability of cells to divide, which is known as the Hayflick limit[173]. A normal, somatic cell can only divide a certain number of times before it stops dividing and enters a state called senescence. This limit is named after the scientist Leonard Hayflick, who first described it in 1961[173]. The Hayflick limit is the maximum number of divisions a normal somatic cell can undergo before it stops dividing and enters senescence, largely due to telomere shortening. This phenomenon plays a role in aging and cancer prevention but also highlights the potential risks of uncontrolled cell proliferation in diseases like cancer[173,174].

This process helps prevent the chromosome ends from being recognized as natural breaks, thereby avoiding the activation of DNA damage checkpoints. Telomeric shelterin proteins play a key role here, preventing DNA damage response pathways and ensuring chromosome stability by inhibiting inappropriate DNA fusion.

Oxidative stress is also a decisive factor in the aging process. This is caused by the accumulation of reactive oxygen species (ROS), which cause cellular damage and impair the function of mitochondria. However, recent studies emphasize that oxidative damage is not the sole cause of aging, but must be considered as part of a network of interactions[175].

SIRT1 (Sirtuin 1) is a NAD-dependent enzyme from the group of deacetylases, which plays a crucial role in aging by regulating cellular processes that influence longevity, stress resistance, and metabolic homeostasis. SIRT1 enhances DNA repair mechanisms and helps maintain genomic stability, which is critical for slowing the aging process[176,177]. For example, it deacetylates proteins involved in DNA repair, such as Ku70 and TP53, reducing DNA damage accumulation[178,179]. The SIRT1 expression goes down by age, which could already shown in

UdRPCs from our lab[180]. The expression and activity of SIRT1 can also be influenced by sex-specific factors, with studies suggesting that there are differences in how males and females regulate and utilize SIRT1. Sex-specific regulatory effects of SIRT1, show that estrogen in females[181] and testosterone in male mices[182] both play significant roles in modulating SIRT1 expression, thereby influencing aging, metabolic health, and longevity. Estradiol, a potent form of estrogen, activates SIRT1 through its interaction with estrogen receptors, leading to increased NAD^+ levels and enhanced SIRT1 activity, which has beneficial effects on several tissues involved in aging[183]. Testosterone also plays a role in modulating SIRT1 expression, though its effects are less well-studied compared to estradiol[184]. These sex differences can be linked to various hormonal, genetic, and physiological factors.

1.9 Induced pluripotent stem cell

The discovery of induced pluripotent stem cells (iPSC) by Takahashi and Yamanaka was based on the retroviral introduction of four key transcription factors: OCT4, SOX2, KLF4 and c-MYC, known as Yamanaka factors[185].

These proteins play a central role in the reprogramming of somatic cells to a pluripotent state. This process involves profound changes at the molecular level that restructure the epigenetic and transcriptional network of cells. Epigenetic modifications, such as DNA methylation and chromatin remodeling, are crucial for the establishment and maintenance of the pluripotent state. In differentiated cells, the promoter region of genes that mediate pluripotency (e.g. OCT4 and NANOG) is strongly methylated and therefore inactive. During reprogramming, the Yamanaka factors remove these epigenetic barriers. These include DNA demethylation and histone modification. Studies have shown that TET1 (ten-eleven translocation enzyme 1) is regulated by OCT4 and plays a key role in the activation of pluripotency genes[186]. During reprogramming, the chromatin of differentiation-specific genes is compacted by the activity of histone deacetylases (HDACs) and polycomb repressor complexes (PRCs). At the same time, pluripotency genes are activated by histone acetyltransferases (HATs) and the activity of trithorax group proteins that promote H3K4 methylation[187]. The Yamanaka factors initiate reprogramming by activating central regulators of the pluripotency network. OCT4 and SOX2 form a heterodimeric complex that directly activates pluripotency genes. At the same time, they repress genes associated with cell differentiation[185]. OCT4 and SOX2 act synergistically on the promoter regions of NANOG and LIN28 to establish pluripotent identity. KLF4 supports reprogramming by activating anti-apoptotic genes, thereby increasing the survival rate of cells

during the stressful reprogramming process. In addition, KLF4 contributes to the loosening of chromatin and facilitates access to pluripotency genes[188]. C-MYC, an oncogene, promotes reprogramming through global chromatin openings and activation of metabolic pathways required for energy supply during cell remodeling. It increases the efficiency of reprogramming but carries an increased risk of tumor formation[189]. At the molecular level, iPSCs switch from an oxidative metabolism (characteristic of differentiated cells) to a glycolytic metabolism, which is typical of pluripotent stem cells. This is mediated by the upregulation of factors such as HIF1α and the reprogramming of mitochondrial dynamics[190]. This metabolic adaptation is crucial for supporting the energetic requirements of the reprogramming process. Finally, the generated cells possess properties typical of pluripotent embryonic stem cells. Characteristic properties include the unlimited capacity for self-renewal, the capacity to spontaneously generate into cell types of all three germ layers through the formation of embryoid bodies[191], telomerase activity and the expression of specific surface markers of human embryonic stem cells (hESCs), including SSEA3/4, TRA-1-60, TRA-1-81 and alkaline phosphatase[191,192]. Another characteristic feature is the ability to form teratomas after transplantation, a phenomenon that has also been demonstrated in human iPSCs[191]. IPS cells are a revolutionary tool in modern biology and medicine. Their flexibility, versatility, and ethical advantages make them a central field of research with the potential to fundamentally transform healthcare.

1.10 Immortalization of cell lines

Human cells have a limited lifespan, which is manifested in cell culture by proliferation arrest[173]. There are various methods to make cells immortal or immortalized using this natural process, including through human telomerase or the SV40 polyomavirus. Furthermore, the reprogramming of iPSCs, as described in the preceding chapter, also constitutes a form of immortalization[193].

1.10.1 Immortalization with human telomerase

Telomeres are repetitive nucleotide sequences (TTAGGG)_n, located at the ends of chromosomes that protect the chromosome from degradation, prevent fusion with neighboring chromosomes and help maintain genomic stability[194]. They play a critical role in the cell cycle, aging, and the development of diseases, particularly cancer. The telomerase plays a crucial role in maintaining the length of telomeres, the protective caps at the ends of chromosomes,

which naturally shorten with each cell division of normal somatic cells[195,196]. On cause for cellular senescence is telomere shortening. Due to the limitations of DNA polymerase in fully replicating linear DNA ends, telomeres progressively shorten with each replication cycle by approximately 50 base pairs per year because DNA polymerase cannot fully replicate the ends of chromosomes (the "end-replication problem")[197,198]. This state as already described in chapter 1.7, is called the Hayflick limit[173].

To overcome the Hayflick limit, cells can restore telomere length through the telomerase enzyme complex. Telomerase comprises multiple subunits, including the RNA component hTR (or TERC), which provides a template for new telomere synthesis, and the catalytic subunit hTERT, which drives telomere elongation[199,200]. The expression of *hTERT* mRNA correlates strongly with telomerase activity. Approximately 20 *hTERT* transcripts are necessary to generate between 100 and 500 active telomerase complexes[201].

Introducing hTERT into human cells has been linked to telomere lengthening, increased cell proliferation, and reduced rates of telomere shortening and senescence[195].

However, it should be noted that cells overexpressing *hTERT* have an increased likelihood of developing genomic instability, which can lead to chromosomal aberrations and aneuploidies[202].

Frequent cellular division is associated with an increased risk of DNA damage accumulation, which can disrupt genomic integrity and promote instability[203]. Furthermore, this can lead to changes in gene expression, such as cells with high amounts of DNA damage often showing a change in metabolism, leading to increased glycolysis, known as the Warburg effect[204]. Telomerase reactivation is also found in many cancers and a mechanism for oncogenic transformation.

1.10.2 Immortalization with SV40

For several decades, it is known that transfecting cells with the simian virus 40 (SV40) lead to cellular immortalization. Immortalization with SV40 a polyomavirus is a commonly used method for extending the lifespan of mammalian cells that can cause cells to bypass normal cellular senescence, allowing continuous proliferation.

SV40-induced immortalization proceeds as a two-step model, as simian virus 40 large T antigen (SV40 LT) alone is not sufficient for immortalization[205,206]. The large T antigen is a crucial component in the virus's ability to replicate and is a well-studied oncoprotein in cancer research. Therefore, different SV40 sequences were used, such as an intact genome, using

constructs with an origin defect for human cells[207] or cloned as individual cDNAs encoding for the whole genome[208].

In the first phase (lifespan extension), the cells proliferate for a limited number of population doublings beyond the point at which untreated cells can proliferate.
This is mainly due to the ability of the large SV40-T antigen (LTAg) to bind to and inactivate the protein products of the *TP53* and retinoblastoma genes (*RB1*)[209,210]. These two proteins normally restrict the cell cycle, preventing uncontrolled proliferation. Once the large T antigen binds to pRB-1, the transcription factor E2F-1 is released from pRB-1[211]. By inactivating p53 and pRB1, the SV40 large T antigen prevents cells from undergoing cell cycle arrest or apoptosis, two major barriers to cellular immortalization.
Especially, the inhibition of pRB1 has been linked to causing cells to proceed through the G1/S checkpoint, enabling DNA synthesis and cell cycle progression[212].
As already mentioned, the SV40 large T alone is not sufficient. Also, the small t-antigen (t) is required. Both the SV40 large T-antigen (LT) and small t-antigen (t) are critical for inducing a transformation phenotype, which refers to the process by which normal cells are converted into cancerous cells. Together, these two viral proteins work synergistically to drive the transformation of host cells by disrupting key cellular mechanisms that regulate growth and prevent malignancy.
The second phase (immortalization) only occurs in a small minority of cells, and cell hybridization analyses indicate that this is due to gene inactivation[213].
The genes involved are currently unknown, but chromosomal localization data are accumulating and should allow their cloning and characterization soon.
Immortalized cell lines are widely used in cancer research, drug development, and basic studies of cellular mechanisms because the transformed cells largely maintain many of their original cell characteristics and allow for prolonged experimental study by retaining their proliferation capacity. As already described in section 1.9.1, this method also has disadvantages such as genomic instability, loss of differentiation capacity, metabolic changes, tumourigenicity, loss of cell-cell communication and altered stress response must also be checked in advance.

2 Aim of this work

Formerly, disease modeling of the kidney has been extremely difficult due to the challenge of obtaining cells derived from the kidney.

Urine provides a non-invasive source of a variety of renal cells, which is a promising alternative to study the biology not only certain kidney diseases such as acute kidney injury, chronic kidney disease, APOL1-mediated disease, Bartter syndrome, High blood pressure, or sickle cell disease but also similarities between kidney and brain and emphasizes the need for further investigation to validate their therapeutic use in the future.

So far, studies using podocytes and tubular cells usually require the isolation of those cells from the glomeruli[214,215]. Therefore, obtaining urine-derived progenitor cells, which can either be used to generate iPSCs or directly differentiated into the aforementioned cell types, provides a unique source to fuel this research. The loss of podocytes is considered crucial for the development of glomerulosclerosis. Damaging effects on podocytes lead to loss of structural integrity of actin filaments in their foot processes, resulting in loss of cytoskeletal stability and detachment of the foot processes from the glomerular basement membrane. In this context, the types of podocyte damage are extremely diverse.

Depending on the amount of cell detachment, the foot processes of podocytes lose contact with the basement membrane and the podocytes are released into the Bowman's capsular space. Further, they are excreted with the urine[216,217]. The damage to the glomeruli is proportional to the degree of podocyte loss, whereby these play a significant role in the genesis of a large proportion of chronic kidney diseases[53].

Abnormalities in the glomerular filtration barrier can lead to the development of proteinuria, which is still reversible in the early stages but cannot be cured over time despite therapy[217]. Proteinuria is a generalized term and can range from albuminuria to massive nephrotic syndrome. Albuminuria is characteristic of both primary (idiopathic, kidney-limited), e.g. FSGS[218] and secondary, associated with systemic diseases, e.g. diabetic nephropathy[219] , proteinuric glomerulopathies and is characteristic of CKD. Consequently, albuminuria in patients with CKD is a predictor of end-stage renal disease progression and is associated with an increased risk of cardiovascular disease.

The RAAS plays a crucial role in blood pressure regulation and renal hemodynamics. Activation of the RAAS leads to vasoconstriction and sodium retention, which help maintain blood pressure during states of hypovolemia or hypotension. However, these adaptations can significantly alter renal blood flow and intraglomerular pressure, imposing osmotic and mechanical stress on podocytes. Persistent activation of the RAAS is fundamental to the pathogenesis of podocyte damage[50,51]. Podocytes, specialized epithelial cells forming the filtration barrier in the glomerulus, are particularly sensitive to such stress. Increased intraglomerular pressure stretches the glomerular basement membrane and places mechanical strain on podocytes, potentially disrupting their structure and function. Additionally, osmotic stress from altered solute concentrations in the glomerular filtrate can impair podocyte metabolism and cytoskeletal integrity.

Over time, chronic RAAS activation and the associated hemodynamic changes can lead to podocyte detachment, foot process effacement, and depletion. These injuries weaken the filtration barrier, resulting in proteinuria and progressive glomerular damage. If unchecked, these processes may culminate in glomerulosclerosis and chronic kidney disease, illustrating the deleterious effects of prolonged RAAS-mediated stress on podocyte health.

Worldwide, around 9.4 million deaths per year are attributable to high blood pressure, which can result in cardiovascular disease and kidney failure. This makes high blood pressure an important modifiable risk factor for mortality[220].

RAAS blockade by ACE inhibitors or AGTR1 antagonists, including losartan, has a positive effect that has been clinically confirmed[51,54]. In the 1990s, the development of orally active, non-peptide, selective AGTR1 blockers began with the synthesis of losartan, which is used worldwide for the treatment of several glomerular diseases[55].

Not only the RAAS) play a crucial role in podocyte injury and the development of CKD, but JAK1-mediated signaling has also emerged as a significant contributor to inflammation and fibrosis, two core mechanisms driving CKD progression[133]. Particularly important in this context is the APOL1 gene, whose risk variants cause a toxic gain-of-function effect, especially in podocytes, resulting in cellular injury. Numerous studies have demonstrated that APOL1 expression is upregulated by pro-inflammatory cytokines such as IFN-γ, a process that is directly mediated through the JAK-STAT signaling cascade[112,114,136,140–144]. This highlights targeted modulation of this pathway as a promising therapeutic strategy. Preclinical studies have shown that blocking JAK1 can reduce inflammation and attenuate renal fibrosis. In this regard, baricitinib—an oral, selective inhibitor of JAK1 and JAK2—has

emerged as a promising candidate. Baricitinib specifically inhibits JAK1 and JAK2, leading to downstream suppression of inflammatory gene transcription, reduced tissue damage, and decreased APOL1 expression in kidney cells. Experimental models have demonstrated that baricitinib reduces APOL1-induced cytotoxicity and alleviates podocyte injury[112,118,136,145]. Functional studies of APOL1 have mainly relied on overexpression models using mice and HEK293 cells engineered to express APOL1-G0, -G1, or -G2 variants[112,126,136,137,221–224]. While these models offer valuable mechanistic insights, they lack the distinctive characteristics of human podocytes and the native regulatory context of APOL1.

In this study, various renal diseases are modelled by using urine-derived renal progenitor cells (UdRPCs). Therefore, UdRPCs have been differentiated into human podocytes and tubular cells and reprogrammed into patient-derived induced pluripotent stem cells.
The focus of this PhD thesis is on the potential of SIX2-positive UdRPCs in modelling AKI, CKD, GS and BS. We have shown that SIX2-positive UdRPCs are able to differentiate into different cell types along the renal lineage such as podocytes for example. One use of the differentiated podocytes is to study the effect of the drug losartan on podocyte damage induced for example by ANGII as it is observed in hypertension. The focus of my PhD thesis lies on the investigation of cytoskeletal changes by quantitative PCR (qPCR), Western blot, and immunofluorescence stainings.
Another use of the podocytes is to study the effect of the JAK1/2 inhibitor baricitinib and IFN-γ on kidney fibrosis using podocyte generated from urine of a West African male. The genetic background of the APOL1 variant in connection with renal fibrosis is being investigated. The focus of my PhD thesis here was to show the successful generation of a partially reprogrammed cell line and to present it in parallel as a potential cell model for APOL1-associated disease in particular kidney inflammation and fibrosis by qPCR, fluorescence-activated cell sorting (FACS), Western blot, and immunofluorescence stainings.
Furthermore, the generation of iPSC from Bartter syndrome patients enables us to analyze this disease through an easily accessible, non-invasive resource, the urine. Furthermore, this avoids ethical concerns, which normally come along side with invasive sample collection methods. To show that UdRPCs also have therapeutic properties and are useful in transplantation medicine, UdRPCs derived from a healthy individuum were injected into mice and their regenerative effect on kidney injury induced by ischemia reperfusion injury (IRI) was analyzed by blood serum of the transplanted mice.

3 Publications

3.1 Derivation of the Immortalized Cell Line UM51-PrePodo-hTERT and Its Responsiveness to Angiotensin II and Activation of the RAAS Pathway

Lars Erichsen, Lea Doris Friedel Kloss, **Chantelle Thimm**, Martina Bohndorf, Kira Schichel, Wasco Wruck and James Adjaye

Cells 2023, Volume 12, 342, Article ID 12030342

Abstract:

Recent demographic studies predict there will be a considerable increase in the number of elderly people within the next few decades. Aging has been recognized as one of the main risk factors for the world's most prevalent diseases such as neurodegenerative disorders, cancer, cardiovascular disease, and metabolic diseases. During the process of aging, a gradual loss of tissue volume and organ function is observed, which is partially caused by replicative senescence. The capacity of cellular proliferation and replicative senescence is tightly regulated by their telomere length. When telomere length is critically shortened with progressive cell division, cells become proliferatively arrested, and DNA damage response and cellular senescence are triggered, whereupon the Hayflick limit is attained at this stage. Podocytes are a cell type found in the kidney glomerulus where they have major roles in blood filtration. Mature podocytes are terminal differentiated cells that are unable to undergo cell division in vivo. For this reason, the establishment of primary podocyte cell cultures has been very challenging. In our present study, we present the successful immortalization of a human podocyte progenitor cell line, of which the primary cells were isolated directly from the urine of a 51-year-old male. The immortalized cell line was cultured over the course of one year (~100 passages) with high proliferation capacity, endowed with contact inhibition and P53 expression. Furthermore, by immunofluorescence-based expression and quantitative real-time PCR for the podocyte markers CD2AP, LMX1B, NPHS1, SYNPO and WT1, we confirmed the differentiation capacity of the immortalized cells. Finally, we evaluated and confirmed the responsiveness of the immortalized cells on the main mediator angiotensin II (ANGII) of the

renin–angiotensin system (RAAS). In conclusion, we have shown that it is possible to bypass cellular replicative senescence (Hayflick limit) by TERT-driven immortalization of human urine-derived pre-podocyte cells from a 51-year-old African male.

Author contribution of C.T. included 25%:

I was responsible for the establishment and maintenance of the cell culture system, including the cultivation of UdRPCs and immortalized UdRPCs (UM51 hTERT). I carried out the induction of podocyte differentiation as well as the stimulation experiments using angiotensin II and the angiotensin receptor blocker losartan. As part of the experimental workflow, I isolated RNA and protein for subsequent my following qPCR (quantitative PCR) and Western blot analyses. In addition, I performed the immunofluorescence staining procedures. For all datasets I generated, I conducted the corresponding statistical analyses and prepared the quantitative evaluation of the results. I designed and executed the experiments and analyzed them in the relation to our research hypothesis. Furthermore, I contributed to the manuscript revision process by discussing and jointly addressing the reviewers' comments together with J.A. and L.E.

Status: Published in Cells.

DOI: doi.org/10.3390/cells12030342

This article is an open access article distributed under the terms and conditions of the Creative Commons Attribution (CC BY) 4.0 license, which permits unrestricted use, distribution, and reproduction in any medium, provided the original work is properly cited.

cells

MDPI

Article

Derivation of the Immortalized Cell Line UM51-PrePodo-hTERT and Its Responsiveness to Angiotensin II and Activation of the RAAS Pathway

Lars Erichsen [1], Lea Doris Friedel Kloss [1], Chantelle Thimm [1], Martina Bohndorf [1], Kira Schichel [1], Wasco Wruck [1] and James Adjaye [1,2,*]

[1] Institute for Stem Cell Research and Regenerative Medicine, Medical Faculty, Heinrich-Heine University Duesseldorf, 40225 Duesseldorf, Germany
[2] EGA Institute for Women's Health, University College London, 86-96 Chenies Mews, London WC1E 6HX, UK
* Correspondence: james.adjaye@med.uni-duesseldorf.de

Abstract: Recent demographic studies predict there will be a considerable increase in the number of elderly people within the next few decades. Aging has been recognized as one of the main risk factors for the world's most prevalent diseases such as neurodegenerative disorders, cancer, cardiovascular disease, and metabolic diseases. During the process of aging, a gradual loss of tissue volume and organ function is observed, which is partially caused by replicative senescence. The capacity of cellular proliferation and replicative senescence is tightly regulated by their telomere length. When telomere length is critically shortened with progressive cell division, cells become proliferatively arrested, and DNA damage response and cellular senescence are triggered, whereupon the "Hayflick limit" is attained at this stage. Podocytes are a cell type found in the kidney glomerulus where they have major roles in blood filtration. Mature podocytes are terminal differentiated cells that are unable to undergo cell division in vivo. For this reason, the establishment of primary podocyte cell cultures has been very challenging. In our present study, we present the successful immortalization of a human podocyte progenitor cell line, of which the primary cells were isolated directly from the urine of a 51-year-old male. The immortalized cell line was cultured over the course of one year (~100 passages) with high proliferation capacity, endowed with contact inhibition and P53 expression. Furthermore, by immunofluorescence-based expression and quantitative real-time PCR for the podocyte markers CD2AP, LMX1B, NPHS1, SYNPO and WT1, we confirmed the differentiation capacity of the immortalized cells. Finally, we evaluated and confirmed the responsiveness of the immortalized cells on the main mediator angiotensin II (ANGII) of the renin–angiotensin system (RAAS). In conclusion, we have shown that it is possible to bypass cellular replicative senescence (Hayflick limit) by TERT-driven immortalization of human urine-derived pre-podocyte cells from a 51-year-old African male.

Keywords: podocytes; renin–angiotensin-system; human telomerase

check for updates

Citation: Erichsen, L.; Kloss, L.D.F.; Thimm, C.; Bohndorf, M.; Schichel, K.; Wruck, W.; Adjaye, J. Derivation of the Immortalized Cell Line UM51-PrePodo-hTERT and Its Responsiveness to Angiotensin II and Activation of the RAAS Pathway. *Cells* **2023**, 12, 342. https://doi.org/10.3390/cells12030342

Received: 17 November 2022
Revised: 12 January 2023
Accepted: 14 January 2023
Published: 17 January 2023

Copyright: © 2023 by the authors. Licensee MDPI, Basel, Switzerland. This article is an open access article distributed under the terms and conditions of the Creative Commons Attribution (CC BY) license (https://creativecommons.org/licenses/by/4.0/).

1. Introduction

Podocytes are a distinct cell type within the kidney glomerulus. Their major task is the filtration of blood to generate urine, and thereby retaining plasma proteins [1]. Therefore, they are part of the glomerular filtration barrier, together with glomerular epithelial cells (GECs) and the glomerular basement membrane (GBM) [2]. To execute this complex task, podocytes need to be terminally differentiated and develop an elaborate and highly specialized actin cytoskeleton. A typical podocyte morphology is composed of three major segments, the cell body, major processes and foot processes (FPs) [3]. Major processes are connected to the cell body of podocytes and can split into foot processes. Neighboring foot processes from different podocytes form an inter-digitating pattern, which is bridged by slit diaphragms (SDs) [4].

During development of the human kidney, the precursor cells of podocytes arise from SIX2-positive renal progenitor cells. Subsequent developmental processes are then needed to acquire the terminally differentiated state and maturity [4,5]. Glomerular development proceeds in four stages: the renal vesicle stage, the S-shaped body stage, the capillary loop stage, and the maturing-glomeruli stage [6,7]. During the S-shaped body stage, podocyte precursors are simply undifferentiated epithelial cells, with apically located tight junctions [8] and prominent mitotic activity [9]. During this specific time point, expression of podocalyxin (PODXL) [10] and the tight junction protein ZO-1 [11] are initiated, while expression of the podocyte transcription factor WT1 is the highest expression level [12]. When these immature podocytes enter the capillary loop stage, their mitotic activity is abolished and they begin to establish their complex actin cytoskeleton, including the appearance of FPs and the reorganization of cell–cell junctions into glomerular slit diaphragms (SD) [8]. The filtration slits are formed by the spatial formation of the FPs. These are spanned by the SD, which is similar to an adherens junctions structure [13]. For the formation of SD, the protein nephrin (NPHS1) is required, which is additionally associated with the actin cytoskeleton and, thus, contributes to the actin dynamics of podocytes and the formation of FPs [14].

The phenotypical changes occurring between the S-shaped body stage and the capillary loop stage are accompanied by synaptopodin (SYNPO) [15] and vimentin [16] expression. Therefore, both have been recognized as key markers of differentiated post-mitotic podocytes [15,17,18], which cannot be detected in undifferentiated or dedifferentiated cells [19,20].

Numerous kidney diseases, such as chronic kidney disease, membranous nephropathy, congenital nephrotic syndrome and Alport syndrome are associated with proteinuria and or hematuria, which is mainly caused by defects in the GBM or alterations in the structure and or function of the podocytes. Modelling of these pathological conditions has been very challenging. One obvious drawback of studying human podocytopathies is the limited proliferation capacity of these cells. This was further aggravated by the fact that the derivation of kidney-originating cells is very challenging. This is particularly true for podocytes since their complex architecture is not well preserved from kidney biopsy tissue [17]. For these reasons, disease modelling of human kidney alterations is often studied in animal models which only replicate human conditions to a limited extent. Therefore, other models have been implemented to study human kidney disease, such as the temperature-sensitive SV40 conditionally immortalized podocyte cell line [17] (UdRPCs, Rahman et al.; and many iPSC-based differentiation protocols for cells of kidney origin, Erichsen et al. [21–25]).

Telomeres are GT-rich repeats $(TTAGGG)_n$ at chromosome ends in human and other vertebrates [26,27]. These structures are established by the enzyme telomerase. Telomerase is an RNA-dependent DNA polymerase [28] consisting of two essential components. The first is the functional RNA component (*hTR* or *hTERC*), which serves as template for telomere synthesis, and the second is the catalytic domain with reverse transcriptase activity (hTERT) [29–32]. While pluripotent stem cells possess high telomerase activity, the level drops during differentiation into somatic cells. hTERT remains active in some tissues (e.g., germ cells) and a selection of cell populations [33]. The activity is regulated to meet the demand of proliferation to facilitate specific cellular functions, while simultaneously serving as a barrier against carcinogenesis by inducing senescence [34,35]. Numerous mammalian and human cell types have been immortalized by using either hTERT transfection [36–39] or by the introduction of viral oncogenes, such as SV40 Large-T antigen, adenovirus E1A and E1B, papilloma virus E6 and E7, CELO virus orf22 and GAM-1. In contrast with hTERT transfections, the main drawback of these viral oncogenes is that the generated cell lines often lose cell cycle and apoptosis control due to the inhibition of the pRB and p53 pathways, respectively, which ultimately results in malignant cell transformation [37,40].

Here, we describe the successful immortalization of a human podocyte progenitor cell line, obtained directly from urine. The cells showed a stable morphology and prolifera-

tion capacity in vitro for more than one year in culture. They expressed typical podocyte markers, such as SYNPO, NPHS1 and WT1, and upon our recently reported differentiation protocol [41], their proliferation capacity was retained, and they expressed several podocyte markers such as SYNPO. Due to their high proliferation capacity and their ease of handling, our immortalized UM51-hTERT-Pre-Podo cell line offers a unique tool for studying nephrogenesis and kidney-associated diseases.

2. Material and Methods

2.1. Cell Culture Conditions

The cell line UM51-PrePodo was derived from the urine of a 51-year-old male of African origin. The cells were cultured, and differentiation was induced as described in [41]. Immortalization of the cells was achieved by cationic polymer transfection of the pCDNA-3xHA-hTERT plasmid with Xfect (Takara BIO INC, Kusatsu, Shiga Prefecture, Japan). The plasmid pCDNA-3xHA-hTERT was obtained from (Addgene plasmid # 51637; http://n2t.net/addgene:51637; RRID: Addgene_51637; accessed 12 January 2023) [42]. In brief, 2 µg of the plasmid was incubated at RT for 10 min with 100 µL of transfection buffer and 1 µL of transfection reagent. After incubation, the mix was added to at least 50% confluent 6 well of UM51-PrePodo, growing as a monolayer. In another transfection, 2 µg of the commercial pmaxGFP Vector (Lonza, Basel, Switzerland) was incubated at RT for 10 min with 100 µL of transfection buffer and 1 µL of transfection reagent. After incubation, the mix was added to at least 50% confluent 6 well of UM51-PrePodo-hTERT, growing as monolayer.

2.2. Immunofluorescence-Based Detection of Protein Expression

Cells were fixed with 4% paraformaldehyde (PFA) (Polysciences, Warrington, FL, USA). Unspecific binding sites were blocked by incubation with blocking buffer, containing 10% normal goat or donkey serum, 1% BSA, 0.5% Triton, and 0.05% Tween, for 2 h at room temperature. Incubation of the primary antibody was performed at 4 °C overnight in staining buffer (blocking buffer diluted 1:1 with PBS). After at least 16 h of incubation, the cells were washed three times with PBS/0.05% Tween and incubated with a 1:500 dilution of secondary antibodies. After three additional washing steps with PBS/0.05% Tween, the cell and nuclei were stained with Hoechst 1:5000 (Thermo Fisher Scientific, Waltham, MA, USA). Images were captured using a fluorescence microscope (LSM700; Zeiss, Oberkochen, Germany) with Zenblue software (Zeiss). Individual channel images were processed and merged with Fiji. Detailed information of the used antibodies is given in Supplementary Table S1.

2.3. Western Blotting

Protein isolation was performed by lysis of the cells in RIPA buffer (Sigma-Aldrich, St. Louis, MO, USA), supplemented with complete protease and phosphatase inhibitors (Roche, Basel, Switzerland). Proteins were resolved on a 7.5% Bis-Tris gel and blotted onto a 0.45 µm nitrocellulose membrane (GE Healthcare Life Sciences, Chalfont St. Giles, UK). After blocking the membranes with 5% skimmed milk in Tris-buffered Saline Tween (TBS-T), they were incubated overnight with the respective primary antibodies (Supplementary Table S1). Membranes were washed 3× for 10 min with TBS-T. Secondary antibody incubation was performed for 1 h at RT, and membranes were subsequently washed 3× for 10 min with TBS-T. Amersham ECL Prime Western Blotting Detection Reagent was used for the chemiluminescent detection (GE Healthcare Life Sciences) and captured with the imaging device Fusion FX.

2.4. Southern Blotting

Genomic DNA isolation was performed with the DNeasy® Blood & Tissue Kit (Qiagen, Hilden, Germany) according to the manufacturer's instructions. An amount of 10 µg of the isolated DNA was digested by incubation with EcoRI and HindIII overnight and separated

on a 1% agarose gel for 2 h. Prior to blotting of the DNA onto a positively charged nylon membrane (GE Healthcare Life Sciences), the in-gel DNA was denaturated by incubation in 0.25 M HCL solution for 5 min, followed by 2×/15 min in denaturation solution and 2×/15 min in neutralization solution. DNA transfer was carried out overnight at room temperature with 10× saline-sodium citrate (SSC) buffer. Subsequently the membrane was fixed at 120 °C for 20–35 min and washed twice with SSC. Telomere fragments were detected by a prehybridization step with DIG Easy Hyb Granules for 1 h and by the actual hybridization of the membrane with a solution containing Telomere Probe dissolved 1:5000 in DIG Easy Hyb granules (Sigma Aldrich) at 42 °C overnight. Two stringent washing steps were performed after hybridization, blocking was performed in blocking solution followed by Anti-DIG antibody solution. For detection, the membranes were washed in detection buffer for 5 min, and 1 mL substrate solution was added. Pictures were taken with the imaging device Fusion FX after an incubation period of at least 5 min.

2.5. Relative Quantification of Podocyte-Associated Gene Expression by Real-Time PCR

Real-time PCR of podocyte-associated gene expression was performed as follows.

An amount of 1 µg of RNA was used as input for reverse transcription in a volume of 10 µL. Real-time measurements were carried out on the Step One Plus Real-Time PCR Systems using 1:10 diluted template cDNA in a MicroAmp Fast Optical 384 Well Reaction Plate and Power Sybr Green PCR Master Mix (Applied Biosystems, Foster City, CA, USA). The amplification conditions were denatured at 95 °C for 13 min followed by 37 cycles of 95 °C for 50 s, 60 °C for 45 s and 72 °C for 30 s. Primer sequences are listed in Supplementary Table S2.

2.6. Resazurin Assay

Proliferation of UM51-PrePodo cells grown in proliferation medium and advanced RPMI was measured with a resazurin assay (Sigma-Aldrich) according to the manufacturer's instructions.

In brief, these were: Per condition (PM/adv. RPMI) 50,00 cells were seeded in 500 µL of the respective medium in triplicate. An amount of 10× Resazurin solution was mixed with the two media in a 1:10 dilution, and cells were incubated at 37 °C and 5% CO_2 for 2 h. An amount of 200 µL medium for each condition was transferred into a 96-well plate and absorbance at 570 and 600 nm was measured with Plate Reader AF2200 (Eppendorf, Hamburg, Germany).

2.7. Statistics

Data are presented as arithmetic means and standard error. In total, three independent experiments were performed and used for the calculation of mean values. Statistical significance was calculated using the two sample Student's *t*-test with a significance threshold of $p = 0.05$.

3. Results

3.1. Successful Immortalization of UM51-PrePodo Primary Cells

UM51-PrePodo cells were isolated directly from human urine as described in [43]. The cells were transfected with the plasmid pCDNA-3xHA-hTERT [42]. Immortalization was achieved after four months, and the cells referred to as UM51-PrePodo-hTERT. This cell line exhibited a much faster proliferation capacity compared with the original primary cells UM51-PrePodo, and kept proliferating for more than six months, while showing a similar morphology (Figure 1A). Both cell lines grew as monolayers, showed contact inhibition and a cobblestone-like morphology typical for epithelial cells. We further analyzed P53 expression and phosphorylation by immunofluorescence-based protein detection (Figure 1B). While most cells expressed P53, only a small percentage were positively stained for phosphorylated P53. Since the transfected hTERT protein was N-terminally tagged with 3× HA, successful transfection of the cells was evaluated by Western blotting and

immunocytochemistry with a primary antibody recognizing the HA-tag (Figure 1C,E). Generally, the transformed cells tended to appear a little smaller and more elongated than UM51-PrePodo. Since ectopic expression of hTERT has been associated with chromosomal alterations and genomic instabilities [44–47], we analyzed the karyotype of UM51-PrePodo-hTERT (Figure 1D). In total, 20 metaphases were analyzed and a hypertriploid karyotype with several chromosomal alterations was observed in all of them. Since alterations of this magnitude might have an impact on transcriptional activity, we could not exclude the probability of cancerous transformation. The immunofluorescence-based analyses detected expression of the HA-tag in UM51-PrePodo-hTERT. Furthermore, Western blot analysis revealed a band at approximately 80 kDa in the protein lysate of UM51-PrePodo-hTERT, which was absent in the non-transfected cell line UM51-PrePodo. ß-Actin was used as loading control and detected at size of 45 kDa (full size Western blot images are given in Supplementary Figure S1). In addition, hTERT gene expression was determined by quantitative real-time PCR, revealing a 132-fold increase in mRNA expression (Figure 1F). The telomere length of UM51-PrePodo-hTERT cells in comparison with the primary UM51-PrePodo cells was evaluated by Southern blotting. Terminal restriction fragments (TRF) containing telomeres and a sub-telomeric region were detected in the control DNA originating from an immortal cell line as supplied by Sigma Aldrich, the induced pluripotent stem cell line A4, as well as the UM51-PrePodo and UM51-PrePodo-hTERT (Figure 1G). TRFs of the A4 cell line were found to be the longest at approximately 13.9 kbp, followed by the control with a fragment size of 7.4 kbp, UM51-PrePodo of 6.3 kbp, and UM51-PrePodo-hTERT had the shortest TRFs with a length of 1.2 kb.

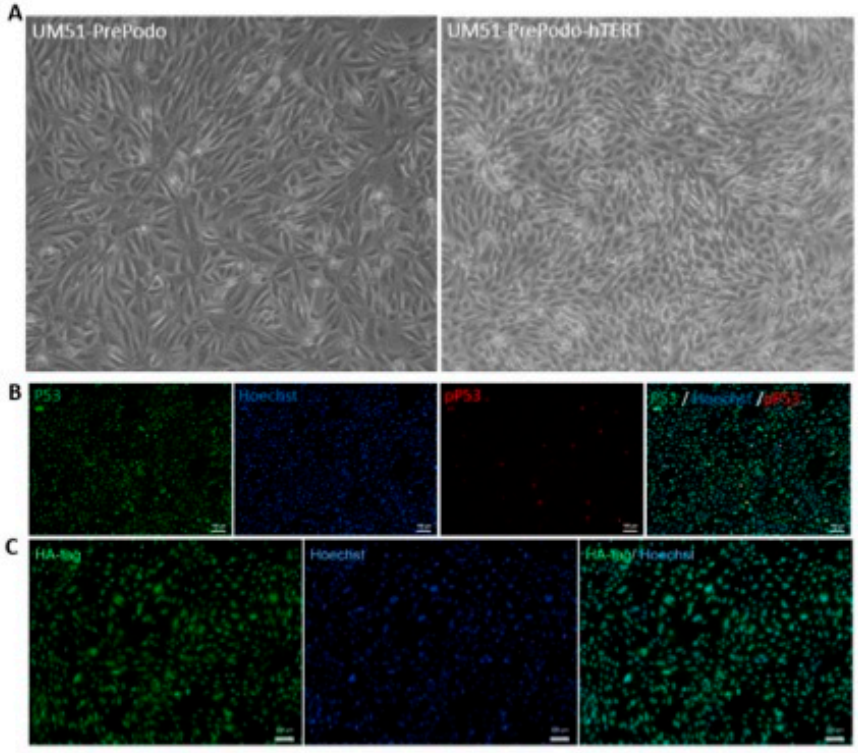


Figure 1. *Cont.*

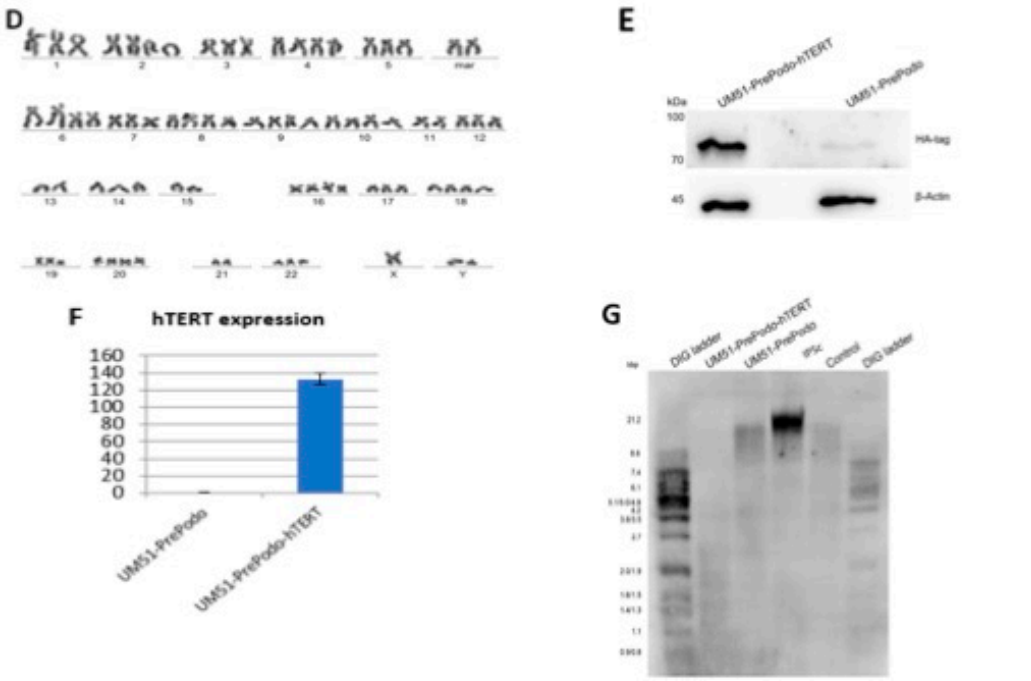


Figure 1. Successful immortalization of the UM51-PrePodo cell line. The UM51-PrePodo cell line was successfully immortalized by transfection with the pCDNA-3xHA-hTERT plasmid. Morphology after transfection as observed by light microscopy (**A**). P53 and phosphorylated P53 expression in the immortalized cells were monitored by immunofluorescent-based detection (**B**) (scale bars: 100 µm). Integration of the plasmid was visualized by immunofluorescence-based and Western blot detection of the HA-tag (**C**,**E**). Karyotyping of UM51-PrePodo-hTERT revealed a hypertriploid karyotype with several alterations (**D**). Expression of the hTERT gene was determined by quantitative real-time PCR (**F**). Telomere length was measured by Southern blotting (**G**).

3.2. Characterization UM51-PrePodo-hTERT

To determine the effect of hTERT-driven immortalization of the primary UM51-PrePodo cells on their differentiation capacity, we performed immunofluorescence-based detection of WT1 and NPHS1 protein and real-time PCR based detection of mRNA expression for the genes *WT1*, *NPHS1*, *CD2AP*, *CD24* and *CD106* (Figure 2A–E). As indicated by the immunofluorescence staining, the primary UM51-PrePodo cells, as well as the immortalized UM51-PrePodo-hTERT cell line, both expressed key podocyte proteins WT1 and NPHS1 (Figure 2A–D). The comparison between the primary and the immortalized cell line by real-time PCR based detection revealed a significant increase in mRNA expression for *WT1*, *NPHS1* and *CD106*, by 0.77 ($p = 0.001$), 2.83 ($p = 0.03$) and 1.66-fold ($p = 0.05$), respectively, and a significant downregulation of *CD2AP* and *CD24*, by 0.57 ($p = 0.05$) and 0.52 ($p = 0.05$) in the immortalized cells. To test transfection efficacy of the UM51-PrePodo-hTERT cell line, we cationic polymer transfected freshly plated cells at approximately 60–70% confluency with the pmaxGFP Vector, and obtained 70% GFP positive cells after 24 h (Supplementary Figure S2).

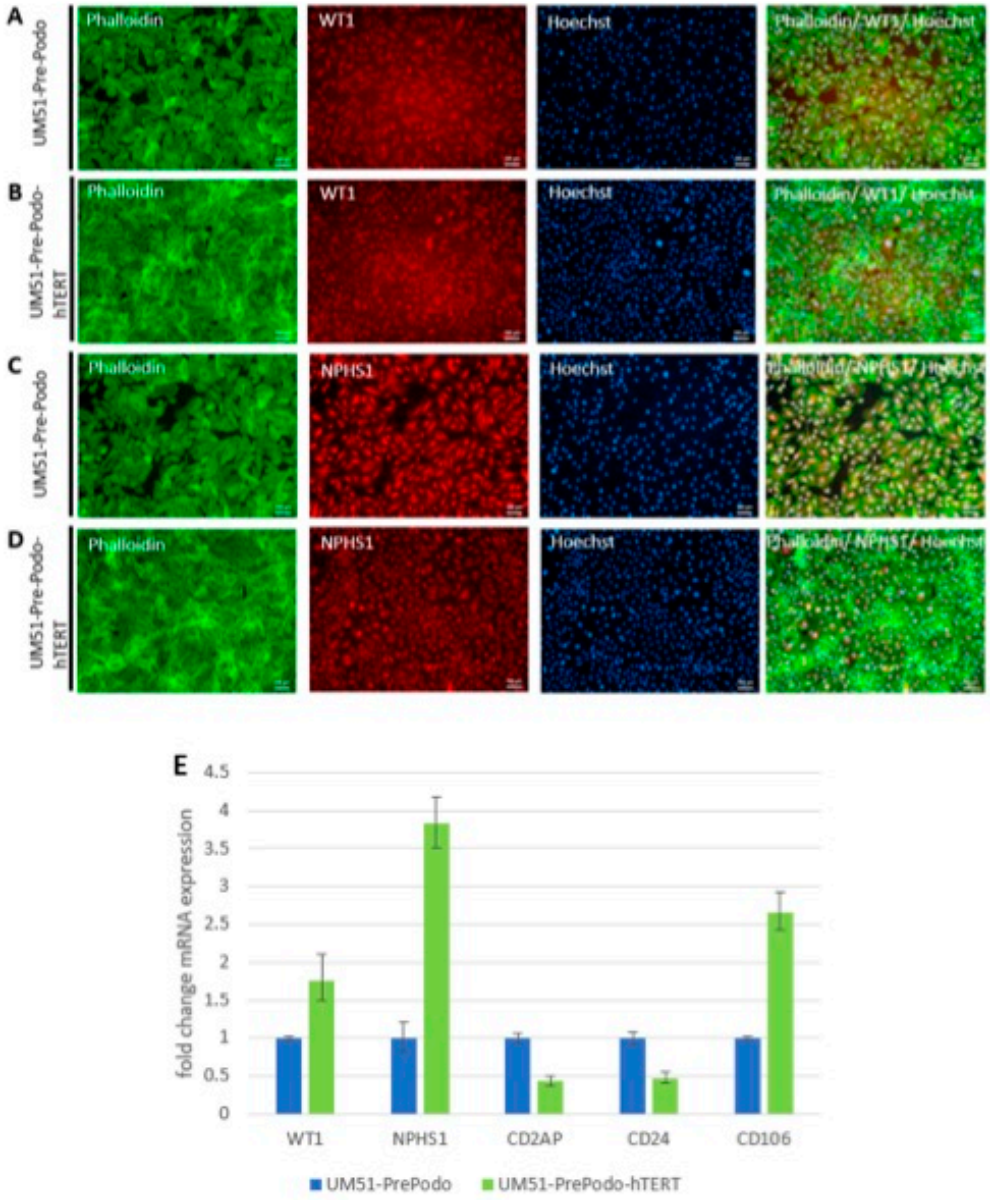


Figure 2. Characterization of immortalized UM51-PrePodo-hTERT. WT1 and NPHS1 expression in the parental UM51-PrePodo as well as the immortalized UM51-PrePodo-hTERT cells were evaluated by immunofluorescence-based detection (**A**–**D**) (scale bars: 100 µm). Immunofluorescence-based detection of the parental UM51-PrePodo is given in (**A**,**C**), while UM51-PrePodo-hTERT is given in (**B**,**D**). Cytoskeleton was stained with phalloidin. mRNA expression of *WT1*, *NPHS1*, *CD2AP*, *CD24* and *CD106* was determined by quantitative real-time PCR (**E**).

3.3. Culturing UM51-PrePodo-hTERT in adv. RPMI Initiates Podocyte Differentiation

We recently reported a detailed protocol for the differentiation of SIX2-positive urine derived renal progenitor cells (UdRPCs) into mature podocytes [41]. We applied this protocol to differentiate the UM51-PrePodo-hTERT cell line into podocytes. To determine the proliferation rate of UM51-PrePodo-hTERT cultured under the differentiation conditions, we applied a resazurin assay for 72 h (Figure 3A). The fold-change of normalized absorbance was found to increase in UM51-PrePodo-hTERT cultured in PM medium by 0.8-fold after 48 h and by additional 0.74-fold after 72 h. In contrast, UM51-PrePodo-hTERT cultured in adv. RPMI medium showed only minor changes in absorbance with 0.03-fold increase after 48 h and 0.13-fold increase after 72 h. The difference in proliferation rate was also observed using light microscopy (Supplementary Figure S3). While UM51-PrePodo-hTERT cells cultured in proliferation medium were at 100% confluency after 72 h, cells cultured in advanced RPMI were approximately 60% confluent. Relative protein expression normalized to ß-ACTIN for the HA-tag, for the key podocyte marker SYNPO as well as P53, were detected by Western blotting (Figure 3B). All proteins were detected at the expected sizes of 80 kDa for the HA-tag, 50 kDA for LMX1B, 100 kDA for NPHS1, 110 kDa for SYNPO, 53 kDa for p53, and 45 kDa for ß-ACTIN. While the most significant difference in protein expression was observed for SYNPO with a 4.8-fold increase ($p = 0.04$), HA-tag expression decreased with a fold change of 0.6 ($p = 0.05$). Interestingly, the protein level of P53 was unaffected by the culturing medium (full size Western blot images are given in Supplementary Figure S4). Expression of the differentiated podocyte marker SYNPO and the proliferation marker KI-67 were assessed by immunofluorescence-based protein detection (Figure 3C–F). KI-67-protein was detected in the nuclei of UM51-PrePodo-hTERT cells cultured in PM (Figure 3C) as well as adv. RPMI medium (Figure 3D). As expected, a lower percentage of cells grown in adv. RPMI expressed the proliferation marker than cells cultured in PM—3.8% compared with 13.9%, respectively (Figure 3G). While UM51-PrePodo-hTERT cells grown in PM lacked SYNPO protein expression (Figure 3E), a clear signal could be detected in cells grown in adv. RPMI (Figure 3F). Additionally, we measured the expression of *CD24, CD106, SYNPO, P53* and *KI67* by quantitative real-time PCR (Figure 3H). In accordance with the Western blot and immunofluorescence-based protein detection, the mRNA level of *SYNPO* was found to be significantly increased (3.2-fold; $p = 0.01$), while *P53* and *KI67* were found to be downregulated (0.41, $p = 0.01$ and 0.82-fold, $p = 0.01$, respectively). Furthermore, mRNA expression of the surface marker CD106 was found to be significantly downregulated (0.74-fold, $p = 0.04$) and CD24 expression was found to be unaltered.

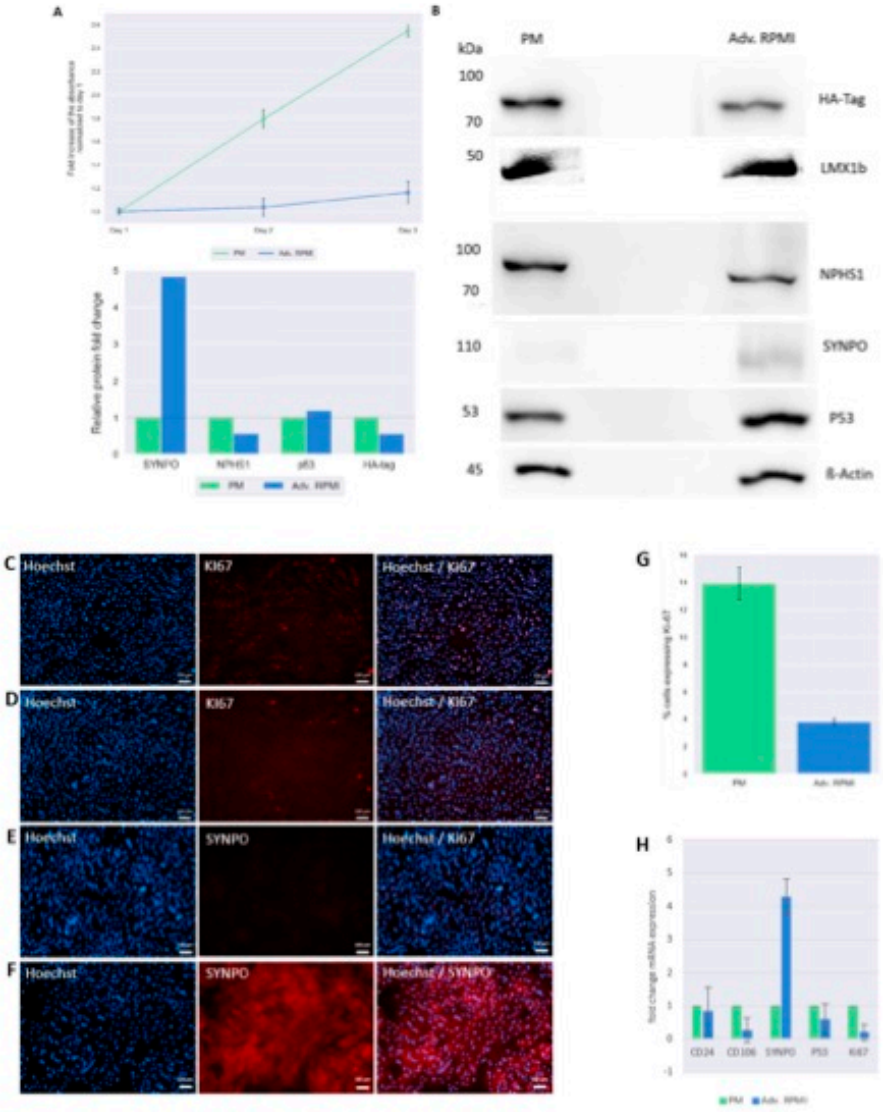


Figure 3. Culturing UM51-PrePodo-hTERT in adv. RPMI initiates podocyte differentiation. Proliferation of immortalized UM51-PrePodo-hTERT cells cultured in PM and adv. RPMI medium was assessed by a resazurin assay (**A**). Relative protein expression normalized to ß-ACTIN for the HA-tag, LMX1B, NPHS1, SYNPO and P53 was detected by Western blot (**B**). Ki-67 and SYNPO expression in UM51-PrePodo-hTERT cultured in PM and adv. RPMI were detected by immunofluorescence-based staining (**C**–**F**). Immunofluorescence-based detection of UM51-PrePodo-hTERT cells grown in PM are given in (**C**,**E**), while cells grown in adv. RPMI are given in (**D**,**F**) (scale bars: 100 µm). Percentage of UM51-PrePodo-hTERT cells cultured in proliferation medium and advanced RPMI expressing the proliferation marker Ki-67 is given in (**G**). mRNA expression of *CD24*, *CD106*, *SYNPO*, *P53 and KI67* was determined by quantitative real-time PCR (**H**).

3.4. Comparative Transcriptome Analysis of Urine Derived Renal Progenitor Cells UM51 with the Immortalized UM51-PrePodo-hTERT Cell Line

After the successful immortalization of UM51-PrePodo into UM51-PrePodo-hTERT and differentiation with adv. RPMI, we performed a comparative transcriptome analysis. Hierarchical clustering analysis comparing the transcriptomes of UM51-PrePodo and UM51 podocytes with their respective immortalized counterpart revealed a distinct expression pattern of wild type and immortalized cells (Figure 4A). By comparing the expressed genes (det-p < 0.05), we found that 582 were exclusively expressed in the UM51-PrePodo and 703 in UM51-PrePodo-hTERT grown in PM (Figure 4B). In total, 13,914 genes were found to be expressed in common between UM51-PrePodo and UM51-PrePodo-hTERT grown in PM (Figure 4B). After differentiation of UM51-PrePodo and UM51-PrePodo-hTERT by culturing the cells in adv. RPMI supplemented with 30 µM retinoic acid, transcriptome data revealed 880 genes to be exclusively expressed in UM51 podocytes and 460 in UM51-PrePodo-hTERT grown in adv. RPMI (Figure 4C). In total, 13,922 genes were found to be expressed in common between UM51-PrePodo-hTERT grown in adv. RPMI and UM51-PrePodo-hTERT grown in PM (Figure 4D). In total, 13,699 genes were found to be expressed in common between UM51-Podocytes and UM51-PrePodo-hTERT grown in adv. RPMI (Figure 4C). By comparing the expressed genes (det-p < 0.05), 237 were exclusively expressed in the UM51-PrePodo-hTERT grown in adv. RPMI and 695 in UM51-PrePodo-hTERT grown in PM (Figure 4D). Wild-type cells and their immortalized counterparts share many of the most over-represented GO BP-terms, such as regulation of ion transport, regulation of organic acid transport and developmental processes. The most over-represented GO BP-terms exclusive to UM51-PrePodo were associated with planar cell polarity involved in axis elongation and skin development. In comparison, the most over-represented GO BP-terms exclusively expressed in the immortalized UM51-PrePodo-hTERT cells grown in PM were associated with cell-cycle checkpoints, nuclear division, regulation of mitotic cycle and DNA replication (Figure 4E). The most over-represented GO BP-terms exclusive to UM51 podocytes were associated with regulation of ion transport, heterophilic cell–cell adhesion via plasma membrane cell adhesion molecules, and regulation of system processes. In comparison, the most over-represented GO BP-terms exclusively expressed in the immortalized UM51-PrePodo-hTERT cells grown in adv. RPMI were associated with chromosome segregation, cell-cycle checkpoints, DNA replication, cell cycle and regulation of DNA replication (Figure 4F). The full gene list can be found in Supplementary Table S3. UM51-PrePodo-hTERT cells grown in both media shared many of the most over-represented GO BP-terms, such as cell junction organization, urogenital system development, potassium ion transport and GPCR ligand binding. The most over-represented GO BP-terms exclusive to UM51-PrePodo-hTERT grown in adv. RPMI were associated with specification of animal organ identity and chemotaxis. In comparison, the most over-represented GO BP-terms exclusively expressed in the immortalized UM51-PrePodo-hTERT cells grown in PM were associated with embryonic pattern specification, embryonic organ development and positive regulation of cell–cell adhesion (Figure 4G). The full gene list can be found in Supplementary Table S4. Additionally, the transcriptomes of UM51-PrePodo and the immortalized UM51-PrePodo-hTERT grown in PM and adv. RPMI were compared with expressed genes in iPS cell-derived podocytes, kidney biopsy isolated human glomeruli, and mouse podocytes (Figure 4H), as reported by Sharmin et al. [48]. This analysis revealed that many key genes associated with podocyte function and structure were upregulated upon differentiation with adv. RMPI, such as *SYNPO*, *NPHS1*, *NPHS2*, *LAMC1*, *INF2*, *SPARC*, *WT1* and *PODXL*.

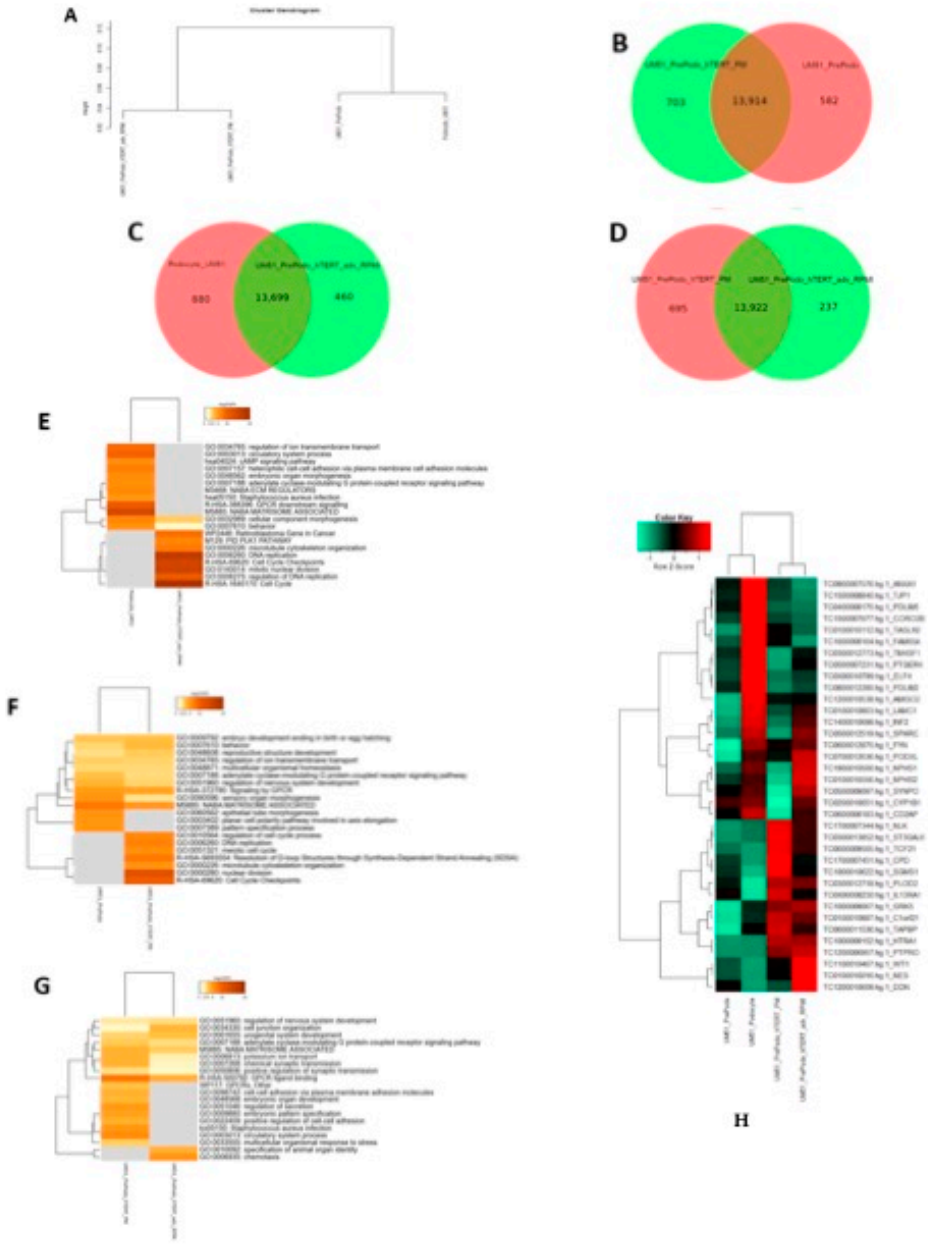


Figure 4. Comparative transcriptome and gene ontology analysis of urine-derived renal progenitor UM51 and derived immortalized UM51-PrePodo-hTERT. A hierarchical cluster dendrogram revealed distinct clusters of immortalized and wild type cells (**A**). Expressed genes (det-p < 0.05) in UdRPCs and podocytes compared in the Venn diagrams (**B**–**D**), showed distinct (582 in UM51-PrePodo; 703 in

UM51-PrePodo-hTERT in PM; 880 in Podocyte UM51; 460 in UM51-PrePodo-hTERT in adv. RPMI; 605 in UM51-PrePodo-hTERT in PM; and 237 UM51-PrePodo-hTERT in adv. RPMI) and overlapping (13,914, 13,699 and 13,922) gene expression patterns. The most over-represented GO BP-terms exclusive in either UM51-PrePodo or UM51-PrePodo-hTERT in PM are shown in (**E**). The most over-represented GO BP-terms exclusive in either podocytes UM51 or UM51-PrePodo-hTERT are shown in (**F**) (full gene list can be found in Supplementary Table S3). The most over-represented GO BP-terms exclusive in either UM51-PrePodo or UM51-PrePodo-hTERT in adv. RPMI are shown in (**G**) (full gene list can be found in Supplementary Table S4). A heatmap comparing UM51-PrePod and UM51-PrePodo-hTERT in PM with their differentiated counterpart UM51-PrePodo-hTERT in adv. RPMI for a gene set commonly expressed in iPS cell-derived podocytes, kidney biopsy isolated human glomeruli and mouse podocytes is shown in (**H**).

3.5. Effects of Angiotensin II on the Differentiated UM51-Pre-Podo-hTERT Podocytes

We recently showed that angiotensin II (ANGII) treatment in UdRPC-differentiated podocytes triggered disruption of the cytoskeleton, resulting in the inhibition of the podocyte spreading and subsequent loss of foot processes as observed by a round and condensed morphology [41]. To evaluate the effect of ANGII on the differentiated podocytes derived from the UM51-Pre-Podo-hTERT cell line, we treated the cells with 100 µM ANGII for 24 h and with a combination of 100 µM ANGII and 1 µM of the selective, competitive angiotensin II receptor type 1 antagonist Losartan for 24 h. After 24 h, dynamic changes in morphology and a significant downregulation of α–ACTININ expression was observed in cells treated with 100 µM ANGII by immunofluorescence-based detection (Figure 5A). While all untreated podocytes stained positive for α–ACTININ, only a limited number of cells appeared to express α–ACTININ after 24 h of ANGII treatment. Furthermore, the control podocytes showed the typical "fried egg" podocyte morphology, whereas in ANG II treated podocytes, a more rounded and condensed morphology was observed. To confirm that the disruptive effect was indeed mediated by ANGII, the effects on the cytoskeleton were evaluated by gene-specific mRNA expression of ANGII receptors, *AGTR1* and *AGTR2*, as well as *SNYPO* and *NPHS1* (Figure 5B–E). All genes were found to be significantly upregulated ($p < 0.05$) upon 100 µM ANGII for 24 h except *NPHS1*, which was found to be significantly downregulated ($p = 0.03$). These findings indicated that the effect was mediated via both receptors. ANGII treatment upregulated *AGTR1* expression by 0.4-fold (Figure 5B) and *AGTR2* by 0.8-fold (Figure 5C). Interestingly, *SNYPO* was also found to be upregulated by 0.5-fold upon ANGII treatment (Figure 5D), while *NPHS1* was found to be downregulated by 0.4-fold. When cells were treated with a combination of 100 µM ANGII and 1 µM Losartan, the expression of all genes was significantly ($p < 0.05$) upregulated, while the expression of *AGTR2*, *NPHS1* and *SYNPO* was found to be increased by 0.7-, 1.4- and 0.8-fold. Interestingly, mRNA expression of *AGTR1* was significantly upregulated by 24-fold. Furthermore, the Losartan treatment rescued the ANGII-induced disruption of the cytoskeleton as indicated by immunofluorescence-based detection of α–ACTININ expression (Figure 5A). Higher magnification pictures of podocyte cytoskeleton and cytoskeletal changes can be found in Supplementary Figure S5. Additionally, the significant upregulation of SYNPO ($p = 0.03$) for both treatments was also confirmed by Western blotting (Figure 5E).

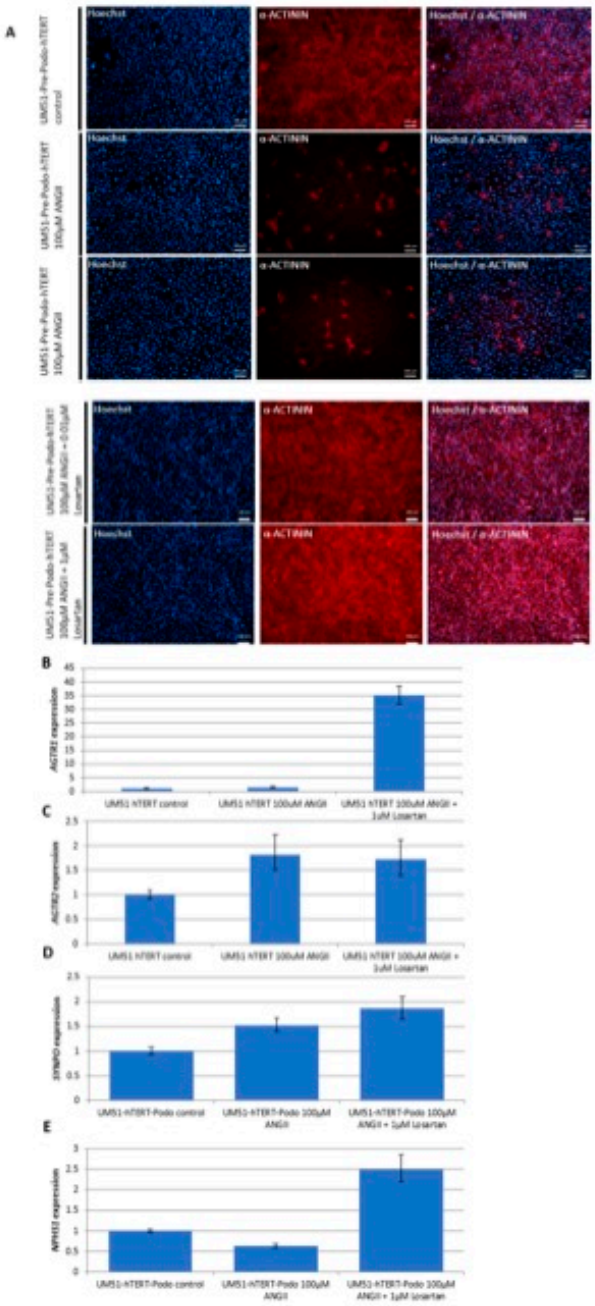


Figure 5. *Cont.*

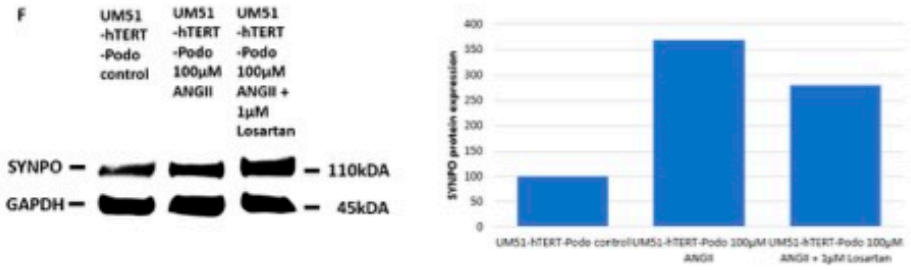


Figure 5. Effects of angiotensin II on the differentiated UM51-Pre-Podo-hTERT cultured in adv. RPMI. UM51-Pre-Podo-hTERT cultured in adv. RPMI supplemented with 30 µM retinoic acid was treated with 100 µM ANGII for 24 h or a combination of 48 h 1 µM Losartan and 24 h 100 µM ANGII. The top panel shows the control morphology. The next two panels show morphology changes after 24 h of 100 µM ANGII treatment, and the last two panels show the morphology for the combination of Losartan and ANGII. The cytoskeleton was visualized by immunofluorescence-based detection of α –ACTININ in red (**A**) (scale bars: 50 µm). Expression of ANGII receptors *AGTR1* (**B**), *AGTR2* (**C**) and expression of podocyte marker *SYNPO* (**D**), and NPHS1 (**E**) were determined by quantitative real-time PCR normalized with the ribosomal encoding gene-RPL0. Expression of the podocyte marker synaptopodin was determined by Western blotting (**F**).

4. Discussion

Podocytes are a cell type found in the kidney glomerulus, where they have major implications in blood filtration. Since mature podocytes are terminal differentiated cells that are unable to undergo cell division in vivo [13], establishing podocyte cell cultures has been very challenging. In the present manuscript, we have described the successful immortalization of a human podocyte progenitor cell line UM51-PrePodo-hTERT, where the primary cells were isolated directly from the urine of a male of African origin. UM51-PrePodo-hTERT was cultured over the course of one year (~100 passages) with high proliferation capacity. Numerous cell lines have been immortalized by overexpression of hTERT, leading to chromosomal aneuploidies and alterations in gene expression [49,50]. Even though UM51-PrePodo-hTERT has a hypertriploid karyotype, the cells showed contact inhibition and P53 expression and activation, indicating that the cells had not lost cell-cycle checkpoints or undergone cancerous transformation—even though they share a characteristic of malignant cells, which for the most part bear short telomeres, and telomerase activity is observed in 85–90% of all human cancers [34,51].

Comparison of the transcriptomes pertaining to podocytes differentiated from UM51-PrePodo-hTERT with previously reported datasets of iPSC–derived podocytes, biopsy-derived human glomeruli, and mouse podocytes [48], revealed distinct clustering of UdR-PCs and their differentiated counterparts, whereas most of the genes were found to be upregulated after our podocyte differentiation protocol. These results confirmed the differentiation capacity of UM51-PrePodo-hTERT into mature podocytes—based on both protein and mRNA expression of LMX1B, NPHS1, SYNPO and WT1. Interestingly, by employing our recently published podocyte differentiation protocol [41], the proliferation capacity of UM51-PrePodo-hTERT was diminished and a significant upregulation of SYNPO expression was observed. SYNPO has been recognized as a key marker of differentiated post-mitotic podocytes [15,17,18], which cannot be detected in undifferentiated or dedifferentiated cells [19,20]. Furthermore, cells in the glomerulus expressing CD133, CD24 and CD166 have been recognized as being highly proliferative, while cells expressing only CD133 and CD24 show lower proliferative capacity and a committed phenotype towards differentiation [52]. Noteworthily, we detected a downregulation of CD24 after immortalization. A study carried out by Paranjape et al. introducing either hTERT or SV40 into human cells, also reported a generation of a cell population with lower levels

of CD24. Therefore, we concluded that the observed CD24 downregulation was caused by the introduction of hTERT and subsequently the immortalization process [46]. Taken together, these two findings, expression of SYNPO and loss of CD24 by cultivation of the UM51-PrePodo-hTert line in adv. RPMI and RA, confirm the differentiation potential of this cell line into podocytes.

We propose that UM51-PrePodo-hTERT can: (a) be differentiated into mature podocytes, and (b) exit the hTERT-driven cell-cycle progression and enter the G_O phase. Of note, during nephron development, podocytes lose their mitotic activity [4] and SYNPO expression is first detectable during the capillary loop stage [15]. This transition is reflected by our KI-67 and SYNPO stainings in the UM51-hTERT-Pre-Podo cells cultured in adv. RPMI.

Finally, we evaluated the responsiveness of UM51-PrePodo-hTERT to angiotensin II (ANGII) which is a key mediator of the renin–angiotensin system (RAS) [1,41]. Elevated levels of ANGII have been identified as a main risk factor for the initiation and progression of chronic kidney disease (CKD). Increased ANGII concentrations are associated with the downregulation of nephrin and synaptopodin expression in podocytes [53,54], leading to podocyte injury [55] and subsequent apoptosis [56]. We observed a disruptive effect of ANGII on the cytoskeleton of podocytes derived from UM51-PrePodo-hTERT, which was accompanied by upregulation of the two angiotensin II receptors, AGTR1 and AGTR2. Here, it is interesting to note that most cells completely downregulated α-ACTININ expression while SYNPO expression was found to be upregulated. This might be explained by the duration of the differentiation. The cells were cultured in adv. RPMI for seven days, in which not all cells entered the quiescent state, as indicated by our KI-67 staining and proliferation assay. This makes it tempting to speculate that the hTERT-driven immortalization sustains a subpopulation of the immortalized cells in a proliferative state, which, then triggered by the culture condition, enables the podocyte lineage a specific gene expression repertoire.

There are currently numerous angiotensin receptor blockers (ARBs) and angiotensin-converting enzyme inhibitors (ACEIs) in clinical use for the treatment of a variety of renal diseases [57,58]. A universal ARB is Losartan, an anti-hypertensive agent. Losartan is used for the management of hypertension, as well as for other therapeutic indications. Its action is based on reversing the effects of ANG II on AGTR1 by the selective masking of AGTR1. Our data provide evidence that the addition of Losartan can counteract the downregulation of the slit diaphragm protein NPHS1 induced by ANG II, thus, leading to the restoration of podocyte architecture by the upregulated expression of nephrin. From this, it can be deduced that Losartan can efficiently reduce ANGII binding to AGTR1.The activation of AGTR2 has been linked to vasodilation, development, cell differentiation, tissue repair and apoptosis [59,60]. Therefore, the masking of AGTR1 and, therefore, the hypothesized hyperactivation of AGTR2, might restore the expression levels of podocyte-specific genes back to the differentiated healthy state.

To summarize, we have described the successful immortalization of the very first male African Pre-Podocyte cell line—UM51-Pre-Podo-hTERT—which grew as a monolayer, and showed contact inhibition and a cobblestone-like morphology typical for epithelial cells. UM51-Pre-Podo-hTERT can be: (a) efficiently transfected as shown by GFP-encoding vector expression, and (b) differentiated into mature podocytes, thus, is amenable for studying nephrogenesis and associated diseases, thus, obviating the need of iPSCs. Furthermore, the responsiveness of the derived podocytes to ANGII implies potential applications in kidney-associated disease modelling, nephrotoxicity studies and drug screening.

Supplementary Materials: The following supporting information can be downloaded at: https://www.mdpi.com/article/10.3390/cells12030342/s1, Figure S1: Complete Western blot images for the detection of the HA-tag in the cell lines UM51-PrePodo-hTERT and UM51-PrePodo: (A) HA-tag, (B) β-Actin; Figure S2: Transfection of UM51-PrePodo-hTERT with the TurboGFP-vector; Figure S3: Morphology of UM51-PrePodo-hTERT cells cultured in proliferation medium (right) and advanced RPMI (left) during the resazurin assay; Figure S4: Complete Western blot images for the comparison of UM51-PrePodo-hTERT cultured in proliferation medium (PM) and advanced RPMI (Adv. RPMI): (A) HA-tag, (B) SYNPO, (C) P53, (D) β-Actin and (E) LMX1b; Figure S5: Higher magnification of podocyte cytoskeleton remodeling after treatment with ANGII stained with α-Actinin (A); Table S1: antibodies; Table S2: RT-qPCR Primers; Table S3: UM51 PrePodo vs UM51 PrePodo Htert Analysis Report; Table S4: UM51 Podo vs UM51 PrePodo Htert adv RPMI metascape result.

Author Contributions: Conceptualization, J.A.; methodology, L.E., L.D.F.K., C.T., K.S. and M.B.; software, W.W.; validation, L.E., L.D.F.K. and C.T.; formal analysis, L.E., C.T. and W.W.; investigation, L.E., L.D.F.K. and C.T.; resources, J.A.; data curation, L.E., L.D.F.K., C.T., K.S. and W.W.; writing—original draft preparation, L.E.; writing—review and editing, J.A.; visualization, L.E., L.D.F.K. and W.W.; supervision, J.A.; project administration, J.A.; funding acquisition, J.A. All authors have read and agreed to the published version of the manuscript.

Funding: J.A. acknowledges the medical faculty of Heinrich Heine University for financial support.

Institutional Review Board Statement: In this study, urine samples were collected with the informed consent of the donors and the written approval (ethical approval number: 5704) of the ethical review board of the medical faculty of Heinrich Heine University, Düsseldorf, Germany. All methods were carried out in accordance with the approved guidelines. The medical faculty of Heinrich Heine University approved all experimental protocols.

Informed Consent Statement: In this study, urine samples were collected with the informed consent of the donors and approved by the local ethical board, with ethical approval number 5704.

Data Availability Statement: Raw data are available upon request.

Acknowledgments: James Adjaye acknowledges funding from the medical faculty of Heinrich Heine University, Duesseldorf, Germany.

Conflicts of Interest: The authors declare no conflict of interest.

References

1. Patel, S.; Rauf, A.; Khan, H.; Abu-Izneid, T. Renin-angiotensin-aldosterone (RAAS): The ubiquitous system for homeostasis and pathologies. *Biomed. Pharmacother.* **2017**, *94*, 317–325. [CrossRef] [PubMed]
2. Kawachi, H.; Miyauchi, N.; Suzuki, K.; Han, G.D.; Orikasa, M.; Shimizu, F. Role of podocyte slit diaphragm as a filtration barrier. *Nephrology (Carlton)* **2006**, *11*, 274–281. [CrossRef] [PubMed]
3. Scott, R.P.; Quaggin, S.E. Review series: The cell biology of renal filtration. *J. Cell Biol.* **2015**, *209*, 199–210. [CrossRef]
4. Mundel, P.; Kriz, W. Structure and function of podocytes: An update. *Anat. Embryol.* **1995**, *192*, 385–397. [CrossRef] [PubMed]
5. Hyodo, T.; Naguro, T.; Kameie, T.; Iino, A.; Miyagawa, I. Scanning and transmission electron-microscopic study of the development of the podocyte in the human fetus. *Pediatr. Nephrol.* **1997**, *11*, 133–139. [CrossRef]
6. Saxén, L.; Sariola, H. Early organogenesis of the kidney. *Pediatr. Nephrol.* **1987**, *1*, 385–392. [CrossRef]
7. Sorokin, L.; Ekblom, P. Development of tubular and glomerular cells of the kidney. *Kidney Int.* **1992**, *41*, 657–664. [CrossRef]
8. Reeves, W.; Caulfield, J.P.; Farquhar, M.G. Differentiation of epithelial foot processes and filtration slits: Sequential appearance of occluding junctions, epithelial polyanion, and slit membranes in developing glomeruli. *Lab. Investig.* **1978**, *39*, 90–100.
9. Nagata, M.; Nakayama, K.-I.; Terada, Y.; Hoshi, S.; Watanabe, T. Cell Cycle Regulation and Differentiation in the Human Podocyte Lineage. *Am. J. Pathol.* **1998**, *153*, 1511–1520. [CrossRef]
10. Schnabel, E.; Dekan, G.; Miettinen, A.; Farquhar, M.G. Biogenesis of podocalyxin–the major glomerular sialoglycoprotein–in the newborn rat kidney. *Eur. J. Cell Biol.* **1989**, *48*, 313–326.
11. Schnabel, E.; Anderson, J.M.; Farquhar, M.G. The tight junction protein ZO-1 is concentrated along slit diaphragms of the glomerular epithelium. *J. Cell Biol.* **1990**, *111*, 1255–1263. [CrossRef] [PubMed]
12. Mundlos, S.; Pelletier, J.; Darveau, A.; Bachmann, M.; Winterpacht, A.; Zabel, B. Nuclear localization of the protein encoded by the Wilms' tumor gene WT1 in embryonic and adult tissues. *Development* **1993**, *119*, 1329–1341. [CrossRef]
13. Greka, A.; Mundel, P. Cell biology and pathology of podocytes. *Annu. Rev. Physiol.* **2012**, *74*, 299–323. [CrossRef] [PubMed]

14. Kestilä, M.; Lenkkeri, U.; Männikkö, M.; Lamerdin, J.; McCready, P.; Putaala, H.; Ruotsalainen, V.; Morita, T.; Nissinen, M.; Herva, R.; et al. Positionally Cloned Gene for a Novel Glomerular Protein—Nephrin—Is Mutated in Congenital Nephrotic Syndrome. *Mol. Cell* **1998**, *1*, 575–582. [CrossRef] [PubMed]
15. Mundel, P.; Gilbert, P.; Kriz, W. Podocytes in glomerulus of rat kidney express a characteristic 44 KD protein. *J. Histochem. Cytochem.* **1991**, *39*, 1047–1056. [CrossRef]
16. Holthöfer, H.; Miettinen, A.; Lehto, V.P.; Lehtonen, E.; Virtanen, I. Expression of vimentin and cytokeratin types of intermediate filament proteins in developing and adult human kidneys. *Lab. Investig.* **1984**, *50*, 552–559.
17. Saleem, M.A.; O'Hare, M.J.; Reiser, J.; Coward, R.J.; Inward, C.D.; Farren, T.; Xing, C.Y.; Ni, L.; Mathieson, P.W.; Mundel, P. A conditionally immortalized human podocyte cell line demonstrating nephrin and podocin expression. *J. Am. Soc. Nephrol.* **2002**, *13*, 630–638. [CrossRef]
18. Mundel, P.; Heid, H.W.; Mundel, T.M.; Krüger, M.; Reiser, J.; Kriz, W. Synaptopodin: An actin-associated protein in telencephalic dendrites and renal podocytes. *J. Cell Biol.* **1997**, *139*, 193–204. [CrossRef]
19. May, C.J.; Saleem, M.; Welsh, G.I. Podocyte dedifferentiation: A specialized process for a specialized cell. *Front. Endocrinol. (Lausanne)* **2014**, *5*, 148. [CrossRef]
20. Shankland, S.J.; Pippin, J.W.; Reiser, J.; Mundel, P. Podocytes in culture: Past, present, and future. *Kidney Int.* **2007**, *72*, 26–36. [CrossRef]
21. Freedman, B.S.; Brooks, C.R.; Lam, A.Q.; Fu, H.; Morizane, R.; Agrawal, V.; Saad, A.F.; Li, M.K.; Hughes, M.R.; Werff, R.V.; et al. Modelling kidney disease with CRISPR-mutant kidney organoids derived from human pluripotent epiblast spheroids. *Nat. Commun.* **2015**, *6*, 8715. [CrossRef] [PubMed]
22. Morizane, R.; Lam, A.Q.; Freedman, B.S.; Kishi, S.; Valerius, M.T.; Bonventre, J.V. Nephron organoids derived from human pluripotent stem cells model kidney development and injury. *Nat. Biotechnol.* **2015**, *33*, 1193–1200. [CrossRef]
23. Taguchi, A.; Kaku, Y.; Ohmori, T.; Sharmin, S.; Ogawa, M.; Sasaki, H.; Nishinakamura, R. Redefining the in vivo origin of metanephric nephron progenitors enables generation of complex kidney structures from pluripotent stem cells. *Cell Stem Cell* **2014**, *14*, 53–67. [CrossRef] [PubMed]
24. Takasato, M.; Er, P.X.; Chiu, H.S.; Maier, B.; Baillie, G.J.; Ferguson, C.; Parton, R.G.; Wolvetang, E.J.; Roost, M.S.; Chuva de Sousa Lopes, S.M.; et al. Kidney organoids from human iPS cells contain multiple lineages and model human nephrogenesis. *Nature* **2015**, *526*, 564–568. [CrossRef]
25. Nguyen, L.; Wruck, W.; Erichsen, L.; Graffmann, N.; Adjaye, J. The Nephrotoxin Puromycin Aminonucleoside Induces Injury in Kidney Organoids Differentiated from Induced Pluripotent Stem Cells. *Cells* **2022**, *11*, 635. [CrossRef]
26. Makarov, V.L.; Hirose, Y.; Langmore, J.P. Long G Tails at Both Ends of Human Chromosomes Suggest a C Strand Degradation Mechanism for Telomere Shortening. *Cell* **1997**, *88*, 657–666. [CrossRef]
27. Wright, W.E.; Tesmer, V.M.; Huffman, K.E.; Levene, S.D.; Shay, J.W. Normal human chromosomes have long G-rich telomeric overhangs at one end. *Genes Dev.* **1997**, *11*, 2801–2809. [CrossRef]
28. Greider, C.W.; Blackburn, E.H. Identification of a specific telomere terminal transferase activity in tetrahymena extracts. *Cell* **1985**, *43*, 405–413. [CrossRef]
29. Harrington, L.; Zhou, W.; McPhail, T.; Oulton, R.; Yeung, D.S.; Mar, V.; Bass, M.B.; Robinson, M.O. Human telomerase contains evolutionarily conserved catalytic and structural subunits. *Genes Dev.* **1997**, *11*, 3109–3115. [CrossRef] [PubMed]
30. Kilian, A.; Bowtell, D.D.; Abud, H.E.; Hime, G.R.; Venter, D.J.; Keese, P.K.; Duncan, E.L.; Reddel, R.R.; Jefferson, R.A. Isolation of a candidate human telomerase catalytic subunit gene, which reveals complex splicing patterns in different cell types. *Hum. Mol. Genet.* **1997**, *6*, 2011–2019. [CrossRef]
31. Lingner, J.; Hughes, T.R.; Shevchenko, A.; Mann, M.; Lundblad, V.; Cech, T.R. Reverse transcriptase motifs in the catalytic subunit of telomerase. *Science* **1997**, *276*, 561–567. [CrossRef] [PubMed]
32. Meyerson, M.; Counter, C.M.; Eaton, E.N.; Ellisen, L.W.; Steiner, P.; Caddle, S.D.; Ziaugra, L.; Beijersbergen, R.L.; Davidoff, M.J.; Liu, Q.; et al. hEST2, the Putative Human Telomerase Catalytic Subunit Gene, Is Up-Regulated in Tumor Cells and during Immortalization. *Cell* **1997**, *90*, 785–795. [CrossRef] [PubMed]
33. Wright, W.E.; Piatyszek, M.A.; Rainey, W.E.; Byrd, W.; Shay, J.W. Telomerase activity in human germline and embryonic tissues and cells. *Dev. Genet.* **1996**, *18*, 173–179. [CrossRef]
34. Shay, J.W.; Bacchetti, S. A survey of telomerase activity in human cancer. *Eur. J. Cancer* **1997**, *33*, 787–791. [CrossRef] [PubMed]
35. Kim, S.H.; Kaminker, P.; Campisi, J. TIN2, a new regulator of telomere length in human cells. *Nat. Genet.* **1999**, *23*, 405–412. [CrossRef]
36. Bodnar, A.G.; Ouellette, M.; Frolkis, M.; Holt, S.E.; Chiu, C.P.; Morin, G.B.; Harley, C.B.; Shay, J.W.; Lichtsteiner, S.; Wright, W.E. Extension of life-span by introduction of telomerase into normal human cells. *Science* **1998**, *279*, 349–352. [CrossRef]
37. Hahn, W.C. Immortalization and transformation of human cells. *Mol. Cells* **2002**, *13*, 351–361.
38. Meyerson, M. Telomerase enzyme activation and human cell immortalization. *Toxicol. Lett.* **1998**, *102–103*, 41–45. [CrossRef]
39. Vaziri, H.; Benchimol, S. Reconstitution of telomerase activity in normal human cells leads to elongation of telomeres and extended replicative life span. *Curr. Biol.* **1998**, *8*, 279–282. [CrossRef]
40. Hahn, W.C.; Counter, C.M.; Lundberg, A.S.; Beijersbergen, R.L.; Brooks, M.W.; Weinberg, R.A. Creation of human tumour cells with defined genetic elements. *Nature* **1999**, *400*, 464–468. [CrossRef]
41. Erichsen, L.; Thimm, C.; Bohndorf, M.; Rahman, M.S.; Wruck, W.; Adjaye, J. Activation of the Renin-Angiotensin System Disrupts the Cytoskeletal Architecture of Human Urine-Derived Podocytes. *Cells* **2022**, *11*, 1095. [CrossRef] [PubMed]

42. Venteicher, A.S.; Meng, Z.; Mason, P.J.; Veenstra, T.D.; Artandi, S.E. Identification of ATPases pontin and reptin as telomerase components essential for holoenzyme assembly. *Cell* **2008**, *132*, 945–957. [CrossRef] [PubMed]
43. Rahman, M.S.; Wruck, W.; Spitzhorn, L.-S.; Nguyen, L.; Bohndorf, M.; Martins, S.; Asar, F.; Ncube, A.; Erichsen, L.; Graffmann, N.; et al. The FGF, TGFβ and WNT axis Modulate Self-renewal of Human SIX2+ Urine Derived Renal Progenitor Cells. *Sci. Rep.* **2020**, *10*, 739. [CrossRef]
44. Bikkul, M.U.; Faragher, R.G.A.; Worthington, G.; Meinke, P.; Kerr, A.R.W.; Sammy, A.; Riyahi, K.; Horton, D.; Schirmer, E.C.; Hubank, M.; et al. Telomere elongation through hTERT immortalization leads to chromosome repositioning in control cells and genomic instability in Hutchinson-Gilford progeria syndrome fibroblasts, expressing a novel SUN1 isoform. *Genes Chromosomes Cancer* **2019**, *58*, 341–356. [CrossRef] [PubMed]
45. Kan, C.-Y.; Wen, V.W.; Pasquier, E.; Jankowski, K.; Chang, M.; Richards, L.A.; Kavallaris, M.; MacKenzie, K.L. Endothelial cell dysfunction and cytoskeletal changes associated with repression of p16(INK4a) during immortalization. *Oncogene* **2012**, *31*, 4815–4827. [CrossRef]
46. Paranjape, A.N.; Mandal, T.; Mukherjee, G.; Kumar, M.V.; Sengupta, K.; Rangarajan, A. Introduction of SV40ER and hTERT into mammospheres generates breast cancer cells with stem cell properties. *Oncogene* **2012**, *31*, 1896–1909. [CrossRef]
47. Schütze, D.M.; Krijgsman, O.; Snijders, P.J.F.; Ylstra, B.; Weischenfeldt, J.; Mardin, B.R.; Stütz, A.M.; Korbel, J.O.; de Winter, J.P.; Meijer, C.J.L.M.; et al. Immortalization capacity of HPV types is inversely related to chromosomal instability. *Oncotarget* **2016**, *7*, 37608–37621. [CrossRef]
48. Sharmin, S.; Taguchi, A.; Kaku, Y.; Yoshimura, Y.; Ohmori, T.; Sakuma, T.; Mukoyama, M.; Yamamoto, T.; Kurihara, H.; Nishinakamura, R. Human Induced Pluripotent Stem Cell-Derived Podocytes Mature into Vascularized Glomeruli upon Experimental Transplantation. *J. Am. Soc. Nephrol.* **2016**, *27*, 1778–1791. [CrossRef]
49. Lindvall, C.; Hou, M.; Komurasaki, T.; Zheng, C.; Henriksson, M.; Sedivy, J.M.; Björkholm, M.; Teh, B.T.; Nordenskjöld, M.; Xu, D. Molecular characterization of human telomerase reverse transcriptase-immortalized human fibroblasts by gene expression profiling: Activation of the epiregulin gene. *Cancer Res.* **2003**, *63*, 1743–1747.
50. Twine, N.A.; Harkness, L.; Adjaye, J.; Aldahmash, A.; Wilkins, M.R.; Kassem, M. Molecular Phenotyping of Telomerized Human Bone Marrow Skeletal Stem Cells Reveals a Genetic Program of Enhanced Proliferation and Maintenance of Differentiation Responses. *JBMR Plus* **2018**, *2*, 257–267. [CrossRef]
51. Kim, N.W.; Piatyszek, M.A.; Prowse, K.R.; Harley, C.B.; West, M.D.; Ho, P.L.; Coviello, G.M.; Wright, W.E.; Weinrich, S.L.; Shay, J.W. Specific association of human telomerase activity with immortal cells and cancer. *Science* **1994**, *266*, 2011–2015. [CrossRef] [PubMed]
52. Angelotti, M.L.; Ronconi, E.; Ballerini, L.; Peired, A.; Mazzinghi, B.; Sagrinati, C.; Parente, E.; Gacci, M.; Carini, M.; Rotondi, M.; et al. Characterization of renal progenitors committed toward tubular lineage and their regenerative potential in renal tubular injury. *Stem Cells* **2012**, *30*, 1714–1725. [CrossRef]
53. Liu, X.; Zhang, H.; Wang, Q.; Yu, K.; Wang, R.; Sun, J. Blockade of vascular endothelial growth factor-A/receptor 2 exhibits a protective effect on angiotensin-II stimulated podocytes. *Mol. Med. Rep.* **2015**, *12*, 4340–4345. [CrossRef] [PubMed]
54. Jia, J.; Ding, G.; Zhu, J.; Chen, C.; Liang, W.; Franki, N.; Singhal, P.C. Angiotensin II infusion induces nephrin expression changes and podocyte apoptosis. *Am. J. Nephrol.* **2008**, *28*, 500–507. [CrossRef] [PubMed]
55. Rüster, C.; Wolf, G. Renin-angiotensin-aldosterone system and progression of renal disease. *J. Am. Soc. Nephrol.* **2006**, *17*, 2985–2991. [CrossRef] [PubMed]
56. Ding, G.; Reddy, K.; Kapasi, A.A.; Franki, N.; Gibbons, N.; Kasinath, B.S.; Singhal, P.C. Angiotensin II induces apoptosis in rat glomerular epithelial cells. *Am. J. Physiol. Renal Physiol.* **2002**, *283*, F173–F180. [CrossRef]
57. Molnar, M.Z.; Kalantar-Zadeh, K.; Lott, E.H.; Lu, J.L.; Malakauskas, S.M.; Ma, J.Z.; Quarles, D.L.; Kovesdy, C.P. Angiotensin-converting enzyme inhibitor, angiotensin receptor blocker use, and mortality in patients with chronic kidney disease. *J. Am. Coll. Cardiol.* **2014**, *63*, 650–658. [CrossRef]
58. Brar, S.; Ye, F.; James, M.T.; Hemmelgarn, B.; Klarenbach, S.; Pannu, N. Association of Angiotensin-Converting Enzyme Inhibitor or Angiotensin Receptor Blocker Use with Outcomes after Acute Kidney Injury. *JAMA Intern. Med.* **2018**, *178*, 1681–1690. [CrossRef]
59. Kaschina, E.; Unger, T. Angiotensin AT1/AT2 receptors: Regulation, signalling and function. *Blood Press.* **2003**, *12*, 70–88. [CrossRef]
60. Stegbauer, J.; Coffman, T.M. New insights into angiotensin receptor actions: From blood pressure to aging. *Curr. Opin. Nephrol. Hypertens.* **2011**, *20*, 84–88. [CrossRef]

Disclaimer/Publisher's Note: The statements, opinions and data contained in all publications are solely those of the individual author(s) and contributor(s) and not of MDPI and/or the editor(s). MDPI and/or the editor(s) disclaim responsibility for any injury to people or property resulting from any ideas, methods, instructions or products referred to in the content.

3.2 Modelling APOL1-mediated kidney inflammation and fibrosis using a partially reprogrammed urine derived SIX2-positive renal progenitor cell line

Chantelle Thimm, Rosanne Mack, Osmond Adjei-Aruna, Wasco Wruck and James Adjaye

BioRxiv, 2025

Abstract:

Background

CKD affects approximately 850 million people worldwide and is a leading cause of mortality. Podocytes, cells in the kidney are terminally differentiated and incapable of division *in vivo* making the establishment of primary cultures particularly challenging. The ability of cells to proliferate and avoid senescence is closely linked to telomere length. When telomere length becomes critically reduced, it results in cellular senescence.

Methods

We present the successful rejuvenation of a human SIX2-positive renal progenitor cell line derived from the urine of a 30-year-old West African male (UM30-OSN). To achieve partial reprogramming, plasmids expressing the Yamanaka factors OCT4, SOX2, NANOG, c-Myc, and KLF4 were employed.

Results

UM30-OSN expresses the pluripotency-associated marker SSEA4, renal stem cell markers such as SIX2, CD133 and CD24, determined by immunofluorescence, FACS and qPCR. Expression analysis revealed downregulation of senescence markers p21and p53 and upregulation of proliferation-associated genes PCNA, KI67 and TERT, confirming rejuvenation.

Upon podocyte differentiation, UM30-OSN cells expressed podocyte-specific markers NPHS1, NPHS2, SYNPO and CD2AP. Comparative transcriptome analyses revealed a correlation co-efficiency (R^2 = 0.88) with the immortal podocyte line AB 8/13.

To demonstrate the usefulness of UM30-OSN to model APOL1-mediated kidney disease, we investigated the effects of Interferon-γ (IFN-γ) on UM30-OSN derived podocytes and evaluated

the potential of the JAK1/JAK2 inhibitor Baricitinib to mitigate IFN-γ–induced cellular responses. IFN-γ stimulation resulting in increased phosphorylation of STAT1, activation of APOL1, upregulation of pro-inflammatory and fibrotic markers such as, IL-6, TGF-β, Vimentin, Fibronectin, and morphological changes indicative of cell stress. Pre-treatment with Baricitinib effectively inhibited STAT1 phosphorylation, reduced expression of pro-inflammatory and fibrosis-associated genes, and preserved podocyte morphology.

Conclusion
Given their robust proliferation capacity, UM30-OSN cells represent a valuable additional model for investigating kidney-associated diseases such the contribution of APOL1 high-risk variants to kidney injury and fibrosis.

Author contribution of C.T. included 80%:

I was responsible for establishing and maintaining the cell culture systems, which included the cultivation of UdRPCs, iPSCs, and the UM30-OSN cell line. I carried out the induction of podocyte differentiation and the execution of stimulation experiments employing IFN-γ and the JAK/STAT-pathway inhibitor Baricitinib on UM30-OSN podocytes.

For the characterization of the newly generated UM30-OSN cell line, I performed immunofluorescence staining, DNA isolation for semi-quantitative PCR/exogenous PCR and APOL1 genotyping, as well as RNA isolation for both NGS (next-generation sequencing) and qPCR. I also prepared protein lysates and conducted the Western blot analyses. The APOL1 genotyping was performed by D.K, A.K and K.B.. In addition, I carried out all immunofluorescence stainings, RNA isolations, and qPCRs for further phenotypic characterization. For the FACS (Fluorescence-activated cell sorting) analyses, I performed the immunofluorescence staining, and the operation of the machine was carried out under the supervision of N.G. For the IFN-γ and Baricitinib treatment experiments, I isolated RNA and protein samples, R.M. provided additional support during protein extraction. I collected all RNA samples designated for NGS, after which W.W. (Bioinformatician) processed and analyzed the raw sequencing data. I subsequently performed further analyses, including functional enrichment analysis using Metascape. For all datasets generated in the course of the study, I carried out the respective statistical analyses and prepared the quantitative evaluation of the results. I contributed to the conceptualization, designed and executed the experiments and

interpreted the results to my research hypothesis. I generated and designed all figures and schematic illustrations, compiled and analyzed the complete dataset, and wrote the original manuscript. I further revised and finalized the manuscript in response to the reviewers' comments with J.A..

Status: Published in Stem Cell Research and Therapy.

DOI: 10.1186/s13287-025-04710-x

This article is an open access article distributed under the terms and conditions of the Creative Commons Attribution (CC BY) 4.0 license, which permits unrestricted use, distribution, and reproduction in any medium, provided the original work is properly cited.

bioRxiv preprint doi: https://doi.org/10.1101/2025.07.28.667124; this version posted July 29, 2025. The copyright holder for this preprint (which was not certified by peer review) is the author/funder, who has granted bioRxiv a license to display the preprint in perpetuity. It is made available under aCC-BY-NC 4.0 International license.

Title page

Title:

Modelling APOL1-mediated kidney inflammation and fibrosis using a partially reprogrammed urine derived SIX2-positive renal progenitor cell line.

Chantelle Thimm[1], Rosanne Mack[1], Osmond Adjei-Aruna[1], Wasco Wruck[1], James Adjaye[1,2*]

[1] Institute for Stem Cell Research and Regenerative Medicine, Medical Faculty, Heinrich Heine University Düsseldorf, 40225 Düsseldorf, Germany.

[2] EGA Institute for Women's Health, Zayed Centre for Research into Rare Diseases in Children (ZCR), University College London (UCL), 20 Guilford Street, London WC1N 1DZ, UK

*Correspondence: James.Adjaye@med.uni-duesseldorf.de

Abstract

Background

CKD affects approximately 850 million people worldwide and is a leading cause of mortality. Podocytes, cells in the kidney are terminally differentiated and incapable of division *in vivo* making the establishment of primary cultures particularly challenging. The ability of cells to proliferate and avoid senescence is closely linked to telomere length. When telomere length becomes critically reduced, it results in cellular senescence.

Methods

We present the successful rejuvenation of a human SIX2-positive renal progenitor cell line derived from the urine of a 30-year-old West African male (UM30-OSN). To achieve partial reprogramming, plasmids expressing the Yamanaka factors OCT4, SOX2, NANOG, c-Myc, and KLF4 were employed.

Results

UM30-OSN expresses the pluripotency-associated marker SSEA4, renal stem cell markers such as SIX2, CD133 and CD24, determined by immunofluorescence, FACS and qPCR.

bioRxiv preprint doi: https://doi.org/10.1101/2025.07.28.667124; this version posted July 29, 2025. The copyright holder for this preprint (which was not certified by peer review) is the author/funder, who has granted bioRxiv a license to display the preprint in perpetuity. It is made available under aCC-BY-NC 4.0 International license.

Expression analysis revealed downregulation of senescence markers p21and p53 and upregulation of proliferation-associated genes PCNA, KI67 and TERT, confirming rejuvenation.
Upon podocyte differentiation, UM30-OSN cells expressed podocyte-specific markers NPHS1, NPHS2, SYNPO and CD2AP. Comparative transcriptome analyses revealed a correlation co-efficiency (R^2 = 0.88) with the immortal podocyte line AB 8/13.
To demonstrate the usefulness of UM30-OSN to model APOL1-mediated kidney disease, we investigated the effects of Interferon-γ (IFN-γ) on UM30-OSN derived podocytes and evaluated the potential of the JAK1/JAK2 inhibitor Baricitinib to mitigate IFN-γ–induced cellular responses. IFN-γ stimulation resulting in increased phosphorylation of STAT1, activation of APOL1, upregulation of pro-inflammatory and fibrotic markers such as, IL-6, TGF-β, Vimentin, Fibronectin, and morphological changes indicative of cell stress. Pre-treatment with Baricitinib effectively inhibited STAT1 phosphorylation, reduced expression of pro-inflammatory and fibrosis-associated genes, and preserved podocyte morphology.

Conclusion
Given their robust proliferation capacity, UM30-OSN cells represent a valuable additional model for investigating kidney-associated diseases such the contribution of APOL1 high-risk variants to kidney injury and fibrosis.

Keywords: Partial reprogramming, rejuvenation, nephrogenesis, Interferon-γ, Baricitinib, JAK/STAT signaling pathway, APOL1-mediated kidney disease, fibrosis, inflammation, SIX2-positive renal progenitor cell line.

Background

Kidneys comprise approximately one million nephrons, which play vital roles in regulating systemic pH, maintaining fluid homeostasis, filtration of blood and electrolyte balance. Each nephron consists of a renal corpuscle, which includes the glomerular filtration barrier and a complex renal tubular system. The glomerular filtration barrier is formed by podocytes, which are highly specialized epithelial cells that envelop the glomerular capillaries and extend into the urinary space of Bowman's capsule. These cells possess a large cell body with numerous foot processes that interdigitate with those of adjacent podocytes. These lamellipodia-like extensions form intercellular junctions across the slit diaphragm, ensuring selective permeability based on molecular size during glomerular filtration. Several podocyte-specific genes have been identified, whose protein products are critical for the integrity and function of the filtration barrier. These include NPHS2 (Podocin), NPHS1 (Nephrin), CD2AP (CD2-associated protein) and SYNPO (Synaptopodin).

bioRxiv preprint doi: https://doi.org/10.1101/2025.07.28.667124; this version posted July 29, 2025. The copyright holder for this preprint (which was not certified by peer review) is the author/funder, who has granted bioRxiv a license to display the preprint in perpetuity. It is made available under aCC-BY-NC 4.0 International license.

Currently, animal models, including rats and mice, are extensively utilized in the study of kidney diseases.

However, these models exhibit significant anatomical, histological, and molecular differences compared to human kidneys. This discrepancy underscores the urgent need for more physiologically relevant human experimental models.

To date, the use of induced pluripotent stem cells (iPSCs), and the temperature-sensitive SV40 conditionally immortalized cell lines has become widespread in kidney-associated research [1–4].

The growth-promoting effect of the SV40 DNA sequence was first reported in 1965 [5]. This immortalized ability was first described in detail by Chang et al. in 1984 [6], for which the tumor (T) antigen and the small T antigen appear to be responsible. The small T antigen facilitates the replication of the viral genome and can accelerate the G1 and S phases of the cell cycle. In parallel, the T antigen interacts with the tumor suppressor retinoblastoma family (pRB) and p53 [7].

In earlier studies have shown that it is possible to rejuvenate adult somatic cells by transient over expression of the Yamanaka factors without the sole dependence on SV40 T antigen [8].

Interferon-gamma (IFN-γ) acts as a pivotal pro-inflammatory cytokine implicated in immune-mediated kidney diseases. It activates JAK/STAT signalling, inducing transcription of inflammatory and pro-fibrotic genes such as APOL1, which is strongly associated with increase the risk of kidney damage, including fibrosis, leading to chronic kidney disease (CKD) and potentially kidney failure in individuals of West African descent carrying the G1 or G2 risk variants [9–11]. Functional investigation of APOL1 has largely relied on over-expression models in mice and HEK293 cells to over-express APOL1-G0, -G1, or -G2 variants. These studies revealed mitochondrial dysfunction, altered gene expression profiles, and impaired respiration in HEK cells over-expressing G1 or G2 variants [11–13]. Although these models provide valuable mechanistic insights, they lack the characteristic features of human podocytes and the native regulatory context of APOL1.

APOL1 gene variants are associated with an increased risk of kidney disease, particularly in individuals of African origin. These variants can lead to various forms of kidney disease, including focal segmental glomerulosclerosis (FSGS), collapsing glomerulopathy, hypertensive nephropathy, CKD and end-stage kidney failure [14–18]. The development of renal fibrosis characterizes CKD. Regardless of the primary cause, renal fibrosis is the hallmark of progressive CKD[19]. Fibrogenesis is initiated in response to chronic kidney damage; following renal injury, profibrotic factors are produced by injured tubular epithelial cells and infiltrating inflammatory cells that stimulate signaling events leading to ECM production. APOL1 risk variants are linked to accelerated fibrosis in the kidneys, contributing to the progression of

bioRxiv preprint doi: https://doi.org/10.1101/2025.07.28.667124; this version posted July 29, 2025. The copyright holder for this preprint (which was not certified by peer review) is the author/funder, who has granted bioRxiv a license to display the preprint in perpetuity. It is made available under aCC-BY-NC 4.0 International license.

kidney disease[20], which has been shown in human cellular[21] and mouse models[22]. In a transgenic mouse model expressing the podocyte-specific APOL1-G2 risk variant (G2APOL1), these variants led to activation of STING and NLRP3 inflammasomes. Triggered pronounced renal fibrosis, increased albuminuria and impaired renal function[22].

In the present study, we used rejuvenated SIX2-positive renal progenitor cells derived from the urine of a male donor of West African ancestry, differentiated into podocytes (UM30-OSN). This model combines genetic authenticity with the physiological relevance of podocytes and enables, for the first time, the investigation of IFN-γ–induced APOL1 regulation and the mechanisms of Baricitinib action in a more disease-relevant cellular context.

These cells exhibit stable morphology and proliferation capacity *in vitro* for over one year of culture. The UM30-OSN cell line expresses the homeodomain transcriptional regulator SIX2, representing a multipotent, self-renewing progenitor population capable of differentiating into all nephron cell types [23,24]. We further analyzed gene and protein expression, morphological cellular changes, and activation of the JAK/STAT signaling pathway, as well as the ability of Baricitinib to suppress these IFN-γ–mediated effects.

Due to their high proliferation capacity and ease of handling, our immortalized male UM30-OSN cell line of West African origin, which we believe is one of its kind, provides a unique tool for studying the molecular basis of APOL1-mediated inflammation and fibrosis in the kidney.

Methods

Cell Culture Conditions

Urine-derived renal progenitor cells (UdRPCs) of a 30-year old man (UM30) were isolated and maintained in proliferation medium (PM) as described in Rahman et al [25]. Furthermore, approximately 250,000 SIX2-positive urine-derived cells from UM30 were immortalized by nucleofection of an episomal not integrative plasmid-based ectopic expression of Yamanaka reprogramming factors co-expressed SV40 large T antigen, which inactivates the tumor suppressors pRB and p53 (UM30-OSN)[26,27]. For more efficiency, pathway inhibitions: TGFβ /SB431245 (Stemgent #04-0014), MEK/PD0325901 (Stemgent #04-0006) and GSK3β/CHIR99021 (Stemgent #04-0004) were added. Cells were cultured for 24 h in PM supplemented with 10 µM Y27632 on Matrigel® at 37 ◦C and 5 % CO2. After 24 h, the medium was changed to StemMACS iPS-Brew XF Medium (Miltenyi Biotec, Bergisch Gladbach,Germany) with daily medium changes. Besides the well-defined iPSC colonies clusters of partially reprogrammed cells were identified. These rapidly proliferating cells are still mesenchymal unlike iPSCs and they resemble the primary urine cells. These clusters were

bioRxiv preprint doi: https://doi.org/10.1101/2025.07.28.667124; this version posted July 29, 2025. The copyright holder for this preprint (which was not certified by peer review) is the author/funder, who has granted bioRxiv a license to display the preprint in perpetuity. It is made available under aCC-BY-NC 4.0 International license.

picked and expanded on plastic, cultured at 37 °C, 5% CO2. The cells were cultured in proliferation medium (PM) composed of 50% DMEM high Glucose (Gibco®, life technologies, California) and 50% Keratinocyte growth basal medium (Lonza, Basel, Switzerland) supplemented with 5 ng/ml bFGF. The DMEM high Glucose medium is supplemented with 10% fetal bovine serum (Gibco®), 0.1% Non-Essential Amino Acid (Gibco®), 0.5% Glutamax (Gibco®) and 1% Penicillin and Streptomycin (Gibco®). Differentiation into podocytes followed our previously published protocols [2,28,29]. In brief, 25,000 cells per 6-well and 100,000 cells per 12-well were first cultured for 24 h in PM on Corning® Collagen I (Merck, Darmstadt, Deutschland) coated plates till approximately 70% confluent. On the next day, the medium was replaced with Advanced RPMI 1640 (Gibco®) supplemented with 10% fetal bovine serum, 1% Penicillin and Streptomycin, and 30 µM retinoic acid (Sigma-Aldrich Chemistry, Steinheim, Germany). After seven days the typical podocyte morphology was observed.

We used the already established human immortal cell line (AB 8/13) described by Saleem et. al. as a reference cell line [3]. The human immortal cell line are expanded at 33°C, 5% CO2 on plastic. The cells were cultured in RPMI 1640 (Gibco®, life technologies, California) supplemented with 10% fetal bovine serum (Gibco®,) and 1% Penicillin and Streptomycin (Gibco®,). For further differentiation into podocytes, the cells were seeded on Corning® Collagen I (Merck, Darmstadt, Deutschland) coated plates. Both UM30-OSN and AB 8/13 were cultured in podocyte differentiation medium- Advanced RPMI 1640 (Gibco®) supplemented with 10% fetal bovine serum, 1% Penicillin and Streptomycin, and 30 µM retinoic acid (Sigma-Aldrich Chemistry, Steinheim, Germany) at 37 °C, 5% CO2 for approximately 14 days. The medium was changed every third day.

To investigate the effect of IFN-γ on UM30-OSN podocytes, we pre-treated them for 24 h with or without 1 µM Baricitinib (Medchemexpress #HY-15315) followed by an additional 24 h treatment of 100 ng/ml IFN-γ (Thermofisher #300-02-100UG).

RNA isolation

For RNA isolation from the various cell lines, the ZYMO Research Kit Direct-zol™ RNA Miniprep R20 was utilized following the manufacturer's protocol. Cells were detached by adding Tryple E and incubated for 5 min. Afterwards, a centrifuging step was added 4 mins 1000 g. Cell pellet was resuspend in 350 µl volume of 95–100% ethanol (EtOH) and thoroughly mixed by pipetting. The resulting solution was transferred to a Zymo-Spin™ column and centrifuged at 12,000 g for 30 seconds at 4 °C. To degrade genomic DNA, the column was washed with RNA Wash Buffer and centrifuged again at 12,000 g for 30 seconds at 4 °C. Subsequently, the column was treated with DNA digestion mix (1:16 dilution of DNase I in DNA Digestion Buffer) for 15 minutes. Following digestion, the column was rinsed twice with RNA

bioRxiv preprint doi: https://doi.org/10.1101/2025.07.28.667124; this version posted July 29, 2025. The copyright holder for this preprint (which was not certified by peer review) is the author/funder, who has granted bioRxiv a license to display the preprint in perpetuity. It is made available under aCC-BY-NC 4.0 International license.

Prewash Buffer, each followed by centrifugation at 12,000 g for 30 seconds at 4 °C. A final wash with RNA Wash Buffer was performed, including a 2-minute centrifugation step. After drying the column by centrifuging for 1 minute, it was transferred to a fresh RNase-free Eppendorf tube. RNA was eluted by adding 35 µL of DNase/RNase-free water to the column and centrifuging for 1 minute at 16,000 g. The eluted RNA samples were immediately placed on ice, and concentrations measured with a Nanodrop device.

Relative Quantification of podocyte-associated gene expression by real-time PCR

This followed our previously published protocols[2,28,29]. In brief, Quantitative real-time PCR of podocyte-associated gene expression was performed as follows:
Samples were run in triplicate on a 384-well reaction plate and Power Sybr Green PCR Master Mix (Applied Biosystems, Foster City, CA, USA) using Step One Plus Real-Time PCR systems. The amplification conditions were denaturation at 95 °C for 13 min followed by 37 cycles of 95 °C for 50 s, 60 °C for 45 s, and 72 °C for 30 s. Primer sequences are listed in supplemental table S2. Results were analyzed by the $2^{-\Delta\Delta\text{-CT}}$ method and specified in the fold change expression.

FACS

UM30-OSN cells were washed with PBS and incubated for approximately 5 min at 37 °C, 5% CO2 in 0.25% Trypsin EDTA. The reaction was stopped with 1:2 DMEM and the cell suspension was transferred to a 15 ml Falcon. This was followed by centrifugation at 1000x g for 4 min. The resulting cell pellet was resuspended with 1 – 2 ml 3% BSA and was blocked for 20 min. at room temperature. Cells were then separated using a 0.4 µM mesh strainer (Thermo Fisher Scientific, Massachusetts, USA) and placed in FACS tubes (Corning, New York, USA,). Afterward 3 ml of MACS buffer (0.5 % BSA, 2 mM EDTA, PBS) were added to each tube followed by an additional centrifugation step. The cells were resuspended at up to $1x10^7$ cells / ml in 4% PFA (Polysciences, Warrington, FL, USA) and incubated for 20 min at room temperature. Followed by two washing steps with PBS. After each washing step the cells were centrifuged at 1000x g for 10 min. Afterwards the cells were diluted in 98 µl MACS Buffer and 2 µl of the primary antibody CD133 (Thermo Fisher Scientific, Massachusetts, USA), CD24 (Thermo Fisher Scientific, Massachusetts, USA) and SIX2 (Abnova, Heidelberg, Germany). The antibody was incubated overnight at 4 °C. Cells were washed by adding 1 – 2 ml MACS Buffer and centrifuged at 1000x g for 10 min. The supernatant was completely aspirated followed by 1 h incubation of the secondary antibodies at room temperature in the dark. 0.2 µl of the secondary antibody Alexa 555 and 647 (Thermo Fisher Scientific, Massachusetts, USA)

bioRxiv preprint doi: https://doi.org/10.1101/2025.07.28.667124; this version posted July 29, 2025. The copyright holder for this preprint (which was not certified by peer review) is the author/funder, who has granted bioRxiv a license to display the preprint in perpetuity. It is made available under aCC-BY-NC 4.0 International license.

was diluted in 100 µl MACS Buffer for each tube. The cells were washed once with 0.05% Tween-20 diluted in PBS. The cell pellets were then resuspended in a suitable amount of MACS Buffer Measurement of fluorescence intensity was demonstrated using Beckman Gallios Flow Cytometer (Beckman Coulter). In each case, 30,000 cells were measured, and data were analyzed using FlowJo software (BD Biosciences). Detailed information on the antibodies used can be found in supplementary table 1.

Immunofluorescence-based staining

For the immunocytochemistry, urine-derived cells were fixed with 4% paraformaldehyde (PFA) (Polysciences, Warrington, FL, USA). Followed by three wash steps with PBS for 5 min each. To block unspecific binding sites, the fixed cells were incubated with a blocking buffer containing 10% normal goat or donkey serum, 1% BSA, and 0.5% Triton X-100. (Sigma-Aldrich Chemistry,) and 0.05% Tween-20 (Sigma-Aldrich Chemistry,) for 2 h at room temperature. The primary antibodies were diluted in blocking buffer according to supplemental table 1 and incubated at 4 °C overnight. The following day, the cells were washed once with 0.05% Tween-20 diluted in PBS and two times with PBS only. After washing them, the fluorochrome-conjugated secondary antibody and HOECHST (1:5000) (Thermo Fisher Scientific, Waltham, MA, USA), were added and incubated for 1 h at room temperature protected from light. The secondary antibodies were diluted in blocking buffer according to supplemental table 1. Visualization of cells employed a fluorescence microscope (LSM700).

Western Blot Analysis

Podocytes were lysed in RIPA buffer (Sigma-Aldrich Chemistry) containing 5 M NaCl, 1% NP-40, 0.5% DOC, 0.1% SDS, 1 mM EDTA, 50 mM Tris, pH 8.0, and freshly added 10 µL/mL protease- and phosphatase inhibitor (Sigma-Aldrich). 20 µg of each obtained protein lysate was dissolved in a 10% sodium dodecyl sulfate PAGE gel and transferred to an Immobilon-P membrane (Merck Millipore, Burlington, VT, USA). The membranes were incubated with the primary antibody overnight at 4 °C. Then washed three times with 0.1% Tween-20 in Tris-buffered saline followed by 1 h incubation of the secondary antibodies at room temperature. For visualization of the blotted proteins the Pierce™ ECL Western Blotting Substrate solutions from Thermo Fisher were used (Thermo Fisher Scientific, Massachusetts, USA).
were used. Both solutions were diluted 1:1. Quantification was carried out with ImageJ. Detailed information on the antibodies used can be found in the supplementary table 1.

Microarrayrray and bulk NGS analysis

For the microarray and NGS experiments, 1 µg RNA preparations were hybridized on the Human Clariom S Gene Expression Array (Affymetrix, Thermo Fisher Scientific, Waltham, MA,

bioRxiv preprint doi: https://doi.org/10.1101/2025.07.28.667124; this version posted July 29, 2025. The copyright holder for this preprint (which was not certified by peer review) is the author/funder, who has granted bioRxiv a license to display the preprint in perpetuity. It is made available under aCC-BY-NC 4.0 International license.

USA) and were used for a 3'RNA-Seq assay on an Illumina NextSeq2000 sequencing system at the core facility Biomedizinisches Forschungszentrum (BMFZ) of Heinrich Heine University- Düsseldorf.

The fastq files containing the RNA-seq raw data were aligned against the GRCh38 genome via the software HISAT2 [30] using the parametrization suggested by Barruzzo et al. [31]: hisat2 -p 7 -N 1 -L 20 -i S,1,0.5 -D 25 -R 5 --mp 1,0 --sp 3,0 -x hisatindex/grch38_r109 -U input.fastq.gz -S output.sam. The resulting BAM files were sorted using the SAMtools software [32] and the reads were condensed to counts per gene with the subread (1.6.1) featurecounts routine [33] using the ENSEMBL annotation file Homo_sapiens.GRCh38.109.gtf. The resulting table of counts per gene were imported into the R/Bioconductor [34] and normalized with the voom [35] algorithm from the limma package [36] filtering expressed genes (counts per million > 1 in at least one sample). Affymetrix raw data was normalized via the Robust Multi-array Average (RMA) method from the R/Bioconductor package oligo [37]. Gene expression heatmaps were generated using the heatmap.2 function from the gplots package [38] employing Pearson correlation or Euclidean distance as distance measures . Gene expression was dissected in Venn diagrams drawn with the Venn Diagram package [39] . Genes were considered expressed when their detection-p-value, calculated as described before [40], was less than 0.05 in microarrays or when there was more than 1 read in NGS data. The subsets of genes obtained from the Venn diagram analysis were analyzed for over-representation of gene ontologies (GOs) using the GOstats R package [41] and KEGG (Kyoto Encyclopedia of Genes and Genomes) pathways [42]. The n=60 most significant pathways and GO terms ($p < 0.05$) were visualized via the R package ggplot2 [43] in dotplots indicating p-value, number and ratio of involved genes. Gene expression data will be available online in the National Centre of Biotechnology Information (NCBI) Gene Expression Omnibus.

Ethical Statement

In this study, urine samples were collected with the informed consent of the donors and the written approval (Ethical approval Number: 2017-2457_3) of the ethical review board of the medical faculty of Heinrich Heine University, Düsseldorf, Germany. All methods were carried out in accordance with the approved guidelines. The medical faculty of Heinrich Heine University approved all experimental protocols. All patients provided written informed consent.

Statistics

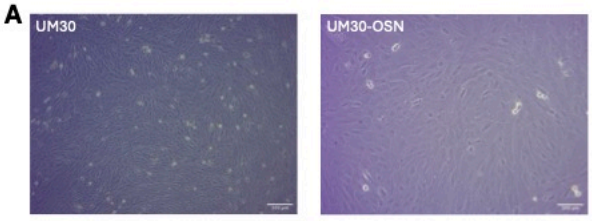
All samples were analyzed in triplicate. The mean value of these was used for the calculations. The statistical significance was calculated using the two-sample Student's *t*-test with a significance threshold $p = 0.05$. Data regarding the Baricitinib and IFN-γ treatment were

bioRxiv preprint doi: https://doi.org/10.1101/2025.07.28.667124; this version posted July 29, 2025. The copyright holder for this preprint (which was not certified by peer review) is the author/funder, who has granted bioRxiv a license to display the preprint in perpetuity. It is made available under aCC-BY-NC 4.0 International license.

298 analyzed using one-way ANOVA to assess statistical significance between groups. A p-value
299 of < 0.05 was considered statistically significant. All experiments were analyzed n=3.
300
301 **Results**
302 **Successful immortalization of UM30-OSN**
303 UM30-OSN cells were isolated directly from the urine of a 30-year-old West African male as
304 described in Rahman et. al. [25]. The cells were transfected with the episomal-based plasmids
305 pEP4EO2SCK2MEN2L and pEP4EO2SET2K as in our previous iPSC lab resource
306 publications [27,44] (Supplementary Figure S2).The vectors express SV40 and the
307 reprogramming factors- OCT4, NANOG, c-MYC, KLF4 and SOX2. The immortalized cells are
308 referred to as UM30-OSN, characterized by rapid proliferation than the primary UdRPCs, no
309 morphological changes and full retention of the SIX2-positive mesenchymal progenitor cell
310 characteristics. The proliferating cells were maintained for over a year without apparent
311 morphological changes (Figure 1A). Because immortalization is associated with chromosomal
312 alterations and genomic instabilities [45], we comparatively analysed the karyotype of UM30-
313 OSN and the immortal podocyte cell line- AB 8/13 at the Institute of Human Genetics of the
314 University Hospital Düsseldorf (Supplementary Figure S3).
315 The primary cells-UM30 and the immortalized counterpart- UM30-OSN cell line grow as
316 monolayers with typical rice grain morphologies (Figure 1A).
317 The absence of plasmids used in partial reprogramming was confirmed by
318 immunofluorescence staining, quantitative real-time PCR, heatmap displayed the expression
319 levels of OCT4, SOX2, NANOG and semi-quantitative PCR (Figure 1B). For comparison, an
320 in-house induced pluripotent stem cell line (iPSC) UM51 iPSC was used as a control cell line
321 to demonstrate that UM30-OSN is not pluripotent (Figure 1B), quantitative real-time PCR
322 results (Figure 1C) and a heatmap of *OCT4, SOX2, NANOG, CDH1* and *VIM* (Figure 1D). For
323 the semi-quantitative PCR, primers were designed, which amplified the exogenous OCT4
324 (Figure 1E).
325 Similar to the stable established cell line UM51 iPSC, the UM30-OSN cell line did not show a
326 comparable band to the positive plasmid controls at 657 bp.
327 The immunocytochemistry-based expression detection was negative for OCT4, SOX2 and
328 NANOG compared to the UM51 iPSC cell line (Figure 1B), therefore confirming the absence
329 of the plasmids and therefore partial and not fully reprogrammed (Figure 1C). After the
330 successful immortalization of UM30-OSN, we performed a comparative transcriptome
331 analysis. Hierarchical clustering analysis comparing the transcriptomes of urine-derived renal
332 progenitor UM30, the immortalized UM30-OSN cell line, and UM51 iPSC (Figure 1F). The
333 UM50 iPSC cell line [27] serves as a direct comparison between a fully reprogrammed iPSC
334 and the partially reprogrammed UM30-OSN. The correlation table indicates a positive

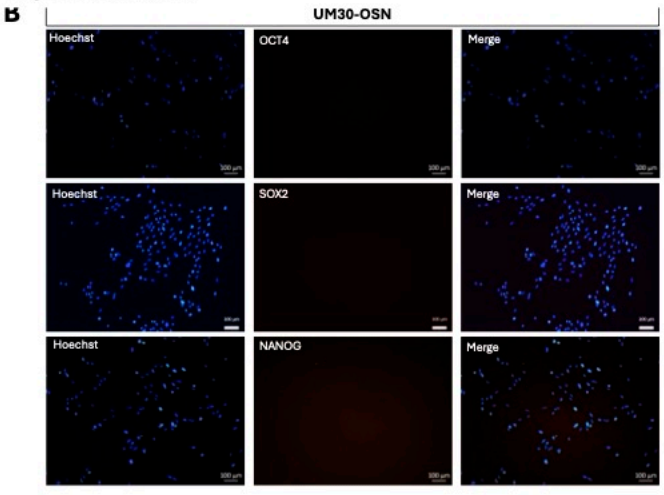
bioRxiv preprint doi: https://doi.org/10.1101/2025.07.28.667124; this version posted July 29, 2025. The copyright holder for this preprint (which was not certified by peer review) is the author/funder, who has granted bioRxiv a license to display the preprint in perpetuity. It is made available under aCC-BY-NC 4.0 International license.

335 relationship between UM30 and UM30-OSN (R^2 = 0.90), which confirms the origin of the
336 UM30-OSN (Figure 1G). The correlation co-efficient between UM30, UM30-OSN and UM51
337 iPSC is 0.85 (Figure 1G).
338
339 Additionally, a Venn diagram-based transcriptome comparison was carried out between
340 UM30-OSN, UdRPC UM30 and UM51 iPSC (Figure 1H). A total 12904 genes were expressed
341 in common expressed in all cell lines. Comparing the expressed genes (det-p < 0.05), 154
342 genes are exclusively expressed in UdRPC UM30, 153 genes in UM30-OSN and 307 genes
343 in the UM51 iPSC (Figure 1H). Figure 1 represents a metascape analysis of the 80 genes only
344 expressed in the UM51 iPSC and the UdRPC UM30, with GO:BP terms and pathways related
345 to e.g. diencephalon development, regulation of body fluid levels and metal ion transport. The
346 exclusive GO:BP terms and pathways related to the 123 genes exclusively expressed in the
347 UM51 iPSC and UM30-OSN are e.g. cell morphogenesis, positive regulation of cell
348 development and cell junction organization.
349 The full gene list of GOs and associated genes are in Supplementary table S4A.



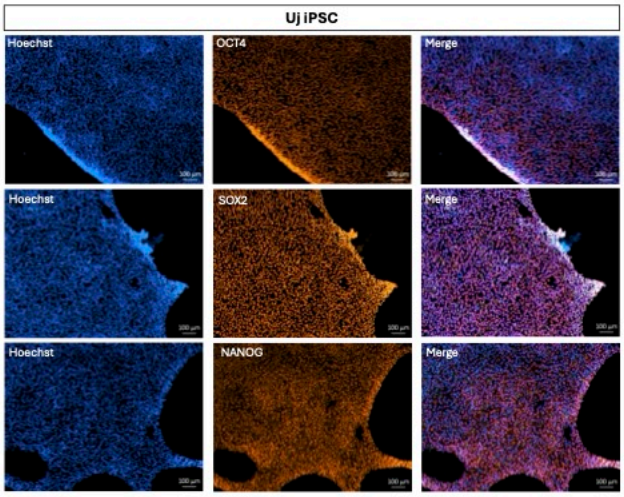
350

Figure 1. continued



351

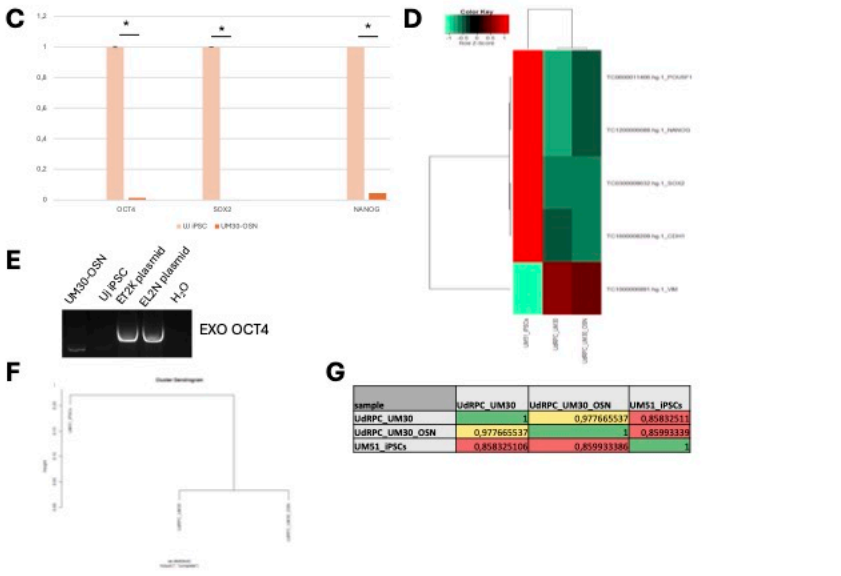
bioRxiv preprint doi: https://doi.org/10.1101/2025.07.28.667124; this version posted July 29, 2025. The copyright holder for this preprint (which was not certified by peer review) is the author/funder, who has granted bioRxiv a license to display the preprint in perpetuity. It is made available under aCC-BY-NC 4.0 International license.



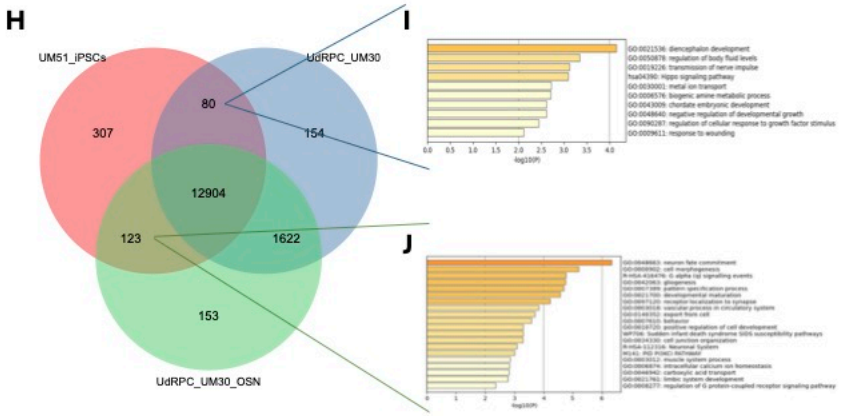
352
353

Figure 1. continued

bioRxiv preprint doi: https://doi.org/10.1101/2025.07.28.667124; this version posted July 29, 2025. The copyright holder for this preprint (which was not certified by peer review) is the author/funder, who has granted bioRxiv a license to display the preprint in perpetuity. It is made available under aCC-BY-NC 4.0 International license.



354



355

356

357 **Figure 1: Successful immortalized UM30-OSN cell line derived from human urine.**

358 **(A)** The UM30-OSN cell line was partially reprogrammed using episomal plasmids encoding the Yamanaka factors. Light
359 microscopy revealed morphological changes typical of early reprogramming stages.
360 **(B)** The absence of full pluripotency was confirmed by immunofluorescence staining for OCT4, SOX2, and NANOG (scale bars:
361 100 µm).
362 **(C)** qPCR analysis further validated the lack of expression of these pluripotency markers.
363 **(D)** A heatmap displayed the expression levels of OCT4, SOX2, NANOG, E-CAD, and VIM, comparing UM30-OSN to a

bioRxiv preprint doi: https://doi.org/10.1101/2025.07.28.667124; this version posted July 29, 2025. The copyright holder for this preprint (which was not certified by peer review) is the author/funder, who has granted bioRxiv a license to display the preprint in perpetuity. It is made available under aCC-BY-NC 4.0 International license.

laboratory-derived induced pluripotent stem cell line (UM51-iPSC) used as a reference. **(E)** The absence of episomal plasmids was confirmed by semi-quantitative PCR targeting exogenous sequences. **(F–G)** A cluster dendrogram and correlation matrix demonstrated the transcriptional relationship between UM51-iPSC, UdRPC-UM30, and UM30-OSN**. (H)** Venn diagram-based transcriptome comparison was carried out between UM30-OSN, UdRPC UM30 and UM51 iPSC. **(I)** Metascape analysis of the 80 genes common expressed in the UM51 iPSC and UdRPC-UM30**. (J)** Metascape analysis carried out with the 123 genes exclusively expressed in the UM51-iPSC and UM30-OSN.

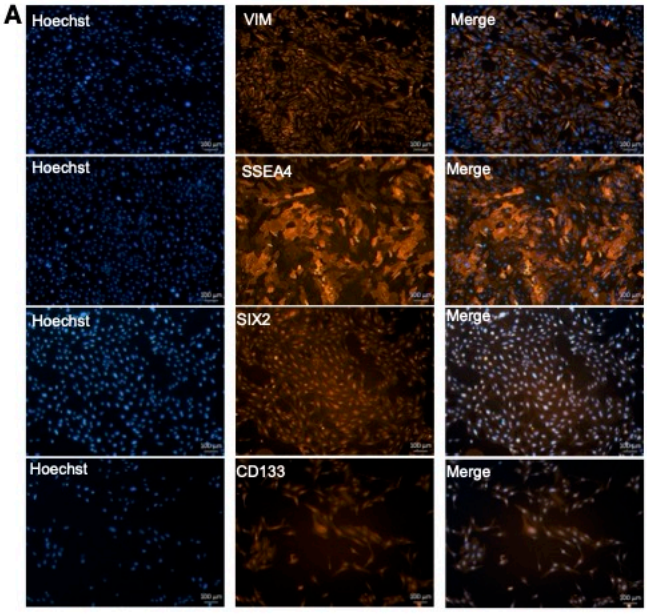
Characterization UM30-OSN

To determine the renal origin of UM30-OSN and thus its differentiation capacity, we performed immunofluorescence-based detection of the proteins, SSEA4 as a pluripotency marker, Vimentin as a cytoskeletal protein of mesenchymal cells, CD133 (Prominin-1) as a stem cell self-renewal marker and SIX2 as a multipotent self-renewing renal progenitor marker (Figure 2A).

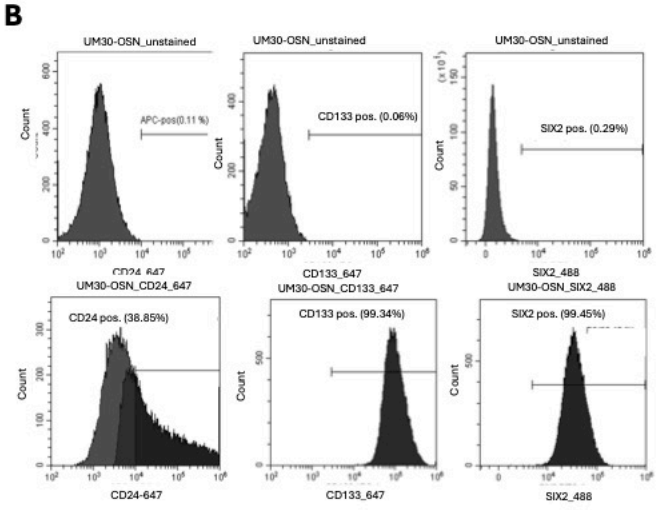
To further confirm stemness, fluorescence-activated cell analysis (FACS) was also performed (Figure 2B) and this revealed that approximately 99.45% of the cells express SIX2, CD133 (99.34%) and the renal progenitor cell surface marker CD24 (38.85%).

Immortalized cell lines are characterized by a high proliferation rate, which can be analyzed not only morphologically but also at the cellular level. Based on this, we comparatively analyzed the expression of the cell cycle-associated genes- *P53, P21, KI67, PCNA*, and *TERT* in UM30-OSN and UM30. UM30-OSN showed a significantly higher expression of *PCNA* (2.9-fold), *KI67* (2.0-fold), hTERT (1.77-fold), whilst the expression of P53 and P21 were downregulated by 0.44-fold and 0.11-fold respectively (Figure 2C).

bioRxiv preprint doi: https://doi.org/10.1101/2025.07.28.667124; this version posted July 29, 2025. The copyright holder for this preprint (which was not certified by peer review) is the author/funder, who has granted bioRxiv a license to display the preprint in perpetuity. It is made available under aCC-BY-NC 4.0 International license.



386



387

388 **Figure 2.** continued

389

390

bioRxiv preprint doi: https://doi.org/10.1101/2025.07.28.667124; this version posted July 29, 2025. The copyright holder for this preprint (which was not certified by peer review) is the author/funder, who has granted bioRxiv a license to display the preprint in perpetuity. It is made available under aCC-BY-NC 4.0 International license.

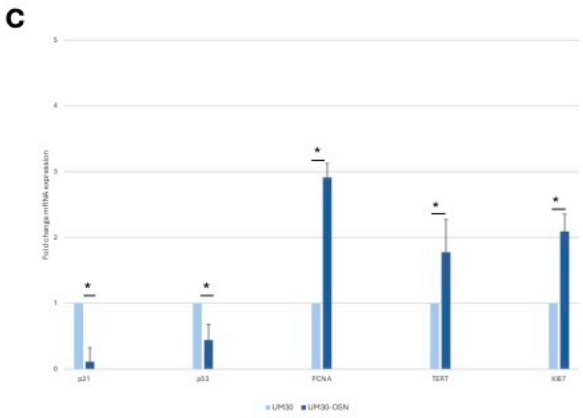


Figure 2: Characterization of immortalized UM30-OSN cell line.
(A) The renal progenitor origin of the urine-derived UM30-OSN cell line was confirmed by immunocytochemistry for the renal stem cell markers SIX2 and CD133, the mesenchymal marker Vimentin, and the pluripotency marker SSEA4. **(B)** Flow cytometry (FACS) further validated the expression of SIX2, CD24, and CD133. **(C)** Quantitative real-time PCR was used to assess the expression of cell cycle-related genes, including p21, p53, hTERT, PCNA, and KI67. Gene expression levels were normalized to the housekeeping gene glycerinaldehyd-3-phosphat-Ddehydrogenase (GAPDH).

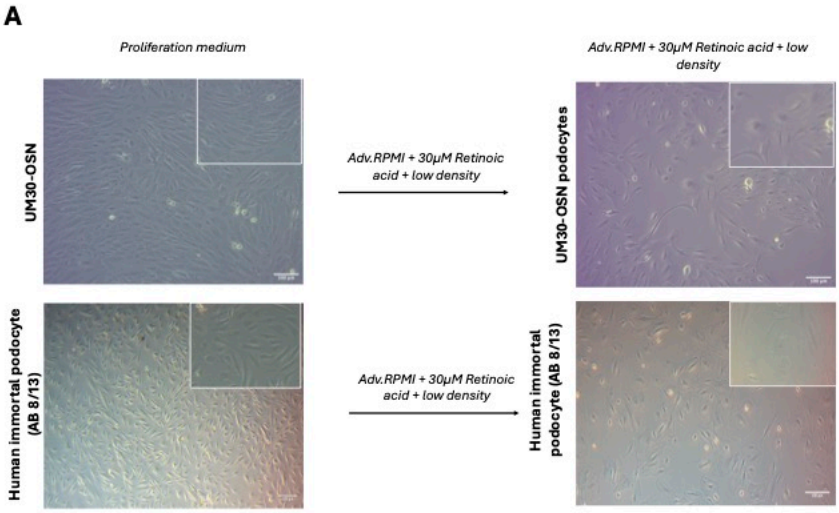
Differentiation potential of UM30-OSN into human podocytes

UM30-OSN were differentiated into podocytes following our previously published protocols [28,29] (Figure 3A). The human immortal podocyte (AB 8/13) cell line was used for comparison and benchmarking [3]. Characterization and assessment of successful differentiation were demonstrated by immunocytochemistry, quantitative real-time PCR, and Western blotting (Figure 3B-D). Expression of podocyte markers NPHS1, NPHS2 and SYNPO were detected only upon podocyte differentiation of UM30-OSN.

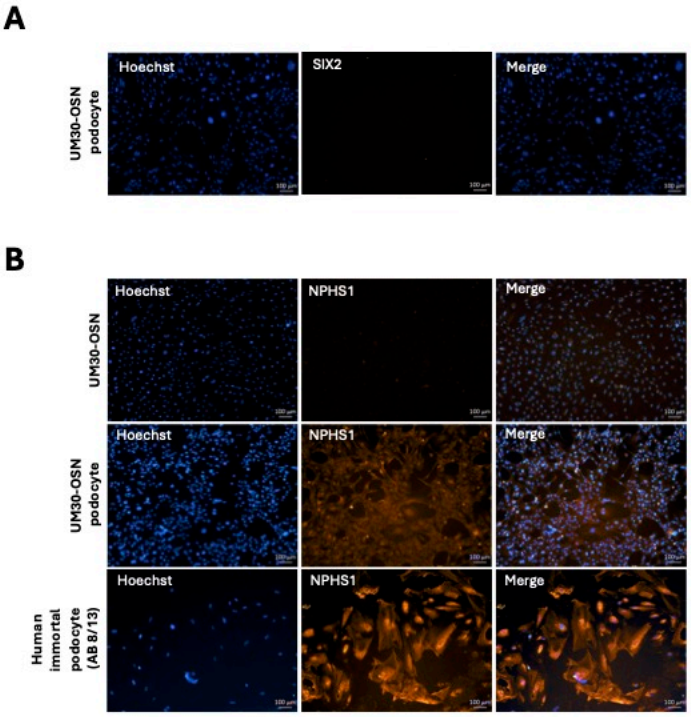
On the mRNA level, UM30-OSN podocytes show increased expression of the podocyte markers *NPHS1* (34.11 fold), *NPHS2* (4.19 fold), *CD2AP* (2.59 fold) and *SYNPO* (1.17 fold) compared to the undifferentiated UM30-OSN (Figure 3C).

Elevated mRNA expression of the podocyte markers *NPHS1* (3.37 fold), *NPHS2* (4.44 fold), *CD2AP* (0.90 fold) and *SYNPO* (1.10 fold) was also demonstrated in the immortal podocytes (AB 8/13) cultured at 37C compared cells cultured at 33C (Figure 3C). These results corroborate the protein-based analyses (Figure 3D). The housekeeping protein Glyceraldehyde -3-phosphate-dehydrogenase (GAPDH) served as loading control.

bioRxiv preprint doi: https://doi.org/10.1101/2025.07.28.667124; this version posted July 29, 2025. The copyright holder for this preprint (which was not certified by peer review) is the author/funder, who has granted bioRxiv a license to display the preprint in perpetuity. It is made available under aCC-BY-NC 4.0 International license.



415



416

Figure 3. continued

bioRxiv preprint doi: https://doi.org/10.1101/2025.07.28.667124; this version posted July 29, 2025. The copyright holder for this preprint (which was not certified by peer review) is the author/funder, who has granted bioRxiv a license to display the preprint in perpetuity. It is made available under aCC-BY-NC 4.0 International license.

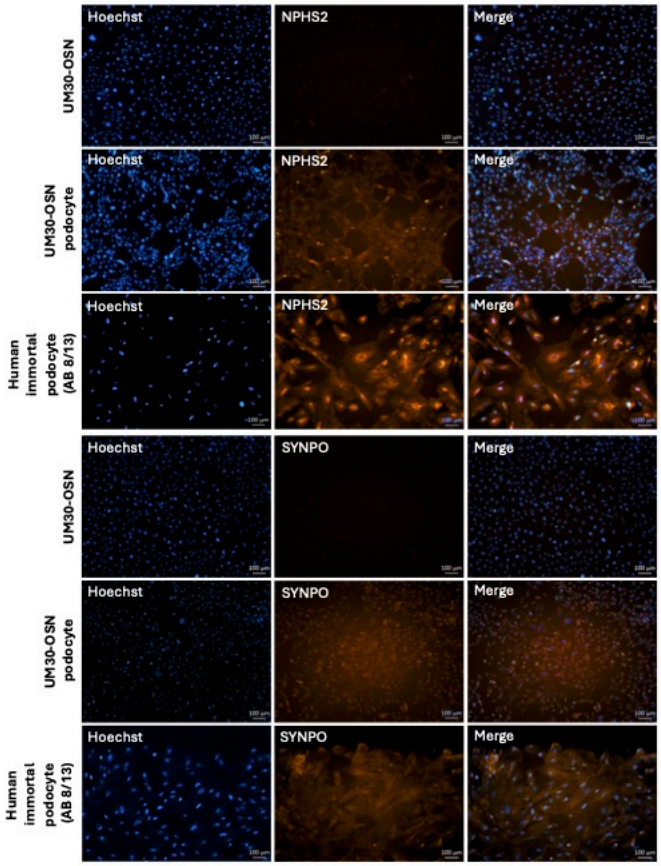


Figure 3. continued

bioRxiv preprint doi: https://doi.org/10.1101/2025.07.28.667124; this version posted July 29, 2025. The copyright holder for this preprint (which was not certified by peer review) is the author/funder, who has granted bioRxiv a license to display the preprint in perpetuity. It is made available under aCC-BY-NC 4.0 International license.

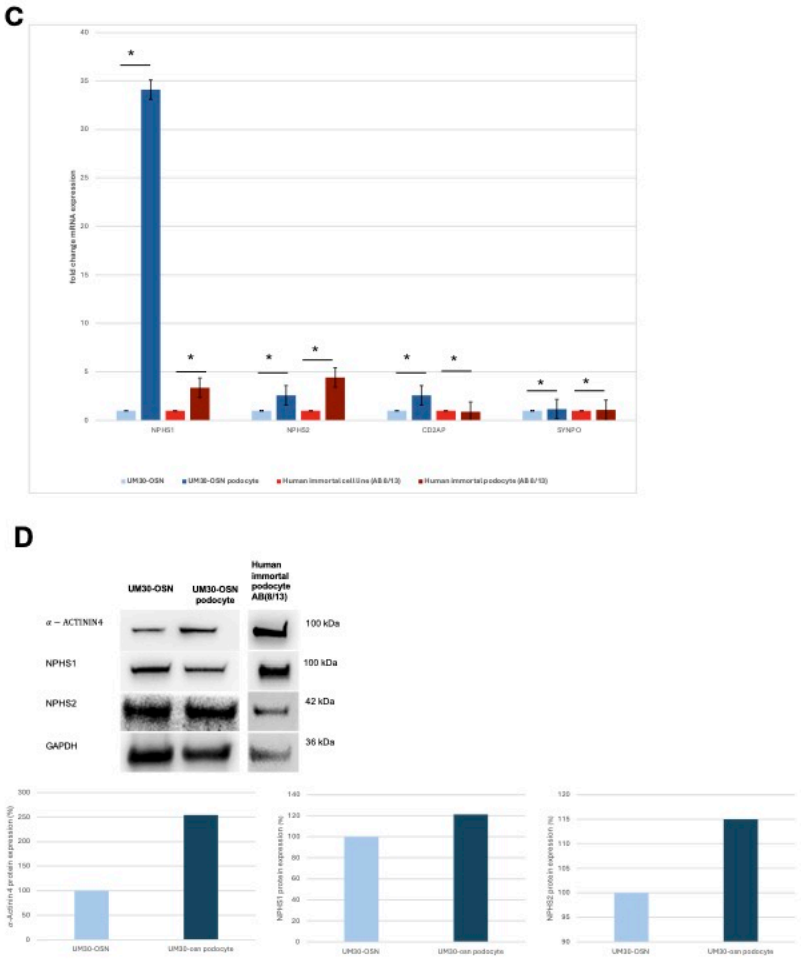


Figure 3: Culturing UM30-OSN Cells in advanced RPMI + RA induces podocyte differentiation. **(A)** UM30-OSN cells and human immortalized podocytes (AB8/13) were cultured in advanced RPMI medium supplemented with 30 µM retinoic acid (RA) to promote differentiation into mature podocytes. Light microscopy revealed the characteristic "fried egg" morphology. **(B)** Immunofluorescence staining confirmed the expression of podocyte-specific markers, including NPHS1, NPHS2 and α-ACTININ4 (scale bars: 100 µm). **(C)** Quantitative real-time PCR and **(D)** Western blot analysis further validated marker gene expression. GAPDH served as the internal control for normalization.

bioRxiv preprint doi: https://doi.org/10.1101/2025.07.28.667124; this version posted July 29, 2025. The copyright holder for this preprint (which was not certified by peer review) is the author/funder, who has granted bioRxiv a license to display the preprint in perpetuity. It is made available under aCC-BY-NC 4.0 International license.

Comparative transcriptome and Gene Ontology analysis of podocytes differentiated from UM30, UM30-OSN and the immortal AB 8/13 cell line.

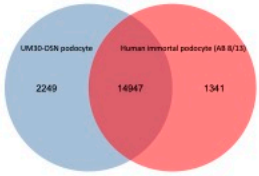
Hierarchical cluster analysis was carried out to compare similarities between their transcriptomes (Figure 4A, 4B). The correlation table shows a higher correlation co-efficient between UM30 and UM30-OSN podocytes as expected (R^2 = 0.94). However, this value drops to 0.88 when comparing UM30 and AB 8/13 podocytes (Figure 4B). Additionally, a Venn diagram-based transcriptome comparison was carried out between UM30-OSN and AB 8/13 podocytes (Figure 4C). A total of 14947 genes were detected as expressed in common expressed in both podocyte lines (Figure 4C). Comparing the expressed genes (det-p < 0.05), 1341 genes are exclusively expressed in AB 8/13 podocytes and 2249 genes in UM30-OSN podocytes (Figure 4C).

The common GO:BP terms and pathways related to the 14947 genes expressed in both podocyte cell lines are associated with cell division, cell cycle and cellular senescence (Figure 4D-E). The entire GO BP-terms and KEGG pathway is presented in Supplemental Table S3 and S5. Metascape analysis related to the 1341 genes exclusively expressed in the human immortal pododcyte line (AB 8/13) are e.g. mesenchymal development, calcium signaling and neuronal system. In parallel the exclusive GO:BP terms and pathways of the UM30-OSN podocytes related to the 2249 genes are e.g. regulation of membrane potential, synapse organization, cell-cell-adhesion and synaptic membrane adhesion. The full gene list can be found in Supplementary Table S4B.

A



C



B

sample	Human immortal podocyte (AB 8/13)	UM30-OSN podocyte	UM30 podocyte
Human immortal podocyte (AB 8/13)	1	0,881970953	0,888595999
UM30-OSN podocyte	0,881970953	1	0,941835589
UM30 podocyte	0,888595999	0,941835589	1

Figure 4. continued

bioRxiv preprint doi: https://doi.org/10.1101/2025.07.28.667124; this version posted July 29, 2025. The copyright holder for this preprint (which was not certified by peer review) is the author/funder, who has granted bioRxiv a license to display the preprint in perpetuity. It is made available under aCC-BY-NC 4.0 International license.

D

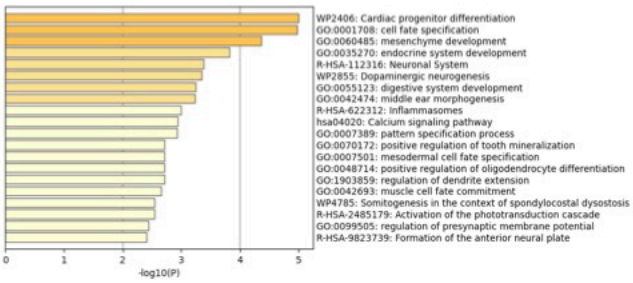
GOID	BP-Term	Pvalue
GO:0033036	*macromolecule localization*	5,97996E-82
GO:0006725	*cellular aromatic compound metabolic process*	1,31947E-74
GO:0071840	*cellular component organization or biogenesis*	2,9107E-72
GO:0034654	*nucleobase-containing compound biosynthetic process*	7,90636E-70
GO:1901360	*organic cyclic compound metabolic process*	1,48744E-69
GO:0006996	*organelle organization*	9,57561E-51
GO:0044085	*cellular component biogenesis*	1,95608E-45
GO:0043933	*protein-containing complex organization*	1,47907E-39
GO:0043687	*post-translational protein modification*	4,48241E-37
GO:0051234	*establishment of localization*	1,37372E-33
GO:0051301	*cell division*	2,92061E-32
GO:0051173	*positive regulation of nitrogen compound metabolic process*	3,11463E-31
GO:0031325	*positive regulation of cellular metabolic process*	1,07077E-29
GO:0043043	*peptide biosynthetic process*	3,98891E-28
GO:0090304	*nucleic acid metabolic process*	2,48169E-26
GO:0051128	*regulation of cellular component organization*	1,05876E-25
GO:0007049	*cell cycle*	1,27959E-25
GO:0051254	*positive regulation of RNA metabolic process*	2,44866E-25
GO:0019637	*organophosphate metabolic process*	2,81412E-25

E

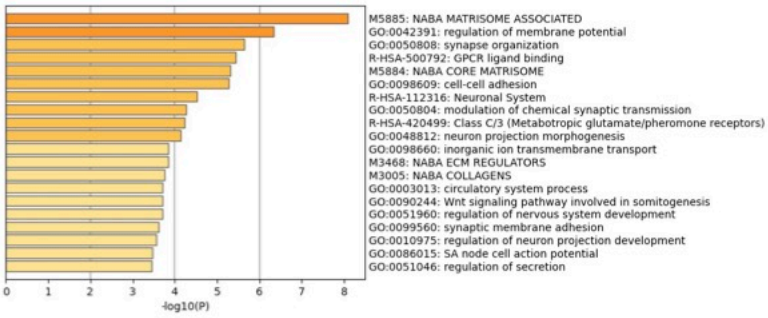
KeggID	Kegg name	p_hyper
hsa05168	*Herpes simplex virus 1 infection - Homo sapiens (human)*	3,4906E-23
hsa04120	*Ubiquitin mediated proteolysis - Homo sapiens (human)*	4,0855E-19
hsa04141	*Protein processing in endoplasmic reticulum - Homo sapiens (human)*	6,2256E-17
hsa04144	*Endocytosis - Homo sapiens (human)*	6,9096E-17
hsa04110	*Cell cycle - Homo sapiens (human)*	1,6022E-15
hsa05132	*Salmonella infection - Homo sapiens (human)*	6,402E-15
hsa04140	*Autophagy - animal - Homo sapiens (human)*	1,0985E-13
hsa01100	*Metabolic pathways - Homo sapiens (human)*	2,2101E-13
hsa05210	*Colorectal cancer - Homo sapiens (human)*	2,4237E-13
hsa03013	*Nucleocytoplasmic transport - Homo sapiens (human)*	3,4272E-13
hsa04218	*Cellular senescence - Homo sapiens (human)*	3,748E-13

453

F



G



454
455
456 **Figure 4.** continued
457

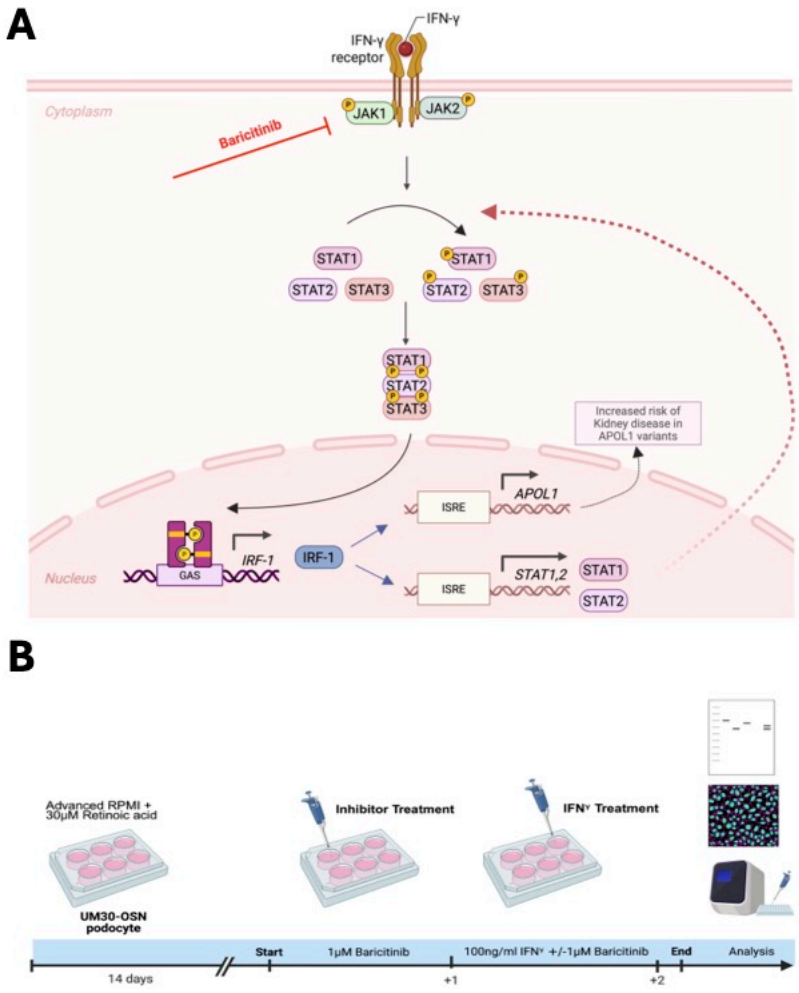
bioRxiv preprint doi: https://doi.org/10.1101/2025.07.28.667124; this version posted July 29, 2025. The copyright holder for this preprint (which was not certified by peer review) is the author/funder, who has granted bioRxiv a license to display the preprint in perpetuity. It is made available under aCC-BY-NC 4.0 International license.

Figure 4: Comparative transcriptome and Gene Ontology analysis of human podocyte cell lines.
(A) A cluster diagram between the human immortal podocytes (AB 8/13), urine-derived UM30 podocytes and the UM30-OSN-derived podocytes was performed. **(B)** The correlation table between the UM30-OSN and the immortal podocytes (AB 8/13) revealed a correlation coefficient of 0.88. **(C)** A Venn diagram was performed and shows 14947 common genes expressed in common between the two cell types. **(D-E)** The common GO BP-terms and KEGG pathways between the immortal podocytes (AB 8/13) and UM30-OSN podocytes are associated with cell cycle, cell division and cellular senescence. **(F)** Metascape analysis of the 1341 genes only expressed in the immortal podocytes (AB 8/13). **(G)** Shows the exclusively 2249 genes expressed only in the UM30-OSN podocytes by metascape analysis.

Modulation of APOL Gene Expression and Kidney Injury Markers by IFN-γ and Baricitinib in Human UM30-OSN Podocytes

Upon IFN-γ binding, the canonical signaling cascade is initiated via the JAK/STAT pathway, predominantly through activation of JAK1 and JAK2, which are linked to the intracellular domains of the IFN-γ receptor (Figure 5A). To investigate the effect of IFN-γ on the UM30-OSN podocytes, the cells were pre-treated with or without the JAK1/2 inhibitor -Baricitinib upon IFN-γ stimulation (Figure 5B). Baricitinib inhibited IFN-γ-induced morphological and molecular alterations in UM30-OSN podocytes. Treatment of UM30-OSN podocytes with 100 ng/ml IFN-γ for 24 hours led to a pronounced increase in rounded, detached cells compared to the untreated control, as observed by light microscopy. Co-treatment with Baricitinib significantly reduced the number of detached cells, resulting in a morphology comparable to that of control cells (Figure 5C). To assess the molecular response to IFN-γ and its modulation by Baricitinib, we analyzed the expression of IFN-γ-responsive genes- APOL1, MAPK8, STAT3 and kidney injury markers Cycs, IL-6, NGAL, CLU, Caspase-1, TGF-β and Gasdermin D using quantitative real-time PCR (Figure 5D). IFN-γ treatment significantly upregulated several of these genes including APOL1, whereas co-treatment with Baricitinib largely attenuated this induction, restoring expression levels closer to those of the control. Western blot analysis confirmed the transcriptional findings at the protein level. IFN-γ induced phosphorylation of STAT1 (p-STAT1) thus leading to activated expression of APOL1 and down-regulation of the podocyte marker- α-ACTININ4. Baricitinib co-treatment reversed these effects, preserving α-ACTININ4 expression and reducing APOL1 and p-STAT1 to near-baseline levels (Figure 5E). Immunofluorescence staining for fibrosis-associated proteins Fibronectin, α-SMA, and Vimentin further supported the deleterious effects of IFN-γ. All three markers were upregulated following IFN-γ treatment, thus indicating a shift towards a pro-fibrotic phenotype. This effect was absent in control and Baricitinib-treated cells, suggesting a protective role of Baricitinib against IFN-γ-induced fibrosis (Figure 5F).

bioRxiv preprint doi: https://doi.org/10.1101/2025.07.28.667124; this version posted July 29, 2025. The copyright holder for this preprint (which was not certified by peer review) is the author/funder, who has granted bioRxiv a license to display the preprint in perpetuity. It is made available under aCC-BY-NC 4.0 International license.



493

494 **Figure 5.** continued

bioRxiv preprint doi: https://doi.org/10.1101/2025.07.28.667124; this version posted July 29, 2025. The copyright holder for this preprint (which was not certified by peer review) is the author/funder, who has granted bioRxiv a license to display the preprint in perpetuity. It is made available under aCC-BY-NC 4.0 International license.

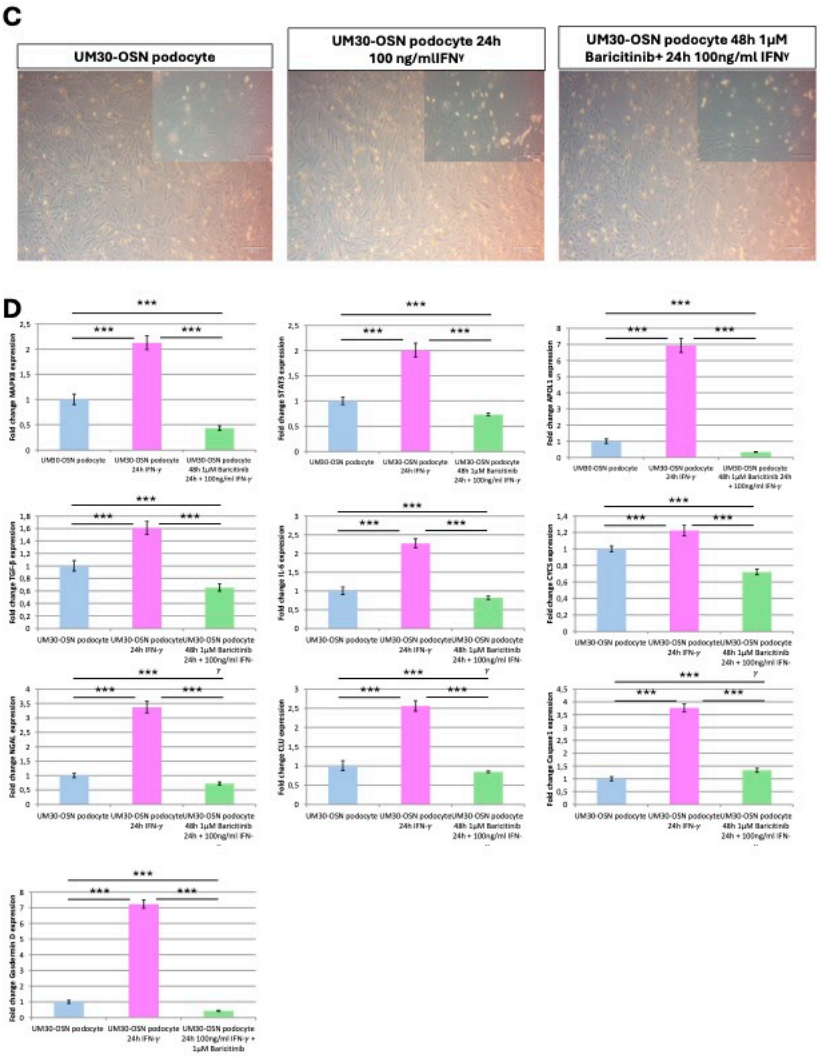
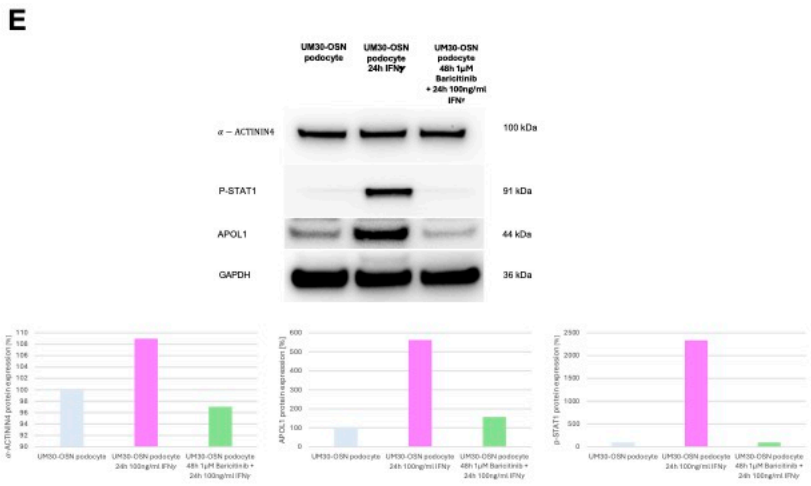
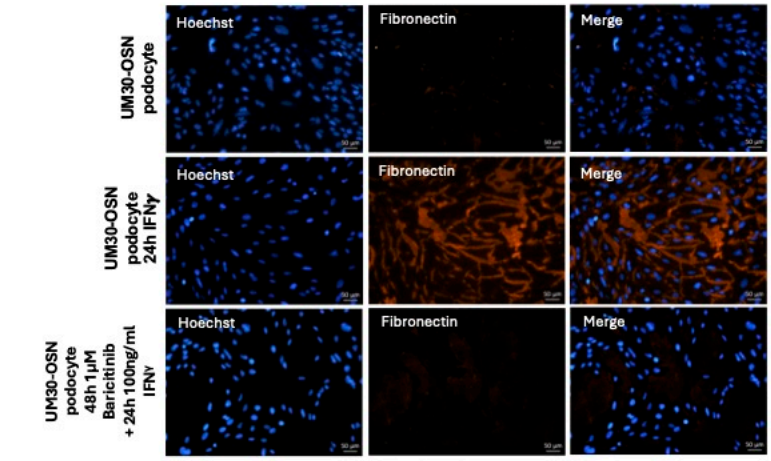


Figure 5. continued

bioRxiv preprint doi: https://doi.org/10.1101/2025.07.28.667124; this version posted July 29, 2025. The copyright holder for this preprint (which was not certified by peer review) is the author/funder, who has granted bioRxiv a license to display the preprint in perpetuity. It is made available under aCC-BY-NC 4.0 International license.



499



500
501

Figure 5. continued

bioRxiv preprint doi: https://doi.org/10.1101/2025.07.28.667124; this version posted July 29, 2025. The copyright holder for this preprint (which was not certified by peer review) is the author/funder, who has granted bioRxiv a license to display the preprint in perpetuity. It is made available under aCC-BY-NC 4.0 International license.

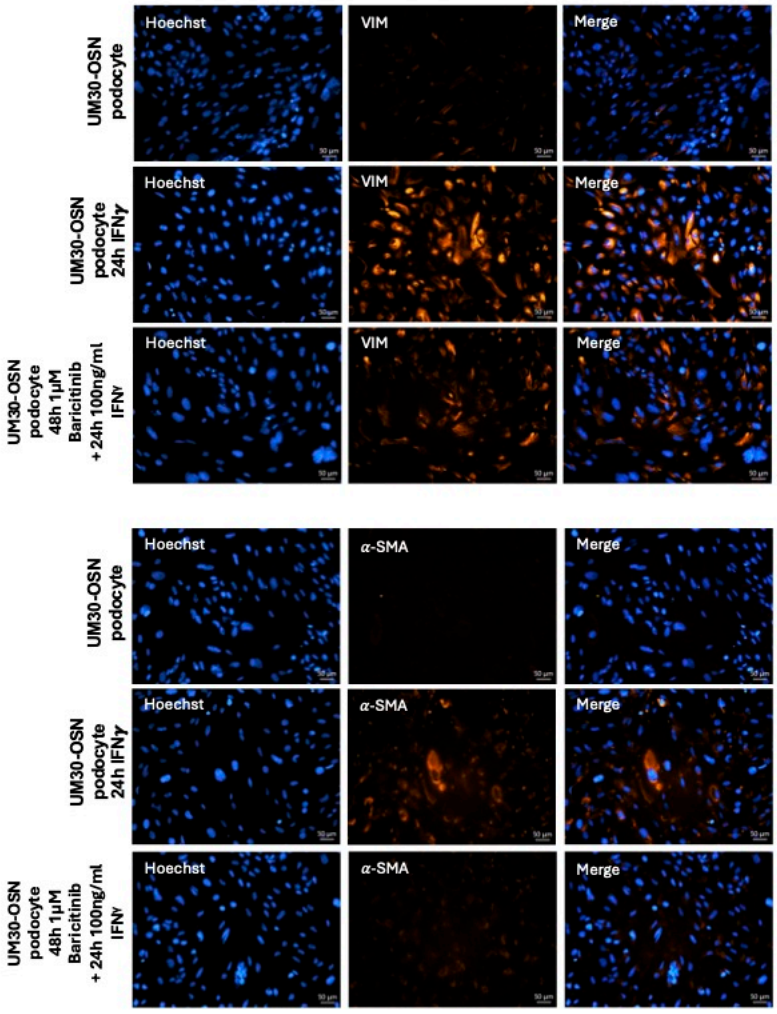


Figure 5: Effects of IFNγ and Baricitinib on UM30-OSN podocytes APOL gene expression and kidney injury marker. (A) Schematic representation of the IFN-γ signaling pathway. Binding of interferon-gamma (IFN-γ) to its heterodimeric receptor, composed of IFNGR1 and IFNGR2, induces receptor dimerization and subsequent activation of the associated Janus kinases JAK1 and JAK2 via transphosphorylation. This leads to the recruitment and phosphorylation of the signal transducers STAT1, STAT2, and STAT3. Phosphorylated STATs dimerize and translocate into the nucleus, where they bind specific DNA elements such as GAS or ISRE sequences and activate the transcription of target genes (e.g., IRF-1, STAT1/2, APOL1). Baricitinib inhibits upstream signaling by selectively blocking JAK1/JAK2 activity, thereby suppressing STAT activation and downstream gene expression. (B) Experimental setup using immortalized urine-derived renal progenitor cells differentiated into podocytes (UM30-OSN). After 14 days of podocyte differentiation, cells were pre-treated with or without 1 µM Baricitinib for 24 h, followed by stimulation with 100 ng/ml IFN-γ for an additional 24 h. Subsequent analyses were performed on both RNA and protein levels.

bioRxiv preprint doi: https://doi.org/10.1101/2025.07.28.667124; this version posted July 29, 2025. The copyright holder for this preprint (which was not certified by peer review) is the author/funder, who has granted bioRxiv a license to display the preprint in perpetuity. It is made available under aCC-BY-NC 4.0 International license.

(C) A 24-hour treatment with 100 ng/ml IFN-γ resulted in an increased number of rounded (detached) cells compared to untreated controls, as visualized by light microscopy. The combination of IFN-γ with Baricitinib significantly reduced the number of rounded cells, resembling the control condition. (D) The expression of IFN-γ-associated genes such as APOL1, MAPK8, STAT3, and kidney injury markers such as Cycs, IL-6, NGAL, CLU, Caspase-1, TGF-β, and Gasdermin D was analyzed by quantitative real-time PCR under all three conditions. (E) Western blot analysis was performed to assess protein levels of the podocyte marker alpha-ACTININ4, APOL1, and phosphorylated STAT1 (p-STAT1). (F) Immunofluorescence-based detection of Fibronectin, alpha-SMA, and Vimentin indicated fibrosis-like tendencies upon IFN-γ treatment, evidenced by the upregulated expression of all three proteins. No such upregulation was observed in control or Baricitinib co-treated cells (Scale bars: 100 µm). Figure 5A-B were created in https://BioRender.com.

Discussion

As mature podocytes are terminally differentiated cells, it is not possible for them to undergo cell division and therefore have a limited life-span in culture[46]. To circumvent this shortfall, we previously established protocols for isolating highly proliferative SIX2-positive urine derived progenitor cells [25] and others have also isolated urine-derived epithelial cells [47]. As these cells also have are endowed limited life-span in culture, this has been by-passed by immortalizations for use in further studies related to nephrogenesis and modelling kidney-associated diseases [1–3,47–49]. The available cell lines have so far been derived from individuals of Caucasian heritage, except the UM51 hTERT [2].

In the present manuscript, we present the successful immortalization of a human SIX2-positive renal progenitor cell line derived from the urine of a 30-year-old West African male (UM30-OSN). These cells show stable morphology and proliferation for over one year in culture (~100 passages). To achieve partial reprogramming and immortalization, plasmids encoding SV40 and the reprogramming factors- OCT4, SOX2, NANOG, cMyc, and KLF4 were employed.

The conferral of unlimited cell division is associated with chromosomal alterations and genomic instabilities [50,51]. In the UM30-OSN these are also present in some cases, whereby P53, P21 as well as PCNA and KI67 expression and their activation and downregulation indicate intact cell cycle checkpoints.

The comparison of the transcriptomes of UM30, UM30-OSN and the UM51 iPSC showed a clear separation, in which UM30-OSN clustered closer to the primary UdRPCs UM30 than to the iPSC.

UM30-OSN retains its renal origin due to partial reprogramming. This is confirmed by the expression of vimentin and renal progenitor stem cell, SIX2 and cell surface markers CD24, CD133 [36]. The lack of expression of the pluripotency markers- POU5F1, NANOG, SOX2 and CDH1 further confirms that UM30-OSN is not pluripotent.

Shared KEGG pathways and GO-Biological Process (GO-BP) terms identified in both immortalized AB8/13 podocytes and UM30-OSN podocytes are associated with cell division, cell cycle regulation, and cellular senescence. These biological processes are well-established hallmarks of cellular immortalization, thereby supporting the molecular basis of the

bioRxiv preprint doi: https://doi.org/10.1101/2025.07.28.667124; this version posted July 29, 2025. The copyright holder for this preprint (which was not certified by peer review) is the author/funder, who has granted bioRxiv a license to display the preprint in perpetuity. It is made available under aCC-BY-NC 4.0 International license.

554 immortalization observed in these cell lines [52]. Differentiation into mature podocytes was shown
555 based on protein and mRNA expression of Nephrin (NPHS1), Podocin (NPHS2),
556 Synaptopodin (SYNPO) and CD2-associated protein (CD2AP). According to the present
557 findings, numerous podocyte-specific genes have been identified whose products play an
558 important role in maintaining the filtration barrier. Near to the extracellular proteins of the slit
559 membrane is the hairpin-like transmembrane protein NPHS2 with two cytoplasmic ends, which
560 is expressed within the glomerulus only in podocytes [53]. An interaction between NPHS2,
561 NPHS1 and CD2AP has already been demonstrated [54,55]. This highly conserved complex,
562 through which podocytes are connected to cell-cell contacts, controls podocyte function [56,57].
563 Besides the essential components of the podocyctic slit membrane, the components the
564 podocytic cytoskeleton and associated molecules are necessary for a mature podocyte.
565 SYNPO a protein that interacts with several cytoskeletal and membrane-associated molecules
566 is restricted expressed in differentiated podocytes in the kidney [58]. It has relevance in the
567 maintenance of podocyte morphology.
568
569 Thus, the expression of podocyte-specific genes, by culturing UM30-OSN in adv. RPMI and
570 RA, confirm the differentiation potential of this cell line into podocytes.
571 In summary, we have successfully described the first male African cell line UM30-OSN
572 immortalized with SV40 and the reprogramming factors OCT4, SOX2, NANOG, cMyc and
573 KLF4. These grow as monolayers and have a rice grain-like morphology. and can be
574 differentiated into mature podocytes amenable for studying nephrogenesis and its kidney-
575 associated diseases.Thus, in addition to iPSC and the human immortal (AB 8/13) podocytes,
576 they serve as an additional cell culture option with a major advantage of West African origin.
577
578 Beyond highlighting UM30-OSN cells as a viable alternative to commonly used cell lines of
579 Caucasian origin such as HEK and the immortalized podocyte cells, our study also supports
580 their application as a disease-relevant *in vitro* model for investigating APOL1-associated
581 nephropathies.
582 In this study, we demonstrate that Baricitinib effectively counteracts the harmful effects of IFN-
583 γ on human urine-derived UM30-OSN podocytes, both at the molecular and morphological
584 levels. Treatment with IFN-γ led to marked changes in cell morphology, including detachment
585 and rounding, along with increased expression of APOL1 and other markers associated with
586 cellular stress, inflammation, and fibrosis. Our findings are consistent with previous reports
587 describing IFN-γ as a potent inducer of APOL1 expression via activation of the JAK/STAT
588 signaling pathway [11,16,59–62].
589 Specifically, we demonstrated that IFN-γ induces a characteristic rounding and detachment of
590 podocytes, accompanied by upregulation of fibrosis markers such as Fibronectin, α-SMA, and

bioRxiv preprint doi: https://doi.org/10.1101/2025.07.28.667124; this version posted July 29, 2025. The copyright holder for this preprint (which was not certified by peer review) is the author/funder, who has granted bioRxiv a license to display the preprint in perpetuity. It is made available under aCC-BY-NC 4.0 International license.

591 Vimentin, as well as APOL1 and additional stress- and inflammation-associated genes, such
592 as STAT3, IL-6, MAPK8, Caspase-1, and Gasdermin D. In particular Caspase-1 and
593 Gasdermin D are associated with cellular immune response and inflammatory reactions and
594 are key players in the pyroptosis signaling pathway, a form of programmed cell death [63,64].
595
596 These findings are similar with previously reported mechanisms by which IFN-γ promotes a
597 pro-fibrotic and cytotoxic environment mediated through activation of the JAK/STAT signaling
598 pathway.[11,65].
599 Baricitinib effectively prevented these IFN-γ-induced effects. Podocyte morphological integrity
600 was preserved, APOL1 expression and STAT1 phosphorylation were reduced, and fibrosis
601 markers remained at baseline levels. This protective effect is consistent with observations in
602 human kidney biopsies and podocyte models, where Baricitinib has been shown to reduce
603 cytotoxicity and APOL1 expression under pro-inflammatory conditions [10]. Mechanistically, our
604 Western blot results showing reduced p-STAT1 expression confirm effective blockade of the
605 JAK/STAT phosphorylation cascade, which plays a central role in APOL1 transcription and
606 downstream cellular injury. These findings highlight the therapeutic potential of Baricitinib in
607 APOL1-associated kidney diseases, as applied in the Phase 2 clinical JUSTICE trial, which
608 evaluated its efficacy in reducing proteinuria in individuals carrying high-risk APOL1 genotypes
609 [60].
610
611 **Conclusion**
612 In conclusion, our results confirm that IFN-γ induces a pro-fibrotic and APOL1-driven stress
613 response in UM30-OSN derived podocytes via JAK/STAT signaling. Baricitinib acts as an
614 effective inhibitor of this signaling cascade, highlighting its strong potential as a therapeutic
615 option for APOL1-associated kidney diseases. Ultimately, this study not only underscores the
616 utility of the urine-derived immortalized UM30-OSN cell line, but also establishes its relevance
617 as a valuable *in vitro* model for investigating APOL1-mediated kidney diseases such as
618 fibrosis.
619 Figure 6 is a graphical summary of this study.

bioRxiv preprint doi: https://doi.org/10.1101/2025.07.28.667124; this version posted July 29, 2025. The copyright holder for this preprint (which was not certified by peer review) is the author/funder, who has granted bioRxiv a license to display the preprint in perpetuity. It is made available under aCC-BY-NC 4.0 International license.

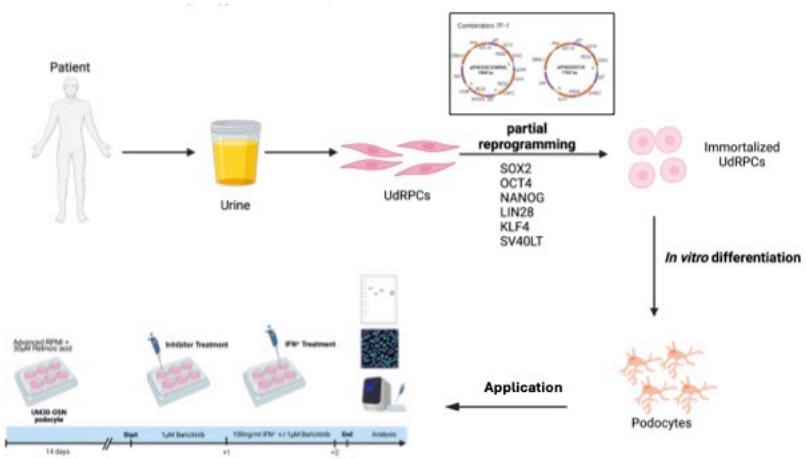


Figure 6: Generation of Immortalized SIX2⁺ Renal progenitor Cells from urine of a West African male. SIX2-positive urine-derived renal progenitor cells (UdRPCs) from a 30 years old male of west African origin were isolated from his urine samples and subjected to episomal-based cellular reprogramming. Although full pluripotency was not induced, the cells acquired a significantly enhanced proliferative capacity compared to primary UdRPCs. Notably, this immortalized cell population retains the ability to differentiate into functional human podocytes, offering a robust and scalable model for renal research. For further application, the human podocytes were treated with and without 1μM Baricitinib, followed by a 24h stimulation with 100ng/ml IFNγ. UM30-OSN represents and a disease-relevant model for studying APOL1-mediated kidney fibrosis. The figure was created using BioRender (https://BioRender.com.)

Declarations

Author Contributions: Conceptualization, J.A.; methodology, C.T., R.M.; bioinformatics, W.W.; formal analysis, C.T.; investigation, C.T., W.W.; resources, J.A., O.A.; data curation, C.T.; writing—original draft preparation,
C.T.; writing—review and editing, C.T. and J.A.; visualization, C.T.; supervision, J.A.; project administration, J.A; funding acquisition, J.A. All authors have read and agreed to the published version of the manuscript.

Funding: J.A. acknowledges the medical faculty of Heinrich Heine University for financial support.

Institutional Review Board Statement: The study was conducted in accordance with the written approval (Ethical approval Number: 2017-2457_3) of the ethical review board of the medical faculty of Heinrich Heine University, Düsseldorf, Germany. All methods were carried out in accordance with the approved guidelines. Medical faculty of Heinrich Heine University approved all experimental protocols.

Informed Consent Statement: In this study, urine samples were collected with the informed consent of the donors.

bioRxiv preprint doi: https://doi.org/10.1101/2025.07.28.667124; this version posted July 29, 2025. The copyright holder for this preprint (which was not certified by peer review) is the author/funder, who has granted bioRxiv a license to display the preprint in perpetuity. It is made available under aCC-BY-NC 4.0 International license.

650 **Data Availability Statement:** Gene expression data will be available online in the National
651 Centre of Biotechnology Information (NCBI) Gene Expression Omnibus under the number
652 GSE299018.
653
654

655 **Acknowledgments:** James Adjaye acknowledges funding from the medical faculty of
656 Heinrich Heine University, Duesseldorf, Germany. Dr. Ania Koziell and Professor Saleem
657 Moin provided the human immortal cell line (AB 8/13). Dr. Nina Graffmann assisted with the
658 FACs analyses. Martina Bohndorf assisted by initiating the partial reprogramming
659 experiments.

660 **Conflicts of Interest:** The authors declare no conflict of interest.
661
662 **Supplementary Materials**
663 Supplementary Table S1: Used antibodies.
664 Supplementary Table S2: Used qPCR primers.
665 Supplementary Table S3: gostats.
666 Supplementary Table S4: full gene list.
667 Supplementary Table S5: KEGG signaling pathways.
668 Supplementary Figure S1: uncropped western blot images.
669 Supplementary Figure S2: Plasmid maps.
670 Supplementary Figure S3: Karyogramm of UdRPC UM30-OSN and immortal cell line
671 (AB 8/13).
672
673

674 References

675 1. Sakairi T, Abe Y, Kajiyama H, et al. Conditionally immortalized human podocyte cell
676 lines established from urine. *Am J Physiol-Ren Physiol*. 2010;298(3):F557-F567.
677 doi:10.1152/ajprenal.00509.2009
678 2. Erichsen L, Kloss LDF, Thimm C, et al. Derivation of the immortalized cell line-
679 UM51-PrePodo-hTERT and its responsiveness to Angiotensin II and activation of RAAS.
680 *Cells*. 2023;12(3). doi:10.3390/cells12030342
681 3. Saleem MA, O'Hare MJ, Reiser J, et al. A Conditionally Immortalized Human
682 Podocyte Cell Line Demonstrating Nephrin and Podocin Expression. *J Am Soc Nephrol*.
683 2002;13(3):630-638. doi:10.1681/ASN.V133630
684 4. Pereira EM, Labilloy A, Eshbach ML, et al. Characterization and phosphoproteomic
685 analysis of a human immortalized podocyte model of Fabry disease generated using
686 CRISPR/Cas9 technology. *Am J Physiol-Ren Physiol*. 2016;311(5):F1015-F1024.
687 doi:10.1152/ajprenal.00283.2016
688 5. Black PH, Rowe WP. Increase of malignant potential of BHK-21 cells by SV40 DNA
689 without persistent new antigen. *Proc Natl Acad Sci*. 1965;54(4):1126-1133.
690 doi:10.1073/pnas.54.4.1126
691 6. Chang LS, Pater MM, Hutchinson NI, Mayorca GD. Transformation by purified early
692 genes of simian virus 40. *Virology*. 1984;133(2):341-353. doi:10.1016/0042-6822(84)90400-8
693 7. Ahuja D, Sáenz-Robles MT, Pipas JM. SV40 large T antigen targets multiple cellular
694 pathways to elicit cellular transformation. *Oncogene*. 2005;24(52):7729-7745.
695 doi:10.1038/sj.onc.1209046

bioRxiv preprint doi: https://doi.org/10.1101/2025.07.28.667124; this version posted July 29, 2025. The copyright holder for this preprint (which was not certified by peer review) is the author/funder, who has granted bioRxiv a license to display the preprint in perpetuity. It is made available under aCC-BY-NC 4.0 International license.

8. Browder KC, Reddy P, Yamamoto M, et al. In vivo partial reprogramming alters age-associated molecular changes during physiological aging in mice. *Nat Aging*. 2022;2(3):243-253. doi:10.1038/s43587-022-00183-2
9. Ma L, Chou JW, Snipes JA, et al. APOL1 Renal-Risk Variants Induce Mitochondrial Dysfunction. *J Am Soc Nephrol*. 2017;28(4):1093-1105. doi:10.1681/asn.2016050567
10. Nystrom SE, Li G, Datta S, et al. JAK inhibitor blocks COVID-19 cytokine–induced JAK/STAT/APOL1 signaling in glomerular cells and podocytopathy in human kidney organoids. *JCI Insight*. 2022;7(11). doi:10.1172/jci.insight.157432
11. Juliar BA, Stanaway IB, Sano F, et al. Interferon-γ induces combined pyroptotic angiopathy and APOL1 expression in human kidney disease. *Cell Rep*. 2024;43(6):114310. doi:10.1016/j.celrep.2024.114310
12. Datta S, Kataria R, Zhang JY, et al. Kidney Disease-Associated APOL1 Variants Have Dose-Dependent, Dominant Toxic Gain-of-Function. *J Am Soc Nephrol JASN*. 2020;31(9):2083-2096. doi:10.1681/ASN.2020010079
13. Vandorpe DH, Heneghan JF, Waitzman JS, et al. Apolipoprotein L1 (APOL1) cation current in HEK-293 cells and in human podocytes. *Pflugers Arch*. 2023;475(3):323-341. doi:10.1007/s00424-022-02767-8
14. Sampson MG, Robertson CC, Martini S, et al. Integrative Genomics Identifies Novel Associations with APOL1 Risk Genotypes in Black NEPTUNE Subjects. *J Am Soc Nephrol*. 2016;27(3):814-823. doi:10.1681/asn.2014111131
15. Kopp JB, Winkler CA, Zhao X, et al. Clinical Features and Histology of Apolipoprotein L1-Associated Nephropathy in the FSGS Clinical Trial. *J Am Soc Nephrol*. 2015;26(6):1443-1448. doi:10.1681/asn.2013111242
16. Olabisi OA, Zhang JY, VerPlank L, et al. APOL1 kidney disease risk variants cause cytotoxicity by depleting cellular potassium and inducing stress-activated protein kinases. *Proc Natl Acad Sci*. 2016;113(4):830-837. doi:10.1073/pnas.1522913113
17. Pollak MR, Friedman DJ. APOL1 and APOL1-Associated Kidney Disease: A Common Disease, an Unusual Disease Gene – Proceedings of the Henry Shavelle Professorship. *Glomerular Dis*. Published online January 25, 2023:75-87. doi:10.1159/000529227
18. Ge M, Molina J, Ducasa GM, et al. APOL1 risk variants affect podocyte lipid homeostasis and energy production in focal segmental glomerulosclerosis. *Hum Mol Genet*. 2021;30(3-4):182-197. doi:10.1093/hmg/ddab022
19. Lee SY, Kim SI, Choi ME. Therapeutic targets for treating fibrotic kidney diseases. *Transl Res*. 2015;165(4):512-530. doi:10.1016/j.trsl.2014.07.010
20. Singhal PC, Skorecki K. APOL1 Dynamics in Diabetic Kidney Disease and Hypertension. *Biomolecules*. 2025;15(2):205. doi:10.3390/biom15020205
21. Daneshpajouhnejad P, Kopp JB, Winkler CA, Rosenberg AZ. The evolving story of apolipoprotein L1 nephropathy: the end of the beginning. *Nat Rev Nephrol*. 2022;18(5):307-320. doi:10.1038/s41581-022-00538-3
22. Wu J, Raman A, Coffey NJ, et al. The key role of NLRP3 and STING in APOL1-associated podocytopathy. *J Clin Invest*. 2021;131(20). doi:10.1172/jci136329
23. Kobayashi A, Valerius MT, Mugford JW, et al. Six2 defines and regulates a multipotent self-renewing nephron progenitor population throughout mammalian kidney development. *Cell Stem Cell*. 2008;3(2):169-181. doi:10.1016/j.stem.2008.05.020
24. Self M, Lagutin OV, Bowling B, et al. Six2 is required for suppression of nephrogenesis and progenitor renewal in the developing kidney. *EMBO J*. 2006;25(21):5214-5228. doi:10.1038/sj.emboj.7601381
25. Rahman MS, Wruck W, Spitzhorn LS, et al. The FGF, TGFβ and WNT axis Modulate Self-renewal of Human SIX2 + Urine Derived Renal Progenitor Cells. *Scientific Reports*. 2020;10(1):739. doi:10.1038/s41598-020-57723-2

bioRxiv preprint doi: https://doi.org/10.1101/2025.07.28.667124; this version posted July 29, 2025. The copyright holder for this preprint (which was not certified by peer review) is the author/funder, who has granted bioRxiv a license to display the preprint in perpetuity. It is made available under aCC-BY-NC 4.0 International license.

747 26. Thimm C, Zhong C, Wruck W, et al. Generation of a Bartter syndrome type 3 patient-
748 derived induced pluripotent stem cell line ISRM-BS3-UM18-iPSC (HHUUKDi014-A). *Stem*
749 *Cell Res*. 2025;87:103760. doi:10.1016/j.scr.2025.103760
750 27. Bohndorf M, Ncube A, Spitzhorn LS, Enczmann J, Wruck W, Adjaye J. Derivation
751 and characterization of integration-free iPSC line ISRM-UM51 derived from SIX2-positive
752 renal cells isolated from urine of an African male expressing the CYP2D6 *4/*17 variant
753 which confers intermediate drug metabolizing activity. *Stem Cell Res* . 2017;25:18-21.
754 28. Erichsen L, Thimm C, Bohndorf M, Rahman MS, Wruck W, Adjaye J. Activation of
755 the Renin–Angiotensin System Disrupts the Cytoskeletal Architecture of Human Urine-
756 Derived Podocytes. *Cells*. 2022;11:1095. doi:https://doi.org/10.3390/ cells11071095
757 29. Thimm C, Erichsen L, Wruck W, Adjaye J. Unveiling Angiotensin II and Losartan-
758 Induced Gene Regulatory Networks Using Human Urine-Derived Podocytes. *Int J Mol Sci*.
759 2023;24(13):10551. doi:10.3390/ijms241310551
760 30. Kim D, Langmead B, Salzberg SL. HISAT: a fast spliced aligner with low memory
761 requirements. *Nat Methods*. 2015;12(4):357-360. doi:10.1038/nmeth.3317
762 31. Baruzzo G, Hayer KE, Kim EJ, Di Camillo B, FitzGerald GA, Grant GR. Simulation-
763 based comprehensive benchmarking of RNA-seq aligners. *Nat Methods*. 2017;14(2):135-139.
764 doi:10.1038/nmeth.4106
765 32. Li H, Handsaker B, Wysoker A, et al. The Sequence Alignment/Map format and
766 SAMtools. *Bioinforma Oxf Engl*. 2009;25(16):2078-2079. doi:10.1093/bioinformatics/btp352
767 33. Liao Y, Smyth GK, Shi W. featureCounts: an efficient general purpose program for
768 assigning sequence reads to genomic features. *Bioinforma Oxf Engl*. 2014;30(7):923-930.
769 doi:10.1093/bioinformatics/btt656
770 34. Gentleman RC, Carey VJ, Bates DM, et al. Bioconductor: open software development
771 for computational biology and bioinformatics. *Genome Biol*. 2004;5(10):R80. doi:10.1186/gb-
772 2004-5-10-r80
773 35. Law CW, Chen Y, Shi W, Smyth GK. voom: precision weights unlock linear model
774 analysis tools for RNA-seq read counts. *Genome Biol*. 2014;15(2):R29. doi:10.1186/gb-2014-
775 15-2-r29
776 36. Smyth GK. Linear Models and Empirical Bayes Methods for Assessing Differential
777 Expression in Microarray Experiments. *Stat Appl Genet Mol Biol*. 2004;3(1).
778 doi:10.2202/1544-6115.1027
779 37. Carvalho BS, Irizarry RA. A framework for oligonucleotide microarray preprocessing.
780 *Bioinformatics*. 2010;26(19):2363-2367. doi:10.1093/bioinformatics/btq431
781 38. Warnes GR, Bolker B, Bonebakker L, et al. *Gplots: Various R Programming Tools for*
782 *Plotting Data*.; 2015. http://CRAN.R-project.org/package=gplots
783 39. Chen H, Boutros PC. VennDiagram: a package for the generation of highly-
784 customizable Venn and Euler diagrams in R. *BMC Bioinformatics*. 2011;12(1):35.
785 doi:10.1186/1471-2105-12-35
786 40. Graffmann N, Ring S, Kawala MA, et al. Modeling Nonalcoholic Fatty Liver Disease
787 with Human Pluripotent Stem Cell-Derived Immature Hepatocyte-Like Cells Reveals
788 Activation of PLIN2 and Confirms Regulatory Functions of Peroxisome Proliferator-
789 Activated Receptor Alpha. *Stem Cells Dev*. 2016;25(15):1119-1133.
790 doi:10.1089/scd.2015.0383
791 41. Falcon S, Gentleman R. Using GOstats to test gene lists for GO term association.
792 *Bioinforma Oxf Engl*. 2007;23(2):257-258. doi:10.1093/bioinformatics/btl567
793 42. Kanehisa M, Furumichi M, Tanabe M, Sato Y, Morishima K. KEGG: new
794 perspectives on genomes, pathways, diseases and drugs. *Nucleic Acids Res*.
795 2017;45(D1):D353-D361. doi:10.1093/nar/gkw1092
796 43. Wickham H. *Ggplot2: Elegant Graphics for Data Analysis*. Springer; 2009.
797 44. Ncube A, Bewersdorf L, Spitzhorn LS, et al. Generation of two Alpha-I antitrypsin

bioRxiv preprint doi: https://doi.org/10.1101/2025.07.28.667124; this version posted July 29, 2025. The copyright holder for this preprint (which was not certified by peer review) is the author/funder, who has granted bioRxiv a license to display the preprint in perpetuity. It is made available under aCC-BY-NC 4.0 International license.

798 deficiency patient-derived induced pluripotent stem cell lines ISRM-AATD-iPSC-1
799 (HHUUKDi011-A) and ISRM-AATD-iPSC-2 (HHUUKDi012-A). *Stem Cell Res*.
800 2023;71:103171. doi:10.1016/j.scr.2023.103171
801 45. Hanahan D, Weinberg RA. Hallmarks of Cancer: The Next Generation. *Cell*.
802 2011;144(5):646-674. doi:10.1016/j.cell.2011.02.013
803 46. Greka A, Mundel P. Cell Biology and Pathology of Podocytes. *Annu Rev Physiol*.
804 2012;74(1):299-323. doi:10.1146/annurev-physiol-020911-153238
805 47. Bondue T, Arcolino FO, Veys KRP, et al. Urine-Derived Epithelial Cells as Models
806 for Genetic Kidney Diseases. *Cells*. 2021;10(6):1413. doi:10.3390/cells10061413
807 48. Racusen LC, Wilson PD, Hartz PA, Fivush BA, Burrow CR, Philip WTTAOET.
808 Renal proximal tubular epithelium from patients with nephropathic cystinosis: Immortalized
809 cell lines as in vitro model systems. *Kidney Int*. 1995;48(2):536-543. doi:10.1038/ki.1995.324
810 49. Wieser M, Stadler G, Jennings P, et al. hTERT alone immortalizes epithelial cells of
811 renal proximal tubules without changing their functional characteristics. *Am J Physiol-Ren*
812 *Physiol*. 2008;295(5):F1365-F1375. doi:10.1152/ajprenal.90405.2008
813 50. Yoshioka K ichi. Development of cancer-initiating cells and immortalized cells with
814 genomic instability. *World J Stem Cells*. 2015;7(2):483. doi:10.4252/wjsc.v7.i2.483
815 51. He Z, Wilson A, Rich F, et al. Chromosomal instability and its effect on cell lines.
816 *Cancer Rep*. 2023;6(6). doi:10.1002/cnr2.1822
817 52. Shay JW, Wright WE. Senescence and immortalization: role of telomeres and
818 telomerase. *Carcinogenesis*. 2005;26(5):867-874. doi:10.1093/carcin/bgh296
819 53. Boute N, Gribouval O, Roselli S, et al. NPHS2, encoding the glomerular protein
820 podocin, is mutated in autosomal recessive steroid-resistant nephrotic syndrome. *Nature*
821 *Genetics*. Published online 2000:349-354.
822 54. Schwarz K, Simons M, Reiser J, et al. Podocin, a raft-associated component of the
823 glomerular slit diaphragm, interacts with CD2AP and nephrin. *JCI*. Published online
824 2001:1621-1629.
825 55. Martin C, Jones N. Nephrin Signaling in the Podocyte: An Updated View of Signal
826 Regulation at the Slit Diaphragm and Beyond. *frontiers in Endocrinology*. 2018;(9).
827 doi:10.3389/fendo.2018.00302
828 56. Huber TB. *Molekulare Pathogenese Der Proteinurie*. Thieme; 2008. Accessed August
829 21, 2021. https://www.thieme-connect.com/products/ejournals/abstract/10.1055/s-2008-
830 1075673
831 57. Li C, Ruotsalainen V, Tryggvason K, Shaw A, Miner J. CD2AP is expressed with
832 nephrin in developing podocytes and is found widley in mature kidney and elsewhere. *The*
833 *American Journal of Physiology - Renal Physiology*. Published online 2000:785-792.
834 doi:091.036.155.088
835 58. Shankland S, Pippin J, Reiser J, Mundel P. Podocytes in cultue: past, present, and
836 future. *Kidney international*. Published online 2007:26-36.
837 59. Datta S, Antonio BM, Zahler NH, et al. APOL1-mediated monovalent cation transport
838 contributes to APOL1-mediated podocytopathy in kidney disease. *J Clin Invest*. 2024;134(5).
839 doi:10.1172/jci172262
840 60. Olabisi OA, Barrett NJ, Lucas A, et al. Design and Rationale of the Phase 2 Baricitinib
841 Study in Apolipoprotein L1–Mediated Kidney Disease (JUSTICE). *Kidney Int Rep*.
842 2024;9(9):2677-2684. doi:10.1016/j.ekir.2024.06.033
843 61. Vasquez-Rios G, De Cos M, Campbell KN. Novel Therapies in APOL1-Mediated
844 Kidney Disease: From Molecular Pathways to Therapeutic Options. *Kidney Int Rep*.
845 2023;8(11):2226-2234. doi:10.1016/j.ekir.2023.08.028
846 62. Nichols B, Jog P, Lee JH, et al. Innate immunity pathways regulate the nephropathy
847 gene Apolipoprotein L1. *Kidney Int*. 2015;87(2):332-342. doi:10.1038/ki.2014.270
848 63. Shi J, Zhao Y, Wang K, et al. Cleavage of GSDMD by inflammatory caspases

bioRxiv preprint doi: https://doi.org/10.1101/2025.07.28.667124; this version posted July 29, 2025. The copyright holder for this preprint (which was not certified by peer review) is the author/funder, who has granted bioRxiv a license to display the preprint in perpetuity. It is made available under aCC-BY-NC 4.0 International license.

849 determines pyroptotic cell death. *Nature*. 2015;526(7575):660-665. doi:10.1038/nature15514
850 64. Dai C, Krantz SB. Interferon γ Induces Upregulation and Activation of Caspases 1, 3,
851 and 8 to Produce Apoptosis in Human Erythroid Progenitor Cells. *Blood*. 1999;93(10):3309-
852 3316. doi:10.1182/blood.v93.10.3309.410k04_3309_3316
853 65. Tao J, Mariani L, Eddy S, et al. JAK-STAT signaling is activated in the kidney and
854 peripheral blood cells of patients with focal segmental glomerulosclerosis. *Kidney Int*.
855 2018;94(4):795-808. doi:10.1016/j.kint.2018.05.022

856

857 **Supplementary Materials**

858 **Supplementary Table S1: Used antibodies.**

859 **Supplementary Table S2: Used qPCR primers.**

860 **Supplementary Table S3: gostats.**

861 **Supplementary Table S4: full gene list. (a) full gene list corresponding to the Venn diagram**
862 **presented in Figure 4C, showing the differences of the UM30-OSN and human immortal**
863 **podocyte (AB 8/13) and their similarities. (b) full gene list corresponding to Figure 1H**
864 **showing the differences between UM30, UM30-OSN and the UM51 iPSC and their**
865 **similarities.**

866 **Supplementary Table S5: KEGG signaling pathways.**

867 **Supplementary Figure S1: uncropped western blot images.**

868 **Supplementary Figure S2: Plasmid maps.**

869 **Supplementary Figure S3: Karyogramm of UdRPC UM30-OSN and immortal cell line (AB**
870 **8/13).**

3.3 Activation of the Renin-Angiotensin System Disrupts the Cytoskeletal Architecture of Human Urine-Derived Podocytes

Lars Erichsen, **Chantelle Thimm**, Martina Bohndorf, Md Shaifur Rahman, Wasco Wruck and James Adjaye

Cells 2022, Volume 11, 1095, Article ID 11071095

Abstract:

High blood pressure is one of the major public health problems that causes severe disorders in several tissues including the human kidney. One of the most important signaling pathways associated with the regulation of blood pressure is the renin–angiotensin system (RAS), with its main mediator angiotensin II (ANGII). Elevated levels of circulating and intracellular ANGII and aldosterone lead to pro-fibrotic, -inflammatory, and -hypertrophic milieu that causes remodeling and dysfunction in cardiovascular and renal tissues. Furthermore, ANGII has been recognized as a major risk factor for the induction of apoptosis in podocytes, ultimately leading to chronic kidney disease (CKD). In the past, disease modeling of kidney-associated diseases was extremely difficult, as the derivation of kidney originated cells is very challenging. Here we describe a differentia- tion protocol for reproducible differentiation of sine oculis homeobox homolog 2 (SIX2)-positive urine-derived renal progenitor cells (UdRPCs) into podocytes bearing typical cellular processes. The UdRPCs-derived podocytes show the activation of the renin–angiotensin system by being responsive to ANGII stimulation. Our data reveal the ANGII-dependent downregulation of nephrin (*NPHS1)* and synaptopodin (*SYNPO)*, resulting in the disruption of the podocyte cytoskeletal architecture, as shown by immunofluorescence-based detection of α-Actinin. Furthermore, we show that the cytoskeletal disruption is mainly mediated through angiotensin II receptor type 1 (AGTR1) signaling and can be rescued by AGTR1 inhibition with the selective, competitive angiotensin II receptor type 1 antagonist, losartan. In the present manuscript we confirm and propose UdRPCs differentiated to podocytes as a unique cell type useful for studying nephrogenesis and associated diseases. Furthermore, the responsiveness of UdRPCs-derived podocytes to ANGII implies potential applications in nephrotoxicity studies and drug screening.

Author contribution of C.T. included 20%:

I was responsible for the establishment and maintenance of the cell culture system, including the cultivation of UdRPCs. I carried out the induction of podocyte differentiation as well as the stimulation experiments using angiotensin II and the angiotensin receptor blocker losartan.

As part of the experimental workflow, I isolated RNA and protein for subsequent my following qPCR and western blot analyses. In addition, I performed the immunofluorescence staining procedures.

For all my generated datasets, I conducted the corresponding statistical analyses and prepared the quantitative evaluation of the results. I designed and executed my experiments and analyzed them in the relation to our research hypothesis.

Status: Published in Cells.

DOI: doi.org/10.3390/cells11071095

This article is an open access article distributed under the terms and conditions of the Creative Commons Attribution (CC BY) 4.0 license, which permits unrestricted use, distribution, and reproduction in any medium, provided the original work is properly cited.

cells

MDPI

Article

Activation of the Renin–Angiotensin System Disrupts the Cytoskeletal Architecture of Human Urine-Derived Podocytes

Lars Erichsen, Chantelle Thimm, Martina Bohndorf, Md Shaifur Rahman, Wasco Wruck and James Adjaye *

Institute for Stem Cell Research and Regenerative Medicine, Medical Faculty, Heinrich-Heine-University Düsseldorf, 40225 Düsseldorf, Germany; lars.erichsen@uni-duesseldorf.de (L.E.); chantelle.thimm@uni-duesseldorf.de (C.T.); martina.bohndorf@med.uni-duesseldorf.de (M.B.); mdshaifur@gmail.com (M.S.R.); wasco.wruck@med.uni-duesseldorf.de (W.W.)
* Correspondence: james.adjaye@med.uni-duesseldorf.de

Abstract: High blood pressure is one of the major public health problems that causes severe disorders in several tissues including the human kidney. One of the most important signaling pathways associated with the regulation of blood pressure is the renin–angiotensin system (RAS), with its main mediator angiotensin II (ANGII). Elevated levels of circulating and intracellular ANGII and aldosterone lead to pro-fibrotic, -inflammatory, and -hypertrophic milieu that causes remodeling and dysfunction in cardiovascular and renal tissues. Furthermore, ANGII has been recognized as a major risk factor for the induction of apoptosis in podocytes, ultimately leading to chronic kidney disease (CKD). In the past, disease modeling of kidney-associated diseases was extremely difficult, as the derivation of kidney originated cells is very challenging. Here we describe a differentiation protocol for reproducible differentiation of sine oculis homeobox homolog 2 (SIX2)-positive urine-derived renal progenitor cells (UdRPCs) into podocytes bearing typical cellular processes. The UdRPCs-derived podocytes show the activation of the renin–angiotensin system by being responsive to ANGII stimulation. Our data reveal the ANGII-dependent downregulation of nephrin (*NPHS1*) and synaptopodin (*SYNPO*), resulting in the disruption of the podocyte cytoskeletal architecture, as shown by immunofluorescence-based detection of α-Actinin. Furthermore, we show that the cytoskeletal disruption is mainly mediated through angiotensin II receptor type 1 (AGTR1) signaling and can be rescued by AGTR1 inhibition with the selective, competitive angiotensin II receptor type 1 antagonist, losartan. In the present manuscript we confirm and propose UdRPCs differentiated to podocytes as a unique cell type useful for studying nephrogenesis and associated diseases. Furthermore, the responsiveness of UdRPCs-derived podocytes to ANGII implies potential applications in nephrotoxicity studies and drug screening.

Keywords: renal differentiation; podocytes; disease modeling; renin–angiotensin system

check for updates

Citation: Erichsen, L.; Thimm, C.; Bohndorf, M.; Rahman, M.S.; Wruck, W.; Adjaye, J. Activation of the Renin–Angiotensin System Disrupts the Cytoskeletal Architecture of Human Urine-Derived Podocytes. *Cells* **2022**, *11*, 1095. https://doi.org/10.3390/cells11071095

Academic Editor: Laura Lasagni

Received: 17 February 2022
Accepted: 21 March 2022
Published: 24 March 2022

Publisher's Note: MDPI stays neutral with regard to jurisdictional claims in published maps and institutional affiliations.

Copyright: © 2022 by the authors. Licensee MDPI, Basel, Switzerland. This article is an open access article distributed under the terms and conditions of the Creative Commons Attribution (CC BY) license (https://creativecommons.org/licenses/by/4.0/).

1. Introduction

The kidney glomerulus or renal corpuscle consists of a glomerular tuft and the Bowman's capsule. Its major task is the filtration of blood to generate urine. The glomerulus consists of distinct cell types: endothelial cells, mesangial cells, parietal epithelial cells of Bowman's capsule, and podocytes, which are attached to the outer part of the glomerular basement membrane (GBM). Podocytes are pericyte-like cells with a complex cellular organization. Key characteristics are the cell body with major and minor foot processes (FPs) [1]. The FPs contain a highly organized actin-based cytoskeleton, essential for maintaining the complex architecture typical of podocytes. Alpha-actinin-4 (ACTN4) and synaptopodin (SYNPO) are both highly expressed in podocyte foot processes. ACTN4 functions as cross-linkers of F-actin filaments in order to bundle them and thereby enhance podocyte signaling and mobility [2,3]. Filtration slits are formed by the spatial arrangement of FPs of

neighboring podocytes, and each of these slits is bridged by the so called glomerular slit diaphragm (SD), which is a comparable structure to the adherens junctions [1]. The most abundant proteins that contribute to SD formation are nephrin (NPHS1) [4] and podocin (NPHS2) [5]. Furthermore, nephrin is also associated with the actin cytoskeleton, thereby contributing to podocyte actin dynamics and FPs formation [6]. Together the FPs and SD help to establish the filtration barrier of the kidney with its selective permeability.

High blood pressure is one of the major public health problems, causing severe disorders in several tissues including heart, brain, and kidney [7]. One of the most important signaling pathways in blood pressure regulation is the renin–angiotensin system (RAS), with its main mediator angiotensin II (ANGII). At the molecular level, ANGII signaling is mediated by two classes of receptors angiotensin II receptor type 1/2 (AGTR1 and AGTR2). Both receptors are expressed in a wide variety of tissues (including the heart, kidney, blood vessels, adrenal glands, and cardiovascular control centers in the brain) and upon stimulation control vasoconstriction [8,9]. Human podocytes express both types of ANGII receptors and are indeed effector cells for this peptide [10]. Furthermore, elevated levels of ANGII have been identified as a main risk factor for the initiation and progression of chronic kidney disease (CKD). Increased ANGII concentrations are associated with the downregulation of nephrin and synaptopodin expression in podocytes [11,12]. The depletion of NPHS1 and SNYPO is causative for podocyte injury [13], which is typically associated with marked albuminuria [1] and increased podocyte apoptosis [14]. This is especially crucial since podocytes are terminal differentiated cells that are unable to undergo cell division in vivo [1]. As a result of this, the replenishment capabilities of podocytes are limited and expose the glomerulus vulnerable to exogenous noxae. Long lasting hazardous cues, such as high blood pressure, can manifest in the significant loss of podocytes, which is a hallmark in the development of CKD [15] and glomerulosclerosis [16]. Furthermore, it has been recognized that AGTR1 is associated with mechanisms and processes leading to injury of podocytes, preceding glomerular crescent formation [17], and that podocyte injury is causative for crescentic glomerulonephritis [18,19].

In the past, disease modeling for kidney-associated diseases was extremely difficult, as the derivation of kidney-originated cells is very challenging. This is particularly true for podocytes since their complex architecture is not well preserved from kidney biopsy tissue [20]. To model podocyte-related diseases, researchers either used an immortalized podocyte cell line [20–22] or induced pluripotent stem cell (iPSC)-based models [23–27]. Meanwhile, the first approach shows the typical drawback of immortalized cells (namely, chromosomal aneuploidies), thus making these cells prone to cancerous transformation. The iPSC-based differentiation approach is very expensive and time-consuming to differentiate.

We recently reported human urine as a non-invasive source of renal stem cells with regenerative potential [28]. The urine-derived renal progenitor cells (UdRPCs) express renal stem cell markers such as sine oculis homeobox homolog 2 (SIX2), Cbp/P300-interacting transactivator, with Glu/Asp rich carboxy-terminal domain 1 (CITED1), Wilms tumor 1 (WT1), CD133, CD24, and CD106. Stimulation of UdRPCs with the glycogen synthase kinase-3 beta (GSK3ß)-inhibitor (CHIR99021) induced differentiation into renal epithelial proximal tubular cells. In the present study, we provide a detailed protocol for the direct differentiation of SIX2-positive UdRPCs into podocytes with typical cellular processes without the need of immortalized cells or pluripotent stem cells. We provide the full characterization of the generated podocytes at the transcriptome, secretome, and cellular level. Furthermore, with ANGII treatment, we demonstrate the responsiveness of the podocytes to the renin–angiotensin system (RAS) with a downregulated expression of NPHS1 and SYNPO.

Our data demonstrate and establish human urine-derived podocytes as a valuable in vitro model for studying podocyte injury, loss, and ultimately CKD. In addition, we hypothesize that the cells can also be used for further drug testing and eventually for kidney-associated regenerative therapies.

2. Material and Methods

2.1. Cell Culture Conditions

UdRPCs were cultured in proliferation medium (PM) composed of 50% DMEM high glucose and 50% keratinocyte medium supplemented with 5% FCS, 0.5% NEAA, 0.25% Gtx, and 0.5% penicillin and streptomycin at 37 °C (Gibco, Carlsbad, CA, USA) under hypoxic conditions. For differentiation, the cells were seeded at low (50,000 cells) and high density (350,000 cells) in 6- or 12-well plates coated with 0.2% type 1 collagen (Gibco) and grown in PM for 24 h. After this, the medium was changed to advanced RPMI (Gibco) supplemented with 0.5% FCS, 1% penicillin and streptomycin, and 30 µM retinoic acid. Typical podocyte morphology was observed after 7 days. ANG II and losartan (Sigma-Aldrich, St. Louis, MO, USA) were diluted in the culture medium to a final concentration of 100 µM (ANGII) or 0.01 µM (losartan). Cells were incubated for 6 h and 24 h with ANGII and 48h with losartan, and the conditioned medium was kept for secretome analyses.

2.2. Relative Quantification of Podocyte Associated Gene Expression by Real-Time PCR

Real-time PCR of podocyte associated gene expression was performed as follows:

Real-time measurements were carried out on the Step One Plus Real-Time PCR Systems using MicroAmp Fast optical 384 well reaction plate and Power Sybr Green PCR Master Mix (Applied Biosystems, Foster City, CA, USA). The amplification conditions were denaturation at 95 °C for 13 min followed by 37 cycles of 95 °C for 50 s, 60 °C for 45 s, and 72 °C for 30 s. Primer sequences are listed in Supplementary Table S1. Results were analyzed by the $2^{-\Delta\Delta\text{-CT}}$ method [29].

2.3. Bisulfite Genomic Sequencing

Bisulfite sequencing was performed following bisulfite conversion with the EpiTec Kit (Qiagen, Hilden, Germany) as described [30]. Primers were designed after excluding pseudogenes or other closely related genomic sequences that could interfere with specific amplification by amplicon and primer sequences comparison in the BLAT sequence data base (https://genome.ucsc.edu/FAQ/FAQblat.html last accessed 27 January 2021). PCR primers are listed in Supplementary Table S2.

Briefly, the amplification conditions were denaturation at 95 °C for 13 min followed by 37 cycles of 95 °C for 50 s, 54 °C for 45 s, and 72 °C for 30 s. The amplification product is 270 bp in size. Amplification products were cloned into pCR2.1 vector using the TA Cloning Kit (Invitrogen, Carlsbad, CA, USA) according to the manufacturer's instructions. On average, 30 clones were sequenced using the BigDye Terminator Cycle Sequencing Kit (Applied Biosystems) on a DNA analyzer 3700 (Applied Biosystems) with M13 primer to obtain a representative methylation profile of each sample. The 5′-regulatory gene sequences referred to the +1 transcription start of the following sequence:

Homo sapiens WT1 transcription factor (WT1), RefSeqGene (LRG_525) on chromosome 11; NCBI Reference Sequence: NG_009272.1;

Homo sapiens NPHS2, podocin (NPHS2), RefSeqGene (LRG_887) on chromosome 1; NCBI Reference Sequence: NG_007535.1;

2.4. Immunofluorescence Staining

Cells were fixed with 4% paraformaldehyde (PFA) (Polysciences, Warrington, FL, USA). To block unspecific binding sites, the fixed cells were incubated with blocking buffer containing 10% normal goat or donkey serum, 1% BSA, 0.5% Triton, and 0.05% Tween for 2 h at room temperature. Incubation of the primary antibody was performed at 4 °C overnight in staining buffer (blocking buffer diluted 1:1 with PBS). After at least 16 h of incubation, the cells were washed three times with PBS/0.05% Tween and incubated with a 1:500 dilution of secondary antibodies dilution. Afterwards, the cells were washed again three times with PBS/0.05% Tween, nuclei were stained with Hoechst 1:5000 (Thermo Fisher Scientific, Waltham, MA, USA), and podocyte cytoskeleton was stained with Alexa Flour 488 phalloidin (Thermo Fisher Scientific) (1:400). Images were captured using a fluo-

rescence microscope (LSM700; Zeiss, Oberkochen, Germany) with Zenblue software (Zeiss). Individual channel images were processed and merged with Fiji. Detailed information on the used antibodies are given in Supplementary Table S3.

2.5. Microarray Data Analyses

Total RNA (1 µg) preparations were hybridized on the PrimeView Human Gene Expression Array (Affymetrix, Thermo Fisher Scientific, USA) at the core facility Biomedizinisches Forschungszentrum (BMFZ) of the Heinrich Heine University Düsseldorf. The raw data were imported into the R/Bioconductor environment and further processed with the package affy using background correction, logarithmic (base 2) transformation, and normalization with the robust multi-array average (RMA) method. The heatmap.2 function from the gplots package was applied for cluster analysis and to generate heatmaps using Pearson correlation as similarity measure. Gene expression was detected using a detection *p*-value threshold of 0.05. Differential gene expression was determined via the *p*-value from the limma package, which was adjusted for false discovery rate using the q value package. Thresholds of 1.33 and 0.75 were used for up-/downregulation of ratios and 0.05 for *p*-values. Venn diagrams were generated with the Venn diagram package. Subsets from the Venn diagrams were used for follow-up GO and pathway analyses as described by Zhou et al. [31]. Gene expression data will be available online at the National Centre of Biotechnology Information (NCBI) Gene Expression Omnibus. For the principal component analysis (PCA), expression data were filtered for a coefficient of variation greater than 0.3. The PCA was carried out with the R Built-in function prcomp, and the first two principal components were plotted.

2.6. Secretome Analyses

Conditioned media from control podocytes as well as ANG II-treated cells were analyzed using the Proteome Profiler Human Kidney Biomarker Array Kit distributed by Research And Diagnostic Systems, Inc. (Minneapolis, MN, USA) as described by the manufacturer. Obtained images were analyzed by using the ImageJ software [32] with the microarray profile plugin by Bob Dougherty and Wayne Rasband (https://www.optinav.info/MicroArray_Profile.html last accessed 20 October 2021). The integrated density generated by the microarray profile plugin function Measure RT was used for follow-up processing, which was performed in the R/Bioconductor environment [33]. Arrays were normalized employing the robust spline normalization from the Bioconductor lumi package [34]. A threshold for background intensities was defined at 5% of the range between maximum and minimum intensity and a detection *p*-value was calculated according to the method described in Graffmann et al. [35].

2.7. Cluster Analysis of the Renin–Angiotensin Pathway

Pathways and associated genes were downloaded from the KEGG database [36] in July 2020 and annotated with official gene symbols. Genes from the KEGG pathway hsa04614 renin–angiotensin system were extracted from the microarray data normalized with the RMA method from the package oligo [37] in R/Biocondcutor [33] as described above and subjected to the R heatmap function using Pearson correlation as similarity measure and color scaling per row.

2.8. Western Blot Analysis

Podocytes were lysed in lysis buffer containing 5 M NaCl, 1% NP-40, 0.5% DOC, 0.1% SDS, 1 mM EDTA, 50 mM Tris, pH 8.0, and freshly added 10 µL/mL protease- and phosphatase inhibitor (Sigma Aldrich). An amount of 20 µg of the obtained protein lysate was resolved in a 10% sodium dodecyl sulfate-PAGE gel and transferred onto Immobilon-P membrane (Merck Millipore, Burlington, VT, USA). Membranes were probed with primary antibody at 4 °C overnight, washed three times with 0.1% Tween-20 in Tris-buffered saline, and incubated with secondary antibody for 1 h at room temperature. The signals were

visualized with enhanced luminescence Western Bright Quantum (Advansta, Bering Dr, San Jose, CA, USA) and quantified using ImageJ [38]. Detailed Information of the used antibodies are given in Supplementary Table S3.

2.9. Statistics

Data are presented as arithmetic means + standard error. In total, three independent experiments were performed and used for the calculation of mean values. Statistical significance was calculated using the two-sample Student's *t*-test or the one-way ANOVA test [39] with a significance threshold $p = 0.05$.

2.10. Albumin Endocytosis Assay

The functionality of podocyte differentiated from urine-derived renal progenitor cells was analyzed employing the albumin endocytosis assay. In brief, podocytes were plated at low density of 10% in a 12-well plate coated with 0.2% type 1 collagen. Forty-eight hours later, the cells were washed with 1x PBS and replaced with podocyte culture medium supplemented with 20 µg/mL of BSA-Alexa Fluor™ 488 and incubated at 37 °C for 60 min. After incubation, the cells were washed 3x with cold PBS and fixed with 4% PFA for 15 min. Finally, the images were taken at the excitation wavelength of 488 nm and an emission wavelength of 540 nm using a LSM700 florescence microscope.

3. Results

3.1. Generation of Human Podocytes from Urine-Derived Renal Progenitor Cells Is Enhanced by Retinoic Acid

We recently reported a "rice grain" fibroblast-like morphology resembling MSCs isolated directly from urine samples of four male (UM) and six female (UF) donors. These cells express the renal stem cell markers SIX2, CITED1 WT1, CD133, CD24, and CD106, and we referred to these cells as urine-derived renal progenitor cells (UdRPCs) [28]. UdRPCs maintain their stem cell features for almost 12 passages (Figure 1a). So far, we have established a differentiation protocol leading to renal epithelial proximal tubular lineage by supplementation with the GSK3ß-inhibitor (CHIR99021) or to podocytes as described in Figure 1a. UdRPCs acquire the typical podocyte "fried egg" shape morphology after 7 days when cultured at 70% confluency in adv. RPMI medium supplemented with retinoic acid (RA). This protocol was applied to cells isolated from human urine of several individuals (age ranged between 27 and 76 years), resulting in the robust generation of podocytes, which was enhanced by the addition of 30 µM rentinoic acid to the culture medium (Figure 1a). For further analysis we evaluated mRNA expression of the two most abundant proteins within the FPs and SD of human podocytes, nephrin (*NPHS1*) and synaptopodin (*SYNPO*), respectively, by quantitative real-time PCR. We analyzed mRNA expression of podocytes derived from five individuals with and without the addition of 30 µM retinoic acid—three males (UM27, UM48, and UM51) and two females (UF31 and UF45)—and compared them to their undifferentiated counterparts. Since the undifferentiated control was set to one for all cell lines, we decided in terms of illustrative purposes to only show one column representative of all the controls. The comparison between both culture conditions (with and without the addition of RA) by the one-way ANOVA test revealed no significant changes between the podocytes and their differentiated counterparts, with *p*-values of *NPHS1* = 0.174381 and SYNPO = 0.173116. Additionally, the transcriptional changes for *NPHS1* and *SYNPO* were found to be not significantly upregulated, while cells were grown under adv. RPMI conditions without the addition of RA in comparison with their undifferentiated counterparts ($p = 0.16$) by a two-sample Student's t-test. In contrast, the expression of *NPHS1* ($p = 0.05$) and *SYNPO* ($p = 0.04$) was found to be significantly upregulated, ranging from 1.4-fold to 11.6-fold for NPHS1 and 1.1-fold to 3.9-fold for *SYNPO* in the RA-differentiated podocytes compared with the respective UdRPCs (Figure 1b,c) by a two-sample Student's t-test. These findings highlight the importance of the addition of retinoic acid during the differentiation of UdRPCs into podocytes. These findings were

confirmed by immunofluorescence blot-based detection of expression of nephrin (NPHS1), podocin (NPHS2), and synaptopodin (SYNPO), as well as Western blot-based detection for nephrin and synaptopodin (Figure 2a,b and supplementary Figures S8 and S9) in all five analyzed cell lines, except for nephrin expression in the UF45-derived podocytes. While podocytes cultured in adv. RPMI already showed expression of all three proteins, which were necessary for podocyte functionality, the addition of retinoic acid significantly increased the protein expression levels of nephrin ($p = 0.04$), with fold changes ranging from 1.4 to 14.95, and a strong trend towards significance for synaptopodin ($p = 0.12$) with fold changes ranging from 1.5 to 7.8 was observed (Figure 2a,b and Supplementary Figure S1j). Of note, different expression levels for nephrin and synaptopodin were detected between the used cell lines, which might reflect individual variabilities based on age, ethnicity, and sex. Additionally, we measured the expression of LIM homeobox transcription factor 1, beta (*LMX1b)* and *WT1* within the UM51 podocytes with and without the addition of retinoic acid by quantitative real-time PCR and nephrin, podocin, and CD2-associated protein (CD2AP) expression by immunofluorescence-based detection (Supplementary Figure S6a–h). While the addition of retinoic acid had only minor impact on the expression of *LMX1b* and *WT1* (both with a fold change of 0.2), the expression levels of CD2AP were found to be highly increased. To show methylation changes within the 5′-regulatory region of the key podocyte transcription factor WT1, we applied bisulfite genomic sequencing. In total, a 270 bp long WT1 promoter fragment spanning 19 cytosine-phosphatidyl-guanine-(CpG)-dinucleotides was analyzed. We found, that the undifferentiated UdRPCs UM51 had a dense methylation pattern at CpG position 12 and 13 of the 5′-regulatory region (Figure 2c). Upon applying our differentiation protocol, methylated DNA at the respective positions for UM51-derived podocytes was found to be almost completely lost. As a mark of renal cell functionality, albumin endocytosis was observed after exogenous BSA was supplemented to the culture medium (Supplementary Figure S10).

3.2. Comparative Transcriptome Analysis of Urine-Derived Renal Progenitor Cells with Their Podocyte Counterparts

After the successful and reproducible differentiation of UdRPCs into podocytes, we performed a comparative transcriptome analysis of UF45, UM48, and UM51. Hierarchical clustering analysis comparing the transcriptomes of UdRPCs with podocytes revealed a distinct expression pattern of both cell types (Figure 3a). By comparing the expressed genes (det-$p < 0.05$), 250 were exclusively expressed in the UdRPCs and 600 in podocytes (Figure 3b). The most over-represented gene ontology and biological processes (GO BP)-terms exclusive to UdRPCs were associated with cell division and activation of the pre-replicative complex. In comparison, the most over-represented GO-BP terms exclusive to podocytes were associated with cell fate commitment, cell morphogenesis, and regulation of ion transport (Figure 3c). In total, 13,762 genes were found to be expressed in common between UdRPCs and podocytes; of these, 671 were upregulated and 904 were downregulated in podocytes (Figure 3b). The downregulated genes were again associated with cell cycle processes and methylation (Figure 3e). In contrast, upregulated genes were associated with cell adhesion, positive regulation of cell migration, cell substrate adhesion, morphogenesis of an epithelium, and regulation of cytokine production (Figure 3d). Furthermore, genes annotated under the GO-BP term morphogenesis of an epithelium are known to be critical effectors either for epithelial–mesenchymal transition (EMT) or mesenchymal–epithelial transition (MET). The generated podocytes expressed numerous genes that were annotated with neuronal GO-BP terms, such as axonogenesis, axon guidance, chemotaxis, and regulation of axonogenesis (Supplementary Table S4). Furthermore, we analyzed the expression of several solute carrier (SLC) family members (Supplementary Figure S2). Both analyses revealed distinct expression patterns of UdRPCs and their differentiated counterparts. In particular, the SLC genes were found to be exclusively upregulated in podocytes. Key genes associated with the podocyte morphology, such as podocalyxin (*PODXL)*, *NPHS1*, *NPHS2*, and *SYNPO*, were found to be upregulated in the differentiated podocytes of all three

individuals. Interestingly undifferentiated UdRPCs expressed *CD2AP* (an important stabilizer of the slit diaphragm), which was highly upregulated by our differentiation protocol (Supplementary Figure S1e–f). In addition, our results provide detailed information about genes exclusively expressed in human UdRPCs that are mesenchymal and differentiated podocytes that are epithelial (Supplementary Tables S4–S6 and S10).

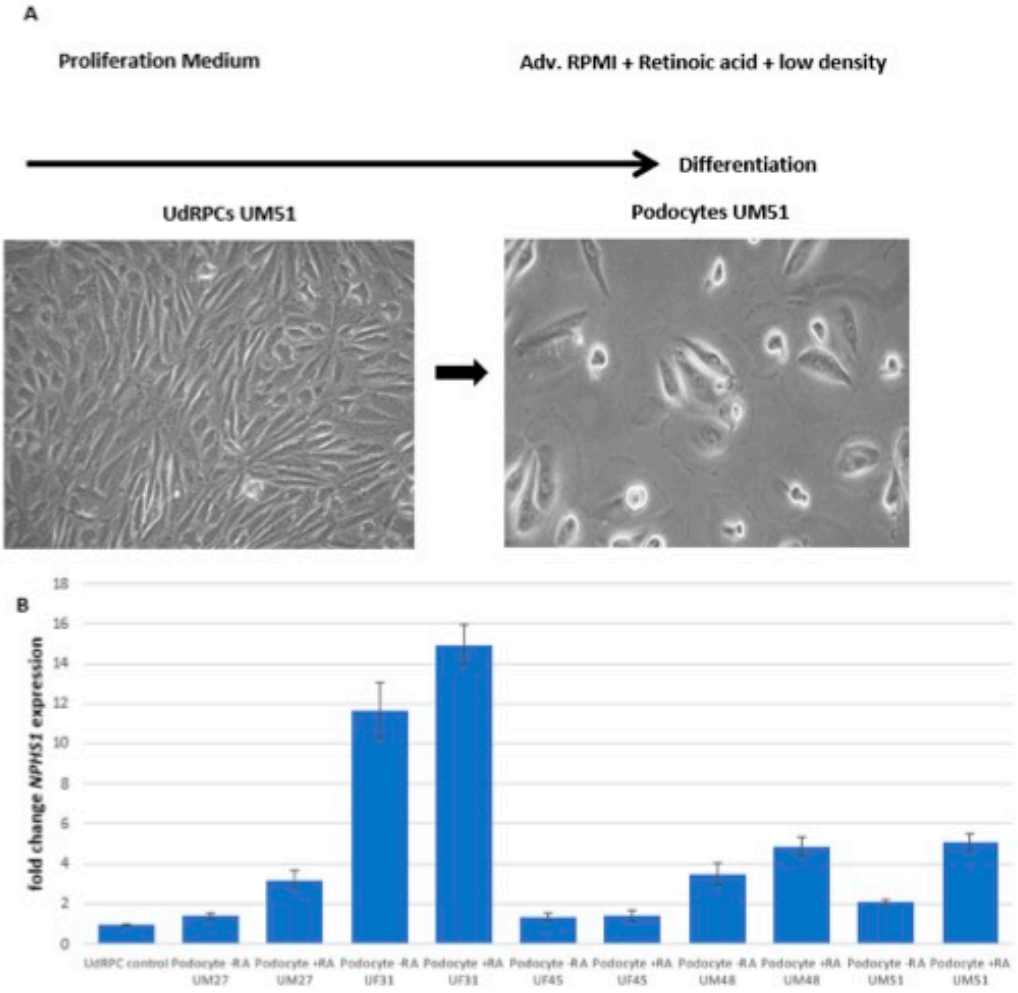


Figure 1. *Cont.*

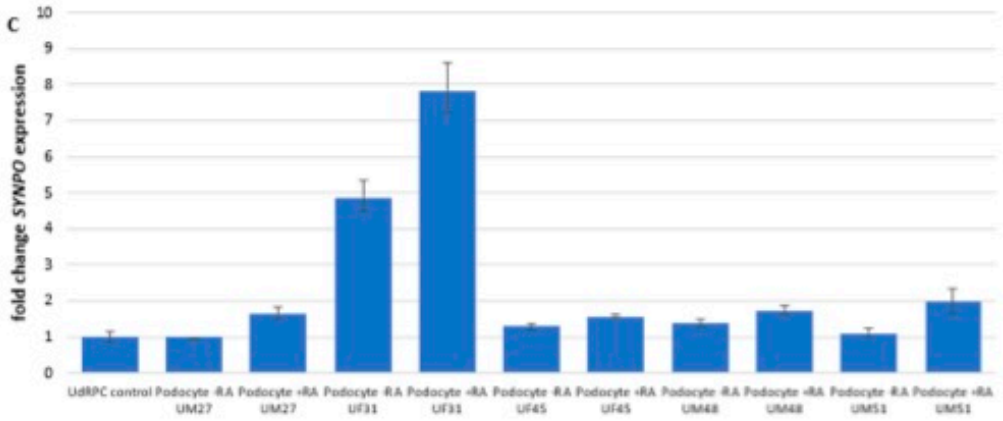


Figure 1. Derivation of mature and functional podocytes from human urine-derived renal progenitor cells. The self-renewal capacity of UdRPCs is maintained by proliferation medium. Differentiation of UdRPCs into podocytes is induced by low density cultivation in adv. RPMI supplemented with 30 µM retinoic acid (**A**). Expression of the podocyte associated genes NPHS1 (**B**) and SYNPO (**C**) was determined by quantitative real-time PCR.

3.3. *Effect of Angiotensin II (ANGII) on Podocyte Morphology and Expression of Podocyte-Specific Genes*

Elevated levels of ANGII have been identified as a main risk factor for the initiation and progression of chronic kidney disease (CKD); furthermore, increased ANGII concentrations are associated with the downregulation of nephrin and synaptopodin expression in podocytes [11,12]. To evaluate the capacity of our generated podocytes modelling of acute and chronic kidney injury, we prepared a final concentration of 100 µM ANGII in adv. RPMI medium supplemented with 30 µM retinoic acid and treated podocytes derived from three individuals—two-males African (UM48 and UM51) and one female Caucasian (UF45)—cultured under low density conditions for 6 h and 24 h, respectively. This analysis was performed for podocytes cultured under low (Figure 4) as well as high cell density (Supplementary Figure S1). After 6 h, dynamic changes in morphology could be observed by immunofluorescence-based detection of α-actinin expression (Figure 4a and Supplementary Figure S3a). While untreated podocytes showed the typical "fried egg" morphology, ANG II-treated podocytes derived from all three individuals underwent massive disruption of the cytoskeleton, resulting in the inhibition of podocyte spreading and subsequent loss of cellular processes, as observed by the round and condensed morphology (Figure 4a and Supplementary Figure S3a). To confirm that the disruptive effect is indeed mediated by ANGII, the effects on the cytoskeleton were evaluated by gene-specific mRNA expression of both ANGII receptors (*AGTR1* and *AGTR2*), as well as podocyte key structural proteins *NPHS1* and *SNYPO* (Figure 4b–e). Both receptors were found not to be significantly regulated (*AGTR1* $p = 0.48$ and *AGTR2* $p = 0.44$) upon ANGII treatment. While *AGTR1* expression showed a trend of downregulation with fold changes ranging between 0.6 and 0.9, *AGTR2* was found to be upregulated with fold changes ranging between 1.2 and 2.2 in podocytes derived under low density cultivation from all three individuals after 6 h (Figure 4b,c). Interestingly when the cells were cultured under high density conditions, both receptors seemed to be upregulated due to the ANGII treatment after 6 h, with the only exception for *AGTR2* in UF45 podocytes (Supplementary Figure S3b,c). When the ANGII treatment was prolonged to 24 h, the mRNA expression level of *AGTR1* was still downregulated in UM48 podocytes cultured under low density conditions (fold change 0.6), at a similar level as in 6 h, while UM51 podocytes showed a modest 2.6-fold increase,

and in podocytes, UF45 *AGTR1* expression was highly increased by 8.6-fold. Furthermore, *AGTR2* mRNA expression was found to be elevated after 24 h in all three derived podocytes, with fold change increases ranging from 1.2 to 21.1. The mRNA expression of *NPHS1* and *SYNPO* was significantly downregulated, as revealed by the one-way ANOVA test ($p = 0.03$ and 0.04 respectively) upon ANGII treatment in all individuals and culture conditions, except for the *SYNPO* expression in podocytes UF45 under high density cultivation, which was upregulated (Figure 4d,e and Supplementary Figure S3d,e), with fold changes ranging between 0.1 and 0.8 for *NPHS1* and 0.2 and 0.8 for *SYNPO*. Podocytes cultured under low density conditions showed only minor changes in *NPHS1* and *SYNPO* expression after 6 h of ANGII treatment, while mRNA expression in UM51 and UM48 podocytes cultured under high density was found to be downregulated by 2.6- and 1.7-fold (*NPHS1*) and 2.6- and 1-fold (*SYNPO*), respectively (Supplementary Figure S3b,c). When ANGII treatment was prolonged to 24 h under low density conditions, UM48 and UM51 podocytes both showed downregulated expression of *NPHS1* expression, 0.9-fold and 3-fold, respectively. In contrast, expression of *SYNPO* remained at similar levels seen in 6 h of ANGII treatment. To evaluate whether the transcriptional changes of cytoskeleton-associated genes could be in part mediated by epigenetic modifications, we applied bisulfite genomic sequencing to analyze the methylation status of a CpG-rich region of the *NPHS2* promoter. In total, a 415 bp long *NPHS2* fragment 11 bp upstream of the TSS, spanning 23 CpG-dinucleotides, was analyzed, and this revealed a lack of methylation changes occurring during 6 h of ANGII treatment in UM51 podocyte (Supplementary Figure S4). Activation of the angiotensin receptors has been linked to the regulation of many biological processes. While AGTR1 mediates cellular functions such as vasoconstriction, cell proliferation, nephrosclerosis, vascular media hypertrophy, endothelial dysfunction, inflammation, and immune responses and promotes aging, signaling trough AGTR2 has been linked to vasodilation, development, cell differentiation, tissue repair, and apoptosis [40,41]. To evaluate whether the disruptive effect of ANGII is mediated by AGTR1 signaling, we treated the UM51 podocytes with a 0.01 µM solution of the selective, competitive angiotensin II receptor type 1 antagonist losartan in combination with 100 µM ANGII. Strikingly, we found a significant upregulation of podocyte key structural proteins *NPHS1* ($p = 0.03$, fold change 24) and *SNYPO* ($p = 0.04$; fold change 6.7) within the podocytes UM51 treated with 0.01 µM losartan compared with cells only treated with ANGII and control podocytes (Figure 4g,h) by a two-sample Student's *t*-test. While synaptopodin also showed a significant increase in protein expression, as detected by Western blot analysis ($p = 0.01$), nephrin protein expression was found to be still downregulated by ANGII, but to a much lower extend compared to ANGII treatment alone (Figure 4f and Supplementary Figure S5). To conclude, our data indicate that the cytoskeletal disruption was mainly mediated through AGTR1 signaling and that it could be rescued by the addition of the competitive angiotensin II receptor type 1 antagonist losartan.

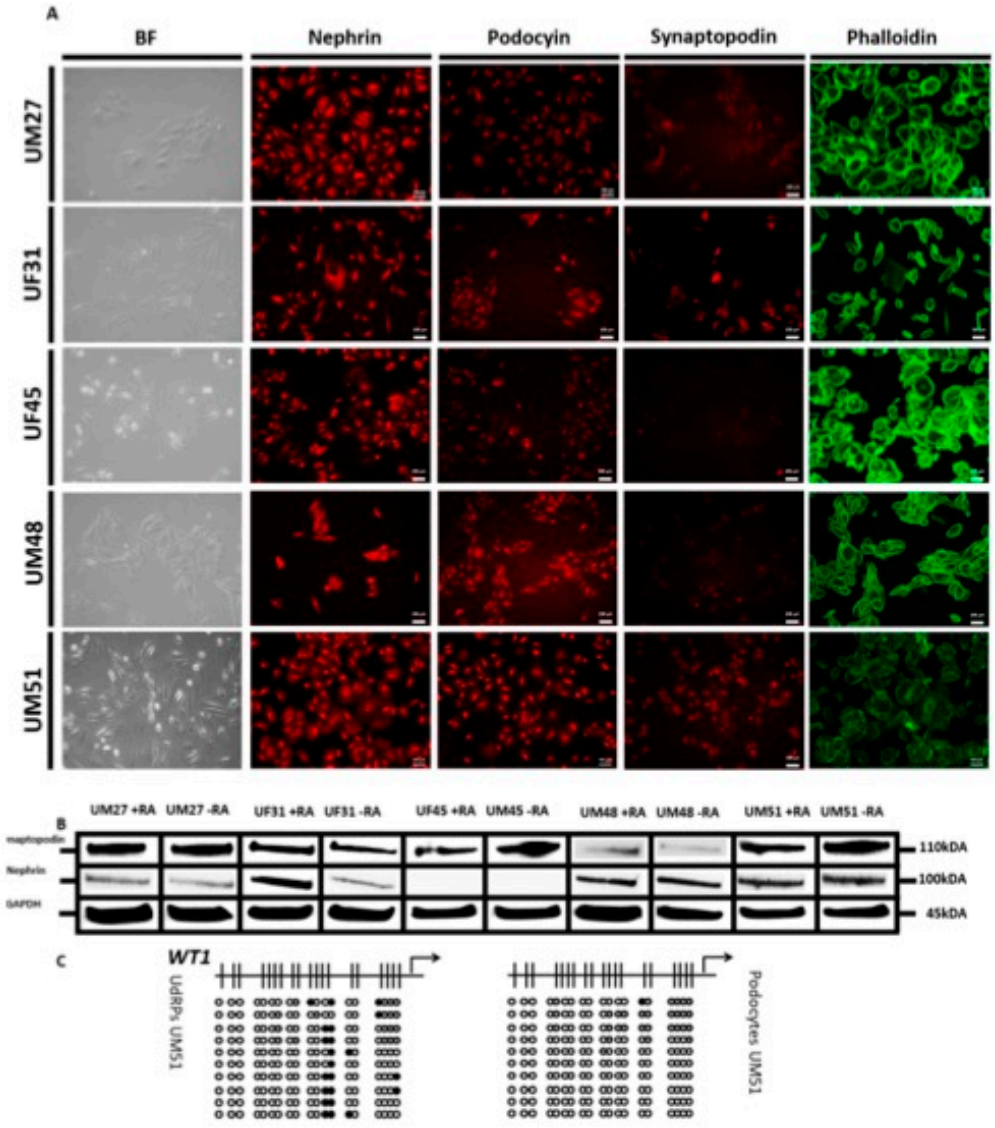


Figure 2. Retinoic acid enhances the maturation of UdRPC-derived podocytes. UdRPCs differentiated into podocytes by low density cultivation in advanced RPMI medium supplemented and with 30 µM retinoic acid. Immunofluorescence-based detection of nephrin, podocin, and synaptopodin expression. Podocyte cytoskeleton was stained with phalloidin (**A**). Expression of podocyte markers nephrin and synaptopodin was determined by Western blot-based detection (**B**). Bisulfite genomic sequencing of a 270 bp long WT1 promoter fragment, spanning 19 CpG-dinucleotides, provides detailed information about the dynamic DNA methylation changes occurring during the differentiation process into podocytes (**C**). Black, white, and grey circles refer to methylated, unmethylated, and undefined CpG dinucleotides, respectively. UdRPCs show dense methylation patterns at CpG position 12 and 13, whilst differentiated podocytes show a lack of methylation.

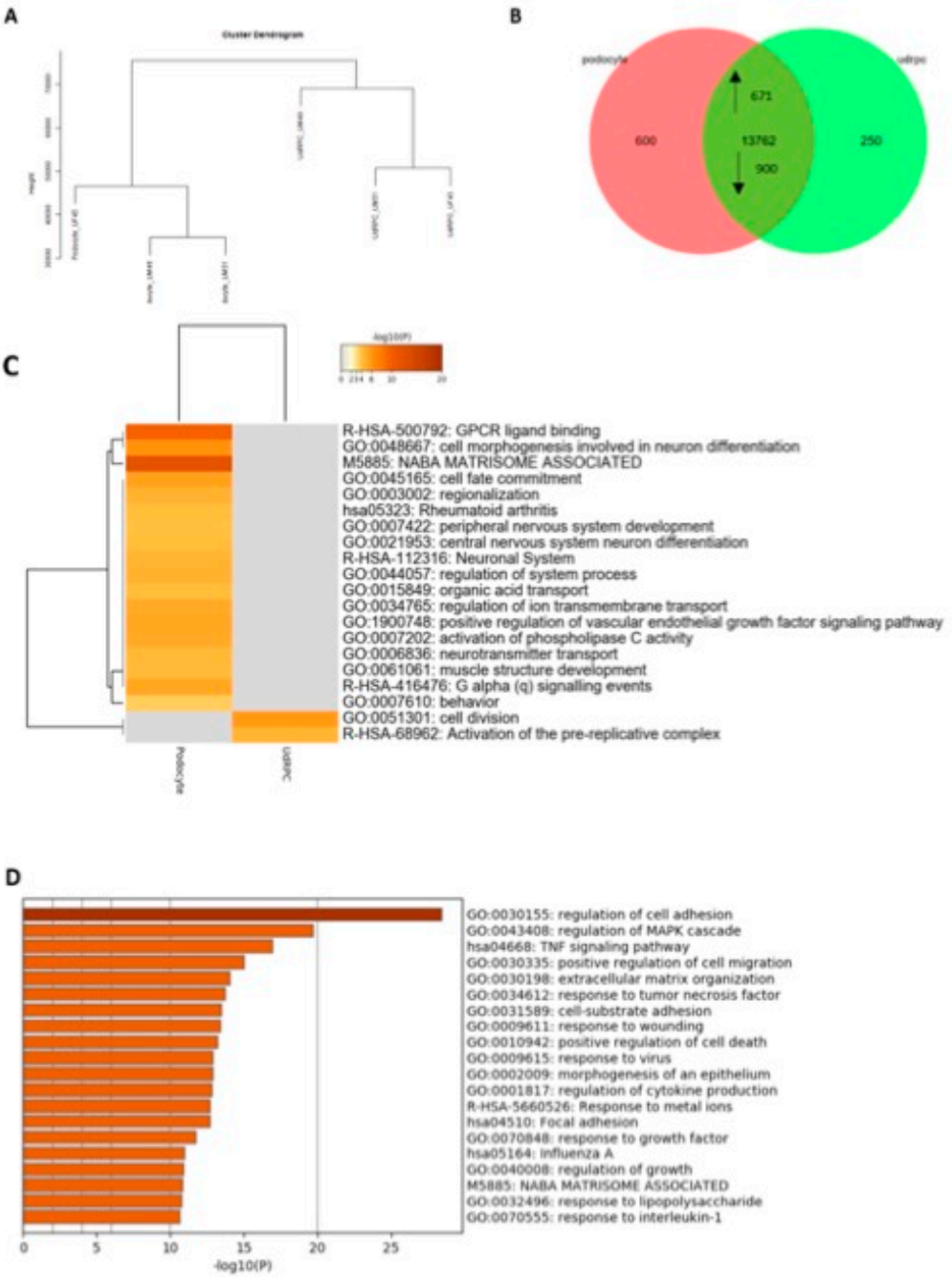


Figure 3. *Cont.*

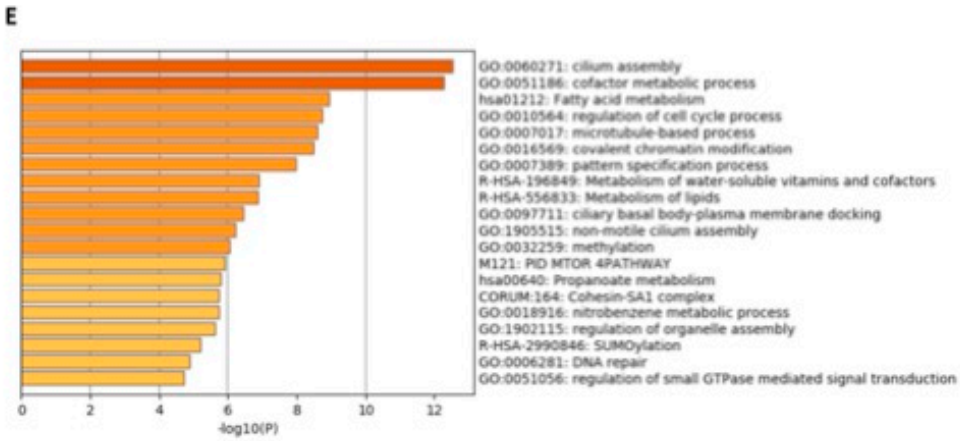


Figure 3. Comparative transcriptome and Gene Ontology analysis of urine-derived renal progenitors UF45, UM 48, UM51, and derived podocytes. A hierarchical cluster dendrogram revealed distinct clusters of UdRPCs and their derived podocytes. (**A**). Expressed genes (det-$p < 0.05$) in UdRPCs and podocytes compared in the Venn diagram (**B**) show distinct (600 in podocytes; 200 in UdRPCs) and overlapping (13,762) gene expression patterns. Of the overlapping genes, 671 are upregulated and 900 are downregulated in podocytes. The most over-represented GO-BP terms exclusive in either UdRPCs or podocytes are shown in (**C**) and include cell division and activation of the pre-replicative complex for the UdRPCs and cell fate commitment, cell morphogenesis, and regulation of ion transport for the podocytes. The upregulated 671 genes in podocytes, are associated with cell adhesion, positive regulation of cell migration, cell substrate adhesion, morphogenesis of an epithelium, and regulation of cytokine production (**D**), while downregulated 900 genes are associated with cell cycle processes and methylation (**E**).

3.4. Effects of Angiotensin II on the Transcriptome and Secretome of Urine-Derived Podocytes

To further investigate the effect of ANGII, we performed a comparative transcriptome analysis of UM48 and UM51 podocytes grown under high density conditions after 6 h and 24 h of ANGII treatment ($n = 2$ biological replicates per genotype). Hierarchical clustering and principal component analysis (PCA) comparing the transcriptomes of non-treated and treated podocytes revealed distinct transcriptomes for the three conditions—without treatment and 6 h and 24 h of ANGII treatment, respectively (Figure 5a and Supplementary Figure S11). Interestingly, while podocytes treated for 6 h seem to cluster rather by their genetic background, the cells treated for 24 h formed a distinct cluster. Further analyses identified 478 genes (det-$p < 0.05$) exclusively expressed under the control conditions and 63 genes under the 6 h angiotensin conditions (Figure 5b). The most over-represented GO-BP terms derived from the 478 genes are associated with growth and locomotion (Figure 5d). In contrast, the most over-represented GO-BP terms linked to the 63 genes are associated with immune system process, response to stimulus, and cell proliferation (Figure 5d). In total, 13,783 non-regulated genes were found to be expressed in common between both conditions. By comparing the expressed genes (det-$p < 0.05$) after 24 h of ANGII treatment, 339 genes were found to be exclusively expressed in the control podocytes and 335 genes in the treated cells (Figure 5c). The most over-represented GO-BP terms of the 339 genes are associated with multi-organism process, multicellular organismal process, and locomotion (Figure 5e). In contrast the most over-represented GO-BP terms linked to the 335 genes are associated with cell proliferation and immune system process (Figure 5e). The full gene list can be found in Supplementary Table S7a,b. In total 13,922 genes were found to be expressed in common between both conditions, from which 1287 were upregulated and 1100 downregulated after 24 h of ANGII treatment

(Supplementary Tables S8 and S9). The upregulated genes are associated with cell cycle, DNA repair, cell cycle phase transition, methylation, and regulation of cellular response to stress (Figure 5f). Interestingly genes annotated for the GO-BP terms cell cycle and methylation were also found in the undifferentiated UdRPCs. The downregulated genes after 24 h ANGII treatment are associated with regulation of cell adhesion, cell junction organization, axonogenesis, actin cytoskeleton organization, and tissue and gland morphogenesis (Figure 5g). Finally, expression of numerous genes annotated under the GO-BP term actin cytoskeleton organization were downregulated upon 24 h ANGII treatment and revealed a distinct clustering of UdRPCs, podocytes and podocytes treated with ANGII for 24 h. The full gene list is given in Supplementary Tables S4, S9 and S11. It is interesting to note that most of these genes also showed basal levels of expression in undifferentiated UdRPCs. These findings further emphasize the disruptive effect of ANGII on the cytoskeleton of podocytes, as it has been observed by immunofluorescence-based detection of protein expression and q-RT PCR. An overview of the KEGG annotated renin–angiotensin system is given in Supplementary Figure S6.

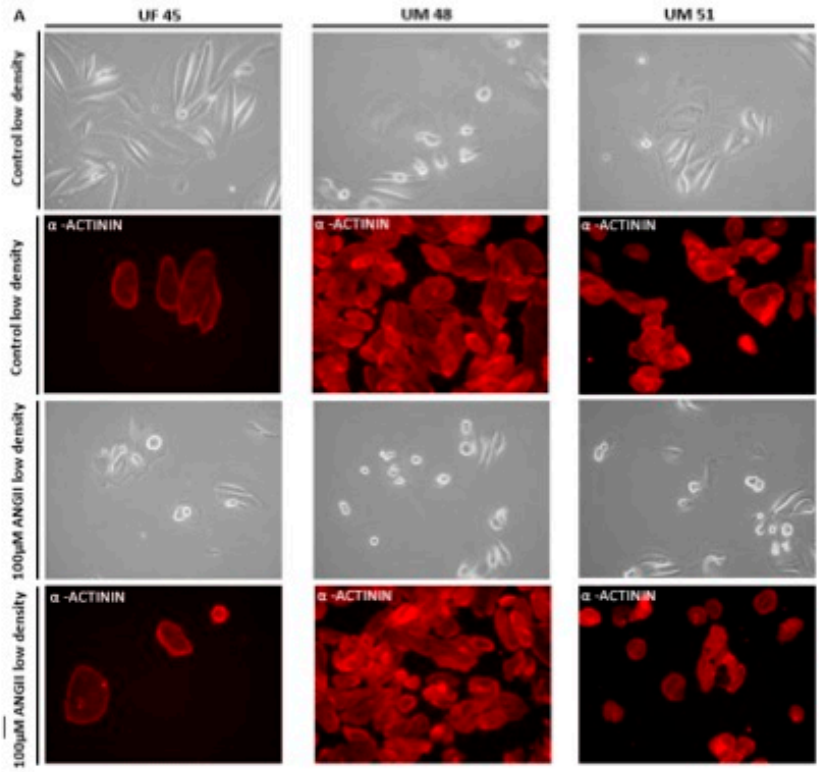


Figure 4. *Cont.*

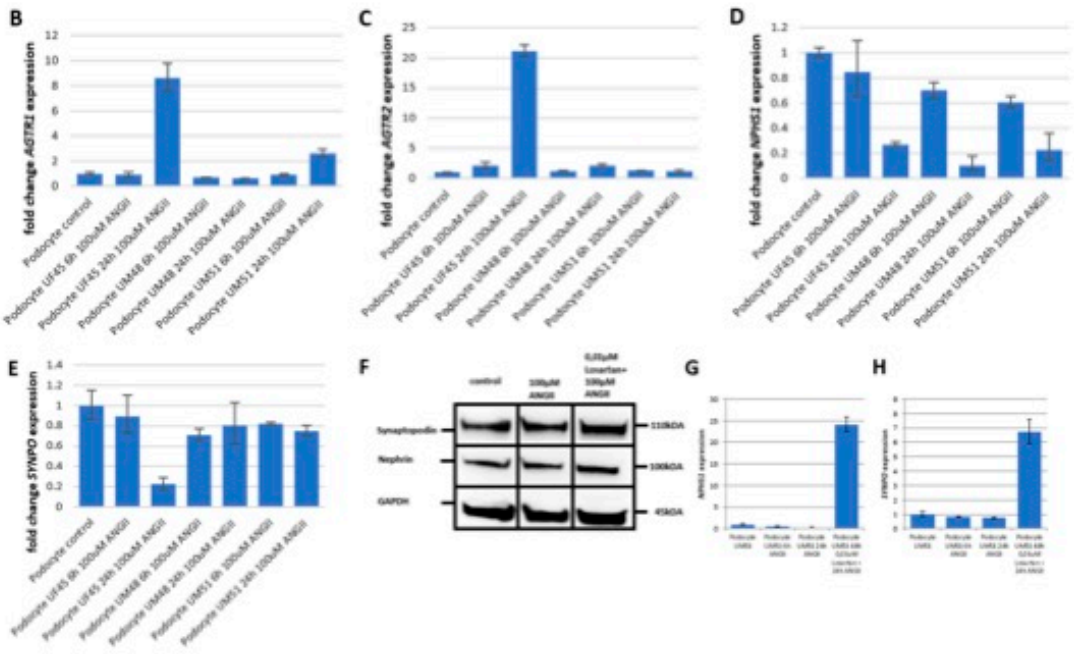


Figure 4. Dynamic changes in the morphology of human urine-derived podocytes post treatment with angiotensin II (ANGII) after 6 h and 24 h and is rescued by losartan. UdRPC-differentiated podocytes from UF45, UM48, and UM51. The top panel (phase contrast) shows the typical "fried egg" shaped podocyte morphology. The lower two panels show morphology changes after 6 h of 100 µM ANGII treatment. Podocyte cytoskeleton was visualized by immunofluorescence-based detection of α-actinin in red (**A**). ANG II interferes with the cytoskeleton of the podocytes, inhibiting podocyte spreading and leading to the observed roundish phenotype. Expression of ANGII receptors *AGTR1* (**B**), and *AGTR2* (**C**) and expression podocyte markers *NPHS1* (**D**,**G**) and *SYNPO* (**E**,**H**) were determined by quantitative real-time PCR normalized with the ribosomal encoding gene-RPL0. An overview of the KEGG-annotated renin–angiotensin system is given in Supplementary Figure S5. Expression of podocyte markers nephrin and synaptopodin was determined by Western blot-based detection (**F**).

By analyzing the secretomes of podocytes with and without 6 h and 24 h of ANGII treatment, a plethora of significantly regulated secreted factors, specific for human kidney and associated with renal diseases, were identified (Supplementary Figure S7). In accord with the transcriptome data, only minor changes after 6 h of ANGII treatment could be observed, with only ANPEP being significantly altered. Major changes within the secretome were manifested after 24 h, resulting in a significant upregulation of EGF, EGFR, and RBP4 in podocytes UF45; adiponectin (ADIPOQ), membrane alanyl aminopeptidase (ANPEP), annexin A5 (ANXA5), cellular communication network factor 1 (CCN1), epidermal growth factor (EGF), epidermal growth factor receptor (EGFR), fatty acid-binding protein 1 (FABP1), alpha 2-HS glycoprotein (AHSG), lipocalin 2 (LCN2), advanced glycosylation end-product specific receptor (AGER), retinol-binding protein 4 (RBP4), serpin family A member 3 (SERPINA3), tumor necrosis factor alpha (TNFA), vascular cell adhesion molecule 1 (VCAM1), and vascular endothelial growth factor (VEGF) in podocytes UM48 and ANPEP, C-X-C motif chemokine ligand 16 (CXCL16), CCN1, dipeptidyl peptidase 4 (DDP4), alpha 2-HS glycoprotein (AHSG), LCN2 and VEGF in podocytes UM51. Additionally, AGER and

VEGF in podocytes UF45, renin (REN) in podocytes UM48, and kallikrein-related peptidase 3 (KLK3) in podocytes UM51 were found to be significantly downregulated.

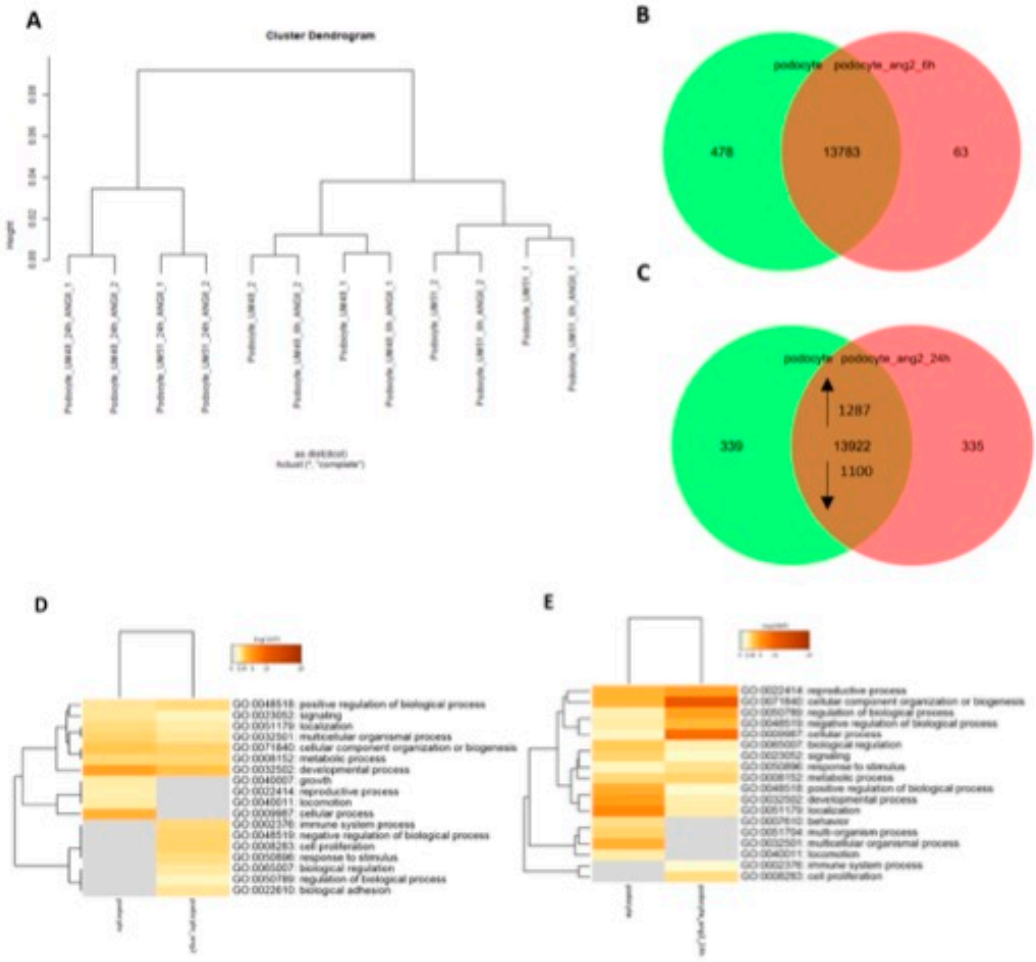


Figure 5. *Cont.*

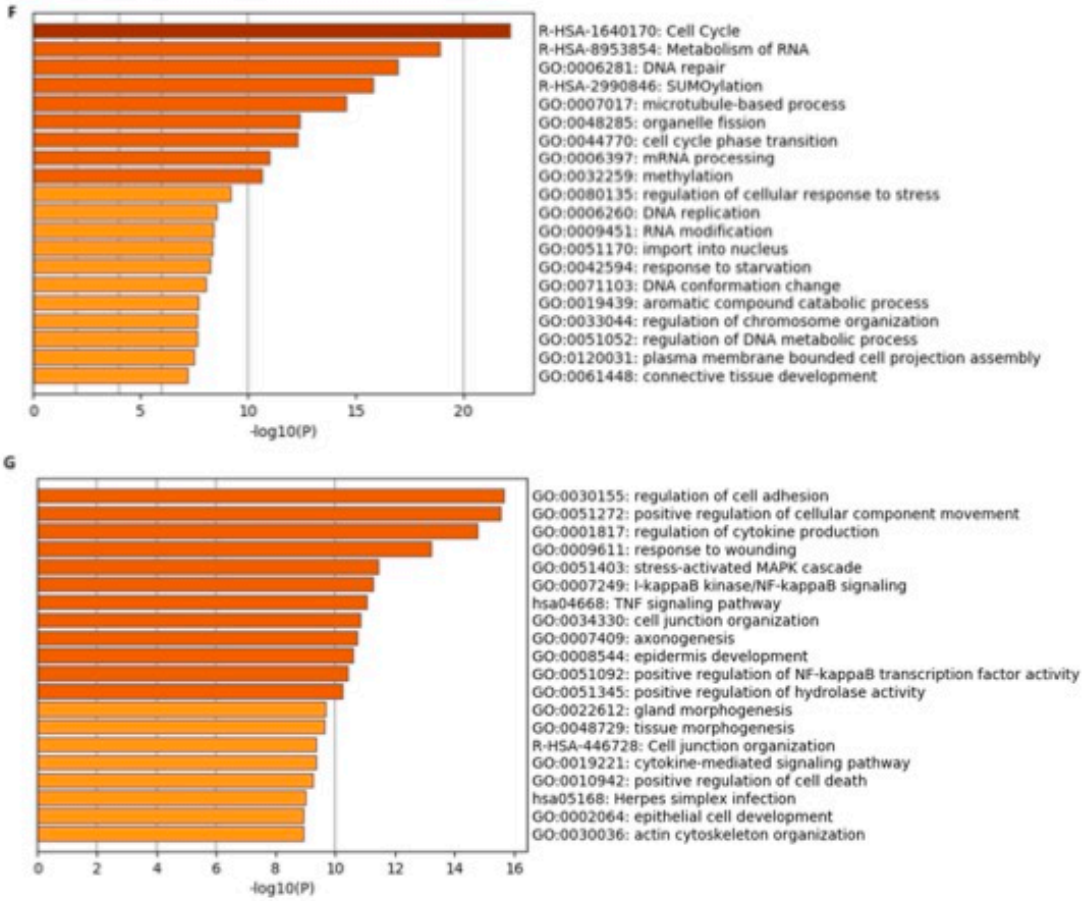


Figure 5. Comparative transcriptome and Gene Ontology analysis of untreated podocytes UM48 and UM51 and treated with angiotensin II for 6 h and 24 h. Podocytes were treated with ANGII (100 µM) for 6 h and 24 h. The hierarchical cluster dendrogram revealed 2 distinct clusters—24 h treated and 6 h treated and untreated cells as a cluster. (**A**). Expressed genes (det-$p < 0.05$) in podocytes and after ANGII treatment are compared by Venn diagrams after 6 h (**B**) and 24 h (**C**), revealing unique and overlapping expression patterns. The most over-represented GO-BP terms (13922 genes) common in either condition are shown in (**D**) after 6 h of treatment and (**E**) after 24 h. The terms include locomotion, growth, immune system process, response to stimulus biological adhesion, metabolic process, and cell proliferation for the treated podocytes. The 10 most over-represented GO-BP terms in the upregulated (1287) and downregulated (1100) genes in podocytes treated for 24 h with ANGII in comparison with untreated cells are shown in (**F**). The upregulated genes are associated with cell cycle, DNA repair, cell cycle phase transition, methylation, and regulation of cellular response to stress, while downregulated genes are associated with regulation of cell adhesion, cell junction organization, axonogenesis, actin cytoskeleton organization, and tissue and gland morphogenesis (**G**).

4. Discussion

The kidney glomerulus or renal corpuscle consists of a glomerular tuft and the Bowman's capsule. Its major task is the filtration of blood to generate urine, and it consists

of four distinct cell types of endothelial cells, mesangial cells, parietal epithelial cells of Bowman's capsule, and podocytes. In the present manuscript, we present a differentiation protocol for the successful and reproducible differentiation of UdRPCs into podocytes. These podocytes have the typical architecture and express podocyte-specific proteins synaptopodin, nephrin, and podocin, which are necessary for the establishment of either the slit diaphragm or the foot processes. The comparison of the transcriptomes pertaining to UdRPC-differentiated podocytes with previously reported datasets of iPSC-derived podocytes, biopsy-derived human glomeruli, and mouse podocytes [25] revealed distinct clustering of UdRPCs and their differentiated counterparts, whereas most of the genes were found to be upregulated after our differentiation protocol. As it has been reported by Ronconi et al., the addition of retinoic acid greatly enhanced the differentiation of UdRPCs into podocytes [42]. Furthermore, genes that are exclusively expressed or upregulated (det-$p < 0.05$) after our differentiation protocol, but that are not on the reported list [25], have been shown to be critical for podocyte morphology and/or function. Unique genes from our data that are associated with the filtration barrier or cytoskeleton of podocytes include the genes C-X3-C motif chemokine ligand 1 (*CX3CL1)* [43], dynamin3 (*DNM3)* [44], dipeptidyl peptidase 4 (*DPP4)* [45], and neurexin 1 (*NRXN1)* [46]. Unique genes from our data that are associated with podocyte function or survival include brain-derived neurotrophic factor *(BDNF)* [47], C-X-C motif chemokine ligand 16 (*CXCL16)* [48], glutamate ionotropic receptor AMPA type subunit 3 (*GRIA3)* [49], platelet-derived growth factor C (*PDGF-C)* [50], RAB3A, member RAS oncogene family *(RAB3A)* [51], and vascular endothelial growth factor C (*VEGF-C)* [52]. Members of the semaphorin gene family *SEMA3A* and *SEMA3C* were also significantly upregulated. Both are guidance proteins that are expressed during kidney development and that regulate kidney vascular patterning, endothelial cell migration, survival, uteric bud branching, and podocyte–endothelial crosstalk [53]. In a mouse model of semaphorin3a gain- and loss-of-function experiments revealed a dose-dependent role of semaphorin3a in podocyte differentiation and establishment of the glomerular filtration barrier [54].

During renal development, the glomerulus is established in four stages: the renal vesicle stage, the S-shaped body stage, the capillary loop stage, and the maturing-glomeruli stage [55]. This developmental process is initiated by the metanephric mesenchyme. It induces the ureteric bud epithelium to grow and finally to branch and form the collecting duct system of the kidney. Hereby, the mesenchymal cells of the metanephric mesenchyme have to form the polarized epithelial cells of the renal vesicle and therefore undergo a process that is referred to as mesenchymal-to-epithelial transition (MET) [56]. The podocytes in the glomerulus are generated by a population of cells within the parietal epithelium. These cells are thought to migrate into the glomerular tuft and then to differentiate into the mesenchyme-like podocytes [57,58]. Therefore, the maturation of podocytes is associated with a physiological epithelial-to-mesenchymal transition [1]. These developmental processes were also reflected in our transcriptome data. Genes that were upregulated in the derived podocytes were annotated with the GO-BP terms such as axon guidance and chemotaxis, thus enabling speculation that this might reflect the migration process during podocyte maturation. In addition, as differentiation into podocytes also involves both MET and EMT, it is not surprising that the upregulated dataset consists of numerous critical effectors for both processes; for instance, *wnt-1* has been reported to be a major driver of MET [59]. Interestingly, the genes caveolin 1 (*Cav1)* and discs large MAGUK scaffold protein 1 (*Dlg1)* have been linked to kidney development and renal pathological conditions in mice [56,60]. Further signs of EMT/MET are the differential expression of cell–cell contact-associated markers and functional changes associated with the conversion between mobile and stationary cells [61]. Confirmation that these changes are induced by our differentiation protocol is reflected in the podocyte upregulated dataset by the annotated GO-BP terms cell adhesion and cell substrate adhesion, as well as by the podocyte exclusive expression of the collagens *COL12A1* and *COL14A1*.

Developmental processes are regulated by epigenetic mechanisms, and these are of fundamental importance for cellular differentiation [62]. Epigenetic remodeling is associated with the establishment and removal of histone modifications and DNA-methylation to generate the cell type-specific epigenome. The epigenetic remodeling needed for the differentiation of UdRPCs into podocytes is also reflected by our transcriptome data. We observed downregulation of the de novo DNA-methyltransferase 3a (*DNMT3a*) as well as Tet methylcytosine dioxygenase 2 (*TET2*) in podocytes. Whilst DNMT3a is required for the establishment of CpG methylation during embryogenesis [63], the members of the Tet family are needed for the initiation of demethylation [64,65]. This targeted epigenetic remodeling during the differentiation process is manifested at the *WT1* promoter, as observed by bisulfite sequencing, therefore lending support to the speculation that this process is mediated by TET2. Furthermore, genes associated with the polycomb repressive complex, enhancer of zeste 1 polycomb repressive complex 2 subunit (*EZH1*) and SUZ12 polycomb repressive complex 2 subunit (*SUZ12*) [66], were also found to be downregulated. Specifically, EZH1 has been reported to be important for the maintenance of stem cell identity and execution of pluripotency [67]. Podocytes are terminally differentiated cells, which are unable to undergo cell division in vivo [1].

Of note, the derived podocytes were found to have upregulated the mRNA expression of several solute carrier family members (SLC) (Supplementary Figure S3). To our knowledge, this is the first report describing the expression of SLCs in human urine-derived podocytes. We propose that the abundance of solute carrier family members is due to the increase in transmembrane transport, as indicated by our podocyte exclusive GO-BP terms, regulation of ion transmembrane transport, neurotransmitter transport, organic acid transport, and chemical synaptic transmission. Furthermore, SLCs have been shown to be involved in human diseases and drug targets, thus establishing our human urine-derived podocytes as a valuable cellular tool for studying SLCs in renal development and under pathological conditions [68].

The major implications of the renin–angiotensin system (RAS) in humans are the maintenance of plasma sodium concentration, arterial blood pressure, and extracellular volume. Activation of the RAS leads to hypertension, cell proliferation, inflammation, and fibrosis and therefore has implications for all tissues of the body [69]. Angiotensin receptors and especially AGTR1 in the kidney have been reported to be primarily causative for hypertension in mammals [70] and are associated with renal sodium handling. AGTRs therefore have been recognized to be commonly expressed in several segments of the nephron, including the thick ascending limb, distal tubule, collecting duct, and renal vasculature [71–76]. The stimulation of these receptors has been linked to renal vasoconstriction and reduced medullary blood flow, diminishing the renal capacity of sodium handling [77–79] and leading to podocyte injury and loss [15]. As has been found in rats, ANG II-induced hypertension is associated with reduced glomerular filtration rate [80], leading to reductions in filtered load and therefore contributing to an enhanced sodium reabsorption and a reduced sodium excretion [81]. The main mediator of RAS is ANGII, and it has been shown that ANG receptors within the kidney are the main mediators of hypertension [70]. Elevated levels of circulating and intracellular ANGII and aldosterone lead to pro-fibrotic, -inflammatory, and -hypertrophic milieu that causes remodeling and dysfunction in cardiovascular and renal tissues [82]. Employing immunofluorescence-based protein expression detection, we observed cytoskeletal changes in the normal morphology of podocytes, leading to the inhibition of podocyte spreading and downregulated expression of *NPHS1* and *SYNPO*. The downregulated expression of nephrin and synaptopodin has been reported as a hallmark of podocyte injury [13] and is causative for the disruption of foot processes (FPs) and the slit diaphragm (SD). This effect is also probably due to the downregulated expression of numerous genes associated with the GO-BP-actin cytoskeleton organization (Figure 5g and Supplementary Table S9). As an example instance, alpha-actinin-4 (ACTN4) is highly expressed in podocyte FPs, and NPHS1 is connected to the actin cytoskeleton, thus contributing to podocyte actin dynamics, signaling, and mobility [2,3,6]. More evidence

that ANGII affects the cytoskeleton of podocytes is represented by the downregulated GO-BP associated with calcium-independent cell–cell adhesion via plasma membrane cell-adhesion molecules (Figure 5g and Supplementary Table S9). The interaction of calcium signaling and actin dynamics is needed for the plasticity of the actin-based FP and SD of podocytes and is nicely reviewed in [83]. Furthermore, our transcriptome data unveiled the downregulated expression of Coronin 2B (*CORO2B*), DPP4, E74-like ETS transcription factor 3 (*ELF3*), low-density lipoprotein receptor (*LDLR*), Kruppel-like factor 4 (*KLF4*), Roundabout guidance receptor 1 (*ROBO1*), and Wnt family member 7A (*WNT7A*). These genes have been linked to podocyte injury and filtration barrier impairments [22,45,84–88]. Of note, *KLF4* has been shown to directly regulate *NPHS1* expression [45], thus suggesting that the disruptive effect of ANGII might be amongst others also mediated by KLF4. In the upregulated gene set numerous genes associated with cell cycle initiation and DNA double strand repair, such as FA complementation group D2 (*FANCD2*), MutS homolog 2 (*MSH2*), WD repeat domain 7 (*WDR7*), and X-ray repair cross-complementing 4 (*XRCC4*) (Figure 5f and Supplementary Table S8). In a mouse model of Brand et al., it was shown that ANGII is indeed able to induce DNA damage via a dose-dependent increase in oxidative stress, which results in DNA damage [89]. Furthermore, elevated levels of activating transcription factor 4 (*ATF4*), endothelin 1 (*EDN-1*), transforming growth factor beta 2 (*TGFB*) 2, and Polo-like kinase 2 (*PLK2*) have all been linked to podocyte injury and loss of key proteins necessary for the maintenance of the podocyte architecture [90–93]. Most of the cytoskeleton-related genes that were downregulated upon ANGII treatment in podocytes had lower levels of expression in the undifferentiated UdRPCs. Although the expression of Ankyrins, Collagens, keratins, and Semaphorins has been linked to kidney development and functionality [44,53,54,94], to our knowledge only Semaphorins have been reported to be involved in kidney injury [53,95,96]. Of note, numerous members of the sodium and chloride symporter family SLC6 [68] are highly upregulated in the differentiated podocytes (Supplementary Figure S2), while upon ANGII stimulation, upregulated expression of AGTR1 and 2 was observed. Furthermore, signaling through both receptors has been linked to the mediation of many biological functions, such as AGTR1 mediating vasoconstriction, cell proliferation, nephrosclerosis, vascular media hypertrophy, endothelial dysfunction, inflammation, and immune responses and promoting aging; and signaling trough AGTR2 has been linked to vasodilation, development, cell differentiation, tissue repair, and apoptosis [40,41]. Of note, it is important to highlight that the observations after 6 and 24 h exposure of podocytes to ANGII, as presented in this manuscript, reflect a physiological adaption of the cells to the exogenous stressor. However, it is probable that a pathological phenotype might arise if the cells are continuously challenged. This question will be addressed in future studies. Our data shows that the addition of losartan was sufficient to rescue (SYNPO) or mitigate (NPHS1) the cytoskeletal disruption induced by ANGII. This indicates that the disruption of podocyte cytoskeleton is mediated through AGTR1 signaling, while the activation of the AGTR2 receptor induces developmental processes and cell differentiation. In the clinic, angiotensin receptor blockers (ARBs) as well as angiotensin-converting enzyme inhibitor (ACEI) have proven to lower the mortality rates of patients suffering from acute kidney disease (AKI) [97] as well as CKD [98]. However, some patients who received this medication also developed a higher risk to be hospitalized for renal causes [97], which makes monitoring of renal-specific complications caused by these medications a necessity. A proposed method for monitoring disease progression and the effect of different medications is the number of urinary podocytes [99] and proteinuria [100]. In clinical use, ACEIs have been proven to reduce the number of urinary podocytes [99] and the application of ARBs, such as losartan, reduced proteinuria [101,102]. Mechanistically, losartan has been reported to exert its positive effects by interacting with distinct cellular mechanisms and processes, such as decreasing mTOR and AKT phosphorylation [103], downregulating the cell membrane-associated calcium channels [104], or the stabilizing the solute carrier family member GLUT1 [105]. Our data presented in this manuscript propose another possible renal protective mechanism—namely, the preservation of the complex

podocyte architecture by upregulation of *SYNPO* and *NPHS1* expression. This might retain podocyte function and prevent apoptosis, thereby slowing down the progression of CKD. Taken together, UdRPCs can be obtained from any patient by a non-invasive method and rapidly differentiated into podocytes, offering a unique tool for personalized medicine, such as drug-based screening for toxicological aspects. Furthermore, we conclude that our findings offer the possibility of establishing biomarkers indicative of differentiation of UdRPCs into podocytes, as well as being indicative of the initiation and progression of CKD.

To summarize, we have described a differentiation protocol for the successful and reproducible differentiation of SIX2-positive urine-derived renal progenitor cells (UdRPCs) from two African (48 and 51 years) and one Caucasian (27 years) male and one African (31 years) and Caucasian (45 years) female into podocytes. We have shown the potential of UdRPCs for studying nephrogenesis and associated diseases, thus obviating the need for iPSCs. Furthermore, the responsiveness of UdRPC-derived podocytes to ANGII implies potential applications in nephrotoxicity studies and drug screening. Figure 6 presents a graphical summary of this study.

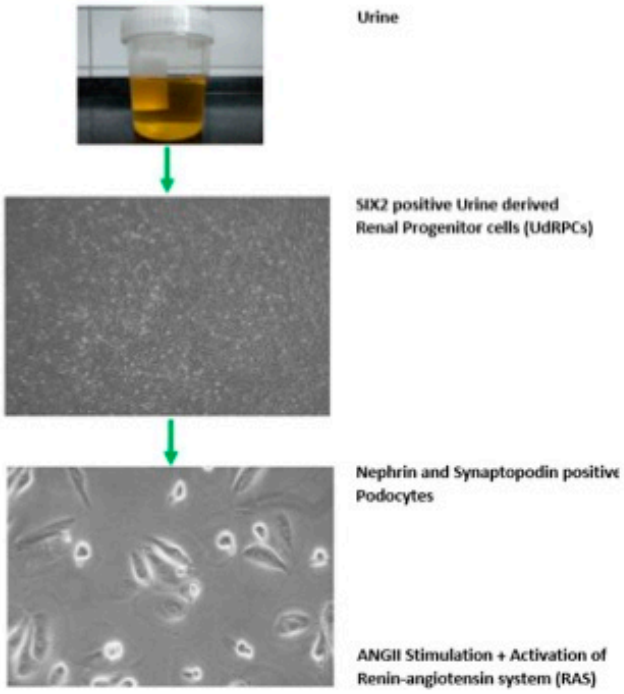


Figure 6. *Cont.*

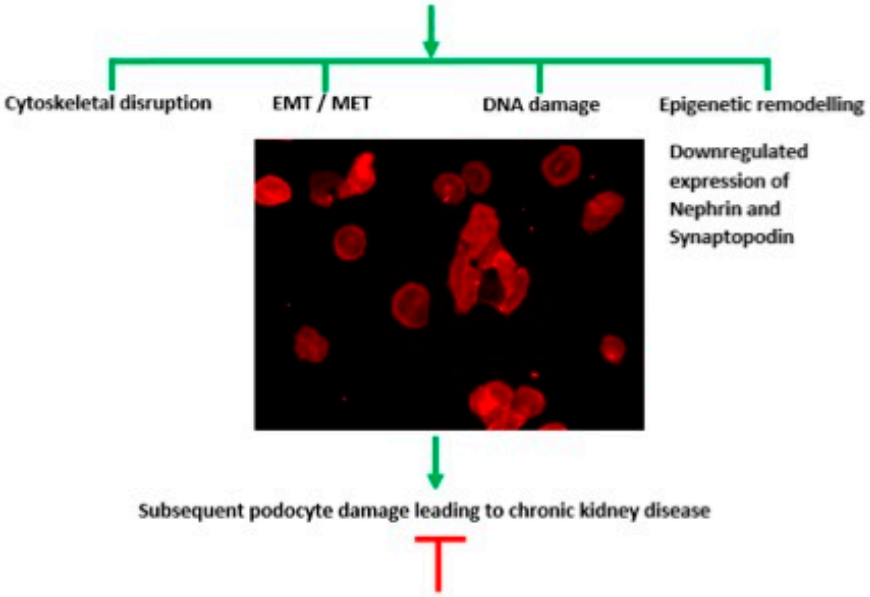


Figure 6. Graphical summary of this study. SIX2-positive renal progenitor cells were isolated directly from human urine and cultured in proliferation medium. UdRPCs differentiated into podocytes, by low density cultivation in advanced RPMI medium supplemented with 30 µM retinoic acid. Stimulation with 100 µM ANGII results in cytoskeletal remodeling. Furthermore, the transcriptome revealed altered expression of genes associated with epigenetic remodeling, DNA damage response, EMT, and MET. ANGII activated the renin–angiotensin system, resulting in podocyte damage and loss and ultimately leading to chronic kidney disease.

Supplementary Materials: The following supporting information can be downloaded at: https://www.mdpi.com/article/10.3390/cells11071095/s1. Figure S1: Retinoic acid enhances the maturation of UdRPC-derived podocytes; Figure S2: iPS cell–derived podocytes, kidney biopsy isolated human glomeruli, and mouse podocytes and Solute Carrier (SLC) Family members, reveals distinct expression patterns of UdRPCs and their differentiated counterparts; Figure S3: Dynamic changes in the morphology of human urine derived podocytes after treatment with Angiotensin II (ANGII) after 6 h; Figure S4: DNA Methylation changes at the NPHS1 promoter upon 6 h of ANGII treatment; Figure S5: Dynamic changes in the morphology of human urine derived podocytes post treatment with Angiotensin II (ANGII) after 6 h and 24 h and is rescued by Losartan; Figure S6: Kegg-pathway Renin-Angiotensin system; Figure S7: Secretome membranes and analysis of podocytes with and without 6 h and 24 h of Angiotensin II treatment; Figure S8: Full size Western blot figures for A = GAPDH, B = NPHS1 and C = SYNPO; Figure S9: Full size Western blot figures for A = GAPDH, B = NPHS1 and C = SYNPO; Figure S10: Albumin uptake assay in UM51 podocytes; Figure S11: Principal component analysis of podocytes UM48 and UM51 with and without 6 h and 24 h of ANGII treatment. Table S1: RT-qPCR Primers; Table S2: bisulfite sequencing primers; Table S3: antibodies; Table S4: UdRPC vs podocyte; Table S5: Podocyte up; Table S6: Podocyte down; Table S7: Podocyte vs. 24 h angII; Table S8: 24 h angII up; Table S9: 24 h angII down; Table S10: differentially expressed genes podocyte and udrpcs; Table S11: differentially expressed genes podocytes and podocytes treated with angII.

Author Contributions: Conceptualization, J.A.; methodology, J.A., L.E., C.T., M.B., M.S.R. and W.W.; bioinformatics, W.W.; validation, L.E. and W.W.; formal analysis, L.E., C.T. and W.W.; investigation, L.E., C.T., M.B., M.S.R. and W.W.; resources, J.A.; data curation, L.E.; writing—original draft preparation, L.E.; writing—review and editing, L.E. and J.A.; visualization, L.E.; supervision, J.A.; project administration, J.A; funding acquisition, J.A. All authors have read and agreed to the published version of the manuscript.

Funding: J.A. acknowledges the medical faculty of Heinrich Heine University for financial support.

Institutional Review Board Statement: The study was conducted in accordance with the written approval (Ethical approval Number: 5704) of the ethical review board of the medical faculty of Heinrich Heine University, Düsseldorf, Germany. All methods were carried out in accordance with the approved guidelines. Medical faculty of Heinrich Heine University approved all experimental protocols.

Informed Consent Statement: In this study, urine samples were collected with the informed consent of the donors.

Data Availability Statement: Microarray data generated for this study are available at NCBI GEO under the accession number GSE171240.

Acknowledgments: James Adjaye acknowledges funding from the medical faculty of Heinrich Heine University, Duesseldorf, Germany.

Conflicts of Interest: The authors declare no conflict of interest.

References

1. Greka, A.; Mundel, P. Cell biology and pathology of podocytes. *Annu. Rev. Physiol.* **2012**, *74*, 299–323. [CrossRef] [PubMed]
2. Critchley, D.R. Focal adhesions—The cytoskeletal connection. *Curr. Opin. Cell Biol.* **2000**, *12*, 133–139. [CrossRef] [PubMed]
3. El-Husseini, A.E.; Kwasnicka, D.; Yamada, T.; Hirohashi, S.; Vincent, S.R. BERP, a novel ring finger protein, binds to alpha-actinin-4. *Biochem. Biophys. Res. Commun.* **2000**, *267*, 906–911. [CrossRef] [PubMed]
4. Kestilä, M.; Lenkkeri, U.; Männikkö, M.; Lamerdin, J.; McCready, P.; Putaala, H.; Ruotsalainen, V.; Morita, T.; Nissinen, M.; Herva, R.; et al. Positionally Cloned Gene for a Novel Glomerular Protein—Nephrin—Is Mutated in Congenital Nephrotic Syndrome. *Mol. Cell* **1998**, *1*, 575–582. [CrossRef] [PubMed]
5. Boute, N.; Gribouval, O.; Roselli, S.; Benessy, F.; Lee, H.; Fuchshuber, A.; Dahan, K.; Gubler, M.C.; Niaudet, P.; Antignac, C. NPHS2, encoding the glomerular protein podocin, is mutated in autosomal recessive steroid-resistant nephrotic syndrome. *Nat. Genet.* **2000**, *24*, 349–354. [CrossRef] [PubMed]
6. Tryggvason, K.; Pikkarainen, T.; Patrakka, J. Nck links nephrin to actin in kidney podocytes. *Cell* **2006**, *125*, 221–224. [CrossRef]
7. Carey, R.M.; Whelton, P.K. Prevention, Detection, Evaluation, and Management of High Blood Pressure in Adults: Synopsis of the 2017 American College of Cardiology/American Heart Association Hypertension Guideline. *Ann. Intern. Med.* **2018**, *168*, 351–358. [CrossRef]
8. Ito, M.; Oliverio, M.I.; Mannon, P.J.; Best, C.F.; Maeda, N.; Smithies, O.; Coffman, T.M. Regulation of blood pressure by the type 1A angiotensin II receptor gene. *Proc. Natl. Acad. Sci. USA* **1995**, *92*, 3521–3525. [CrossRef] [PubMed]
9. Shanmugam, S.; Sandberg, K. Ontogeny of angiotensin II receptors. *Cell Biol. Int.* **1996**, *20*, 169–176. [CrossRef] [PubMed]
10. Sharma, M.; Sharma, R.; Greene, A.S.; McCarthy, E.T.; Savin, V.J. Documentation of angiotensin II receptors in glomerular epithelial cells. *Am. J. Physiol.* **1998**, *274*, F623–F627. [CrossRef] [PubMed]
11. Jia, J.; Ding, G.; Zhu, J.; Chen, C.; Liang, W.; Franki, N.; Singhal, P.C. Angiotensin II infusion induces nephrin expression changes and podocyte apoptosis. *Am. J. Nephrol.* **2008**, *28*, 500–507. [CrossRef] [PubMed]
12. Liu, X.; Zhang, H.; Wang, Q.; Yu, K.; Wang, R.; Sun, J. Blockade of vascular endothelial growth factor-A/receptor 2 exhibits a protective effect on angiotensin-II stimulated podocytes. *Mol. Med. Rep.* **2015**, *12*, 4340–4345. [CrossRef] [PubMed]
13. Rüster, C.; Wolf, G. Renin-angiotensin-aldosterone system and progression of renal disease. *J. Am. Soc. Nephrol.* **2006**, *17*, 2985–2991. [CrossRef] [PubMed]
14. Ding, G.; Reddy, K.; Kapasi, A.A.; Franki, N.; Gibbons, N.; Kasinath, B.S.; Singhal, P.C. Angiotensin II induces apoptosis in rat glomerular epithelial cells. *Am. J. Physiol. Ren. Physiol.* **2002**, *283*, F173–F180. [CrossRef]
15. Kriz, W.; Gretz, N.; Lemley, K.V. Progression of glomerular diseases: Is the podocyte the culprit? *Kidney Int.* **1998**, *54*, 687–697. [CrossRef]
16. Fukuda, A.; Wickman, L.T.; Venkatareddy, M.P.; Sato, Y.; Chowdhury, M.A.; Wang, S.Q.; Shedden, K.A.; Dysko, R.C.; Wiggins, J.E.; Wiggins, R.C. Angiotensin II-dependent persistent podocyte loss from destabilized glomeruli causes progression of end stage kidney disease. *Kidney Int.* **2012**, *81*, 40–55. [CrossRef] [PubMed]

17. Hidaka, T.; Suzuki, Y.; Yamashita, M.; Shibata, T.; Tanaka, Y.; Horikoshi, S.; Tomino, Y. Amelioration of crescentic glomerulonephritis by RhoA kinase inhibitor, Fasudil, through podocyte protection and prevention of leukocyte migration. *Am. J. Pathol.* **2008**, *172*, 603–614. [CrossRef]
18. Bariéty, J.; Bruneval, P.; Meyrier, A.; Mandet, C.; Hill, G.; Jacquot, C. Podocyte involvement in human immune crescentic glomerulonephritis. *Kidney Int.* **2005**, *68*, 1109–1119. [CrossRef]
19. Morioka, Y.; Koike, H.; Ikezumi, Y.; Ito, Y.; Oyanagi, A.; Gejyo, F.; Shimizu, F.; Kawachi, H. Podocyte injuries exacerbate mesangial proliferative glomerulonephritis. *Kidney Int.* **2001**, *60*, 2192–2204. [CrossRef]
20. Saleem, M.A.; O'Hare, M.J.; Reiser, J.; Coward, R.J.; Inward, C.D.; Farren, T.; Xing, C.Y.; Ni, L.; Mathieson, P.W.; Mundel, P. A conditionally immortalized human podocyte cell line demonstrating nephrin and podocin expression. *J. Am. Soc. Nephrol.* **2002**, *13*, 630–638. [PubMed]
21. Srivastava, T.; Sharma, M.; Yew, K.-H.; Sharma, R.; Duncan, R.S.; Saleem, M.A.; McCarthy, E.T.; Kats, A.; Cudmore, P.A.; Alon, U.S.; et al. LPS and PAN-induced podocyte injury in an in vitro model of minimal change disease: Changes in TLR profile. *J. Cell Commun. Signal.* **2013**, *7*, 49–60. [CrossRef] [PubMed]
22. Yang, Y.; Yang, Q.; Yang, J.; Ma, Y.; Ding, G. Angiotensin II induces cholesterol accumulation and injury in podocytes. *Sci. Rep.* **2017**, *7*, 10672. [CrossRef] [PubMed]
23. Musah, S.; Dimitrakakis, N.; Camacho, D.M.; Church, G.M.; Ingber, D.E. Directed differentiation of human induced pluripotent stem cells into mature kidney podocytes and establishment of a Glomerulus Chip. *Nat. Protoc.* **2018**, *13*, 1662–1685. [CrossRef]
24. Freedman, B.S.; Brooks, C.R.; Lam, A.Q.; Fu, H.; Morizane, R.; Agrawal, V.; Saad, A.F.; Li, M.K.; Hughes, M.R.; Werff, R.V.; et al. Modelling kidney disease with CRISPR-mutant kidney organoids derived from human pluripotent epiblast spheroids. *Nat. Commun.* **2015**, *6*, 8715. [CrossRef] [PubMed]
25. Sharmin, S.; Taguchi, A.; Kaku, Y.; Yoshimura, Y.; Ohmori, T.; Sakuma, T.; Mukoyama, M.; Yamamoto, T.; Kurihara, H.; Nishinakamura, R. Human Induced Pluripotent Stem Cell-Derived Podocytes Mature into Vascularized Glomeruli upon Experimental Transplantation. *J. Am. Soc. Nephrol.* **2016**, *27*, 1778–1791. [CrossRef] [PubMed]
26. Taguchi, A.; Kaku, Y.; Ohmori, T.; Sharmin, S.; Ogawa, M.; Sasaki, H.; Nishinakamura, R. Redefining the in vivo origin of metanephric nephron progenitors enables generation of complex kidney structures from pluripotent stem cells. *Cell Stem Cell* **2014**, *14*, 53–67. [CrossRef] [PubMed]
27. Takasato, M.; Er, P.X.; Chiu, H.S.; Maier, B.; Baillie, G.J.; Ferguson, C.; Parton, R.G.; Wolvetang, E.J.; Roost, M.S.; Chuva de Sousa Lopes, S.M.; et al. Kidney organoids from human iPS cells contain multiple lineages and model human nephrogenesis. *Nature* **2015**, *526*, 564–568. [CrossRef] [PubMed]
28. Rahman, M.S.; Wruck, W.; Spitzhorn, L.-S.; Nguyen, L.; Bohndorf, M.; Martins, S.; Asar, F.; Ncube, A.; Erichsen, L.; Graffmann, N.; et al. The FGF, TGFβ and WNT axis Modulate Self-renewal of Human SIX2+ Urine Derived Renal Progenitor Cells. *Sci. Rep.* **2020**, *10*, 739. [CrossRef] [PubMed]
29. Schmittgen, T.D.; Livak, K.J. Analyzing real-time PCR data by the comparative C(T) method. *Nat. Protoc.* **2008**, *3*, 1101–1108. [CrossRef] [PubMed]
30. Santourlidis, S.; Trompeter, H.-I.; Weinhold, S.; Eisermann, B.; Meyer, K.L.; Wernet, P.; Uhrberg, M. Crucial role of DNA methylation in determination of clonally distributed killer cell Ig-like receptor expression patterns in NK cells. *J. Immunol.* **2002**, *169*, 4253–4261. [CrossRef] [PubMed]
31. Zhou, Y.; Zhou, B.; Pache, L.; Chang, M.; Khodabakhshi, A.H.; Tanaseichuk, O.; Benner, C.; Chanda, S.K. Metascape provides a biologist-oriented resource for the analysis of systems-level datasets. *Nat. Commun.* **2019**, *10*, 1523. [CrossRef] [PubMed]
32. Schneider, C.A.; Rasband, W.S.; Eliceiri, K.W. NIH Image to ImageJ: 25 years of image analysis. *Nat. Methods* **2012**, *9*, 671–675. [CrossRef] [PubMed]
33. Gentleman, R.C.; Carey, V.J.; Bates, D.M.; Bolstad, B.; Dettling, M.; Dudoit, S.; Ellis, B.; Gautier, L.; Ge, Y.; Gentry, J.; et al. Bioconductor: Open software development for computational biology and bioinformatics. *Genome Biol.* **2004**, *5*, R80. [CrossRef]
34. Du, P.; Kibbe, W.A.; Lin, S.M. lumi: A pipeline for processing Illumina microarray. *Bioinformatics* **2008**, *24*, 1547–1548. [CrossRef]
35. Graffmann, N.; Ring, S.; Kawala, M.-A.; Wruck, W.; Ncube, A.; Trompeter, H.-I.; Adjaye, J. Modeling Nonalcoholic Fatty Liver Disease with Human Pluripotent Stem Cell-Derived Immature Hepatocyte-Like Cells Reveals Activation of PLIN2 and Confirms Regulatory Functions of Peroxisome Proliferator-Activated Receptor Alpha. *Stem Cells Dev.* **2016**, *25*, 1119–1133. [CrossRef]
36. Kanehisa, M.; Furumichi, M.; Tanabe, M.; Sato, Y.; Morishima, K. KEGG: New perspectives on genomes, pathways, diseases and drugs. *Nucleic Acids Res.* **2017**, *45*, D353–D361. [CrossRef]
37. Carvalho, B.S.; Irizarry, R.A. A framework for oligonucleotide microarray preprocessing. *Bioinformatics* **2010**, *26*, 2363–2367. [CrossRef]
38. Gassmann, M.; Grenacher, B.; Rohde, B.; Vogel, J. Quantifying Western blots: Pitfalls of densitometry. *Electrophoresis* **2009**, *30*, 1845–1855. [CrossRef]
39. Miller, R.G. *Beyond Anova: Basics of Applied Statistics*, 1st ed.; Chapman & Hall: London, UK, 1997; ISBN 9780412070112.
40. Stegbauer, J.; Coffman, T.M. New insights into angiotensin receptor actions: From blood pressure to aging. *Curr. Opin. Nephrol. Hypertens.* **2011**, *20*, 84–88. [CrossRef]
41. Kaschina, E.; Unger, T. Angiotensin AT1/AT2 receptors: Regulation, signalling and function. *Blood Press.* **2003**, *12*, 70–88. [CrossRef]

42. Ronconi, E.; Sagrinati, C.; Angelotti, M.L.; Lazzeri, E.; Mazzinghi, B.; Ballerini, L.; Parente, E.; Becherucci, F.; Gacci, M.; Carini, M.; et al. Regeneration of glomerular podocytes by human renal progenitors. *J. Am. Soc. Nephrol.* **2009**, *20*, 322–332. [CrossRef] [PubMed]
43. Katsuyama, K.; Fujinaka, H.; Yamamoto, K.; Nameta, M.; Yaoita, E.; Yoshida, Y.; Tomizawa, S.; Uchiyama, M.; Yamamoto, T. Expression of the chemokine fractalkine (FKN/CX3CL1) by podocytes in normal and proteinuric rat kidney glomerulus. *Nephron Exp. Nephrol.* **2009**, *113*, e45–e56. [CrossRef] [PubMed]
44. Miao, J.; Fan, Q.; Cui, Q.; Zhang, H.; Chen, L.; Wang, S.; Guan, N.; Guan, Y.; Ding, J. Newly identified cytoskeletal components are associated with dynamic changes of podocyte foot processes. *Nephrol. Dial. Transpl.* **2009**, *24*, 3297–3305. [CrossRef]
45. Nistala, R.; Habibi, J.; Aroor, A.; Sowers, J.R.; Hayden, M.R.; Meuth, A.; Knight, W.; Hancock, T.; Klein, T.; DeMarco, V.G.; et al. DPP4 inhibition attenuates filtration barrier injury and oxidant stress in the zucker obese rat. *Obesity* **2014**, *22*, 2172–2179. [CrossRef]
46. Saito, A.; Miyauchi, N.; Hashimoto, T.; Karasawa, T.; Han, G.D.; Kayaba, M.; Sumi, T.; Tomita, M.; Ikezumi, Y.; Suzuki, K.; et al. Neurexin-1, a presynaptic adhesion molecule, localizes at the slit diaphragm of the glomerular podocytes in kidneys. *Am. J. Physiol. Regul. Integr. Comp. Physiol.* **2011**, *300*, R340-8. [CrossRef]
47. Endlich, N.; Lange, T.; Kuhn, J.; Klemm, P.; Kotb, A.M.; Siegerist, F.; Kindt, F.; Lindenmeyer, M.T.; Cohen, C.D.; Kuss, A.W.; et al. BDNF: mRNA expression in urine cells of patients with chronic kidney disease and its role in kidney function. *J. Cell. Mol. Med.* **2018**, *22*, 5265–5277. [CrossRef]
48. Gutwein, P.; Abdel-Bakky, M.S.; Schramme, A.; Doberstein, K.; Kämpfer-Kolb, N.; Amann, K.; Hauser, I.A.; Obermüller, N.; Bartel, C.; Abdel-Aziz, A.-A.H.; et al. CXCL16 is expressed in podocytes and acts as a scavenger receptor for oxidized low-density lipoprotein. *Am. J. Pathol.* **2009**, *174*, 2061–2072. [CrossRef]
49. Li, Z.; Chen, H.; Zhong, F.; Zhang, W.; Lee, K.; He, J.C. Expression of Glutamate Receptor Subtype 3 Is Epigenetically Regulated in Podocytes under Diabetic Conditions. *Kidney Dis.* **2019**, *5*, 34–42. [CrossRef]
50. Eitner, F.; Ostendorf, T.; Kretzler, M.; Cohen, C.D.; Eriksson, U.; Gröne, H.-J.; Floege, J. PDGF-C expression in the developing and normal adult human kidney and in glomerular diseases. *J. Am. Soc. Nephrol.* **2003**, *14*, 1145–1153. [CrossRef]
51. Rastaldi, M.P.; Armelloni, S.; Berra, S.; Calvaresi, N.; Corbelli, A.; Giardino, L.A.; Li, M.; Wang, G.Q.; Fornasieri, A.; Villa, A.; et al. Glomerular podocytes contain neuron-like functional synaptic vesicles. *FASEB J.* **2006**, *20*, 976–978. [CrossRef]
52. Müller-Deile, J.; Worthmann, K.; Saleem, M.; Tossidou, I.; Haller, H.; Schiffer, M. The balance of autocrine VEGF-A and VEGF-C determines podocyte survival. *Am. J. Physiol. Ren. Physiol.* **2009**, *297*, F1656–F1667. [CrossRef]
53. Reidy, K.; Tufro, A. Semaphorins in kidney development and disease: Modulators of ureteric bud branching, vascular morphogenesis, and podocyte-endothelial crosstalk. *Pediatr. Nephrol.* **2011**, *26*, 1407–1412. [CrossRef] [PubMed]
54. Reidy, K.J.; Villegas, G.; Teichman, J.; Veron, D.; Shen, W.; Jimenez, J.; Thomas, D.; Tufro, A. Semaphorin3a regulates endothelial cell number and podocyte differentiation during glomerular development. *Development* **2009**, *136*, 3979–3989. [CrossRef] [PubMed]
55. Saxén, L.; Sariola, H. Early organogenesis of the kidney. *Pediatr. Nephrol.* **1987**, *1*, 385–392. [CrossRef] [PubMed]
56. Naim, E.; Bernstein, A.; Bertram, J.F.; Caruana, G. Mutagenesis of the epithelial polarity gene, discs large 1, perturbs nephrogenesis in the developing mouse kidney. *Kidney Int.* **2005**, *68*, 955–965. [CrossRef] [PubMed]
57. Smeets, B.; Uhlig, S.; Fuss, A.; Mooren, F.; Wetzels, J.F.M.; Floege, J.; Moeller, M.J. Tracing the origin of glomerular extracapillary lesions from parietal epithelial cells. *J. Am. Soc. Nephrol.* **2009**, *20*, 2604–2615. [CrossRef]
58. Appel, D.; Kershaw, D.B.; Smeets, B.; Yuan, G.; Fuss, A.; Frye, B.; Elger, M.; Kriz, W.; Floege, J.; Moeller, M.J. Recruitment of podocytes from glomerular parietal epithelial cells. *J. Am. Soc. Nephrol.* **2009**, *20*, 333–343. [CrossRef]
59. Hay, E.D.; Zuk, A. Transformations between epithelium and mesenchyme: Normal, pathological, and experimentally induced. *Am. J. Kidney Dis.* **1995**, *26*, 678–690. [CrossRef]
60. Strippoli, R.; Loureiro, J.; Moreno, V.; Benedicto, I.; Pérez Lozano, M.L.; Barreiro, O.; Pellinen, T.; Minguet, S.; Foronda, M.; Osteso, M.T.; et al. Caveolin-1 deficiency induces a MEK-ERK1/2-Snail-1-dependent epithelial-mesenchymal transition and fibrosis during peritoneal dialysis. *EMBO Mol. Med.* **2015**, *7*, 102–123. [CrossRef]
61. Yang, J.; Weinberg, R.A. Epithelial-mesenchymal transition: At the crossroads of development and tumor metastasis. *Dev. Cell* **2008**, *14*, 818–829. [CrossRef]
62. Berdasco, M.; Esteller, M. Aberrant epigenetic landscape in cancer: How cellular identity goes awry. *Dev. Cell* **2010**, *19*, 698–711. [CrossRef] [PubMed]
63. Jair, K.-W.; Bachman, K.E.; Suzuki, H.; Ting, A.H.; Rhee, I.; Yen, R.-W.C.; Baylin, S.B.; Schuebel, K.E. De novo CpG island methylation in human cancer cells. *Cancer Res.* **2006**, *66*, 682–692. [CrossRef] [PubMed]
64. Tahiliani, M.; Koh, K.P.; Shen, Y.; Pastor, W.A.; Bandukwala, H.; Brudno, Y.; Agarwal, S.; Iyer, L.M.; Liu, D.R.; Aravind, L.; et al. Conversion of 5-methylcytosine to 5-hydroxymethylcytosine in mammalian DNA by MLL partner TET1. *Science* **2009**, *324*, 930–935. [CrossRef] [PubMed]
65. Ito, S.; D'Alessio, A.C.; Taranova, O.V.; Hong, K.; Sowers, L.C.; Zhang, Y. Role of Tet proteins in 5mC to 5hmC conversion, ES-cell self-renewal and inner cell mass specification. *Nature* **2010**, *466*, 1129–1133. [CrossRef]
66. Klutstein, M.; Nejman, D.; Greenfield, R.; Cedar, H. DNA Methylation in Cancer and Aging. *Cancer Res.* **2016**, *76*, 3446–3450. [CrossRef]

67. Shen, X.; Liu, Y.; Hsu, Y.-J.; Fujiwara, Y.; Kim, J.; Mao, X.; Yuan, G.-C.; Orkin, S.H. EZH1 mediates methylation on histone H3 lysine 27 and complements EZH2 in maintaining stem cell identity and executing pluripotency. *Mol. Cell* **2008**, *32*, 491–502. [CrossRef]
68. César-Razquin, A.; Snijder, B.; Frappier-Brinton, T.; Isserlin, R.; Gyimesi, G.; Bai, X.; Reithmeier, R.A.; Hepworth, D.; Hediger, M.A.; Edwards, A.M.; et al. A Call for Systematic Research on Solute Carriers. *Cell* **2015**, *162*, 478–487. [CrossRef]
69. Patel, S.; Rauf, A.; Khan, H.; Abu-Izneid, T. Renin-angiotensin-aldosterone (RAAS): The ubiquitous system for homeostasis and pathologies. *Biomed. Pharmacother.* **2017**, *94*, 317–325. [CrossRef]
70. Crowley, S.D.; Gurley, S.B.; Herrera, M.J.; Ruiz, P.; Griffiths, R.; Kumar, A.P.; Kim, H.-S.; Smithies, O.; Le, T.H.; Coffman, T.M. Angiotensin II causes hypertension and cardiac hypertrophy through its receptors in the kidney. *Proc. Natl. Acad. Sci. USA* **2006**, *103*, 17985–17990. [CrossRef]
71. Barreto-Chaves, M.L.; Mello-Aires, M. Effect of luminal angiotensin II and ANP on early and late cortical distal tubule HCO3- reabsorption. *Am. J. Physiol.* **1996**, *271*, F977–F984. [CrossRef]
72. Kwon, T.-H.; Nielsen, J.; Kim, Y.-H.; Knepper, M.A.; Frøkiaer, J.; Nielsen, S. Regulation of sodium transporters in the thick ascending limb of rat kidney: Response to angiotensin II. *Am. J. Physiol. Ren. Physiol.* **2003**, *285*, F152–F165. [CrossRef]
73. Rocque, B.L.; Babayeva, S.; Li, J.; Leung, V.; Nezvitsky, L.; Cybulsky, A.V.; Gros, P.; Torban, E. Deficiency of the planar cell polarity protein Vangl2 in podocytes affects glomerular morphogenesis and increases susceptibility to injury. *J. Am. Soc. Nephrol.* **2015**, *26*, 576–586. [CrossRef] [PubMed]
74. Tojo, A.; Tisher, C.C.; Madsen, K.M. Angiotensin II regulates H(+)-ATPase activity in rat cortical collecting duct. *Am. J. Physiol.* **1994**, *267*, F1045–F1051. [CrossRef] [PubMed]
75. Xie, K.; Xu, C.; Zhang, M.; Wang, M.; Min, L.; Qian, C.; Wang, Q.; Ni, Z.; Mou, S.; Dai, H.; et al. Yes-associated protein regulates podocyte cell cycle re-entry and dedifferentiation in adriamycin-induced nephropathy. *Cell Death Dis.* **2019**, *10*, 915. [CrossRef]
76. Wang, T.; Giebisch, G. Effects of angiotensin II on electrolyte transport in the early and late distal tubule in rat kidney. *Am. J. Physiol.* **1996**, *271*, F143–F149. [CrossRef]
77. Faubert, P.F.; Chou, S.Y.; Porush, J.G. Regulation of papillary plasma flow by angiotensin II. *Kidney Int.* **1987**, *32*, 472–478. [CrossRef]
78. Hall, J.E. Control of sodium excretion by angiotensin II: Intrarenal mechanisms and blood pressure regulation. *Am. J. Physiol.* **1986**, *250*, R960–R972. [CrossRef]
79. Ruan, X.; Oliverio, M.I.; Coffman, T.M.; Arendshorst, W.J. Renal vascular reactivity in mice: AngII-induced vasoconstriction in AT1A receptor null mice. *J. Am. Soc. Nephrol.* **1999**, *10*, 2620–2630.
80. Wang, C.T.; Zou, L.X.; Navar, L.G. Renal responses to AT1 blockade in angiotensin II-induced hypertensive rats. *J. Am. Soc. Nephrol.* **1997**, *8*, 535–542.
81. Wang, C.T.; Chin, S.Y.; Navar, L.G. Impairment of pressure-natriuresis and renal autoregulation in ANG II-infused hypertensive rats. *Am. J. Physiol. Ren. Physiol.* **2000**, *279*, F319–F325. [CrossRef]
82. Ames, M.K.; Atkins, C.E.; Pitt, B. The renin-angiotensin-aldosterone system and its suppression. *J. Vet. Intern. Med.* **2019**, *33*, 363–382. [CrossRef] [PubMed]
83. Greka, A.; Mundel, P. Calcium regulates podocyte actin dynamics. *Semin. Nephrol.* **2012**, *32*, 319–326. [CrossRef] [PubMed]
84. Hayashi, K.; Sasamura, H.; Nakamura, M.; Azegami, T.; Oguchi, H.; Sakamaki, Y.; Itoh, H. KLF4-dependent epigenetic remodeling modulates podocyte phenotypes and attenuates proteinuria. *J. Clin. Investig.* **2014**, *124*, 2523–2537. [CrossRef] [PubMed]
85. He, W.; Kang, Y.S.; Dai, C.; Liu, Y. Blockade of Wnt/β-catenin signaling by paricalcitol ameliorates proteinuria and kidney injury. *J. Am. Soc. Nephrol.* **2011**, *22*, 90–103. [CrossRef]
86. Liu, J.; Hou, W.; Guan, T.; Tang, L.; Zhu, X.; Li, Y.; Hou, S.; Zhang, J.; Chen, H.; Huang, Y. Slit2/Robo1 signaling is involved in angiogenesis of glomerular endothelial cells exposed to a diabetic-like environment. *Angiogenesis* **2018**, *21*, 237–249. [CrossRef]
87. Sakurai, A.; Ono, H.; Ochi, A.; Matsuura, M.; Yoshimoto, S.; Kishi, S.; Murakami, T.; Tominaga, T.; Nagai, K.; Abe, H.; et al. Involvement of Elf3 on Smad3 activation-dependent injuries in podocytes and excretion of urinary exosome in diabetic nephropathy. *PLoS ONE* **2019**, *14*, e0216788. [CrossRef]
88. Schwarz, A.; Möller-Hackbarth, K.; Ebarasi, L.; Unnersjö Jess, D.; Zambrano, S.; Blom, H.; Wernerson, A.; Lal, M.; Patrakka, J. Coro2b, a podocyte protein downregulated in human diabetic nephropathy, is involved in the development of protamine sulphate-induced foot process effacement. *Sci. Rep.* **2019**, *9*, 8888. [CrossRef]
89. Brand, S.; Amann, K.; Schupp, N. Angiotensin II-induced hypertension dose-dependently leads to oxidative stress and DNA damage in mouse kidneys and hearts. *J. Hypertens.* **2013**, *31*, 333–344. [CrossRef]
90. Fuchshofer, R.; Ullmann, S.; Zeilbeck, L.F.; Baumann, M.; Junglas, B.; Tamm, E.R. Connective tissue growth factor modulates podocyte actin cytoskeleton and extracellular matrix synthesis and is induced in podocytes upon injury. *Histochem. Cell Biol.* **2011**, *136*, 301–319. [CrossRef]
91. Kang, M.-K.; Park, S.-H.; Kim, Y.-H.; Lee, E.-J.; Antika, L.D.; Kim, D.Y.; Choi, Y.-J.; Kang, Y.-H. Chrysin ameliorates podocyte injury and slit diaphragm protein loss via inhibition of the PERK-eIF2α-ATF-CHOP pathway in diabetic mice. *Acta Pharmacol. Sin.* **2017**, *38*, 1129–1140. [CrossRef]
92. Qi, H.; Casalena, G.; Shi, S.; Yu, L.; Ebefors, K.; Sun, Y.; Zhang, W.; D'Agati, V.; Schlondorff, D.; Haraldsson, B.; et al. Glomerular Endothelial Mitochondrial Dysfunction Is Essential and Characteristic of Diabetic Kidney Disease Susceptibility. *Diabetes* **2017**, *66*, 763–778. [CrossRef] [PubMed]

93. Zou, H.-H.; Yang, P.-P.; Huang, T.-L.; Zheng, X.-X.; Xu, G.-S. PLK2 Plays an Essential Role in High D-Glucose-Induced Apoptosis, ROS Generation and Inflammation in Podocytes. *Sci. Rep.* **2017**, *7*, 4261. [CrossRef] [PubMed]
94. Stankewich, M.C.; Moeckel, G.W.; Ji, L.; Ardito, T.; Morrow, J.S. Isoforms of Spectrin and Ankyrin Reflect the Functional Topography of the Mouse Kidney. *PLoS ONE* **2016**, *11*, e0142687. [CrossRef]
95. Fu, Y.; Wang, C.; Zhang, D.; Chu, X.; Zhang, Y.; Li, J. miR-15b-5p ameliorated high glucose-induced podocyte injury through repressing apoptosis, oxidative stress, and inflammatory responses by targeting Sema3A. *J. Cell. Physiol.* **2019**, *234*, 20869–20878. [CrossRef]
96. Aggarwal, P.K.; Veron, D.; Thomas, D.B.; Siegel, D.; Moeckel, G.; Kashgarian, M.; Tufro, A. Semaphorin3a promotes advanced diabetic nephropathy. *Diabetes* **2015**, *64*, 1743–1759. [CrossRef]
97. Brar, S.; Ye, F.; James, M.T.; Hemmelgarn, B.; Klarenbach, S.; Pannu, N. Association of Angiotensin-Converting Enzyme Inhibitor or Angiotensin Receptor Blocker Use with Outcomes After Acute Kidney Injury. *JAMA Intern. Med.* **2018**, *178*, 1681–1690.
98. Molnar, M.Z.; Kalantar-Zadeh, K.; Lott, E.H.; Lu, J.L.; Malakauskas, S.M.; Ma, J.Z.; Quarles, D.L.; Kovesdy, C.P. Angiotensin-converting enzyme inhibitor, angiotensin receptor blocker use, and mortality in patients with chronic kidney disease. *J. Am. Coll. Cardiol.* **2014**, *63*, 650–658.
99. Nakamura, T.; Ushiyama, C.; Suzuki, S.; Hara, M.; Shimada, N.; Sekizuka, K.; Ebihara, I.; Koide, H. Effects of angiotensin-converting enzyme inhibitor, angiotensin II receptor antagonist and calcium antagonist on urinary podocytes in patients with IgA nephropathy. *Am. J. Nephrol.* **2000**, *20*, 373–379. [CrossRef]
100. Zandi-Nejad, K.; Eddy, A.A.; Glassock, R.J.; Brenner, B.M. Why is proteinuria an ominous biomarker of progressive kidney disease? *Kidney Int. Suppl.* **2004**, *66*, S76–S89.
101. Lin, S.-L.; Chen, Y.-M.; Chiang, W.-C.; Wu, K.-D.; Tsai, T.-J. Effect of pentoxifylline in addition to losartan on proteinuria and GFR in CKD: A 12-month randomized trial. *Am. J. Kidney Dis.* **2008**, *52*, 464–474. [CrossRef]
102. Horita, Y.; Tadokoro, M.; Taura, K.; Suyama, N.; Taguchi, T.; Miyazaki, M.; Kohno, S. Low-dose combination therapy with temocapril and losartan reduces proteinuria in normotensive patients with immunoglobulin a nephropathy. *Hypertens. Res.* **2004**, *27*, 963–970. [PubMed]
103. Mavroeidi, V.; Petrakis, I.; Stylianou, K.; Katsarou, T.; Giannakakis, K.; Perakis, K.; Vardaki, E.; Stratigis, S.; Ganotakis, E.; Papavasiliou, S.; et al. Losartan affects glomerular AKT and mTOR phosphorylation in an experimental model of type 1 diabetic nephropathy. *J. Histochem. Cytochem.* **2013**, *61*, 433–443. [PubMed]
104. Chi, X.; Hu, B.; Yu, S.Y.; Yin, L.; Meng, Y.; Wang, B.; Yang, J.; Lin, J.; Huang, D.; Chen, L. Losartan treating podocyte injury induced by Ang II via downregulation of TRPC6 in podocytes. *J. Renin Angiotensin Aldosterone Syst.* **2015**, *16*, 1118–1124.
105. Yu, S.Y.; Qi, R.; Zhao, H. Losartan reverses glomerular podocytes injury induced by AngII via stabilizing the expression of GLUT1. *Mol. Biol. Rep.* **2013**, *40*, 6295–6301. [CrossRef]

3.4 Unveiling Angiotensin II and Losartan-Induced Gene Regulatory Networks Using Human Urine-Derived Podocytes

Chantelle Thimm, Lars Erichsen, Wasco Wruck and James Adjaye

International Journal of Molecular Sciences 2023, Volume 24, 10551,
Article ID: 241310551

Abstract:

Podocytes are highly specialized cells that play a pivotal role in the blood filtration process in the glomeruli of the kidney, and their dysfunction leads to renal diseases. For this reason, the study and application of this cell type is of great importance in the field of regenerative medicine. Hypertension is mainly regulated by the renin–angiotensin–aldosterone system (RAAS), with its main mediator being angiotensin II (ANG II). Elevated ANG II levels lead to a pro-fibrotic, inflammatory, and hypertrophic milieu that induces apoptosis in podocytes. The activation of RAAS is critical for the pathogenesis of podocyte injury; as such, to prevent podocyte damage, patients with hypertension are administered drugs that modulate RAAS signaling. A prime example is the orally active, non-peptide, selective angiotensin-II-type I receptor (AGTR1) blocker losartan. Here, we demonstrate that SIX2-positive urine-derived renal progenitor cells (UdRPCs) and their immortalized counterpart (UM51-hTERT) can be directly differentiated into mature podocytes. These podocytes show activation of RAAS after stimulation with ANG II, resulting in ANG II-dependent upregulation of the expression of the angiotensin-II-type I receptor, AGTR1, and the downregulated expression of the angiotensin-II-type II receptor 2 (AGTR2). The stimulation of podocytes with losartan counteracts ANG II-dependent changes, resulting in a dependent favoring of the specific receptor from AGTR1 to AGTR2. Transcriptome analysis revealed 94 losartan-induced genes associated with diverse biological processes and pathways such as vascular smooth muscle contraction, the oxytocin signaling pathway, renin secretion, and ECM-receptor interaction. Co-stimulation with losartan and ANG II induced the exclusive expression of 106 genes associated with DNA methylation or demethylation, cell differentiation, the developmental process, response to muscle stretch, and calcium ion transmembrane transport. These findings highlight the usefulness of UdRPC-

derived podocytes in studying the RAAS pathway and nephrotoxicity in various kidney diseases.

Author contribution of C.T. included 80%:

I was responsible for establishing and maintaining the cell culture systems, which included the cultivation of primary and immortalized UdRPCs. I further carried out the induction of podocyte differentiation and the execution of stimulation experiments employing ANG II and Losartan.
I performed immunofluorescence staining, RNA isolation for both (NGS and my follow-up qPCR experiment. I also prepared protein lysates and conducted the western blot analyses.
I collected all samples designated for NGS, after which W.W. processed and analyzed the raw sequencing data. I subsequently performed further analyses, including functional enrichment analysis using Metascape. For all datasets generated in the course of the study, I carried out the respective statistical analyses and prepared the quantitative evaluation of the results.
I contributed to the conceptualization, designed and executed the experiments and interpreted the results to my research hypothesis.
I generated and designed all figures and schematic illustrations, compiled and analyzed the complete dataset, and wrote the original manuscript. I further revised and finalized the manuscript in response to the reviewers' comments with L.E. and J.A..

Status: Published in International Journal of Molecular Sciences.

DOI: doi.org/10.3390/ijms241310551

This article is an open access article distributed under the terms and conditions of the Creative Commons Attribution (CC BY) 4.0 license, which permits unrestricted use, distribution, and reproduction in any medium, provided the original work is properly cited.

International Journal of
Molecular Sciences

MDPI

Article

Unveiling Angiotensin II and Losartan-Induced Gene Regulatory Networks Using Human Urine-Derived Podocytes

Chantelle Thimm [1], Lars Erichsen [1], Wasco Wruck [1] and James Adjaye [1,2,*]

[1] Institute for Stem Cell Research and Regenerative Medicine, Medical Faculty, Heinrich-Heine University Düsseldorf, 40225 Düsseldorf, Germany; chantelle.thimm@uni-duesseldorf.de (C.T.); lars.erichsen@uni-duesseldorf.de (L.E.); wasco.wruck@med.uni-duesseldorf.de (W.W.)
[2] EGA Institute for Women's Health, Zayed Centre for Research into Rare Diseases in Children (ZCR), University College London (UCL), 20 Guilford Street, London WC1N 1DZ, UK
* Correspondence: james.adjaye@med.uni-duesseldorf.de

Abstract: Podocytes are highly specialized cells that play a pivotal role in the blood filtration process in the glomeruli of the kidney, and their dysfunction leads to renal diseases. For this reason, the study and application of this cell type is of great importance in the field of regenerative medicine. Hypertension is mainly regulated by the renin–angiotensin–aldosterone system (RAAS), with its main mediator being angiotensin II (ANG II). Elevated ANG II levels lead to a pro-fibrotic, inflammatory, and hypertrophic milieu that induces apoptosis in podocytes. The activation of RAAS is critical for the pathogenesis of podocyte injury; as such, to prevent podocyte damage, patients with hypertension are administered drugs that modulate RAAS signaling. A prime example is the orally active, non-peptide, selective angiotensin-II-type I receptor (AGTR1) blocker losartan. Here, we demonstrate that SIX2-positive urine-derived renal progenitor cells (UdRPCs) and their immortalized counterpart (UM51-hTERT) can be directly differentiated into mature podocytes. These podocytes show activation of RAAS after stimulation with ANG II, resulting in ANG II-dependent upregulation of the expression of the angiotensin-II-type I receptor, AGTR1, and the downregulated expression of the angiotensin-II-type II receptor 2 (AGTR2). The stimulation of podocytes with losartan counteracts ANG II-dependent changes, resulting in a dependent favoring of the specific receptor from AGTR1 to AGTR2. Transcriptome analysis revealed 94 losartan-induced genes associated with diverse biological processes and pathways such as vascular smooth muscle contraction, the oxytocin signaling pathway, renin secretion, and ECM-receptor interaction. Co-stimulation with losartan and ANG II induced the exclusive expression of 106 genes associated with DNA methylation or demethylation, cell differentiation, the developmental process, response to muscle stretch, and calcium ion transmembrane transport. These findings highlight the usefulness of UdRPC-derived podocytes in studying the RAAS pathway and nephrotoxicity in various kidney diseases.

Keywords: urine; podocytes; disease modeling; renin–angiotensin–aldosterone system; kidney; losartan; hypertension

check for updates

Citation: Thimm, C.; Erichsen, L.; Wruck, W.; Adjaye, J. Unveiling Angiotensin II and Losartan-Induced Gene Regulatory Networks Using Human Urine-Derived Podocytes. *Int. J. Mol. Sci.* **2023**, *24*, 10551. https://doi.org/10.3390/ijms241310551

Academic Editors: Marcus Brand and Giovana S. Di Marco

Received: 7 June 2023
Revised: 20 June 2023
Accepted: 21 June 2023
Published: 23 June 2023

Copyright: © 2023 by the authors. Licensee MDPI, Basel, Switzerland. This article is an open access article distributed under the terms and conditions of the Creative Commons Attribution (CC BY) license (https://creativecommons.org/licenses/by/4.0/).

1. Introduction

Kidneys perform numerous essential tasks in the human body; these are filtration of the urine to dispose of urinary components such as urea, uric acid, and creatine into the urine [1]. They regulate the homeostasis of electrolytes such as sodium, potassium, calcium, magnesium, and phosphate. Additionally, kidneys adjust the acid–base balance and control blood pressure by regulating the synthesis of calcitriol, erythropoietin, and renin [1].

Podocytes are highly differentiated and specialized cells located on the outside of the glomerular capillaries that project into the urinary cavity of Bowman's capsule. They have a large cell body from which numerous foot processes taper around the glomerular capillaries. Adjacent podocytes thus form lamellipodia-like foot processes, between which

an interdigitating cell–cell contact is formed to ensure the size selectivity of glomerular filtration via the slit membrane. Numerous podocyte-specific genes have been identified whose products play important roles in maintaining the filtration barrier. There is a highly conserved complex consisting of Podocin (*NPHS2*), Nephrin (*NPHS1*), KIRREL1 (*NEPH1*), and CD2-associated protein (*CD2AP*) through which podocytes are connected to cell–cell contacts and control podocyte function [2–4]. The morphology of podocytes, which form the filtration slits with their primary and secondary foot processes, can only be maintained by a mature internal support network.

The renin–angiotensin–aldosterone system (RAAS) is a cascade that contributes to various systematic and localized processes. Among the systematic processes is the regulation of blood pressure. The octapeptide angiotensin II (ANG II) is the biological effector of the renin–angiotensin system and regulates blood pressure and extracellular volume. Angiotensin II acts on the two subtypes of angiotensin II receptors AT1 (AGTR1) and AT2 (AGTR2). Based on this, AGTRs were shown to be expressed in various segments of the nephron in the distal tubule, collecting duct, and renal vasculature [5–10]. The binding of ANG II to the AGTR1 activates four classical signaling cascades, including phospholipase A2, phospholipase C, phospholipase D, and L-type calcium channels, and normally blocks the adenylate cycle [11,12]. Stimulation of these signaling pathways via renal AGTR1 initiates vasoconstriction, sodium re-absorption, protein synthesis, and cellular growth [13,14]. AGTR2 receptors are comparable to AGTR1 receptors in their structure, tissue expression, signaling pathways, and functions. The activation of AGTR2 mediates K+ channel activity via the G protein G1 and activates protein tyrosine phosphatase (PTP), which leads to a reduction in MAPK- activity or ERK1 [15,16]. It should be noted that in the human kidney, the expression of AGTR1 is 8–10-fold higher at the mRNA level compared to AGTR2. Moreover, the activation of AGTR2 leads to increased bradykinin production, which induces vasodilation via the NO/cGMP pathway [13].

Persistent activation of the RAAS is critical for the pathogenesis of podocyte injury and causes proteinuria. ANG II stimulation triggered the downregulation of *ACTN4* and decreased expression of focal adhesion in podocytes [17]. In summary, with sustained RAAS activation, the phenotype induced by ANG II shifts from dynamic stability to adaptive migration, which can eventually lead to podocyte depletion with high actin cytoskeletal turnover and consequent podocyte depletion and focal segmental glomerulosclerosis [18,19]. The beneficial effects of RAAS modulation on proteinuria reduction, whether occurring via ACE inhibitors (e.g., Ramipril, Benazapril, and Captopril) or AGTR1 antagonists (e.g., losartan, Candesartan, and Irbesartan), are confirmed by clinical evidence [20,21]. ACE inhibitors and AGTR1 antagonists are these days indispensable in the management of hypertension and blood pressure. In the 1990s, the development of orally active, non-peptide, selective AGTR1 blockers began with the synthesis of losartan [22]. In contrast to the application of ACE inhibitors, AGTR1 blockers do not prevent the formation of ANG II, but rather the binding of the peptide to AGTR1. With respect to AGTR1 binding inhibition, the increase in ANG I leads to an increase in ANG II levels, which can bind freely to AGTR2 or other receptor subtypes [14,23].

We previously reported human urine as a non-invasive source of renal stem cells with regenerative potential. These urine-derived renal progenitor cells (UdRPCs) express, among others, the renal stem cell markers sine oculis homeobox homolog 2 (SIX2), Cbp/P300-interacting transactivator with Glu/Asp rich carboxy-terminal domain 1 (CITED1), Wilms tumor 1 (WT1), CD133, CD24, and CD106 [24]. Recently, we established a protocol that leads to the differentiation of human UdRPCs into mature podocytes with typical cellular processes. We reported the full characterization of the generated podocytes at the transcriptome, secretome, and cellular levels [19]. Furthermore, we showed that ANG II-stimulation of the podocytes activated the renin–angiotensin aldosterone system, resulting in a downregulated expression of NPHS1 [19]. This subsequently leads to cytoskeletal changes and increased AGTR1 expression and downregulation of AGTR2 expression.

In the current study, we demonstrate that losartan counteracts ANG II-dependent molecular changes by elevating the expression of podocyte-specific markers such as NPHS1.

Additionally, cells treated simultaneously with ANG II and losartan undergo receptor-usage switching from AGTR1 to AGTR2. We carried out a transcriptome analysis of human urine-derived podocytes stimulated with 100 µM ANG II with and without 1 µM losartan. To date, transcriptome data derived from podocytes treated with losartan are restricted to rodents [25–27]. Our current data re-affirms that human urine-derived podocytes are a valuable in vitro model for dissecting RAAS, studying podocyte-associated diseases, and drug screening, thus complementing the use of pluripotent stem cells.

2. Results

2.1. Losartan Rescues ANG II Induced Down-Regulation of NPHS1 Expression

In a previous manuscript, we reported the existence of urine-derived renal progenitor cells (UdRPCs) inherently capable of differentiating into podocytes [19,24,28]. UdRPCs adopt the typical "fried egg" morphology typical of podocytes after seven days of continuous culturing in adv. RPMI medium supplemented with 30 µM retinoic acid (RA). We previously showed the expression of foot processes and slit-diaphragm-associated proteins-NPHS1 [19]. Furthermore, because these cells have been shown to be responsive to angiotensin II (ANG II) [20], we applied the angiotensin II receptor type I blocker losartan to investigate its protective effect on UdRPC-derived podocytes treated with ANG II.

For the investigation, the optimal concentration of losartan was tested with and without ANG II. Based on these findings, a losartan concentration of 1 µM and a cell density of 60–70% were used in all further experiments. Therefore, the urine-derived podocytes were pre-treated with 1 µM losartan for 24 h, thereafter 100 µM ANG II was added for another 24 h.

We differentiated primary SIX2-positive UdRPC UM51 and the transformed counterpart UM51-hTERT into podocytes [28]. The expression of NPHS1 was analyzed to confirm the differentiation of both cell types into mature podocytes, and phalloidin staining was employed to reveal cytoskeletal morphologies (Figure 1A,B). The addition of ANG II for 24 h induced rounded-up morphological changes in some cells, but all cells expressed NPHS1 (Figure 1A,B).

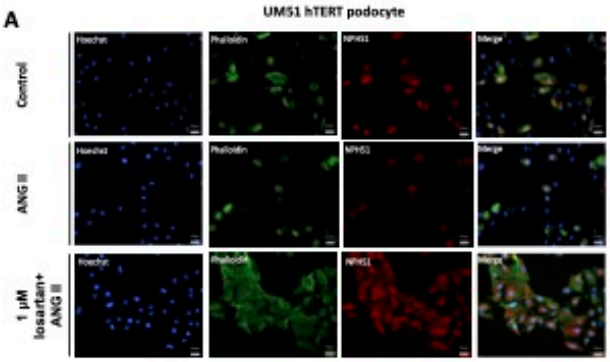


Figure 1. *Cont.*

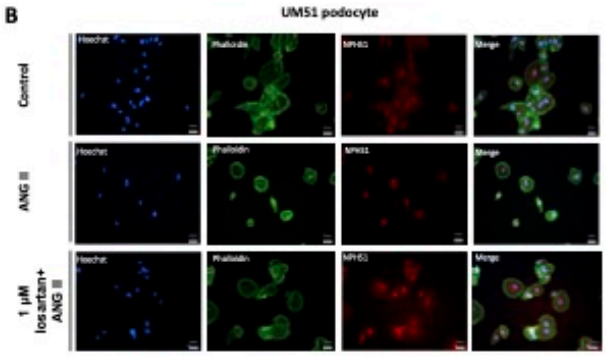


Figure 1. Losartan enhances NPHS1 expression in UdRPC-derived podocytes. UM51 and immortalized UM51-hTERT were differentiated into podocytes by culturing at 60–70% density in advanced RPMI medium supplemented with 30 µM RA. Podocytes were pre-treated with 1 µM losartan for 24 h and subsequently treated with 100 µM ANG II for a further 24 h. NPHS1 was expressed at both losartan concentrations and some cells adopted a rounded morphology ($n = 3$). (**A**) corresponds to the UM51 hTERT cell line and (**B**) the primary UM51 podocytes.

2.2. The Effect of Angiotensin II and Losartan on the Expression of Angiotensin Receptor Type 1 and 2

High ANG II concentrations impart a strong vasoconstriction effect that is associated with an increase in blood pressure. To assess the effect of ANG II and the ability of the generated podocytes to model RAAS with the involvement of AGTR1 and AGTR2, a final concentration of 100 µM ANG II in adv. RPMI supplemented with 30 µM RA for 24 h was used to treat the cells. The gene-specific mRNA expression of AGTR1, AGTR2 receptors, and NPHS1 were analyzed via qRT-PCR (Figure 2A–C). The expression of AGTR1 tended to be upregulated by 24 h of ANG II treatment in the UM51 podocytes and UM51 hTERT podocytes. In the UM51 podocytes, we observed a significant increase in the AGTR1 expression after ANG II treatment ($p = 0.002$). In contrast, the addition of 1 µM losartan induced a slight significant downregulation of AGTR1 ($p < 0.05$) compared to ANG II treatment (Figure 2A). The expression of AGTR2 was significantly downregulated after 24 h of ANG II treatment in UM51 ($p = 0.007$) while in UM51, hTERT podocyte mRNA expression was slightly increased (Figure 2B).

Furthermore, the expression of the podocyte structural protein NPHS1 was analyzed using RT-PCR and Western blotting. We show that NPHS1 expression is significantly downregulated in the UM51 hTERT podocytes by ANG II treatment for 24 h ($p = 0.02$) (Figure 2C). As hypothesized, this transcriptional downregulation was counteracted by losartan, leading to a significant increase in NPHS1 ($p < 0.05$) expression in both cell lines (Figure 2C). To further confirm the effect of losartan, the protein expression of AGTR1, AGTR2, and NPHS1 were determined using Western blot analysis. ANG II treatment increased AGTR1 expression and induced a concomitant downregulation of AGTR2 (Figure 2D). This effect is counteracted by the addition of losartan, resulting in a significant decrease in AGTR1 ($p = 0.004$ and $p = 0.01$) expression compared with ANG II treatment (Figure 2D). In parallel, AGTR2 expression significantly increased compared to ANG II treatment ($p = 0.003$ and $p = 0.004$) (Figure 2D). We propose that losartan modulates the expression of both receptors, with a bias, however, towards the AGTR2 downstream signaling pathway.

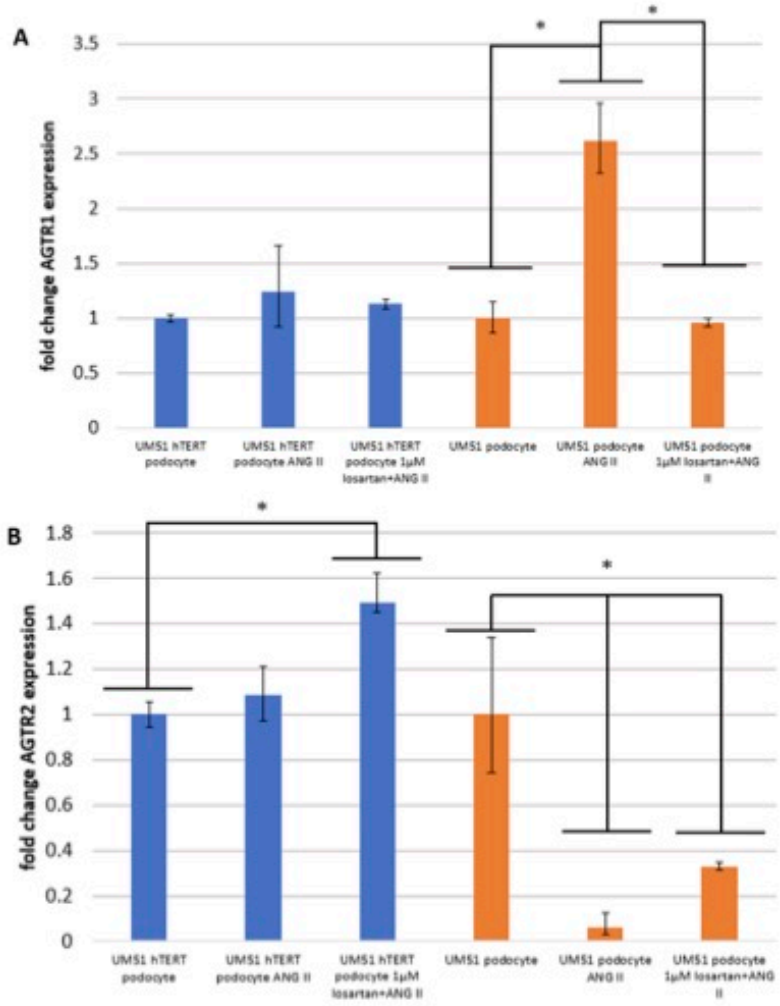


Figure 2. *Cont.*

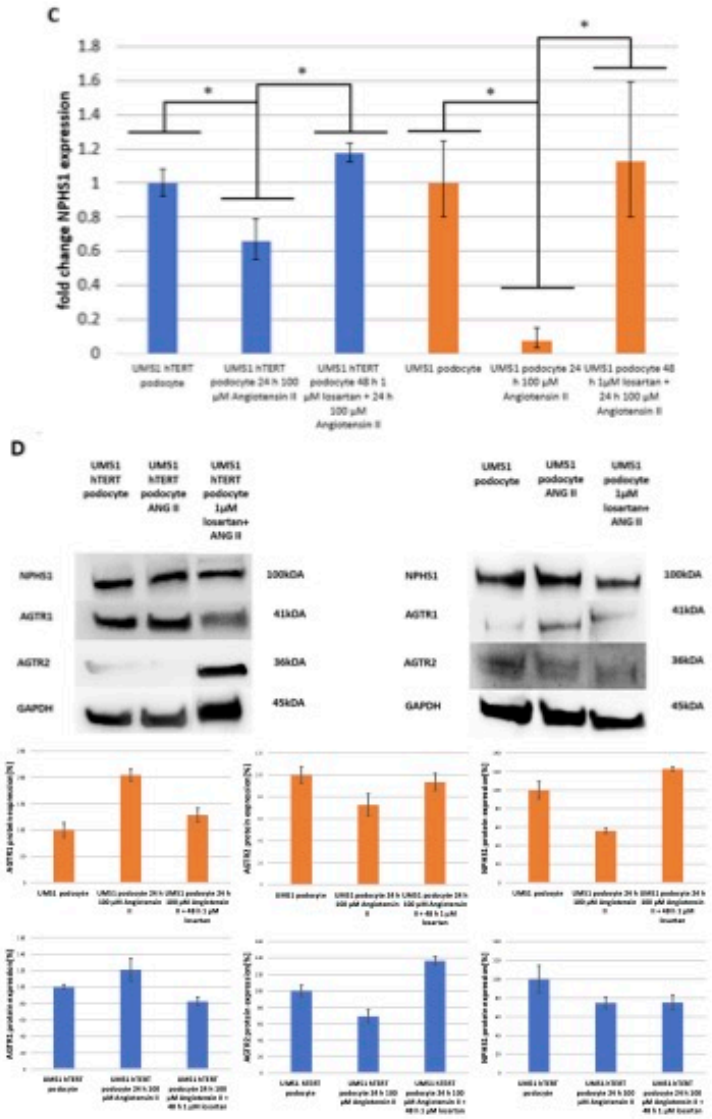
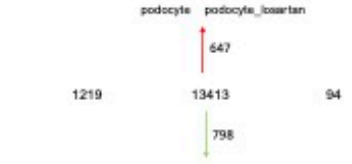


Figure 2. Stimulation of podocytes with losartan and Ang II induced changes in the expression of angiotensin receptors I and II. Urine-derived renal progenitor cells UM51 and immortalized UM51-hTERT were differentiated into podocytes. The RAAS-associated receptors AGTR1 (**A**,**D**), AGTR2 (**B**,**D**), and NPHS1(**C**,**D**) were analyzed via qPCR (**A**–**C**) and Western blotting (**D**). Expression of Glyceraldehyde-3-phosphate dehydrogenase (GAPDH) was used for normalization. Full uncropped Western blot images are presented in Supplementary Figure S1A,B. To normalize the quantitative real-time PCR, the ribosomal encoding gene RPL0 was used. Primary UM51 podocytes are depicted in orange and the immortalized UM51-hTERT podocytes are represented in blue ($n = 3$). The statistical significance was calculated using the two-sample Student's *t*-test with a significance threshold $p = 0.05$ is marked by an asterisk (*).

2.3. Comparative Transcriptome Analysis of Urine-Derived Podocytes Treated with and without Losartan

The podocytes were treated with 100 µM ANG II or 1 µM losartan or the combination of 100 µM ANG II and 1µM losartan, and we performed a comparative transcriptome analysis. Hierarchical clustering analysis comparing the transcriptomes revealed a distinct expression pattern for all treatments compared to the untreated control podocytes (Supplementary Figure S2A,B). A total of 13,413 genes were detected as expressed in both the untreated and 1 µM losartan treated podocytes. Comparing the expressed genes (det-$p < 0.05$), 1219 are exclusively expressed in the untreated control podocytes and 94 in the podocytes treated with losartan alone (Figure 3A). The most over-represented GO BP-terms exclusive to untreated podocytes are associated with the regulation of system processes, epithelial cell differentiation, negative regulation of cell population proliferation, and cytokine–cytokine receptor interaction (Supplementary Table S3, sheet 1). In comparison, podocytes treated with 1 µM losartan showed the most over-represented GO BP-terms associated with regulation of monoatomic ion transmembrane transporter activity, cell morphogenesis involved in neuron differentiation, and cell–cell communication (Figure 3B,D). The significant genes and associated KEGG pathways revealed vascular smooth muscle contraction, the oxytocin signaling pathway, renin secretion, and ECM-receptor interaction (Figure 3C). The entire KEGG pathway is presented in Supplementary Table S5 and Supplementary Figure S3A,B. Figure 3D represents an overview of the exclusive GO BP-terms for losartan alone used in this study. The full gene lists can be found in Supplementary Table S4.

A



B

GoID	BP-Term	Pvalue
GO:0019935	*cyclic-nucleotide-mediated signaling*	0.00332
GO:0022898	*regulation of transmembrane transporter activity*	0.00372
GO:0032414	*positive regulation of ion transmembrane transporter activity*	0.00381
GO:0043951	*negative regulation of cAMP-mediated signaling*	0.00382
GO:0043508	*negative regulation of JUN kinase activity*	0.00177
GO:1904064	*positive regulation of cation transmembrane transport*	0.00277
GO:0032793	*positive regulation of CREB transcription factor activity*	0.00277
GO:0007194	*negative regulation of adenylate cyclase activity*	0.00306
GO:1900273	*positive regulation of long-term synaptic potentiation*	0.00336
GO:0042326	*negative regulation of phosphorylation*	0.00392

C

KeggID	Kegg name	p_hyper
hsa04270	*Vascular smooth muscle contraction - Homo sapiens (human)*	0.022129
hsa04921	*Oxytocin signaling pathway - Homo sapiens (human)*	0.031091
hsa04924	*Renin secretion - Homo sapiens (human)*	0.037974
hsa04512	*ECM-receptor interaction - Homo sapiens (human)*	0.058788

Figure 3. *Cont.*

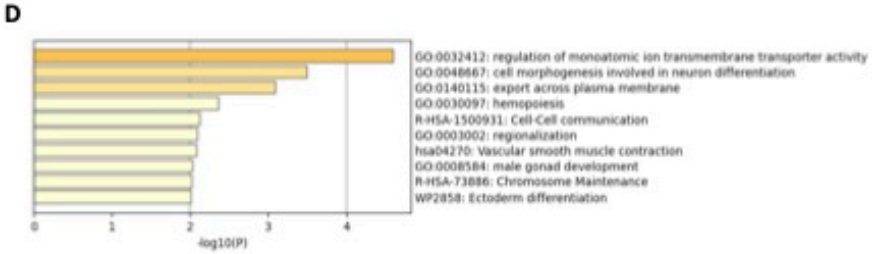


Figure 3. Transcriptome analysis of urine-derived podocytes treated with and without losartan. Comparative transcriptome and Gene Ontology analysis of urine-derived UM51 podocytes treated with and without 1 µM losartan. Expressed genes (det- $p < 0.05$) in UM51 derived podocytes treated with and without 1 µM losartan compared in the Venn diagram (**A**) show distinct (1219 in untreated podocytes and 94 in podocytes treated with 1 µM losartan) gene expression patterns. In total, 13,413 genes were found to be expressed in common between untreated podocytes and podocytes treated with 1 µM losartan. Podocytes treated with 1 µM losartan showed the most over-represented GO BP-terms associated with regulation of monoatomic ion transmembrane transporter activity, cell morphogenesis involved in neuron differentiation, and cell–cell communication (**B**,**D**). The 94 significant genes associated with KEGG pathways revealed vascular smooth muscle contraction, oxytocin signaling pathway, renin secretion, and ECM-receptor interaction (**C**).

2.4. Comparative Transcriptome Analysis of Urine-Derived Podocytes Treated with Angiotensin II and the Combination of Angiotensin II and Losartan

We detected 13,131 genes as co-expressed between podocytes treated with 100 µM ANG II and the combination of 100 µM ANG II and 1 µM losartan (Figure 4A). In total, 1243 genes were exclusively expressed in podocytes treated with ANG II alone. In the combination of ANG II and losartan, 106 unique genes were expressed (Figure 4A). The most over-represented GO BP-terms exclusive to podocytes treated with 100 µM ANG II are associated with cell division, regulation of cell cycle process, renal system development, metal ion transport, and regulation of hormone levels (Supplementary Table S3, sheet 4). In comparison, podocytes treated with the combination of 100 µM ANG II and 1 µM losartan showed the most over-represented GO BP-terms associated with extracellular matrix organization, metal ion transport, DNA methylation or demethylation, cell differentiation, developmental process, response to muscle stretch, calcium ion transmembrane transport, and regulation of cytokine production involved in inflammatory response (Figure 4B,D). The significant genes and associated KEGG pathways revealed including protein digestion and absorption, pancreatic secretion, and primary immunodeficiency, amongst others. (Figure 4C). The entire KEGG pathway is presented in Supplementary Table S5.

To summarize, our results provide detailed information on ANG II and losartan-induced gene expression and associated signaling pathways. The full gene lists can be found in Supplementary Table S4.

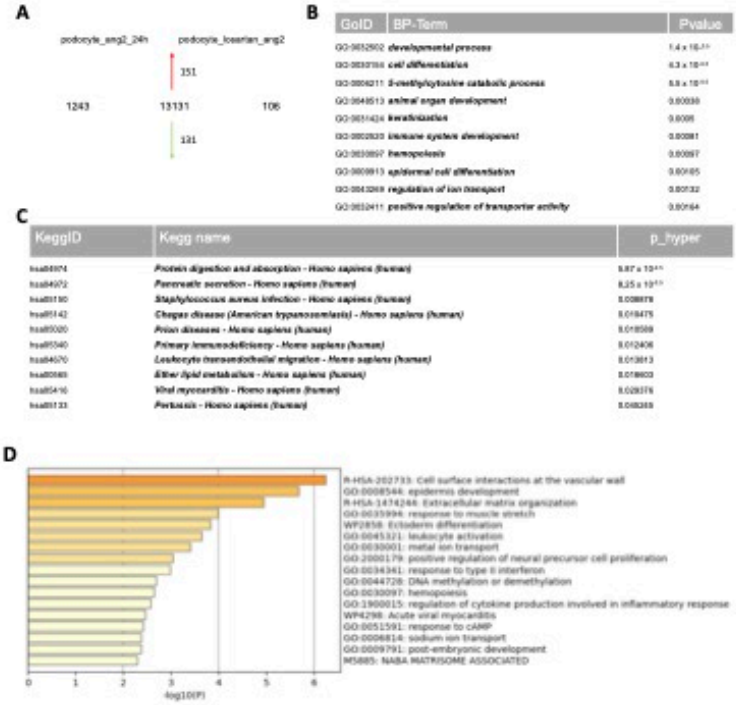


Figure 4. Transcriptome analysis of urine-derived podocytes stimulated with ANG II and losartan. Comparative transcriptome and Gene Ontology analysis of urine-derived UM51 podocytes stimulated with 100 µM ANG II with and without 1 µM losartan. Expressed genes (det-$p < 0.05$) in UM51 derived podocytes treated with 100 µM ANG II and with and without 1 µM losartan compared in the Venn diagram (**A**) show distinct (1243 in podocytes only treated with 100 µM ANG II; 106 in podocytes treated with the combination of 100 µM ANG II and 1µM losartan) gene expression patterns. We found 13,131 genes to be expressed in common between podocytes treated with 100 µM ANG II and podocytes treated with the combination of 100 µM ANG II and 1 µM losartan. Podocytes treated with the combination of 100 µM ANG II and 1 µM losartan showed the most over-represented GO BP-terms associated with extracellular matrix organization, metal ion transport, DNA methylation or demethylation, and regulation of cytokine production involved in inflammatory response and response to cAMP (**B**,**D**). KEGG pathway analyses revealed, for example, protein digestion and absorption, pancreatic secretion, and primary immunodeficiency (**C**).

3. Discussion

The epithelial cells of the glomerulus called podocytes are highly differentiated and specialized cells that are located on the outside of the glomerular capillaries and project into the urinary cavity of Bowman's capsule. They have a large cell body from which numerous foot processes taper around the glomerular capillaries. Worldwide, 1.28 billion adults aged 30–79 years are afflicted with elevated blood pressure [29]. Uncontrolled high blood pressure causes serious damage to the heart and kidneys that eventually leads to death. RAAS represents a key mechanism in the regulation of blood pressure and the electrolyte and fluid balance of the organism. Activation of the RAAS is mediated by two receptors, angiotensin II receptor type I and II. Studies suggest that AGTR1 in the kidney is responsible for hypertension in mammals [30]. Based on this, AGTRs were shown to be expressed in various segments of the nephron in the distal tubule, collecting duct, and renal

vasculature [5–10]. The stimulation of AGTR1, which is expressed 8–10 fold higher at the mRNA level than AGTR2 in the human kidney, is accompanied by renal vasoconstriction, which consequently impairs the capacity of the kidney to process sodium by decreasing medullary blood flow [31]. Additionally, other groups have reported that ANG II can induce damage to and the subsequent loss of podocytes [32]. AGTR1 can be activated by the main mediator of the RAAS, namely ANG II. An increased amount of circulating and intracellular ANG II and aldosterone causes a pro-fibrotic, -inflammatory, and -hypertrophic milieu that triggers the remodeling and dysfunction of the podocyte cytoskeleton.

To date, human induced pluripotent stem cells (iPSCs) derived from somatic cells are available and serve to study nephrogenesis and various kidney associated diseases such as hypertension [33–37]. In the present study, we investigated gene-regulatory networks induced by ANGII and losartan employing our previously established podocyte differentiation protocol based on urine-derived nephron progenitor cells (UdRPCs) [19,28]. We specifically modeled the RAAS pathway using our established primary SIX2-positive UM51 and the transformed counterpart UM51-hTERT cell line. In our previous work, immunofluorescence-based protein detection, Western blotting, and RT-PCR were used to observe a change in the podocyte cytoskeleton after 24 h of ANG II treatment [19]. ANG II treatment led to the alteration of the podocyte-specific fried-egg morphology to a rounded-cell morphology. It is known that downregulation in the expression of podocyte-specific genes, such as NPHS1, is associated with podocyte injury [38]. Consequently, there is a disturbance of the foot processes and the slit diaphragm [39,40]. An upregulation in angiotensin II receptor type I expression was shown after 24 h treatment with ANG II. The biological function of this receptor is associated with the mediation of vasoconstriction, cell proliferation, nephrosclerosis, hypertrophy of vascular media, endothelial dysfunction, inflammation and immune responses, and promotion of aging [11,41]. It is questionable whether podocytes can adapt their phenotype and whether the observed changes even remain chronic when stimulated with ANG II over a longer period. Currently, numerous angiotensin receptor blockers (ARB) and angiotensin converting enzyme inhibitors (ACEI) are used in the clinic to manage a variety of renal disorders; one of these ARBs is losartan. It is an anti-hypertensive agent from the group of sartans used to treat hypertension, heart failure, and diabetic nephropathy. Its action is based on reversing the effects of ANG II at AGTR1 by blocking AGTR1 [42]. ANG II signaling through AGTR2 has been associated with vasodilatation, development, cell differentiation, tissue repair, and apoptosis [11].

The use of losartan allowed us to determine whether the cytoskeletal change was mediated by ANGII induced signaling through AGTR1. The present data indicate that the addition of losartan is sufficient to counteract the cytoskeletal restructuring induced by ANG II by rescuing NPHS1 expression. It is interesting to note that losartan causes a redistribution of the expression of AGTR1 and AGTR2. From this, it can be concluded that losartan can efficiently block binding to AGTR1, causing ANG II to bind with a higher preference, presumably to AGTR2. Furthermore, this indicates that activated angiotensin receptors trigger a signaling cascade into the nucleus to augment their own transcriptional and translational expression. AGTR2 appears to reintroduce cells into differentiation, again upregulating the expression of podocyte-specific genes.

The 1243 genes that were upregulated in the podocytes treated with ANG II are annotated with GO-BP terms such as renal system development, cell division, metal ion transport, calcium signaling pathway, and regulation of the cell cycle process, suggesting that these cells might dedifferentiate and lose their cell type-specific properties by signaling through AGTR1. Podocytes are terminally differentiated cells that do not undergo cell division in vivo. Therefore, a process of dedifferentiation is needed when kidney damage occurs. This process has been described for many renal pathologies, such as diabetes and lupus nephritis, and is even discussed as a potential biomarker [43]. In our model, we hypothesize that this dedifferentiation might reflect the need for highly differentiated podocytes to re-enter the cell cycle to regenerate tissue because of ANGII-induced damage.

In comparison, GO-BP terms for losartan treatment included cell–cell communication, vascular smooth muscle contraction, oxytocin signaling pathways, and renin secretion. These include the calmodulin-like 4 (CALML4), natriuretic peptide A (NPPA), and protein phosphatase 1 regulatory subunit 12B (PPP1R12B) genes. The blockade of AGTR1 and the resulting signaling through AGTR2 seem to lead to vasodilation and reduction in vascular tone [44–46]. In addition, metal ion transport seems to play an essential role in the distinct signaling cascades of the receptors and the conformation of ANGII itself [10,47]. More precisely, the interaction of metal ions with the imidazole moiety of His-6 of ANGII has been shown to influence the conformation of human ANG II [47]. ANG II-stimulated podocytes show upregulated expression of genes including adrenoceptor alpha 1A (*ADRA1A*) and shroom family member 2 (*SHROOM2*). Like AGTR1, the alpha-adrenergic receptor *ADRA1A* mediates its action through association with G-proteins that activate a phosphatidylinositol calcium second messenger system. These in turn activate mitogenic responses and regulate the growth and proliferation mediated by Klf15 in the kidney [48]. Additionally, the loss of foot processes may be explained by *SHROOM2*, which is involved in endothelial cell morphology changes during cell spreading [49].

Some of the losartan-induced 94 genes are associated with the GO-BP term metal ion transport, which includes *LCK*, *NPPA*, *CCL3*, *SLC10A1*, *SLC12A3*, *CACNA1H*, *CATSPER1*, *LRRC38*, *HEPHL1*, *CFTR*, *TMC8*, *CSRP3*, *DMD*, and *MMP9*. These genes have been reported to contribute to reduction in inflammation and oxidative stress [50]. ARBs prevent abnormal iron deposition in the interstitium, correct chronic hypoxia, reduce the expression of heme oxygenase and p47phox, and inhibit pentosidine formation [51]. *NPPA*, for example, is responsible for extracellular fluid volume and electrolyte homeostasis. This signaling cascade can apparently be activated by the addition of losartan and seems to play a major role in hypertension [45,52,53]. The inhibition of tyrosine kinase activity by *LCK* results in a reduction in oxidative stress as described by Alqarni [54]. Interestingly, the inhibition of metal ions catalyzes oxidation of ascorbic acid, and abnormal depositing of metal ions in the interstitium is unique to ARBs, but not to calcium channel blockers (CCBs) and ß blockers (BBs). This might imply superior renal protective effects of ARBS related to the prevention of oxidative stress.

The 106 genes associated with the co-stimulation of losartan and ANG II are annotated with GO-BP terms such as extracellular matrix organization, metal ion transport, DNA methylation or demethylation, cell differentiation, developmental process, response to muscle stretch, regulation of cytokine production involved in inflammatory response, and calcium ion transmembrane transport. It has already been reported that podocytes expresse the transient receptor proteins TRPC3, TRPC4, TRPC5, and TRPC6 [55,56]. Under normal conditions, these receptors mediate calcium influx into podocytes, by which they can adapt their cytoskeleton to environmental cues. This actin remodeling is Ca^{2+} dependent. As early as 1978, Kerjaschik was the first to propose that the Ca^{2+} increase in podocytes is one of the first events leading to podocyte injury [57]. AGTR1 serves as an upstream receptor for both TRPC5 and TRPC6 in podocytes [58]. It was previously suggested that the activation of Calcineurin appears to be downstream of the AGTR1 signaling pathway via ANG II [59,60]. Upstream of AGTR1, G protein-coupled receptors activate phospholipase C, which grants Ca^{2+} influx via TRPC5/TRPC6. This cascade enables the downstream transcription of Calcineurin. AGTR1, TRPC, Calcineurin, and the actin cytoskeleton form a linear signaling cascade in which ANG II activates Calcineurin in a TRPC5-dependent manner [58]. Changed calcium influx leads to the loss of podocyte foot processes and the downregulation of SYNPO as well as TRPC6 [61]. This downregulation of the podocyte-specific marker SYNPO was already demonstrated in one of our previous manuscripts [28]. The effect of ANG II on human urine-derived podocytes is also reflected in our data, in which calcium signaling is associated with ANG II treatment. ANGII induced activation of AGTR1 signaling is reflected by the biological effects of AGTR1, which initiates proliferation as well as calcium-dependent changes in cellular morphology. Another possible mode of action was revealed by a study carried out by Schenk et al. [62]. Here, the authors showed the protein expression and phosphorylation of LCP1 in ANGII treated podocytes

through AGTR1 activation [62]. It is known that LCP1 is involved in actin-bundling and that this function is impaired by increased calcium concentrations [63]. A well-documented biological effect of ANG II signaling via AGTR2 is vasodilation, which is highlighted by our transcriptome data [13,46].

Transcriptome analysis revealed 94 losartan-induced genes associated with diverse biological processes and pathways such as vascular smooth muscle contraction, the oxytocin signaling pathway, renin secretion, and ECM-receptor interaction. Co-stimulation with losartan and ANG II induced exclusive expression of 106 genes associated with extracellular matrix organization, metal ion transport, DNA methylation or demethylation, cell differentiation, the developmental process, response to muscle stretch, calcium ion transmembrane transport, and the regulation of cytokine production involved in the inflammatory response.

These findings highlight the usefulness of human urine-derived podocytes in studying nephrogenesis, kidney-associated diseases such as hypertension, the RAAS pathway, nephrotoxicity, and drug screening. Figure 5 presents a graphical summary of this study.

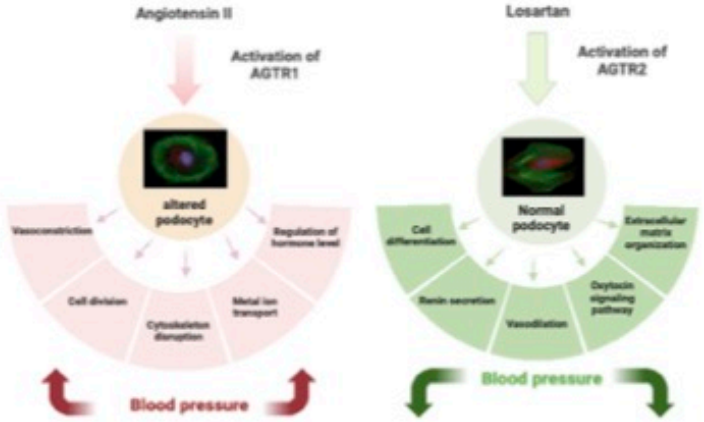


Figure 5. Biological consequences of ANG II binding on angiotensin II type I and II receptors. The renin–angiotensin–aldosterone system (RAAS) is a bio-enzymatic cascade that contributes to various systematic and localized processes. The octapeptide angiotensin II (ANG II) is the biological effect of the RAAS and regulates blood pressure and extracellular volume. ANG II can bind two types of receptors that are involved in the regulation of renal hemodynamics and tubular function. These effects are dependent on binding to the two subtypes of receptors angiotensin receptors type I (AGTR1) and angiotensin receptors type II (AGTR2). ANGII binding and signaling through AGTR1 is associated with cell division, cytoskeleton disruption, vasoconstriction, metal ion transport, and regulation of hormone levels, e.g., estrogen or cholecystokinin. The development of orally active, non-peptide, selective AGTR1 blockers began with the synthesis of losartan. Preventing the binding of ANGII to AGTR1 leads to binding and signaling through AGTR2, which is associated with vasodilation, renin secretion, cell differentiation, extracellular matrix organization, and activation of the oxytocin signaling pathway [64].

4. Materials and Methods

4.1. Cell Culture Conditions

Urine-derived renal progenitor cells (UdRPCs) of a 51-year-old male (UM51) were isolated as described in Rahman et al. [24]. Further, the UM51 cell line was immortalized with an hTERT-expressing plasmid (UM51 hTERT) [28]. The cell lines were cultured on 0.2% type 1 collagen (Thermo Fisher Scientific, Waltham, MA, USA) coated 6- or 12-well plates at 37 °C under hypoxic conditions. The cells were cultured in Proliferation Medium

(PM) composed of 50% DMEM high-glucose (Gibco) and 50% keratinocyte growth basal medium (Lonza, Basel, Switzeland) supplemented with 5% fetal bovine serum (Gibco), 0.5% Non-Essential Amino Acid (Gibco), 0.25% Glutamax (Gibco), and 0.5% penicillin and streptomycin (Gibco). For further differentiation into podocytes, the cells were seeded at a low density (50,000 cells per 6-well) and cultured for 24 h in PM. On the next day, the medium was exchanged to Advanced RPMI 1640 (Gibco) supplemented with 0.5% fetal bovine serum, 1% penicillin and streptomycin, and 30 µM retinoic acid (Sigma-Aldrich Chemistry, Steinheim, Germany). After 7 days, the typical podocyte morphology was observed. Losartan (Sigma-Aldrich Chemistry) and ANG II (Sigma-Aldrich Chemistry) were diluted using Advanced RPMI 1640 to a final concentration of 100 µM ANG II or 1 µM losartan. First, the cells were incubated for 24 h with 1 µM losartan and then for 24 h with ANG II.

4.2. Immunofluorescence Staining

For the immunocytochemistry, the podocytes were fixed with 4% paraformaldehyde (PFA) (Polysciences, Warrington, FL, USA) followed by three wash steps with PBS for 5 min each. To block unspecific binding sites, the fixed cells were incubated with blocking buffer containing 10% normal goat or donkey serum, 1% BSA, 0.5% Triton X-100 (Sigma-Aldrich Chemistry) and 0.05% Tween-20 (Sigma-Aldrich Chemistry) for 2 h at room temperature. The primary antibodies were diluted in blocking buffer according to Supplementary Table S1 and incubated at 4 °C overnight. On the following day, the cells were washed once with 0.05% Tween-20 diluted in PBS and two times with PBS only. After washing them, a fluorochrome conjugated secondary antibody together with HOECHST (1:5000) (Thermo Fisher Scientific, Waltham, MA, USA) were added and incubated for 1 h at room temperature protected from light. The secondary antibodies were diluted in blocking buffer according to Supplementary Table S1. After three consecutive washing steps, the visualization was performed by using a fluorescence microscope (LSM700).

4.3. Relative Quantification of Podocyte-Associated Gene Expression via Real-Time PCR

Quantitative PCR was performed using podocyte-specific genes and angiotensin II receptors of type I and II. The samples were run in triplicate on a 384-well reaction plate and Power Sybr Green PCR Master Mix (Applied Biosystems, Foster City, CA, USA) using Step One Plus Real-Time PCR systems. The amplification conditions were denaturation at 95 °C for 13 min followed by 37 cycles of 95 °C for 50 s, 60 °C for 45 s, and 72 °C for 30 s. To normalize the quantitative real-time PCR, the ribosomal encoding gene-RPL0 was used. The primer sequences are listed in Supplementary Table S2. The results were analyzed using the $2^{-\Delta\Delta CT}$ method and specified by fold change expression. The samples were run in independent experiments three times. The mean value of these experiments was used for the calculations. The statistical significance was calculated using the Two-Sample test assuming unequal variances [65] with a significance threshold $p = 0.05$.

4.4. Western Blot Analysis

The podocytes were lysed in RIPA buffer (Sigma-Aldrich Chemistry) containing 5 M NaCl, 1% NP-40, 0.5% DOC, 0.1% SDS, 1 mM EDTA, 50 mM Tris, pH 8.0, and freshly added 10 µL/mL protease and phosphatase inhibitor (Sigma-Aldrich). We dissolved 20 µg of each obtained protein lysate in a 10% sodium dodecyl sulfate PAGE gel and then transferred it to an Immobilon-P membrane (Merck Millipore, Burlington, VT, USA). The membranes were incubated with the primary antibody overnight at 4 °C, then washed three times with 0.1% Tween-20 in Tris-buffered saline followed by 1 h of incubation of the secondary antibodies at room temperature. For visualization of the blotted proteins, Pierce™ ECL Western Blotting Substrate solutions from Thermofisher (Thermo Fisher Scientific, Waltham, MA, USA) were used. The quantification was carried out with ImageJ. Detailed information on the antibodies used can be found in Supplementary Table S1.

4.5. Microarray Data Analyses

For the microarray experiments, 1 µg RNA preparations were hybridized on the Human Clariom S Gene Expression Array (Affymetrix, Thermo Fisher Scientific, Waltham, MA, USA) at the core facility Biomedizinisches Forschungszentrum (BMFZ) of the Heinrich Heine University Düsseldorf. The raw data were imported into the R/Bioconductor environment [66] and further processed with the package oligo [67] using background correction, logarithmic (base 2) transformation, and normalization with the robust multi-array average (RMA) method. Venn diagrams were generated with the Venn diagram package. Subsets from the Venn diagrams were used for follow-up GO and pathway analyses [68]. Heatmaps were drawn with the R package gplots [69] using Pearson correlation as similarity measure and color scaling per gene.

Gene expression data will be available online in the National Centre of Biotechnology Information (NCBI) Gene Expression Omnibus.

4.6. Ethics Statement

In this study, urine samples were collected with the informed consent of the donors and the written approval (Ethical approval Number: 5704) of the ethical review board of the medical faculty of Heinrich Heine University, Düsseldorf, Germany. All methods were carried out in accordance with the approved guidelines. The medical faculty of Heinrich Heine University approved all experimental protocols.

4.7. Statistics

Data are presented as arithmetic means + standard error. In total, three independent experiments were performed and used for the calculation of mean values. The statistical significance was calculated using the two-sample Student's *t*-test with a significance threshold $p = 0.05$.

Supplementary Materials: The following supporting information can be downloaded at: https://www.mdpi.com/article/10.3390/ijms241310551/s1.

Author Contributions: Conceptualization, J.A.; methodology, J.A., C.T., L.E., and W.W.; bioinformatics, W.W.; formal analysis, C.T., L.E., and W.W.; investigation, C.T., L.E., and W.W.; resources, J.A.; data curation, C.T.; writing—original draft preparation, C.T.; writing—review and editing, C.T., L.E., and J.A.; visualization, C.T.; supervision, J.A.; project administration, J.A.; funding acquisition, J.A. All authors have read and agreed to the published version of the manuscript.

Funding: J.A. acknowledges the medical faculty of Heinrich Heine University for financial support.

Institutional Review Board Statement: This study was conducted in accordance with the written approval (Ethical approval Number: 5704) of the ethical review board of the medical faculty of Heinrich Heine University, Düsseldorf, Germany. All methods were carried out in accordance with the approved guidelines. The medical faculty of Heinrich Heine University approved all experimental protocols.

Informed Consent Statement: In this study, urine samples were collected with the informed consent of the donors.

Data Availability Statement: Not applicable.

Acknowledgments: James Adjaye acknowledges funding from the medical faculty of Heinrich Heine University, Duesseldorf, Germany.

Conflicts of Interest: The authors declare no conflict of interest.

References

1. Schmidt, R.F.; Lang, F.; Heckmann, M. *Physiologie des Menschen*, 31st ed.; Springer: Berlin/Heidelberg, Germany, 2017; ISBN 978-3-662-54121-0.
2. Schwarz, K.; Simons, M.; Reiser, J.; Saleem, M.; Faul, C.; Kriz, W.; Shaw, A.; Holzmann, L.; Mundel, P. Podocin, a raft-associated component of the glomerular slit diaphragm, interacts with CD2AP and nephrin. *J. Clin. Investig.* **2001**, *108*, 1621–1629. [CrossRef] [PubMed]
3. Martin, C.; Jones, N. Nephrin Signaling in the Podocyte: An Updated View of Signal Regulation at the Slit Diaphragm and Beyond. *Front. Endocrinol.* **2018**, *9*, 302. [CrossRef]
4. Li, C.; Ruotsalainen, V.; Tryggvason, K.; Shaw, A.; Miner, J. CD2AP is expressed with nephrin in developing podocytes and is found widely in mature kidney and elsewhere. *Am. J. Physiol. Renal Physiol.* **2000**, *279*, F785–F792. [CrossRef]
5. Barreto-Chaves, M.L.; Mello-Aires, M. Effect of luminal angiotensin II and ANP on early and late cortical distal tubule HCO3- reabsorption. *Am. J. Physiol.* **1996**, *271*, F977–F984. [CrossRef]
6. Kwon, T.-H.; Nielsen, J.; Kim, Y.-H.; Knepper, M.A.; Frøkiaer, J.; Nielsen, S. Regulation of sodium transporters in the thick ascending limb of rat kidney: Response to angiotensin II. *Am. J. Physiol.* **2003**, *285*, F152–F165. [CrossRef] [PubMed]
7. Rocque, B.L.; Babayeva, S.; Li, J.; Leung, V.; Nezvitsky, L.; Cybulsky, A.V.; Gros, P.; Torban, E. Deficiency of the Planar Cell Polarity Protein Vangl2 in Podocytes Affects Glomerular Morphogenesis and Increases Susceptibility to Injury. *J. Am. Soc. Nephrol.* **2015**, *26*, 576–586. [CrossRef]
8. Tojo, A.; Tisher, C.C.; Madsen, K.M. Angiotensin II regulates H(+)-ATPase activity in rat cortical collecting duct. *Am. J. Physiol.* **1994**, *267*, F1045–F1051. [CrossRef]
9. Xie, K.; Xu, C.; Zhang, M.; Wang, M.; Min, L.; Qian, C.; Wang, Q.; Ni, Z.; Mou, S.; Dai, H.; et al. Yes-associated protein regulates podocyte cell cycle re-entry and dedifferentiation in adriamycin-induced nephropathy. *Cell Death Dis.* **2019**, *10*, 915. [CrossRef] [PubMed]
10. Wang, T.; Giebisch, G. Effects of angiotensin II on electrolyte transport in the early and late distal tubule in rat kidney. *Am. J. Physiol.* **1996**, *271*, F143–F149. [CrossRef] [PubMed]
11. Kaschina, E.; Unger, T. Angiotensin AT1/AT2 receptors: Regulation, signalling and function. *Blood Press.* **2003**, *12*, 70–88. [CrossRef]
12. Savoia, C.; Burger, D.; Nishigaki, N.; Montezano, A.; Touyz, R.M. Angiotensin II and the vascular phenotype in hypertension. *Comb. Univ. Press* **2011**, *13*, 11. [CrossRef]
13. Siragy, H.M. AT1 and AT2 Receptor in the Kidney: Role in Health and Disease. *Semin. Nephrol.* **2004**, *24*, 93–100. [CrossRef] [PubMed]
14. Ames, M.; Atkins, C.; Pitt, B. The renin-angiotensin-aldosterone system and its suppression. *J. Vet. Intern. Med.* **2019**, *33*, 363–382. [CrossRef] [PubMed]
15. Berry, C.; Touyz, A.F.; Dominiczak, R.; Webb, C.; Johns, D.G. Angiotensin receptors: Signaling, vascular pathophysiology, and interactions with ceramide. *Am. J. Physiol. Heart Circ. Physiol.* **2001**, *281*, H2337–H2365. [CrossRef] [PubMed]
16. Widdop, R.; Jones, E.; Hannan, R.; Gaspari, T. Angiotensin AT2 receptors: Cardiovascular hope or hype? *Br. J. Pharmacol.* **2003**, *140*, 809–824. [CrossRef] [PubMed]
17. Macconi, D.; Abbate, M.; Morigi, M.; Angioletti, S.; Mister, M.; Buelli, S.; Bonomelli, M.; Mundel, P.; Endlich, K.; Remuzzi, A.; et al. Permselective Dysfunction of Podocyte-Podocyte Contact upon Angiotensin II Unravels the Molecular Target for Renoprotective Intervention. *Am. J. Pathol.* **2006**, *168*, 1073–1085. [CrossRef]
18. Suzuki, K.; Han, G.D.; Miyauchi, N.; Hashimoto, T.; Nakatsue, T.; Fujioka, Y.; Koike, H.; Shimizu, F.; Kawachi, H. Angiotensin II Type 1 and Type 2 Receptors Play Opposite Roles in Regulating the Barrier Function of Kidney Glomerular Capillary Wall. *Am. J. Pathol.* **2007**, *170*, 1841–1853. [CrossRef]
19. Erichsen, L.; Thimm, C.; Bohndorf, M.; Rahman, M.S.; Wruck, W.; Adjaye, J. Activation of the Renin–Angiotensin System Disrupts the Cytoskeletal Architecture of Human Urine-Derived Podocytes. *Cells* **2022**, *11*, 1095. [CrossRef]
20. Remuzzi, G.; Benigni, A.; Remuzzi, A. Mechanisms of progression and regression of renal lesions of chronic nephropathies and diabetes. *J. Clin. Investig.* **2006**, *116*, 288–296. [CrossRef]
21. Currie, G.; Delles, C. Proteinuria and its relation to cardiovascular disease. *Int. J. Nephrol. Renovasc. Dis.* **2014**, *7*, 13–24. [CrossRef]
22. Ferrario, C. Role of Angiotensin II in Cardiovascular Disease—Therapeutic Implications of More Than a Century of Research. *JRAAS* **2006**, *7*, 3–145. [CrossRef] [PubMed]
23. Atlas, S. The Renin-Angiotensin Aldosterone System: Pathophysiological Role and Pharmacologic Inhibition. *J. Manag. Care Pharm.* **2007**, *13*, 9–20. [CrossRef] [PubMed]
24. Rahman, M.S.; Wruck, W.; Spitzhorn, L.-S.; Nguyen, L.; Bohndorf, M.; Martins, S.; Asar, F.; Ncube, A.; Erichsen, L.; Graffmann, N.; et al. The FGF, TGFβ and WNT axis Modulate Self-renewal of Human SIX2 + Urine Derived Renal Progenitor Cells. *Sci. Rep.* **2020**, *10*, 739. [CrossRef]
25. Onoda, N.; Kawabata, A.; Hasegawa, K.; Sakakura, M.; Urakawa, I.; Seki, M.; Zenkoh, J.; Suzuki, A.; Suzuki, Y. Spatial and single-cell transcriptome analysis reveals changes in gene expression in response to drug perturbation in rat kidney. *DNA Res.* **2022**, *29*, dsac007. [CrossRef] [PubMed]

26. Komers, R.; Xu, B.; McClelland, A.; Kantharidis, P.; Mittal, A.; Cohen, H.T.; Cohen, D.M. Transcriptome-Based Analysis of Kidney Gene Expression Changes Associated with Diabetes in OVE26 Mice, in the Presence and Absence of Losartan Treatment. *PLoS ONE* **2014**, *9*, e96987. [CrossRef]
27. Omachi, K.; Kaseda, S.; Yokota, T.; Kamura, M.; Teramoto, K.; Kuwazuru, J.; Kojima, H.; Nohara, H.; Koyama, K.; Ohtsuki, S.; et al. Metformin ameliorates the severity of experimental Alport syndrome. *Sci. Rep.* **2021**, *11*, 7053. [CrossRef]
28. Erichsen, L.; Kloss, L.D.F.; Thimm, C.; Bohndorf, M.; Schichel, K.; Wruck, W.; Adjaye, J. Derivation of the immortalized cell line-UM51-PrePodo-hTERT and its responsiveness to Angiotensin II and activation of RAAS. *Cells* **2023**, *12*, 342. [CrossRef]
29. Hypertension. Available online: https://www.who.int/news-room/fact-sheets/detail/hypertension#:~:text=For%20most%20people%2C%20the%20goal,vessels%20and%20prevent%20kidney%20damage (accessed on 25 May 2023).
30. Crowley, S.D.; Gurley, S.B.; Herrera, M.J.; Ruiz, P.; Griffiths, R.; Kumar, A.P.; Kim, H.-S.; Smithies, O.; Le, T.H.; Coffman, T.M. Angiotensin II causes hypertension and cardiac hypertrophy through its receptors in the kidney. *Proc. Natl. Acad. Sci. USA* **2006**, *47*, 17985–17990. [CrossRef]
31. Sobczuk, P.; Szczylik, C.; Porta, C.; Czarnecka, A.M. Renin angiotensin system deregulation as renal cancer risk factor. *Oncol. Lett.* **2017**, *14*, 5059–5068. [CrossRef] [PubMed]
32. Reiser, J.; Mundel, P. Dual effects of RAS blockade on blood pressure and podocyte function. *Curr. Hypertens. Rep.* **2007**, *9*, 403–408. [CrossRef]
33. Nguyen, L.; Wruck, W.; Erichsen, L.; Graffmann, N.; Adjaye, J. The Nephrotoxin Puromycin Aminonucleoside Induces Injury in Kidney Organoids Differentiated from Induced Pluripotent Stem Cells. *Cells* **2022**, *11*, 635. [CrossRef] [PubMed]
34. Lau, R.W.K.; Fisher, C.; Phan, T.K.; Ozkocak, D.C.; Selby, J.; Saini, S.; Mukundan, S.; Wise, A.F.; Savige, J.; Poon, I.K.H.; et al. Modelling X-linked Alport Syndrome With Induced Pluripotent Stem Cell-Derived Podocytes. *Kidney Int. Rep.* **2021**, *6*, 2912–2917. [CrossRef]
35. Ciampi, O.; Iacone, R.; Longaretti, L.; Benedetti, V.; Graf, M.; Magnone, M.C.; Patsch, C.; Xinaris, C.; Remuzzi, G.; Benigni, A.; et al. Generation of functional podocytes from human induced pluripotent stem cells. *Stem Cell Res.* **2016**, *17*, 130–139. [CrossRef] [PubMed]
36. De Carvalho Ribeiro, P.; Oliveira, L.F.; Filho, M.A.; Caldas, H.C. Differentiating Induced Pluripotent Stem Cells into Renal Cells: A New Approach to Treat Kidney Diseases. *Stem Cell Res.* **2020**, *2020*, 8894590. [CrossRef]
37. Yanofsky, S.M.; Dugas, C.M.; Katsurada, A.; Liu, J.; Saifudeen, Z.; El-Dahr, S.S.; Satou, R. Angiotensin II biphasically regulates cell differentiation in human iPSC-derived kidney organoids. *Am. J. Physiol. Renal Physiol.* **2021**, *321*, 559–571. [CrossRef]
38. Rüster, C.; Wolf, G. Renin-angiotensin-aldosterone system and progression of renal disease. *J. Am. Soc. Nephrol.* **2006**, *17*, 2985–2991. [CrossRef] [PubMed]
39. Liu, Y.; Liang, W.; Yang, Y.; Pan, Y.; Yang, Q.; Chen, X.; Singhal, P.C.; Ding, G. IQGAP1 regulates actin cytoskeleton organization in podocytes through interaction with nephrin. *Cell Signal* **2015**, *27*, 867–877. [CrossRef]
40. Yang, Q.; Ma, Y.; Liu, Y.; Lian, W.; Chen, X.; Ren, Z.; Wang, H.; Singhal, P.C.; Ding, G. Angiotensin II down-regulates nephrin–Akt signaling and induces podocyte injury: Roleof c-Abl. *Mol. Biol. Cell* **2016**, *27*, 197–208. [CrossRef]
41. Stegbauer, J.; Coffman, T.M. New insights into angiotensin receptor actions: From blood pressure to aging. *Curr. Opin. Nephrol. Hypertens.* **2011**, *20*, 84–88. [CrossRef]
42. McIntyre, M.; Caffe, S.E.; Michalak, R.A.; Reid, J.L. Losartan, an Orally Active Angiotensin (AT,) Receptor Antagonist: A Review of Its Efficacy and Safety in Essential Hypertension. *Pharmacol. Ther.* **1997**, *74*, 181–194. [CrossRef]
43. Perez-Hernandez, J.; Olivares, M.D.; Forner, M.J.; Chaves, F.J.; Cortes, R.; Redon, J. Urinary dedifferentiated podocytes as a non-invasive biomarker of lupus nephritis. *Nephrol. Dial. Transplant.* **2016**, *31*, 780–789. [CrossRef]
44. Rabow, S.; Hjorth, U.; Schönbeck, S.; Olofsson, P. Effects of oxytocin and anaesthesia on vascular tone in pregnant women: A randomised double-blind placebo-controlled study using non-invasive pulse wave analysis. *BMC Pregnancy Childbirth* **2018**, *18*, 453. [CrossRef]
45. Song, W.; Wang, H.; Wu, Q. Atrial natriuretic peptide in cardiovascular biology and disease (NPPA). *Gene* **2015**, *569*, 1–6. [CrossRef] [PubMed]
46. Lartey, J.; Taggart, J.; Robson, S.; Taggart, M. Altered Expression of Human Smooth Muscle Myosin Phosphatase Targeting (MYPT) Isovariants with Pregnancy and Labor. *PLoS ONE* **2016**, *11*, e0164352. [CrossRef] [PubMed]
47. Basosi, R.; Gaggelli, E.; Valensin, G. The effect of binding divalent metal ions on the conformation of human angiotensin-II in solution as probed by nuclear and electron paramagnetic resonance investigations. *J. Inorg. Biochem.* **1984**, *20*, 263–268. [CrossRef] [PubMed]
48. Suzuki, N.; Kanai, A.; Suzuki, Y.; Ogino, H.; Ochi, H. Adrenergic receptor signaling induced by Klf15, a regulator of regeneration enhancer, promotes kidney reconstruction. *Proc. Natl. Acad. Sci. USA* **2022**, *119*, e2204338119. [CrossRef] [PubMed]
49. Farber, M.J.; Rizaldy, R.; Hildebrand, J.D. Shroom2 regulates contractility to control endothelial morphogenesis. *Mol. Biol. Cell* **2011**, *22*, 795–805. [CrossRef] [PubMed]
50. Rehman, A.; Leibowitz, A.; Yamamoto, N.; Rautureau, Y.; Paradis, P.; Schiffrin, E.L. Angiotensin Type 2 Receptor Agonist Compound 21 Reduces Vascular Injury and Myocardial Fibrosis in Stroke-Prone Spontaneously Hypertensive Rats. *Hypertension* **2012**, *59*, 291–299. [CrossRef] [PubMed]
51. Izuhara, Y.; Nangaku, M.; Inagi, R.; Tominaga, N.; Aizawa, T.; Kurokawa, K.; van Ypersele de Strihou, C.; Miyata, T. Renoprotective Properties of Angiotensin Receptor Blockers beyond Blood Pressure Lowering. *J. Am. Soc. Nephrol.* **2005**, *16*, 3631–3641. [CrossRef]

52. Zhang, H.; Mo, X.; Zhou, Z.; Zhu, Z.; HuangFu, X.; Xu, T.; Wang, A.; Guo, Z. Associations among NPPA gene polymorphisms, serum ANP levels, and hypertension in the Chinese Han population. *J. Hum. Hypertens.* **2019**, *33*, 641–647. [CrossRef]
53. Potter, L.R.; Yoder, A.R.; Flora, D.R.; Antos, L.K.; Dickey, D.M. Natriuretic Peptides: Their Structures, Receptors, Physiologic Functions and Therapeutic Applications. In *Handbook of Experimental Pharmacology*; Springer: Berlin/Heidelberg, Germany, 2009; pp. 341–366. [CrossRef]
54. Alqarni, S.A.; Bineid, A.; Ahmad, S.F.; Al-Harbi, N.O.; Alqahtani, F.; Ibrahim, K.E.; Ali, N.; Nadeem, A. Blockade of Tyrosine Kinase, LCK Leads to Reduction in Airway Inflammation through Regulation of Pulmonary Th2/Treg Balance and Oxidative Stress in Cockroach Extract-Induced Mouse Model of Allergic Asthma. *Metabolites* **2022**, *12*, 793. [CrossRef] [PubMed]
55. Hall, G.; Wang, L.; Spurrney, R.F. TRPC Channels in Proteinuric Kidney Diseases. *Cells* **2019**, *9*, 44. [CrossRef] [PubMed]
56. Reiser, J.; Polu, K.R.; Möller, C.C.; Kenlan, P.; Altintas, M.M.; Wei, C.; Faul, C.; Herbert, S.; Villegas, I.; Avila-Casadoq, C.; et al. TRPC6 is a glomerular slit diaphragm-associated channel required for normal renal function. *Nat. Genet.* **2005**, *37*, 739–744. [CrossRef] [PubMed]
57. Kerjaschki, D. Polycation-induced dislocation of slit daiphragms and formation of cell junctions in rat kidney glomeruli: The effects of low temperature, divalent cations, colchicine, and cytochalasin B. *Lab. Investig.* **1978**, *39*, 430–440. [PubMed]
58. Tian, D.; Jacobo, S.M.P.; Billing, D.; Rozkalne, A.; Gage, S.D.; Anagnostou, T.; Pavenstädt, H.; Hsu, H.-H.; Schlondorff, J.; Ramos, A.; et al. Antagonistic Regulation of Actin Dynamics and Cell Motility by TRPC5 and TRPC6 Channels. *Sci. Signal.* **2011**, *3*, ra77. [CrossRef]
59. Kuwahara, K.; Wang, Y.; McAnally, J.; Richardson, J.A.; Bassel-Duby, R.; Hill, J.; Olson, E. TRCP6 fulfills a calcineurin signaling circuit during pathologic carciac remodeling. *J. Clin. Investig.* **2006**, *116*, 3114–3126. [CrossRef] [PubMed]
60. Binz-Lotter, J.; Jüngst, C.; Rinschen, M.M.; Koehler, S.; Zentis, P.; Schauss, A.; Schermer, B.; Benzing, T.; HAckl, M.J. Injured Podocytes Are Sensitized to Angiotensin II–Induced Calcium Signaling. *J. Am. Soc. Nephrol.* **2020**, *31*, 532–542. [CrossRef] [PubMed]
61. Faul, C.; Donnelly, M.; Merscher-Gomez, S.; Chang, Y.H.; Franz, S.; Delfgaauw, J.; Chang, J.-M.; Choi, H.Y.; Campbell, K.N.; Kim, K.; et al. The actin cytoskeleton of kidney podocytes is a direct target of the antiproteinureic effect of cyclosporine A. *Nat. Med.* **2008**, *14*, 931–938. [CrossRef]
62. Schenk, L.K.; Möller-Kerutt, A.; Klosowski, R.; Wolters, D.; Schaffner-Reckinger, E.; Weide, T.; Pavenstädt, H.; Vollenbröker, B. Angiotensin II regulates phosphorylation of actin-associated proteins in human podocytes. *FASEB J.* **2017**, *31*, 5019–5035. [CrossRef]
63. Namba, Y.; Ito, M.; Shigesada, K.; Maruyama, K. Human T cell L-plastin bundles actin filaments in a calcium-dependent manner. *J. Biochem.* **1992**, *112*, 503–507. [CrossRef]
64. Adapted from "Mechanisms of Cancer-Associated Fibroblast Activation", by BioRender.com. 2023. Available online: https://app.biorender.com/biorender-templates (accessed on 1 January 2023).
65. Miller, R.G., Jr. *Beyond Anova: Basics of Applied Statistics*; Reissue Edition; Routledge: London, UK, 1997; ISBN 978-0-412-07011-2.
66. Gentleman, R.C.; Carey, V.J.; Bates, D.M.; Bolstad, B.; Dettling, M.; Dudoit, S.; Ellis, B.; Gautier, L.; Ge, Y.; Gentry, J.; et al. Bioconductor: Open software development for computational biology and bioinformatics. *Genome Biol.* **2004**, *5*, R80. [CrossRef] [PubMed]
67. Carvalho, B.S.; Irizarry, R.A. A frameowrk for oligonucleotide microarray preprocessing. *Bioinformatics* **2010**, *26*, 2363–2367. [CrossRef] [PubMed]
68. Zhou, Y.; Zhou, B.; Pache, L.; Chang, M.; Khodabakhshi, A.H.; Tanaseichuk, O.; Benner, C.; Chanda, S.K. Metascape provides a biologist-oriented resource for the analysis of systems-level datasets. *Nat. Commun.* **2019**, *10*, 1523. [CrossRef] [PubMed]
69. Warnes, G.R.; Bolker, B.; Bonebakker, L.; Gentleman, R.; Liaw, W.H.A.; Lumley, T.; Maechler, M.; Magnusson, A.; Moeller, S.; Schwartz, M. *Gplots: Various R Programming Tools for Plotting Data*; R Package Version: Vienna, Austria, 2015.

Disclaimer/Publisher's Note: The statements, opinions and data contained in all publications are solely those of the individual author(s) and contributor(s) and not of MDPI and/or the editor(s). MDPI and/or the editor(s) disclaim responsibility for any injury to people or property resulting from any ideas, methods, instructions or products referred to in the content.

3.5 Secreted Cytokines within the Urine of AKI Patients Modulate TP53 and SIRT1 Levels in a Human Podocyte Cell Model

Lars Erichsen, **Chantelle Thimm,** Wasco Wruck , Daniela Kaierle, Manon Schless, Laura Huthmann, Thomas Dimski, Detlef Kindgen-Milles, Timo Brandenburger and James Adjaye

International Journal of Molecular Sciences 2023, Volume 24, 8228, Article ID 24098228

Abstract:

Acute kidney injury (AKI) is a major kidney disease with a poor clinical outcome. It is a common complication, with an incidence of 10–15% of patients admitted to hospital. This rate even increases for patients who are admitted to the intensive care unit, with an incidence of >50%. AKI is characterized by a rapid increase in serum creatinine, decrease in urine output, or both. The associated symptoms include feeling sick or being sick, diarrhoea, dehydration, decreased urine output (although occasionally the urine output remains normal), fluid retention causing swelling in the legs or ankles, shortness of breath, fatigue and nausea. However, sometimes acute kidney injury causes no signs or symptoms and is detected by lab tests. Therefore, the identification of cytokines for the early detection and diagnosis of AKI is highly desirable, as their application might enable the prevention of the progression from AKI to chronic kidney disease (CKD). In this study, we analysed the secretome of the urine of an AKI patient cohort by employing a kidney-biomarker cytokine assay. Based on these results, we suggest ADIPOQ, EGF and SERPIN3A as potential cytokines that might be able to detect AKI as early as 24 h post-surgery. For the later stages, as common cytokines for the detection of AKI in both male and female patients, we suggest VEGF, SERPIN3A, TNFSF12, ANPEP, CXCL1, REN, CLU and PLAU. These cytokines in combination might present a robust strategy for identifying the development of AKI as early as 24 h or 72 h post-surgery. Furthermore, we evaluated the effect of patient and healthy urine on human podocyte cells. We conclude that cytokines abundant in the urine of AKI patients trigger processes that are needed to repair the damaged nephron and activate TP53 and SIRT1 to maintain the balance between proliferation, angiogenesis, and cell cycle arrest.

Author contribution of C.T. included 30%:

Patients urine included in the AKI cohort were clinically recruited by D.K., M.S., L.H., T.D., D.KM. and T.B.. Together with L.E., I collected, sorted, and pooled the patient urine samples, which I subsequently analyzed using the Proteome Profiler Human Kidney Biomarker Kit. I was responsible for establishing and maintaining the cell culture system, which included the cultivation of immortalized UdRPCs (UM51 hTERT) as well as the differentiation into podocytes and the processing and treatment of urine samples obtained from patients with acute kidney injury (AKI). In addition, I performed immunofluorescence staining and isolated RNA for my follow-up qPCR analysis. I prepared protein lysates and performed Western blot analysis. For all datasets I generated in the course of the study, I carried out the respective statistical analyses and prepared the quantitative evaluation of the results. Furthermore, I generated the schematic illustration and designed and executed the experiments and analyzed them in the relation to our research hypothesis with L.E.

Status: Published in International Journal of Molecular Sciences

DOI: doi.org/10.3390/ijms24098228

This article is an open access article distributed under the terms and conditions of the Creative Commons Attribution (CC BY) 4.0 license, which permits unrestricted use, distribution, and reproduction in any medium, provided the original work is properly cited.

International Journal of *Molecular Sciences*

MDPI

Article

Secreted Cytokines within the Urine of AKI Patients Modulate TP53 and SIRT1 Levels in a Human Podocyte Cell Model

Lars Erichsen [1], Chantelle Thimm [1], Wasco Wruck [1], Daniela Kaierle [2], Manon Schless [2], Laura Huthmann [2], Thomas Dimski [2], Detlef Kindgen-Milles [2], Timo Brandenburger [2] and James Adjaye [1,3,*]

[1] Institute for Stem Cell Research and Regenerative Medicine, Medical Faculty, Heinrich-Heine University Düsseldorf, 40225 Düsseldorf, Germany
[2] Department of Anesthesiology, University Hospital Düsseldorf, Heinrich-Heine University Duesseldorf, Moorenstr. 5, 40225 Düsseldorf, Germany
[3] Zayed Centre for Research into Rare Diseases in Children (ZCR), EGA Institute for Women's Health, University College London (UCL), 20 Guilford Street, London WC1N 1DZ, UK
* Correspondence: james.adjaye@med.uni-duesseldorf.de or j.adjaye@ucl.ac.uk

Abstract: Acute kidney injury (AKI) is a major kidney disease with a poor clinical outcome. It is a common complication, with an incidence of 10–15% of patients admitted to hospital. This rate even increases for patients who are admitted to the intensive care unit, with an incidence of >50%. AKI is characterized by a rapid increase in serum creatinine, decrease in urine output, or both. The associated symptoms include feeling sick or being sick, diarrhoea, dehydration, decreased urine output (although occasionally the urine output remains normal), fluid retention causing swelling in the legs or ankles, shortness of breath, fatigue and nausea. However, sometimes acute kidney injury causes no signs or symptoms and is detected by lab tests. Therefore, the identification of cytokines for the early detection and diagnosis of AKI is highly desirable, as their application might enable the prevention of the progression from AKI to chronic kidney disease (CKD). In this study, we analysed the secretome of the urine of an AKI patient cohort by employing a kidney-biomarker cytokine assay. Based on these results, we suggest ADIPOQ, EGF and SERPIN3A as potential cytokines that might be able to detect AKI as early as 24 h post-surgery. For the later stages, as common cytokines for the detection of AKI in both male and female patients, we suggest VEGF, SERPIN3A, TNFSF12, ANPEP, CXCL1, REN, CLU and PLAU. These cytokines in combination might present a robust strategy for identifying the development of AKI as early as 24 h or 72 h post-surgery. Furthermore, we evaluated the effect of patient and healthy urine on human podocyte cells. We conclude that cytokines abundant in the urine of AKI patients trigger processes that are needed to repair the damaged nephron and activate TP53 and SIRT1 to maintain the balance between proliferation, angiogenesis, and cell cycle arrest.

Keywords: acute kidney injury; cytokines; TP53; SIRT1

check for updates

Citation: Erichsen, L.; Thimm, C.; Wruck, W.; Kaierle, D.; Schless, M.; Huthmann, L.; Dimski, T.; Kindgen-Milles, D.; Brandenburger, T.; Adjaye, J. Secreted Cytokines within the Urine of AKI Patients Modulate TP53 and SIRT1 Levels in a Human Podocyte Cell Model. *Int. J. Mol. Sci.* **2023**, *24*, 8228. https://doi.org/10.3390/ijms24098228

Academic Editors: Giovana S. Di Marco and Marcus Brand

Received: 20 March 2023
Revised: 26 April 2023
Accepted: 28 April 2023
Published: 4 May 2023

Copyright: © 2023 by the authors. Licensee MDPI, Basel, Switzerland. This article is an open access article distributed under the terms and conditions of the Creative Commons Attribution (CC BY) license (https://creativecommons.org/licenses/by/4.0/).

1. Introduction

The understanding of the ethology underlying AKI has fundamentally changed in recent years [1,2]. In the past, research focused on the most severe impairment of the kidney. More recent studies have provided evidence that even minor injuries or impairments of kidney function can lead to severe consequences, such as changes in serum creatinine (sCr) and/or urine secretion (UO) [3]. Today, the term acute kidney injury (AKI) is used for a major kidney disease with a poor clinical outcome. It is characterised as an abrupt (within hours or days) decline in renal function, which includes structural damage to the nephron as well as loss of functionality. It is a common complication in patients admitted to the hospital, with an incidence of 10–15% [4]. This rate even increases for patients who are admitted to the intensive care unit, with the incidence rising to >50% [5]. The classification of AKI includes pre-renal AKI, acute post-renal obstructive nephropathy, and

intrinsic acute kidney disease. Of these, only the latter represents a true renal disease, whereas pre- and post-renal AKI are the result of extra-renal disease leading to a decreased glomerular filtration rate (GFR). If these pre- and/or post-renal conditions persist, they eventually develop into cellular damage to the kidney and thus intrinsic renal disease [3]. The current diagnostic approach for AKI is based on an acute decrease in the GFR reflected in an acute increase in the sCr level and/or a decrease in the UO value over a given time interval [3]. According to the current Kidney Disease: Improving Global Outcomes (KDIGO) guidelines, the definition of AKI is classified into three distinct stages: stage 1: creatinine >1.5 times baseline or an increase of $\geq$0.3 mg/dL within any 48 h period, or a urine volume <0.5 mL/kg for 6–12 h; stage 2: creatinine $\geq$2.0 times baseline or a urine volume <0.5 mL/kg for $\geq$12 h; and stage 3: creatinine >3.0 times baseline or increased to $\geq$4.0 mg/dL or acute dialysis, or a urine volume <0.3 mL/kg for $\geq$24 h [6]. If these conditions persist for up to seven days, the pathological conditions are referred to as AKI. Between 7 and 90 days, the conditions are referred to as acute kidney disease (AKD), and if they exceed 90 days, chronic kidney disease (CKD) has manifested [7]. In terms of their clinical presentation, kidney diseases are very difficult to identify because, except for urinary tract obstructions, they do not cause any specific signs or symptoms [7]. Furthermore, diagnosis of AKI is hindered by the fact that specific syndromes often co-exist (as reviewed in [7]) or AKI arises as part of other syndromes, such as heart or liver failure or sepsis. In addition, 40% of all AKI cases in the hospital are related to surgical procedures [8], with AKI being associated with cardiac surgery with an incidence ranging from 7 to 40% [9–12].

Therefore, non-invasive biomarkers for the early detection of AKI are urgently needed. This might improve patient outcomes in the intensive care unit and reduce the risk of progression from AKI to CKD and, ultimately, end-stage kidney disease (ESKD).

Under healthy physiological conditions, kidney cells divide at very low rates [13,14]. In contrast, several studies have reported a dramatic increase in proliferating cells after AKI, which can also be accompanied by transient dedifferentiation [14,15] to repair the injured nephron. This repair process has been identified to be possibly maladaptive, depending on the severity of the injury, involving increased DNA damage and cellular senescence [16]. Therefore, it is not surprising that TP53 and its downstream target, TP21, were found to be upregulated in the kidney after AKI and that inhibition or gene deletion reduces kidney lesions [17–21]. Interestingly, using P53 inhibitors after unilateral ischemia reperfusion injury resulted in reduced fibrosis [20]. Despite this progress in understanding the role of TP53 in the pathology of kidney injury, the underlying mechanism in the progress remains largely unknown. The NAD+-dependent class III histone deacetylase SIRT1 is involved in many biological processes, including DNA damage repair and TP53 activation [22,23]. Furthermore, SIRT1 has been reported to play a protective role in many diseases, including AKI [24–26].

In the present study, we screened urine from intensive care patients who developed AKI 24 h and 72 h post-surgery for established kidney biomarkers by employing a kidney-injury cytokine assay. We identified ADIPOQ, EGF and SERPIN3A to be upregulated in urine derived from AKI patients as early as 24 h post-surgery. At 72 h post-surgery, the common cytokines upregulated in the urine samples of both male female patients include VEGF, SERPIN3A, TNFSF12, ANPEP, CXCL1, REN, CLU and PLAU. Furthermore, we applied the urine to our recently published hTERT immortalized podocyte cell line [27] and evaluated the effects of the urine on TP53 and SIRT1 expression.

2. Results

2.1. *Identification of Cytokines Upregulated in Urine Derived from AKI Patients 24 h Post-Operation*

Urine samples from six stage 2/3 AKI patients and six patients without AKI were collected 24 h post-surgery at the clinic for anaesthesiology at Heinrich-Heine University Düsseldorf. The patients without AKI were aged between 55 and 75 years—three males

and three females. The AKI patients were aged between 34 and 84 years, with the same sex distribution (see Table 1). The urine samples were incubated individually on the human kidney biomarker array, and scanned images are shown in Supplementary Figure S1. The results are shown in Figure 1. As shown in the dendrogram (Figure 1A), except for P100_M34_AKI3, the samples segregated into two distinct clusters of AKI (red) and healthy controls (blue). The clustering of the AKI group could even further be sub-divided into male and female. Interestingly, the cytokines in the healthy urine seem to be more equally distributed between the genders according to the dendrogram. The heatmap (Figure 1B) and the barplots (Figure 1C,D) show the cytokines found to be significantly regulated as detected by the array.

Table 1. Patient cohort.

Parameter	No AKI (n = 6)	AKI 2 and 3 (n = 6)	p-Value
Age [years]	68 ± 8	69 ± 18	0.37
Gender			
Female [%]	3 (50)	3 (50)	1.0
Male [%]	3 (50)	3 (50)	1.0
Comorbidities			
Obesity [%]	2 (33)	3 (50)	1.0
Hypertension [%]	5 (93)	4 (67)	1.0
Diabetes Mellitus [%]	2 (33)	2 (33)	1.0
CKD [%]	0 (0)	2 (33)	0.455
Preoperative creatinine [mg/dL]	1.18 ± 0.44	1.85 ± 0.90	0.126
Operation time [minutes]	282 ± 66	287 ± 86	0.699
CPB time [minutes]	191 ± 65	170 ± 51	0.589
X-clamp [minutes]	109 ± 33	103 ± 52	1.0
Creatinine postop. [mg/dL]	1.2 ± 0.34	1.43 ± 0.42	0.268
Creatinine on day 3 [mg/dL]	1.08 ± 0.50	2.03 ± 1.29	0.097
Lactate postop. [mmol/L]	2.5 ± 0.9	7.5 ± 3.2	**0.004**
Lactate on day 3 [mmol/L]	2.2 ± 2.5	1.7 ± 0.5	0.296
APACHE-II postop.	26 ± 2	32 ± 3	**0.008**
Ventilation [hours]	20 ± 8	186 ± 253	**0.020**
LOICUS [days]	2 ± 2	13 ± 11	**0.014**
LOHS [days]	18 ± 12	42 ± 20	**0.030**
Last creatinine [mg/dL]	1.03 ± 0.33	2.07 ± 0.72	**0.016**
Mortality in hospital	0 (0)	1 (17)	1.0

Matched no AKI vs. AKI stage 2 and 3 data are expressed as the mean ± standard deviation or number (percentage). A statistical analysis was performed with the Mann–Whitney U test to compare the variables between the two groups; the association between the categorical variables and the two groups (no AKI vs. AKI patients) was tested with the Chi-squared test. For all the tests, p-values < 0.05 were considered significant. LOICUS = length of intensive care unit stay after surgery; LOHS = length of hospital stay; X-clamp = aortic cross-clamping.

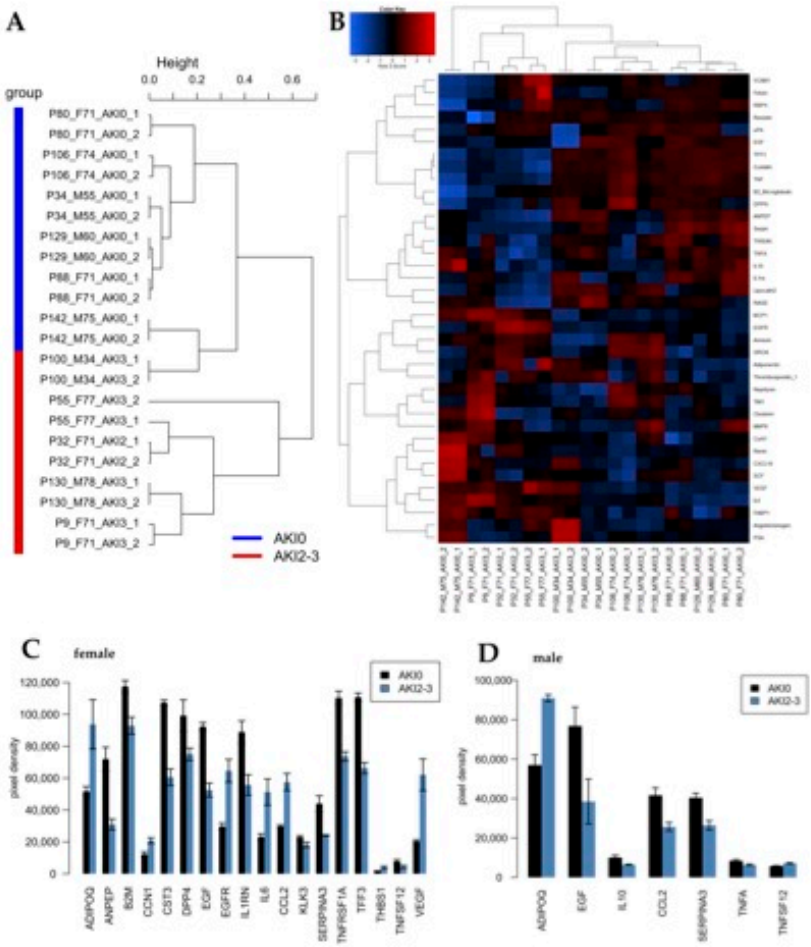


Figure 1. AKI cytokines identified in patients 24 h post-surgery. (**A**) Experiments clustered into CKD ($n = 6$) and healthy control ($n = 6$) based on the global kidney cytokine expression. (**B**) Heatmap and (**C**) barplot of markers in females and barplot of markers in males (**D**). The histograms represent means and the error bars standard errors of the mean ($n = 3$). The cytokines depicted here were differentially upregulated with a *p*-value (test of the R package limma (Smyth 2004 [28])) $p < 0.05$ and a ratio > 1.2, or downregulated with a $p < 0.05$, FDR < 0.25 and ratio < 0.8333.

In the female patients, adiponectin (ADIPOQ), cellular communication network factor 1 (CCN1), epidermal growth factor receptor (EGFR), interleukin 6 (IL6), CC-chemokine ligand 2 (CCL2), thrombospondin 1 (THBS1) and vascular endothelial growth factor (VEGF) were found to be upregulated, while alanyl aminopeptidase (ANPEP), β2-mikroglobulin (B2M), cystatin C (CST3), dipeptidylpeptidase-4 (DDP4), epidermal growth factor (EGF), interleukin 1 receptor antagonist (IL1RN), kallikrein-related peptidase 3 (KLK3), serpin family A member 3 (SERPIN3A), tumour necrosis factor receptor superfamily member 1A (TNFRSF1A), trefoil factor 3 (TFF3) and tumour necrosis factor ligand superfamily member 12 (TNFSF12) were found to be downregulated.

In the male patients, adiponectin (ADIPOQ) and tumour necrosis factor ligand superfamily member 12 (TNFSF12) were found to be upregulated, while epidermal growth factor (EGF), interleukin 10 (IL10), CC-chemokine ligand 2 (CCL2), serpin family A member 3 (SERPIN3A) and tumour necrosis factor alpha (TNFA) were found to be downregulated.

2.2. Identification of Cytokines Upregulated in Urine Derived from AKI Patients 72 h Post-Operation

Urine samples from the same six AKI and non-AKI patients were collected 72 h post-surgery. The patient characteristics were similar between the AKI and non-AKI patients (e.g., age, gender, comorbidities; Table 1). The intra-operative data (operation time, cross-clamp time and time on cardiopulmonary bypass) were also comparable. The creatinine levels, as expected, were higher in the AKI group, and so were the lengths of the intensive care and hospital stays. The urine samples were pooled (based on gender and disease state) and incubated on the human kidney biomarker array. The results are shown in Figure 2, while scanned images are shown in Supplementary Figure S2. As shown in the dendrogram (Figure 2A), the samples segregated into two distinct clusters, with the male AKI samples (black) being closer but distinct from the healthy controls (red) when compared to the female AKI samples (blue). The heatmap (Figure 2B) and the barplots (Figure 2C,D) show the cytokines significantly regulated ($p < 0.05$) as detected by the array. In the female patients, alanyl aminopeptidase (ANPEP), chemokine (C-X-C motif) ligand 1 (CXCL1), interleukin 1 receptor antagonist (IL1RN), renin (REN) and vascular endothelial growth factor (VEGF) were found to be upregulated, while β2-mikroglobulin (B2M), clusterin (CLU), epidermal growth factor (EGF), CC-chemokine ligand 2 (CCL2), matrix metallopeptidase 9 (MMP-9), membrane metalloendopeptidase (MME), kallikrein-related peptidase 3 (KLK3), advanced glycosylation end-product specific receptor (AGER), serpin family A member 3 (SERPIN3A), tumour necrosis factor ligand superfamily member 12 (TNFSF12) and plasminogen activator urokinase (PLAU) were found to be downregulated. In the male patients, alanyl aminopeptidase (ANPEP), epidermal growth factor receptor (EGFR), alpha 2-HS glycoprotein (AHSG), chemokine (C-X-C motif) ligand 1 (CXCL1), CC-chemokine ligand 2 (CCL2), renin (REN) and vascular endothelial growth factor (VEGF) were found to be upregulated, while annexin A5 (ANXA5), clusterin (CLU), cellular communication network factor 1 (CCN1), interleukin 1 receptor antagonist (IL1RN), interleukin 6 (IL6), interleukin 10 (IL10), SKP1-CUL1-F-box protein (SKP1), serpin family A member 3 (SERPIN3A), tumour necrosis factor ligand superfamily member 12 (TNFSF12) and plasminogen activator urokinase (PLAU) were found to be downregulated.

2.3. Effect of AKI Stage 2/3 Urine on Podocytes

A number of the chemokines, such as VEGF and EGFR, that were found to be upregulated are capable of either activating or being activated by either TP53 [29–32] or SIRT1 [33,34]. To test the hypothesis that the chemokines found to be upregulated in the AKI stage 2/3 urine have a direct influence on the expression levels of TP53 and SIRT1, we incubated our recently published immortalized podocyte cell line UM51 Htert [27] with a medium composed of 10% of the patient urine 72 h post-surgery for 120 h. The relative protein expression normalized to GAPDH for TP53 and SIRT1 and the phosphorylation levels of histone 2A (pH2A.X), which is an established biomarker of DNA damage [35], were detected by Western blotting (Figure 3A), and full images of the Western blots are shown in Supplementary Figure S3. All the proteins were detected at the expected sizes of 110 kDa for SIRT1, 15 kDa for pH2A.X, 53 kDa for p53 and 38 kDa for GAPDH. While the SIRT1 expression was not detectable in the podocytes under control conditions, it significantly increased in the podocytes incubated with healthy urine to 600% ($p < 0.01$) and was even found to be further elevated when the podocytes were incubated with AKI stage 2/3 urine to 1051% ($p < 0.01$). In contrast, the TP53 levels were found to be significantly downregulated by 85% when the cells were incubated with healthy urine ($p > 0.05$). When the cells were incubated with the AKI stage 2/3 urine, the TP53 expression was found to be

significantly upregulated to 150% ($p < 0.05$). Accordingly, the phosphorylation levels of H2A.X were found to be upregulated under both conditions, with healthy urine increasing the phosphorylation levels by 280% and the AKI 2/3 urine by 700%. Both changes were found to be significant ($p < 0.05$). The qRT-PCR analysis of TP53 and SIRT1 (Figure 3B) revealed that the mRNA expression of both was upregulated in the podocytes treated with human urine. Healthy urine induced a 2.5-fold increase in the TP53 mRNA expression and a 1.7-fold increase in the TP51 expression, while AKI stage 2/3 urine induced an upregulation of the TP53 mRNA by 3.5-fold and the SIRT1 mRNA by 4.2-fold. Finally, we applied immunofluorescence-based detection of TP53 to the cells exposed to AKI 2/3 urine (Figure 3C), revealing an increase in positively stained cells.

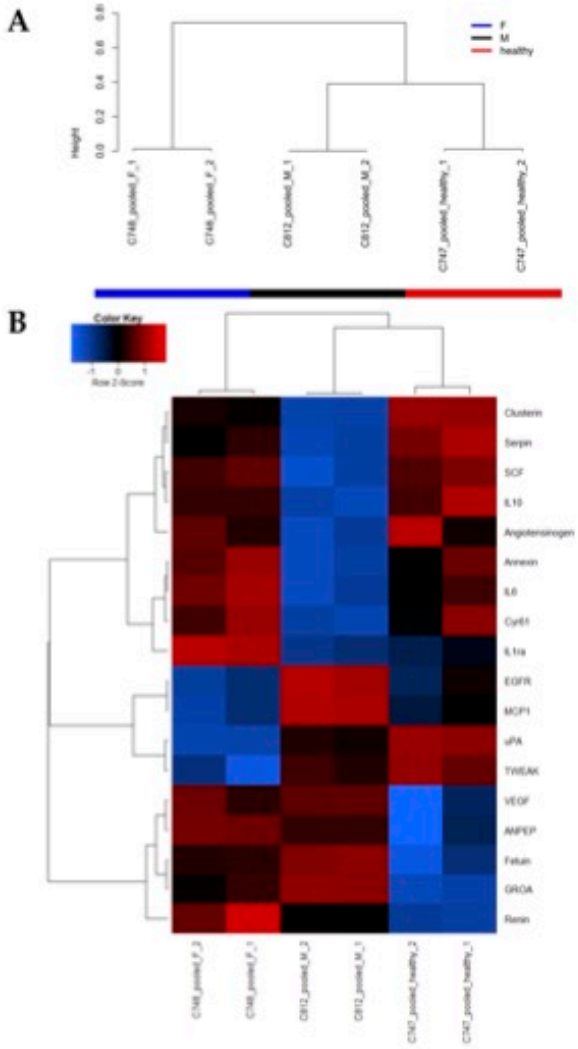


Figure 2. *Cont.*

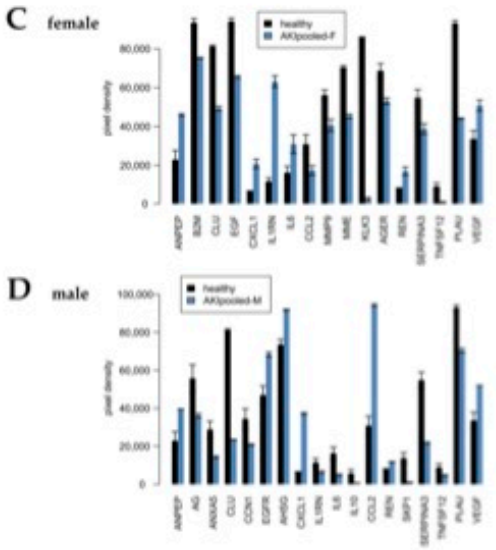


Figure 2. AKI cytokines identified in patients 72 h post-surgery. (**A**) Experiments clustered into CKD ($n = 6$) and healthy control ($n = 6$) based on the global kidney cytokine expression. (**B**) Heatmap and (**C**) barplot of markers in females and barplot of markers in males (**D**). The histograms represent means and the error bars standard errors of the mean of technical duplicates ($n = 2$). The cytokines depicted here were differentially upregulated with a p-value (test of the R package limma) $p < 0.05$ and a ratio > 1.2, or downregulated with a $p < 0.05$, FDR < 0.25 and ratio < 0.8333.

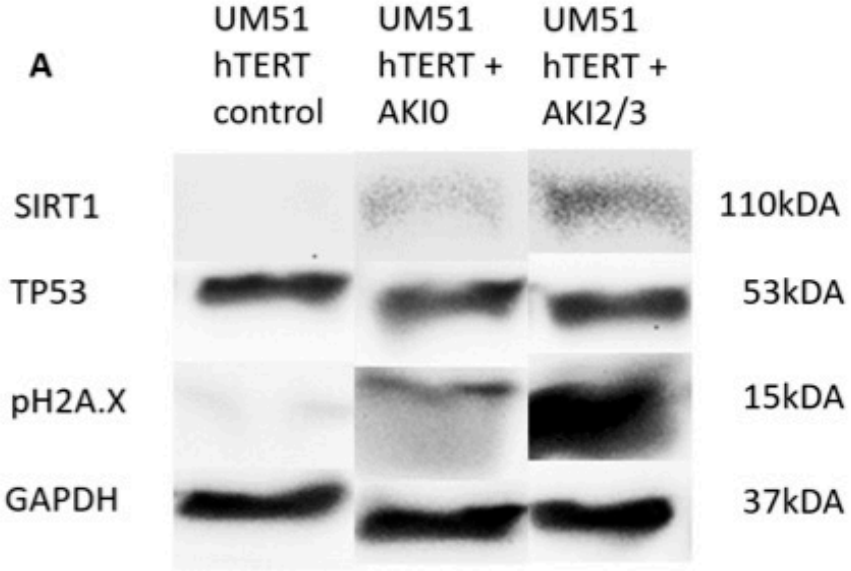


Figure 3. *Cont.*

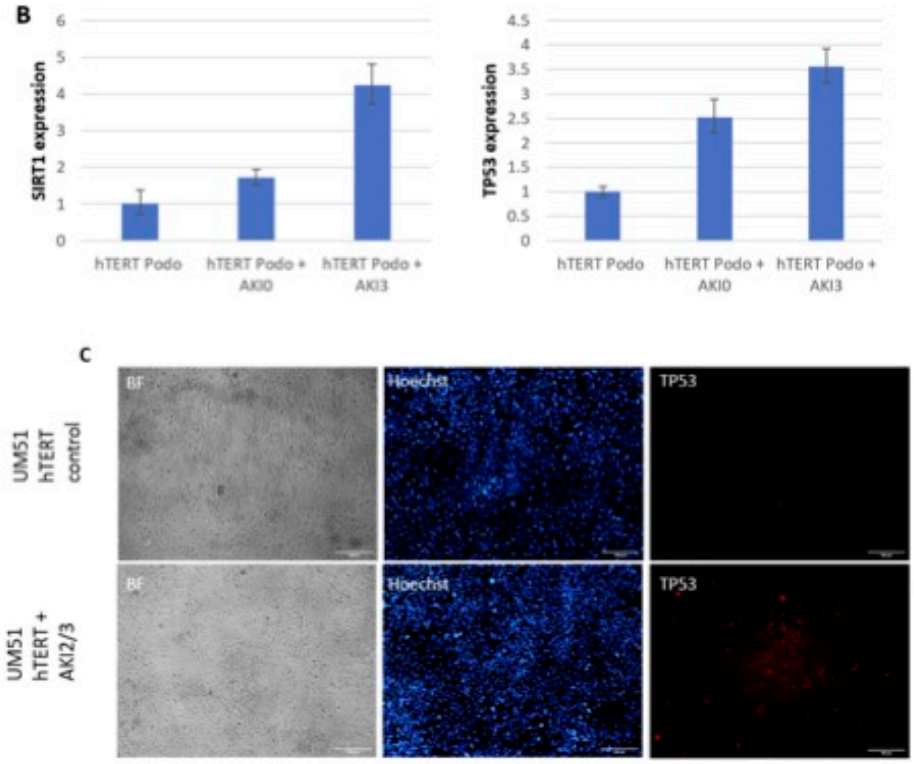


Figure 3. Upregulation of TP53 and SIRT1 induced by AKI stage 2/3 urine in podocytes. The podocytes were incubated with 72 h post-surgery healthy ($n = 6$) and AKI stage 2/3 urine ($n = 6$) for 5 days. The relative protein expression normalized to GAPDH for SIRT1, TP53 and H2A.X phosphorylation was detected by Western blot (**A**). The mRNA expression of TP53 and SIRT1 was determined by quantitative real-time PCR (**B**). The TP53 expression in the podocytes exposed to AKI 2/3 urine was detected by immunofluorescence-based staining (**C**). Scale bars indicate 100 µm.

3. Discussion

In this study, by comparing the urine-secreted cytokines of non-AKI and AKI 2/3-patients after cardiac surgery, we identified a panel of cytokine specifically upregulated in the urine derived from AKI patients. Since kidney diseases can be difficult to identify in the clinic because they do not cause any specific signs or symptoms [7], and as AKI can arise as part of other syndromes such as heart or liver failure and sepsis, the variability between individuals and genders has to be accounted for. Since we only had access to a limited sample pool for this study, we aimed at excluding individual variability by pooling the samples. Gender-specific analyses were carried out to avoid variations due to the influence of sex hormones, such as testosterone and oestradiol, in the modulation of SIRT1 expression [36–38]. While the male urine samples 24 h post-surgery revealed only seven cytokines as significantly altered, the female urine samples contained a plethora of significantly altered cytokines. The common cytokines in both the female and male urine samples provided 24 h post-surgery were the upregulation of adiponectin (ADIPOQ) and the downregulation of epidermal growth factor (EGF) and serpin family A member 3 (SERPIN3A). In contrast, the analysis of the urine from the stage 2/3 AKI patients 72 h post-surgery showed a dramatic increase in the regulated cytokines. Here, the male and female samples showed

the upregulation of vascular endothelial growth factor (VEGF), alanyl aminopeptidase (ANPEP), chemokine (C-X-C motif), ligand 1 (CXCL1) and renin (REN), while clusterin (CLU), SERPIN3A, plasminogen activator urokinase (PLAU) and tumour necrosis factor ligand superfamily member 12 (TNFSF12) were found to be downregulated. Of note, the upregulation of ADIPOQ detected in the 24 post-surgery urine was reduced after 72 h. The same trend was observed for EGF in the female urine, while the downregulation was persistent in the male AKI urine samples 72 h post-surgery. Interestingly, the downregulation of secreted interleukin 10 was only observed in the male AKI urine samples 24 h and 72 h post-surgery. Based on these results, we suggest ADIPOQ, EGF and SERPIN3A as potential cytokines that might be able to detect AKI as early as 24 h post-surgery. For the later stages, as common cytokines for the detection of AKI in both male and female patients, we propose VEGF, SERPIN3A, TNFSF12, ANPEP, CXCL1, REN, CLU and PLAU. These markers in combination might present a robust strategy for diagnosing AKI as early as 24 h or 72 h post-surgery. Many of these cytokines have already been described in the context of AKI [39–41]. The full list of significantly regulated cytokines is given in Table 2.

At the molecular level, ADIPOQ might be of special interest, since it has been described to directly regulate the expression of three of the identified cytokines that were upregulated 72 h post-surgery, namely CXCL1, VEGF and RENIN.

In cancer cells, adiponectin has been shown to induce CXCL1 secretion and thereby promote tumour angiogenesis [29]. In addition, CXCL1 has been reported to stimulate angiogenesis via the VEGF pathway [42,43], and it has even been suggested as a biomarker for patients suffering from colon cancer [44]. Furthermore, it has been shown that inhibition of the renin–angiotensin system results in significantly increased adiponectin levels [45]. Therefore, we propose that the observed upregulation of secreted RENIN in the AKI urine samples 72 h post-surgery might be causative for the downregulation of secreted ADIPOQ, while the early upregulation of secreted ADIPOQ results in the activation of the angiogenesis-related genes CXCL1 and VEGF, thus reflecting the initiation of the repair processes in the damaged nephron. For instance, VEGF has been shown to be an important mediator of the early and late phase of renal protective action after AKI in the context of stem cell treatment [40].

EGF and EGFR both have been associated with AKI, and low levels of EGF have been reported to be predictive of AKI in newborns [46,47]. Of note, EGF has been reported to induce several matrix metalloproteinases [48] and, therefore, the identified downregulation of EGF might be causative for the also observed downregulation of MME and MMP9 in the female AKI urine 72 h post-surgery. EGFR has been reported to play an important role in renal recovery from AKI through PI3K-AKT-dependent YAP activation [49]. Indeed, the EGFR promoter bears several p53-responsive elements [50], and it has been reported that renal fibrosis is associated with EGFR and p53 activation [51]. Interestingly, the FDA approved test "NephroCheck®", which is in clinical use and predicts the risk of developing moderate to severe AKI within 24 h [52], uses the following two biomarkers: tissue inhibitor of metalloproteinase 2 (TIMP-2) and insulin-like growth factor binding protein 7 (IGFBP7). Both are secreted by renal tubular cells in response to cellular stress and are involved in G1-phase cell-cycle arrest [53]. This is achieved by the transcriptional activation of p27 via TIMP-2 and p53 and p21 via IGFBP7 [54,55], further highlighting the involvement of TP53 activation in the clinical manifestation of AKI. Another study carried out by Montero et al. also documented that VEGF and p53 expression levels are significantly correlated and can be used as independent prognostic factors [30]. Our results suggest that secreted EGFR and VEGF are sufficient for the upregulation of p53 mRNA and protein levels in our immortalized podocyte cell line, although further experiments need to be conducted to verify this hypothesis. Furthermore, another study carried out by Pierzchalski et al. showed that p53 is able to induce apoptosis via the activation of the renin–angiotensin system [31]. In two recent studies carried out in our laboratory, we demonstrated the devastating effect of the activated renin–angiotensin system on podocyte morphology and functionality [27,56]. Therefore, we propose that the observed upregulated

secretion of EGFR and VEGF mainly triggers angiogenesis and the activation of p53 and the renin–angiotensin system. This mode of action might be a plausible explanation for the progression from AKI to CKD. Considering the constant secretion of these factors, they should be investigated in urine samples from patients with AKI for more than three days after surgery and in patients who progress to CKD. Interestingly, our recently published study investigating the secretome of urine from a CKD patient cohort from Ghana revealed the downregulation of secreted EGFR and VEGF [57]. This makes it tempting to speculate that EGFR and VEGF might also be involved as initiators of AKI and downregulated in the progression to CKD. In particular, VEGF, in the context of CKD, has been shown to have therapeutic potential by inducing renal recovery [58]. The exact mechanism underlying this protective effect of VEGF is unknown, although kidney tissue after AKI is characterized by impaired endothelial proliferation and mesenchymal transition—both contribute to vascular refraction and, subsequently, to the progression to CKD [59]. So far, the clinical diagnosis and monitoring of AKI is based on the clearance of urea and creatinine [2]. This means that an impairment of the filtration barrier of the nephron already has happened, and the repair process of the kidney is monitored. A clear advantage of a cytokine dosage-based approach is the possible detection of the development of AKI prior to or at the onset of reduced kidney function. This might be especially true since we found an accumulation of ADIPOQ in the urine of patients who developed AKI as early as 24 h post-surgery. This factor is known to upregulate cytokines such as VEGF, CXCL1 and REN in a feed-forward cycle and, therefore, activate distinct pathways that are known to contribute towards the development and progression of AKI. By detecting the accumulation of urine-secreted cytokines such as ADIPQ as early as possible, therapeutic approaches to prevent the breakdown of the filtration barrier might be initiated, with great benefits for the patients. Nevertheless, this needs to be evaluated in further studies. Another great benefit of a cytokine-based approach is that the test can be conducted in a non-invasive, fast and cheap manner by simply collecting the urine and detecting the aberrant regulated cytokines on a suitable device, such as a flow cell.

Finally, we found an upregulation of SIRT1 in the podocytes incubated with the patient-derived urine, which was found to be even more pronounced when AKI stage 2/3 urine was used. SIRT1 has been reported to be renal-protective during AKI [24,60]. This protective effect might be caused by two distinct pathways that are regulated by SIRT1 activity. First, p53 is a direct substrate of the deacetylation activity of SIRT1 by regulating p53 activity, since p53 acetylation promotes the transactivation of numerous genes regulating cell-cycle arrest, apoptosis and metabolic targets [61]. In this context, it has been shown that SIRT1 overexpression promotes cellular survival in the presence of a cellular stressor [62,63]. The second pathway directly influenced by SIRT1 is the renin–angiotensin pathway [34]. In this context, the overexpression of SIRT1 has been reported to attenuate angiotensin II-induced vascular remodelling and hypertension [64], which might be caused by SIRT1-induced downregulation of the angiotensin II type 1 receptor (AGTR1) [65]. SIRT1 has been reported to increase the lifespan in lower organisms, such as *Caenorhabditis elegans* [66] and *Drosophila melanogaster* [67], and recently, we reported the age-associated decline in SIRT1 mRNA and protein in urine-derived renal progenitor cells [68]. Since AKI has been described as a condition of renal senescence [69], the expression level of SIRT1 seems to be of major importance for the prevention of AKI. Nevertheless, this study is limited by the small sample size. This is especially true with regard to the complex nature of human urine, which contains a plethora of cytokines and molecules harbouring possible mechanistic influences on the observed results. Therefore, further experiments in which the cells are exposed to recombinant EGFR or VEGF should be conducted, although that is beyond the limits of the current study.

Table 2. Summary of the identified cytokines for the early diagnosis of AKI.

Cytokine	Female 24 h Post-Surgery	Male 24 h Post-Surgery	Female 72 h Post-Surgery	Male 72 h Post-Surgery
ADIPOQ	Up	Up		
CCN1	Up			Down
EGFR	Up			Up
IL6	Up			
CCL2	Up	Down	Down	Up
THBS1	Up			
VEGF	Up		Up	Up
ANPEP	Down			
B2M	Down		Down	
CST3	Down			
DDP4	Down			
EGF	Down	Down	Down	
IL1RN	Down		Up	Down
KLK3	Down			
SERPIN3A	Down	Down	Down	Down
TNFRSF1A	Down			
TTF3	Down			
TNFSF12	Down	Up	Down	Down
IL10		Down		Down
TNFA		Down		
ANPEP			Up	Up
CXCL1			Up	Up
REN			Up	Up
CLU			Down	Down
MMP9			Down	
MME			Down	
KLK3			Down	
AGER			Down	
PLAU			Down	Down
AHSG				Up
ANXA5				Down
IL6				Down
SKP1				Down

In summary, we propose putative urine-based cytokines (24 and 72 h post-surgery) for the detection of AKI, which are male-enriched (AHSG), female-enriched (CCN1, IL6, CCL2, THBS1, IL1RN) and common in both (VEGF, SERPIN3A, TNFSF12, ANPEP, CXCL1, REN, CLU and PLAU). Furthermore, mechanistically, the cytokines ADIPOQ, EGF, EGFR, REN and VEGF present in the urine of AKI stage 2/3 patients trigger processes such as angiogenesis that are needed to repair the damaged nephron and the activation of p53 and SIRT1 to maintain the balance between proliferation, angiogenesis, repair and cell-cycle arrest. On this basis, we propose a specific signalling cascade induced by damage to the kidney, resulting in the establishment and propagation of AKI (Figure 4).

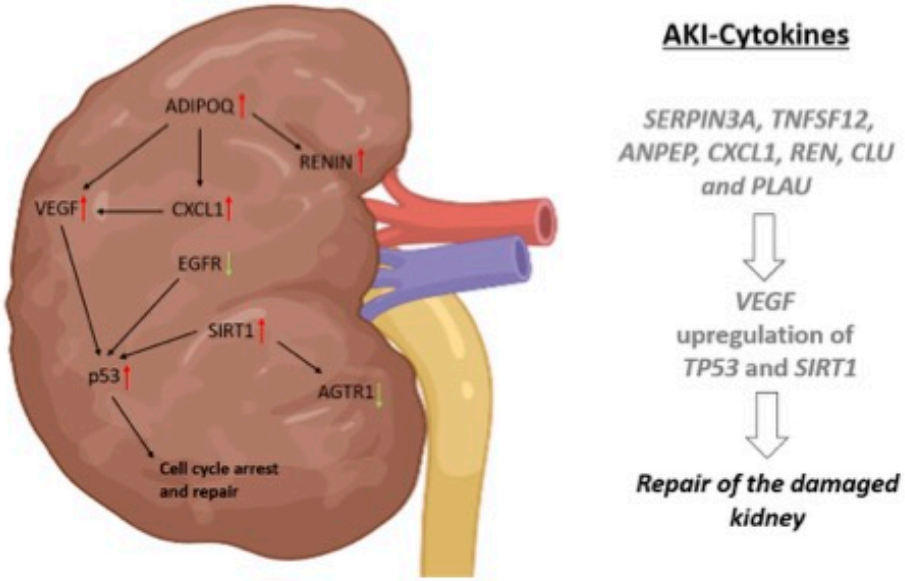


Figure 4. Proposed AKI signalling cascade. Urine-containing cytokines for the detection of AKI, which are male-enriched (AHSG), female-enriched (CCN1, IL6, CCL2, THBS1, IL1RN) and common in both (VEGF, SERPIN3A, TNFSF12, ANPEP, CXCL1, REN, CLU and PLAU). Furthermore, mechanistically, the cytokines ADIPOQ, EGF, EGFR, REN and VEGF present in the urine of AKI 2/3 patients trigger processes such as angiogenesis that are needed to repair the damaged nephron and the activation of TP53 and SIRT1 to maintain the balance between proliferation, angiogenesis, repair and cell-cycle arrest. Upregulated Cyokines and Proteins are indicated by a red arrow, while downregulated ones are indicated by a green arrow. Created with BioRender.com.

4. Materials and Methods

4.1. Study Design

After approval by the local ethics committee of Heinrich-Heine University Duesseldorf, Germany (local trial number 5803, clinicaltrials.gov: NCT03089242), adult patients scheduled for cardiac surgery were enrolled after they had provided written informed consent to participate in the study.

Urinary samples from 6 patients with moderate to severe AKI (AKI stage 2 or 3) and from 6 matched controls (heart surgery, no AKI post-operatively) were centrifuged (3500 rpm, 5 min) and stored until further analysis.

4.2. Secretome Analyses

The urine samples were analysed using the Proteome Profiler Human Kidney Biomarker Array Kit (#ARY019) distributed by Research and Diagnostic Systems, Inc. (Minneapolis, MN, USA), as described by the manufacturer and in our previous publication [57]. In brief, the membranes were blocked with the provided blocking buffer and each urine sample was incubated with 15 µL of reconstituted Detection Antibody Cocktail for 1 h at room temperature. After removing the blocking buffer, the urine samples were incubated on the membranes at 4 °C overnight on a rocking platform. After three consecutive washing steps, each for 10 min at room temperature on a rocking platform, the membranes were incubated with the diluted Streptavidin–HRP antibody mix. After three consecutive washing steps, each for 10 min at room temperature on a rocking platform, the fluorescence signals were

visualized with enhanced luminescence (WesternBright Quantum, Advansta, San Jose, CA, USA).

The obtained images were analyzed using Image J software [70] with the Microarray Profile plugin by Bob Dougherty and Wayne Rasband (https://www.optinav.info/MicroArray_Profile.html accessed on 10 March 2023). The integrated density generated by the Microarray Profile plugin function Measure RT was used for the follow-up processing, which was performed in the R/Bioconductor environment [71]. The arrays were normalized by employing the Robust Spline Normalization from the Bioconductor lumi package [72]. The threshold for background intensities was defined at 5% of the range between the maximum and minimum intensity, and the detection p-value was calculated according to the method described in Graffmann et al. [73]. Cytokines detected in the AKI and control condition with a p-value from the R package limma of less than 0.05 controlled for the false discovery rate (FDR < 0.25) and with a ratio greater than 1.2 (inverse ratio < 0.8333 for downregulation) were considered upregulated [28].

4.3. Cell Culture Conditions

The cell line UM51-hTERT was derived and cultured as described in ref. [27]. For the experiments, the non-AKI and AKI 2/3 patient urine samples obtained 72 h post-surgery were pooled and mixed with the culture medium to a final concentration of 10%. This concentration was observed to be acceptable for cell culture experiments in terms of a lack of contamination and cell death. The cells were incubated with this medium for five days.

4.4. Relative Quantification of Podocyte-Associated Gene Expression by Real-Time PCR

The real-time PCR of the podocyte-associated gene expression was performed as follows. Real-time measurements were carried out on the Step One Plus Real-Time PCR Systems using a MicroAmp Fast Optical 384 Well Reaction Plate and Power Sybr Green PCR Master Mix (Applied Biosystems, Foster City, CA, USA). The amplification conditions were denaturation at 95 °C for 13 min, followed by 37 cycles of 95 °C for 50 s, 60 °C for 45 s and 72 °C for 30 s. The primer sequences are listed in Supplementary Table S1.

4.5. Immunofluorescence-Based Detection of Protein Expression

The cells were fixed with 4% paraformaldehyde (PFA) (Polysciences, WA, USA). The unspecific binding sites were blocked by incubation with blocking buffer containing 10% normal goat or donkey serum, 1% BSA, 0.5% triton, and 0.05% tween for 2 h at room temperature. Incubation of the primary antibody was performed at 4 °C overnight in staining buffer (blocking buffer diluted 1:1 with PBS). After at least 16 h of incubation, the cells were washed three times with PBS/0.05% tween and incubated with a 1:500 dilution of secondary antibodies. After three additional washing steps with PBS/0.05% tween, the cell and nuclei were stained with Hoechst 1:5000 (Thermo Fisher Scientific, Waltham, MA, USA). Images were captured using a fluorescence microscope (LSM700; Zeiss, Oberkochen, Germany) with Zenblue software (Zeiss). Individual channel images were processed and merged with Fiji. Detailed information on the used antibodies is given in Supplementary Table S2.

4.6. Western Blotting

Protein isolation was performed via lysis of the cells in RIPA buffer (Sigma-Aldrich, St. Louis, MO, USA) supplemented with complete protease and phosphatase inhibitors (Roche, Basel, Switzerland). The proteins were separated on a 7.5% Bis-Tris gel and blotted onto a 0.45 µm nitrocellulose membrane (GE Healthcare Life Sciences, Chalfont St. Giles, UK). After blocking the membranes with 5% skimmed milk in Tris-buffered saline tween (TBS-T), they were incubated overnight with the respective primary antibodies (Supplementary Table S1). The membranes were washed 3× for 10 min with TBS-T. Secondary antibody incubation was performed for 1 h at RT and the membranes were subsequently washed 3× for 10 min with TBS-T. Amersham ECL Prime Western Blotting

Detection Reagent was used for the chemiluminescent detection (GE Healthcare Life Sciences) and captured with the imaging device Fusion FX.

4.7. Statistics

The data are presented as arithmetic means + standard error. In total, three independent experiments were performed and used for the calculation of the mean values. Statistical significance was calculated using the two-sample Student's *t*-test or with Mann–Whitney U test to compare the variables between the two patient groups. The association between the categorical variables and the two groups (no AKI vs. AKI patients) was tested with the Chi-squared test. For all the tests, p-values < 0.05 were considered significant.

Supplementary Materials: The following supporting information can be downloaded at https://www.mdpi.com/article/10.3390/ijms24098228/s1.

Author Contributions: Conceptualization, J.A.; methodology, J.A., L.E., C.T. and W.W.; bioinformatics, W.W.; sample collection: D.K., M.S., L.H., T.D. and D.K.-M. validation, L.E. and W.W.; formal analysis, L.E., C.T. and W.W.; investigation, L.E., C.T. and W.W.; resources, J.A.; data curation, L.E.; writing—original draft preparation, L.E.; writing—review and editing, L.E., T.B. and J.A.; visualization, L.E.; supervision, J.A.; project administration, J.A.; funding acquisition, J.A. All authors have read and agreed to the published version of the manuscript.

Funding: J.A. acknowledges the medical faculty of Heinrich-Heine University for financial support.

Institutional Review Board Statement: The study was conducted in accordance with the written approval (Ethical approval Number: clinicaltrials.gov NCT03089242) of the ethical review board of the medical faculty of Heinrich Heine University, Düsseldorf, Germany. All methods were carried out in accordance with the approved guidelines. Medical faculty of Heinrich Heine University approved all experimental protocols.

Informed Consent Statement: In this study, urine samples were collected with the informed consent of the donors.

Data Availability Statement: All data is available.

Conflicts of Interest: The authors declare no conflict of interest.

References

1. Eknoyan, G. Emergence of the concept of acute renal failure. *Am. J. Nephrol.* **2002**, *22*, 225–230. [CrossRef] [PubMed]
2. Kellum, J.A.; Ronco, C.; Bellomo, R. Conceptual advances and evolving terminology in acute kidney disease. *Nat. Rev. Nephrol.* **2021**, *17*, 493–502. [CrossRef] [PubMed]
3. Makris, K.; Spanou, L. Acute Kidney Injury: Definition, Pathophysiology and Clinical Phenotypes. *Clin. Biochem. Rev.* **2016**, *37*, 85–98. [PubMed]
4. Al-Jaghbeer, M.; Dealmeida, D.; Bilderback, A.; Ambrosino, R.; Kellum, J.A. Clinical Decision Support for In-Hospital AKI. *J. Am. Soc. Nephrol.* **2018**, *29*, 654–660. [CrossRef] [PubMed]
5. Hoste, E.A.J.; Bagshaw, S.M.; Bellomo, R.; Cely, C.M.; Colman, R.; Cruz, D.N.; Edipidis, K.; Forni, L.G.; Gomersall, C.D.; Govil, D.; et al. Epidemiology of acute kidney injury in critically ill patients: The multinational AKI-EPI study. *Intensive Care Med.* **2015**, *41*, 1411–1423. [CrossRef]
6. Khwaja, A. KDIGO clinical practice guidelines for acute kidney injury, Nephron. *Clin. Pract.* **2012**, *120*, c179–c184.
7. Ronco, C.; Bellomo, R.; Kellum, J.A. Acute kidney injury. *Lancet* **2019**, *394*, 1949–1964. [CrossRef]
8. Thakar, C.V. Perioperative acute kidney injury. *Adv. Chronic Kidney Dis.* **2013**, *20*, 67–75. [CrossRef]
9. Antunes, P.E.; Prieto, D.; Ferrão de Oliveira, J.; Antunes, M.J. Renal dysfunction after myocardial revascularization. *Eur. J. Cardio Thorac. Surg. Off. J. Eur. Assoc. Cardio-Thorac. Surg.* **2004**, *25*, 597–604. [CrossRef]
10. Chertow, G.M.; Lazarus, J.M.; Christiansen, C.L.; Cook, E.F.; Hammermeister, K.E.; Grover, F.; Daley, J. Preoperative renal risk stratification. *Circulation* **1997**, *95*, 878–884. [CrossRef]
11. Chertow, G.M.; Levy, E.M.; Hammermeister, K.E.; Grover, F.; Daley, J. Independent association between acute renal failure and mortality following cardiac surgery. *Am. J. Med.* **1998**, *104*, 343–348. [CrossRef]
12. Ostermann, M.E.; Taube, D.; Morgan, C.J.; Evans, T.W. Acute renal failure following cardiopulmonary bypass: A changing picture. *Intensive Care Med.* **2000**, *26*, 565–571. [CrossRef] [PubMed]
13. Nadasdy, T.; Laszik, Z.; Blick, K.E.; Johnson, L.D.; Silva, F.G. Proliferative activity of intrinsic cell populations in the normal human kidney. *J. Am. Soc. Nephrol.* **1994**, *4*, 2032–2039. [CrossRef] [PubMed]

14. Witzgall, R.; Brown, D.; Schwarz, C.; Bonventre, J.V. Localization of proliferating cell nuclear antigen, vimentin, c-Fos, and clusterin in the postischemic kidney. Evidence for a heterogenous genetic response among nephron segments, and a large pool of mitotically active and dedifferentiated cells. *J. Clin. Investig.* **1994**, *93*, 2175–2188. [CrossRef] [PubMed]
15. Lin, F.; Moran, A.; Igarashi, P. Intrarenal cells, not bone marrow-derived cells, are the major source for regeneration in postischemic kidney. *J. Clin. Investig.* **2005**, *115*, 1756–1764. [CrossRef]
16. Canaud, G.; Bonventre, J.V. Cell cycle arrest and the evolution of chronic kidney disease from acute kidney injury. *Nephrol. Dial. Transplant. Off. Publ. Eur. Dial. Transpl. Assoc. Eur. Ren. Assoc.* **2015**, *30*, 575–583. [CrossRef]
17. Clements, M.E.; Chaber, C.J.; Ledbetter, S.R.; Zuk, A. Increased cellular senescence and vascular rarefaction exacerbate the progression of kidney fibrosis in aged mice following transient ischemic injury. *PLoS ONE* **2013**, *8*, e70464. [CrossRef]
18. Molitoris, B.A.; Dagher, P.C.; Sandoval, R.M.; Campos, S.B.; Ashush, H.; Fridman, E.; Brafman, A.; Faerman, A.; Atkinson, S.J.; Thompson, J.D.; et al. siRNA targeted to p53 attenuates ischemic and cisplatin-induced acute kidney injury. *J. Am. Soc. Nephrol.* **2009**, *20*, 1754–1764. [CrossRef]
19. Wei, Q.; Dong, G.; Yang, T.; Megyesi, J.; Price, P.M.; Dong, Z. Activation and involvement of p53 in cisplatin-induced nephrotoxicity. *Am. J. Physiol. Ren. Physiol.* **2007**, *293*, F1282–F1291. [CrossRef]
20. Zhou, L.; Fu, P.; Huang, X.R.; Liu, F.; Lai, K.N.; Lan, H.Y. Activation of p53 promotes renal injury in acute aristolochic acid nephropathy. *J. Am. Soc. Nephrol.* **2010**, *21*, 31–41. [CrossRef]
21. Yang, L.; Besschetnova, T.Y.; Brooks, C.R.; Shah, J.V.; Bonventre, J.V. Epithelial cell cycle arrest in G2/M mediates kidney fibrosis after injury. *Nat. Med.* **2010**, *16*, 535–543. [CrossRef]
22. Deng, C.-X. SIRT1, is it a tumor promoter or tumor suppressor? *Int. J. Biol. Sci.* **2009**, *5*, 147–152. [CrossRef] [PubMed]
23. Han, M.-K.; Song, E.-K.; Guo, Y.; Ou, X.; Mantel, C.; Broxmeyer, H.E. SIRT1 regulates apoptosis and Nanog expression in mouse embryonic stem cells by controlling p53 subcellular localization. *Cell Stem Cell* **2008**, *2*, 241–251. [CrossRef] [PubMed]
24. Raji-amirhasani, A.; Khaksari, M.; Darvishzadeh Mahani, F.; Hajializadeh, Z. Activators of SIRT1 in the kidney and protective effects of SIRT1 during acute kidney injury (AKI) (effect of SIRT1 activators on acute kidney injury). *Clin. Exp. Nephrol.* **2021**, *25*, 807–821. [CrossRef] [PubMed]
25. Kim, J.-Y.; Jo, J.; Kim, K.; An, H.-J.; Gwon, M.-G.; Gu, H.; Kim, H.-J.; Yang, A.Y.; Kim, S.-W.; Jeon, E.J.; et al. Pharmacological Activation of Sirt1 Ameliorates Cisplatin-Induced Acute Kidney Injury by Suppressing Apoptosis, Oxidative Stress, and Inflammation in Mice. *Antioxidants* **2019**, *8*, 322. [CrossRef]
26. Mahani, F.D.; Khaksari, M.; Raji-Amirhasani, A. Renoprotective effects of estrogen on acute kidney injury: The role of SIRT1. *Int. Urol. Nephrol.* **2021**, *53*, 2299–2310. [CrossRef]
27. Erichsen, L.; Kloss, L.D.F.; Thimm, C.; Bohndorf, M.; Schichel, K.; Wruck, W.; Adjaye, J. Derivation of the Immortalized Cell Line UM51-PrePodo-hTERT and Its Responsiveness to Angiotensin II and Activation of the RAAS Pathway. *Cells* **2023**, *12*, 342. [CrossRef]
28. Smyth, G.K. Linear models and empirical bayes methods for assessing differential expression in microarray experiments. *Stat. Appl. Genet. Mol. Biol.* **2004**, *3*, 3. [CrossRef]
29. Cai, L.; Xu, S.; Piao, C.; Qiu, S.; Li, H.; Du, J. Adiponectin induces CXCL1 secretion from cancer cells and promotes tumor angiogenesis by inducing stromal fibroblast senescence. *Mol. Carcinog.* **2016**, *55*, 1796–1806. [CrossRef]
30. Montero, E.; Abreu, C.; Tonino, P. Relationship between VEGF and p53 expression and tumor cell proliferation in human gastrointestinal carcinomas. *J. Cancer Res. Clin. Oncol.* **2008**, *134*, 193–201. [CrossRef]
31. Pierzchalski, P.; Reiss, K.; Cheng, W.; Cirielli, C.; Kajstura, J.; Nitahara, J.A.; Rizk, M.; Capogrossi, M.C.; Anversa, P. p53 Induces myocyte apoptosis via the activation of the renin-angiotensin system. *Exp. Cell Res.* **1997**, *234*, 57–65. [CrossRef] [PubMed]
32. Tiwari, N.; Marudamuthu, A.S.; Tsukasaki, Y.; Ikebe, M.; Fu, J.; Shetty, S. p53- and PAI-1-mediated induction of C-X-C chemokines and CXCR2: Importance in pulmonary inflammation due to cigarette smoke exposure. *Am. J. Physiol. Lung Cell. Mol. Physiol.* **2016**, *310*, L496–L506. [CrossRef] [PubMed]
33. Zhang, H.; He, S.; Spee, C.; Ishikawa, K.; Hinton, D.R. SIRT1 mediated inhibition of VEGF/VEGFR2 signaling by Resveratrol and its relevance to choroidal neovascularization. *Cytokine* **2015**, *76*, 549–552. [CrossRef]
34. Chandel, N.; Ayasolla, K.; Wen, H.; Lan, X.; Haque, S.; Saleem, M.A.; Malhotra, A.; Singhal, P.C. Vitamin D receptor deficit induces activation of renin angiotensin system via SIRT1 modulation in podocytes. *Exp. Mol. Pathol.* **2017**, *102*, 97–105. [CrossRef] [PubMed]
35. Georgoulis, A.; Vorgias, C.E.; Chrousos, G.P.; Rogakou, E.P. Genome Instability and γH2AX. *Int. J. Mol. Sci.* **2017**, *18*, 1979. [CrossRef] [PubMed]
36. Bendale, D.S.; Karpe, P.A.; Chhabra, R.; Shete, S.P.; Shah, H.; Tikoo, K. 17-β Oestradiol prevents cardiovascular dysfunction in post-menopausal metabolic syndrome by affecting SIRT1/AMPK/H3 acetylation. *Br. J. Pharmacol.* **2013**, *170*, 779–795. [CrossRef]
37. Ota, H.; Akishita, M.; Akiyoshi, T.; Kahyo, T.; Setou, M.; Ogawa, S.; Iijima, K.; Eto, M.; Ouchi, Y. Testosterone deficiency accelerates neuronal and vascular aging of SAMP8 mice: Protective role of eNOS and SIRT1. *PLoS ONE* **2012**, *7*, e29598. [CrossRef]
38. Yu, X.; Zheng, J.; Cai, T.; Wang, Z.; Zhu, G. Testosterone antagonizes paraquat-induced cardiomyocyte senescence via the mIGF-1/SIRT1 signaling pathway. *Braz. J. Med. Biol. Res.* **2020**, *53*, e9849. [CrossRef]
39. Ucero, A.C.; Benito-Martin, A.; Fuentes-Calvo, I.; Santamaria, B.; Blanco, J.; Lopez-Novoa, J.M.; Ruiz-Ortega, M.; Egido, J.; Burkly, L.C.; Martinez-Salgado, C.; et al. TNF-related weak inducer of apoptosis (TWEAK) promotes kidney fibrosis and Ras-dependent proliferation of cultured renal fibroblast. *Biochim. Biophys. Acta* **2013**, *1832*, 1744–1755. [CrossRef]

40. Tögel, F.; Zhang, P.; Hu, Z.; Westenfelder, C. VEGF is a mediator of the renoprotective effects of multipotent marrow stromal cells in acute kidney injury. *J. Cell. Mol. Med.* **2009**, *13*, 2109–2114. [CrossRef]
41. Sharma, N.; Anders, H.-J.; Gaikwad, A.B. Fiend and friend in the renin angiotensin system: An insight on acute kidney injury. *Biomed. Pharmacother.* **2018**, *110*, 764–774. [CrossRef]
42. Ma, C.; Liu, G.; Liu, W.; Xu, W.; Li, H.; Piao, S.; Sui, Y.; Feng, W. CXCL1 stimulates decidual angiogenesis via the VEGF-A pathway during the first trimester of pregnancy. *Mol. Cell. Biochem.* **2021**, *476*, 2989–2998. [CrossRef] [PubMed]
43. Wei, Z.-W.; Xia, G.-K.; Wu, Y.; Chen, W.; Xiang, Z.; Schwarz, R.E.; Brekken, R.A.; Awasthi, N.; He, Y.-L.; Zhang, C.-H. CXCL1 promotes tumor growth through VEGF pathway activation and is associated with inferior survival in gastric cancer. *Cancer Lett.* **2015**, *359*, 335–343. [CrossRef]
44. Divella, R.; Daniele, A.; DE Luca, R.; Simone, M.; Naglieri, E.; Savino, E.; Abbate, I.; Gadaleta, C.D.; Ranieri, G. Circulating Levels of VEGF and CXCL1 Are Predictive of Metastatic Organotropismin in Patients with Colorectal Cancer. *Anticancer Res.* **2017**, *37*, 4867–4871. [PubMed]
45. Nakagawa, N.; Yao, N.; Hirayama, T.; Ishida, M.; Ishida, H.; Wada, A.; Fujino, T.; Saijo, Y.; Kikuchi, K.; Hasebe, N. Potential impact of renin-angiotensin system inhibitors and calcium channel blockers on plasma high-molecular-weight adiponectin levels in hemodialysis patients. *Hypertens. Res. Off. J. Jpn. Soc. Hypertens.* **2011**, *34*, 592–598. [CrossRef] [PubMed]
46. Hoffman, S.B.; Massaro, A.N.; Soler-García, A.A.; Perazzo, S.; Ray, P.E. A novel urinary biomarker profile to identify acute kidney injury (AKI) in critically ill neonates: A pilot study. *Pediatr. Nephrol.* **2013**, *28*, 2179–2188. [CrossRef]
47. Askenazi, D.J.; Koralkar, R.; Hundley, H.E.; Montesanti, A.; Parwar, P.; Sonjara, S.; Ambalavanan, N. Urine biomarkers predict acute kidney injury in newborns. *J. Pediatr.* **2012**, *161*, 270–275.e1. [CrossRef]
48. Staun-Ram, E.; Goldman, S.; Shalev, E. p53 Mediates epidermal growth factor (EGF) induction of MMP-2 transcription and trophoblast invasion. *Placenta* **2009**, *30*, 1029–1036. [CrossRef]
49. Chen, J.; You, H.; Li, Y.; Xu, Y.; He, Q.; Harris, R.C. EGF Receptor-Dependent YAP Activation Is Important for Renal Recovery from AKI. *J. Am. Soc. Nephrol.* **2018**, *29*, 2372–2385. [CrossRef]
50. Sheikh, M.S.; Carrier, F.; Johnson, A.C.; Ogdon, S.E.; Fornace, A.J. Identification of an additional p53-responsive site in the human epidermal growth factor receptor gene promotor. *Oncogene* **1997**, *15*, 1095–1101. [CrossRef]
51. Samarakoon, R.; Dobberfuhl, A.D.; Cooley, C.; Overstreet, J.M.; Patel, S.; Goldschmeding, R.; Meldrum, K.K.; Higgins, P.J. Induction of renal fibrotic genes by TGF-β1 requires EGFR activation, p53 and reactive oxygen species. *Cell. Signal.* **2013**, *25*, 2198–2209. [CrossRef] [PubMed]
52. Vijayan, A.; Faubel, S.; Askenazi, D.J.; Cerda, J.; Fissell, W.H.; Heung, M.; Humphreys, B.D.; Koyner, J.L.; Liu, K.D.; Mour, G.; et al. Clinical Use of the Urine Biomarker TIMP-2 × IGFBP7 for Acute Kidney Injury Risk Assessment. *Am. J. Kidney Dis. Off. J. Natl. Kidney Found.* **2016**, *68*, 19–28. [CrossRef] [PubMed]
53. Ortega, L.M.; Heung, M. The use of cell cycle arrest biomarkers in the early detection of acute kidney injury. Is this the new renal troponin? *Nefrologia* **2018**, *38*, 361–367. [CrossRef] [PubMed]
54. Wang, W.; Saad, A.; Herrmann, S.M.; Eirin Massat, A.; McKusick, M.A.; Misra, S.; Lerman, L.O.; Textor, S.C. Changes in inflammatory biomarkers after renal revascularization in atherosclerotic renal artery stenosis. *Nephrol. Dial. Transplant. Off. Publ. Eur. Dial. Transpl. Assoc. Eur. Ren. Assoc.* **2016**, *31*, 1437–1443. [CrossRef]
55. Kashani, K.; Al-Khafaji, A.; Ardiles, T.; Artigas, A.; Bagshaw, S.M.; Bell, M.; Bihorac, A.; Birkhahn, R.; Cely, C.M.; Chawla, L.S.; et al. Discovery and validation of cell cycle arrest biomarkers in human acute kidney injury. *Crit. Care* **2013**, *17*, R25. [CrossRef] [PubMed]
56. Erichsen, L.; Thimm, C.; Bohndorf, M.; Rahman, M.S.; Wruck, W.; Adjaye, J. Activation of the Renin-Angiotensin System Disrupts the Cytoskeletal Architecture of Human Urine-Derived Podocytes. *Cells* **2022**, *11*, 1095. [CrossRef]
57. Wruck, W.; Boima, V.; Erichsen, L.; Thimm, C.; Koranteng, T.; Kwakyi, E.; Antwi, S.; Adu, D.; Adjaye, J. Urine-based detection of biomarkers indicative of chronic kidney disease in a patient cohort from Ghana. *J. Pers. Med.* **2022**, *13*, 38. [CrossRef]
58. Engel, J.E.; Williams, E.; Williams, M.L.; Bidwell, G.L.; Chade, A.R. Targeted VEGF (Vascular Endothelial Growth Factor) Therapy Induces Long-Term Renal Recovery in Chronic Kidney Disease via Macrophage Polarization. *Hypertension* **2019**, *74*, 1113–1123. [CrossRef]
59. Basile, D.P.; Friedrich, J.L.; Spahic, J.; Knipe, N.; Mang, H.; Leonard, E.C.; Changizi-Ashtiyani, S.; Bacallao, R.L.; Molitoris, B.A.; Sutton, T.A. Impaired endothelial proliferation and mesenchymal transition contribute to vascular rarefaction following acute kidney injury. *Am. J. Physiol. Ren. Physiol.* **2011**, *300*, F721–F733. [CrossRef]
60. Hasegawa, K.; Wakino, S.; Yoshioka, K.; Tatematsu, S.; Hara, Y.; Minakuchi, H.; Sueyasu, K.; Washida, N.; Tokuyama, H.; Tzukerman, M.; et al. Kidney-specific overexpression of Sirt1 protects against acute kidney injury by retaining peroxisome function. *J. Biol. Chem.* **2010**, *285*, 13045–13056. [CrossRef]
61. Lee, J.T.; Gu, W. SIRT1: Regulator of p53 Deacetylation. *Genes Cancer* **2013**, *4*, 112–117. [CrossRef] [PubMed]
62. Niederer, F.; Ospelt, C.; Brentano, F.; Hottiger, M.O.; Gay, R.E.; Gay, S.; Detmar, M.; Kyburz, D. SIRT1 overexpression in the rheumatoid arthritis synovium contributes to proinflammatory cytokine production and apoptosis resistance. *Ann. Rheum. Dis.* **2011**, *70*, 1866–1873. [CrossRef] [PubMed]
63. Hasegawa, K.; Wakino, S.; Yoshioka, K.; Tatematsu, S.; Hara, Y.; Minakuchi, H.; Washida, N.; Tokuyama, H.; Hayashi, K.; Itoh, H. Sirt1 protects against oxidative stress-induced renal tubular cell apoptosis by the bidirectional regulation of catalase expression. *Biochem. Biophys. Res. Commun.* **2008**, *372*, 51–56. [CrossRef]

64. Gao, P.; Xu, T.-T.; Lu, J.; Li, L.; Xu, J.; Hao, D.-L.; Chen, H.-Z.; Liu, D.-P. Overexpression of SIRT1 in vascular smooth muscle cells attenuates angiotensin II-induced vascular remodeling and hypertension in mice. *J. Mol. Med.* **2013**, *92*, 347–357. [CrossRef] [PubMed]
65. Miyazaki, R.; Ichiki, T.; Hashimoto, T.; Inanaga, K.; Imayama, I.; Sadoshima, J.; Sunagawa, K. SIRT1, a longevity gene, downregulates angiotensin II type 1 receptor expression in vascular smooth muscle cells. *Arterioscler. Thromb. Vasc. Biol.* **2008**, *28*, 1263–1269. [CrossRef] [PubMed]
66. Tissenbaum, H.A.; Guarente, L. Increased dosage of a sir-2 gene extends lifespan in Caenorhabditis elegans. *Nature* **2001**, *410*, 227–230. [CrossRef]
67. Wood, J.G.; Rogina, B.; Lavu, S.; Howitz, K.; Helfand, S.L.; Tatar, M.; Sinclair, D. Sirtuin activators mimic caloric restriction and delay ageing in metazoans. *Nature* **2004**, *430*, 686–689. [CrossRef]
68. Erichsen, L.; Adjaye, J. Crosstalk between age accumulated DNA-damage and the SIRT1-AKT-GSK3ß axis in urine derived renal progenitor cells. *Aging* **2022**, *14*, 8179–8204. [CrossRef]
69. Andrade, L.; Rodrigues, C.E.; Gomes, S.A.; Noronha, I.L. Acute Kidney Injury as a Condition of Renal Senescence. *Cell Transplant.* **2018**, *27*, 739–753. [CrossRef]
70. Schneider, C.A.; Rasband, W.S.; Eliceiri, K.W. NIH Image to ImageJ: 25 years of image analysis. *Nat. Methods* **2012**, *9*, 671–675. [CrossRef]
71. Gentleman, R.C.; Carey, V.J.; Bates, D.M.; Bolstad, B.; Dettling, M.; Dudoit, S.; Ellis, B.; Gautier, L.; Ge, Y.; Gentry, J.; et al. Bioconductor: Open software development for computational biology and bioinformatics. *Genome Biol.* **2004**, *5*, R80. [CrossRef] [PubMed]
72. Du, P.; Kibbe, W.A.; Lin, S.M. lumi: A pipeline for processing Illumina microarray. *Bioinformatics* **2008**, *24*, 1547–1548. [CrossRef] [PubMed]
73. Graffmann, N.; Ring, S.; Kawala, M.-A.; Wruck, W.; Ncube, A.; Trompeter, H.-I.; Adjaye, J. Modeling Nonalcoholic Fatty Liver Disease with Human Pluripotent Stem Cell-Derived Immature Hepatocyte-Like Cells Reveals Activation of PLIN2 and Confirms Regulatory Functions of Peroxisome Proliferator-Activated Receptor Alpha. *Stem Cells Dev.* **2016**, *25*, 1119–1133. [CrossRef] [PubMed]

Disclaimer/Publisher's Note: The statements, opinions and data contained in all publications are solely those of the individual author(s) and contributor(s) and not of MDPI and/or the editor(s). MDPI and/or the editor(s) disclaim responsibility for any injury to people or property resulting from any ideas, methods, instructions or products referred to in the content.

3.6 Urine-Based Detection of Biomarkers Indicative of Chronic Kidney Disease in a Patient Cohort from Ghana

Wasco Wruck, Vincent Boima, Lars Erichsen, **Chantelle Thimm**, Theresa Koranteng, Edward Kwakyi, Sampson Antwi, Dwomoa Adu and James Adjaye

Journal of Personalized Medicine 2023, Volume 13, 38, Article ID 13010038

Abstract:

Chronic kidney disease (CKD) is a global health burden with a continuously increasing prevalence associated with an increasing incidence of diabetes and hypertension in aging populations. CKD is characterized by low glomerular filtration rate (GFR) and other renal impairments including proteinuria, thus implying that multiple factors may contribute to the etiology this disease. While there are indications of ethnic differences, it is hard to disentangle these from confounding social factors. Usually, CKD is detected in later stages of the disease when irreversible renal damage has already occurred, thus suggesting a need for early non-invasive diagnostic markers. In this study, we explored the urine secretome of a CKD patient cohort from Ghana with 40 gender-matched patients and 40 gender-matched healthy controls employing a kidney injury and a more general cytokine assay. We identified panels of kidney-specific cytokine markers, which were also gender-specific, and a panel of gender-independent cytokine markers. The gender-specific markers are IL10 and MME for male and CLU, RETN, AGER, EGFR and VEGFA for female. The gender-independent cytokine markers were APOA1, ANGPT2, C5, CFD, GH1, ICAM1, IGFBP2, IL8, KLK4, MMP9 and SPP1 (up-regulated) and FLT3LG, CSF1, PDGFA, RETN and VEGFA (down-regulated). APOA1—the major component of HDL particles—was up-regulated in Ghanaian CKD patients and its co-occurrence with APOL1 in a subpopulation of HDL particles may point to specific CKD-predisposing APOL1 haplotypes in patients of African descent—this, however, needs further investigation. The identified panels, though preliminary, lay down the foundation for the development of robust CKD-diagnostic assays.

Author contribution of C.T. included 30%:

Patients urine included in the CKD cohort were clinically recruited by V.B., T.K., E.K., S.A., D.A. and J.A. Together with L.E., I collected, sorted, and pooled the CKD patient urine samples, which I subsequently analyzed using the Proteome Profiler Human Kidney Biomarker Kit and the Proteome Profiler Human Cytokine Array Kit. Furthermore, I contributed to the manuscript revision process by discussing and jointly addressing the reviewers' comments together with W.W., J.A. and L.E.

Status: Published in the Journal of Personalized Medicine

DOI: doi.org/10.3390/ jpm13010038

This article is an open access article distributed under the terms and conditions of the Creative Commons Attribution (CC BY) 4.0 license, which permits unrestricted use, distribution, and reproduction in any medium, provided the original work is properly cited.

Journal of *Personalized Medicine*

MDPI

Article

Urine-Based Detection of Biomarkers Indicative of Chronic Kidney Disease in a Patient Cohort from Ghana

Wasco Wruck [1], Vincent Boima [2], Lars Erichsen [1], Chantelle Thimm [1], Theresa Koranteng [3], Edward Kwakyi [2], Sampson Antwi [4], Dwomoa Adu [2] and James Adjaye [1,5,*]

[1] Institute for Stem Cell Research and Regenerative Medicine, Medical Faculty, Heinrich Heine University, Moorenstr. 5, 40225 Düsseldorf, Germany
[2] Department of Medicine & Therapeutics, University of Ghana Medical School, College of Health Sciences, Box 4236, University of Ghana, Accra P.O. Box LG 1181, Ghana
[3] NHS-Clover Health Centre, Equitable House, 10 Woolich New Road, Woolich, London SE18 6AB, UK
[4] Department of Child Health, School of Medical Sciences, Kwame Nkrumah University of Science and Technology, Komfo Anokye Teaching Hospital, Kumasi P.O. Box KS 9265, Ghana
[5] EGA Institute for Women's Health, University College London, 86-96 Chenies Mews, London WC1E 6HX, UK
* Correspondence: james.adjaye@med.uni-duesseldorf.de

Abstract: Chronic kidney disease (CKD) is a global health burden with a continuously increasing prevalence associated with an increasing incidence of diabetes and hypertension in aging populations. CKD is characterized by low glomerular filtration rate (GFR) and other renal impairments including proteinuria, thus implying that multiple factors may contribute to the etiology this disease. While there are indications of ethnic differences, it is hard to disentangle these from confounding social factors. Usually, CKD is detected in later stages of the disease when irreversible renal damage has already occurred, thus suggesting a need for early non-invasive diagnostic markers. In this study, we explored the urine secretome of a CKD patient cohort from Ghana with 40 gender-matched patients and 40 gender-matched healthy controls employing a kidney injury and a more general cytokine assay. We identified panels of kidney-specific cytokine markers, which were also gender-specific, and a panel of gender-independent cytokine markers. The gender-specific markers are IL10 and MME for male and CLU, RETN, AGER, EGFR and VEGFA for female. The gender-independent cytokine markers were APOA1, ANGPT2, C5, CFD, GH1, ICAM1, IGFBP2, IL8, KLK4, MMP9 and SPP1 (up-regulated) and FLT3LG, CSF1, PDGFA, RETN and VEGFA (down-regulated). APOA1—the major component of HDL particles—was up-regulated in Ghanaian CKD patients and its co-occurrence with APOL1 in a subpopulation of HDL particles may point to specific CKD-predisposing APOL1 haplotypes in patients of African descent—this, however, needs further investigation. The identified panels, though preliminary, lay down the foundation for the development of robust CKD-diagnostic assays.

Keywords: CKD; biomarkers; Ghana; urine; cytokines; VEGFA; inflammation

check for updates

Citation: Wruck, W.; Boima, V.; Erichsen, L.; Thimm, C.; Koranteng, T.; Kwakyi, E.; Antwi, S.; Adu, D.; Adjaye, J. Urine-Based Detection of Biomarkers Indicative of Chronic Kidney Disease in a Patient Cohort from Ghana. *J. Pers. Med.* **2023**, *13*, 38. https://doi.org/10.3390/jpm13010038

Academic Editor: Marijn Speeckaert

Received: 10 November 2022
Revised: 7 December 2022
Accepted: 22 December 2022
Published: 24 December 2022

Copyright: © 2022 by the authors. Licensee MDPI, Basel, Switzerland. This article is an open access article distributed under the terms and conditions of the Creative Commons Attribution (CC BY) license (https://creativecommons.org/licenses/by/4.0/).

1. Introduction

Chronic kidney disease (CKD) is defined by a glomerular filtration rate (GFR) < 60 mL/min per 1.73 m^2 or the presence of kidney damage predominantly manifested by proteinuria for 3 months or more [1,2].

Protein in urine as an indicator of kidney damage is often measured by the urine albumin-to-creatinine ratio (UACR). Proteinuria and decreased GFR directly reflect physical properties of the filter between blood and urine constituted by an endothelial layer, the glomerular basement membrane (GMB) and podocytes. This filter is coarse at the endothelial side and fine at the podocytes and works in the dimension of nanometers in addition to a negative polarity. Thus, bigger and negatively charged molecules, such as most proteins under physiological conditions, cannot traverse this barrier. In proteinuria, larger proteins, such as albumin, immunoglobulins G and M and α1-microglobulin, β2-microglobulin,

correlating with the severity of histologic lesions [3], can traverse. These proteins can, as a consequence, impair the re-absorption of other smaller molecules by the proximal tubular epithelial cells and in final stages lead to toxic damage [3].

The increasing prevalence of CKD is largely influenced by the increase of diabetes and hypertension among the aging population [4,5]. Although substantial percentages of CKD patients will progress to more severe disease stages requiring dialysis or transplantation, most patients die of associated cardiovascular disease (CVD) than of end-stage renal disease (ESRD) [6]. Although diabetes is the most common cause of CKD, it is not clear why only 30% of patients with type 1 and 25 to 40% of patients with type 2 diabetes progress to nephropathy irrespective of glycemic control [4,7,8].

Ethnic differences have been reported for diabetic nephropathy, particularly in Pima Indians [4], and for focal segmental glomerulosclerosis (FSGS) in patients of African descent, who have higher frequencies of the FSGS-predisposing APOL1 G1 and G2 haplotypes, which on the other hand confer advantages against the sleeping sickness-causing parasite—Trypanosoma brucei brucei [9]. A body of literature reports gender differences in CKD [10–12], resulting in phenomena including gender-specific prevalence in dialysis and mortality rates. The causes of these differences have not been fully elucidated. However, differences in the levels of sex hormones and in the Renin-Angiotensin system may play major roles, as well as behavioral compliance with the dialysis treatment, medication and lifestyle restrictions.

Biomarkers for the early diagnosis of CKD are urgently needed and studies aiming at their identification have been performed using serum [13] as well as urine samples [14,15]. While there are several reports focusing on single or only few proteins [16–18], to our knowledge, there has been only one other study investigating CKD urine samples with a cytokine array, which, however, was on a distinct platform not specific for kidney injury markers [19]. This study identified higher levels of MMP9, MCP-1, RANTES, tissue inhibitor of metalloproteinase (TIMP) 1, TNF-alpha, vascular endothelial growth factor (VEGF), E-selectin, Fas, intercellular adhesion molecule 1, interleukin 2, matrix metalloproteinase (MMP) 2 and transforming growth factor beta and lower levels of urinary vascular cell adhesion molecule 1 and platelet-derived growth factor in CKD [19].

In this study, aimed at gender-neutral and -specific CKD biomarker identification, we investigated proteins secreted into the urine of a cohort of CKD patients and healthy controls from Ghana using a general (Human XL) assay and a kidney injury-specific cytokine assay.

2. Materials and Methods

Participants in the present study were recruited from two academic medical centers in urban regions of Ghana between 2012–2017. Persons with kidney disease were individuals aged 1–74 years with estimated glomerular filtration rate (eGFR) < 60 mL/min/1.73 m^2 (creatinine based chronic kidney disease epidemiology [CKD-EPI] collaboration equation without race adjustment) [1] or albumin/creatinine ratio $\geq$ 3.0 mg/mmol (30 mg/g), and persons with a confirmed diagnosis of membranous glomerulonephritis, focal and segmental glomerulosclerosis/minimal change disease (FSGS/MCD) or childhood onset nephrotic syndrome. The CKD-EPI equation without the race adjustment was used in adults and the Schwartz formula [20] in children aged less than 16 years. We excluded persons with obstructive uropathy, kidney tumors, multiple myeloma, polycystic kidney disease and women who were pregnant. Healthy persons without CKD were defined as individuals with eGFR $\geq$ 60 mL/min/1.73 m^2 and albumin/creatinine ratio < 3.0 mg/mmol (<30 mg/g). Random urine samples were collected from cases and controls and aliquots of 10 mLs were taken into cryovials. All participants of this study are from African ancestry. We were anticipating that ancestry might lead to some differences due to higher prevalences of genetic variants, such as the known APOL1 risk haplotype [9,21], which through regulatory networks might also affect the biomarker signatures.

2.1. Ethics Statement

Ethics approval was obtained locally at each clinical site. The approval number for the Case-Control study is: GHSERC: 07/03/2013. Written informed consent was obtained from all participants. Participants unable or unwilling to give consent or who were institutionalized were excluded.

2.2. Cytokine Assay Experiments

The urine samples were analyzed using the Human Kidney Biomarker Array (ARY019) as well as the Human XL Cytokine Array kit (ARY022B) from Research And Diagnostic Systems, Inc. (Minneapolis, MN, USA), according to the manufacturer's protocols. For the experiment series 1, the urine samples (control and CDK) were pooled prior to analysis. In the experiment series 2, we analyzed another pool of urine samples (control and CDK).

In the experiment series 3, urine from one individual male control sample was compared to the pooled male and female CKD samples. For each membrane, 1 mL of urine was incubated overnight at 4 °C on the respective membranes. Detection was carried out using a streptavidin-HRP and the ECL Prime WesternfBlot-Detectionreagent (Merck, Darmstadt, Germany) detection reagents. The obtained signal was analyzed using FIJI/ImageJ software [22].

2.3. Image Analysis of Cytokine Assays

Scanned images of the cytokine assays were read into the FIJI/ImageJ software [22]. The semi-automatic grid finding was based on pre-processing via Gaussian blur (size 4) and local maxima finding as described in Steinfath et al. [23]. Local maxima were detected via the FIJI function "Find Maxima" and exported to a file in the csv format. The csv file containing the local maxima was imported into the R programming environment to detect the corners and interpolate the grid with the pre-defined size between the corners. The interpolation routine took into account alleyways between blocks within the grid and adjusted grid positions to local maxima, where existent. For positions without detected local maxima, the interpolated values were used. Grid positions were read into the FIJI Microarray Profile plugin by Bob Dougherty and Wayne Rasband (https://www.optinav.info/MicroArray_Profile.htm, accessed on 21 December 2022), which was employed to quantify the integrated densities of the spots. Grid positions were annotated with the cytokine identifiers provided in the manuals of the manufacturer (Proteome Profiler Array from R & D Systems, Human XL Cytokine Array Kit, Catalog Number ARY022B and Human Kidney Biomarker Array Kit, Catalog Number ARY019).

2.4. Data Analysis of Cytokine Assays

Integrated densities of the spots quantified by the FIJI Microarray plugin were imported into the R/Bioconductor [24] environment for further processing. Data were normalized via the Robust Spline Normalization from the R/Bioconductor package lumi [25]. Cytokines were considered expressed when their integrated density was significantly ($p < 0.05$) over the background spots, which were determined as spots with the minimum density plus 0.05 (max_density–min_density). Differential expression was assessed via the moderated t-test from the Bioconductor *limma* package [26]. Limma p-values were adjusted for the false discovery rate (FDR) by the method described by Benjamini and Hochberg [27]. Cytokines were considered as differentially expressed based on the criteria: detection p-value < 0.05 in at least one condition, ratio < 0.667 (down-regulated), ratio > 1.5 (up-regulated), limma-p-value < 0.05, FDR < 0.25. Heatmaps were generated with the function *heatmap.2* from the *gplots* package [28] using Pearson correlation as similarity measure. Bar plots were generated with the R-builtin function *barplot*. Dendrograms were produced via the R package *dendextend* [29] using Pearson correlation as the similarity measure and complete linkage as the agglomeration method.

3. Results

3.1. Patient Characteristics

Urine samples from CKD patients aged 6–71 years and control urine samples from probands with no history of CKD aged 11–68 were used (Table 1). The urine samples were collected in Ghana at the University of Ghana Medical School. Decisive criteria for the choice of CKD urine samples were the glomerular filtration rate (GFR) < 60 mL/min per 1.73 m^2, which is documented for CKD [29]. Furthermore, CKD is associated with an elevated albumin creatine ratio (ACR) < 300 mg/g [30]. In experiment series 1, urine samples of patients from group 1 were investigated, in experiment series 2, urine samples of patients from group 2 were investigated and in experiment series 3, urine samples of patients from group 1 were investigated.

3.2. Strategy for the Identification of CKD Markers

Figure 1 shows the workflow used for identifying the CKD biomarkers. In the first phase, experiment series 1 and 2 were performed on the kidney-injury cytokine assay platform. Each experiment series consisted of 10 pooled male CKD urine samples, 10 pooled female CKD urine samples, 10 pooled male healthy control urine samples and 10 pooled female healthy control urine samples. Series 1 and 2 differed by the selection of distinct individuals. In the second phase, experiment series 3 was performed on the Human cytokine XL assay platform. The experiment series consisted of 10 pooled male CKD urine samples, 10 pooled female CKD urine samples and 1 male healthy control sample.



Figure 1. Workflow for the identification of CKD biomarkers. The pipeline employed the Human Kidney Biomarker Array in phase 1 of experiment series 1 and 2 and the human XL cytokine assay in phase 2 with experiment series 3. Pools of 10 male and 10 female urine samples were used for CKD patients and healthy controls.

3.3. Identification of CKD Biomarkers Using the Human Kidney Biomarker Array

Figure 2 shows results of experiment series 1 on the kidney cytokine assay and the identified CKD biomarkers. At the global level of the kidney cytokine expression, the data segregated (Figure 2A) into two distinct clusters of CKD (male and female) and healthy control (male and female). The heatmap (Figure 2B) and barplot (Figure 2C) show biomarkers which were found up-regulated (up) in males (M): CLU, CXCL1, IL1RN, IL10, RBP4 and SKP1, as well as biomarkers which were down-regulated (down): DPP4, EGFR, MME, MMP9 and VEGF. The heatmap (Figure 2D) and barplot (Figure 2E) show biomarkers which were found up-regulated (up) in females (F): ANPEP, ANXA5, B2M, CCL2, CCN1, CLU, CXCL16, CST3, DPP4, EGF, IL6, IL10, HAVCR1, KLK3, LCN2, MMP9, PLAU, RETN, SERPINA3, SKP1, TNFA, TNFSRF1A and TTF3, as well as biomarkers which were down-regulated (down): AGER, EGFR, FABP1 and VEGF.

Table 1. Characteristics of the patient cohort and the healthy individual cohort utilized in the cytokine assay analyses.

Group 1															
	Control female				Control male				CKD female				CKD male		
Age	eGFR (mL/min per 1–73 m^2)	number	Albumine creatine ratio (g/mmol)	Age	eGFR (mL/min per 1–73 m^2)	number	Albumine creatine ratio (g/mmol)	Age	eGFR (mL/min per 1–73 m^2)	number	Albumine creatine ratio (g/mmol)	Age	eGFR (mL/min per 1–73 m^2)	number	Albumine creatine ratio (g/mmol)
39	169.45	52815	0.68	11	70.77	52803	0.4	69	3	52866	107.25	24	84.05	52852	123.34
39	94.85	21206	1.11	26	153.98	52833	1.6	28	29	21245	8.27	41	123.38	52840	10.61
46	131.85	52855	0.85	46	92.64	52856	0.93	65	49	52838	1.67	28	153.97	52829	1925.38
47	145.27	52805	0.47	47	120.56	52839	1.06	49	51	52973	30.68	25	181.34	52830	17.89
20	134.71	21227	0.81	47	85.62	52839	1.06	38	75	52845	13.79	48	11.04	52842	2.69
24	74.53	21246	0.51	57	160.36	52777	1.03	39	92	21240	119.93	47	30.99	52875	0.91
25	113.26	21216	0.19	57	136.93	52823	0.48	25	93	52854	3.76	48	11.04	52842	2.69
70	134.61	52778	0.3	66	145.09	52818	0.67	35	99	21244	11.23	60	22.58	52828	87.79
51	150.26	52757	0.32	67	83.58	21241	0.36	46	114	52827	141.83	60	54.94	52862	3.05
50	119.12	21225	0.35	68	102.38	52861	1.71	60	123	52871	82.99	65	4.95	52832	0.54

Group 2															
	Control female				Control male				CKD female				CKD male		
Age	eGFR (mL/min per 1–73 m^2)	number	Albumine creatine ratio (g/mmol)	Age	eGFR (mL/min per 1–73 m^2)	number	Albumine creatine ratio (g/mmol)	Age	eGFR (mL/min per 1–73 m^2)	number	Albumine creatine ratio (g/mmol)	Age	eGFR (mL/min per 1–73 m^2)	number	Albumine creatine ratio (g/mmol)
33	185.43	52768	1.32	17	72.7	21210	0.26	65	1	52865	0.68	22	157.26	52843	2.55
4	85.97	52811	0.71	18	83.16	21223	2.02	22	3	52877	0.62	24	19.68	52844	0.97
14	92.56	21213	0.52	21	165.3	21232	1.24	71	11	52834	0.91	28	5.37	52864	5.03
16	75.12	21214	0.37	24	153.06	21212	0.26	7	14	21237	0.68	33	194.92	52831	10
16	68.11	52812	2.51	33	217.41	52804	1.21	30	17	52859	1.04	35	24.3	52873	1.2
18	78.64	21231	0.86	37	151.17	21235	0.88	50	26	21238	0.6	37	13.96	52870	1.08
20	129.93	21229	0.76	48	123.11	21243	1.14	71	35	52867	0.53	39	5.92	21248	2.08
27	140.59	21218	1.92	49	68.92	52728	0.52	62	41	21249	2.78	39	8.5	52879	0.57
62	153.39	52825	1.84	59	85.61	52759	0.89	28	46	52857	46.4	44	5.15	52835	4.33
21	91.94	21217	0.78	63	87.59	52772	1.36	35	17	52858	7.2	59	3.07	52869	0.51

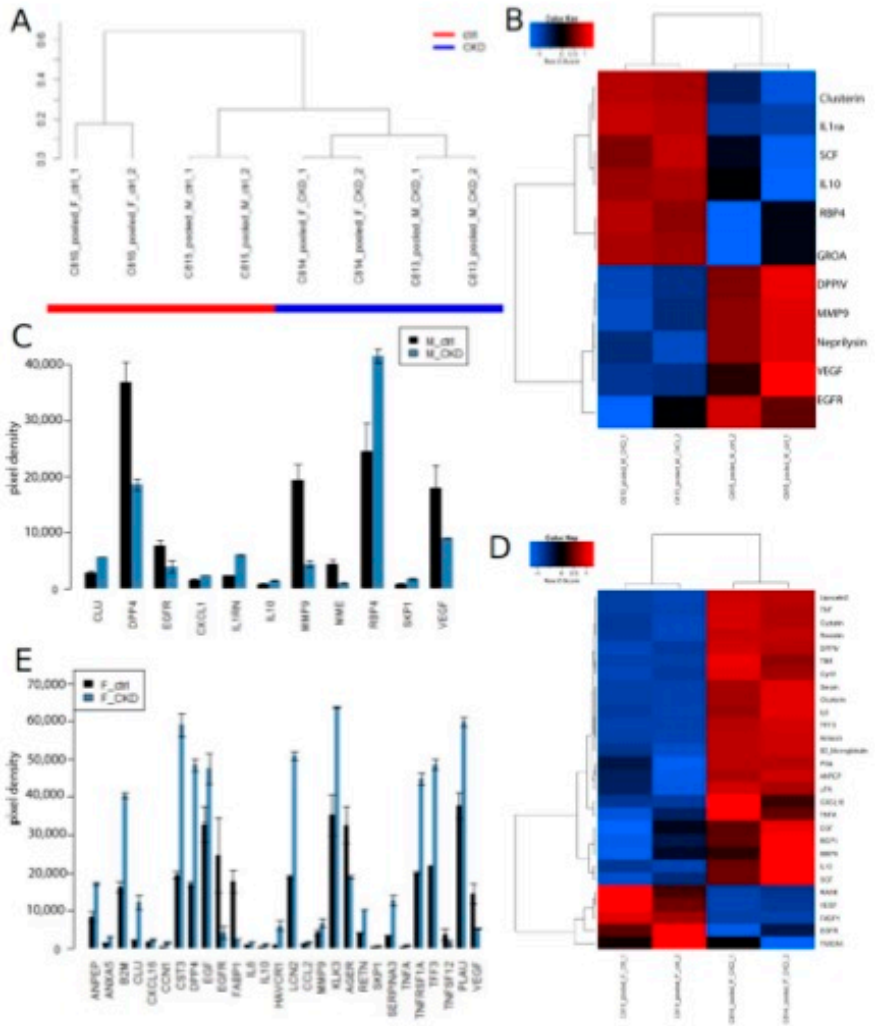


Figure 2. CKD biomarkers identified on the Human Kidney Biomarker Array in experiment se-ries 1. (**A**) Experiments cluster into CKD and healthy control based on the global kidney cytokine expression. (**B**) Heatmap and (**C**) barplot of markers in males (M) that were up-regulated (up): CLU, CXCL1, IL1RN, IL10, RBP4 and SKP1, and down-regulated (down): DPP4, EGFR, MME, MMP9 and VEGF. (**D**) Heatmap and (**E**) barplot of markers in females (F) that were up-regulated (up): ANPEP, ANXA5, B2M, CCL2, CCN1, CLU, CXCL16, CST3, DPP4, EGF, IL6, IL10, HAVCR1, KLK3, LCN2, MMP9, PLAU, RETN, SERPINA3, SKP1, TNFA, TNFSRF1A and TTF3, and down-regulated (down): AGER, EGFR, FABP1 and VEGF.

Figure 3 shows the results of experiment series 2 on the Human Kidney Biomarker Array and the identified CKD biomarkers. On the global level of kidney cytokine expression, the experiments clustered heterogeneously with respect to CKD and gender (Figure 3A). The heatmap (Figure 3B) and barplot (Figure 3C) show markers which were found up-

regulated (up) in males (M): ADIPOQ, AG, ANXA5, CCN1, FABP1, IL10, LCN2, MMP9, RETN, SERPINA3, TNFA, TNFSF12 and VEGF, and which were down-regulated (down): AGER, AHSG, ANPEP, CLU, CXCL16, MME and RBP4. The heatmap (Figure 3D) and barplot (Figure 3E) show markers which were found up-regulated (up) in females (F): AG, AHSG, CLU, IL1RN, MME, RETN, TNFSF12 and VCAM1, and which were down-regulated (down): ADIPOQ, AGER, ANPEP, ANXA5, CCL2, CCN1, EGFR, IL6, MMP9, PLAU and VEGF.

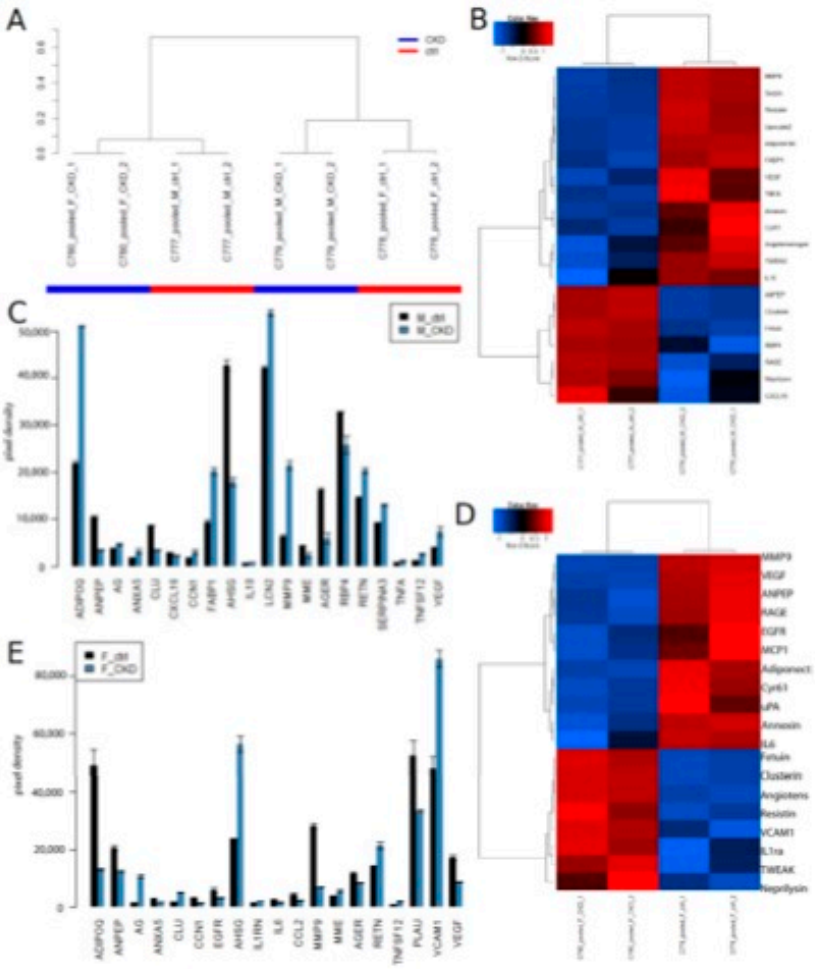


Figure 3. CKD biomarkers identified on the Human Kidney Biomarker Array in experiment series 2. (**A**) experiments cluster heterogeneously based on the global kidney cytokine expression. (**B**) Heatmap and (**C**) barplot of biomarkers in males (M) that were up-regulated (up): ADIPOQ, AG, ANXA5, CCN1, FABP1, IL10, LCN2, MMP9, RETN, SERPINA3, TNFA, TNFSF12 and VEGF, and down-regulated (down): AGER, AHSG, ANPEP, CLU, CXCL16, MME and RBP4. (**D**) Heatmap and (**E**) barplot of biomarkers in females (F) that were up-regulated (up): AG, AHSG, CLU, IL1RN, MME, RETN, TNFSF12 and VCAM1, and down-regulated (down): ADIPOQ, AGER, ANPEP, ANXA5, CCL2, CCN1, EGFR, IL6, MMP9, PLAU and VEGF.

3.4. Summary of the Identified CKD Biomarkers in Experiment Series 1 and 2

Table 2 shows a summary of the CKD biomarkers identified in experiment series 1 and 2 for male CKD patients. Biomarkers identified in common in both series are underlined and in bold font. In both series, IL10 was shown to be up-regulated and MME was shown to be down-regulated in CKD.

Table 2. CKD markers identified in male CKD patients in experiment series 1 and 2.

Cytokine	CKD_M_ExpSeries1	CKD_M_ExpSeries2
ADIPOQ		up
AG		up
AGER		down
AHSG		down
ANPEP		down
ANXA5		up
CCN1		up
CLU	up	down
CXCL1	up	
CXCL16		down
DPP4	down	
EGFR	down	
FABP1		up
IL1RN	up	
IL10	**up**	**up**
LCN2		up
MME	**down**	**down**
MMP9	down	up
RBP4	up	down
RETN		up
SERPINA3		up
SKP1	up	
TNFA		up
TNFSF12		up
VEGF	down	up

Table 3 shows a summary of the CKD biomarkers identified in experiment series 1 and 2 for female CKD patients. Biomarkers identified in common in both series are underlined and in bold format. In both series, CLU and RETN were shown to be up-regulated and AGER, EGFR and VEGF were shown to be down-regulated in CKD.

3.5. Identification of CKD Biomarkers on the Human XL Cytokine Assay

After identification of CKD biomarkers on the Human Kidney Biomarker Array we set out to identify CKD-associated cytokines which include both pro-and anti-inflammatory molecules. Figure 4 shows results from experiment series 3 on the human XL cytokine assay and the identified CKD inflammation-associated biomarkers. On the global level of cytokine expression, the data segregated (Figure 4A) into two clusters of CKD (male and female) and healthy control (male). The heatmap (Figure 4B) and barplot (Figure 4C) show biomarkers which were found to be up-regulated (up) or down-regulated (down) in males

(M). The heatmap (Figure 4D) and barplot (Figure 4E) show markers which were found up-regulated (up) or down-regulated in females (F). Interestingly, we found a large overlap between up-and down-regulated cytokines between both genders. Some biomarkers that were up-regulated in experiment series 3 overlapped between females (F) and males (M) in CKD: APOA1 (up), ANGPT2 (up), C5 (up), CFD (up), GH1 (up), ICAM1 (up), IGFBP2 (up), IL8 (up), KLK4 (up), MMP9 (up) and SPP1 (up). Other markers that were down-regulated in experiment series 3 overlapped between female (F) and male (M) in CKD: FLT3LG (down), CSF1 (down), PDGFA (down), RETN (down) and VEGFA (down).

Table 3. CKD markers identified in female CKD patients in experiment series 1 and 2.

Cytokine	CKD_F_ExpSeries1	CKD_F_ExpSeries2
ADIPOQ		down
AG		up
AGER	down	down
AHSG		up
ANPEP	up	down
ANXA5	up	down
B2M	up	
CCL2	up	down
CCN1	up	down
CLU	up	up
CST3	up	
CXCL16	up	
DPP4	up	
EGF	up	
EGFR	down	down
FABP1	down	
IL1RN		up
IL6	up	down
IL10	up	
HAVCR1	up	
KLK3	up	
LCN2	up	
MME		up
MMP9	up	down
PLAU	up	down
RETN	up	up
SERPINA3	up	
SKP1	up	
TNFA	up	
TNFSF12		up
TNFRSF1A	up	
TTF3	up	
VCAM1		up
VEGF	down	down

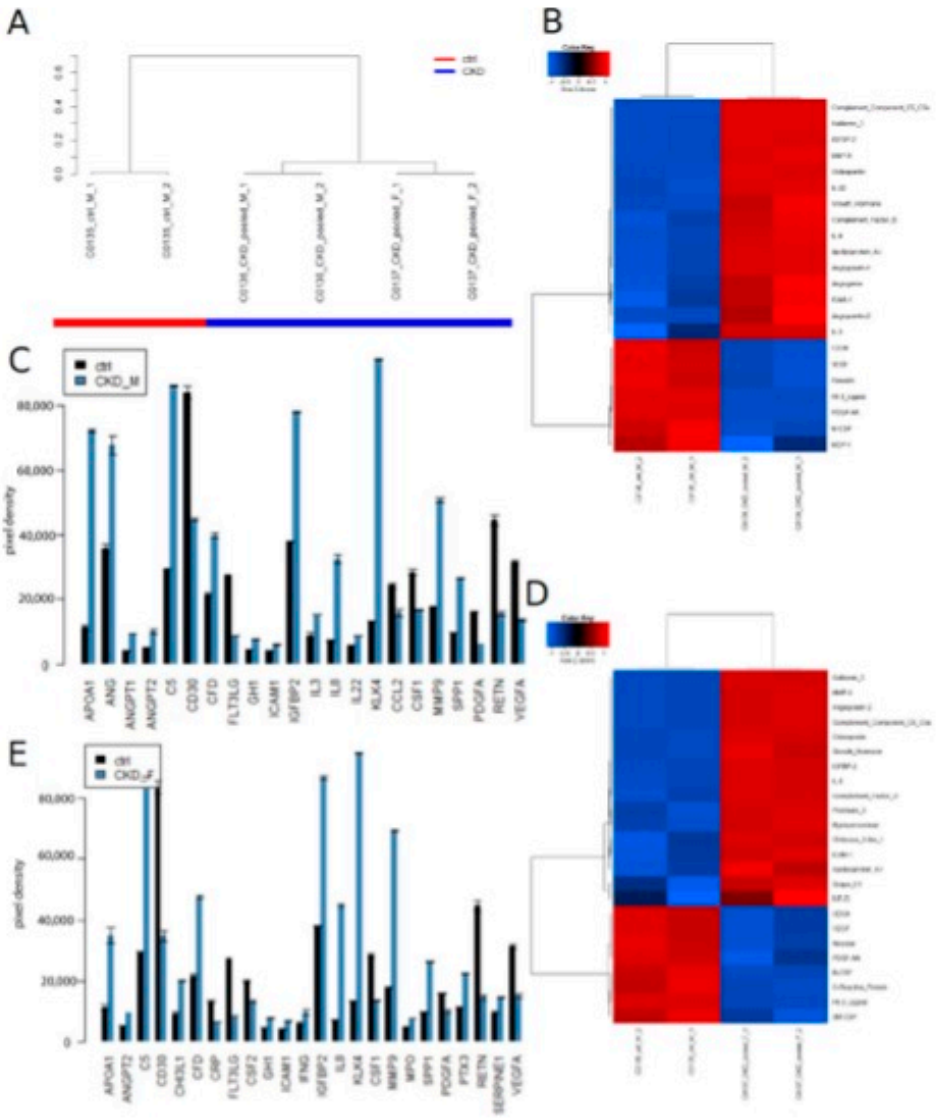


Figure 4. CKD biomarkers identified on the Human XL cytokine assay in experiment series 3 show significant overlap between males and females. (**A**) Data cluster into CKD and healthy control based on global cytokine expression. (**B**) Heatmap and (**C**) barplot of markers in males (M) that were up-regulated (up) or down-regulated (down). (**D**) Heatmap and (**E**) barplot of markers in females (F) that were up-regulated (up) or down-regulated (down). Markers in experiment series 3 that overlapped between females (F) and males (M) that were up-regulated in CKD: APOA1 (up), ANGPT2 (up), C5 (up), CFD (up), GH1 (up), ICAM1 (up), IGFBP2 (up), IL8 (up), KLK4 (up), MMP9 (up) and SPP1 (up). Markers in experiment series 3 that overlapped between females (F) and males (M) that were down-regulated in CKD: FLT3LG (down), CSF1 (down), PDGFA (down), RETN (down) and VEGFA (down).

Table 4 shows a summary of CKD markers identified in experiment series 3 for male and female CKD patients and independent of gender, taking the mean of male and female values. Markers identified as overlapping in males and females are underlined and in bold format. This summary table highlights the large overlap between male and female CKD markers on the human XL cytokine platform.

Table 4. CKD-associated cytokine biomarkers identified as common and specific between males and females, based on experiment series 3.

Cytokine	CKD_mean_M_F_ExpSeries3	CKD_M_ExpSeries3	CKD_F_ExpSeries3
APOA1	**up**	**up**	**up**
ANG		**up**	
ANGPT1		**up**	
ANGPT2	**up**	**up**	**up**
C5	**up**	**up**	**up**
CD3	**down**		**down**
CHI3L1	**up**		**up**
CFD	**up**	**up**	**up**
CRP	**down**		**down**
FLT3LG	**down**	**down**	**down**
CSF2	**down**		**down**
GH1	**up**	**up**	**up**
ICAM1	**up**	**up**	**up**
IFNG	**up**		**up**
IGFBP2	**up**	**up**	**up**
IL3		**up**	
IL8	**up**	**up**	**up**
IL22		**up**	
KLK4	**up**	**up**	**up**
CCL2		**down**	
CSF1	**down**	**down**	**down**
MMP9	**up**	**up**	**up**
MPO	**up**		**up**
SPP1	**up**	**up**	**up**
PDGFA	**down**	**down**	**down**
PTX3	**up**		**up**
RETN	**down**	**down**	**down**
SERPINE1	**up**		**up**
VEGFA	**down**	**down**	**down**

3.6. Protein Interaction Network

Based on the identified differentially regulated cytokines, we set out to identify and characterize a protein interaction network involved in the inflammatory pathophysiology of CKD. Figure 5A shows the Protein interaction network generated via the STRING online tool [31]. Via the STRING tool, enriched disease associations with *Leukostasis* and *Artery Disease* (Figure 5C) were determined and a table of enriched Gene ontology Biological

Processes was created (Figure 5D, top 25 terms sorted by strength is shown). These pointed to the inflammatory response and included the highlighted term *Regulation of kidney development* (strength = 1.8, false discovery rate = 0.0024). The proteins associated with the regulation of kidney development (PDGFA, MMP9, VEGFA) are highlighted in the network in Figure 5B.



Figure 5. CKD biomarkers identified on the Human XL cytokine assay interact in a network regulating the inflammatory response affecting kidney development. (**A**) STRING protein interaction network (PPI) of CKD biomarkers identified on the Human XL cytokine assay. (**B**) PPI highlighting proteins involved in the regulation of kidney development. (**C**) Disease associations found enriched by the STRING tool are *Leukostasis* and *Artery Disease*. (**D**) Gene ontology Biological Processes found enriched point to the inflammatory response and include *the regulation of kidney development*.

4. Discussion

In this two-phase analysis of cytokines in the urine of CKD patients and healthy individuals from Ghana, we identified urine-based cytokine biomarkers for CKD. In the first phase, which was performed on a Human Kidney Biomarker Array, we found variability

between males and females and also between the two experimental series, which consisted of pooled urine samples from distinct individuals. This variability is a reflection of heterogeneity within biomarkers associated with CKD, which comprises a broad spectrum of distinct diseases, such as diabetic nephropathy and focal segmental glomerulosclerosis. Furthermore, there is much diversity in the genetic background of CKD and recent findings on biomarkers associated with hitherto neglected areas, such as telomeres, CNVs, mtDNA variants and sex chromosomes [32], which may gain attention in the future. This may also help to explain the high heredity estimated at 30–75%, which at the moment is incompletely understood [32]. A further aspect of heterogeneity is found in the definitions of CKD, which on the one hand have to cope with the complexity of the disease, but on the other hand, lead to strongly deviating assessments of CKD progression [33]. Among the kidney-associated cytokines, we identified as variable between genders and experimental series LCN2 (alias NGAL; up-regulated in male in experiment series 1 and in female in experiment series 2, not significant in the others), which should be highlighted. NGAL had been established as marker of acute kidney injury, but several problems, including its unpredictable release, have led to increasing concerns about its diagnostic value [34].

For the sake of robustness, only biomarkers regulated in the same direction in both experiment series are listed. The CKD biomarkers in male are: IL10 (Interleukin-10, up-regulated) and MME (Membrane metalloendopeptidase, down-regulated). Sinuani et al. reported that IL10, through increased proliferation of mesangial cells and mediated by several other cytokines, induces progression of renal failure [35]. Dedicated single nucleotide polymorphisms (SNPs) in the MME gene have been associated with a higher risk for diabetic nephropathy in female diabetes type 1 patients [36]. The CKD biomarkers in females are: CLU (Clusterin), RETN (Resistin, up-regulated), AGER (advanced glycosylation end-product specific receptor, alias RAGE), EGFR (epidermal growth factor receptor) and VEGFA (vascular endothelial growth factor A, alias VEGF, down-regulated). CLU has been reported to be elevated in kidney disease [37,38], although Guo et al. found that CLU deficiency exacerbates renal inflammation and tissue fibrosis after ischemia-reperfusion injury in mice [39]. For Resistin, there are reports on elevated levels in CKD, which are associated with decreased glomerular filtration rate and inflammation [40]. AGER/RAGE was reported to be elevated in the serum of CKD patients [41]. Up-regulation of EGFR has been described for CKD, but EGFR inhibition in models of acute kidney injury (AKI) may also have deleterious effects [42].

In the second phase, we used a more general cytokine (human XL) assay and found a high percentage of cytokine biomarkers overlapping between both genders. The CKD biomarkers regulated in the same direction between male and female are: APOA1, ANGPT2, C5, CFD, GH1, ICAM1, IGFBP2, IL8, KLK4, MMP9 and SPP1 (up-regulated) and FLT3LG, CSF1, PDGFA, RETN and VEGFA (down-regulated).

Interestingly, APOA1 is connected to APOL1, which has been associated with FSGS in haplotypes carried by patients of African descent. APOL1 is bound to HDL particles, of which APOA1 is the major protein component, but only 10% of APOA1-containing HDL particles have APOL1 [21]. We still need to confirm if these APOL1-positive HDL particles play a special role in CKD. In comparison to the first phase, where we saw strong gender-specific differences, in the second phase, we identified nearly the same markers regulated in the same direction for both males and females. The large number of gender-specific differences found on the Human Kidney Biomarker Array in the first phase is in line with reports of gender differences in kidney function [43] and kidney disease [11]. It is tempting to speculate that the more general cytokines measured on the human XL assay reflect more gender-independent inflammatory processes which precede CKD.

Cytokines detected as differentially regulated on the Human XL cytokine assay as well as the Human Kidney Biomarker Array were RETN (Resistin, down-regulated on the Human XL cytokine assay), MMP9 (metalloproteinase 9, up-regulated on the Human XL cytokine assay) and VEGFA (down-regulated on the Human XL cytokine assay). VEGFA was regulated in the same direction on the Human Kidney Biomarker Array (down), while

MMP9 was up-regulated in males in series 2 and females in series 1 and down-regulated in males in series 1 and females in series 2; however, RETN, in contrast to the XL assay, was up-regulated. As mentioned above for RETN, there are reports on elevated levels in CKD [40]. MMP9 is described to be up-regulated in early stages of the disease and down-regulated in later stages [44]. In our cohorts, this might reflect the predominantly late disease stages in the distinct cohorts. For VEGFA, there are conflicting data on the regulation in diabetic nephropathy going from up-regulation in rat models and also diabetic patients [45], to no effect [46], to down-regulation when diabetic nephropathy leads to glomerusclerosis [45]. For glomerusclerosis and tubulorinterstitial fibrosis down-regulation has been reported [45].

We compared our detected biomarkers with association loci from GWAS and found that VEGFA, which we detected as a biomarker, had been identified in GWAS for an association with eGFR [47] and also in a further study by the CKD consortium for an association with CKD, which, while not having a significant *p*-value, nevertheless pointed in the same direction [48]. Furthermore, we found that CST3, which we found up-regulated in females on the Human Kidney biomarker array (Figure 2E), was detected to be associated with eGFR via GWAS by Köttgen et al. [47].

We anticipate that our detected biomarkers may foster the mechanistic understanding of the development of CKD and further help to enable an earlier detection of the disease and in cases not detected by the conventional markers. CKD diagnosis mainly relies on GFR estimation indicating kidney dysfunction or albuminuria indicating kidney damage [49]. GFR estimations are hampered by limitations of creatinine [50]. Albumin does not work as a marker in the non-albuminuric cases highly prevalent in non-diabetic CKD [17,51,52], but is also common in diabetic CKD [16,49,53].

5. Conclusions

We conclude that our two-phase cytokine analysis of urine samples from CKD patients and healthy controls from Ghana has revealed panels of kidney-specific cytokine biomarkers which are also gender-specific and a panel of gender-independent cytokine markers. The gender-specific markers are IL10 and MME for males and CLU, RETN, AGER, EGFR and VEGFA for females. The gender-independent cytokine markers were APOA1, ANGPT2, C5, CFD, GH1, ICAM1, IGFBP2, IL8, KLK4, MMP9 and SPP1 (up-regulated) and FLT3LG, CSF1, PDGFA, RETN and VEGFA (down-regulated).

Supplementary Materials: The following supporting information can be downloaded at: https://www.mdpi.com/article/10.3390/jpm13010038/s1, Table S1: mean values and statistical test results of male patients CKD vs. healthy control in experiment series 1 on kidney cytokine array. Table S2: mean values and statistical test results of female patients CKD vs. healthy control in experiment series 1 on kidney cytokine array. Table S3: mean values and statistical test results of male patients CKD vs. healthy control in experiment series 2 on kidney cytokine array. Table S4: mean values and statistical test results of female patients CKD vs. healthy control in experiment series 2 on kidney cytokine array. Table S5: mean values and statistical test results of male patients CKD vs. healthy control in experiment series 3 on Human XL cytokine array. Table S6: mean values and statistical test results of female patients CKD vs. healthy control in experiment series 3 on Human XL cytokine array. Table S7: statistical test results of mean of male and female patients CKD vs. healthy control in experiment series 3 on Human XL cytokine array. Figure S1: Scanned kidney cytokine arrays of experiment series 1. Figure S2: Scanned kidney cytokine arrays of experiment series 2. Figure S3: Scanned kidney cytokine arrays of experiment series 3.

Author Contributions: J.A. and V.B. conceived the study. V.B., D.A., T.K., S.A. and E.K. recruited the patients and healthy individuals and collected the urine samples. W.W. analyzed the data and wrote the manuscript. L.E. and C.T. performed the cytokine assays and co-wrote the manuscript. J.A. supervised the work, co-wrote the manuscript and gave the final approval. All authors have read and agreed to the published version of the manuscript.

Funding: James Adjaye acknowledges support from the Medical faculty of Heinrich-Heine University, Duesseldorf. Vincent Boima acknowledges support from the University of Ghana Medical School and all participants who consented to participate in this study.

Institutional Review Board Statement: Ethics approval was obtained locally at each clinical site. The approval number for the Case-Control study is: GHSERC: 07/03/2013.

Informed Consent Statement: Written informed consent was obtained from all participants. Participants unable or unwilling to give consent or institutionalized were excluded.

Data Availability Statement: Datasets for the analysis of cytokine assays were generated during the current study. The datasets are available in the Supplementary Materials data of this work.

Conflicts of Interest: The authors declare no competing interest.

References

1. Levey, A.S.; Coresh, J. Chronic Kidney Disease. *Lancet* **2012**, *379*, 165–180. [CrossRef] [PubMed]
2. Levey, A.S.; Coresh, J.; Balk, E.; Kausz, A.T.; Levin, A.; Steffes, M.W.; Hogg, R.J.; Perrone, R.D.; Lau, J.; Eknoyan, G.; et al. National Kidney Foundation Practice Guidelines for Chronic Kidney Disease: Evaluation, Classification, and Stratification. *Ann. Intern. Med.* **2003**, *139*, 137–147. [CrossRef]
3. D'Amico, G.; Bazzi, C. Pathophysiology of Proteinuria. *Kidney Int.* **2003**, *63*, 809–825. [CrossRef] [PubMed]
4. Schena, F.P.; Gesualdo, L. Pathogenetic Mechanisms of Diabetic Nephropathy. *J. Am. Soc. Nephrol.* **2005**, *16*, S30–S33. [CrossRef] [PubMed]
5. Webster, A.C.; Nagler, E.V.; Morton, R.L.; Masson, P. Chronic Kidney Disease. *Lancet* **2017**, *389*, 1238–1252. [CrossRef]
6. Remuzzi, G. Mechanisms of Progression and Regression of Renal Lesions of Chronic Nephropathies and Diabetes. *J. Clin. Investig.* **2006**, *116*, 288–296. [CrossRef]
7. The Diabetes Control and Complications (DCCT) Research Group. Effect of Intensive Therapy on the Development and Progression of Diabetic Nephropathy in the Diabetes Control and Complications Trial. *Kidney Int.* **1995**, *47*, 1703–1720. [CrossRef]
8. Dronavalli, S.; Duka, I.; Bakris, G.L. The Pathogenesis of Diabetic Nephropathy. *Nat. Clin. Pract. Endocrinol. Metab.* **2008**, *4*, 444–452. [CrossRef]
9. D'Agati, V.D.; Kaskel, F.J.; Falk, R.J. Focal Segmental Glomerulosclerosis. *N. Engl. J. Med.* **2011**, *365*, 2398–2411. [CrossRef]
10. Cobo, G.; Hecking, M.; Port, F.K.; Exner, I.; Lindholm, B.; Stenvinkel, P.; Carrero, J.J. Sex and Gender Differences in Chronic Kidney Disease: Progression to End-Stage Renal Disease and Haemodialysis. *Clin. Sci.* **2016**, *130*, 1147–1163. [CrossRef]
11. Iseki, K. Gender Differences in Chronic Kidney Disease. *Kidney Int.* **2008**, *74*, 415–417. [CrossRef] [PubMed]
12. Carrero, J.J. Gender Differences in Chronic Kidney Disease: Underpinnings and Therapeutic Implications. *Kidney Blood Press. Res.* **2010**, *33*, 383–392. [CrossRef] [PubMed]
13. Goek, O.-N.; Döring, A.; Gieger, C.; Heier, M.; Koenig, W.; Prehn, C.; Römisch-Margl, W.; Wang-Sattler, R.; Illig, T.; Suhre, K.; et al. Serum Metabolite Concentrations and Decreased GFR in the General Population. *Am. J. Kidney Dis.* **2012**, *60*, 197–206. [CrossRef]
14. Saulnier, P.-J.; Darshi, M.; Wheelock, K.M.; Looker, H.C.; Fufaa, G.D.; Knowler, W.C.; Weil, E.J.; Tanamas, S.K.; Lemley, K.V.; Saito, R.; et al. Urine Metabolites Are Associated with Glomerular Lesions in Type 2 Diabetes. *Metabolomics* **2018**, *14*, 84. [CrossRef] [PubMed]
15. Posada-Ayala, M.; Zubiri, I.; Martin-Lorenzo, M.; Sanz-Maroto, A.; Molero, D.; Gonzalez-Calero, L.; Fernandez-Fernandez, B.; de la Cuesta, F.; Laborde, C.M.; Barderas, M.G.; et al. Identification of a Urine Metabolomic Signature in Patients with Advanced-Stage Chronic Kidney Disease. *Kidney Int.* **2014**, *85*, 103–111. [CrossRef] [PubMed]
16. Abbasi, F.; Moosaie, F.; Khaloo, P.; Firouzabadi, F.D.; Abhari, S.M.F.; Atainia, B.; Ardeshir, M.; Nakhjavani, M.; Esteghamati, A. Neutrophil Gelatinase-Associated Lipocalin and Retinol-Binding Protein-4 as Biomarkers for Diabetic Kidney Disease. *Kidney Blood Press. Res.* **2020**, *45*, 222–232. [CrossRef]
17. Peralta, C.A.; Katz, R.; Bonventre, J.V.; Sabbisetti, V.; Siscovick, D.; Sarnak, M.; Shlipak, M.G. Associations of Urinary Levels of Kidney Injury Molecule 1 (KIM-1) and Neutrophil Gelatinase-Associated Lipocalin (NGAL) with Kidney Function Decline in the Multi-Ethnic Study of Atherosclerosis (MESA). *Am. J. Kidney Dis. Off. J. Natl. Kidney Found.* **2012**, *60*, 904–911. [CrossRef] [PubMed]
18. Feldreich, T.; Carlsson, A.C.; Helmersson-Karlqvist, J.; Risérus, U.; Larsson, A.; Lind, L.; Ärnlöv, J. Urinary Osteopontin Predicts Incident Chronic Kidney Disease, While Plasma Osteopontin Predicts Cardiovascular Death in Elderly Men. *Cardiorenal Med.* **2017**, *7*, 245–254. [CrossRef] [PubMed]
19. Liu, B.-C.; Zhang, L.; Lv, L.-L.; Wang, Y.; Liu, D.; Zhang, X. Application of Antibody Array Technology in the Analysis of Urinary Cytokine Profiles in Patients with Chronic Kidney Disease. *Am. J. Nephrol.* **2006**, *26*, 483–490. [CrossRef]
20. Schwartz, G.J.; Muñoz, A.; Schneider, M.F.; Mak, R.H.; Kaskel, F.; Warady, B.A.; Furth, S.L. New Equations to Estimate GFR in Children with CKD. *J. Am. Soc. Nephrol. JASN* **2009**, *20*, 629–637. [CrossRef]
21. Madhavan, S.M.; O'Toole, J.F. The Biology of APOL1 with Insights into the Association between APOL1 Variants and Chronic Kidney Disease. *Clin. Exp. Nephrol.* **2013**, *18*, 238–242. [CrossRef] [PubMed]

22. Schneider, C.A.; Rasband, W.S.; Eliceiri, K.W. NIH Image to ImageJ: 25 Years of Image Analysis. *Nat. Methods* **2012**, *9*, 671–675. [CrossRef]
23. Steinfath, M.; Wruck, W.; Seidel, H.; Lehrach, H.; Radelof, U.; O'Brien, J. Automated Image Analysis for Array Hybridization Experiments. *Bioinformatics* **2001**, *17*, 634–641. [CrossRef] [PubMed]
24. Gentleman, R.C.; Carey, V.J.; Bates, D.M.; Bolstad, B.; Dettling, M.; Dudoit, S.; Ellis, B.; Gautier, L.; Ge, Y.; Gentry, J.; et al. Bioconductor: Open Software Development for Computational Biology and Bioinformatics. *Genome Biol.* **2004**, *5*, R80. [CrossRef] [PubMed]
25. Du, P.; Kibbe, W.A.; Lin, S.M. Lumi: A Pipeline for Processing Illumina Microarray. *Bioinformatics* **2008**, *24*, 1547–1548. [CrossRef] [PubMed]
26. Smyth, G.K. Linear Models and Empirical Bayes Methods for Assessing Differential Expression in Microarray Experiments. *Stat. Appl. Genet. Mol. Biol.* **2004**, *3*, 1–25. [CrossRef]
27. Benjamini, Y.; Hochberg, Y. Controlling the False Discovery Rate: A Practical and Powerful Approach to Multiple Testing. *J. R. Stat. Soc. Ser. B Methodol.* **1995**, *57*, 289–300. [CrossRef]
28. Warnes, G.R.; Bolker, B.; Bonebakker, L.; Gentleman, R.; Liaw, W.H.A.; Lumley, T.; Maechler, M.; Magnusson, A.; Moeller, S.; Schwartz, M.; et al. Gplots: Various R Programming Tools for Plotting Data. *R Package Ver.* **2015**.
29. Galili, T. Dendextend: An R Package for Visualizing, Adjusting and Comparing Trees of Hierarchical Clustering. *Bioinforma. Oxf. Engl.* **2015**, *31*, 3718–3720. [CrossRef]
30. Levey, A.S.; Becker, C.; Inker, L.A. Glomerular Filtration Rate and Albuminuria for Detection and Staging of Acute and Chronic Kidney Disease in Adults: A Systematic Review. *JAMA* **2015**, *313*, 837–846. [CrossRef]
31. Szklarczyk, D.; Franceschini, A.; Wyder, S.; Forslund, K.; Heller, D.; Huerta-Cepas, J.; Simonovic, M.; Roth, A.; Santos, A.; Tsafou, K.P.; et al. STRING V10: Protein-Protein Interaction Networks, Integrated over the Tree of Life. *Nucleic Acids Res.* **2015**, *43*, D447–D452. [CrossRef] [PubMed]
32. Cañadas-Garre, M.; Anderson, K.; Cappa, R.; Skelly, R.; Smyth, L.J.; McKnight, A.J.; Maxwell, A.P. Genetic Susceptibility to Chronic Kidney Disease–Some More Pieces for the Heritability Puzzle. *Front. Genet.* **2019**, *10*, 453. [CrossRef] [PubMed]
33. Abeysekera, R.A.; Healy, H.G.; Wang, Z.; Cameron, A.L.; Hoy, W.E. Heterogeneity in Patterns of Progression of Chronic Kidney Disease. *Intern. Med. J.* **2021**, *51*, 220–228. [CrossRef] [PubMed]
34. Mårtensson, J.; Bellomo, R. The Rise and Fall of NGAL in Acute Kidney Injury. *Blood Purif.* **2014**, *37*, 304–310. [CrossRef]
35. Sinuani, I.; Beberashvili, I.; Averbukh, Z.; Sandbank, J. Role of IL-10 in the Progression of Kidney Disease. *World J. Transplant.* **2013**, *3*, 91–98. [CrossRef]
36. Zhang, D.; Gu, T.; Forsberg, E.; Efendic, S.; Brismar, K.; Gu, H.F. Genetic and Functional Effects of Membrane Metalloendopeptidase on Diabetic Nephropathy Development. *Am. J. Nephrol.* **2011**, *34*, 483–490. [CrossRef]
37. Fritz, I.B.; Murphy, B. Clusterin Insights into a Multifunctional Protein. *Trends Endocrinol. Metab. TEM* **1993**, *4*, 41–45. [CrossRef]
38. Rogulska, K.; Wojciechowska-Koszko, I.; Dołęgowska, B.; Kwiatkowska, E.; Roszkowska, P.; Kapczuk, P.; Kosik-Bogacka, D. The Most Promising Biomarkers of Allogeneic Kidney Transplant Rejection. *J. Immunol. Res.* **2022**, *2022*, 6572338. [CrossRef]
39. Guo, J.; Guan, Q.; Liu, X.; Wang, H.; Gleave, M.E.; Nguan, C.Y.C.; Du, C. Relationship of Clusterin with Renal Inflammation and Fibrosis after the Recovery Phase of Ischemia-Reperfusion Injury. *BMC Nephrol.* **2016**, *17*, 133. [CrossRef]
40. Axelsson, J.; Bergsten, A.; Qureshi, A.R.; Heimbürger, O.; Bárány, P.; Lönnqvist, F.; Lindholm, B.; Nordfors, L.; Alvestrand, A.; Stenvinkel, P. Elevated Resistin Levels in Chronic Kidney Disease Are Associated with Decreased Glomerular Filtration Rate and Inflammation, but Not with Insulin Resistance. *Kidney Int.* **2006**, *69*, 596–604. [CrossRef]
41. Curran, C.S.; Kopp, J.B. RAGE Pathway Activation and Function in Chronic Kidney Disease and COVID-19. *Front. Med.* **2022**, *9*, 970423. [CrossRef] [PubMed]
42. Rayego-Mateos, S.; Rodrigues-Diez, R.; Morgado-Pascual, J.L.; Valentijn, F.; Valdivielso, J.M.; Goldschmeding, R.; Ruiz-Ortega, M. Role of Epidermal Growth Factor Receptor (EGFR) and Its Ligands in Kidney Inflammation and Damage. *Mediat. Inflamm.* **2018**, *2018*, 8739473. [CrossRef]
43. Sabolić, I.; Asif, A.R.; Budach, W.E.; Wanke, C.; Bahn, A.; Burckhardt, G. Gender Differences in Kidney Function. *Pflüg. Arch.-Eur. J. Physiol.* **2007**, *455*, 397–429. [CrossRef] [PubMed]
44. Cheng, Z.; Limbu, M.H.; Wang, Z.; Liu, J.; Liu, L.; Zhang, X.; Chen, P.; Liu, B. MMP-2 and 9 in Chronic Kidney Disease. *Int. J. Mol. Sci.* **2017**, *18*, 776. [CrossRef] [PubMed]
45. Schrijvers, B.F.; Flyvbjerg, A.; De Vriese, A.S. The Role of Vascular Endothelial Growth Factor (VEGF) in Renal Pathophysiology. *Kidney Int.* **2004**, *65*, 2003–2017. [CrossRef] [PubMed]
46. Shimada, K.; Baba, T.; Neugebauer, S.; Onozaki, A.; Yamada, D.; Midorikawa, S.; Sato, W.; Watanabe, T. Plasma Vascular Endothelial Growth Factor in Japanese Type 2 Diabetic Patients with and without Nephropathy. *J. Diabetes Complicat.* **2002**, *16*, 386–390. [CrossRef]
47. Köttgen, A.; Pattaro, C.; Böger, C.A.; Fuchsberger, C.; Olden, M.; Glazer, N.L.; Parsa, A.; Gao, X.; Yang, Q.; Smith, A.V.; et al. New Loci Associated with Kidney Function and Chronic Kidney Disease. *Nat. Genet.* **2010**, *42*, 376–384. [CrossRef]
48. Böger, C.A.; Gorski, M.; Li, M.; Hoffmann, M.M.; Huang, C.; Yang, Q.; Teumer, A.; Krane, V.; O'Seaghdha, C.M.; Kutalik, Z.; et al. Association of EGFR-Related Loci Identified by GWAS with Incident CKD and ESRD. *PLoS Genet.* **2011**, *7*, e1002292. [CrossRef]
49. Lousa, I.; Reis, F.; Beirão, I.; Alves, R.; Belo, L.; Santos-Silva, A. New Potential Biomarkers for Chronic Kidney Disease Management—A Review of the Literature. *Int. J. Mol. Sci.* **2020**, *22*, 43. [CrossRef]

50. Levey, A.S.; Perrone, R.D.; Madias, N.E. Serum Creatinine and Renal Function. *Annu. Rev. Med.* **1988**, *39*, 465–490. [CrossRef]
51. Coresh, J.; Selvin, E.; Stevens, L.A.; Manzi, J.; Kusek, J.W.; Eggers, P.; Van Lente, F.; Levey, A.S. Prevalence of Chronic Kidney Disease in the United States. *JAMA* **2007**, *298*, 2038–2047. [CrossRef] [PubMed]
52. Kodgirwar, P.S.; Jajoo, S.U.; Jajoo, U.N.; Taksande, B.A.; Gupta, S.S. Nonalbuminuric Chronic Kidney Disease: A Dominant Presentation in Noncommunicable Disease Population of Rural Central India. *J. Fam. Med. Prim. Care* **2018**, *7*, 442–446. [CrossRef]
53. Koye, D.N.; Magliano, D.J.; Reid, C.M.; Jepson, C.; Feldman, H.I.; Herman, W.H.; Shaw, J.E. Risk of Progression of Nonalbuminuric CKD to End-Stage Kidney Disease in People with Diabetes: The CRIC (Chronic Renal Insufficiency Cohort) Study. *Am. J. Kidney Dis.* **2018**, *72*, 653–661. [CrossRef] [PubMed]

Disclaimer/Publisher's Note: The statements, opinions and data contained in all publications are solely those of the individual author(s) and contributor(s) and not of MDPI and/or the editor(s). MDPI and/or the editor(s) disclaim responsibility for any injury to people or property resulting from any ideas, methods, instructions or products referred to in the content.

3.7 Untangling the Uncertain Role of Overactivation of the Renin–Angiotensin–Aldosterone System with the Aging Process Based on Sodium Wasting Human Models

Chantelle Thimm and James Adjaye

International Journal of Molecular Sciences 2024, Volume 25, 9332, Article ID 25179332

Abstract:

Every individual at some point encounters the progressive biological process of aging, which is considered one of the major risk factors for common diseases. The main drivers of aging are oxidative stress, senescence, and reactive oxygen species (ROS). The renin–angiotensin–aldosterone system (RAAS) includes several systematic processes for the regulation of blood pressure, which is caused by an imbalance of electrolytes. During activation of the RAAS, binding of angiotensin II (ANG II) to angiotensin II type 1 receptor (AGTR1) activates intracellular nicotinamide adenine dinucleotide phosphate (NADPH) oxidase to generate superoxide anions and promote uncoupling of endothelial nitric oxide (NO) synthase, which in turn decreases NO availability and increases ROS production. Promoting oxidative stress and DNA damage mediated by ANG II is tightly regulated. Individuals with sodium deficiency-associated diseases such as Gitelman syndrome (GS) and Bartter syndrome (BS) show downregulation of inflammation-related processes and have reduced oxidative stress and ROS. Additionally, the histone deacetylase sirtuin-1 (SIRT1) has a significant impact on the aging process, with reduced activity with age. However, GS/BS patients generally sustain higher levels of sirtuin-1 (SIRT1) activity than age-matched healthy individuals. SIRT1 expression in GS/BS patients tends to be higher than in healthy age-matched individuals; therefore, it can be assumed that there will be a trend towards healthy aging in these patients. In this review, we highlight the importance of the hallmarks of aging, inflammation, and the RAAS system in GS/BS patients and how this might impact healthy aging. We further propose future research directions for studying the etiology of GS/BS at the molecular level using patient-derived renal stem cells and induced pluripotent stem cells.

Author contribution of C.T. included 90%:

I was responsible for the conceptualization of the review, including the delineation of its thematic focus, the formulation of guiding research questions, and the development of the overarching structure.
I wrote the original draft, which I edited and revised with J.A.. Furthermore, I designed all figures, tables and schematic illustrations.

Status: Published in International Journal of Molecular Sciences

DOI: https:// doi.org/10.3390/ijms25179332

This article is an open access article distributed under the terms and conditions of the Creative Commons Attribution (CC BY) 4.0 license, which permits unrestricted use, distribution, and reproduction in any medium, provided the original work is properly cited.

International Journal of *Molecular Sciences*

MDPI

Review

Untangling the Uncertain Role of Overactivation of the Renin–Angiotensin–Aldosterone System with the Aging Process Based on Sodium Wasting Human Models

Chantelle Thimm [1] and James Adjaye [1,2,*]

[1] Institute for Stem Cell Research and Regenerative Medicine, Medical Faculty, Heinrich-Heine University Düsseldorf, 40225 Düsseldorf, Germany
[2] Zayed Centre for Research into Rare Diseases in Children (ZCR), EGA Institute for Women's Health, University College London (UCL), 20 Guilford Street, London WC1N 1DZ, UK
* Correspondence: james.adjaye@med.uni-duesseldorf.de or james.adjaye@ucl.ac.uk

Abstract: Every individual at some point encounters the progressive biological process of aging, which is considered one of the major risk factors for common diseases. The main drivers of aging are oxidative stress, senescence, and reactive oxygen species (ROS). The renin–angiotensin–aldosterone system (RAAS) includes several systematic processes for the regulation of blood pressure, which is caused by an imbalance of electrolytes. During activation of the RAAS, binding of angiotensin II (ANG II) to angiotensin II type 1 receptor (AGTR1) activates intracellular nicotinamide adenine dinucleotide phosphate (NADPH) oxidase to generate superoxide anions and promote uncoupling of endothelial nitric oxide (NO) synthase, which in turn decreases NO availability and increases ROS production. Promoting oxidative stress and DNA damage mediated by ANG II is tightly regulated. Individuals with sodium deficiency-associated diseases such as Gitelman syndrome (GS) and Bartter syndrome (BS) show downregulation of inflammation-related processes and have reduced oxidative stress and ROS. Additionally, the histone deacetylase sirtuin-1 (SIRT1) has a significant impact on the aging process, with reduced activity with age. However, GS/BS patients generally sustain higher levels of sirtuin-1 (SIRT1) activity than age-matched healthy individuals. SIRT1 expression in GS/BS patients tends to be higher than in healthy age-matched individuals; therefore, it can be assumed that there will be a trend towards healthy aging in these patients. In this review, we highlight the importance of the hallmarks of aging, inflammation, and the RAAS system in GS/BS patients and how this might impact healthy aging. We further propose future research directions for studying the etiology of GS/BS at the molecular level using patient-derived renal stem cells and induced pluripotent stem cells.

Keywords: sodium deficiency diseases; distal convoluted tubules; renin–angiotensin–aldosterone system; ageing; sodium accumulation

check for updates

Citation: Thimm, C.; Adjaye, J. Untangling the Uncertain Role of Overactivation of the Renin–Angiotensin–Aldosterone System with the Aging Process Based on Sodium Wasting Human Models. *Int. J. Mol. Sci.* **2024**, *25*, 9332. https://doi.org/10.3390/ijms25179332

Academic Editor: Jana Tchekalarova

Received: 14 July 2024
Revised: 20 August 2024
Accepted: 24 August 2024
Published: 28 August 2024

Copyright: © 2024 by the authors. Licensee MDPI, Basel, Switzerland. This article is an open access article distributed under the terms and conditions of the Creative Commons Attribution (CC BY) license (https://creativecommons.org/licenses/by/4.0/).

1. Introduction

The kidney is a paired organ associated with the urinary system and performs numerous tasks such as filtration of urine and regulation of homeostasis of electrolytes such as sodium, potassium, calcium, magnesium, and phosphate [1].

The processes involved in the regulation of sodium and water balance, including blood pressure and the glomerular filtration rate, have a decisive influence on sodium and water transport in the renal tubule. An imbalance is accompanied by undesirable consequences. Several diseases are associated with sodium deficiency; these include Gitelman syndrome (GS) and Bartter syndrome (BS) [2–6].

Gitelman syndrome is an autosomal recessive tubular disorder caused by biallelic mutations in a gene encoding the protein that is a sodium–chloride cotransporter. These are responsible for approximately 7–10% of the tubular absorption of electrolytes. GS is

characterized by an increased excretion of magnesium (hypermagnesiuria) and a reduced excretion of calcium (hypocalciuria) in the urine. In addition, GS patients have hypokalemic alkalosis, i.e., a disorder of the acid–base balance and salt loss. Other signs of illness include muscle weakness, fatigue, cramps, and low blood pressure caused by an electrolyte imbalance due to distinct mutations within the SLC12A3 encoding gene [7–9].

Each individual, at some point, encounters the progressive biological process of aging associated with oxidative stress, senescence, and reactive oxygen species (ROS). GS/BS patients show downregulation of inflammation-related processes and have reduced oxidative stress and ROS. In this context, GS and BS patients, in comparison to healthy individuals, sustain higher levels of sirtuin-1 (SIRT1) activity, which seems to have a significant impact on hypertension and the aging process [10–12].

We highlight the importance of the hallmarks of aging and the renin–angiotensin–aldosterone system (RAAS) in Gitelman syndrome patients and how this might impact healthy aging.

2. Gitelman Syndrome

The nephrologist Hillel Jonathan Gitelman first observed patients with various conditions associated with metabolic alkalosis, electrolyte imbalance, and salt wasting in the late 1960s [8]. Gitelman syndrome (GS) (OMIM 263800) is one of the most common renal tubulopathies and is known as familial hypokalemia–hypomagnesemia. It is an autosomal recessive inherited disorder caused by a disturbance in the function of the thiazide-sensitive sodium chloride cotransporter (NCC) in the kidney. In this process, blood levels show magnesium and potassium deficiency, while the urine has high levels of magnesium excretion and decreased excretion of calcium. GS is characterized by metabolic alkalosis, hypomagnesemia, and hypercalciuria. The etiology is a transport defect of the distal convoluted tubule (DCT). It is manifested in adolescence or adulthood and has an estimated prevalence of 1:40,000 Caucasian individuals [13]. It is more prevalent in the Asian population and is estimated at around 1.7 per 1000 people [13]. The actual frequency of GS is difficult to determine in the general population due to its inconspicuousness or misdiagnosis.

The disease is caused by biallelic inactivating mutations within the SLC12A3 encoding gene, which encodes the NCC. Its genomic locus is chromosome 16q13 and it consists of 26 exons that code for 1002 amino acids [9,14,15].

NCC is expressed by cells of the apical membrane lining the distal convoluted tubule [9]. Studies have identified more than 350 distinct mutations within the SLC12A3 encoding gene in GS patients [16–18]. In addition to this, mutations in the cation channel subfamily 6 of the protein Claudin 16 gene (TRPM6), which is involved in magnesium transport in distal tubules [19,20].

The largest proportion of mutations in SLC12A3 is 62.1% missense and nonsense mutations. A missense mutation is when the error in spelling a single base pair creates a different amino acid. If the mutation is meaningless (nonsense mutation), a so-called stop codon results, and the synthesis of the protein is terminated. Furthermore, the splice mutations are present at around 13.5% and small deletions at around 12%. Finally, there are the major deletions and small insertions at 5%. Other mutations account for 7.4% (Figure 1) [18].

The most common mutation is heterozygous, which has a prevalence of 1% in Europe [21]. Studies have shown that homozygous mutations have also been identified in a Spanish cohort [22].

An example of multiple mutations was found in patients in Taiwan. Here, triple mutations in GS patients are presented with a prevalence of approximately 12%, which is certainly due to the higher frequency of heterozygous carriers within the Asian population [23].

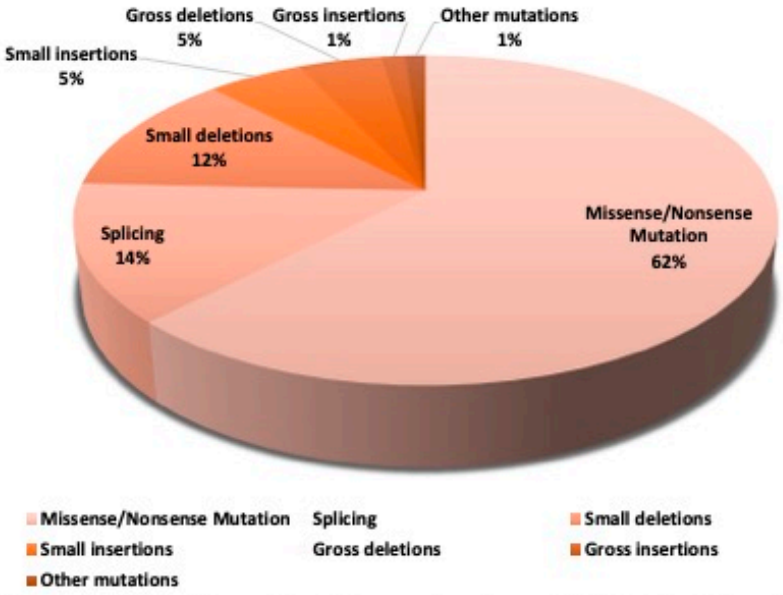


Figure 1. SLC12A3 mutation variants. Gitelman syndrome is caused by biallelic inactivating mutations in the SLC12A3 gene. It consists of 26 exons that code for 1002 amino acids. There are more than 350 different mutations that are caused by missense and nonsense variants, frameshift, splice, and deep intronic variants, as well as large genomic rearrangements. The pie chart represents all variants of mutations in the SLC12A3 gene. The largest population of mutations are missense and nonsense mutations, with a prevalence of approximately 62.1%. The splice mutations are present at approximately 14% and small deletions at around 12%. Major deletions and small insertions make up approximately 5%, whereas the remaining mutation types account for 7.4% [21].

The mutations lead to sodium efflux and activation of adaptive mechanisms such as the RAAS [24]. The NCC is the salt-reabsorptive transporter localized at the apical membrane in the DCT. It has been documented that RAAS is a primary physiological regulator of NCC [25]. The inactivation of NCC leads to the activation of RAAS, which results in reduced tubular reabsorption of sodium and chloride. This deficiency leads to dehydration, which triggers RAAS as a compensatory mechanism. Additionally, low levels of potassium in blood serum have been described, as well as an increase in the levels of renin and aldosterone.

Studies based on GS rodent models revealed that Ca^{2+} deficiency has significant consequences on DCT function as compromised NCC function leads to structural remodeling of DCTs [26]. The disease can be asymptomatic or associated with mild symptoms, such as weakness, fatigue, craving for salt, thirst, or nocturia. GS patients often have transient episodes of muscle weakness and tetany, sometimes combined with abdominal pain, vomiting, and fever [27,28]. The presence of hypocalciuria and hypomagnesemia has high predictive value for the clinical diagnosis of GS [29,30].

If GS is suspected, there are not only clinical complaints but also biochemical criteria, which include chronic hypokalemia (<3.5 mmol/L) and renal potassium loss, determined as a spot urine sample with a potassium/creatinine ratio >2.0 mmol/mol (>18 mmol/g) [31].

Hypocalciuria is determined as a spontaneous urine calcium/creatinine ratio <0.2 mmol/mmol (0.07 mg/mg). GS patients have low urinary calcium excretion [25,32], high fractional magnesium excretion, and hypomagnesemia [8,25].

Metabolic alkalosis, hypomagnesemia <0.7 mmol/L (<1.70 mg/dL) [33], and renal magnesium loss (fractional magnesium excretion >4%) occur in Gitelman syndrome [34]. Gitelman syndrome occurs in both males and females alike.

In adults, additional criteria include fractional chloride excretion >0.5%, normal or low blood pressure, and the absence of morphologic and functional renal abnormalities [11,31] including increased renin activity and aldosterone expression [35].

GS is caused by a variety of mutations within the genes encoding SLC12A3 (thiazide-sensitive sodium chloride cotransporter (NCC): HNF1B (hepatocyte nuclear factor 1β), FXYD2 (sodium/potassium-transporting ATPase gamma chain—a member of the FXYD family of transmembrane proteins), KCNJ10 (ATP-sensitive inward rectifier potassium channel 10, a member of the inward rectifier-type potassium channel family) [16,36–39]. EAST or SeSAME syndrome closely resembles Gitelman syndrome. This is an autosomal recessive disorder caused by mutations within the KCNJ10 gene. EAST is an acronym for epilepsy, ataxia, sensorineural deafness, and (a renal salt-wasting) tubulopathy, and SeSAME stands for seizures, sensorineural deafness, ataxia, mental retardation, and electrolyte imbalance [37,38,40].

Mitochondria are essential components of eukaryotic cells. Mitochondrial DNA (mtDNA) mutations can occur during mitosis, which then results in changes in the degree of heteroplasmy. If the proportion of mtDNA exceeds the threshold value of 60–80% [41], this results in a considerable drop in energy production, leading to the development of metabolic disorders. Pathogenic mtDNA variants of genes encoding the transfer RNAs for phenylalanine (MT-TF) and isoleucine (MT-TI) cause a Gitelman-like syndrome [42].

There is currently no specific therapy, but potassium and magnesium supplementation and a high-salt diet are recommended for all GS patients. To counteract disturbed hormone levels and fluid and electrolyte balance, spironolactone or triamterene are prescribed to GS patients to reduce potassium and magnesium losses [43]. In GS patients, a high dose of potassium chloride is used to combat hypokalemia. Salts with poor absorbable anions such as aspartan should not be administered to patients, as these do not lead to any improvement and may even exacerbate alkalosis.

Children, or even infants, are prescribed a nonsteroidal anti-inflammatory drug (NSAID) known as indomethacin, which is used to treat growth deficits in severe, early-onset forms of the disease [44,45].

3. Bartter Syndrome

In 1962, Bartter et al. identified a new syndrome and named it Bartter syndrome (BS) [46]. BS is one of the rare hereditary renal tubular disorders caused by impaired salt reabsorption in the thick ascending limb (TAL) of the loop of Henle. It is associated with several electrolyte abnormalities including low potassium and chloride, salt wasting, hypokalemia, and metabolic alkalosis with hyperaldosteronism with normal blood pressure and hyperplasia of the juxtaglomerular apparatus (JGA) [46,47].

In contrast to GS, Bartter syndrome is a more severe congenital kidney injury that often manifests itself earlier, usually within the first year of life [48]. BS is a polygenic disease caused by homozygous or mixed heterozygous mutations in one of the following genes: SLC12A1, KCNJ1, CLCNKB, BSND, or CASR (Figure 2).

Depending on the mutated gene and, thus, the affected transporter protein, BS can be divided into at least five subtypes, which are expressed in the tubular epithelial cells of the TAL of the Henle loop. Type I BS is characterized by loss-of-function mutations within the SLC12A1 gene and is known as neonatal Bartter syndrome (hyperprostaglandin E syndrome). This codes for the apical sodium–potassium–chloride cotransporter NKCC2. Type II of BS, also known as neonatal Bartter syndrome, is caused by loss-of-function mutations in the KCNJ1 gene, which codes for the apical inwardly rectifying potassium channel ROMK. BS type III, also known as classic Bartter syndrome, is caused by mutations in the CLCNKB gene, which codes for the basolateral chloride channel ClC-Kb. Distinct variants of chloride channels are present in most organs but CLCNKB, affected here, is

found exclusively in the kidney, so the clinical manifestation of a mutation in this channel is only seen in the kidney [49].

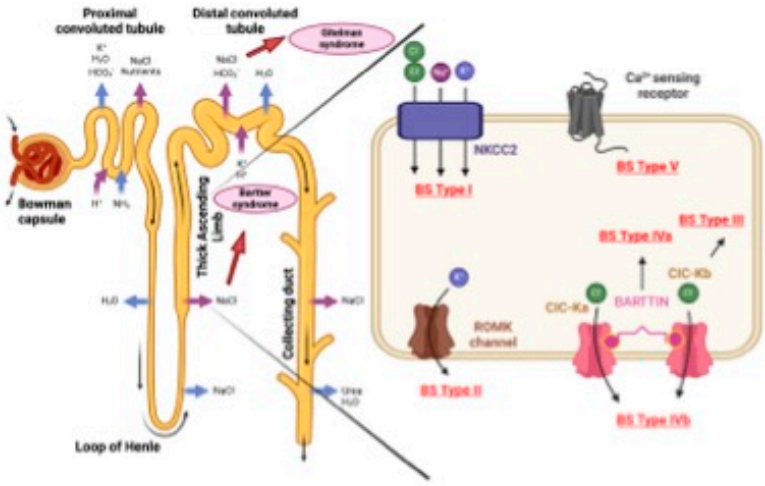


Figure 2. Mutations associated with Bartter syndrome. This is caused by homozygous or mixed heterozygous mutations in one of the following genes: SLC12A1, KCNJ1, CLCNKB, BSND, or CASR. Depending on the mutated gene, BS can be divided into five subtypes: BS type I—SLC12A1 codes for the sodium–potassium–chloride cotransporter NKCC2; BS type II—KCNJ1 codes for the potassium channel ROMK; BS type III—CLCNKB codes for chloride channel ClC-Kb; BS type IVa—BSND codes for barttin, which is a subunit of the chloride channels ClC-Ka and ClC-Kb; BS type IVb—simultaneous mutations in CIC-Ka and CIC-Kb; BS type V—CASR, which encodes the basolateral calcium receptor CASR. The Figure was created with BioRender.com.

Classical Bartter syndrome with sensorineural hearing loss (hyperprostaglandin E syndrome), or BS type IVa, is caused by loss-of-function mutations in the BSND gene, which encodes barttin, a β-subunit for ClC-Ka and ClC-Kb. Parallel to BS type IVa, simultaneous mutations in CIC-Ka and CIC-Kb are present in type IVb. Bartter syndrome type V with hypocalcemia is also known as autosomal dominant hypoparathyroidism. This is characterized by gain-of-function mutations in the Ca^{2+}-sensing receptor CASR, which codes for the basolateral calcium receptor CAS.

Bartter syndrome is an inherited disorder of the renal tubules caused by impaired salt reabsorption. It leads to several electrolyte abnormalities including low potassium and chloride, salt wasting, hypokalemia, and metabolic alkalosis [6,50].

Previously, GS and BS patients were classified based on age, the presence of hypercalciuria, polyhydramnios, or growth retardation, and severity. Based on differences in the metabolism of divalent cations, BS and GS can be distinguished by laboratory measurements, which include urinary Ca^{2+} excretion, Ca^{2+}/creatinine, and serum Mg^{2+}. BS patients tend to have a less severe manifestation compared to GS patients. BS patients have increased urinary calcium excretion and fractional excretion rates, whereas serum magnesium levels are within the normal range [49]. To differentiate between BS and GS, a thiazide test was proposed using a cohort of genetically proven GS and BS patients given oral administration of hydrochlorothiazide (1 mg/kg to 50 mg) [51]. In patients with GS, fractional chloride excretion showed very little change (<2.3%) as the defect was in the thiazide-sensitive Na/Cl cotransporter (NCCT). In contrast, patients with BS showed an increased response to HCO_3 administration, which led to a more pronounced excretion. Despite the successful differentiation between GS and BS, the test is not routinely recommended due to the increased risk of volume depletion [51].

Due to the rare nature of the syndrome, there is only limited clinical information on treatment. Therapeutically, BS patients urgently need sufficient fluid and electrolyte replacement. For newborns, it is important to control the risk of pre-renal failure due to imbalances in fluid homeostasis. The classic pharmacological therapy for BS patients includes the administration of potassium chloride, prostaglandin inhibitors (indomethacin), and aldosterone antagonists (spironolactone) [52,53].

The symptoms of BS patients are initially treated with the help of potassium supplementation. Also, potassium-sparing diuretics such as spironolactone, eplerenone, or amiloride are often prescribed. According to the literature, these diuretics lead to reduced aldosterone levels, which subsequently increases serum potassium and, hence, counteracts metabolic alkalosis. In cases of persistent hypokalemia and or other side effects of medications, potassium-sparing diuretics, renin–angiotensin system blockers, or NSAIDs are also prescribed. Combinations of these medications are also recommended in certain cases [44,47,54]. Angiotensin-converting enzyme inhibitors (ACE inhibitors) are used to correct low K^+ levels or to counteract proteinuria [54,55].

Table 1 provides an overview of the distinct gene variants, clinical symptoms, and treatment options for GS/BS patients.

Table 1. Comparisons between Gitelman and Bartter syndromes.

Gitelman Syndrom				Bartter Syndrom			
Variant	**Gene Mutation/ OMIM**	**Gene Product**	**Clinical Symptoms**	**Variant**	**Gene Mutation/ OMIM**	**Gene Product**	**Clinical Symptoms**
Gitelman syndrome (GS)	*SLC12A3*/ 263800	NCC	• present in later childhood or adulthood with • weakness • hypokalemic alkalosis • hypomagnesemia • hypermagnesemia • hypocalciuria	**Type I (neonatal Bartter syndrome/ hyperprostaglandin E syndrome)**	*SLC12A1*/ 601678	NKCC2	• polyhydramnios • prematurity • hypokalemic • hypochloremic alkalosis • nephrocalcinosis with or without concentrating defect
GS-like syndrome mtDNA	*MT-TF* /590070) *MT-TI*/ 590045	Mitochon-drially encoded TRNA Phen-ylalanine and isoleucine	• dysfunction of oxidative phosphorylation complex IV • reduced maximal mitochondrial respiratory capacity • hypokalemia • hypomagnesemia • arterial hypertension • hypercholesterole-mia	**Type II** (neonatal Bartter syndrome)	*KCNJ1*/ 241200	ROMK1	• polyhydramnios • prematurity • transient hyperkalemia and acidosis • hypokalemic hypochloremic alkalosis • nephrocalcinosis, with or without concentrating defect
EAST syndrome (SeSAME)	*Kir4.1*/ 612780	KCNJ10	• epilepsy • ataxia, • sensorineural deafness • hypokalemic • hypochloremic alkalosis • muscle cramps • paresthesias • nocturia • salt craving • muscle weakness • fatigue	**Type III** (classic Bartter syndrome)	*CLCNKB*/ 607364	CIC-Kb	Variable age at presentation with severity corresponding to type of gene mutation; • hypokalemic • hypochloremic alkalosis

Table 1. *Cont.*

Gitelman Syndrom				Bartter Syndrom			
Variant	**Gene Mutation/ OMIM**	**Gene Product**	**Clinical Symptoms**	**Variant**	**Gene Mutation/ OMIM**	**Gene Product**	**Clinical Symptoms**
Other pathogenic variants		*FXYD2* and *HNF1B*	• sensorineural deafness • epilepsy • ataxia • intellectual disability • diabetes • renal cysts • muscle cramps • paresthesias nocturia • salt craving • muscle weakness • fatigue	**Type IVa (Classical Bartter syndrom with sensorineural hearing loss)**	*BSND*/ 602522	BARTTIN	• polyhydramnios • prematurity • hypokalemic • hypochloremic alkalosis • sensorineural deafness, with or without concentrating defect
				Type IVb	*CLCNKA, CLCNKB*/ 613090	CIC-Ka and CIC-Kb	Polyhydramnios, prematurity, hypokalemic hypochloremic alkalosis, sensorineural deafness, with or without concentrating defect
				Type V (autosomal dominant hypoparathyroidism)	*L125P*/ 601199	CASR	Hypocalcemic hypocalciuria, hypokalemic hypochloremic alkalosis, suppressed PTH
Therapy	Supplementation of: • potassium • potassium chloride • magnesium			Supplementation of: • potassium chloride • sodium • magnesium			
	High-salt diet						
	Potassium-sparing diuretics: • spironolactone • triamterene			Potassium-sparing diuretics: • spironolactone • amiloride			
	Nonsteroidal anti-inflammatory drug (NAID): • Indometacin			Nonsteroidal anti-inflammatory drug (NAID): • Ibuprofen			
	Renin-angiotensin system blocker: • spironolacton • eplerenon			Renin-angiotensin system blocker: • eplerenone			

Gitelman syndrome (GS) and Bartter syndrome (BS) have distinct genetic mutations. BS is divided into five subtypes depending on the affected gene (I, II, III, IVa, IVb, V). NKCC2: furosemide-sensitive sodium–potassium–2-chloride cotransporter; ROMK: renal outer medullary potassium channel; CLC-Kb: chloride channel Kb; CLC-Ka: chloride channel Ka; CaSR: calcium-sensing receptor; Gitelman syndrome is caused by biallelic inactivating mutations in the SLC12A3 gene. NCC: thiazide-sensitive sodium chloride cotransporter. MT-TF: mitochondria-encoded tRNA-Phe (UUU/C)); KCNJ10: Potassium Inwardly Rectifying Channel Subfamily J Member 10; FXYD2: FXYD Domain Containing Ion Transport Regulator 2; HNF1B: hepatocyte nuclear factor 1-beta. Modified version from Fulchiero et al. [56].

4. Aging and RAAS

Aging is a biological process that affects all organizational levels of an organism. The aging process is considered one of the major risk factors for the most prevalent diseases worldwide [57]. The hallmarks of aging contribute to processes leading to the aging phenotype, which include epigenetic alterations, chronic inflammation, dysbiosis, deregulated nutrient sensing, mitochondrial dysfunction, genomic instability, telomere attrition, loss of proteostasis, deregulated macro-autophagy, stem cell exhaustion, altered intercellular communication, and cellular senescence [58–60]. Cellular aging is the result of the accumulation of damaged macromolecules, which are chemically altered by ROS. ROS impairs the integrity and function of mitochondria, resulting in, for example, reduced ATP generation [61].

The RAAS includes several systematic processes for the regulation of blood pressure. This is a consequence of increasing peripheral resistance or vascular tone and cardiac contractility, as well as enhanced water and sodium reabsorption, increased aldosterone secretion, and facilitated catecholamine release from sympathetic nerve terminals [1]. Regulation of hypertension and extracellular volume is regulated by angiotensin II (ANG II)

as the biological effector of RAAS [62–64]. ANG II preferentially binds two subtypes of angiotensin II receptors: AT1 (AGTR1) and AT2 (AGTR2). AGTRs are expressed in various segments of the nephron in the distal tubule, collecting duct, and renal vasculature [65–70]. The known physiological and pathological effects are induced via the AT1 receptor. In humans, AGTR1 receptors are expressed in a wide variety of organs. They are present in glomerular mesangial cells, proximal and distal tubular epithelial cells, medullary interstitial cells, and renal vasculature [71–73]. The binding of ANG II to AGTR1 activates four classical signaling cascades, including phospholipase A2, phospholipase C, phospholipase D, and L-type calcium channels, and normally blocks the adenylate cycle.

ANG II binding to renal AGTR1 initiates vasoconstriction, sodium reabsorption, protein synthesis, and cellular growth [73,74].

In comparison, the activation of AGTR2 mediates K^+ channel activity via the protein-coupled receptors and activates protein tyrosine phosphatase (PTP), which leads to a reduction in the activities of mitogen-activated protein kinase (MAPK) and extracellular signal-regulated kinases ERK1 signaling pathways [75,76]. The activation of AGTR2 leads to increased bradykinin production, which induces vasodilation via the nitric oxide (NO)/cyclic guanosine monophosphate (GMP) pathway [73]. ANG II binding to AGTR2 initiates vasodilation, differentiation, apoptosis, anti-proliferation, and sodium transport imbalance of membrane ionic effects [77].

Both types of receptors are involved in the regulation of renal hemodynamics, tubular function, renal cellular growth, and matrix formation [73].

During activation of RAAS, binding of ANG II to AGTR1 leads intracellular nicotinamide adenine dinucleotide phosphate (NADPH) oxidase to generate superoxide anions and promotes uncoupling of endothelial NO synthase, which in turn decreases NO availability, and increases ROS production. The promotion of oxidative stress and DNA damage mediated by ANG II is tightly regulated. However, if uncontrolled, ANG II-mediated ROS production occurs; this leads to cellular senescence-associated mitochondrial dysfunction, hypertrophy, inflammation, and fibrosis in the kidneys, heart, and brain [78,79]. ANG II-mediated signaling via AGTR1 additionally leads to shortening of telomeres and ultimately glomerular mesangial cell senescence but this can be counteracted by losartan [80].

The mammalian ortholog of the silent information regulator (Sir2) of yeast, SIRT1, is a nicotinamide adenine dinucleotide (NAD)+-dependent class III histone deacetylase involved in many aging-associated processes such as apoptosis, cell differentiation, development, stress response, metabolism, and tumorigenesis [41,81,82]. SIRT1 expression is reduced in senescent mesenchymal stem cells, whereas its over-expression slows the onset of senescence and loss of differentiation capacity [83]. SIRT1 is associated with longevity, and in a hypertensive patient, low SIRT1 levels lead to an acceleration of the aging process [84,85]. The same is true for endothelial progenitor cells induced by ANG II, which presumably have reduced SIRT1 expression [86,87]. To counteract this, studies have been conducted investigating the role of polyphenol resveratrol in relation to hypertension [88,89]. Resveratrol (3,5,4′-trihydroxystilbene) is a polyphenol found in red wine that has several beneficial effects on cardiovascular disease [90,91]. In mammalian cells, resveratrol can promote various cellular functions and signaling pathways including longevity, cell cycle regulation, apoptosis, DNA damage repair, and muscle differentiation through the activation of SIRT1 [92,93]. In a study carried out by Miyazaki et al., resveratrol intake was shown to reduce AGTR1 expression in vascular smooth muscle cells [88]. Furthermore, resveratrol has been shown to downregulate AGTR1 expression via SIRT1 and has beneficial effects on hypertension [88]. Currently, several approaches can be employed to counteract premature aging such as caloric restriction, strength training, or nutrition [94–98]. In DNA repair mutant mice, caloric restriction reduced ROS and other reactive compounds, resulting in lower levels of DNA damage [99].

According to a study by the Robert Koch Institute, around every third person in Germany and, therefore, around 20–30 million German citizens are afflicted with high blood pressure [100]. Worldwide, about a fourth of the world's population is affected. The preva-

lence of high blood pressure increases with age, with almost two-thirds of people aged 65 and over having a diagnosis of high blood pressure [100]. Globally, hypertension is responsible for ten million deaths each year and is a critical risk factor for cardiovascular disease.

Multiple key mechanisms including inflammation, oxidative stress, as well as endothelial dysfunction lead to accelerated aging and hypertension. They can occur either independently or together [101–103]. Hypertension is an age-associated disease, as illustrated in Figure 3.

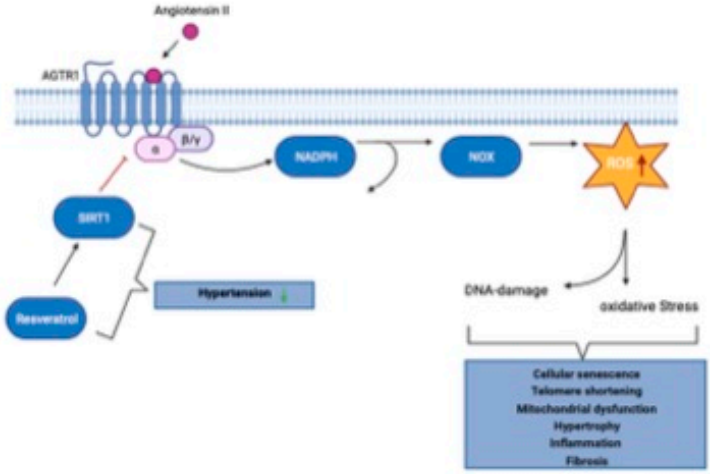


Figure 3. The role of the RAAS in the aging process. Cellular aging and stimulation of RAAS are closely intertwined. Sustained stimulation of angiotensin II (ANG II) receptor type 1 (AGTR1) causes intracellular NADPH oxidase to generate superoxide anions and promote uncoupling of endothelial NO synthase, which in turn decreases NO availability and increases reactive oxygen species (ROS) production. Uncontrolled ANG II-induced ROS production ultimately results in cellular senescence, mitochondrial dysfunction, hypertrophy, inflammation, and fibrosis in the kidney. Sirtuin-1 (SIRT1), involved in many age-associated processes, can counteract the uncontrolled ANG II-induced effects, by regulating the expression of AGTR1. Resveratrol is a natural compound capable of promoting SIRT1 activity and has been shown to have beneficial effects on hypertension. Adapted from "Activation of Protein Kinase C (PKC)", by BioRender.com (2023). The Figure was generated from https://app.biorender.com/biorender-templates accessed on 7 December 2023.

The Hallmarks of Aging in the Etiology of Sodium Deficiency-Associated Diseases

The aging process is one of the main causes of cancer, metabolic disorders, and heart and kidney diseases. Aged tissue is accompanied by a progressive loss of physiological integrity, which leads to dysfunction, and is prone to death. The accumulation of reactive oxygen and nitrogen species (RONS)-induced cellular and organ damage is often associated with aging. RONS are generated by various endogenous and exogenous processes, which are normally neutralized by antioxidant defenses, e.g., lipoic and uric acid and coenzyme Q. When an imbalance occurs between the attack and defense systems, oxidative stress ensues. Oxidative stress is part and parcel associated with various age-related diseases. The formation of RONS can be attributed to endogenous as well as exogenous sources.

Exogenous sources of RONS include tobacco, alcohol, heavy metals, air and water pollution, radiation, etc., which are subsequently converted into free radicals [104]. Endogenous sources include, for example, myeloperoxidase, NADPH oxidase, and ANG II [105]. NADPH is an enzyme complex consisting of several subunits that uses nicotinamide adenine dinucleotide phosphate to produce superoxide anions ($O_2^{\bullet -}$) [106]. Here, most of the di-oxygen is dismutated into hydrogen peroxide [104]. This can form the highly

reactive ROS hydroxyl ion (OH^-) by a Fenton or Haber–Weiss reaction. In addition, nitric oxide, which is formed from L-arginine by nitric oxide synthase (NOS), is also one of the endogenous sources. This can be divided into three main isoforms: epithelial NOS, neuronal NOS, and inducible NOS. Epithelial NOS is associated with vasodilation and vascular regulation and has a fundamental link with RAAS as well as with tubular disorder diseases such as Gitelman syndrome and Bartter syndrome (Figure 4) [107].

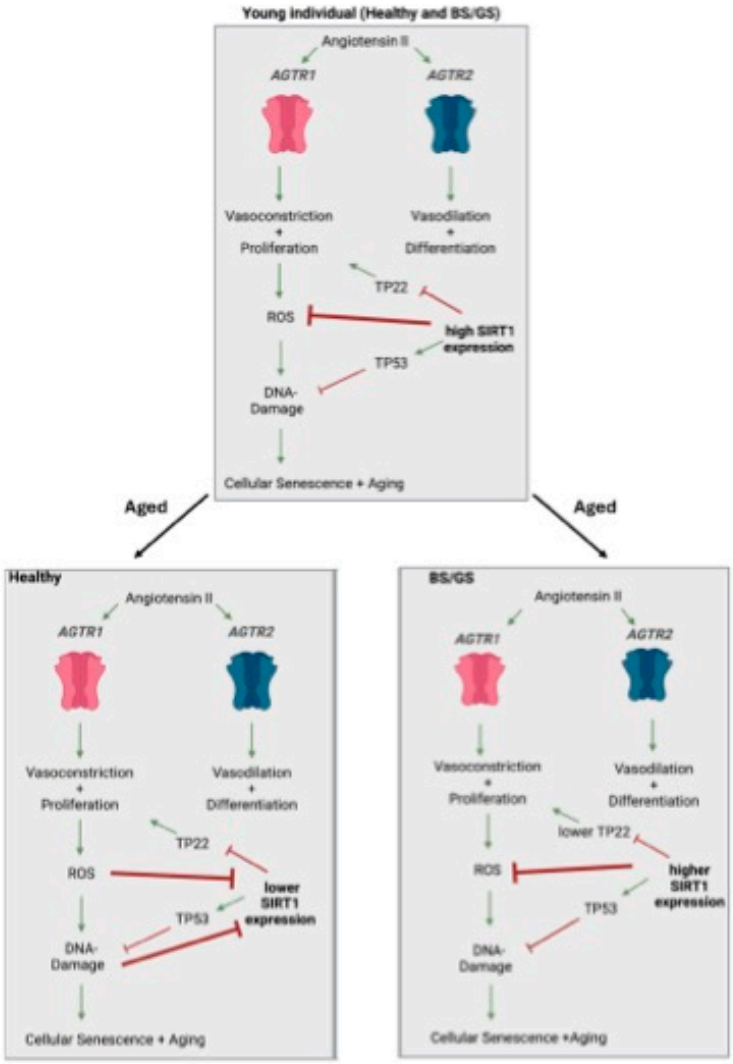


Figure 4. A proposed mechanism of how ROS, SIRT1, and RAAS impinge in Gitelman and Bartter syndromes. Regulation of the renin-angiotensin-aldosterone system (RAAS) is regulated by the octapeptide Angiotensin II (ANGII). In a young individual independent in healthy or in Bartter syndrome (BS)/Gitelman syndrome (GS) patients ANGII binds to either of the two subtypes of

Angiotensin II receptors, AT1 (AGTR1) initiates vasoconstriction and proliferation, and AT2 (AGTR2) initiates vasodilation and differentiation. In a healthy but aged individual, such a stimulatory response of AGTR1 leads to increased arteriolar vasoconstriction, proliferation, and reactive oxygen species (ROS) activation which then induces DNA damage, cellular senescence, and acceleration of the aging process. This process can be reversed/minimized by high levels of sirtuin-1 (SIRT1). It is assumed that GS and BS patients have comparable levels of SIRT1 as seen in young individuals. The figure was created with BioRender.com.

The cortical segments of the nephron have a high density of mitochondria [108,109]. Mitochondria not only play an essential role in the metabolism of the kidney but also signal transmission, and they facilitate stress reactions of kidney cells. Mitochondrial defects such as mutations in nuclear or mtDNA are common causes of mitochondrial dysfunction leading ultimately to the development of multiple kidney diseases [110–112]. In detail, permanent mitochondrial dysfunction can lead to inflammation, oxidative stress, loss in cellular functions and structure of renal cells, as well as reduced adenosine triphosphate (ATP) production [108,113,114]. These consequences are also linked to the aging process.

Mutations within mtDNA can result in Gitelman and Bartter syndromes [42,115,116]. Active mitochondria increase ROS levels, thus activating the RAAS. This is associated with increased NCC activity and, thus, with the regulation of DCT-specific NaCl reabsorption [117].

In a healthy person, kidney function often declines, leading to an accumulation of metabolic waste products and excessive electrolytes. Low potassium concentration associated with excessive salt concentration appears to be a highly prevalent cause of hypertension. High sodium intake induces intra-renal and vascular RAAS activation, which ultimately produces pro-inflammatory and pro-fibrotic conclusions [118–120].

GS and BS patients have salt wasting and are protected from the well-documented increase in sodium reabsorption and retention promoted by ANG II.

GS patients have reduced serum phosphate [121], Ca^{2+} reduction [122], and PKC activation, in contrast to a healthy individual [122–124]. PKC is a negative regulator of endothelial nitric oxide synthase (eNOS) and has a positive effect on vasodilation in GS and BS patients, as evidenced by increased urinary eNOS expression. Thus, it can be concluded that increased eNOS and NO-mediated vasodilation in GS/BS patients is crucial for the response of endothelial cells to increased flow in the brachial artery [11,125,126].

ANG II induces a reduction in the number of endothelial progenitor cells (EPCs), which are crucial for regulating heart diseases such as hypertension [126]. ANG II binding to AGTR1 leads to induced senescence of EPCs in mice and the development of oxidative stress [12].

In GS/BS patients, senescence, as well as the production of oxidative stress, remains under control at non-deleterious levels. It appears that in GS/BS patients, there is drastically reduced hypertension, cardiac remodeling, and the reduction in oxidative stress and its associated proteins despite constitutive RAAS stimulation secondary to salt wasting [12,125]. Mammalian aging is characterized by somatic mutations and other forms of DNA damage such as chromosomal abnormalities [127]. When these changes occur, the cell cycle is arrested in the G1 phase, which is triggered by TP53, TP22, as well as TP16 [81,128].

Four distinct processes can be initiated depending on the cell type, transient cell cycle arrest associated with DNA repair, apoptosis, senescence, or cell differentiation [129]. A connection between TP53 and Gitelman syndrome is currently not established. According to the literature, p22/PRG1 is a novel target gene of p53 target [130]. Caló et al. reported that GS/BS patients have less oxidative stress and low levels of p22 expression [131]. In relation to p53, this may imply that GS/BS patients have lower p53 activity and, consequently, the activation of p22 is lower [86,127,129].

SIRT1 expression in GS/BS patients tends to be higher than in healthy age-matched individuals; therefore, it can be assumed that there will be a trend towards healthy aging (Figure 4) [10].

Regulation of the renin–angiotensin–aldosterone system (RAAS) is regulated by the octapeptide ANG II. In a healthy young individual or in BS/GS syndrome patients, ANG

II binds to either of the two subtypes of angiotensin II receptors, AGTR1 initiates vasoconstriction and proliferation, and AGTR2 initiates vasodilation and differentiation. In a healthy but aged individual, such a stimulatory response of AGTR1 leads to increased arteriolar vasoconstriction, proliferation, and ROS activation, which then induces DNA damage, cellular senescence, and acceleration of the aging process. This process can be reversed/minimized by high levels of SIRT1. It is assumed that GS and BS patients have comparable levels of SIRT1 to those seen in young individuals. The figure was created with BioRender.com.

5. Conclusions

Salt intake is a determinant of high blood pressure and as such has an important role in the sensitivity of hypertensive responses. Salt-sensitive individuals show strong hypertension responses compared to BS/GS patients [132,133].

Several diseases are associated with magnesium deficiency, such as Gitelman and Bartter syndromes. The binding of angiotensin II to AGTR1 leads to ROS production and subsequently to cellular senescence associated with mitochondrial dysfunction, hypertrophy, inflammation, and renal fibrosis [78,79,134]. However, none of these hypertensive consequences have been observed to date in GS/BS patients despite their high-salt medication [135,136]. GS and BS patients show downregulation of inflammation-related processes and have reduced oxidative stress and ROS production. Explanations for this may include the reduced release of messenger substances by AGTR1 [137], reduced Ca^{2+} release and PKC activation [137], or higher SIRT1 expression [10]. SIRT1 expression in GS/BS patients tends to be higher than in healthy age-matched individuals; therefore, it can be assumed that there will be a trend towards healthy aging. As these reports are sparse, more studies are needed to confirm these observations.

Another link can be made to immune deficiency in patients with salt-wasting tubulopathies, including GS [138]. Here, the effects of salt wasting may provide a further link between GS/BS and protection against some effects of aging by analysis of the signaling pathways and excreted proteins. The addition of salt as a therapeutic intervention, which is already used as therapy today, could play a crucial role in this process.

These findings should not only apply to GS/BS but could also provide general links to salt-wasting tubulopathies.

6. The Future Direction of Research

We previously demonstrated that urine can serve as a non-invasive source of bipotential SIX2-positive renal progenitor cells [139], which can be differentiated into renal tubular cells and podocytes [62,63,139]. These cells can be employed for studying kidney-associated aging processes [81] and ANG II-mediated RAAS activation [62,63], and can be reprogrammed into induced pluripotent stem cells to enable studying the effects of a mutation on other cell types [140].

We are currently isolating SIX2-positive urine-derived progenitor cells from GS and BS patients with the aim of differentiating these into either tubular cells or podocytes, which will be ideal for studying the effect of angiotensin II and the RAAS pathway in these patients.

More recently, iPSCs have been generated from GS patients harboring the common Asian mutations [141,142]. GS and BS patient-derived iPSC will enable far-reaching investigations using revolutionized gene editing methods such as Clustered Regularly Interspaced Short Palindromic Repeats (CRISPR) to correct the mutation(s) in the GS/BS patient-derived iPSC lines to provide isogenic disease and healthy lines, which can be differentiated either to tubular cells or podocytes to study disease mechanisms and also toxicology and drug screening. There are GS and BS knockout mice, which can be used to investigate the link between hypertension, oxidative stress, and aging. With these human cellular and mouse models, the path is now paved for increased efforts in uncovering the underlying etiology leading to Gitelman and Bartter syndromes. These cellular models will enable drug

screening/development and toxicology studies, thus leading to better and more targeted treatment options in the near future.

Author Contributions: Conceptualization, C.T. and J.A. Original draft preparation, C.T. Editing, C.T. and J.A. Figures, C.T. All authors have read and agreed to the published version of the manuscript.

Funding: This research was funded by the medical faculty at Heinrich-Heine University, Duesseldorf.

Institutional Review Board Statement: Not applicable.

Acknowledgments: James Adjaye acknowledges funding from the medical faculty of Heinrich Heine University, Duesseldorf, Germany.

Conflicts of Interest: The authors declare no conflicts of interest.

References

1. Fountain, J.H.; Kaur, J.; Lappin, S.L. *Physiology, Renin Angiotensin System*; StatPearls Publishing LLC.: St. Petersburg, FL, USA, 2023.
2. Walsh, S.B.; Unwin, R.J. Renal tubular disorders. *Clin. Med.* **2012**, *12*, 476–479. [CrossRef]
3. Kopp, J.B.; Anders, H.-J.; Susztak, K.; Podestà, M.A.; Remuzzi, G.; Hildebrandt, F.; Romagnani, P. Podocytopathies. *Nat. Rev. Dis. Primers* **2020**, *6*, 68. [CrossRef] [PubMed]
4. Remuzzi, G.; Benigni, A.; Remuzzi, A. Mechanisms of progression and regression of renal lesions of chronic nephropathies and diabetes. *J. Clin. Investig.* **2006**, *116*, 288–296. [CrossRef]
5. Delles, C.; Currie, G. Proteinuria and its relation to cardiovascular disease. *Int. J. Nephrol. Renov. Dis.* **2013**, *7*, 13–24. [CrossRef] [PubMed]
6. da Silva Cunha, T.; Pfefermann Heilberg, I. Bartter syndrome: Causes, diagnosis, and treatment. *Int. J. Nephrol. Renov. Dis.* **2018**, *11*, 291–301. [CrossRef] [PubMed]
7. Cruz, D.N.; Shaer, A.J.; Bia, M.J.; Lifton, R.P.; Simon, D.B. Gitelman's syndrome revisited: An evaluation of symptoms and health-related quality of life. *Kidney Int.* **2001**, *59*, 710–717. [CrossRef]
8. Gitelman, H.J.; Graham, J.B.; Welt, L.G. A new familial disorder characterized by hypokalemia and hypomagnesemia. *.Trans. Assoc. Am. Physicians* **1966**, *79*, 221–235.
9. Simon, D.B.; Nelson-Williams, C.; Bia, M.J.; Ellison, D.; Karet, F.E.; Molina, A.M.; Vaara, I.; Iwata, F.; Cushner, H.M.; Koolen, M.; et al. Gitelman's variant of Bartter's syndrome, inherited hypokalaemic alkalosis, is caused by mutations in the thiazide-sensitive Na-Cl cotransporter. *Nat. Genet.* **1996**, *12*, 24–30. [CrossRef]
10. Davis, P.A.; Pagnin, E.; Dal Maso, L.; Caielli, P.; Maiolino, G.; Fusaro, M.; Rossi, G.P.; Calò, L.A. SIRT1, heme oxygenase-1 and NO-mediated vasodilation in a human model of endogenous angiotensin II type 1 receptor antagonism: Implications for hypertension. *Hypertens. Res.* **2013**, *36*, 873–878. [CrossRef]
11. Ravarotto, V.; Bertoldi, G.; Stefanelli, L.F.; Nalesso, F.; Calò, L.A. Gitelman's and Bartter's Syndromes: From Genetics to the Molecular Basis of Hypertension and More. *Kidney Blood Press. Res.* **2022**, *47*, 556–564. [CrossRef]
12. Ravarotto, V.; Simioni, F.; Sabbadin, C.; Pagnin, E.; Maiolino, G.; Armanini, D.; Caló, L.A. Proinflammatory/profibrotic effects of aldosterone in Gitelman's syndrome, a human model opposite to hypertension. *J. Endocrinol. Investig.* **2019**, *42*, 521–526. [CrossRef] [PubMed]
13. Kondo, A.; Nagano, C.; Ishiko, S.; Omori, T.; Aoto, Y.; Rossanti, R.; Sakakibara, N.; Horinouchi, T.; Yamamura, T.; Nagai, S.; et al. Examination of the predicted prevalence of Gitelman syndrome by ethnicity based on genome databases. *Sci. Rep.* **2021**, *11*, 16099. [CrossRef] [PubMed]
14. San-Cristobal, P.; de los Heros, P.; Ponce-Coria, J.; Moreno, E.; Gamba, G. WNK Kinases, Renal Ion Transport and Hypertension. *Am. J. Nephrol.* **2008**, *28*, 860–870. [CrossRef] [PubMed]
15. Gamba, G. Role of WNK kinases in regulating tubular salt and potassium transport and in the development of hypertension. *Am. J. Physiol.-Ren. Physiol.* **2005**, *288*, 245–252.
16. Takeuchi, Y.; Mishima, E.; Shima, H.; Akiyama, Y.; Suzuki, C.; Suzuki, T.; Kobayashi, T.; Suzuki, Y.; Nakayama, T.; Takeshima, Y.; et al. Exonic Mutations in the SLC12A3 Gene Cause Exon Skipping and Premature Termination in Gitelman Syndrome. *J. Am. Soc. Nephrol.* **2015**, *26*, 271–279.
17. Vargas-Poussou, R.; Dahan, K.; Kahila, D.; Venisse, A.; Riveira-Munoz, E.; Debaix, H.; Grisart, B.; Bridoux, F.; Unwin, R.; Moulin, B.; et al. Spectrum of mutations in Gitelman syndrome. *J. Am. Soc. Nephrol.* **2011**, *22*, 693–703.
18. Stenson, P.D.; Ball, E.V.; Mort, M.; Phillips, A.D.; Shiel, J.A.; Thomas, N.S.T.; Abeysinghe, S.; Krawczak, M.; Cooper, D.N. Human Gene Mutation Database (HGMD): 2003 update. *Hum. Mutat.* **2003**, *21*, 577–581.
19. Hsu, Y.-J.; Hoenderop, J.G.; Bindels, R.J.M. TRP channels in kidney disease. *Biochim. Biophys. Acta* **2007**, *1772*, 928–936.
20. Knoers, N.V.A. Inherited forms of renal hypomagnesemia: An update. *Pediatr. Nephrol.* **2009**, *24*, 697–705. [CrossRef]
21. Ji, W.; Foo, J.N.; O'Roak, B.J.; Zhao, H.; Larson, M.G.; Simon, D.B.; Newton-Chen, C.; State, M.W.; Levy, D.; Lifton, R.P. Rare independent mutations in renal salt handling genes contribute to blood pressure variation. *Nat. Genet.* **2008**, *40*, 592–599. [CrossRef]

22. Herrero-Morín, J.D.; Rodríguez, J.; Coto, E.; Gil-Peña, H.; Alvarez, V.; Espinosa, L.; Loris, C.; Gil-Calvo, M.; Santos, F. Gitelman syndrome in Gypsy paediatric patients carrying the same intron 9 + 1 G>T mutation. Clinical features and impact on quality of life. *Nephrol. Dial. Transplant.* **2011**, *26*, 151–155. [CrossRef]
23. Tseng, M.-H.; Yang, S.-S.; Hsu, Y.-J.; Fang, Y.-W.; Wu, C.-J.; Tsai, J.-D.; Hwang, D.-Y.; Lin, S.-H. Genotype, phenotype, and follow-up in Taiwanese patients with salt-losing tubulopathy associated with SLC12A3 mutation. *J. Clin. Endocrinol. Metab.* **2012**, *97*, 1478–1482. [CrossRef] [PubMed]
24. Wang, L.; Dong, C.; Xi, Y.-G.; Su, X. Thiazide-sensitive Na^+-Cl^- cotransporter: Genetic polymorphisms and human diseases. *Acta Biochim. Biophys. Sin.* **2015**, *47*, 325–334. [CrossRef]
25. Colussi, G.; Macaluso, M.; Brunati, C.; Minetti, L. Calcium metabolism and calciotropic hormone levels in Gitelman's syndrome. *Min. Electrolyte Metab.* **1994**, *20*, 294–301.
26. Loffing, J.; Loffing-Cueni, D.; Valderrabano, V.; Kläusli, L.; Hebert, S.C.; Rossier, B.C.; Hoenderop, J.G.; Bindels, R.J.; Kaissling, B. Distribution of transcellular calcium and sodium transport pathways along mouse distal nephron. *Am. J. Physiol.-Ren. Physiol.* **2001**, *281*, F1021–F1027. [CrossRef]
27. Knoers, N.V.A.M.; Levtchenko, E. Gitelman syndrome. *Orphanet. J. Rare Dis.* **2008**, *3*, 22. [CrossRef] [PubMed]
28. Graziani, G.; Fedeli, C.; Moroni, L.; Cosmai, L.; Badalamenti, S.; Ponticelli, C. Gitelman syndrome: Pathophysiological and clinical aspects*. *QJM Int. J. Med.* **2010**, *103*, 741–748. [CrossRef] [PubMed]
29. Bettinelli, A.; Bianchetti, M.G.; Girardin, E.; Caringella, A.; Cecconi, M.; Appiani, A.C.; Pavanello, L.; Gastaldi, R.; Isimbaldi, C.; Lama, G.; et al. Use of calcium excretion values to distinguish two forms of primary renal tubular hypokalemic alkalosis: Bartter and Gitelman syndromes. *J. Pediatr.* **1992**, *120*, 38–43. [CrossRef]
30. Jeck, N.; Schlingmann, K.P.; Reinalter, S.C.; Kömhoff, M.; Peters, M.; Waldegger, S.; Seyberth, H.W. Salt handling in the distal nephron: Lessons learned from inherited human disorders. *Am. J. Physiol. Regul. Integr. Comp. Physiol.* **2005**, *288*, 782–795. [CrossRef]
31. Blanchard, A.; Bockenhauer, D.; Bolignano, D.; Calò, L.A.; Cosyns, E.; Devuyst, O.; Ellison, D.H.; Karet Frankl, F.E.; Knoers, N.V.A.; Konrad, M.; et al. Gitelman syndrome: Consensus and guidance from a Kidney Disease: Improving Global Outcomes (KDIGO) Controversies Conference. *Kidney Int.* **2017**, *91*, 24–33. [CrossRef]
32. Rudin, A.; Aurell, M.; Wilske, J. Low urinary calcium excretion in Bartter's syndrome. *Scand. J. Urol. Nephrol.* **1988**, *22*, 35–39. [CrossRef] [PubMed]
33. Agus, Z.S. Hypomagnesemia. *J. Am. Soc. Nephrol.* **1999**, *10*, 1616–1622. [CrossRef]
34. Elisaf, M.; Panteli, K.; Theodorou, J.; Siamopoulos, K.C. Fractional excretion of magnesium in normal subjects and in patients with hypomagnesemia. *Magnes. Res.* **1997**, *10*, 315–320.
35. Fuhimura, J.; Nozu, K.; Yamamura, T.; Minamikawa, S.; Nakanishi, K.; Horinouchi, T.; Nagano, C.; Sakakibara, N.; Nakanishi, K.; Shima, Y.; et al. Clinical and Genetic Characteristics in Patients with Gitelman Syndrome. *Kidney Int. Rep.* **2019**, *4*, 119–125. [CrossRef] [PubMed]
36. Adalat, S.; Hayes, W.N.; Bryant, W.; Booth, J.; Woolf, A.S.; Kleta, R.; Subtil, S.; Clissold, R.; Colclough, K.; Ellard, S.; et al. HNF1B Mutations Are Associated with a Gitelman-like Tubulopathy That Develops During Childhood. *Kidney Int. Rep.* **2019**, *4*, 1304–1311. [CrossRef] [PubMed]
37. Bockenhauer, D.; Feather, S.; Stanescu, H.C.; Bandulik, S.; Zdebik, A.A.; Reichold, M.; Tobin, J.; Lieberer, E.; Sterner, C.; Landoure, G.; et al. Epilepsy, ataxia, sensorineural deafness, tubulopathy, and KCNJ10 mutations. *N. Engl. J. Med.* **2009**, *360*, 1960–1970. [CrossRef]
38. Scholl, U.I.; Choi, M.; Liu, T.; Ramaekers, V.T.; Häusler, M.G.; Grimmer, J.; Tobe, S.W.; Farhi, A.; Nelson-Williams, C.; Lifton, R.P. Seizures, sensorineural deafness, ataxia, mental retardation, and electrolyte imbalance (SeSAME syndrome) caused by mutations in KCNJ10. *Proc. Natl. Acad. Sci. USA* **2009**, *106*, 5842–5847. [CrossRef]
39. Mayan, H.; Farfel, Z.; Karlish, S.J.D. Renal Mg handling, FXYD2 and the central role of the Na,K-ATPase. *Physiol. Rep.* **2018**, *6*, e13843. [CrossRef]
40. Suzumoto, Y.; Columbano, V.; Gervasi, L.; Giunta, R.; Mattina, T.; Trimarchi, G.; Capolongo, G.; Simeoni, M.; Perna, A.F.; Zacchia, M.; et al. A case series of adult patients affected by EAST/SeSAME syndrome suggests more severe disease in subjects bearing *KCNJ10* truncating mutations. *Intractable Rare Dis. Res.* **2021**, *10*, 95–101. [CrossRef]
41. Finkel, T.; Deng, C.-X.; Mostoslavsky, R. Recent progress in the biology and physiology of sirtuins. *Nature* **2009**, *460*, 587–591. [CrossRef]
42. Viering, D.; Schlingmann, K.P.; Hureaux, M.; Nijenhuis, T.; Mallett, A.; Chan, M.M.Y.; van Beek, A.; van Eerde, A.; Coulibaly, J.-M.; Vallet, M.; et al. Gitelman-Like Syndrome Caused by Pathogenic Variants in mtDNA. *J. Am. Soc. Nephrol.* **2022**, *33*, 305–325.
43. Yang, L.; Fan, J.; Liu, Y.; Ren, Y.; Liu, Z.; Fu, H.; Qi, H.; Yang, J. Case report: Gitelman syndrome with diabetes: Confirmed by both hydrochlorothiazide test and genetic testing. *Medicine* **2023**, *102*, e33959.
44. Nuñez-Gonzale, L.; Carrera, N.; Garcia-Gonzale, M.A. Molecular Basis, Diagnostic Challenges and Therapeutic Approaches of Bartter and Gitelman Syndromes: A Primer for Clinicians. *Int. J. Mol. Sci.* **2021**, *22*, 11414. [CrossRef] [PubMed]
45. Liaw, L.C.; Banerjee, K.; Coulthard, M.G. Dose related growth response to indometacin in Gitelman syndrome. *Arch. Dis. Child* **1999**, *81*, 508–510. [PubMed]
46. Bartter, F.C.; Pronove, P.; Gill, J.R.; Maccardle, R.C. Hyperplasia of the juxtaglomerular complex with hyperaldosteronism and hypokalemic alkalosis. A new syndrome. *Am. J. Med.* **1962**, *33*, 811–828.

47. Lee, B.H.; Cho, H.Y.; Lee, H.; Han, K.H.; Kang, H.G.; Ha, I.S.; Lee, J.H.; Park, Y.S.; Shin, J.I.; Lee, D.-Y.; et al. Genetic basis of Bartter syndrome in Korea. *Nephrol. Dial. Transplant.* **2012**, *27*, 1516–1521. [CrossRef]
48. Konrad, M.; Vollmer, M.; Lemmink, H.H.; Van Den Heuvel, L.P.W.J.; Jeck, N.; Vargas-Poussou, R.; Lakings, A.; Ruf, R.; Deschênes, G.; Antignac, C.; et al. Mutations in the chloride channel gene CLCNKB as a cause of classic Bartter syndrome. *J. Am. Soc. Nephrol.* **2000**, *11*, 1449–1459.
49. Kurtz, I. Molecular pathogenesis of Bartter's and Gitelman's syndromes. *Kidney Int.* **1998**, *54*, 1396–1410.
50. Bokhari, S.R.A.; Zulfiqar, H.; Mansur, A. *Bartter Syndrome*; StatPearls Publishing LLC.: St. Petersburg, FL, USA, 2023.
51. Colussi, G.; Bettinelli, A.; Tedeschi, S.; De Ferrari, M.E.; Syrèn, M.L.; Borsa, N.; Mattiello, C.; Casari, G.; Bianchetti, M.G. A thiazide test for the diagnosis of renal tubular hypokalemic disorders. *Clin. J. Am. Soc. Nephrol.* **2007**, *2*, 454–460. [CrossRef]
52. Verberckmoes, R.; van Damme, B.; Clement, J.; Amery, A.; Michielsen, P. Bartter's syndrome with hyperplasia of renomedullary cells: Successful treatment with indomethacin. *Kidney Int.* **1976**, *9*, 302–307. [CrossRef]
53. Nascimento, C.L.P.; Garcia, C.L.; Schvartsman, B.G.S.; Vaisbich, M.H. Treatment of Bartter syndrome. Unsolved issue. *J. Pediatr.* **2014**, *90*, 512–517. [CrossRef]
54. Morales, J.M.; Ruilope, L.M.; Coto, A.; Alcazar, J.M.; Prieto, C.; Nieto, J.; Rodicio, J.L. Long-term enalapril therapy in Bartter's syndrome. *Nephron* **1988**, *48*, 327. [CrossRef]
55. Hené, R.J.; Koomans, H.A.; Dorhout Mees, E.J.; vd Stolpe, A.; Verhoef, G.E.; Boer, P. Correction of Hypokalemia in Bartter's Syndrome by Enalapril. *Am. J. Kidney Dis.* **1987**, *9*, 200–205. [CrossRef]
56. Fulchiero, R.; Seo-Mayer, P. Bartter Syndrome and Gitelman Syndrome. *Pediatr. Clin. N. Am.* **2019**, *66*, 121–134. [CrossRef]
57. Armanios, M.; de Cabo, R.; Mannick, J.; Partridge, L.; van Deursen, J.; Villeda, S. Translational strategies in aging and age-related disease. *Nat. Med.* **2015**, *21*, 1395–1399. [CrossRef]
58. López-Otín, C.; Blasco, M.A.; Partridge, L.; Serrano, M.; Kroemer, G. The Hallmarks of Aging. *Cell* **2013**, *153*, 1194–1217. [CrossRef]
59. Erichsen, L.; Seifert, H.-H.; Schulz, W.A.; Hoffmann, M.J.; Niegisch, G.; Araúzo-Bravo, M.J.; Bendhack, M.L.; Poyet, C.; Hermanns, T.; Beermann, A.; et al. Basic Hallmarks of Urothelial Cancer Unleashed in Primary Uroepithelium by Interference with the Epigenetic Master Regulator ODC1. *Sci. Rep.* **2020**, *10*, 1–10. [CrossRef]
60. López-Otín, C.; Blasco, M.A.; Patridge, L.; Serrano, M.; Kroemer, G. Hallmarks of aging: An expanding universe. *Cell* **2023**, *186*, 243–278. [CrossRef]
61. Sastre, J.; Pallardò, F.V.; Viña, J. Mitochondrial oxidative stress plays a key role in aging and apoptosis. *IUBMB Life* **2000**, *49*, 427–435. [CrossRef]
62. Erichsen, L.; Thimm, C.; Bohndorf, M.; Rahman, M.S.; Wruck, W.; Adjaye, J. Activation of the Renin—Angiotensin System Disrupts the Cytoskeletal Architecture of Human Urine-Derived Podocytes. *Cells* **2022**, *11*, 1095. [CrossRef]
63. Thimm, C.; Erichsen, L.; Wruck, W.; Adjaye, J. Unveiling Angiotensin II and Losartan-Induced Gene Regulatory Networks Using Human Urine-Derived Podocytes. *Int. J. Mol. Sci.* **2023**, *24*, 10551. [CrossRef] [PubMed]
64. Erichsen, L.; Kloss, L.D.F.; Thimm, C.; Bohndorf, M.; Schichel, K.; Wruck, W.; Adjaye, J. Derivation of the immortalized cell line-UM51-PrePodo-hTERT and its responsiveness to Angiotensin II and activation of RAAS. *Cells* **2023**, *12*, 342. [CrossRef] [PubMed]
65. Barreto-Chaves, M.L.; Mello-Aires, M. Effect of luminal angiotensin II and ANP on early and late cortical distal tubule HCO_3-reabsorption. *Am. J. Physiol.* **1996**, *271*, F977–F984. [CrossRef]
66. Kwon, T.-H.; Nielsen, J.; Kim, Y.-H.; Knepper, M.A.; Frøkiaer, J.; Nielsen, S. Regulation of sodium transporters in the thick ascending limb of rat kidney: Response to angiotensin II. *Am. J. Physiol.* **2003**, *285*, F152–F165. [CrossRef]
67. Rocque, B.L.; Babayeva, S.; Li, J.; Leung, V.; Nezvitsky, L.; Cybulsky, A.V.; Gros, P.; Torban, E. Deficiency of the Planar Cell Polarity Protein Vangl2 in Podocytes Affects Glomerular Morphogenesis and Increases Susceptibility to Injury. *J. Am. Soc. Nephrol.* **2015**, *26*, 576–586. [CrossRef]
68. Tojo, A.; Tisher, C.C.; Madsen, K.M. Angiotensin II regulates H(+)-ATPase activity in rat cortical collecting duct. *Am. J. Physiol.* **1994**, *267*, F1045–F1051. [CrossRef]
69. Xie, K.; Xu, C.; Zhang, M.; Wang, M.; Min, L.; Qian, C.; Wang, Q.; Ni, Z.; Mou, S.; Dai, H.; et al. Yes-associated protein regulates podocyte cell cycle re-entry and dedifferentiation in adriamycin-induced nephropathy. *Cell Death Dis.* **2019**, *10*, 915. [CrossRef] [PubMed]
70. Wang, T.; Giebisch, G. Effects of angiotensin II on electrolyte transport in the early and late distal tubule in rat kidney. *Am. J. Physiol.* **1996**, *271*, F143–F149. [CrossRef] [PubMed]
71. Zhuo, J.; Maric, C.; Harris, P.J.; Alcorn, D.; Mendelsohn, F. Localization and Functional Properties of Angiotensin II AT1 Receptors in the Kidney: Focus on Renomedullary Interstitial Cells. *Hypertens. Res.* **1997**, *20*, 233–250. [CrossRef]
72. Gasparo, M.; Unger, T. International Union of Pharmacology. XXIII. The Angiotensin II Receptors. Pharmacological Reviews 2000. Available online: https://www.researchgate.net/publication/12344120 (accessed on 22 August 2021).
73. Siragy, H.M. AT1 and AT2 Receptor in the Kidney: Role in Health and Disease. *Semin. Nephrol.* **2004**, *24*, 93–100. [CrossRef]
74. Ames, M.; Atkins, C.; Pitt, B. The renin-angiotensin-aldosterone system and its suppression. *J. Vet. Intern. Med.* **2019**, *33*, 363–382. [CrossRef] [PubMed]
75. Berry, C.; Touyz, A.F.; Dominiczak, R.; Webb, C.; Johns, D.G. Angiotensin receptors: Signaling, vascular pathophysiology, and interactions with ceramide. *Am. J. Physiol. Heart Circ. Physiol.* **2001**, *281*, H2337–H2365. [CrossRef]

76. Widdop, R.; Jones, E.; Hannan, R.; Gaspari, T. Angiotensin AT2 receptors: Cardiovascular hope or hype? *Br. J. Pharmacol.* **2003**, *140*, 809–824. [CrossRef]
77. Nouet, S.; Nahmias, C. Signal Transduction from the Angiotensin II AT2 Receptor. *Trends Endocrinol. Metab.* **2000**, *11*, 1–6. [CrossRef] [PubMed]
78. Gilliam-Davis, S.; Payne, V.S.; Kasper, S.O.; Tommasi, E.N.; Robbins, M.E.; Diz, D.I. Long-term AT1 receptor blockade improves metabolic function and provides renoprotection in Fischer-344 rats. *Am. J. Physiol. Heart Circ. Physiol.* **2007**, *293*, H1327–H1333. [CrossRef]
79. Herbert, K.E.; Mistry, Y.; Hastings, R.; Poolman, T.; Niklason, L.; Williams, B. Angiotensin II-mediated oxidative DNA damage accelerates cellular senescence in cultured human vascular smooth muscle cells via telomere-dependent and independent pathways. *Circ. Res.* **2008**, *102*, 201–208. [CrossRef] [PubMed]
80. Feng, X.; Wang, L.; Li, Y. Change of telomere length in angiotensin II-induced human glomerular mesangial cell senescence and the protective role of losartan. *Mol. Med. Rep.* **2011**, *4*, 255–260.
81. Erichsen, L.; Adjaye, J. Crosstalk between age accumulated DNA-damage and the SIRT1-AKT-GSK3ß axis in urine derived renal progenitor cells. *Aging* **2022**, *14*, 8179–8204. [CrossRef]
82. Brooks, C.; Gu, W. How does SIRT1 affect metabolism, senescence and cancer? *Nat. Rev. Cancer* **2009**, *9*, 123–128. [CrossRef]
83. Yuan, H.-F.; Zhai, C.; Yan, X.-L.; Zhao, D.-D.; Wang, J.-X.; Zeng, Q.; Chen, L.; Nan, X.; He, L.-J.; Li, S.-T.; et al. SIRT1 is required for long-term growth of human mesenchymal stem cells. *J. Mol. Med.* **2012**, *90*, 389–400. [CrossRef]
84. Chen, C.; Zhou, M.; Ge, Y.; Wang, X. SIRT1 and aging related signaling pathways. *Mech. Ageing Dev.* **2020**, *187*, 111215. [CrossRef] [PubMed]
85. Satoh, A.; Brace, C.S.; Rensing, N.; Clifton, P.; Wozniak, D.; Herzog, E.D.; Yamada, K.A.; Imai, S. Sirt1 extends life span and delays aging in mice through the regulation of Nk2 homeobox 1 in the DMH and LH. *Cell Metab.* **2013**, *18*, 416–430. [CrossRef]
86. Peng, J.; Hu, C.-P.; Li, Y.-J. Reply to 'Number and function of circulating endothelial progenitor cells and calcitonin gene-related peptide in hypertension: Support from and opportunities in Bartter's and Gitelman's syndromes patients'. *J. Hypertens.* **2010**, *28*, 2171.
87. Liu, T.; Yang, Q.; Zhang, X.; Qin, R.; Shan, W.; Zhang, H.; Chen, X. Quercetin alleviates kidney fibrosis by reducing renal tubular epithelial cell senescence through the SIRT1/PINK1/mitophagy axis. *Life Sci.* **2020**, *257*, 118116. [CrossRef]
88. Miyazaki, R.; Ichiki, T.; Hashimoto, T.; Inanaga, K.; Imayama, I.; Sadoshima, J.; Sunagawa, K. SIRT1, a Longevity Gene, Downregulates Angiotensin II Type 1 Receptor Expression in Vascular Smooth Muscle Cells. *Arter. Thromb. Vasc. Biol.* **2008**, *28*, 1263–1269. [CrossRef]
89. Jang, I.-A.; Kim, E.N.; Lim, J.H.; Kim, M.Y.; Ban, T.H.; Yoon, H.E.; Park, C.W.; Chang, Y.S.; Choi, B.S. Effects of Resveratrol on the Renin-Angiotensin System in the Aging Kidney. *Nutrients* **2018**, *10*, 1741. [CrossRef]
90. Jang, M.; Cai, L.; Udeani, G.O.; Slowing, K.V.; Thomas, C.F.; Beecher, C.W.; Fong, H.H.; Farnsworth, N.R.; Kinghorn, A.D.; Mehta, R.G.; et al. Cancer chemopreventive activity of resveratrol, a natural product derived from grapes. *Science* **1997**, *275*, 218–220. [CrossRef] [PubMed]
91. Wang, Q.; Xu, J.; Rottinghaus, G.E.; Simonyi, A.; Lubahn, D.; Sun, G.Y.; Sun, A.Y. Resveratrol protects against global cerebral ischemic injury in gerbils. *Brain Res.* **2002**, *958*, 439–447. [CrossRef] [PubMed]
92. Dryden, S.C.; Nahhas, F.; Nowak, J.E.; Goustin, A.-S.; Tainsky, M.A. Role for human SIRT2 NAD-dependent deacetylase activity in control of mitotic exit in the cell cycle. *Mol. Cell Biol.* **2003**, *23*, 3173–3185. [CrossRef]
93. Blander, G.; Guarente, L. The Sir2 family of protein deacetylases. *Annu. Rev. Biochem.* **2004**, *73*, 417–435. [CrossRef]
94. Nishikori, S.; Yasuda, J.; Murata, K.; Takegaki, J.; Harada, Y.; Shirai, Y.; Fujita, S. Resistance training rejuvenates aging skin by reducing circulating inflammatory factors and enhancing dermal extracellular matrices. *Sci. Rep.* **2023**, *13*, 10214. [CrossRef] [PubMed]
95. Aversa, Z.; White, T.A.; Heeren, A.A.; Hulshizer, C.A.; Saul, D.; Zhang, X.; Molina, A.J.; Redman, L.M.; Martin, C.K.; Racette, S.B.; et al. Calorie restriction reduces biomarkers of cellular senescence in humans. *Aging Cell* **2023**, *23*, e14038. [CrossRef]
96. Dorling, J.L.; Martin, C.K.; Redman, L.M. Calorie restriction for enhanced longevity: The role of novel dietary strategies in the present obesogenic environment. *Ageing Res. Rev.* **2020**, *64*, 101038. [CrossRef] [PubMed]
97. Flanagan, E.W.; Most, J.; Mey, J.T.; Redman, L.M. Calorie Restriction and Aging in Humans. *Annu. Rev. Nutr.* **2020**, *40*, 105–133. [CrossRef] [PubMed]
98. Hurley, B.F.; Hanson, E.D.; Sheaff, A.K. Strength Training as a Countermeasure to Aging Muscle and Chronic Disease. *Sports Med.* **2012**, *41*, 289–306. [CrossRef]
99. Vermeij, W.P.; Dollé, M.E.T.; Reiling, E.; Jaarsma, D.; Payan-Gomez, C.; Bombardieri, C.R.; Wu, H.; Roks, A.J.M.; Botter, S.M.; van der Eerden, B.C.; et al. Restricted diet delays accelerated ageing and genomic stress in DNA-repair-deficient mice. *Nature* **2016**, *537*, 427–431. [CrossRef] [PubMed]
100. Neuhauser, H.; Kuhnert, R.; Born, S. 12-Monats-Prävalenz von Bluthochdruck in Deutschland. *J. Health Monit.* **2017**, *2*, 57–63.
101. Higashi, Y.; Kihara, Y.; Noma, K. Endothelial dysfunction and hypertension in aging. *Hypertens. Res.* **2012**, *35*, 1039–1047. [CrossRef]
102. Buford, T.W. Hypertension and aging. *Ageing Res. Rev.* **2016**, *26*, 96–111. [CrossRef]
103. Zhongjie, S. Aging, Arterial Stiffness, and Hypertensio. *Hypertension* **2015**, *65*, 252–256.
104. Genestra, M. Oxyl radicals, redox-sensitive signalling cascades and antioxidants. *Cell Signal* **2007**, *19*, 1807–1819. [CrossRef]

105. Salisbury, D.; Bronas, U. Reactive oxygen and nitrogen species: Impact on endothelial dysfunction. *Nurs. Res.* **2015**, *64*, 53–66. [CrossRef] [PubMed]
106. Shen, J.; Rastogi, R.; Geng, X.; Ding, Y. Nicotinamide adenine dinucleotide phosphate oxidase activation and neuronal death after ischemic stroke. *Neural. Regen. Res.* **2019**, *14*, 948–953. [PubMed]
107. Guo, D.; Liang, S.; Wang, S.; Tang, C.; Yao, B.; Wan, W.; Zhang, H.; Jiang, H.; Ahmed, A.; Zhang, Z.; et al. Role of epithelial Na+ channels in endothelial function. *J. Cell Sci.* **2016**, *129*, 290–297. [PubMed]
108. Bhargava, P.; Schnellmann, R.G. Mitochondrial energetics in the kidney. *Nat. Rev. Nephrol.* **2017**, *13*, 629–646. [CrossRef]
109. Wang, Z.; Ying, Z.; Bosy-Westphal, A.; Zhang Schautz, B.; Later, W.; Heymsfield, S.B.; Müller, M.J. Specific metabolic rates of major organs and tissues across adulthood: Evaluation by mechanistic model of resting energy expenditure. *Am. J. Clin. Nutr.* **2010**, *92*, 1369–1377. [CrossRef]
110. Bhatia, D.; Capili, A.; Choi, M.E. Mitochondrial dysfunction in kidney injury, inflammation, and disease: Potential therapeutic approaches. *Kidney Res. Clin. Pract.* **2020**, *39*, 244–258. [CrossRef]
111. Emma, F.; Montini, G.; Parikh, S.; Salviati, L. Mitochondrial dysfunction in inherited renal disease and acute kidney injury. *Nat. Rev. Nephrol.* **2016**, *12*, 267–280. [CrossRef]
112. Galvan, D.L.; Green, N.H.; Danesh, F.R. The hallmarks of mitochondrial dysfunction in chronic kidney disease. *Kidney Int.* **2017**, *92*, 1051–1057. [CrossRef]
113. Honda, T.; Hirakawa, Y.; Nangaku, M. The role of oxidative stress and hypoxia in renal disease. *Kidney Res. Clin. Pract.* **2019**, *38*, 414–426. [CrossRef]
114. Zhan, M.; Brooks, C.; Liu, F.; Dong, Z. Mitochondrial dynamics: Regulatory mechanisms and emerging role in renal pathophysiology. *Kidney Int.* **2013**, *83*, 568–581. [CrossRef] [PubMed]
115. Goto, Y.; Itami, N.; Kajii, N.; Tochimaru, H.; Endo, M.; Horai, S. Renal tubular involvement mimicking Bartter syndrome in a patient with Kearns-Sayre syndrome. *J. Pediatr.* **1990**, *116*, 904–910. [CrossRef] [PubMed]
116. Emma, F.; Pizzini, C.; Tessa, A.; Di Giandomenico, S.; Onetti-Muda, A.; Santorelli, F.M.; Bertini, E.; Rizzoni, G. "Bartter-like" phenotype in Kearns-Sayre syndrome. *Pediatr. Nephrol.* **2006**, *21*, 355–360. [CrossRef]
117. Gonzalez-Vicente, A.; Hong, N.; Garvin, J.L. Effects of reactive oxygen species on renal tubular transport. *Am. J. Physiol. Renal. Physiol.* **2019**, *317*, F444–F455. [CrossRef] [PubMed]
118. Kwakernaak, A.J.; Waanders, F.; Slagman, M.C.J.; Dokter, M.M.; Laverman, G.D.; de Boer, R.A.; Navis, G. Sodium restriction on top of renin-angiotensin-aldosterone system blockade increases circulating levels of N-acetyl-seryl-aspartyl-lysyl-proline in chronic kidney disease patients. *J. Hypertens.* **2013**, *31*, 2425–2432. [CrossRef]
119. Kobori, H.; Nishiyama, A.; Abe, Y.; Navar, L.G. Enhancement of Intrarenal Angiotensinogen in Dahl Salt-Sensitive Rats on High Salt Diet. *Hypertension* **2003**, *41*, 592–597. [CrossRef]
120. Kocks, M.; Buikema, H.; Gschwend, S.; Boomsma, F.; de Zeeuw, D.; Navis, G. High Dietary Sodium Blunts Effects of Angiotensin-converting Enzyme Inhibition on Vascular Angiotensin I–to–Angiotensin II Conversion in Rats. *J. Cardiovasc. Pharmacol.* **2003**, *42*, 601–606. [CrossRef]
121. Verploegen, M.; Vargas-Poussou, R.; Walsh, S.B.; Alpay, H.; Amouzegar, A.; Ariceta, G.; Atmis, B.; Francesco, E.; Nijenhuis, T. Parathyroid hormone and phosphate homeostasis in patients with Bartter and Gitelman syndrome: An international cross-sectional study. *Nephrol. Dial. Transplant.* **2022**, *37*, 2474–2486. [CrossRef]
122. Calò, L.A.; Ceolotto, G.; Milani, M.; Pagnin, E.; van den Heuvel, L.P.; Sartori, M.; Davis, P.A.; Costa, R.; Semplicini, A. Abnormalities of Gq-mediated cell signaling in Bartter and Gitelman syndromes. *Kidney Int.* **2001**, *60*, 882–889. [CrossRef]
123. Virgilio, D.; Calò, L.A.; Favaro, S.; Borsatti, A. Resting and stimulated cytosolic free calcium levels in neutrophils from patients with Bartter's syndrome. *Clin. Sci.* **1987**, *72*, 483–488. [CrossRef]
124. Calò, L.A.; D'Angelo, A.; Cantaro, S.; Rizzolo, M.; Favaro, S.; Antonello, A.; Borsatti, A. Intracellular calcium signaling and vascular reactivity in Bartter's syndrome. *Nephron* **1996**, *72*, 570–573. [CrossRef] [PubMed]
125. Calò, L.A.; Puato, M.; Schiavo, S.; Zanardo, M.; Tirrito, C.; Pagnin, E.; Balbi, G.; Davis, P.A.; Palatini, P.; Pauletto, P. Absence of vascular remodelling in a high angiotensin-II state (Bartter's and Gitelman's syndromes): Implications for angiotensin II signalling pathways. *Nephrol. Dial. Transplant.* **2008**, *23*, 2804–2809. [CrossRef] [PubMed]
126. Tura, O.; Mills, N.L.; Hadoke, P.W. Does Bartter's syndrome/Gitelman's syndrome provide a clinical model for investigating the association between calcitonin gene-related peptide and angiotensin II-mediated senescence of endothelial progenitor cells? *J. Hypertens.* **2010**, *28*, 2170–2171. [CrossRef] [PubMed]
127. Calò, L.A.; Davis, P.A. Number and function of circulating endothelial progenitor cells and calcitonin gene-related peptide in hypertension: Support from and opportunities in Bartter's and Gitelman's syndromes patients. *J. Hypertens.* **2012**, *28*, 2169–2170. [CrossRef]
128. Ben-Porath, I.; Weinberg, R.A. When cells get stressed: An integrative view of cellular senescence. *J. Clin. Investig.* **2004**, *113*, 8–13. [CrossRef]
129. Pagnin, E.; Paul, D.; Sartori, M.; Semplicini, A.; Pessina, A.C.; Calò, L.A. Rho kinase and PAI-1 in Bartter's/Gitelman's syndromes relationship to angiotensin II signaling. *J. Hypertens.* **2004**, *22*, 1963–1969. [CrossRef]
130. Schäfer, H.; Trauzold, A.; Sebens, T.; Deppert, W.; Fölsch, U.R.; Schmidt, W.E. The proliferation-associated early response gene p22/PRG1 is a novel p53 target gene. *Oncogene* **1998**, *16*, 2479–2487. [CrossRef]

131. Calò, L.A.; Pagnin, E.; Davis, P.A.; Sartori, M.; Semplicini, A. Oxidative stress-related factors in Bartter's and Gitelman's syndromes: Relevance for angiotensin II signalling. *Nephrol. Dial. Transplant.* **2003**, *18*, 1518–1525. [CrossRef]
132. Morimoto, A.; Uzu, T.; Fujii, T.; Nishimura, M.; Kuroda, S.; Nakamura, S.; Inenaga, T.; Kimura, G. Sodium sensitivity and cardiovascular events in patients with essential hypertension. *Lancet* **1997**, *350*, 1734–1737. [CrossRef]
133. Weinberger, M.H.; Fineberg, N.S.; Fineberg, S.E.; Weinberger, M. Salt sensitivity, pulse pressure, and death in normal and hypertensive humans. *Hypertension* **2001**, *37*, 429–432. [CrossRef]
134. Rajagopalan, S.; Kurz, S.; Münzel, T.; Tarpey, T.; Freeman, B.A.; Griendling, K.K.; Harrison, D.G. Angiotensin II-mediated hypertension in the rat increases vascular superoxide production via membrane NADH/NADPH oxidase activation. Contribution to alterations of vasomotor tone. *J. Clin. Investig.* **1996**, *97*, 1916–1923. [CrossRef] [PubMed]
135. Sartori, M.; Parotto, E.; Bonso, E.; Semplicini, A.; Palatini, P.; Pessina, A.C.; Calò, L.A. Autonomic nervous system function in chronic hypotension associated with Bartter and Gitelman syndromes. *Am. J. Kidney Dis.* **2007**, *49*, 330–335. [CrossRef]
136. Harris, P.J.; Young, J.A. Dose-dependent stimulation and inhibition of proximal tubular sodium reabsorption by angiotensin II in the rat kidney. *Pflugers. Arch.* **1977**, *367*, 295–297. [CrossRef] [PubMed]
137. Calò, L.A.; Davis, P.A.; Rossi, G.P. Understanding the mechanisms of angiotensin II signaling involved in hypertension and its long-term sequelae: Insights from Bartter's and Gitelman's syndromes, human models of endogenous angiotensin II signaling antagonism. *J. Hypertens.* **2014**, *32*, 2109–2119. [CrossRef]
138. Evans, R.D.R.; Antonelou, M.; Sathiananthamoorthy, S.; Rega, M.; Henderson, S.; Ceron-Gutierrez, L.; Barcenas-Morales, G.; Müller, C.A.; Doffinger, R.; Walsh, S.B.; et al. Inherited salt-losing tubulopathies are associated with immunodeficiency due to impaired IL-17 responses. *Nat. Commun.* **2020**, *11*, 4368. [CrossRef] [PubMed]
139. Rahman, M.S.; Wruck, W.; Spitzhorn, L.-S.; Nguyen, L.; Bohndorf, M.; Martins, S.; Asar, F.; Ncube, A.; Erichsen, L.; Graffmann, N.; et al. The FGF, TGFβ and WNT axis Modulate Self-renewal of Human SIX2 + Urine Derived Renal Progenitor Cells. *Sci. Rep.* **2020**, *10*, 739. [CrossRef] [PubMed]
140. Bohndorf, M.; Ncube, A.; Spitzhorn, L.-S.; Enczmann, J.; Wruck, W.; Adjaye, J. Derivation and characterization of integration-free iPSC line ISRM-UM51 derived from SIX2-positive renal cells isolated from urine of an African male expressing the CYP2D6 *4/*17 variant which confers intermediate drug metabolizing activity. *Stem Cell Res.* **2017**, *25*, 18–21. [CrossRef]
141. Guo, X.; Qian, R.; Shan, X.; Yang, L.; Chen, H.; Ding, Y.; Chen, C.; Chu, M.; Lin, J.; Wang, D. Generation of a human induced pluripotent stem cell line (WMUi021-A) from a Gitelman syndrome patient carrying a SLC12A3 gene mutation (c.179C>T). *Stem Cell Res.* **2021**, *53*, 102280. [CrossRef]
142. Lim, S.W.; Shin, Y.J.; Cui, S.; Ko, E.J.; Lee, K.I.; Lee, J.Y.; Chung, B.H.; Yang, C.W. Generation of a human induced pluripotent stem cell line (CMCi002-A) from a patient with Gitelman's syndrome. *Stem Cell Res.* **2020**, *49*, 102110. [CrossRef]

Disclaimer/Publisher's Note: The statements, opinions and data contained in all publications are solely those of the individual author(s) and contributor(s) and not of MDPI and/or the editor(s). MDPI and/or the editor(s) disclaim responsibility for any injury to people or property resulting from any ideas, methods, instructions or products referred to in the content.

3.8 Generation of a Bartter syndrome type 3 patient-derived induced pluripotent stem cell line ISRM-BS3-UM18-iPSC (HHUUKDi014-A)

Chantelle Thimm, Chutong Zhong, Wasco Wruck, Martina Bohndorf, Nina Graffmann, Alessandra Grillo, Anson Tang, Viola D'Ambrosio, Rhys D Evans, Elizabeth R Wan, Keith Siew, Stephan B. Walsh and James Adjaye

Stem Cell Research 2025, Volume 87, 103760, Article ID: 40609324

Abstract:

SIX2-positive urine-derived renal progenitor cells (UdRPCs) were isolated from an 18-year-old Bartter syndrome type 3 (BS3) patient within a homozygous CLCNKB gene deletion. Two episomal-based plasmids expressing OCT4, SOX2, NANOG, KLF4, c-MYC and LIN28 we were able to generate an integration-free induced pluripotent stem cell line (iPSC). Pluripotency was confirmed by fluorescence-activated cell sorting analysis and immunocytochemistry for the markers-OCT4, SOX2, NANOG, TRA-1-60, TRA-1-81 and SSEA4. Embryoid body-based differentiation into the three germ layers was conducted and confirmed by immunocytochemistry. Pluritest analysis revealed a Pearson correlation of 0,93. Short tandem repeat DNA fingerprinting and karyotype analyses were performed.

Author contribution of C.T. included 80%:

Patient recruitment in the clinic was caried out by A.T., V.A., E.W., K.S., R.E.. Isolation of the UdRPCs from urine was carried out by C.Z. and A.G..
I was responsible for establishing and maintaining the cell culture systems, which included the cultivation of UdRPCs and iPSCs. For the characterization of the generated cell line, I isolated RNA and DNA. I conducted FACS analyses, immunofluorescence staining to evaluate phenotypic markers, and STR profiling to verify genomic identity. I examined the integration of exogenous genetic elements via exogenous PCR, and mycoplasma testing I carried out to

ensure culture purity. I additionally performed embryoid body (EB) formation to assess the pluripotency state of the cells under non-adherent conditions. Following EB generation and culture, I conducted immunofluorescence staining to evaluate lineage-specific marker expression. For all datasets generated in the course of the study, I carried out the respective statistical analyses and prepared the quantitative evaluation of the results.
Isolated RNA for NGS, which was analyzed by W.W.
I contributed to the conceptualization, designed and executed the experiments and interpreted the results. I wrote the original draft, which I edited and revised with J.A. Furthermore, I designed all figures.

Status: Published in Stem Cell Research

DOI: 10.1016/j.scr.2025.103760
This article is an open access article distributed under the terms and conditions of the Creative Commons Attribution (CC BY) 4.0 license, which permits unrestricted use, distribution, and reproduction in any medium, provided the original work is properly cited. Published by Elsevier B.V. All rights reserved.

Stem Cell Research 87 (2025) 103760

Contents lists available at ScienceDirect

Stem Cell Research

journal homepage: www.elsevier.com/locate/scr

Lab Resource: Single Cell Line

Generation of a Bartter syndrome type 3 patient-derived induced pluripotent stem cell line ISRM-BS3-UM18-iPSC (HHUUKDi014-A)

Chantelle Thimm [a], Chutong Zhong [c], Wasco Wruck [a], Alessandra Grillo [c], Rosanne Mack [a], Martina Bohndorf [a], Nina Graffmann [a], Anson Tang [c], Viola D'Ambrosio [c], Elizabeth R Wan [c], Keith Siew [c], Rhys D Evans [c], Stephan B. Walsh [c,†], James Adjaye [a,b,*]

[a] Institute for Stem Cell Research and Regenerative Medicine, Medical Faculty, Heinrich-Heine- University Düsseldorf 40225 Düsseldorf, Germany
[b] EGA Institute for Women's Health, Zayed Centre for Research into Rare Diseases in Children (ZCR), University College London (UCL), 20 Guilford Street, London WC1N 1DZ, UK
[c] Department of Renal Medicine, University College London, Royal Free Hospital, London, UK

ABSTRACT

SIX2-positive urine-derived renal progenitor cells (UdRPCs) were isolated from an 18-year-old Bartter syndrome type 3 (BS3) patient within a homozygous CLCNKB gene deletion. Two episomal-based plasmids expressing OCT4, SOX2, NANOG, KLF4, c-MYC and LIN28 we were able to generate an integration-free induced pluripotent stem cell line (iPSC). Pluripotency was confirmed by fluorescence-activated cell sorting analysis and immunocytochemistry for the markers-OCT4, SOX2, NANOG, TRA-1-60, TRA-1-81 and SSEA4. Embryoid body-based differentiation into the three germ layers was the conducted and confirmed by immunocytochemistry. Pluritest analysis revealed a Pearson correlation of 0,93. Short tandem repeat DNA fingerprinting and karyotype analyses were performed.

Unique stem cell line identifier	HHUUKDi014-A https://hpscreg.eu/cell-line/HHUUKDi014-A
Alternative name(s) of stem cell line	ISRM-BS3-UM18-iPSC
Institution	Institute for Stem Cell Research and Regenerative Medicine
Contact information of distributor	James Adjaye, James.Adjaye@med.uni-duesseldorf.de
Type of cell line	iPSC
Origin	Human
Additional origin info required for human ESC or iPSC	Age: 18 Sex: male Ethnicity if known: any other ethnic group
Cell Source	SIX2-positive urine derived renal progenitor cells (UdRPCs)
Clonality	Clonal
Method of reprogramming	Episomal expression of OCT4, SOX2, NANOG, LIN28, c-MYC, KLF-4
Genetic Modification	YES
Type of Genetic Modification	Hereditary.

(continued on next column)

(continued)

Unique stem cell line identifier	HHUUKDi014-A https://hpscreg.eu/cell-line/HHUUKDi014-A
Evidence of the reprogramming transgene loss (including genomic copy if applicable)	PCR
Associated disease	Bartter Syndrome type 3
Gene/locus	Homozygous gene deletion of CLCNKB
Date archived/stock date	30.01.2024
Cell line repository/bank	
Ethical approval	The study was approved under the ethical approval "Identification of genes involved in renal, electrolyte, and urinary tract disorders" (REC reference 05/Q0508/6). The ethic approval was provided by the ethical committee of university College London. The study was also approved under the ethical approval "Isolation, characterization and reprogramming of urine-derived stem cells" (Study number: 2017-2457_3. The ethic approval was provided by the ethical committee of the

(continued on next page)

* Corresponding author at: Institute for Stem Cell Research and Regenerative Medicine, Medical Faculty, Heinrich-Heine- University Düsseldorf, 40225 Düsseldorf, Germany.
E-mail address: james.adjaye@med.uni-duesseldorf.de (J. Adjaye).
[†] Deceased (RIP).

https://doi.org/10.1016/j.scr.2025.103760
Received 16 May 2025; Received in revised form 25 June 2025; Accepted 27 June 2025
Available online 28 June 2025
1873-5061/© 2025 The Authors. Published by Elsevier B.V. This is an open access article under the CC BY license (http://creativecommons.org/licenses/by/4.0/).

(continued)

Unique stem cell line identifier	HHUUKDi014-A https://hpscreg.eu/cell-line/HHUUKDi014-A
	medical faculty of the Heinrich-Heine university Düsseldorf. All patients provided written informed consent.

1. Resource utility

The kidneys of Bartter syndrome (BS) patients excrete excessive electrolytes such as potassium, sodium and chloride due to a congenital defect in the tubules. BS is a rare polygenic disease caused by homozygous or mixed heterozygous mutations in one of the genes: SLC12A1, KCNJ1, CLCNKB, BSND or CASR (Pulchiero and Seo-Mayer, 2019; Thimm and Adjaye, 2024). This iPSC line can be used for studying the etiology of Bartter syndrome at the cellular and molecular level. Table 1

Table 1
Characterization and validation.

Classification	Test	Result	Data
Morphology	Photography Bright field	*Normal*	Fig. 1 *panel A*
Phenotype	*Immunocytochemistry*	*Expression of pluripotency markers: OCT4, NANOG, SOX2, Tra 1–60, SSEA-4, Tra-1–81.*	Fig. 1 *panel D*
	Flow cytometry	1. *Assess 98.3 % of OCT4 positive cells* 2. *Assess 99.6 % of SSEA-4 positive cells*	Fig. 1 *panel E*
Genotype	Karyotype (G-banding) and resolution	*BS3-UM18-iPSC, 46XX Resolution 450–500*	*panel I*
Identity	Microsatellite PCR (mPCR) OR STR analysis	*Not performed* STR analysis by PCR of nine loci, matched.	*N/A* Supplementary *file 2*
Mutation analysis (IF APPLICABLE)	PCR with Sanger Sequencing	*CLCNKB mutation was found, position: 16049-17081nt.*	Fig. 1 *panel G*
	Southern Blot OR WGS	*Not performed*	*N/A*
Microbiology and virology	Mycoplasma	*Mycoplasma testing by RT-PCR*	Supplementary Fig. 1B
Differentiation potential	Embryoid body formation	*Expression of germ layer specific proteins:* *Mesoderm – α-smooth muscle actin (α-SMA), BRACHYURY* *Ectoderm – PAX6, βIII-TUBULIN* *Endoderm – SOX17, AFP*	Fig. 1 *panel F*
Donor screening (OPTIONAL)	HIV 1 + 2 Hepatitis B, Hepatitis C	*Not performed*	*N/A*
Genotype additional info (OPTIONAL)	Blood group genotyping	*Not performed*	*N/A*
	HLA tissue typing	*Not performed*	*N/A*

displays the results of the characterization and validation.

2. Resource details

In 1962, Bartter et al. identified a new syndrome and named it Bartter syndrome (BS). BS is one of the rare hereditary renal tubular disorders caused by impaired salt reabsorption in the thick ascending limb (TAL) of the loop of Henle. It is associated with several electrolyte abnormalities including low potassium and chloride, salt wasting, hypokalemia, and metabolic alkalosis with hyperaldosteronism with normal blood pressure and hyperplasia of the juxtaglomerular apparatus (JGA) (Bartter et al., 1962; Lee et al., 2012; da Silva and Pfefermann, 2018; Bokhari et al., 2023). BS is a polygenic disease caused by homozygous or mixed heterozygous mutations in one of the following genes: SLC12A1, KCNJ1, CLCNKB, BSND, or CASR (Pulchiero and Seo-Mayer, 2019; Thimm and Adjaye, 2024). We generated an iPSC line from a male Bartter syndrome type 3 patient (ISRM-BS3-UM18-iPSC). SIX2-positive urine-derived renal progenitor cells (UdRPCs) were first isolated from the patient and used to generate the described iPSC line. Reprogramming was carried out by nucleofection of the episomal plasmids pEP4EO2SCK2MEN2L and pEP4EO2SET2K (7F1) expressing OCT4, SOX2, NANOG, LIN28, c-MYC and KLF-4 (Supplementary Fig. 1A). The T- 13PC3 (ATCC) program and epithelial cells nucleofection kit were used. The resulting iPSC line has the typical iPSC morphology(Fig. 1A). The renal progenitor origin of UdRPC-BS3-UM18 were confirmed by immunocytochemistry for the renal stem cell marker SIX2 (Fig. 1B). The absence of exogenous OCT4 is shown in Fig. 1C. Pluripotency was confirmed by immunocytochemistry for the pluripotency-regulating transcription factors OCT4, NANOG, SOX2 and cell surface markers SSEA-4, TRA-1–60 and TRA-1–81 (Fig. 1D). Flow cytometry-based detection and quantification of OCT4 and SSEA4 expressing cells was confirmed (Fig. 1E). Pluripotency was also shown in vitro by embryoid body (EB)-based differentiation into the cell types of the three germ layers- endoderm (SOX17, AFP), ectoderm (PAX6, βIII-TUBULIN) and mesoderm (α-SMA –smooth muscle actin, BRACHYURY) (Fig. 1F). The deletion was confirmed by RT-PCR (Fig. 1G). Comparative transcriptome and cluster analysis of the ISRM-BS3-UM18-iPSC and the human embryonic stem cell line H9 revealed a Pearson correlation of 0,93. (Fig. 1H). Chromosomal content analysis counting 24 mitoses revealed a normal karyotype: ISRM-BS3-UM18-iPSC – 46, XY [22] (Fig. 1I). DNA fingerprinting confirmed the identity of ISRM-BS3-UM18-iPSC with the respective parental UdRPC (Supplementary file 2). A PCR-based Mycoplasma contamination test was negative (Supplementary Fig. 1B).

3. Materials and methods

3.1. Cell culture

UdRPCs (BS3-UM18) were isolated from urine samples and expanded as previously described (Bohndorf et al., 2017; Rahman et al., 2020). Cells were cultured on plastic plates in proliferation medium (PM) composed of 50 % DMEM high Glucose (Gibco®, life technologies, California) and 50 % Keratinocyte growth basal medium (Lonza, Basel, Switzerland) supplemented with 5 ng/ml bFGF. The DMEM high Glucose medium is supplemented with 10 % fetal bovine serum (Gibco®,), 0.1 % Non-Essential Amino Acid (Gibco®,), 0.5 % Glutamax (Gibco®,) and 1 % Penicillin and Streptomycin (Gibco®. Cells were cultured at 37 °C, 5 % CO_2 and 5 % O_2. ISRM-BS3-UM18 was cultured in StemMACS iPS-Brew XF Medium (Miltenyi Biotec, Bergisch Gladbach, Germany) with 1 % Penstrep on Matrigel at 37 °C and 5 % CO_2. Cells were split at a 1:6 ratio into new matrigel coated plates. The characterization of the cells was carried out at passage 19.

3.2. Derivation of iPSCs

SIX2-positive BS3-UM18 UdRPC were reprogrammed into iPSCs (Bohndorf et al., 2017; Yu et al., 2011; Ncube et al., 2023) using the Amaxa nucleofector (Lonza, Basel, Switzerland) program T-13PC3 (ATCC). The epithelial cells nucleofection kit from LONZA was used for nucleofecting approximately 3 µg each of the two plasmids pEP4EO2SCK2MEN2L and pEP4EO2SET2K (Supplementary Fig. 1A). In addition, 0.5 µm A83-01, 0.5 µM PD0325901, 10 µM Y-27632, and 3 µM CHIR99021 were supplemented to inhibit TGFß-, MEK-, and Rock-signalling and activate WNT-signalling pathway. Cells were cultured for 24 h in Proliferation medium supplemented with 10 µM Y-27632 on Matrigel® at 37 °C and 5 % CO_2. After 24 h the Medium was changed to StemMACS iPS-Brew XF Medium (Miltenyi Biotec, Bergisch Gladbach, Germany) with daily medium changes. Well-defined iPSC colonies were picked and detached using PBS lacking Mg^{2+} and Ca^{2+} and distributed at a 1:6 ratio into new matrigel coated plates.

3.3. PCR

Supernatants from dense cultures were collected, and PCR was run to confirm the absence of mycoplasma contamination. To confirm the vector dilution, genomic DNA was extracted using the DNeasy Blood and Tissue kit (QIAGEN, Hilden, Germany). PCR was carried out using the GoTaq DNA Polymerase kit (Promega) with exogenous OCT4 primers (Table 1).

3.4. DNA fingerprint analysis

STR analysis was performed using genomic DNA extracted using the DNeasy Blood and Tissue kit (QIAGEN, Hilden, Germany). By using the GoTaq DNA Polymerase kit (Promega), the STR analysis was performed by PCR using the following primers: D16S539, D13S317 and D7S820. RPL0 served as a housekeeping gene for normalization. The PCR program is as followed:

Cycle 1 (x1): 94 °C for 3 min
Cycle 2 (x10): 94 °C for 30 s, 60 °C for 15 s, 70 °C for 45 s
Cycle 3 (x20): 94 °C for 30 s, 60 °C for 15 s, 70 °C for 45 s
Cycle 4 (x1): 60 °C for 30 min
Cycle 5: 4 °C end

Primary BS3-UM18 UdRPC cells was used for comparison-H_2O served as a negative control. The PCR amplicons were resolved by gel electrophoresis using 2.5 % agarose. Primer sequences are shown in Table 1.

3.5. Embryoid body (EB) formation

Embryoid bodies are three-dimensional aggregates that confirm the pluripotent properties of iPSCs. Based on this, EBs were also produced from the cultured iPSCs. First, the iPSCs were cultured on Matrigel-coated plates until they were subconfluent. Then a 6 mm Petri dish (greiner BIO-ONE, Kremsmünster, Austria) was coated with an anti-adherence rinsing solution (Stemcell technologies) for 10 min at 37 °C. The subconfluent wells were transferred 1:1 into a coated Petri dish. The Petri dish was cultivated for 24 h in a low oxygen incubator. As usual, the cells were cultivated in StemMACS iPS-Brew XF medium with 10 µM Y-27632. After 24 h, the cells were transferred to a normoxic incubator on a shaking platform. After approximately three days, the medium was changed to high-glucose DMEM, containing 1 % NEAA, to generate the EBs. After 7 days, the EBs are transferred to a 24-well plate coated with Matrigel and cultured till confluent.

3.6. Immunofluorescence

Cells were fixed with 4 % paraformaldehyde for 15 min at room temperature (RT). Cells were washed three times with PBS. Afterwards an incubation with 0.05 % Tween-20/PBS for 10 min. The cells were treated three times with PBS and continued blocking the cells with 3 % BSA/PBS. Thereafter they were incubated with the respective primary antibodies (Table 2) overnight at 4 °C. Followed by one washing step with Triton x-100/PBS and two washing steps with PBS. The cells were incubated for 2 h with Alexa488 or Alexa555-conjugated secondary antibodies and nuclear Hoechst at RT. Fluorescence images were captured by a LSM700 microscope (Carl Zeiss).

3.7. Flow-cytometry and immunofluorescence-based detection of pluripotency-associated proteins

Cells cultured in 6-well plates were washed twice with PBS. Afterwards they were replaced with 500 µl Triple-E (Gibco®, life technologies, California) for 10 min at 37 °C and 5 % CO_2. in the incubator. The reaction is stopped by 1 ml StemMACS iPS-Brew XF Medium (MiltenyiBiotec, Bergisch Gladbach, Germany). Cells from each 6-well was transferred into FACS-Tubes (Falcon,New York, USA) and centrifuged by 190 g, 5 min. Afterwards the cells were fixed with 4 % paraformaldehyde (polysciences, Illinois, USA) for 15 min at RT. Followed by three washings steps with PBS at 500 g 5 min. Blocking was carried out with 1 – 2 ml 3 % BSA (Sigma-Aldrich, St.Louis, USA) for 1 h at RT. The cells were separated with a 0.4 µm meshstainer (greiner BIO-ONE, Kremsmünster, Austria). Followed by a centrifugation step at 300 g, 10 min, RT. Cell pellet were resuspended with 98 µl. FACS Buffer consisting of 50 ml PBS (−/-), 0.5 % BSA, 2 mM EDTA, which can be stored by 2–8 °C. 2 µl of antibody were added. Incubation was overnight at 4 °C. Cells were washed three times with PBS and diluted in 100 µl FACS Buffer, 0.2 ul of second antibody (Table 2) for 1 h at the shaking plate in the dark, RT. After three washing steps the cell pellet were resuspend in 200–300 µl FACS Buffer and stored at 4 °C.

3.8. Karyotype analysis

Karyotype analysis was performed and evaluated at the Institute of Human Genetics and Anthropology, Heinrich-Heine-University, Düsseldorf.

3.9. NGS analysis

For the NGS experiments, 50 ng RNA preparations were sequenced via 3'RNA-Seq on a Illumina NextSeq 2000 at the core facility Biomedizinisches Forschungszentrum (BMFZ)- Heinrich Heine University Düsseldorf. The reads from the resulting fastq files were aligned against the GRCh38 genome via the HISAT2 (version 2.1.0) software (Kim et al., 2015) and summarized per gene with the subread (1.6.1) featurecounts software (Liao et al., 2014) using the ENSEMBL annotation file Homo_sapiens.GRCh38.109.gtf as described in our previous publication (Martins et al., 2020). The summarized RNA-Seq counts were corrected for batch effects and normalized within the R/Bioconductor (Gentleman et al., 2004) environment using the batch effect removal and voom normalization from the package limma (Smyth, 2004). Dendrograms and correlations were calculated using Pearson correlation as a similarity measure.

3.10. Genotyping

Genotyping was performed by multiplex polymerase chain reaction and next generation sequencing of patient genomic DNA for a panel of genes associated with inherited tubular disease (inclusive of CLCNKB). The panel (R198) of genes associated with tubular disease currently tested can be found at https://panelapp.genomicsengland.co.uk/pan

Table 2
Reagents details.

	Antibodies used for immunocytochemistry/flow-cytometry			
	Antibody	**Dilution**	**Company Cat #**	**RRID**
Characterization	*Mouse-SIX2*	*1:200*	*Abnova #H00010736-M01*	*AB_489974*
Flow Cytometry	*Rabbit anti-OCT4*	*1:50*	*Cell Signaling Technologies #2840S*	*AB_2167691*
Flow Cytometry	*Mouse anti-SSEA4*	*1:50*	*Cell Signaling #MC813*	*AB_4755*
Pluripotency Marker	*Rabbit anti-OCT4*	*1:200*	*Cell Signaling Technologies #2840S*	*AB_2167691*
Pluripotency Marker	*Rabbit anti-SOX2*	*1:200*	*Cell Signaling Technologies #3579S*	*AB_2195767*
Pluripotency Marker	*Rabbit anti-NANOG*	*1:200*	*Cell Signaling Technologies #4903S*	*AB_10559205*
Pluripotency Marker	*Mouse anti-Tra-1–60*	*1:200*	*Cell Signaling Technologies #4746S*	*AB_2119059*
Pluripotency Marker	*Mouse anti-Tra-1–81*	*1:200*	*Cell Signaling Technologies #4745S*	*AB_2119060*
Pluripotency Marker	*Mouse anti-SSEA4*	*1:200*	*Cell Signaling #MC813*	*AB_4755*
e.g. Differentiation Markers	*Rabbit anti-PAX6*	*1:200*	*Cell Signaling #D3A9V*	*AB_60433*
	Mouse anti-αSMA	*1:1000*	*Dako # M0851*	*AB_2223500*
	Mouse anti-IgG-SOX17	*1:50*	*R&D System #AF1924*	*AB_355060*
	Rabbit anti-βIII Tubulin	*1:1000*	*Sy5y # 302,304*	*AB_10805138*
	Rabbit anti-AFP	*1:200*	*Cell Signaling Technology # 21375*	*AB_2209744*
	Rabbit anti-brachyury	*1:200*	*Abcam #ab209665*	*AB_270925*
Secondary antibodies Flow Cytometry	*anti-rabbit- Alexa488*	*1:50*	*Thermo Fisher Scientific # A27034*	*AB_2536097*
Secondary antibody	*anti-rabbit- Alexa488*	*1:500*	*Thermo Fisher Scientific # A27034*	*AB_2536097*
Secondary antibody	*anti-mouse- Alexa555*	*1:500*	*Thermo Fisher Scientific # A21424*	*AB_141780*
Nuclear Co- Staining	*Hoechst*	*1:5000*	*Thermo Fisher Scientific # H3569*	*AB_2651133*
	Primers			
	Target	**Size of band**	**Forward/Reverse primer (5'-3')**	
Episomal plasmid (exogenous)	*OCT4*	*657 bp*	*AGTGAGAGGCAACCTGGAGA/ AGGAACTGCTTCCTTCACGA*	
House-Keeping Genes	*RPLO*	*42 bp*	*TCGAGAATGGCAGCATCTAC/ ATCCGTCTCCACAGACAAGG*	
Mycoplasma: ITW Reagents #A3744	*mycoplasma-specific 16S rRNA gene*	*270 bp*	Negative samples show a 270 bp band only	
		357 bp	Positive ones have two bands 270 bp & 357 bp	
STR analysis	*D16S539*		*GGGGGTCTAAGAGCTTGTAAAAAG GTTTGTGTGTGATCTGTAAGCATGTATC*	
	D13S317		*ACAGAAGTCTGGGATGTGGAGGA GGCAGCCCAAAAAGACAGA*	
	D7S820		*ATGTTGGTCAGGCTGACTATG GATTCCAGATTTATCCTCATTGAC*	
	vWA		*CTAGTGGATGATAAGAATAATCAGTATGTG GGACAGATGATAAATACATAGGATGGATGG*	
	Th01		*ATTCAAAGGGTATCTGGGCTCTGG GTGGGCTGAAAAGCTCCCGATTAT*	
	Amelogenin		*ACCTCATCCTGGGCACCCTGGTT AGGCTTGAGGCCAACCATCAG*	
	D5S818		*GGTGATTTTCCTCTTTGGTATCC AGCCACAGTTTACAAGATTTGTATCT*	
	CSF1		*AACCTGAGTCTGCCAAGGACTAGC TTCCACACACCACTGGCCATCTTC*	
	TPOX		*ACTGGCACAGAAGAGGCACTTAGG GGAGGAACTGGGAACCACACAGGT*	
Genotyping	*CLCNKB 4*	*568 bp*	*GAAGATAAGGCGGGGTTGGGG*	
	Position: 15481-16028nt		*CTTGGGTGAGCAGTGGGGTCC*	
	CLCNKB 5	*507 bp*	*AAATAGCCTTCAGTGTTCAT*	
	Position: 16049-16537nt		*TATGGGGCTATTGTGACTA*	
	CLCNKB 6	*562 bp*	*TAGTCACAATAGCCCCATAG*	
	Position: 16537-17081nt		*AGGAAGCAGCATAAGACG*	

els/292/ (Hureaux et al., 2019; Ashton et al., 2018). In addition the deletion within the CLCNKB gene of the BS3-UM18 UdRPC and the derived iPSC was confirmed by PCR and Sanger sequenced at the core facility- Biomedizinisches Forschungszentrum (BMFZ)-Heinrich Heine University Düsseldorf.

3.11. Patient recruitment

Patients were recruited from the University College London Department of Renal Medicine specialist clinics for renal tubular disorders based at the Royal Free Hospital and Great Ormond Street Hospital. Patients are referred to this clinic with confirmed or possible inherited disorders of tubular function. From our cohort, patients with genotyped Bartter's Syndrome Type 3 [OMIM: 607,364 | GENE: CLCNKB] were selected for isolation of urine-derived cells.

3.12. Ethics

The study was approved under the ethical approval "Identification of genes involved in renal, electrolyte, and urinary tract disorders" (REC reference 05/Q0508/6). The study was also approved under the ethical approval "Isolation, characterization and reprogramming of urine-derived stem cells" (Study number: 2017-2457_3. The ethic approval was provided by the ethical committee of the medical faculty of the

Heinrich Heine university Düsseldorf.
All patients provided written informed consent

4. Funding statement

J.A. acknowledges the medical faculty of Heinrich Heine University for financial support.

CRediT authorship contribution statement

Chantelle Thimm: Writing – review & editing, Writing – original draft, Visualization, Methodology, Investigation, Formal analysis. **Chutong Zhong:** Resources, Methodology, Investigation. **Wasco Wruck:** Software, Formal analysis. **Alessandra Grillo:** Resources, Methodology. **Rosanne Mack:** Methodology. **Martina Bohndorf:** Methodology. **Nina Graffmann:** Methodology. **Anson Tang:** Resources. **Viola D'Ambrosio:** Resources. **Elizabeth R Wan:** Resources. **Keith Siew:** Supervision, Funding acquisition, Conceptualization. **Rhys D Evans:** Resources. **Stephan B. Walsh:** Supervision, Funding acquisition, Conceptualization. **James Adjaye:** Supervision, Project administration, Funding acquisition, Conceptualization.

Declaration of competing interest

The authors declare that they have no known competing financial interests or personal relationships that could have appeared to influence the work reported in this paper.

Acknowledgements

S.B.W., A.G., E.R.W., A.T. are supported by Kidney Research UK grant [RP_017_20190306; TF_007_20191202; ST_001_20221128]. K.S. acknowledges this research was funded in part by the Wellcome Trust [Grant number 110282/Z/15/Z]. For the purpose of open access, the author has applied a CC BY public copyright licence to any Author Accepted Manuscript version arising from this submission.

Appendix A. Supplementary data

Supplementary data to this article can be found online at https://doi.org/10.1016/j.scr.2025.103760.

References

Ashton, E.J., Legrand, A., Benoit, V., Rondelin, I., Venisse, A., Zennaro, M.-C., Jeunemaitre, X., Iancu, D., Van 'T Hoff, W.G., Walsh, S.B., Godefroid, N., Rotthier, A., Del Favero, J., et al., 2018. Simultaneous sequencing of 37 genes identified causative mutations in the majority of children with renal tubulopathies. Kidney Int. 93, 961–967.
Bartter, F.C., Pronove, P., Gill, J.R., Maccardle, R.C., 1962. Hyperplasia of the juxtaglomerular complex with hyperaldosteronism and hypokalemic alkalosis. A New Syndrome. Am. J. Med. 33, 811–828.
Bohndorf, M., Neube, A., Spitzhorn, L.-S., Enczmann, J., Wruck, W., Adjaye, J., 2017. Derivation and characterization of integration-free iPSC line ISRM-UM51 derived from SIX2-positive renal cells isolated from urine of an african male expressing the CYP2D6 *4/*17 variant which confers intermediate drug metabolizing activity. Stem Cell Res. 25, 18–21.
Bokhari, S.R.A., Zulfiqar, H., Mansur, A., 2023. Bartter Syndrome. StatPearls Publishing LLC.
da Silva, C.T., Pfeffermann, H.I., 2018. Bartter syndrome: causes, diagnosis, and treatment. Int. J. Nephrol. Renovasc. Dis. 11, 293–301.
Fulchiero, R., Seo-Mayer, P., 2019. Bartter Syndrome and Gitelman Syndrome. Pediatr. Clin. North Am. 66, 121–134.
Gentleman, R.C., Carey, V.J., Bates, D.M., Bolstad, B., Dettling, M., Dudoit, S., Ellis, B., Gautier, L., Ge, Y., Gentry, J., Hornik, K., Hothorn, T., Huber, W., et al., 2004. Bioconductor: open software development for computational biology and bioinformatics. Genome Biol. 5.
Hureaux, M., Ashton, E., Dahan, K., Houillier, P., Blanchard, A., Cornier, C., Koumakis, E., Iancu, D., Beige, H., Hilbert, P., Rotthier, A., Del Favero, J., Schaefer, F., et al., 2019. High-throughput sequencing contributes to the diagnosis of tubulopathies and familial hypercalciuria in adults. Kidney Int. 96, 1408–1416.
Kim, D., Langmead, B., Salzberg, S.L., 2015. HISAT: a fast spliced aligner with low memory requirements. Nat. Methods 12, 357–360.
Lee, B.H., Cho, H.Y., Lee, H., Han, K.H., Kang, H.G., Ha, I.S., Lee, J.H., Park, Y.S., Shin, J. I., Lee, D.-Y., Kim, S.-Y., Choi, Y., Cheong, H.I., 2012. Genetic basis of Bartter syndrome in Korea. Nöt 27, 1516–1523.
Liao, Y., Smyth, G.K., Shi, W., 2014. featureCounts: an efficient general purpose program for assigning sequence reads to genomic features. Bioinformatics 30, 923–930.
Martins, S., Müller-Schiffmann, A., Erichsen, L., Bohndorf, M., Wruck, W., Sleegers, K., Van Broeckhoven, C., Korth, C., Adjaye, J., 2020. IPSC-Derived Neuronal Cultures Carrying the Alzheimer's Disease Associated TREM2 R47H Variant Enables the Construction of an Aβ-Induced Gene Regulatory Network. Int. J. Mol. Sci. 21, 4516.
Neube, A., Seweradorf, L., Spitzhorn, L.-S., Loerch, C., Bohndorf, M., Graffmann, N., May, L., Amzou, S., Fronzoe, M., Wruck, W., Strnad, P., Adjaye, J., 2023. Generation of two Alpha-1 antitrypsin deficiency patient-derived induced pluripotent stem cell lines ISRM-AATD-iPSC-1 (iHUUKDi011-a) and ISRM-AATD-iPSC-2 (iHUUKDi012-a). Stem Cell Res. 71, 103171.
Rahman, M.S., Wruck, W., Spitzhorn, L.-S., Nguyen, L., Bohndorf, M., Martins, S., Asan, F., Neube, A., Erichsen, L., Graffmann, N., Adjaye, J., 2020. The FGF, TGFβ and WNT axis Modulate Self-renewal of Human SIX2 + Urine Derived Renal Progenitor Cells. Sci. Rep. 10, 739.
Smyth, G.K., 2004. Linear models and empirical bayes methods for assessing differential expression in microarray experiments. Stat. Appl. Genet. Mol. Biol. 3, 1–25.
Thimm, C., Adjaye, J., 2024. Untangling the Uncertain Role of Overactivation of the Renin–Angiotensin–Aldosterone System with the Aging Process based on Sodium Wasting Human Models. Int. J. Mol. Sci. 25, 9332.
Yu J, Chau KF, Vodyanik MA, Jiang J, Jiang Y. Efficient Feeder-Free Episomal Reprogramming with Small Molecules. Pera M, editor. PLoS ONE. 2011; 6: e17557.

Stem Cell Research 87 (2025) 103804

Contents lists available at ScienceDirect

Stem Cell Research

journal homepage: www.elsevier.com/locate/scr

Corrigendum

Corrigendum to "Generation of a Bartter syndrome type 3 patient-derived induced pluripotent stem cell line ISRM-BS3_UM18-iPSC (HHUUKDi014-A)" [Stem Cell Res. 87 (2025) 103760]

Chantelle Thimm [a], Chutong Zhong [c], Wasco Wruck [a], Alessandra Grillo [c], Rosanne Mack [a], Martina Bohndorf [a], Nina Graffmann [a], Anson Tang [c], Viola D'Ambrosio [c], Elizabeth R. Wan [c], Keith Siew [c], Rhys D. Evans [c], Stephan B. Walsh [c,†], James Adjaye [a,b,*]

[a] Institute for Stem Cell Research and Regenerative Medicine, Medical Faculty, Heinrich-Heine- University Düsseldorf 40225 Düsseldorf, Germany
[b] EGA Institute for Women's Health, Zayed Centre for Research into Rare Diseases in Children (ZCR), University College London (UCL), 20 Guilford Street, London WC1N 1DZ, UK
[c] Department of Renal Medicine, University College London, Royal Free Hospital, London, UK

The authors regret that the absence of Fig. 1 was not noticed during the tests.

The Fig. 1 is included here:

DOI of original article: https://doi.org/10.1016/j.scr.2025.103760.
* Corresponding author at: Institute for Stem Cell Research and Regenerative Medicine, Medical Faculty, Heinrich-Heine- University Düsseldorf, 40225 Düsseldorf, Germany.
E-mail address: james.adjaye@med.uni-duesseldorf.de (J. Adjaye).
† Deceased (RIP).

https://doi.org/10.1016/j.scr.2025.103804

1873-5061/© 2025 The Author(s). Published by Elsevier B.V. This is an open access article under the CC BY license (http://creativecommons.org/licenses/by/4.0/).

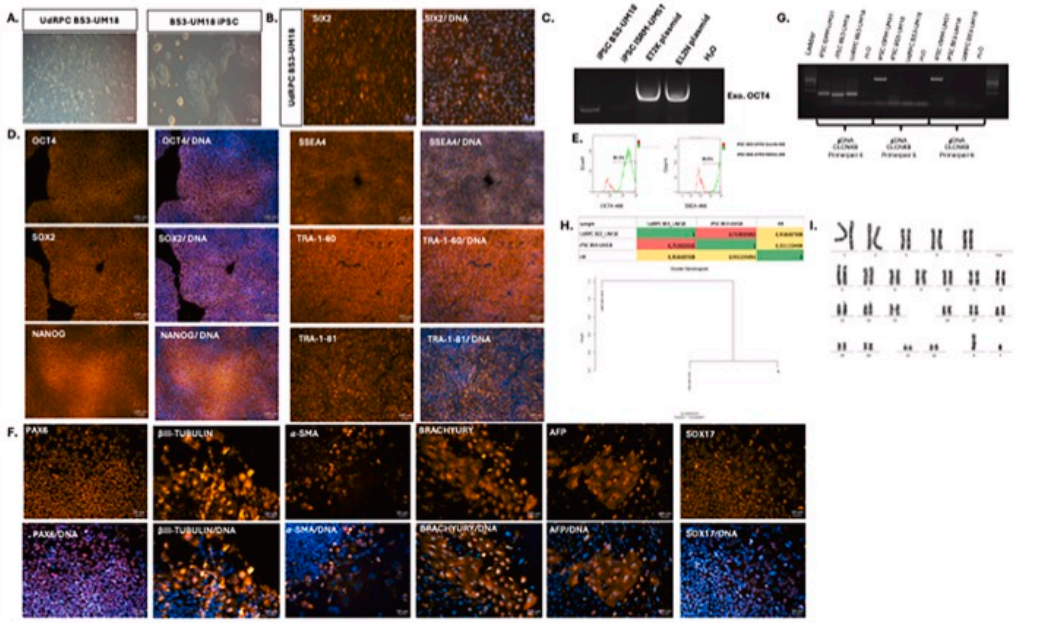


Fig. 1. Characterization of iPSC line *ISRM-BS3-UM18-iPSC*

The authors would like to apologise for any inconvenience caused.

3.9 Evidence for conserved gene expression and biological processes operative in human podocytes and adult brain.

Wasco Wruck*, **Chantelle Thimm*** and James Adjaye

BioRxiv, 2025

Abstract

Background

Podocytes are essential for the proper functioning of the glomerular filtration barrier and are characterized by their intricate structure which includes well-organized primary and secondary footprocesses. The brain expresses podocyte-associated proteins such as Nephrin, and Synaptopodin which are well documented. Processing of information and inter-cellular communication between podocytes and neurons employ similar molecular mechanisms which include actin-based projections, adhesion molecules, and signaling pathways.

Methods

In this study, we analysed brain-associated biological processes, transcription factors and pathwayssignificantly regulated in UdPodocytes, i.e. podocytes differentiated from SIX2-positive UdRPCs(urine-derived renal progenitor cells). We compared gene expression in iPSC-derived brain and kidney organoids with UdPodocytes and mapped the overlapping 344 genes to brain regions via the GTEX (Genotype-Tissue Expression) database and investigated their regulation induced by the mediator of the renin-angiotensin system- angiotensin II (ANG II).

Results

The protein interaction network of UdPodocytes genes associated with brain in GTEX contains modules for pre-synapse, post-synapse, endocrine processes and neural crest differentiation. We also found that the genes overlapping between brain and podocytes are also expressed in iPSC-derived kidney and brain organoids and could map the involved genes to all regions of the brain with the frontal cortex as the most enriched. The genes SUZ*12, NFKB1* and *PAX2* were the most significantly over-represented transcription factors. We independently confirmed the conserved expression of PAX6, KCNQ3, TUJ1,MAP2, TAU and ACTN4 in Udpodocytes as shown by Western blotting, Immunofluorescence and RT-PCR. We further investigated if the conserved genes are also regulated by ANGII. This unveiled genes down-

regulated upon ANGII-stimulation of Udpodocytes to be associated with axon guidance, Calcium , Hippo and cGMP-PKG signaling as over-represented pathways.

Conclusion

In conclusion, we have identified 344 genes with overlapping expression in brain and podocytes. These are mainly associated with synaptic signaling and cell projections. This implies that human urine-derived SIX2-renal progenitor cells differentiated into podocytes can serve as a platform for dissecting and understanding the relevance of conserved biological processes in podocytes, which are currently annotated as neuron projection, axons, neurogenesis and synaptic signaling.

Author contribution of C.T. included 50%:

I was responsible for establishing and maintaining the cell culture systems, which included the cultivation of UdRPCs and their differentiation into podocytes. In addition, I performed immunofluorescence staining, isolated RNA for both semi-quantitative PCR and NGS. I prepared protein lysates and performed western blot analysis. I collected all samples designated for NGS, after which W.W. processed and analyzed the raw sequencing data. I subsequently performed further analyses, including functional enrichment analysis using Metascape. For all datasets I generated in the course of the study, I carried out the respective statistical analyses and prepared the quantitative evaluation of the results. Furthermore, I designed figures. I contributed to the conceptualization, designed and executed the experiments and interpreted the results in relation to our research hypothesis. I wrote the original draft with W.W. I responded to the Reviewer comments and edited together with W.W. and J.A. the manuscript text and figures.

Status: Pre-print available in the open access pre-print BioRxiv
(Under revision in BMC Nephrology).

DOI: https://doi.org/10.1101/2025.03.17.643629

This article is an open access article distributed under the terms and conditions of the Creative Commons Attribution (CC BY) 4.0 license, which permits unrestricted use, distribution, and reproduction in any medium, provided the original work is properly cited.

bioRxiv preprint doi: https://doi.org/10.1101/2025.03.17.643629; this version posted March 17, 2025. The copyright holder for this preprint (which was not certified by peer review) is the author/funder. All rights reserved. No reuse allowed without permission.

Evidence for conserved gene expression and biological processes operative in human podocytes and adult brain.

Wasco Wruck[1,#], Chantelle Thimm[1,#] and James Adjaye[1,2,*]

[1]Institute for Stem Cell Research and Regenerative Medicine, Medical Faculty, Heinrich Heine University, Moorenstr.5, 40225, Düsseldorf, Germany

[2]University College London (UCL) –EGA Institute for Women's Health, Zayed Centre for Research into Rare Diseases in Children (ZCR). 20 Guilford Street, London WC1N 1DZ

[#]Equal contribution

*Correspondence: James.Adjaye@med.uni-duesseldorf.de

Abstract

Background

Podocytes are essential for the proper functioning of the glomerular filtration barrier and are characterized by their intricate structure which includes well-organized primary and secondary foot processes. The brain expresses podocyte-associated proteins such as Nephrin, and Synaptopodin which are well documented. Processing of information and inter-cellular communication between podocytes and neurons employ similar molecular mechanisms which include actin-based projections, adhesion molecules, and signaling pathways.

Methods

In this study, we analysed brain-associated biological processes, transcription factors and pathways significantly regulated in UdPodocytes, i.e. podocytes differentiated from SIX2-positive UdRPCs (urine-derived renal progenitor cells). We compared gene expression in iPSC-derived brain and kidney organoids with UdPodocytes and mapped the overlapping 344 genes to brain regions via the GTEX

bioRxiv preprint doi: https://doi.org/10.1101/2025.03.17.643629; this version posted March 17, 2025. The copyright holder for this preprint (which was not certified by peer review) is the author/funder. All rights reserved. No reuse allowed without permission.

(Genotype-Tissue Expression) database and investigated their regulation induced by the mediator of the renin-angiotensin system- angiotensin II (ANG II)

Results

The protein interaction network of UdPodocytes genes associated with brain in GTEX contains modules for pre-synapse, post-synapse, endocrine processes and neural crest differentiation. We also found that the genes overlapping between brain and podocytes are also expressed in iPSC-derived kidney and brain organoids and could map the involved genes to all regions of the brain with the frontal cortex as the most enriched. The genes SUZ*12, NFKB1* and *PAX2* were the most significantly over-represented transcription factors. We independently confirmed the conserved expression of PAX6, KCNQ3, TUJ1,MAP2, TAU and ACTN4 in Udpodocytes as shown by Western blotting, Immunofluorescence and RT-PCR. We further investigated if the conserved genes are also regulated by ANGII. This unveiled genes down-regulated upon ANGII-stimulation of Udpodocytes to be associated with axon guidance, Calcium , Hippo and cGMP-PKG signaling as over-represented pathways.

Conclusion

In conclusion, we have identified 344 genes with overlapping expression in brain and podocytes. These are mainly associated with synaptic signaling and cell projections. This implies that human urine-derived SIX2-renal progenitor cells differentiated into podocytes can serve as a platform for dissecting and understanding the relevance of conserved biological processes in podocytes which are currently annotated as neuron projection, axons, neurogenesis and synaptic signaling.

Introduction

The central nervous system (CNS) and the kidneys are very closely connected, for example, the CNS provides afferent impulses that regulate and influence renal blood flow, the glomerular filtration rate (GFR) and the sodium balance [1] and Cao et al. report a kidney-brain neural circuit driving kidney

bioRxiv preprint doi: https://doi.org/10.1101/2025.03.17.643629; this version posted March 17, 2025. The copyright holder for this preprint (which was not certified by peer review) is the author/funder. All rights reserved. No reuse allowed without permission.

damage and heart failure [2]. With respect to early development, podocytes and neurons are derived from distinct lineages, neurons arise from the ectodermal germ layer and podocytes from metanephric mesenchyme [3] developing from the intermediate part of the mesoderm germ layer [4] .

The similarity between podocytes and neurons is largely determined by common features of primary processes operative in both cell types as well as the need to exchange signals across membranes in synaptic or synaptic-like constellations [5]. Processing of formation in podocytes and neurons use the same molecular machinery which include actin-based projections such as podocyte foot processes and dendritic spines [6]. These are organized in microtubules (MT) and intermediate filaments for thick processes and actin filaments for thin projections [6]. Further similarity resides in the cell-cell contacts in synapses and the slit diaphragm where adhesion molecules in neurons and podocytes belong to the same families such as Cadherins/Protocadherins, Ig-like proteins, Neurexin and Podocalyxin [7].

Synaptopodin (SYNPO) is an Actin-associated protein that regulates the cytoskeleton in podocytes. It is not only expressed in mature podocytes but also in parts of the cytoskeleton of postsynaptic densities (PSD) and their dendritic spines. Studies have shown that the expression of SYNPO is restricted to a sub-population of cells within the telencephalic synapse [8], [9].

Furthermore, communication between podocytes and other glomerular cells is mediated via signaling mechanisms involving neurotransmitters which are also found in synapses [7] such as the glutamate receptors NMDAR and GRM1. Within podocytes, Nephrin connects these glutamate receptors through scaffolding molecules, such as PSD95, to the actin cytoskeleton of the foot processes [7].

Numerous kidney-associated diseases can result in neuronal damage. A decrease in the glomerular filtration rate (GFR) due to age or disease leads to higher concentration of the filtered waste products in the blood and can cause uremia. This accumulation of uremic substances in the blood can exert toxic effects on neurons such as in uremic encephalopathy, uremic neuropathy and uremic myopathy [10].

bioRxiv preprint doi: https://doi.org/10.1101/2025.03.17.643629; this version posted March 17, 2025. The copyright holder for this preprint (which was not certified by peer review) is the author/funder. All rights reserved. No reuse allowed without permission.

Besides the uremic toxins, oxidative stress, inflammation, and impaired blood circulation and blood brain barrier are factors mediating neurological disorders in kidney diseases, particularly in chronic kidney disease (CKD). On the other hand, leakage in the glomerular filtration barrier which leads to low concentrations of molecules such as Albumin in the blood and high concentrations in the urine are another source of kidney damage such as in diabetic nephropathy.

The similarity between podocytes and neurons manifests directly in diseases associated with calcium signaling. Deregulated or non-functional proteins from the TRPC family are associated with focal segmental glomerulosclerosis (FSGS- TRPC6) and TRCP5 induces pathologically motile podocytes while in brain the loss of TRCP5 can result in deficits in gait and motor coordination [7]. Another disease affecting neurons and podocytes, Charcot-Marie-Tooth neuropathy, often co-occurring with FSGS, is associated with mutations in *INF2* which is involved in regulation of the actin and microtubule cytoskeleton [11]. Interestingly, apart from podocytes, brain dysfunction in tubular and tubulointerstitial diseases is more often seen in disorders of water handling such as Bartter and Gitelman syndromes [12].

In this study, we further investigated similarities between a set of genes expressed in brain and podocytes with respect to neuronal-associated gene ontologies operative in urine-derived podocytes [13]. We also confirmed expression in iPSC-derived brain and kidney organoid cultures and revealed their responsiveness to ANGII-stimulation. Signalling pathways and genes regulatory networks suggest common functionality in brain and podoytes.

Methods

Cell culture conditions

Urine-derived renal progenitor cells (UdRPCs) from distinct individual males with ages 48 and 51 years (UM48, UM51) and 21 and 27year old females (UF21, UF27), were isolated following the protocol detailed by Rahman et al. [14]. These cell cultures were maintained on 6- or 12-well plates uncoated at

bioRxiv preprint doi: https://doi.org/10.1101/2025.03.17.643629; this version posted March 17, 2025. The copyright holder for this preprint (which was not certified by peer review) is the author/funder. All rights reserved. No reuse allowed without permission.

37 °C in a hypoxic environment. Cells were grown in Proliferation Medium (PM), consisting of a 1:1 mixture of DMEM high-glucose (Gibco) and keratinocyte growth basal medium (Lonza, Basel, Switzerland), supplemented with 5% fetal bovine serum (Gibco), 0.5% non-essential amino acids (Gibco), 0.25% Glutamax (Gibco), and 0.5% penicillin-streptomycin (Gibco).

For differentiation into podocytes, cells were seeded at a low density (50,000 cells per 6-well plate) on a Corning® Collagen I (Merck, Darmstadt, Deutschland) coated six or 12-Well plate and cultured for 24 hours in PM. The following day, the medium was replaced with Advanced RPMI 1640 (Gibco) supplemented with 0.5% fetal bovine serum, 1% penicillin-streptomycin, and 30 µM retinoic acid (Sigma-Aldrich Chemistry, Steinheim, Germany). After seven days, cells exhibited the characteristic morphology of podocytes. Furthermore a human SV40-temperature sensitive immortalized podocyte cell line (AB 8/13) [15] was used as an established reference . The cells were first cultured at 33 °C in RPMI 1640 (Gibco). To induce podocyte differentiation and maturation the, cells were seeded on Corning® Collagen I (Merck, Darmstadt, Deutschland) coated dishes and cultured at 37 °C in Advanced RPMI 1640 (Gibco) supplemented with 0.5% fetal bovine serum, 1% penicillin-streptomycin, and 30 µM retinoic acid (Sigma-Aldrich Chemistry, Steinheim, Germany).

Immunofluorescence-based detection of protein expression

Cells were fixed with 4% paraformaldehyde for 15 minutes at room temperature (RT) and subsequently washed three times with PBS. Afterwards the cells were blocked using 3% BSA in PBS. Primary antibodies (detailed in Table S5) were applied, and the cells were incubated overnight at 4 °C. The next day, the cells underwent a single washing step with Triton X-100 in PBS, followed by two washes with PBS. Secondary antibodies (detailed in Table S5) together with Hoechst as a nuclear stain, were applied for 2 hours at RT. Fluorescence imaging was performed using an LSM700 microscope (Carl Zeiss).

bioRxiv preprint doi: https://doi.org/10.1101/2025.03.17.643629; this version posted March 17, 2025. The copyright holder for this preprint (which was not certified by peer review) is the author/funder. All rights reserved. No reuse allowed without permission.

Western Blotting

Podocytes were lysed using RIPA buffer (Sigma-Aldrich Chemistry) supplemented with 5 M NaCl, 1% NP-40, 0.5% DOC, 0.1% SDS, 1 mM EDTA, and 50 mM Tris (pH 8.0), along with freshly added protease and phosphatase inhibitors (10 µL/mL, Sigma-Aldrich). A total of 20 µg of protein from each lysate was resolved on a 10% SDS-PAGE gel and transferred onto an Immobilon-P membrane (Merck Millipore, Burlington, VT, USA). Membranes were incubated overnight at 4 °C with the primary antibody, followed by three washes with 0.1% Tween-20 in Tris-buffered saline. Secondary antibodies were then applied for 1 hour at room temperature. Protein visualization was performed using the Pierce™ ECL Western Blotting Substrate (Thermo Fisher Scientific, Massachusetts, USA), with both solutions mixed at a 1:1 ratio. Quantification of protein bands was conducted using ImageJ software. Further details regarding the antibodies used are available in Supplemental Table S5.

RNA isolation

For RNA isolation from the various cell lines, the ZYMO Research Kit Direct-zol™ RNA Miniprep R20 was utilized following the manufacturer's protocol. Cells were detached by adding Tryple E and incubated for 5 min. Afterwards, a centrifuging step was added 4 mins 1000 g. Cell pellet was resuspend in 350 µl volume of 95–100% ethanol (EtOH) and thoroughly mixed by pipetting. The resulting solution was transferred to a Zymo-Spin™ column and centrifuged at 12,000 g for 30 seconds at 4 °C. To degrade genomic DNA, the column was washed with RNA Wash Buffer and centrifuged again at 12,000 g for 30 seconds at 4 °C. Subsequently, the column was treated with DNA digestion mix (1:16 dilution of DNase I in DNA Digestion Buffer) for 15 minutes. Following digestion, the column was rinsed twice with RNA Prewash Buffer, each followed by centrifugation at 12,000 g for 30 seconds at 4 °C. A final wash with RNA Wash Buffer was performed, including a 2-minute centrifugation step.

bioRxiv preprint doi: https://doi.org/10.1101/2025.03.17.643629; this version posted March 17, 2025. The copyright holder for this preprint (which was not certified by peer review) is the author/funder. All rights reserved. No reuse allowed without permission.

After drying the column by centrifuging for 1 minute, it was transferred to a fresh RNase-free Eppendorf tube. RNA was eluted by adding 35 µL of DNase/RNase-free water to the column and centrifuging for 1 minute at 16,000 g. The eluted RNA samples were immediately placed on ice, and concentrations measured with a Nanodrop device.

Semi-quantitative RT- PCR

1000 ng of RNA sample was used for reverse transcription using the TaqMan Kit following the manufacturer's instructions. PCR was performed using the GoTaq® G2 Hot Start Polymerase Kit from Promega. For each sample, 1 µL cDNA (5 ng/µL) was mixed with 24 µL master mix. As a negative control, 1 µL RNAse-free water was used. As references, commercial RNA samples of Human kidney total RNA (Takara, #636529) and fetal brain (BioChain®) were used. PCR was performed using a thermal cycler under the following conditions, polymerase activation: 95 °C for 2 min; 35 cycles amplification: 95 °C for 30 s, 60 °C for 30 s, 72 °C for 30 s; final elongation: 72 °C for 5 min, and finally held at 4 °C. The PCR product was resolved in a 2% agarose gel by gel electrophoresis. *RPL0* was used as the housekeeping gene.The imaging device Fusion FX was used for visualization.

Acquisition of brain and podocyte transcriptome data

Microarray datasets related to experiments conducted with brain cells and podocytes were downloaded from the public repository at the NCBI GEO (National Center for Biotechnology Information, Gene Expression Omnibus) (Table 1). In order to minimize technical variability only datasets from the same technical platform were employed. Kidney-related datasets are associated with two previous studies from our lab by Erichsen et al. (GSE171240) pertaining to Angiotensin-II-treated podocytes [13] and by Nguyen et al. (GSE186823) containing kidney organoids treated with the nephrotoxin Puromycin Aminonucleoside (PAN) [16]. Brain-related datasets are associated with a previous study from our lab

bioRxiv preprint doi: https://doi.org/10.1101/2025.03.17.643629; this version posted March 17, 2025. The copyright holder for this preprint (which was not certified by peer review) is the author/funder. All rights reserved. No reuse allowed without permission.

pertaining to brain organoids [17] and with datasets associated with genes expressed in brain regions based on RNAseq data from the Genotype-Tissue Expression (GTEx) project [18].

Table 1: Brain and kidney transcriptome datasets from NCBI GEO and other sources used in this study.

dataset	contents	brain/kidney region	platform	PubMedId
GSE279611	control	brain organoids	Affymetrix Human Clariom-S	35269426
GTEx	tissue gene expression	brain regions	RNA-Seq	23715323
GSE171240	ANGII treated podocytes	podocytes	Affymetrix Human Clariom-S	35406662
GSE186823	PAN treated kidney organoids	kidney organoids	Affymetrix Human Clariom-S	35203286
		brain		
		kidney		

Identification of brain-related biological processes in urine-derived podocytes

This study was initiated by the unexpected observation of a plethora of over-represented brain-associated GOs in transcriptomes of urine derived SIX2-positive renal progenitor cells -UdRPCs differentiated into podocytes and stimulated with ANGII [13] . In the gene expression data from our previous study by Rahman et al. [19] genes expressed in UdRPCs and UdPodocytes [13] were compared in a Venn diagram using the VennDiagram package [20] from the R/Bioconductor environment [21]. Gene expression was determined by a detection-p-value < 0.05 as described in our previous publication [22]. Genes exclusively expressed in the UdPodocytes but not in the UdRPCs were subjected to over-representation analysis via the GOstats package [23].

Association of genes with whole brain and brain regions

Genes associated with tissues were downloaded from the GTEX portal (version GTEx_Analysis_v6_RNA-seq_RNA-SeQCv1.1.8_gene_median_rpkm.gct) [18] as median RPKM data

bioRxiv preprint doi: https://doi.org/10.1101/2025.03.17.643629; this version posted March 17, 2025. The copyright holder for this preprint (which was not certified by peer review) is the author/funder. All rights reserved. No reuse allowed without permission.

from RNAseq experiments. From these genes with a median RPKM value five times greater than the mean of all tissues were considered specific for that tissue. Particularly for this study genes associated with brain regions were extracted from the dataset.

Comparison of brain-related genes in urine-derived podocytes to kidney and brain organoids

Genes expressed in kidney as well as brain organoids were extracted from our previous studies based on iPSC-derived kidney [16] and brain organoids [17]. The gene-set expressed in common was compared to the genes we found above exclusively expressed in UdPodocytes in a Venn diagram via the R package VennDiagram [20]. The intersection set from the venn diagram was further refined in a pie-chart for brain regions associated with the contained genes in the GTEX dataset. The pie-chart of brain regions was drawn with the function “pie3D” from the R package “plotrix”. Analysis of transcription factors over-represented in the promoter regions of the intersection gene set was preformed via the EnrichR web tool [24]. Association of genes to GO terms were made via the package “org.Hs.eg.db” from the R/Bioconductor [21]. For determining transcription factors (TFs), the GO terms of category “Molecular Function” with the 20 most associated genes were extracted via ratios dividing the number of associated genes by the total gene number. TFs were taken from the GO terms nucleic acid binding, DNA binding, transcription regulator activity, sequence-specific DNA binding and DNA-binding transcription factor activity, RNA polymerase II-specific. The protein interaction network was constructed using these TFs and Biogrid interactions [25] as described in our previous publication [17].

Comparison of neuron-related genes in urine-derived podocytes to brain-associated genes

Genes associated with whole brain, i.e. all brain regions, in the GTEX dataset were compared to the genes exclusively expressed in UdPodocytes in a Venn diagram via the R package VennDiagram [20].

bioRxiv preprint doi: https://doi.org/10.1101/2025.03.17.643629; this version posted March 17, 2025. The copyright holder for this preprint (which was not certified by peer review) is the author/funder. All rights reserved. No reuse allowed without permission.

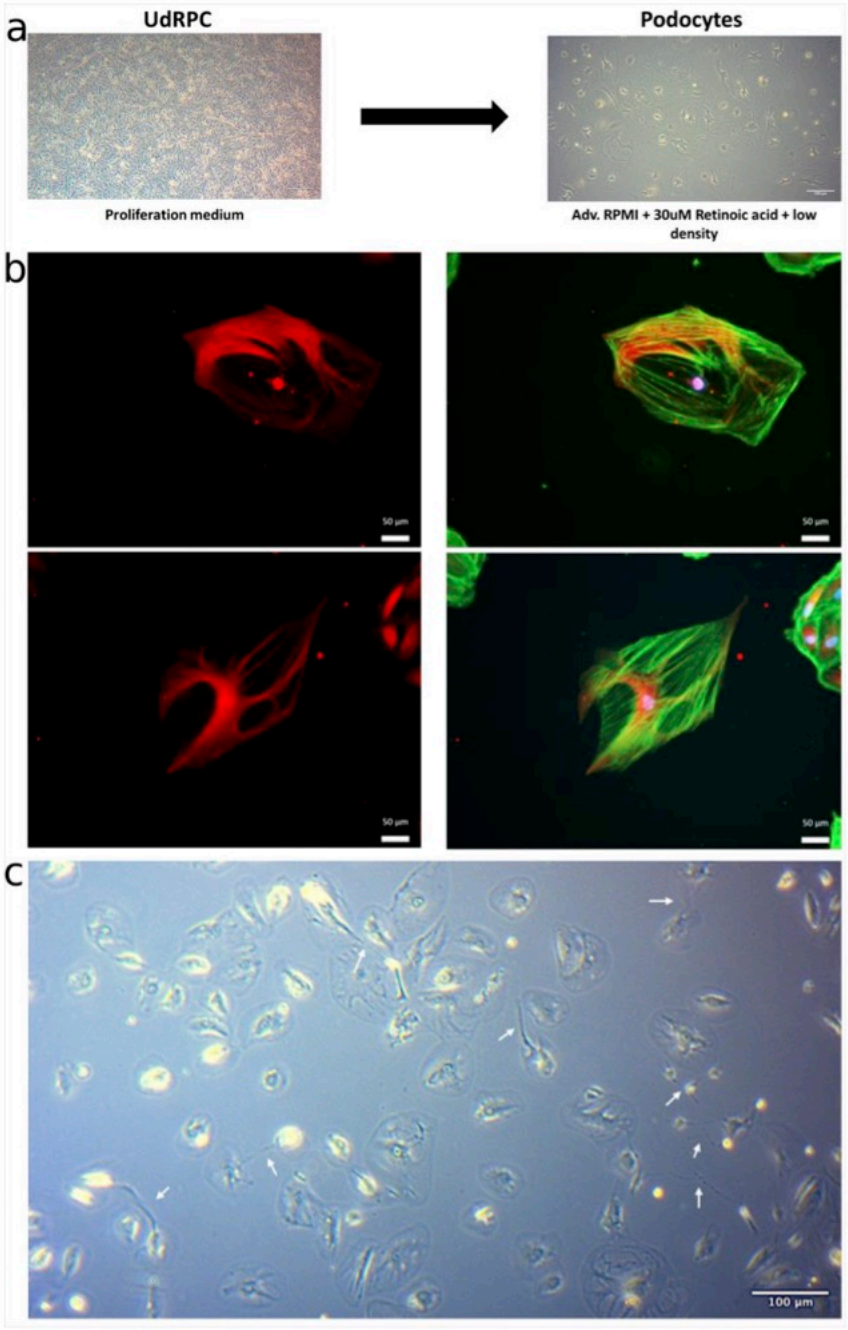
The intersection gene set from the venn diagram was submitted to the STRING-DB web tool [26] to construct a protein interaction network which in turn was used as input for Cytoscape [27]. In Cytoscape a clustering for subnetworks was performed via the plugin MCODE [28]. The sub-networks were highlighted in the whole network and analyzed for enrichment via cytoscape-builtin functions. Most significant terms from the enrichment analysis were plotted as barcharts of negative log10 p-values indicating ratios of involved gene numbers to total gene numbers on a color scale via the R package ggplot2 [29].

Results

Urine-derived Podocytes develop projections with synapses

Urine-derived renal progenitor cells (UdRPCs) were derived from urine and differentiated into podocytes (UdPodocytes) according to the scheme illustrated in Figure 1a [13], [30]. Nephrin (NPHS1) plays a major role in podocyte development and is localised at the slit diaphragm (Figure 1b: NPHS1 - red staining, phalloidin - green staining in UdPodocytes). NPHS1 is expressed in developing brain [31] and we found it up-regulated in kidney organoids [16]. The green phalloidin staining shows the actin filament structure of the podocytes. UdPodocytes can sporadically develop axon-like projections with synapses connecting to other cells (Figure 1c, white arrows pointing to synapses).

bioRxiv preprint doi: https://doi.org/10.1101/2025.03.17.643629; this version posted March 17, 2025. The copyright holder for this preprint (which was not certified by peer review) is the author/funder. All rights reserved. No reuse allowed without permission.



bioRxiv preprint doi: https://doi.org/10.1101/2025.03.17.643629; this version posted March 17, 2025. The copyright holder for this preprint (which was not certified by peer review) is the author/funder. All rights reserved. No reuse allowed without permission.

Figure 1: Podocytes develop projections with synapses.

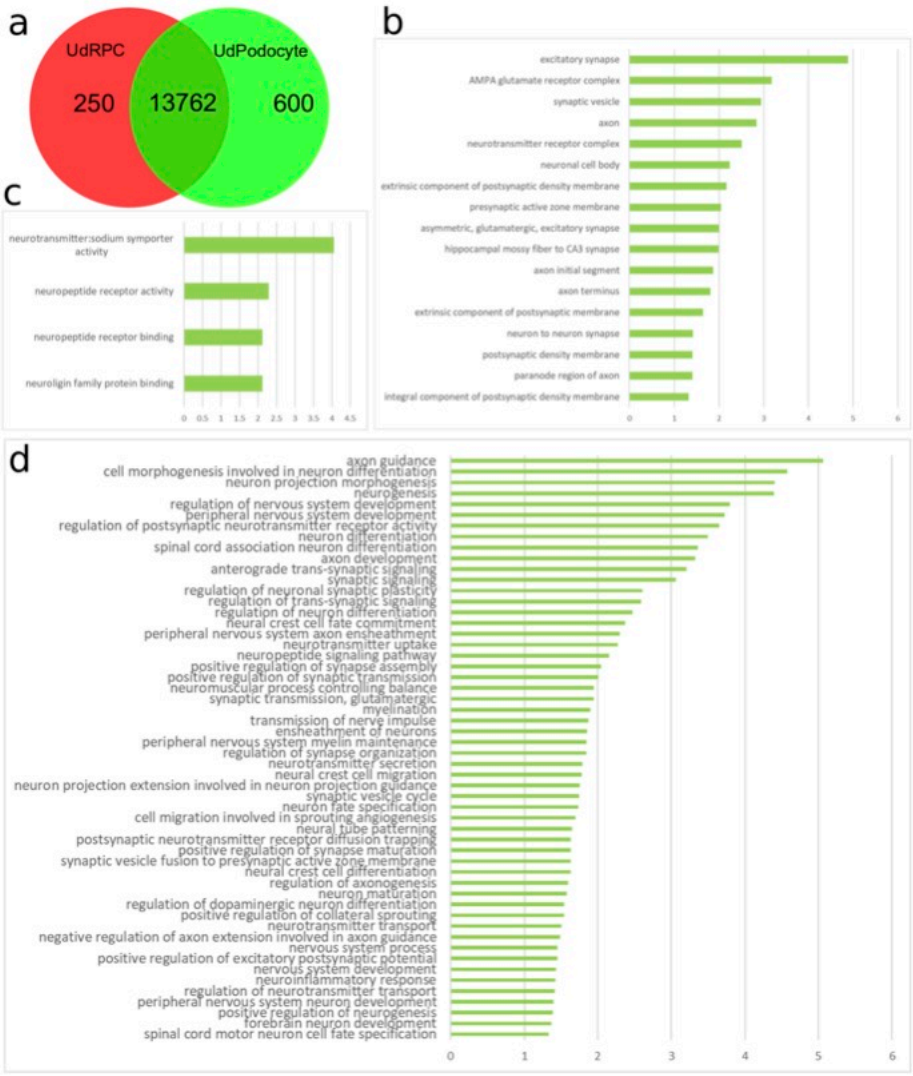
(a) Urine-derived renal progenitor (UdRPCs) were differentiated into UdPodocytes according to this scheme. (b) Nephrin (NPHS1) plays a major role in podocyte development and is found at the slit diaphragm. The staining here shows NPHS1 in red and phalloidin in green in UdPodocytes. (c) Podocytes derived from UdRPCs can develop axon-like projections with synapses inter-connecting other cells (arrows pointing at examples).

Identification of brain-associated biological processes in urine-derived podocytes

This study was initiated by the unexpected observation of a plethora of over-represented brain related GOs in transcriptomes of UdRPCs differentiated into podocytes [13], [30]. A probable explanation for this result is that there is obviously more transcriptome data available of the brain than in the kidney and as such much more GO annotations exist for brain. Nevertheless, these results also demonstrate the similarity in cell-cell communication-associated molecular mechanisms between podocytes and brain. Figure 2 shows neuron-related GO terms extracted from a list of GOs significantly over-represented in urine-derived podocytes (UdPodocytes, 600 genes) extracted from a Venn diagram comparison of expressed genes between urine-derived renal progenitor cells (UdRPCs) and UdPodocytes (Figure 2a, Figure S1). The most significant Cellular Component (CC) is *excitatory synapse* (Figure 2b) the most significant Molecular Function (MF) is *neurotransmitter:sodium symporter activity*. The three most significant Biological Processes in the list of GO terms are *axon guidance, cell morphogenesis involved in neuron differentiation* and *neuron projection morphogenesis* (Figure 2d). A more detailed analyses of the genes associated with *axon guidance* revealed genes encoding Ephrins, Slits, and Semaphorins (Figure S2). These ligands and receptors are responsible for the regulation of the actin cytoskeleton on the one hand and on the other hand for attraction and repulsion. In summary, the GO terms can be categorized into groups related to neurons including amongst others *neurogenesis* and *neuron*

bioRxiv preprint doi: https://doi.org/10.1101/2025.03.17.643629; this version posted March 17, 2025. The copyright holder for this preprint (which was not certified by peer review) is the author/funder. All rights reserved. No reuse allowed without permission.

differentiation, neuron projections including *neuron projection morphogenesis*, axons including *axon guidance* and *axon development* and synapses including *positive regulation of synapse assembly*.



bioRxiv preprint doi: https://doi.org/10.1101/2025.03.17.643629; this version posted March 17, 2025. The copyright holder for this preprint (which was not certified by peer review) is the author/funder. All rights reserved. No reuse allowed without permission.

Figure 2: Brain-associated biological processes are enriched in Urine-derived Podocytes (UdPodocytes). Genes expressed exclusively in UdPodocytes in a Venn diagram comparison (a) with urine-derived SIX2-positive renal progenitor cells (UdRPCs) were subjected to gene ontology (GO) over-representation analysis and brain-related terms were extracted from them. From the resulting list of GOs (b) the cellular components, (c) the molecular functions and (d) the biological processes with a p-value less than 0.05 are plotted here with bars indicating their negative logarithmic (base 10) p-value.

Comparison of brain-associated gene expression in urine-derived podocytes and in iPSC-differentiated brain and kidney organoids

We further compared the genes associated with neuron-related biological processes in urine-derived podocytes detected above with transcriptome data from brain and kidney organoids. Figure 3a shows a venn diagram comparing the genes expressed in kidney and brain organoids with the 600 genes identified to be exclusively expressed in UdPodocytes. The resulting intersection set of 344 genes were mapped to brain regions via associations retrieved from the GTEX database (Figure 3b) showing distribution over multiple brain regions with most hits and most significant over-representation in the frontal cortex (p=0.0006, hypergeometric test). GO analysis via the R package GOStats [23] was applied to detect over-represented GO terms in the 344 genes (Figure 3c). This revealed categories such as *cellular morphogenesis, neuron differentiation, synaptic signaling* and axon *guidance*. In a follow-up REVIGO analysis the "Biological Process"-associated GO terms "*cell projection morphogenesis*" and "*regulation of postsynaptic neurotransmitter receptor activity*" were central hubs (Figure S3). Moreover, Figure 3d and Table S2g depict results of a Metascape analysis based on the 20 GO terms of the category "Molecular Function" with most matches of the 344 genes. (approximately 70% of the 344 genes are associated with binding activity while 25% are associated with catalytic, 13% with hydrolase and 10% with transporter activity) yielding similar results as Figure 3c. Over-representation analysis of the 344 genes with the EnrichR tool [24] revealed SUZ12, NFKB1 and PAX2 as most significantly

bioRxiv preprint doi: https://doi.org/10.1101/2025.03.17.643629; this version posted March 17, 2025. The copyright holder for this preprint (which was not certified by peer review) is the author/funder. All rights reserved. No reuse allowed without permission.

over-represented transcription factors (Table S2c-e) and also transcription factors including PAX6, PAX7, SOX2 and GATA4 associated with TF-associated GO Molecular Functions *DNA-binding, transcription regulator activity, etc.* (Table S2f) which were partially validated via kidney expression in the Protein Atlas [32] (Table S2h). These validated proteins could be connected in a protein interaction network of Biogrid interactions using EGFR and XPO1 as major hubs (Figure S4).

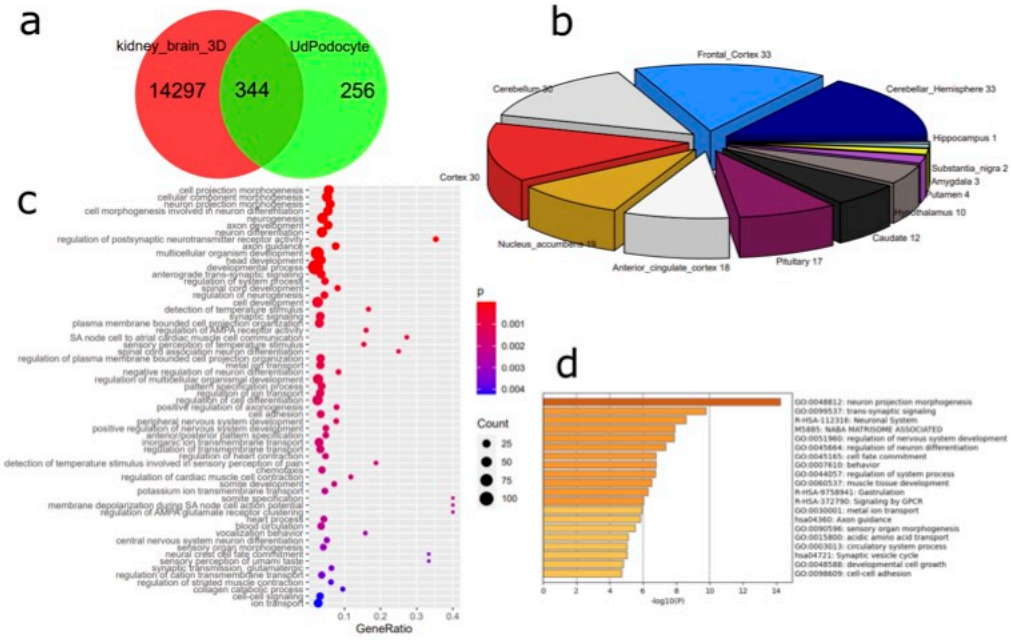


Figure 3: The overlap between urine-derived Podocytes (UdPodocytes) with brain and kidney organoids shows over-representation of the frontal cortex brain region and biological categories such as cellular morphogenesis, neuron differentiation, synaptic signaling and axon guidance. (a) Genes expressed in kidney and brain organoids were compared with the 600 genes identified as exclusively expressed in UdPodocytes resulted in an intersection of 344 genes. (b) The 344 genes map

bioRxiv preprint doi: https://doi.org/10.1101/2025.03.17.643629; this version posted March 17, 2025. The copyright holder for this preprint (which was not certified by peer review) is the author/funder. All rights reserved. No reuse allowed without permission.

to multiple brain regions with most hits in frontal cortex. (c) Results of the GO analysis using the 344 genes expressed in common revealed biological terms from categories such as *cellular morphogenesis, neuron differentiation, synaptic signaling* and *axon guidance*. (d) Mapping genes to the GO: Molecular Function (GO-MF) top category shows that most of the 344 genes are associated with binding and transcription factor activity and submitting the 294 genes associated with the top 20 GO-MFs to Metascape analysis besides similar biological processes as in (c) reveals involvement of the extra-cellular matrisome.

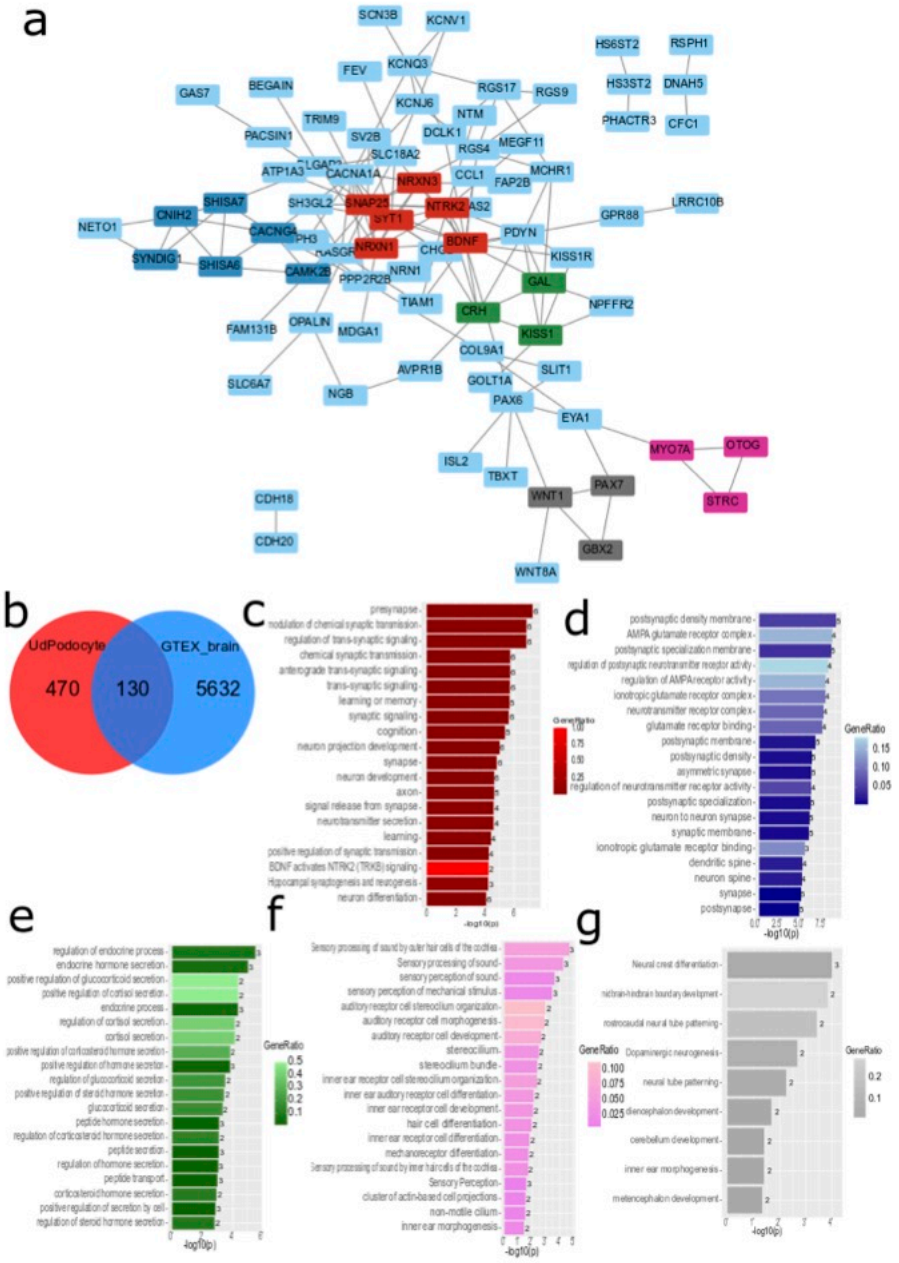
The protein interaction network of UdPodocytes genes associated with brain

Figure 4a shows the protein interaction network of the 130 genes from the intersection set of the venn diagram comparison of genes exclusively expressed in UdPodocytes and genes associated with brain in the GTEX database (Figure 4b). In a REVIGO analysis of the "Biological Process"-associated GO terms found over-represented in the 130 gene-set, "*neurogenesis*" and "*regulation of trans-synaptic signaling*" were central hubs (Figure S5). Furthermore, we submitted the 130 genes to the STRING online database, added no further interacting proteins but removed unconnected proteins. The STRING network was then loaded into Cytoscape and analysed with the MCODE plugin to identify clusters/subnetworks. In Figure 4a the most significant five subnetworks MCODE1-5 are highlighted. Bar charts in Figure 4c-g show biological terms found enriched in the subnetworks MCODE1-5 with the corresponding color. Subnetwork MCODE1 (Figure 4c, red) contains the proteins NTRK2, SNAP25, SYT1, BDNF, NRXN1 and NRXN3 and is most significantly enriched with the GO *presynapse*. Subnetwork MCODE2 (Figure 4d, blue) contains the proteins SYNDIG1, CNIH2, CACNG4, SHISA7, SHISA6 and CAMK2B and is most significantly enriched with the GO *postsynaptic density membrane*. Subnetwork MCODE3 (Figure 4e, green) contains the proteins CRH, GAL and KISS1 and is most significantly enriched with the GO *regulation of endocrine process*. Subnetwork MCODE4 (Figure 4f, violet) contains the proteins MYO7A, OTOG and STRC and is most

bioRxiv preprint doi: https://doi.org/10.1101/2025.03.17.643629; this version posted March 17, 2025. The copyright holder for this preprint (which was not certified by peer review) is the author/funder. All rights reserved. No reuse allowed without permission.

significantly enriched with the GO *Sensory processing of sound by outer hair cells of the cochlea*. Subnetwork MCODE5 (Figure 4g, grey) contains the proteins GBX2, PAX7 and WNT1 and is most significantly enriched with the GO *Neural crest differentiation*. mRNA expression of *KCNQ3, PAX6* and *TUJ1* which are amongst the 130 selected genes were confirmed in four distinct podocyte cultures and the immortalized podocyte cell line (Figure S6, primers used Table S6) and protein expression was confirmed in the Human Protein Atlas (proteinatlas.org) [32] (Figure S7). The expression of RPL0 was measured as a housekeeping gene.

bioRxiv preprint doi: https://doi.org/10.1101/2025.03.17.643629; this version posted March 17, 2025. The copyright holder for this preprint (which was not certified by peer review) is the author/funder. All rights reserved. No reuse allowed without permission.



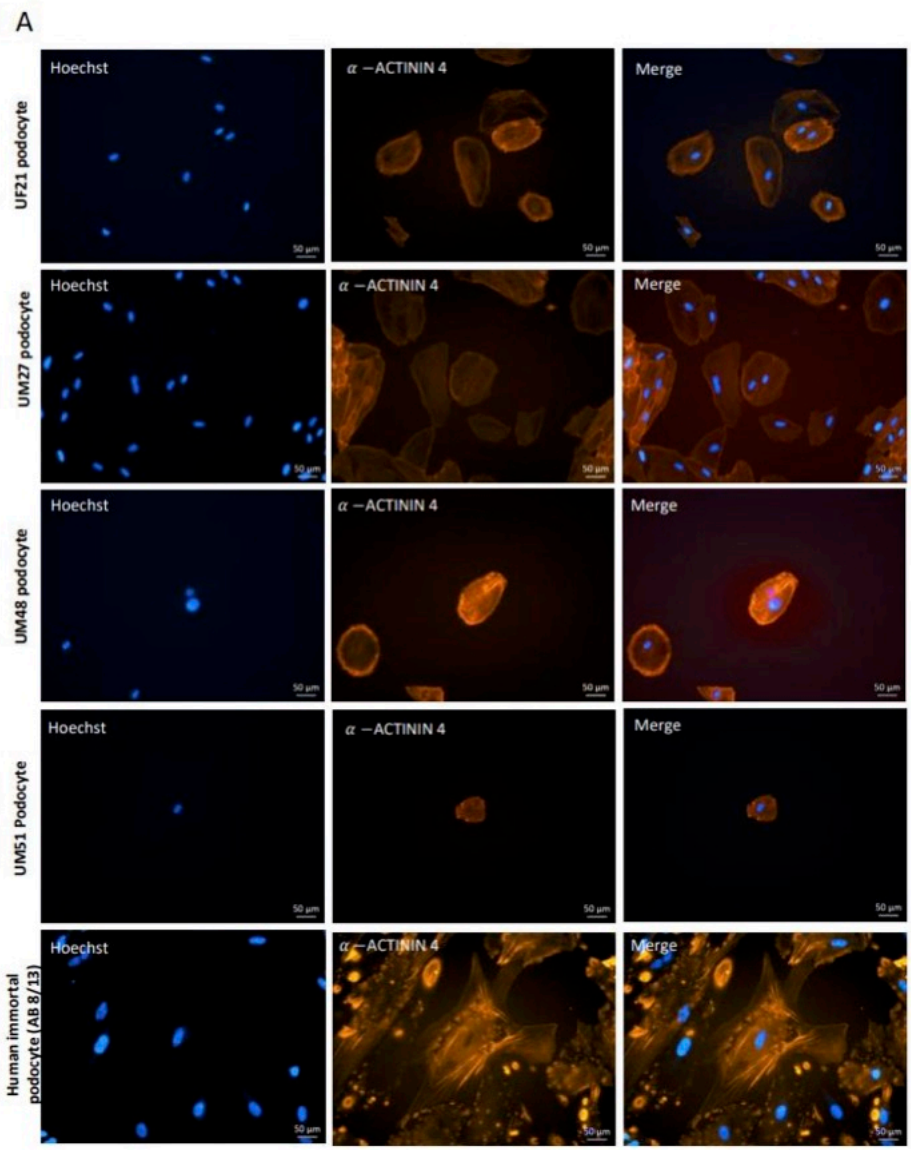
bioRxiv preprint doi: https://doi.org/10.1101/2025.03.17.643629; this version posted March 17, 2025. The copyright holder for this preprint (which was not certified by peer review) is the author/funder. All rights reserved. No reuse allowed without permission.

Figure 4: The protein interaction network of UdPodocytes genes associated with brain in GTEX contains modules for pre-synapse, post-synapse, endocrine processes, cochlea and neural crest differentiation. (a) STRING protein interaction network of 130 genes resulting from the venn diagram comparison of genes exclusively expressed in UdPodocytes and genes associated with brain in the GTEX database (b). Analysis of the STRING network in Cytoscape and MCODE yielded several subnetworks of which the most significant five MCODE1-5 are highlighted. Bar charts in panels (c-g) show biological terms found enriched in the subnetworks MCODE1-5 with the corresponding color. (c) In subnetwork MCODE1 *presynapse* is the most significantly enriched biological term. (d) In subnetwork MCODE2 *postsynaptic density membrane* is the most significantly enriched biological term. (e) In subnetwork MCODE3 *regulation of endocrine process* is the most significantly enriched biological term. (d) In subnetwork MCODE4 *Sensory processing of sound by outer hair cells of the cochlea* is the most significantly enriched biological term. (e) In subnetwork MCODE5 *Neural crest differentiation* is the most significantly enriched biological term.

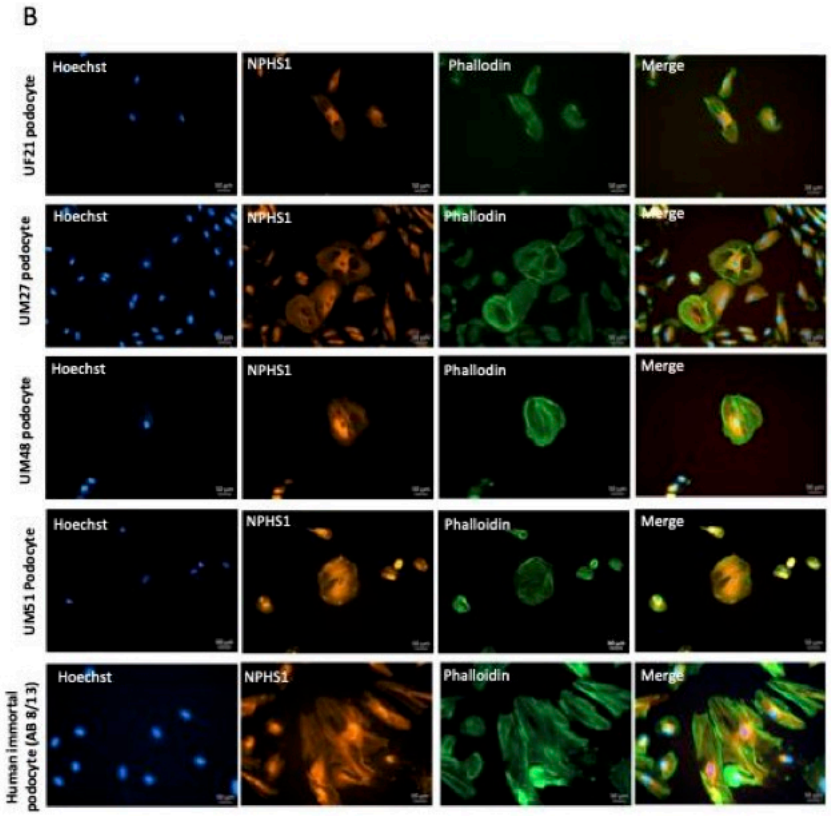
Expression of common brain associated proteins

In our previous manuscripts, we showed the capacity of urine-derived renal progenitors (UdRPCs) to differentiate into podocytes [13], [30], [19],[33] . Figure 5 depicts an immunofluorescence staining confirming the differentiation capacity of all five UdRPC preparations. Two podocyte markers were used, the cytoskeletal protein Alpha Actinin 4 (ACTN4) and the adhesion molecule Nephrin (NPHS1) (Figure 5 A+B). For investigation of common brain-associated proteins, β-Tubulin (TUBB) staining was also performed (Figure 5C). Furthermore, the expression of the podocyte cytoskeletal protein ACTN4 served as reference, TUBB, microtubule-associated TAU (MAPT) and Microtubule Associated Protein 2 (MAP2) were analyzed by Western blotting (Figure 6A-C).

bioRxiv preprint doi: https://doi.org/10.1101/2025.03.17.643629; this version posted March 17, 2025. The copyright holder for this preprint (which was not certified by peer review) is the author/funder. All rights reserved. No reuse allowed without permission.



bioRxiv preprint doi: https://doi.org/10.1101/2025.03.17.643629; this version posted March 17, 2025. The copyright holder for this preprint (which was not certified by peer review) is the author/funder. All rights reserved. No reuse allowed without permission.



bioRxiv preprint doi: https://doi.org/10.1101/2025.03.17.643629; this version posted March 17, 2025. The copyright holder for this preprint (which was not certified by peer review) is the author/funder. All rights reserved. No reuse allowed without permission.

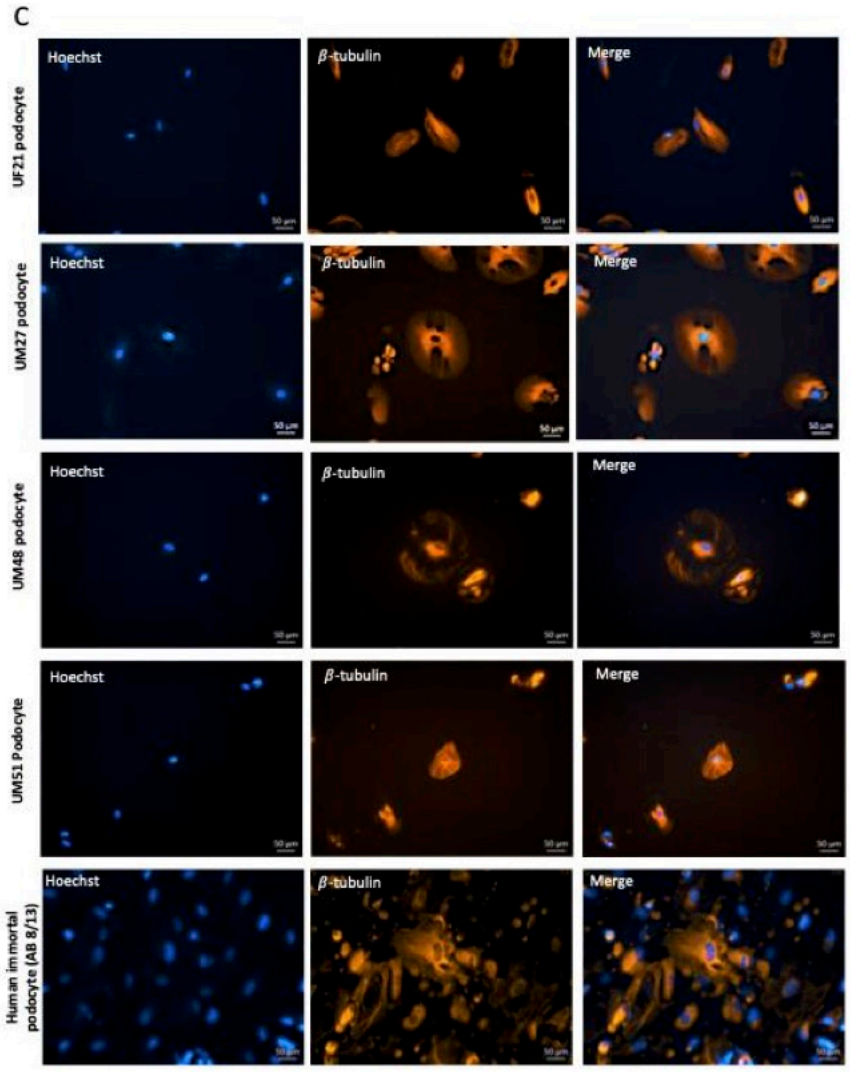


Figure 5: Expression of Alpha-actinin-4 (*ACTN4*), Nephrin (*NPHS1*) and β-TUBULIN (*TUBB*) in human podocytes.

bioRxiv preprint doi: https://doi.org/10.1101/2025.03.17.643629; this version posted March 17, 2025. The copyright holder for this preprint (which was not certified by peer review) is the author/funder. All rights reserved. No reuse allowed without permission.

Urine-derived nephron progenitor cells (UdRPC) and the immortalized podocyte cell line (AB 8/13) were differentiated into podocytes by culturing at 60–70% density in Advanced RPMI supplemented with 30 μM retinoic acid (RA). The typical Podocyte cytoskeleton was visualized by immunofluorescence-based detection of (**A**) Alpha-actinin-4 (ACTN4), and (**B**) Nephrin (NPHS1) combined with the cytoskeleton marker Phalloidin. As a common brain-associated protein (**C**) β-TUBULIN (TUBB) was stained in all five podocyte preparations.

bioRxiv preprint doi: https://doi.org/10.1101/2025.03.17.643629; this version posted March 17, 2025. The copyright holder for this preprint (which was not certified by peer review) is the author/funder. All rights reserved. No reuse allowed without permission.

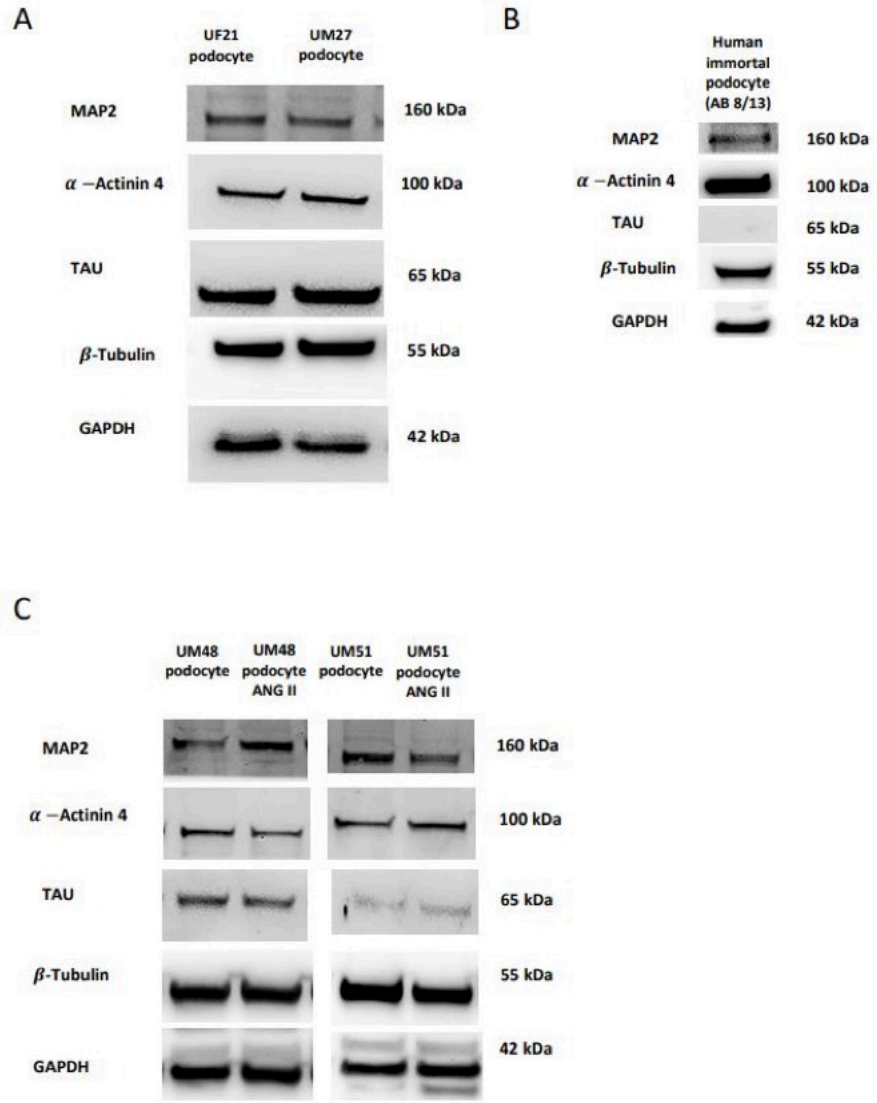


Figure 6: Western Blot analyses of brain-associated proteins expressed in human podocytes. Expression of MAP2, TUBB and TAU were analyzed by Western blotting and the expression of the podocyte markers-ACTN4 was confirmed in all cell cultures. For normalization, expression

bioRxiv preprint doi: https://doi.org/10.1101/2025.03.17.643629; this version posted March 17, 2025. The copyright holder for this preprint (which was not certified by peer review) is the author/funder. All rights reserved. No reuse allowed without permission.

glyceraldehyde-3-phosphate dehydrogenase (GAPDH) was used. Full uncropped Western blot images are presented in Supplementary Figure S8.

Responsiveness of genes expressed in podocytes and brain to the renin-angiotensin-system mediator-ANG II

Figure 7a shows a cluster analysis and heatmap of the 344 genes overlapping between UdPodocytes and kidney and brain organoids in UdPodocytes untreated (ctrl, red color bar), treated 24h with ANGII (blue color bar) and other treatments including the Angiotensin-II-type I receptor (AT1R) antagonist Losartan (no color bar). Following our previous publications showing down-regulation of key molecules of the actin cytoskeleton by ANG II [13] and beneficial effects of the ATR1 blocker - Losartan [30] we were interested in down-regulated gene clusters upon 24h of ANGII treatment. We then used these genes for a follow-up cluster analysis and heatmap (Figure 7b) in UdPodocytes from two individuals untreated (ctrl, red color bar), treated 6h with ANGII (effect not yet apparent, also red color bar) and treated 24h with ANGII (blue color bar). Furthermore, genes from the cluster down-regulated by ANG II were subjected to GO analysis (Figure 7c, Suppl. Table S4) and revealed terms related to *projection morphogenesis, axon development* and *AMPA receptors* among the most significantly over-represented Biological Processes. Over-representation analysis results of KEGG pathways (Figure 7d) included significant ($p < 0.05$) *axon guidance, Hippo signaling, Calcium signaling* and *cGMP-PKG signaling.*

bioRxiv preprint doi: https://doi.org/10.1101/2025.03.17.643629; this version posted March 17, 2025. The copyright holder for this preprint (which was not certified by peer review) is the author/funder. All rights reserved. No reuse allowed without permission.

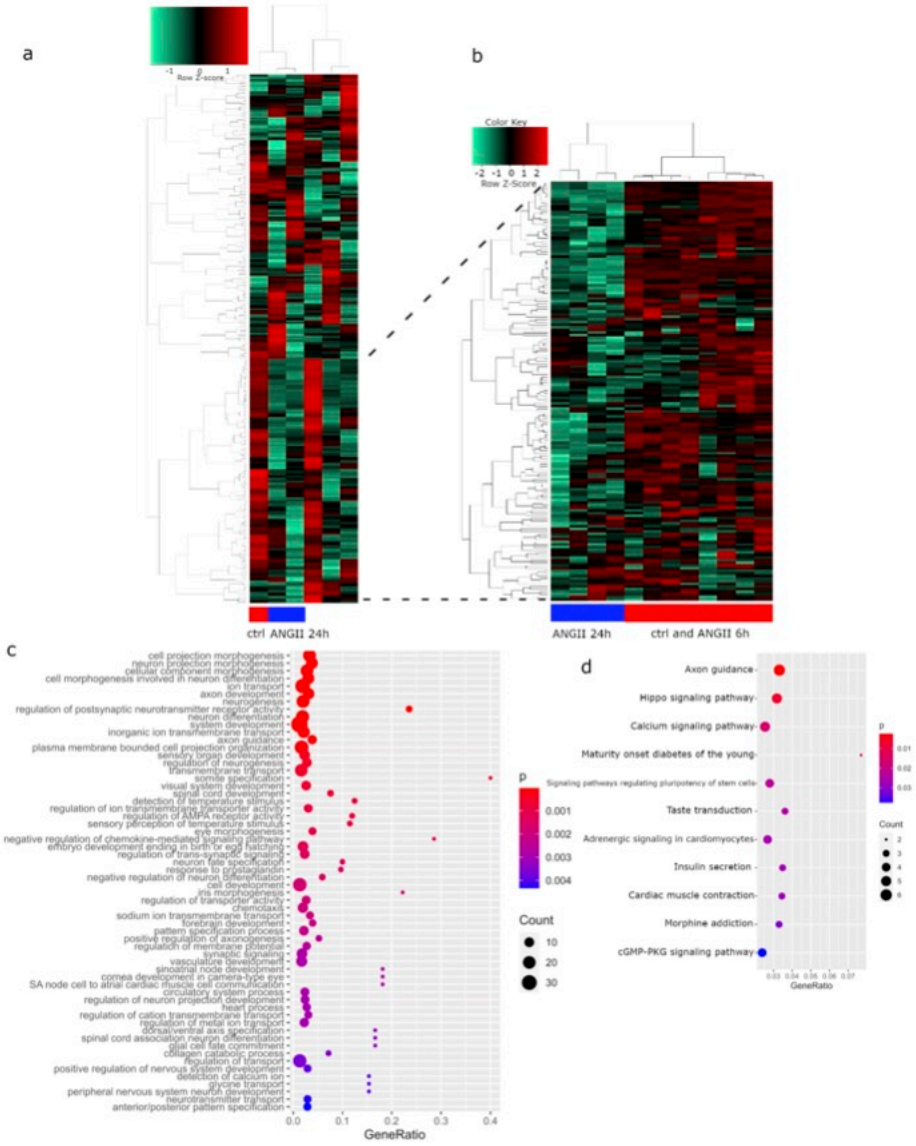


Figure 7: The 344 genes overlapping between UdPodocytes and kidney and brain organoids are responsive to ANGII stimulation. (a) cluster analysis and heatmap of the 344 genes overlapping

bioRxiv preprint doi: https://doi.org/10.1101/2025.03.17.643629; this version posted March 17, 2025. The copyright holder for this preprint (which was not certified by peer review) is the author/funder. All rights reserved. No reuse allowed without permission.

between UdPodocytes and kidney and brain organoids in UdPodocytes untreated (ctrl, red color bar), treated 24h with ANGII (blue color bar) and other treatments including the AT1R antagonist Losartan (no color bar). This cluster analysis dissected one cluster which was down-regulated upon 24h of ANGII treatment and on which we focused in the follow-up analysis. (b) cluster analysis and heatmap in UdPodocytes from two individuals using the genes from the ANGII-down-regulated cluster in UdPodocytes untreated (ctrl, red color bar), treated 6h with ANGII (effect not yet apparent, also red color bar) and treated 24h with ANGII (blue color bar). (c) The 60 most significantly over-represented gene ontologies of type Biological Process include terms related to *projection morphogenesis, axon development* and *AMPA receptors*. (d) KEGG pathways significantly over-represented ($p < 0.05$) include *axon guidance, Hippo signaling, Calcium signaling and cGMP-PKG signaling*.

Comparison of synaptic pathways between brain and podocytes

Figure 8 is an illustration of the 344 genes expressed in common between UdPodocytes, kidney and brain organoids which were found enriched ($p=3.89\ 10^{-4}$, adjusted_p=0.037) in the KEGG pathway hsa04721 *Synaptic vesicle cycle* via EnrichR enrichment analysis. The involved genes were mapped to the pathway chart and marked with red shading. The pathway chart in Figure 8 shows that most genes of the synaptic vesicle cycle are also expressed in podocytes therefore implying overlapping mechanisms in neurotransmitter uptake, Calcium signalling and vesicle processing.

In Figure 9a, genes from the KEGG pathway hsa04728 *Dopaminergic synapse* expressed in common in UdPodocytes, kidney and brain organoids are shown. The EnrichR enrichment analysis identified this pathway as the most significant specific synapse-related pathway (p=0.027, adjusted_p=0.485). The pathway map shows additionally numerous genes of post-synaptic cells are expressed in podocytes and kidney organoids. CACNA1C (indicated in the map as Cav 2.1/2.2) involved in the calcium channels has been reported to be a major player in polycystic kidney disease [34] . In general, ion channels mediate the homeostasis of electrolytes and mutations in the genes coding them may lead to renal

bioRxiv preprint doi: https://doi.org/10.1101/2025.03.17.643629; this version posted March 17, 2025. The copyright holder for this preprint (which was not certified by peer review) is the author/funder. All rights reserved. No reuse allowed without permission.

disease [35], [12]. Furthermore, the KEGG pathway- hsa04724 *Glutamatergic synapse* (p=0.047, adjusted_p=0.485) was found over-represented (Figure 9b) and thus may imply similar mechanisms in podocytes and diverse types of synapses.

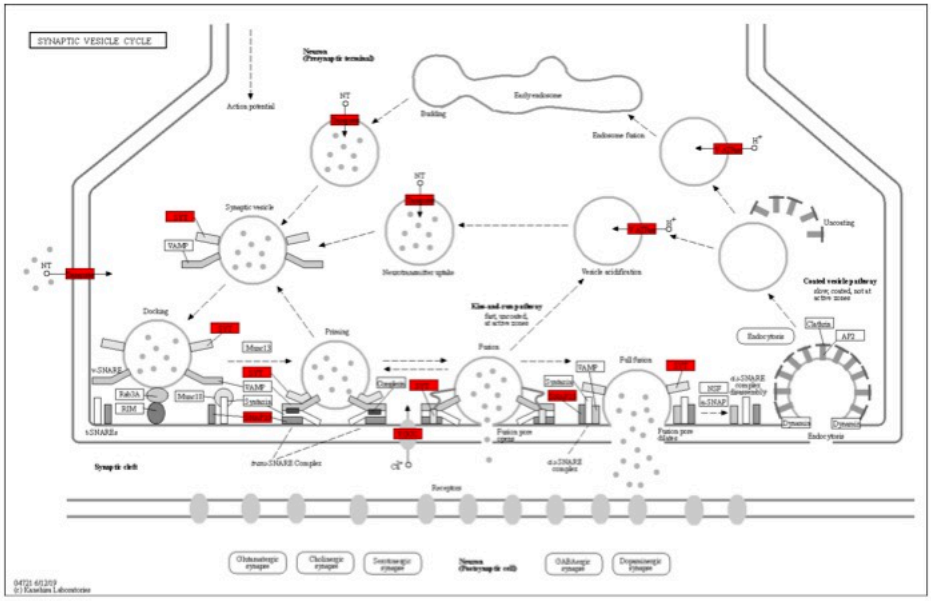
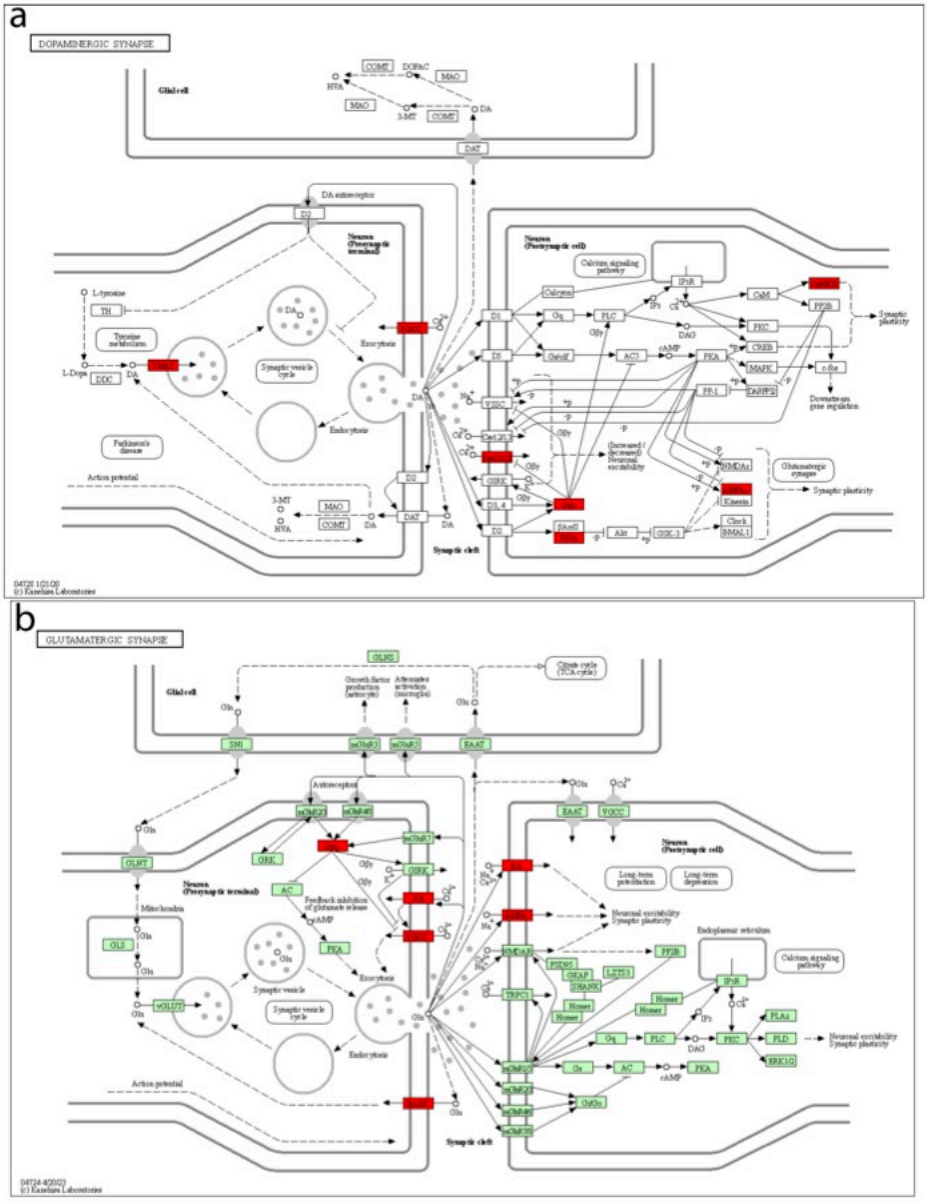


Figure 8: Most genes of the synaptic vesicle cycle are expressed in podocytes and in brain. The 344 genes expressed in UdPodocytes and in kidney as well as in brain organoids were subjected to EnrichR analysis and the KEGG pathway hsa04721 *Synaptic vesicle cycle* was found as one of the most enriched pathways ($p=3.89\ 10^{-4}$, adjusted_p=0.037). Genes in crucial locations of the pathway are involved as illustrated by the boxes with red shading.

bioRxiv preprint doi: https://doi.org/10.1101/2025.03.17.643629; this version posted March 17, 2025. The copyright holder for this preprint (which was not certified by peer review) is the author/funder. All rights reserved. No reuse allowed without permission.



bioRxiv preprint doi: https://doi.org/10.1101/2025.03.17.643629; this version posted March 17, 2025. The copyright holder for this preprint (which was not certified by peer review) is the author/funder. All rights reserved. No reuse allowed without permission.

Figure 9: Genes of the pre- and post-synaptic parts of the Dopaminergic and Glutamatergic synapse are expressed in podocytes and brain. The 344 genes expressed in UdPodocytes and in kidney as well as in brain organoids were subjected to EnrichR analysis and the KEGG pathways (a) hsa04728 *Dopaminergic synapse* (p=0.027, adjusted_p=0.485) and (b) hsa04724 *Glutamatergic synapse* (p=0.047, adjusted_p=0.485) were found amongst the most enriched pathways. Genes in crucial locations of the pathways, e.g. Dopamine uptake into vesicles, synaptic plasticity and calcium signaling, are involved in the Dopaminergic synapse (a) and glutamate receptors of AMPA and kainate types triggering neuronal excitability and synaptic plasticity in the Glutamatergic synapse (b), as illustrated by the boxes with red shading.

Discussion

In this study we compared gene expression in podocytes and brain and unveiled considerable overlap. Starting with genes expressed exclusively in UdPodocytes [13], [30] in comparison to SIX2-posive UdRPCs [19] we identified a plethora of genes over-represented in brain-associated GOs such as *synapses, synaptic signaling, neuron projections/axons* and *myelination*. Our in vitro model revealed expression of Nephrin (NPHS1) and axon-like projections from cells with synapses connecting to other cells upon differentiation of UdRPCs into UdPodocytes (Figure 1). The major function of NPHS1 as a cell adhesion molecule that functions in the glomerular filtration barrier in the kidney has been widely described [36]. Moreover, expression of NPHS1 has been identified in brain [31] where Putaala et al. conclude that it has a developmental role and is mainly expressed in radial glia cells [31] . Li et al. report Nephrin expression close to synaptic proteins in primary neuronal cells and co-immunoprecipitation with synaptic molecules including glutamate receptors and PSD95 and hypothesize that podocytes and brain cells use similar organization and signaling mechanisms [37].

bioRxiv preprint doi: https://doi.org/10.1101/2025.03.17.643629; this version posted March 17, 2025. The copyright holder for this preprint (which was not certified by peer review) is the author/funder. All rights reserved. No reuse allowed without permission.

One crucial player in the organization of foot processes and synapses is ACTN4, which bundles F-actin in the cytoskeleton and cross-links it to developing processes, in neurons and podocytes acting together in a network with glutamate receptors [38], [37]. These control the plasticity of dendritic spines in neurons in response to signaling events [38]. A corresponding mechanism of podocyte glutamatergic signaling participating in the integrity of the glomerular filtration barrier was reported by Giardino et al. who identified foot process effacement in a knock-out mouse model of Rab3a which regulates exocytosis of glutamate [5]. In our human UdPodocyte model, we found ACTN4 expression connecting the cytoskeleton of podocytes.

Another Actin-associated protein SYNPO, which is evident in the present transcriptome data, regulates the cytoskeleton in mature podocytes, where it is essential for the functioning of podocyte foot processes. Previous studies have shown that SYNPO also plays a role in the formation of spine apparatuses in spines of telencephalic neurons, which is involved in synaptic plasticity [8], [9]. Dendritic spines are small thorn-like protrusions found on the dendrites of most of the excitatory neurons in the brain. They are the point of contact between neurons, forming the post-synaptic side of the excitatory synapses, and orchestrate the molecular machinery that allows the transmission of signals from the afferent neurons [39], [40], [41], [42]. The stability of the spines is associated with SYNPO [43] , [44], [45], [46] . Studies have shown that deletion of SYNPO in mice results in deficits in spatial learning [47], [48] . Furthermore, podocytes lacking SYNPO acquire cytoskeletal alterations, which results in damage to the podocytes and disturbance of the foot processes and the slit diaphragm [49], [8] .

ACTN4, microtubule-associated proteins such as TUBB1 and MAPT (TAU) are cytoskeletal-associated proteins expressed in podocytes and down-regulated upon ANGII stimulation [13] TAU links actin and microtubule networks [50], [51] .

bioRxiv preprint doi: https://doi.org/10.1101/2025.03.17.643629; this version posted March 17, 2025. The copyright holder for this preprint (which was not certified by peer review) is the author/funder. All rights reserved. No reuse allowed without permission.

With respect to these partially similar signaling mechanisms in podocytes processes and neuronal synapses, Weide and Huber ask what is pre- and post-synaptic [52] refering to the publication of Giardino et al. who report Myosin IIA at post-synapses and in foot processes [5]. Moreover, Mundel and colleagues report Synaptopodin (SYNPO) at podocyte foot processes and dendritic spines [9] and Kobayashi and colleagues [6] find the typical postsynaptic density protein Densin localised in the cytoplasm beneath the slit membrane.

UdPodocytes constitute a promising model for studying cytoskeletal dynamics in healthy and diseased podocyte.

Genes such as *SERPINI1*, *RSPH1*, *KCNQ3* and *PAX*6 are also expressed in both brain and podocytes (Table S2). PAX6 is a crucial transcription factor associated with brain development and function. It has been shown to regulate genes associated with neural stem and progenitor cells. Studies have shown molecular interactions, such as the regulation of cell-cell adhesion or ion transport [53], [54].

PAX2 and PAX8 are crucial regulators of multiple steps of renal system development [55]. However, to date studies associating PAX6 function in nephrogenesis is lacking. SERPINI1 is a Serine protease inhibitor that inhibits plasminogen activators and plasmin but not thrombin [56], [57], [58], [59], [60]. It is involved in the formation or re-organization of synaptic connections as well as for synaptic plasticity in the adult nervous system and protects neurons from cell damage by tissue-type plasminogen activator and probably plays the same role in kidney.

The gene *KCNQ3,* encodes a potassium channel protein that functions in the regulation of neuronal excitability and is considered to be a key characteristic of activity-dependent synaptic plasticity of neurons [61]. One of the fundamental functions of renal K channels is their role in generating the cell-negative potential that provides one of the main driving forces for the passive movement of charged solutes and carrier molecules across the apical and basolateral membranes of tubule cells [62] .

In-depth analyses of the 600 brain-annotated genes expressed in UdPodocytes revealed GOs such as *excitatory synapse* and *AMPA glutamate receptor complex*. Amongst this list, GRIA3 has been reported

bioRxiv preprint doi: https://doi.org/10.1101/2025.03.17.643629; this version posted March 17, 2025. The copyright holder for this preprint (which was not certified by peer review) is the author/funder. All rights reserved. No reuse allowed without permission.

to be epigenetically down-regulated in podocytes under diabetic conditions [63]. Additionally, we found AMPA receptor over-represented among genes expressed in brain and podocytes and down-regulated upon ANGII stimulation of Upodocytes. AMPA belongs to the group of ionotropic glutamate receptors [64] and the same holds for NMDA receptors which are more intensively studied with regards to their role in regulating ion channels in podocytes [65], [66]. In comparison to neurons, NMDA receptors have overlapping and distinct features in podocytes, e.g. unlike in neurons they are resistant to activation by L-glutamate and L-aspartate and show minimal inactivation upon continuous NMDA supply, but similar to neurons they can be activated by D-aspartate and L-homocysteic acid [65]. Staruschenko et al. propose that NMDA receptors in podocytes are more adapted to slowly flowing metabolites in contrast to fast synaptic signaling processes. Our finding of AMPA receptor expression in podocytes together with Li et al's report of down-regulated AMPA-associated GRIA3 in podocytes under diabetic conditions [63] suggests that further studies investigating the role of AMPA receptors in podocyte physiology will be promising.

A body of publications describe ANGII signaling in the brain and beyond that a brain renin-angiotensin system which despite profound evidence [67], [68], [69] , [70] is also a subject of debate [70]. Persistent activation of ANGII signaling can lead to neurodegeneration and Angiotensin receptor blockers (ARBs) possess therapeutic potential [70]. Besides its role in regulating blood pressure, ANGII has also been reported to act as a neurotransmitter [71] which can interact with glutamate, possibly acting on glutamate receptors and also mediating increase of blood pressure, upon glutamate administration into the paraventricular nucleus (PVN).

We identified Calcium signaling as associated with the ANGII -down-regulated geneset. Greka and Mundel demonstrated that ANGII triggers - Calcium (Ca^{2+}) flow into podocytes via transient receptor potential canonical 6 (TRPC6) and TRPC5 channels and modulate actin cytoskeleton [72], by interacting with Ca^{2+}-activated phosphatase, Calcineurin, and Rho GTPases which are crucial determinants of podocyte function. Impairments in these channels e.g. by mutations in TRPC6 can lead

bioRxiv preprint doi: https://doi.org/10.1101/2025.03.17.643629; this version posted March 17, 2025. The copyright holder for this preprint (which was not certified by peer review) is the author/funder. All rights reserved. No reuse allowed without permission.

to Focal Segmental Glomerusclerosis (FSGS). Besides Calcium signaling, Hippo Signaling, cGMP-PKG signaling and axon guidance pathways were also over-represented. cGMP-bound ion channels regulate sodium uptake and excretion [73]. Chen et al. [74] described YAP and TAZ, as key players in Hippo signaling which are important for the integrity of podocytes and TAZ together with the transcription factor TEAD activate crucial podocyte-associated genes such as *SYNPO*, *ZO-1* and *ZO-2* (synaptopodin, zonula occludens-1, and zonula occludens-2). Interestingly, proteins from the axon guidance pathway were found to be associated with risk of end-stage kidney disease in diabetes [75] . The genes in our ANGII-down-regulated signature are all upstream of the actin-cytoskeleton-regulation complex within the axon guidance pathway thus pointing at down-regulation of actin cytoskeleton by ANGII treatment, in line with our previous publication showing ANGII-dependent downregulation of *NPHS1* and *SYNPO* and subsequent disruption of the podocyte cytoskeletal architecture [13]. Moreover, Shao et al. [76] revealed that HNF1B regulates axon guidance-associated genes in the developing mouse kidney and suggest that axon guidance ligand receptor pairs of neighboring cells, some also from the ureteric bud, may orchestrate kidney development via auto- and paracrine signaling. This may be underlined by Combes et al. 2019 [77] who found axon-guidance associated GDNF-RET ligand receptor crosstalk in single-cell analysis of the developing mouse kidney. Analysing the 600 UdPodocyte-specific genes in the axon guidance pathway revealed numerous ligand receptor pairs which regulate both actin cytoskeleton and are responsible for attraction and repulsion of projections. Tapia et al. [78] described the axon-guidance-associated protein-Semaphorin 3A (SEMA3A) as a repulsive gene leading to foot process effacement and proteinuria upon exogenous induction of SEMA3A. Additionally, Lu and Zhu [79] describe involvement of several Semaphorins in diabetic nephropathy and partially aberrant foot processes in Sema3G-deficient mice. Hashimoto et al. [80] described co-localization of the axon guidance receptor Ephrin-B1 with Nephrin at the slit diaphragm between neighboring foot processes during development and is down-regulated in nephropathy. Furthermore, Wu et al. [81] describe a major role of the axon guidance factors Slit2 and Robo2 in

bioRxiv preprint doi: https://doi.org/10.1101/2025.03.17.643629; this version posted March 17, 2025. The copyright holder for this preprint (which was not certified by peer review) is the author/funder. All rights reserved. No reuse allowed without permission.

podocyte attachment to the glomerular basement membrane and the structural integrity of foot processes. Taken together, it is tempting to speculate that foot processes partly use similar signaling mechanisms as axon guidance for their interdigitation and impairment of these signaling processes and lead to pathologically altered glomerular permeability.

In the follow-up analysis we identified abundant overlap of 344 genes expressed in common in UdPodocytes and in iPSC-derived brain and kidney organoids. The 344 genes expressed in common map to multiple brain regions with most hits in frontal cortex. As transcription factors enriched in the promoter regions of the 344 genes we found SUZ12 most significant (p=8.42x10-22, EnrichR ENCODE and CHEA datasets), NFKB1 (p=2.29x10-3, EnrichR TRANSFAC and JASPAR) and PAX2 (p=1.59x10-3, EnrichR TTRUST). Mapping genes to the GO Molecular Function top category showed that about 70% of the 344 genes are associated with binding activity while about 25% are associated with catalytic activity.

Of note, we identified Brain-derived neurotrophic factor (BDNF) as central protein in one module associated with “pre-synapse” within our protein interaction network of brain-associated UdPodocyte genes (Figure 4a,c). Besides the brain-associated roles of BDNF in synaptic plasticity, learning, memory, behavior, depression and neurodegenerative disorders such as Alzheimer’s disease [82], Endlich and colleagues proposed BDNF as marker for CKD. They found a strong correlation of BDNF expression with the podocyte marker Nephrin, the kidney injury marker KIM-1 and the urinary albumin-to-creatinine ratio in CKD patients [83] . Putatively connected to BDNF’s role in podocyte development, the authors showed de-differentiation of podocytes upon BDNF inhibition. Furthermore, Saito and colleagues reported another protein from this module, Neurexin-1 (NRXN1) known as presynaptic adhesion molecule associated with synaptic differentiation, expressed at the podocyte slit diaphragm, co-localized with Nephrin and CD2AP, and proposed it as marker of podocyte injury [84]. SNAP25, a further protein of this module, as well as BDNF were shown to be correlated with the

bioRxiv preprint doi: https://doi.org/10.1101/2025.03.17.643629; this version posted March 17, 2025. The copyright holder for this preprint (which was not certified by peer review) is the author/funder. All rights reserved. No reuse allowed without permission.

Parkinson's Disease (PD) -associated protein Parkin (PARK2), putatively via ubiquination of p21 and JNK, and inhibition of PARK2 led to down-regulation of BDNF and SNAP25 and impaired neural stem cell differentiation [85]. A study revealing an association between PD and impaired glomerular filtration [86] may be seen in this context.

We conclude that our study has revealed similarities between the transcriptomes of brain and podocytes which can be condensed into gene networks regulating (i) projections such as foot processes, axons and denritic spines implicating modulation of actin cytoskeleton and (ii) signaling pathways such as Calcium-, Hippo- and cGMP- signaling happening at synaptic (e.g. glutamatergic, dopaminergic) or resembling constellations such as the slit diaphragm between interdigitating foot processes.
Interestingly, axon guidance was found as most significant pathway in response to ANG II stimulation of podocytes which might point at similar mechanisms guiding axons and foot processes in kidney development and disease. This was in fact underlined by reports on ligand-receptor crosstalk of axon guidance molecules (GDNF-RET) for the developing kidney and association of axon guidance molecules with risk of end-stage kidney disease in diabetes [79], [87] .
Interestingly, many of the brain-associated biological processes are currently not annotated for kidney. This points to the comparative lack of advancement in the annotation of kidney associated processes. We therefore propose our urine-derived podocyte platform as a non-invasive and easily accessible in vitro model enabling the investigation of the functions of these brain-associated genes and biological processes in healthy and diseased kidneys.

Author contributions

WW and CT analysed the data and wrote the manuscript. JA supervised the work, co-wrote the manuscript and gave the final approval. We thank Leon Szepanowski and Abida Islam Pranty for designing the primers used in this study.

bioRxiv preprint doi: https://doi.org/10.1101/2025.03.17.643629; this version posted March 17, 2025. The copyright holder for this preprint (which was not certified by peer review) is the author/funder. All rights reserved. No reuse allowed without permission.

Competing interests

The authors declare no competing interests.

Acknowledgments

James Adjaye acknowledges financial support from the Medical faculty of the Heinrich-Heine University, Duesseldorf. We thank Prof. Moin Saleem for providing the human kidney-biopsy derived immortalized podocyte cell line used in this study

Data availability

No datasets were generated in the current study. The datasets used for the meta-analysis are available at the National Center for Biotechnology Information (NCBI) Gene expression Omnibus (GEO) accessions referred to in Table 1.

References

1. DiBona GF. Physiology in perspective: *The Wisdom of the Body.* Neural control of the kidney. Am J Physiol-Regul Integr Comp Physiol. 2005;289:R633–41.

2. Cao W, Yang Z, Liu X, Ren S, Su H, Yang B, et al. A kidney-brain neural circuit drives progressive kidney damage and heart failure. Signal Transduct Target Ther. 2023;8:184.

3. Kobayashi A, Valerius MT, Mugford JW, Carroll TJ, Self M, Oliver G, et al. Six2 Defines and Regulates a Multipotent Self-Renewing Nephron Progenitor Population throughout Mammalian Kidney Development. Cell Stem Cell. 2008;3:169–81.

4. Bejoy J, Qian ES, Woodard LE. Accelerated protocol for the differentiation of podocytes from human pluripotent stem cells. STAR Protoc. 2021;2:100898.

5. Giardino L, Armelloni S, Corbelli A, Mattinzoli D, Zennaro C, Guerrot D, et al. Podocyte Glutamatergic Signaling Contributes to the Function of the Glomerular Filtration Barrier. J Am Soc Nephrol. 2009;20:1929–40.

bioRxiv preprint doi: https://doi.org/10.1101/2025.03.17.643629; this version posted March 17, 2025. The copyright holder for this preprint (which was not certified by peer review) is the author/funder. All rights reserved. No reuse allowed without permission.

6. Kobayashi N, Gao S, Chen J, Saito K, Miyawaki K, Li C, et al. Process formation of the renal glomerular podocyte: Is there common molecular machinery for processes of podocytes and neurons? Anat Sci Int. 2004;79:1–10.

7. Armelloni S, Corbelli A, Giardino L, Li M, Ikehata M, Mattinzoli D, et al. Podocytes: recent biomolecular developments. Biomol Concepts. 2014;5:319–30.

8. Ning L, Suleiman HY, Miner JH. Synaptopodin Is Dispensable for Normal Podocyte Homeostasis but Is Protective in the Context of Acute Podocyte Injury. J Am Soc Nephrol. 2020;31:2815–32.

9. Mundel P, Heid HW, Mundel TM, Krüger M, Reiser J, Kriz W. Synaptopodin: An Actin-associated Protein in Telencephalic Dendrites and Renal Podocytes. J Cell Biol. 1997;139:193–204.

10. Jabbari B, Vaziri ND. The nature, consequences, and management of neurological disorders in chronic kidney disease. Hemodial Int. 2018;22:150–60.

11. Boyer O, Nevo F, Plaisier E, Funalot B, Gribouval O, Benoit G, et al. *INF2* Mutations in Charcot–Marie–Tooth Disease with Glomerulopathy. N Engl J Med. 2011;365:2377–88.

12. Viggiano D, Bruchfeld A, Carriazo S, De Donato A, Endlich N, Ferreira AC, et al. Brain dysfunction in tubular and tubulointerstitial kidney diseases. Nephrol Dial Transplant. 2021;37 Supplement_2:ii46–55.

13. Erichsen L, Thimm C, Bohndorf M, Rahman MS, Wruck W, Adjaye J. Activation of the Renin–Angiotensin System Disrupts the Cytoskeletal Architecture of Human Urine-Derived Podocytes. Cells. 2022;11:1095.

14. Rahman MS, Spitzhorn L-S, Wruck W, Hagenbeck C, Balan P, Graffmann N, et al. The presence of human mesenchymal stem cells of renal origin in amniotic fluid increases with gestational time. Stem Cell Res Ther. 2018;9:113.

15. Saleem MA, O'Hare MJ, Reiser J, Coward RJ, Inward CD, Farren T, et al. A Conditionally Immortalized Human Podocyte Cell Line Demonstrating Nephrin and Podocin Expression. J Am Soc Nephrol. 2002;13:630–8.

16. Nguyen L, Wruck W, Erichsen L, Graffmann N, Adjaye J. The Nephrotoxin Puromycin Aminonucleoside Induces Injury in Kidney Organoids Differentiated from Induced Pluripotent Stem Cells. Cells. 2022;11:635.

17. Martins S, Erichsen L, Datsi A, Wruck W, Goering W, Chatzantonaki E, et al. Impaired p53-Mediated DNA Damage Response Contributes to Microcephaly in Nijmegen Breakage Syndrome Patient-Derived Cerebral Organoids. Cells. 2022;11:802.

18. Lonsdale J, Thomas J, Salvatore M, Phillips R, Lo E, Shad S, et al. The Genotype-Tissue Expression (GTEx) project. Nat Genet. 2013;45:580–5.

19. Rahman MS, Wruck W, Spitzhorn L-S, Nguyen L, Bohndorf M, Martins S, et al. The FGF, TGFβ and WNT axis Modulate Self-renewal of Human SIX2+ Urine Derived Renal Progenitor Cells. Sci Rep. 2020;10:739.

bioRxiv preprint doi: https://doi.org/10.1101/2025.03.17.643629; this version posted March 17, 2025. The copyright holder for this preprint (which was not certified by peer review) is the author/funder. All rights reserved. No reuse allowed without permission.

20. Chen H, Boutros PC. VennDiagram: a package for the generation of highly-customizable Venn and Euler diagrams in R. BMC Bioinformatics. 2011;12:35.

21. Gentleman RC, Carey VJ, Bates DM, Bolstad B, Dettling M, Dudoit S, et al. Bioconductor: open software development for computational biology and bioinformatics. Genome Biol. 2004;5:R80.

22. Graffmann N, Ring S, Kawala M-A, Wruck W, Ncube A, Trompeter H-I, et al. Modeling Nonalcoholic Fatty Liver Disease with Human Pluripotent Stem Cell-Derived Immature Hepatocyte-Like Cells Reveals Activation of PLIN2 and Confirms Regulatory Functions of Peroxisome Proliferator-Activated Receptor Alpha. Stem Cells Dev. 2016;25:1119–33.

23. Falcon S, Gentleman R. Using GOstats to test gene lists for GO term association. Bioinforma Oxf Engl. 2007;23:257–8.

24. Kuleshov MV, Jones MR, Rouillard AD, Fernandez NF, Duan Q, Wang Z, et al. Enrichr: a comprehensive gene set enrichment analysis web server 2016 update. Nucleic Acids Res. 2016;44:W90-97.

25. Oughtred R, Stark C, Breitkreutz B-J, Rust J, Boucher L, Chang C, et al. The BioGRID interaction database: 2019 update. Nucleic Acids Res. 2019;47:D529–41.

26. Szklarczyk D, Franceschini A, Wyder S, Forslund K, Heller D, Huerta-Cepas J, et al. STRING v10: protein-protein interaction networks, integrated over the tree of life. Nucleic Acids Res. 2015;43 Database issue:D447-452.

27. Shannon P, Markiel A, Ozier O, Baliga NS, Wang JT, Ramage D, et al. Cytoscape: A Software Environment for Integrated Models of Biomolecular Interaction Networks. Genome Res. 2003;13:2498–504.

28. Bader GD, Hogue CWV. An automated method for finding molecular complexes in large protein interaction networks. BMC Bioinformatics. 2003;4:2.

29. Wickham H. Ggplot2: elegant graphics for data analysis. New York: Springer; 2009.

30. Thimm C, Erichsen L, Wruck W, Adjaye J. Unveiling Angiotensin II and Losartan-Induced Gene Regulatory Networks Using Human Urine-Derived Podocytes. Int J Mol Sci. 2023;24:10551.

31. Putaala H. The murine nephrin gene is specifically expressed in kidney, brain and pancreas: inactivation of the gene leads to massive proteinuria and neonatal death. Hum Mol Genet. 2001;10:1–8.

32. Uhlén M, Fagerberg L, Hallström BM, Lindskog C, Oksvold P, Mardinoglu A, et al. Tissue-based map of the human proteome. Science. 2015;347:1260419.

33. Erichsen L, Kloss LDF, Thimm C, Bohndorf M, Schichel K, Wruck W, et al. Derivation of the Immortalized Cell Line UM51-PrePodo-hTERT and Its Responsiveness to Angiotensin II and Activation of the RAAS Pathway. Cells. 2023;12:342.

34. Jin X, Muntean BS, Aal-Aaboda MS, Duan Q, Zhou J, Nauli SM. L-type calcium channel modulates cystic kidney phenotype. Biochim Biophys Acta BBA - Mol Basis Dis. 2014;1842:1518–26.

35. Kuo IY, Ehrlich BE. Ion Channels in Renal Disease. Chem Rev. 2012;112:6353–72.

bioRxiv preprint doi: https://doi.org/10.1101/2025.03.17.643629; this version posted March 17, 2025. The copyright holder for this preprint (which was not certified by peer review) is the author/funder. All rights reserved. No reuse allowed without permission.

36. Martin CE, Jones N. Nephrin Signaling in the Podocyte: An Updated View of Signal Regulation at the Slit Diaphragm and Beyond. Front Endocrinol. 2018;9.

37. Li M, Armelloni S, Ikehata M, Corbelli A, Pesaresi M, Calvaresi N, et al. Nephrin expression in adult rodent central nervous system and its interaction with glutamate receptors: Nephrin in neurons and podocytes. J Pathol. 2011;225:118–28.

38. Kalinowska M, Chávez AE, Lutzu S, Castillo PE, Bukauskas FF, Francesconi A. Actinin-4 Governs Dendritic Spine Dynamics and Promotes Their Remodeling by Metabotropic Glutamate Receptors. J Biol Chem. 2015;290:15909–20.

39. Gray EG. Electron Microscopy of Synaptic Contacts on Dendrite Spines of the Cerebral Cortex. Nature. 1959;183:1592–3.

40. Hering H, Sheng M. Dentritic spines : structure, dynamics and regulation. Nat Rev Neurosci. 2001;2:880–8.

41. Nimchinsky EA, Sabatini BL, Svoboda K. Structure and Function of Dendritic Spines. Annu Rev Physiol. 2002;64:313–53.

42. McKinney RA. Excitatory amino acid involvement in dendritic spine formation, maintenance and remodelling. J Physiol. 2010;588:107–16.

43. Deller T, Mundel P, Frotscher M. Potential role of synaptopodin in spine motility by coupling actin to the spine apparatus. Hippocampus. 2000;10:569–81.

44. Korkotian E, Segal M. Synaptopodin regulates release of calcium from stores in dendritic spines of cultured hippocampal neurons. J Physiol. 2011;589:5987–95.

45. Perez-Alvarez A, Yin S, Schulze C, Hammer JA, Wagner W, Oertner TG. Endoplasmic reticulum visits highly active spines and prevents runaway potentiation of synapses. Nat Commun. 2020;11:5083.

46. Yap K, Drakew A, Smilovic D, Rietsche M, Paul MH, Vuksic M, et al. The actin-modulating protein synaptopodin mediates long-term survival of dendritic spines. eLife. 2020;9:e62944.

47. Deller T, Korte M, Chabanis S, Drakew A, Schwegler H, Stefani GG, et al. Synaptopodin-deficient mice lack a spine apparatus and show deficits in synaptic plasticity. Proc Natl Acad Sci. 2003;100:10494–9.

48. Jedlicka P, Vlachos A, Schwarzacher SW, Deller T. A role for the spine apparatus in LTP and spatial learning. Behav Brain Res. 2008;192:12–9.

49. Rüster C, Wolf G. Renin-Angiotensin-Aldosterone System and Progression of Renal Disease. J Am Soc Nephrol. 2006;17:2985–91.

50. Elie A, Prezel E, Guérin C, Denarier E, Ramirez-Rios S, Serre L, et al. Tau co-organizes dynamic microtubule and actin networks. Sci Rep. 2015;5:9964.

51. Schell C, Huber TB. The Evolving Complexity of the Podocyte Cytoskeleton. J Am Soc Nephrol JASN. 2017;28:3166–74.

bioRxiv preprint doi: https://doi.org/10.1101/2025.03.17.643629; this version posted March 17, 2025. The copyright holder for this preprint (which was not certified by peer review) is the author/funder. All rights reserved. No reuse allowed without permission.

52. Weide T, Huber TB. Signaling at the Slit: Podocytes Chat by Synaptic Transmission. J Am Soc Nephrol. 2009;20:1862–4.

53. Kikkawa T, Casingal CR, Chun SH, Shinohara H, Hiraoka K, Osumi N. The role of Pax6 in brain development and its impact on pathogenesis of autism spectrum disorder. Brain Res. 2019;1705:95–103.

54. Osumi N, Shinohara H, Numayama-Tsuruta K, Maekawa M. Concise Review: Pax6 Transcription Factor Contributes to both Embryonic and Adult Neurogenesis as a Multifunctional Regulator. Stem Cells. 2008;26:1663–72.

55. Sharma R, Sanchez-Ferras O, Bouchard M. Pax genes in renal development, disease and regeneration. Semin Cell Dev Biol. 2015;44:97–106.

56. Belorgey D, Crowther DC, Mahadeva R, Lomas DA. Mutant Neuroserpin (S49P) that causes familial encephalopathy with neuroserpin inclusion bodies is a poor proteinase inhibitor and readily forms polymers in vitro. J Biol Chem. 2002;277:17367–73.

57. Ricagno S, Caccia S, Sorrentino G, Antonini G, Bolognesi M. Human neuroserpin: structure and time-dependent inhibition. J Mol Biol. 2009;388:109–21.

58. Takehara S, Onda M, Zhang J, Nishiyama M, Yang X, Mikami B, et al. The 2.1-A crystal structure of native neuroserpin reveals unique structural elements that contribute to conformational instability. J Mol Biol. 2009;388:11–20.

59. Noto R, Randazzo L, Raccosta S, Caccia S, Moriconi C, Miranda E, et al. The stability and activity of human neuroserpin are modulated by a salt bridge that stabilises the reactive centre loop. Sci Rep. 2015;5:13666.

60. Osterwalder T, Cinelli P, Baici A, Pennella A, Krueger SR, Schrimpf SP, et al. The axonally secreted serine proteinase inhibitor, neuroserpin, inhibits plasminogen activators and plasmin but not thrombin. J Biol Chem. 1998;273:2312–21.

61. Fitzsimmons SMDD, Oostra E, Postma TS, van der Werf YD, van den Heuvel OA. Repetitive Transcranial Magnetic Stimulation–Induced Neuroplasticity and the Treatment of Psychiatric Disorders: State of the Evidence and Future Opportunities. Biol Psychiatry. 2024;95:592–600.

62. Gurkan S, Estilo GK, Wei Y, Satlin LM. Potassium transport in the maturing kidney. Pediatr Nephrol Berl Ger. 2007;22:915–25.

63. Li Z, Chen H, Zhong F, Zhang W, Lee K, He JC. Expression of Glutamate Receptor Subtype 3 Is Epigenetically Regulated in Podocytes under Diabetic Conditions. Kidney Dis. 2019;5:34–42.

64. Watkins JC, Jane DE. The glutamate story. Br J Pharmacol. 2006;147.

65. Staruschenko A, Ma R, Palygin O, Dryer SE. Ion channels and channelopathies in glomeruli. Physiol Rev. 2023;103:787–854.

66. Anderson M, Suh JM, Kim EY, Dryer SE. Functional NMDA receptors with atypical properties are expressed in podocytes. Am J Physiol-Cell Physiol. 2011;300:C22–32.

bioRxiv preprint doi: https://doi.org/10.1101/2025.03.17.643629; this version posted March 17, 2025. The copyright holder for this preprint (which was not certified by peer review) is the author/funder. All rights reserved. No reuse allowed without permission.

67. Ganten D, Minnich JL, Grenger P, Hayduk K, Brecht HM, Barbeau A, et al. Angiotensin-Forming Enzyme in Brain Tissue. Science. 1971;173:64–5.

68. Wright JW, Harding JW. The brain renin-angiotensin system: a diversity of functions and implications for CNS diseases. Pflugers Arch. 2013;465:133–51.

69. McKinley MJ, Albiston AL, Allen AM, Mathai ML, May CN, McAllen RM, et al. The brain renin–angiotensin system: location and physiological roles. Int J Biochem Cell Biol. 2003;35:901–18.

70. Forrester SJ, Booz GW, Sigmund CD, Coffman TM, Kawai T, Rizzo V, et al. Angiotensin II Signal Transduction: An Update on Mechanisms of Physiology and Pathophysiology. Physiol Rev. 2018;98:1627–738.

71. Ferguson AV, Washburn DLS. Angiotensin II:A peptidergic neurotransmitter in central autonomic pathways. Prog Neurobiol. 1998;54:169–92.

72. Greka A, Mundel P. Balancing calcium signals through TRPC5 and TRPC6 in podocytes. J Am Soc Nephrol JASN. 2011;22:1969–80.

73. Chen Y, Burnett J. Particulate Guanylyl Cyclase A/cGMP Signaling Pathway in the Kidney: Physiologic and Therapeutic Indications. Int J Mol Sci. 2018;19:1006.

74. Chen J, Wang X, He Q, Harris RC. TAZ is important for maintenance of the integrity of podocytes. Am J Physiol-Ren Physiol. 2022;322:F419–28.

75. Satake E, Saulnier P-J, Kobayashi H, Gupta MK, Looker HC, Wilson JM, et al. Comprehensive Search for Novel Circulating miRNAs and Axon Guidance Pathway Proteins Associated with Risk of ESKD in Diabetes. J Am Soc Nephrol. 2021;32:2331–51.

76. Shao A, Gearhart MD, Chan SC, Miao Z, Susztak K, Igarashi P. Multiomics analysis reveals that hepatocyte nuclear factor 1β regulates axon guidance genes in the developing mouse kidney. Sci Rep. 2022;12:17586.

77. Combes AN, Phipson B, Lawlor KT, Dorison A, Patrick R, Zappia L, et al. Single cell analysis of the developing mouse kidney provides deeper insight into marker gene expression and ligand-receptor crosstalk. Development. 2019;146:dev178673.

78. Tapia R, Guan F, Gershin I, Teichman J, Villegas G, Tufro A. Semaphorin3a disrupts podocyte foot processes causing acute proteinuria. Kidney Int. 2008;73:733–40.

79. Lu Q, Zhu L. The Role of Semaphorins in Metabolic Disorders. Int J Mol Sci. 2020;21:5641.

80. Hashimoto T, Karasawa T, Saito A, Miyauchi N, Han GD, Hayasaka K, et al. Ephrin-B1 localizes at the slit diaphragm of the glomerular podocyte. Kidney Int. 2007;72:954–64.

81. Wu M-F, Liao C-Y, Wang L-Y, Chang JT. The role of Slit-Robo signaling in the regulation of tissue barriers. Tissue Barriers. 2017;5:e1331155.

82. Afsar B, Afsar RE. Brain-derived neurotrophic factor (BDNF): a multifaceted marker in chronic kidney disease. Clin Exp Nephrol. 2022;26:1149–59.

bioRxiv preprint doi: https://doi.org/10.1101/2025.03.17.643629; this version posted March 17, 2025. The copyright holder for this preprint (which was not certified by peer review) is the author/funder. All rights reserved. No reuse allowed without permission.

83. Endlich N, Lange T, Kuhn J, Klemm P, Kotb AM, Siegerist F, et al. *BDNF* : mRNA expression in urine cells of patients with chronic kidney disease and its role in kidney function. J Cell Mol Med. 2018;22:5265–77.

84. Saito A, Miyauchi N, Hashimoto T, Karasawa T, Han GD, Kayaba M, et al. Neurexin-1, a presynaptic adhesion molecule, localizes at the slit diaphragm of the glomerular podocytes in kidneys. Am J Physiol-Regul Integr Comp Physiol. 2011;300:R340–8.

85. Park MH, Lee H-J, Lee HL, Son DJ, Ju JH, Hyun BK, et al. Parkin Knockout Inhibits Neuronal Development via Regulation of Proteasomal Degradation of p21. Theranostics. 2017;7:2033–45.

86. Peng H, Wu L, Chen Q, Chen S, Wu S, Shi X, et al. Association between kidney function and Parkinson's disease risk: a prospective study from the UK Biobank. BMC Public Health. 2024;24:2225.

87. The GENIE Consortium, The FinnDiane Study Group, Sambo F, Malovini A, Sandholm N, Stavarachi M, et al. Novel genetic susceptibility loci for diabetic end-stage renal disease identified through robust naive Bayes classification. Diabetologia. 2014;57:1611–22.

Supplementary Material

Supplementary Table 1 (tableS1.xlsx): significantly over-represented GOs in the 600 genes subset only expressed in UdPodocytes from the Venn diagram of UdPodocytes vs. UdRPCs filtered for neuronal terms

Supplementary Table 2 (tableS2.xlsx): (a) subsets from the Venn diagram comparing the 600 genes exclusively expressed in UdPodocytes with genes expressed in kidney and brain organoids. (b) Significantly over-represented GOs in the 344 genes subset expressed in common in UdPodocytes and brain and kidney organoids. (c) enriched transcription factors (TFs) found via the EnrichR analysis of the 344 genes using the ENCODE_and_ChEA dataset. (d) enriched TFs found via the EnrichR analysis of the 344 genes using the TRANSFAC_and_JASPAR dataset. (e) enriched TFs found via the EnrichR analysis of the 344 genes using the TRRUST dataset. (f) 20 most abundant GO Molecular Function (MF) terms amongst the 344 genes. (g) Metascape

bioRxiv preprint doi: https://doi.org/10.1101/2025.03.17.643629; this version posted March 17, 2025. The copyright holder for this preprint (which was not certified by peer review) is the author/funder. All rights reserved. No reuse allowed without permission.

enrichment analysis results of genes in (f). (h) TFs from (f) validated for expression in kidney via the Proteinatlas.

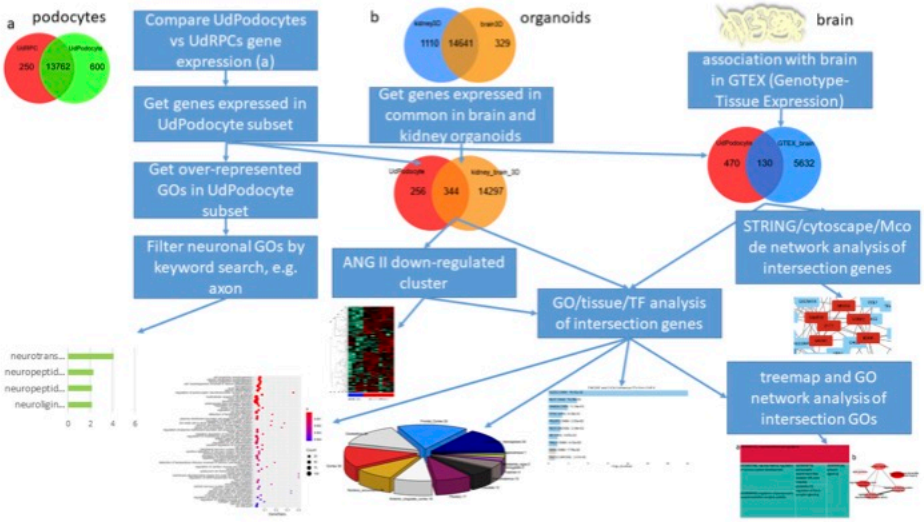
Supplementary Table 3 (tableS3.xlsx): (a) subsets from the Venn diagram comparing the 600 genes exclusively expressed in UdPodocytes with genes expressed in brain in the GTEX database. (b) Significantly over-represented GOs in the 130 genes subset expressed in common in UdPodocytes and GTEX brain

Supplementary Table 4 (tableS4.xlsx): (a) Significantly over-represented GOs in the genes down-regulated upon ANGII treatment amongst the 344 genes expressed in common in UdPodocytes and brain and kidney organoids. (b) GO terms in (a) filtered by neuronal and brain-related key words listed at the bottom of the sheet.

Supplementary Table 5 (tableS5.xlsx): Antibodies used in this study.

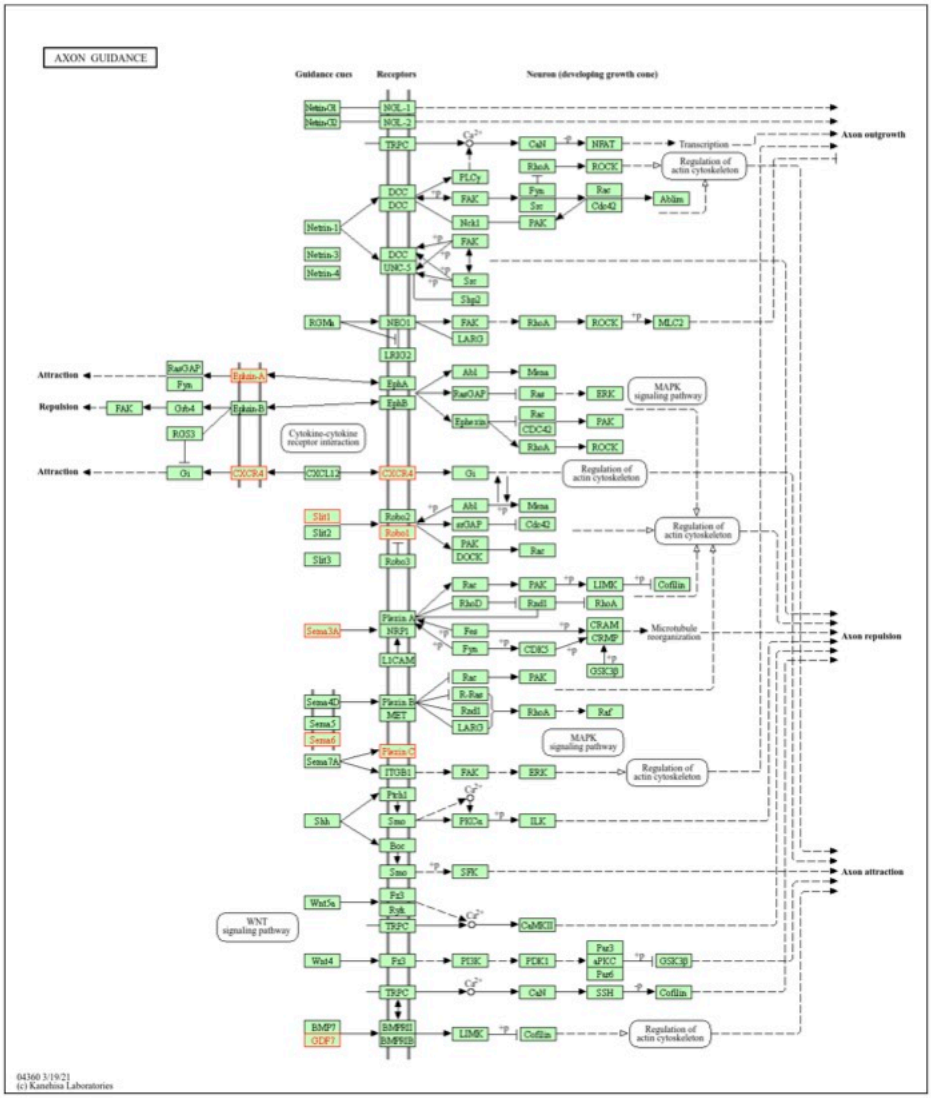
Supplementary Table 6 (tableS6.docx): Primer sequences used in this study.

Supplementary Figures



bioRxiv preprint doi: https://doi.org/10.1101/2025.03.17.643629; this version posted March 17, 2025. The copyright holder for this preprint (which was not certified by peer review) is the author/funder. All rights reserved. No reuse allowed without permission.

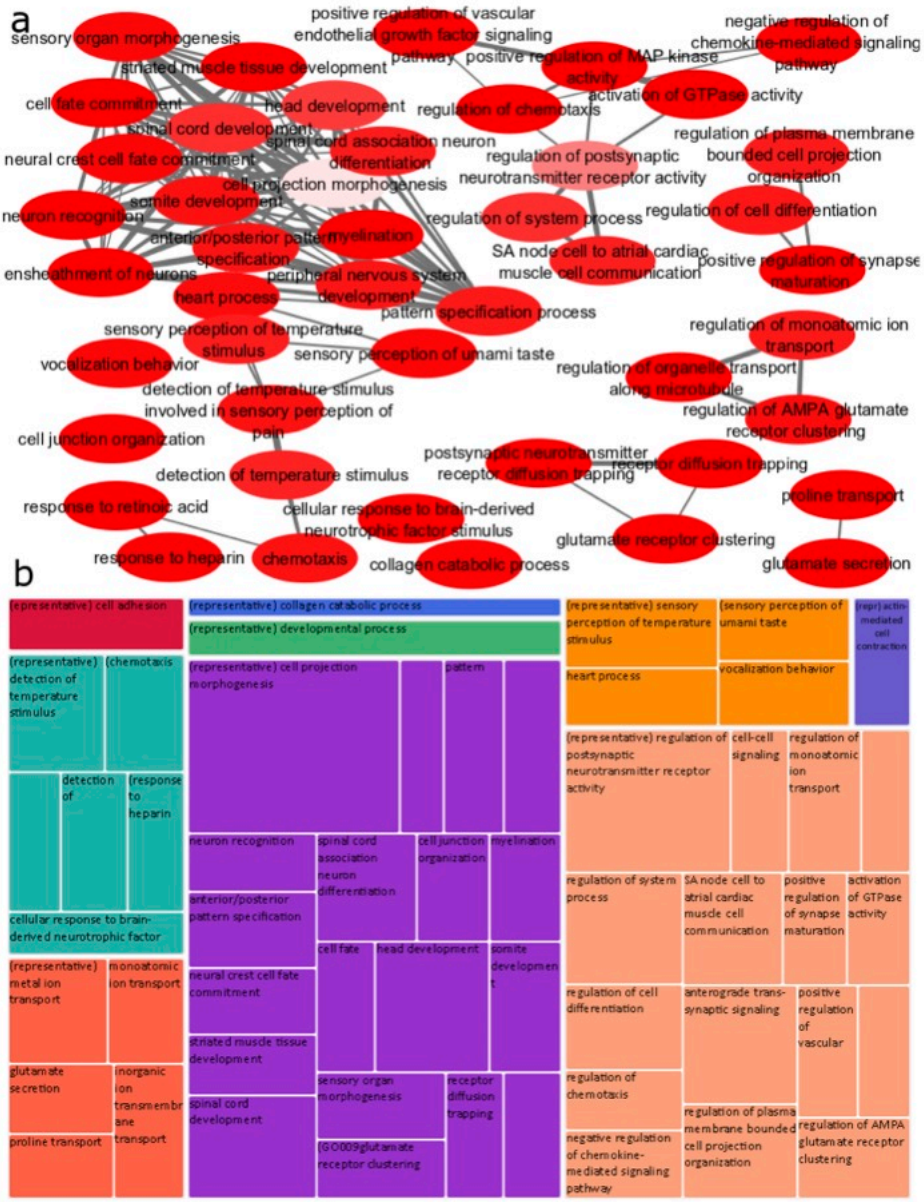
Figure S1: Flow chart of the comparison between brain and podocytes.



bioRxiv preprint doi: https://doi.org/10.1101/2025.03.17.643629; this version posted March 17, 2025. The copyright holder for this preprint (which was not certified by peer review) is the author/funder. All rights reserved. No reuse allowed without permission.

Figure S2: Genes related to the GO term "axon guidance", the most significantly over-represented biological process in the 600 genes exclusively expressed in urine-derived Podocytes (UdPodocytes), marked within the KEGG pathway chart of axon guidance (hsa04360). Several guidance factors, such as ephrins, Slits, and semaphorins are expressed in the UdPodocytes. These ligands and receptors are responsible for the regulation of the actin cytoskeleton on the one hand and on the other hand for attraction of the projection while genes responsible for repulsion are missing. Genes exclusively expressed in the UdPodocytes are marked in red.

bioRxiv preprint doi: https://doi.org/10.1101/2025.03.17.643629; this version posted March 17, 2025. The copyright holder for this preprint (which was not certified by peer review) is the author/funder. All rights reserved. No reuse allowed without permission.



bioRxiv preprint doi: https://doi.org/10.1101/2025.03.17.643629; this version posted March 17, 2025. The copyright holder for this preprint (which was not certified by peer review) is the author/funder. All rights reserved. No reuse allowed without permission.

Figure S3: Overlap between biological processes in urine-derived Podocytes (UdPodocytes) with brain and kidney organoids (344 genes) relates to cell projection morphogenesis and regulation of postsynaptic neurotransmitter receptor activity. (a) The gene ontology network was generated with the tools REVIGO and Cytoscape and summarizes GO-BP (Gene ontologies - Biological Process) terms found over-represented with a p-value < 0.01 in the 344 genes overlapping between UdPodocytes and brain and kidney organoids. Cell projection morphogenesis and regulation of postsynaptic neurotransmitter receptor activity -related terms emerged as representative for their clusters. GOs are represented by the network nodes with light red associated with the highest significance of over-representation of a GO term. The edges refer to similarities between the GO terms. (b) Treemap of the REVIGO tool corresponding to (a) summarizing biological process overlapping between UdPodocytes and brain and kidney organoids.

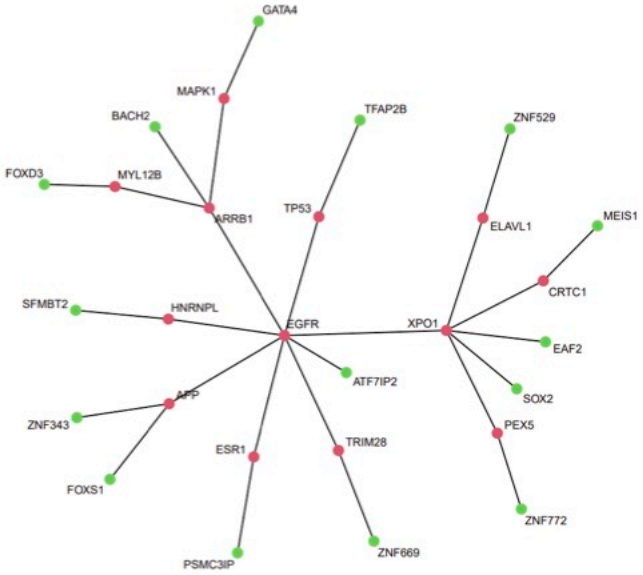
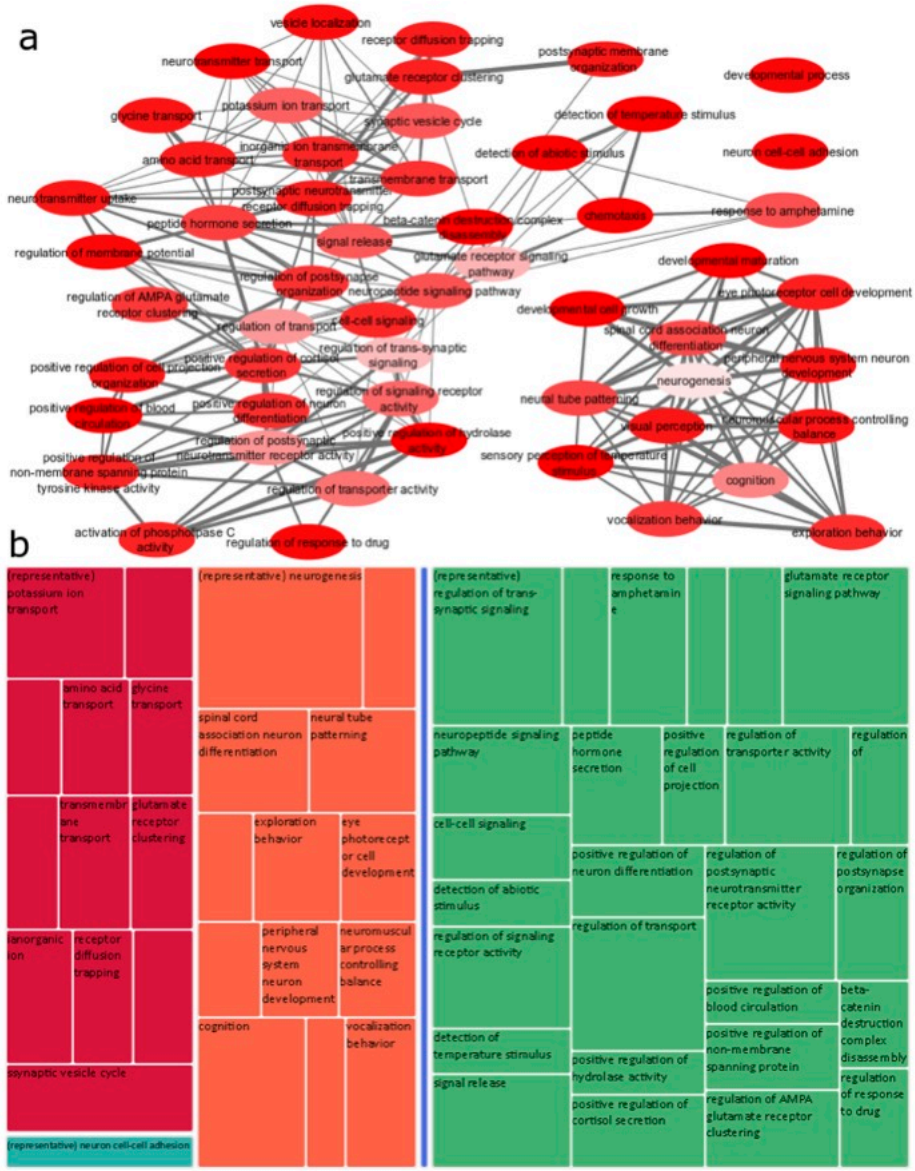


Figure S4: Protein interaction network of Proteinatlas-validated Transcription Factors (TFs) amongst the 344 genes subset expressed in common in UdPodocytes and brain and kidney

bioRxiv preprint doi: https://doi.org/10.1101/2025.03.17.643629; this version posted March 17, 2025. The copyright holder for this preprint (which was not certified by peer review) is the author/funder. All rights reserved. No reuse allowed without permission.

organoids. The TFs validated for expression in the kidney via the Proteinatlas could be connected in a protein interaction network of Biogrid interactions using EGFR and XPO1 as major hubs. Green nodes are the original TFs and red nodes were added via Biogrid interactions.

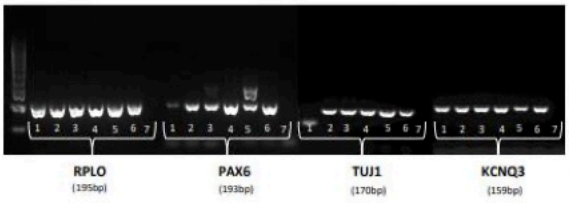
bioRxiv preprint doi: https://doi.org/10.1101/2025.03.17.643629; this version posted March 17, 2025. The copyright holder for this preprint (which was not certified by peer review) is the author/funder. All rights reserved. No reuse allowed without permission.



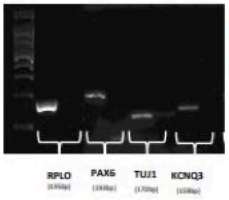
bioRxiv preprint doi: https://doi.org/10.1101/2025.03.17.643629; this version posted March 17, 2025. The copyright holder for this preprint (which was not certified by peer review) is the author/funder. All rights reserved. No reuse allowed without permission.

Figure S5: Overlap between biological processes in urine-derived Podocytes (UdPodocytes) with genes associated with brain in Genotype-Tissue Expression GTEX (130 genes) relates to neurogenesis and regulation of trans-synaptic signaling. (a) The gene ontology network was generated with the tools REVIGO and Cytoscape and summarizes GO-BP (Gene ontologies - Biological Process) terms found over-represented with a p-value < 0.01 in the 130 genes overlapping between UdPodocytes and genes associated with brain in GTEX. Neurogenesis and regulation of trans-synaptic signaling -related terms emerged as representative for their clusters. GOs are represented by the network nodes with light red associated with the highest significance of over-representation of a GO term. The edges refer to similarities between the GO terms. (b) Treemap of the REVIGO tool corresponding to (a) summarizing biological process overlapping between UdPodocytes and brain and kidney organoids.

bioRxiv preprint doi: https://doi.org/10.1101/2025.03.17.643629; this version posted March 17, 2025. The copyright holder for this preprint (which was not certified by peer review) is the author/funder. All rights reserved. No reuse allowed without permission.



Legend:
1. Kidney biopsy
2. UF21 podocyte
3. UM27 podocyte
4. UM48 podocyte
5. UM51 podocyte
6. Fetal brain
7. H_2O



Legend:
1. Human immortal podocyte (AB 8/13)
2. H_2O

Figure S6: RT-PCR measurements of genes expressed in brain and podocytes.

(**A**) RT-PCR measurements of genes *RPLO, PAX6, TUJ1* and *KCNQ3* expressed in brain and podocytes, 1: kidney biopsy, 2: UF21 podocyte, 3: UM27 podocyte, 4: UM48 podocyte, 5: UM51 podocyte, 6: fetal brain, 7: H_2O. Ribosomal protein lateral stalk subunit P0 (RPL0) was used as a housekeeping gene. (**B**) PCR measurements of the genes *RPLO, PAX6, TUJ1* and *KCNQ3* expressed in the human immortal podocyte line (AB 8/13). The loading scheme was as follows: 1. human immortal podocyte line (AB 8/13) and 2. H_2O. For normalization, RPL0 was used.

Figure S7: Protein expression from the Protein Atlas for the relevant proteins (figS7_Proteinatlas_podobrain.pdf).

Figure S8: Complete images of Western Blot analyses of brain-associated proteins expressed in human podocytes (figS8_WB_uncropped.pdf).

3.10 Urinary proteins from Sickle Cell patients induce inflammation and kidney injury via the TGFβ-p53 axis in a podocyte cell culture model.

Wasco Wruck[#], Abida Islam Pranty[#], **Chantelle Thimm[#]**, Christiane Loerch, Rosanne Mack, Theresa Koranteng-Adjaye, Vincent Boima, Yvonne Dei-Adomakoh, Margaret Lartey and James Adjaye

BioRxiv, 2025

Abstract

Background

Sickle cell disease (SCD) is an inherited blood disorder affecting the oxygen-carrying hemoglobin in red blood cells making them deform into a sickle shape. Hemolysis and vaso-occlusion associated with this process can lead to complications in many organs and frequently to renal complications. Numerous factors are considered to contribute towards the development of proteinuria (PU) in SCD including hyperfiltration, ischemia, oxidative stress and decreased nitric oxide (NO) bioavailability but the detailed pathophysiology still needs further elucidation.

Methods

Employing arrays, we investigated cytokines and kidney injury-associated markers in the urine of a cohort of SCD patients from Ghana carrying the SS and SC genotypes which were further sub-divided into groups with proteinuria (SCD_PU) and without proteinuria (SCD).

Results

We identified up- and down-regulated proteins when comparing SCD with and without proteinuria. Amongst these is the well-established kidney injury marker- Clusterin which was up-regulated and could be validated in an ELISA-based assay. Refining the study to the SS and SC genotypes, we identified (and confirmed by ELISA) another established kidney injury marker- NGAL, as up-regulated in both genotypes and SCD with and without proteinuria. Metascape-based analysis of biological processes revealed “Cellular component disassembly” associated with proteins expressed in SCD but not regulated between PU and no PU and “leukocyte chemotaxis” down-regulated in SCD_PU vs. SCD. Interestingly, “Integrin-cell-surface interactions” was associated with proteins up-regulated between SCD_PU vs. SCD which is consistent with endothelial hyperplasia in the setting of glomerular hyperfiltration. To

investigate the effect secreted urine proteins have on human podocytes in vitro, immortalized podocytes supplemented with SCD_PU urine showed elevated p53 levels in both immunofluorescence staining and RT-PCR compared to SCD. Additionally, RT-PCR revealed elevated levels of VEGF, NGAL and the pro-inflammatory proteins-TGFβ, IL6, IL8 and TNFα.
Conclusion
We hypothesize that the increased number of endothelial cells in hyperplasia and hyperfiltration leads to more Integrin-mediated links to podocyte foot processes at the glomerular basement membrane and to glomerular fibrosis. Severe inflammation and kidney injury in SCD_PU patients is induced by the TGFβ-p53 axis.

Author contribution of C.T. included 30%:

Patient recruitment in the clinic was carried out by T.KA., V.B., Y.DA., M.L. and J.A.. I was responsible for establishing and maintaining the cell culture system, which included the cultivation of human immortalized cell line (AB 8/13) as well as the differentiation into podocytes and the processing and treatment of urine samples obtained from patients with and without sickle cell disease. In addition, I performed immunofluorescence staining, isolated RNA and performed qPCR. For all datasets I generated in the course of the study, I carried out the respective statistical analyses and prepared the quantitative evaluation of the results. I contributed to the conceptualization, designed and executed the experiments and interpreted the results to our research hypothesis. I wrote the original draft with W.W. and A.P. and created figures. I responded to the Reviewer comments and dealt with the submission.

Status: Pre-print available in the open access pre-print BioRxiv
(Under revision in BMC Nephrology).

DOI: https://doi.org/10.1101/2025.08.08.669286

This article is an open access article distributed under the terms and conditions of the Creative Commons Attribution (CC BY) 4.0 license, which permits unrestricted use, distribution, and reproduction in any medium, provided the original work is properly cited.

bioRxiv preprint doi: https://doi.org/10.1101/2025.08.08.669286; this version posted August 9, 2025. The copyright holder for this preprint (which was not certified by peer review) is the author/funder. All rights reserved. No reuse allowed without permission.

Urinary proteins from Sickle Cell patients induce inflammation and kidney injury via the TGFβ-p53 axis in a podocyte cell culture model.

Wasco Wruck[1#], Abida Islam Pranty[1#], Chantelle Thimm[1#], Christiane Loerch[1], Rosanne Mack[1], Theresa Koranteng-Adjaye[3], Vincent Boima[4], Yvonne Dei-Adomakoh[5], Margaret Lartey[4], and James Adjaye[1,2*]

[1]Institute for Stem Cell Research and Regenerative Medicine, Medical Faculty, Heinrich Heine University, Moorenstr.5, 40225, Düsseldorf, Germany.

[2]University College London (UCL) –EGA Institute for Women's Health, Zayed Centre for Research into Rare Diseases in Children (ZCR). 20 Guilford Street, London WC1N 1DZ.

[3]Thamesmead Health Centre, 4-5 Thames Reach, London SE28 ONY.

[4]Department of Medicine and Therapeutics, University of Ghana Medical School, College of Health Sciences, University of Ghana, Accra, Ghana

[5]Department of Haematology, University of Ghana Medical School, College of Health Sciences, University of Ghana, Accra, Ghana

[#]Equal contribution

*Correspondence: James.Adjaye@med.uni-duesseldorf.de

Abstract

Background

Sickle cell disease (SCD) is an inherited blood disorder affecting the oxygen-carrying hemoglobin in red blood cells making them deform into a sickle shape. Hemolysis and vaso-occlusion associated with this process can lead to complications in many organs and frequently to renal complications. Numerous factors are considered to contribute towards the development of proteinuria (PU) in SCD including hyperfiltration, ischemia, oxidative stress

bioRxiv preprint doi: https://doi.org/10.1101/2025.08.08.669286; this version posted August 9, 2025. The copyright holder for this preprint (which was not certified by peer review) is the author/funder. All rights reserved. No reuse allowed without permission.

and decreased nitric oxide (NO) bioavailability but the detailed pathophysiology still needs further elucidation.

Methods

Employing arrays, we investigated cytokines and kidney injury-associated markers in the urine of a cohort of SCD patients from Ghana carrying the SS and SC genotypes which were further sub-divided into groups with proteinuria (SCD_PU) and without proteinuria (SCD).

Results

We identified up- and down-regulated proteins when comparing SCD with and without proteinuria. Amongst these is the well-established kidney injury marker- Clusterin which was up-regulated and could be validated in an ELISA-based assay. Refining the study to the SS and SC genotypes, we identified (and confirmed by ELISA) another established kidney injury marker- NGAL, as up-regulated in both genotypes and SCD with and without proteinuria. Metascape-based analysis of biological processes revealed "Cellular component disassembly" associated with proteins expressed in SCD but not regulated between PU and no PU and "leukocyte chemotaxis" down-regulated in SCD_PU vs. SCD. Interestingly, "Integrin-cell-surface interactions" was associated with proteins up-regulated between SCD_PU vs. SCD which is consistent with endothelial hyperplasia in the setting of glomerular hyperfiltration. To investigate the effect secreted urine proteins have on human podocytes in vitro, immortalized podocytes supplemented with SCD_PU urine showed elevated p53 levels in both immunofluorescence staining and RT-PCR compared to SCD. Additionally, RT-PCR revealed elevated levels of VEGF, NGAL and the pro-inflammatory proteins-TGFβ, IL6, IL8 and TNFα.

Conclusion

We hypothesize that the increased number of endothelial cells in hyperplasia and hyperfiltration leads to more Integrin-mediated links to podocyte foot processes at the

bioRxiv preprint doi: https://doi.org/10.1101/2025.08.08.669286; this version posted August 9, 2025. The copyright holder for this preprint (which was not certified by peer review) is the author/funder. All rights reserved. No reuse allowed without permission.

glomerular basement membrane and to glomerular fibrosis. Severe inflammation and kidney injury in SCD_PU patients is induced by the TGFβ-p53 axis.

Introduction

Sickle cell disease (SCD) is a group of inherited blood disorders affecting hemoglobin, the protein in red blood cells (RBCs) that carries oxygen. SCD is primarily caused by a mutation in the beta-globin gene (*HBB*), which is responsible for producing hemoglobin [1]. This mutation results in the production of an abnormal form of hemoglobin, called hemoglobin S (HbS), instead of the normal hemoglobin A (HbA) [2], [3] . HbS leads RBCs to adopt a rigid, sickle-like shape and this deformed shape prevents the cells from easily passing through capillaries, leading to blockages and vaso-occlusion [4] , [1]. SCD impacts multiple body systems, including kidneys, brain, liver, heart, gallbladder, eyes, bones, and joints, characterized by acute episodes of illness and gradual organ damage [4]. Repeated vaso-occlusive episodes and inflammation results in cumulative organ damage, which becomes more evident as individuals get older. Recurrent pain, fatigue, anemia, and increased infection susceptibility are some of the common symptoms manifested in SCD patients, while acute chest syndrome, delayed growth and development, stroke and organ damage are also reported [5], [6], [4]. SCD is more common among individuals from the Mediterranean, Middle East, South Asian, Caribbean, with the highest prevalence amongst individuals of African ancestry. It is also one of the most widespread severe single-gene disorders globally [7] , [4] .

SCD includes several types, with sickle cell anemia (SS) and sickle hemoglobin-C disease (SC) being among the most commonly observed. Patients with sickle cell anemia (HbSS) have homozygous HbS, inheriting one mutated beta-globin gene from each parent. In contrast, individuals with HbSC inherit a different mutation in their beta-globin genes, resulting in the production of both hemoglobin C and hemoglobin S [http://scancainc.org/learn/types-of-sickle-cell-disease/ , accessed March 18 2025], [8], [9] [10]. Patients with an SS genotype have more severe clinical symptoms, while those with an SC genotype manifest milder symptoms [8], [9]

bioRxiv preprint doi: https://doi.org/10.1101/2025.08.08.669286; this version posted August 9, 2025. The copyright holder for this preprint (which was not certified by peer review) is the author/funder. All rights reserved. No reuse allowed without permission.

Nephropathy associated with SCD can lead to a range of renal complications including proteinuria, hyposthenuria, hematuria, renal papillary necrosis, renal tubular disorders, acute and chronic kidney injury, sickle cell glomerulopathy, and renal medullary carcinoma [11]. These kidney impairments often progress to chronic kidney disease (CKD), frequently requiring renal replacement therapy [1], [12], [13]. Findings from epidemiological studies also indicate an association between SCD and the occurrence of proteinuria and microalbuminuria in patients with autosomal dominant polycystic kidney disease (ADPKD) [12], [14], [15].

The pathophysiology of sickle cell nephropathy includes repeated sickling cycles favoured by hypoxic conditions in the renal medulla with vaso-occlusion in the vasa recta [11], [16], [17]. Ataga et al. revealed that prostaglandin release under hypoxic conditions leads to vasodilation and hyperfiltration [17] referring to reports of decreased hyperfiltration in SCD but not healthy control after administration of the prostaglandin inhibitor indomethacin [18]. Hyperfiltration among other factors such as glomerular hypertension and decreased nitric oxide [17] contributes to developing proteinuria although the detailed mechanisms are not fully elucidated.

Approximately 9.1% of the global population is affected by CKD [19]. CKD is linked to a wide range of adverse clinical outcomes, including cardiovascular disease, increased hospitalizations and death [20], [21], [19]. Regardless of the initial diagnosis, CKD shares common pathological mechanisms, including proteinuria, glomerular hyperfiltration, progressive renal scarring, and loss of kidney function [22]. Proteinuria is a condition where excess protein, primarily albumin, leaks into the urine due to kidney damage or dysfunction, disrupting the kidneys' normal filtering process [23], [24]. Proteinuria can mediate inflammation and fibrosis, ultimately leading to kidney failure [24]. It is a well-known marker of kidney damage and is commonly associated with conditions such as CKD, diabetes, hypertension, and distinct immune disorders. Persistent proteinuria is a key indicator of severe CKD and can contribute to a decline in kidney function and increase the risk of cardiovascular disease [25] . Numerous studies have also revealed a correlation between proteinuria levels and an increased risk of cardiovascular disease [22]. Proteinuria is observed in approximately 8% to

bioRxiv preprint doi: https://doi.org/10.1101/2025.08.08.669286; this version posted August 9, 2025. The copyright holder for this preprint (which was not certified by peer review) is the author/funder. All rights reserved. No reuse allowed without permission.

33% of the general population [26], [27], [25]. Given that proteinuria and urinalysis abnormalities, and renal impairment were observed in African SCD patients, urinalysis abnormalities, kidney function assessment should be an active pursuit in patients with SCD [28]. Therefore, in this study we investigated novel urine-based kidney injury biomarkers as additional diagnostic tools for first line screening of SCD patients.

The aim of this study was to further elucidate the etiology of proteinuria in SCD and to identify SCD-associated kidney injury and inflammatory biomarkers based on analysing urinary proteins. We employed a Human XL cytokine and a kidney injury-specific biomarker array-based assay to analyze the expression and levels of urine-shed proteins from a cohort of SCD patients from Ghana. Some patients in the cohort were diagnosed with proteinuria during urine analysis. To validate our findings from the initial array analyses, we performed an ELISA-based quantitative protein analysis for Clusterin and NGAL. We compared SCD patients with and without proteinuria to healthy controls. The study involved urine analysis based on two approaches: pooled urine samples from healthy individuals, SCD patients without, and SCD patients with proteinuria, as well as a genotype-specific (SS, SC) analysis.

Methods and materials

Ethics Statement

Ethics approval for this current analysis was obtained locally from the Korle-Bu Teaching Hospital Institutional Review Board with approval protocol identification number KBTH-IRB/000261/2024. Written informed consent was obtained from all participants. Participants unable or unwilling to give consent or who were institutionalized were excluded.

Participants

The current analysis included data from an initial project involving sickle cell disease patients. The initial study involved known SCD patients attending clinic at the Ghana Institute of Clinical Genetics (GICG) (Sickle Cell Clinic for adolescents and adults) in the Greater Accra Region of

bioRxiv preprint doi: https://doi.org/10.1101/2025.08.08.669286; this version posted August 9, 2025. The copyright holder for this preprint (which was not certified by peer review) is the author/funder. All rights reserved. No reuse allowed without permission.

Ghana between February 2021 to May 2022. The institute attends to SCD patients 13 years and above and its environs on out-patient basis; approximately 50 patients are seen per day. It also receives referrals from other parts of the country. Consented persons with Sickle cell disease aged ≥18 years with and without clinical evidence of proteinuria or albumin/creatinine ratio ≥ 3.0 mg/mmol (30 mg/g) and healthy controls with no evidence of kidney disease were consecutively recruited.

The CKD-EPI equation without the race adjustment was used in adults and the Schwartz formula [29] in children aged less than 16 years. The following people were excluded from the study; pregnant females, smokers, history of recreational drug or alcohol abuse, current over-the-counter drug use, NSAID use within the last three months, persons with acute illness at time of enrollment, history of chronic illness, current evidence or history of renal disease and people who had sickle Cell crises within the last three months. Healthy persons without SCD or CKD were defined as individuals with eGFR 60 mL/min/1.73 m2 and albumin/creatinine ratio < 3.0 mg/mmol (<30 mg/g) and HB electrophoresis negative for sickle cell disease. Random urine samples were collected from cases and controls and aliquots of 10 mLs were taken into cryovials. All participants of this study are from African ancestry.

Urine sample preparation and participant details

This analysis utilized urine samples collected from 10 healthy individuals and 20 patients from a cohort of individuals with sickle cell disease (SCD) in Ghana. Among the SCD patients, 10 were diagnosed with proteinuria and classified as the analysis group SCD with proteinuria (SCD_PU). The participants ranged in age from 18 to 49 years. Urine analysis was conducted using two approaches: pooled urine samples representing healthy individuals, SCD patients, and SCD_PU, as well as a genotype-specific (SS, SC) analysis. For each condition, urine samples from 10 individuals were pooled in equal volumes, and a final volume of 500 µl per condition was used for each of the array experiments. Clinical features of patients whose urine samples were pooled in the SCD_PU, SCD and control groups are listed in Table 1.

bioRxiv preprint doi: https://doi.org/10.1101/2025.08.08.669286; this version posted August 9, 2025. The copyright holder for this preprint (which was not certified by peer review) is the author/funder. All rights reserved. No reuse allowed without permission.

Array-based cytokine and kidney injury biomarker analysis

As with our previous studies using urine samples from AKI and CKD patients [30], [31], the current study used pooled urine samples from healthy individuals, SCD and SCD.PU patients, as well as pools of genotype-specific samples (SS, SC). These were hybridized onto the Human Kidney Biomarker Array (Human Kidney Biomarker Array Kit, Catalog Number ARY019) and the Proteome Profiler Array (Human XL Cytokine Array Kit, Catalog Number ARY022B) from Research And Diagnostic Systems, Inc. (Minneapolis, MN, USA), following the manufacturer's protocol. Images of the hybridized arrays were captured using the Fusion FX instrument (PeqLab, Erlangen, Germany). The detailed workflow of the analyses is depicted in Supplementary Figure 1.

Image analysis of cytokine arrays

The images of the hybridized cytokine assays were imported into the FIJI/ImageJ software [32] for preprocessing, grid-finding and quantification via the FIJI Microarray Profile plugin by Bob Dougherty and Wayne Rasband (https://www.optinav.info/MicroArray_Profile.htm, accessed on 06 January 2025). Details of the image analysis including semi-automatically grid-finding employing an R script for interpolation of missing spots are described in our previous publication [31].

Array data analysis

Quantification results from the microarray plugin within FIJI/ImageJ were imported into the R/Bioconductor [33] environment where they were normalized with the Robust Spline Normalization from the R/Bioconductor package lumi [34]. Up- and down-regulated cytokines for the comparisons SCD vs. control, SCD_PU vs. control, SCD_PU vs SCD and SS vs SC were determined using the criteria: detection-p-value in at least one case < 0.05, p-value from the limma [35] R package < 0.05, false-discovery-rate < 0.25, ratio >1.5 (up-regulation) or ratio

bioRxiv preprint doi: https://doi.org/10.1101/2025.08.08.669286; this version posted August 9, 2025. The copyright holder for this preprint (which was not certified by peer review) is the author/funder. All rights reserved. No reuse allowed without permission.

< 0.6667 (down-regulation). Hierarchical cluster analysis dendrograms and heatmaps were drawn via the heatmap.2 function from the R package gplots [36] using complete linkage as cluster agglomeration method and the Pearson correlation coefficient as similarity measure. Barplots with error bars indicating standard error of the mean were generated via the R methods barplot and arrows.

Enzyme-linked Immunosorbent assay (ELISA)

Secreted Clusterin and Lipocalin-2 (NGAL) detected in pooled urine samples of SCD and SCD_PU patients using the DuoSet ELISA (R&D Systems, Minneapolis, MN, USA) was performed as described by the manufacturer. Optical density was measured using the EPOCH2 spectrophotometer (BioTek, Winooski, Vermont, USA) at 450 nm with wavelength correction at 540 nm. 4-PL curve fitting was performed to calculate concentrations.

Cell culture

The human SV40, temperature sensitive podocyte immortal cell line (AB 8/13) [37] proliferates at 33°C, 5% CO2 on plastic when cultured in RPMI 1640 (Gibco®, life technologies, California) supplemented with 10% fetal bovine serum (Gibco®,) and 1% Penicillin and Streptomycin (Gibco®,).

For differentiation into podocytes we followed our previously published protocols [38], [39] . In brief, the cells were seeded on Corning® Collagen type I (Merck, Darmstadt, Deutschland) coated plates and cultured in the differentiation medium- Advanced RPMI 1640 (Gibco®) supplemented with 10% fetal bovine serum, 1% Penicillin and Streptomycin, and 30 µM retinoic acid (Sigma-Aldrich Chemistry, Steinheim, Germany), incubated at 37 °C, 5% CO2 for 14 days. The medium was changed once a week. After 14 days the podocytes were treated with for 5 days with 30% urine from healthy individuals, sickle cell patients without proteinuria (SCD) and sickle cell patients with proteinuria SCD_PU for 5 days.

bioRxiv preprint doi: https://doi.org/10.1101/2025.08.08.669286; this version posted August 9, 2025. The copyright holder for this preprint (which was not certified by peer review) is the author/funder. All rights reserved. No reuse allowed without permission.

Immunofluoresence-based protein staining

Human immortalized podocytes (AB 8/13) were fixed with 4% paraformaldehyde for 15 min at room temperature (RT). Cells were washed three times with PBS. Afterwards an incubation with 0.05% Tween-20/PBS for 10 minutes. The cells were treated three times with PBS and continued blocking the cells with 3% BSA/PBS. Thereafter they were incubated with the respective primary antibody (Cell signaling; 2527S) diluted 1:200 overnight at 4 °C. Followed by one washing step with Triton x-100/PBS and two washing steps with PBS. The cells were incubated for 1 h with Alexa488-conjugated secondary antibody diluted 1:500 and nuclear Hoechst 1:5000(Thermo Fisher; H3569) at RT. Fluorescence images were captured by a LSM700 microscope (Carl Zeiss).

RNA isolation

For RNA isolation from the human immortalized podocyte cell (AB 8/13) the ZYMO Research Kit Direct-zol™ RNA Miniprep R20 was utilized following the manufacturer's protocol. Cells were detached by adding Tryple E and incubated for 5 min. Afterwards, a centrifuging step of 4 mins 1000 g and the cell pellets processed following manufacturer´s protocol. The RNA was eluted by adding 35 µL of DNase/RNase-free water to the column and centrifuging for 1 minute at 16,000 g. The eluted RNA samples were immediately placed on ice, and concentrations measured with a Nanodrop device.

Real-Time PCR based gene expression quantification of pro-inflammatory and kidney injury-associated genes.

RNA samples were run in triplicate on a 384-well reaction plate with Power Sybr Green PCR Master Mix (Applied Biosystems, Foster City, CA, USA) using Step One Plus Real-Time PCR systems. The amplification conditions were denaturation at 95 ^{0}C for 13 min followed by 35 cycles of 95 ^{0}C for 50 s, 60 ^{0}C for 45 s, and 72 ^{0}C for 30 s. To normalize the quantitative real-time PCR, the ribosomal encoding gene-RPL0 was used. The primer sequences are listed in Supplementary Table S1. The results were analyzed using the $2^{-\Delta\Delta CT}$ method and specified

bioRxiv preprint doi: https://doi.org/10.1101/2025.08.08.669286; this version posted August 9, 2025. The copyright holder for this preprint (which was not certified by peer review) is the author/funder. All rights reserved. No reuse allowed without permission.

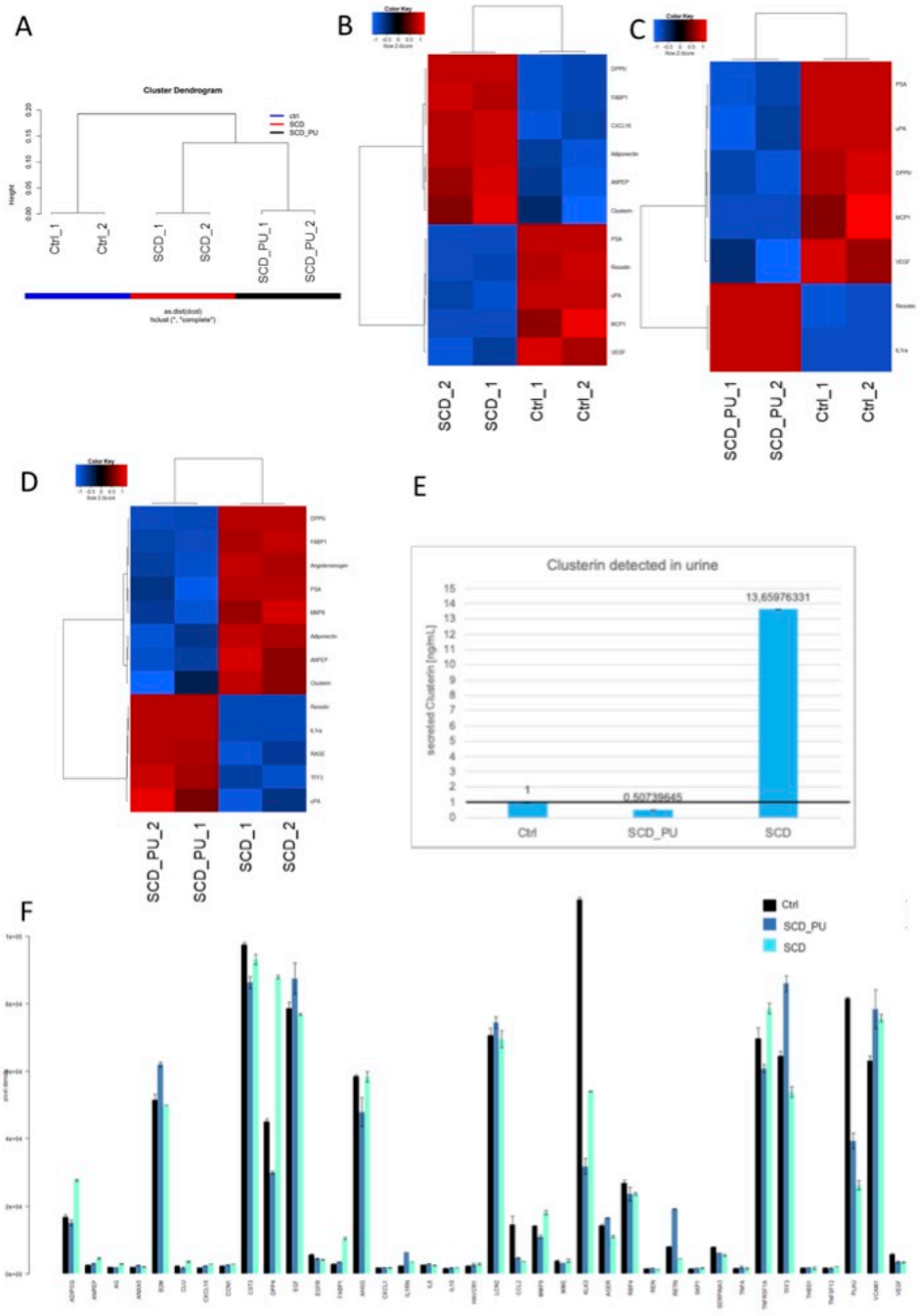
by fold change expression. The samples were run in independent experiments three times. The mean value of these experiments was used for the calculations. The statistical significance was calculated using the Two-Sample test assuming unequal variances [40] with a significance threshold $p = 0.05$.

Results

Comparison of kidney injury markers between SCD with and without Proteinuria

We pooled urine samples from SCD_PU, SCD without proteinuria and healthy controls and analyzed these on the Human Kidney Biomarker Array. Figure 1A shows the cluster dendrogram with separate clusters of SCD with PU (SCD_PU), SCD without PU (SCD) and healthy control (Ctrl). The analysis revealed distinct kidney protein signatures of SCD_PU, SCD and ctrl. The heatmaps in Figure 1B-D distinguish expression of differentially expressed proteins between SCD and Ctrl (B), between SCD_PU and Ctrl (C) and between SCD_PU and SCD (D). Resistin, IL1RA, RAGE, TFF3 and uPA (PLAU) are up-regulated in SCD_PU vs SCD while DPPIV, FABP1, Angiotensinogen, PSA (KLK3), MMP9, Adiponectin, ANPEP and Clusterin are down-regulated. Clusterin had lower expression in SCD_PU than in SCD, in line with reports of Clusterin attenuating kidney disease [41]. We therefore followed-up this protein with ELISA measurements which confirmed higher expression of Clusterin in SCD than in control but lower expression in SCD_PU than in control (Figure 1E). Figure 1F provides a global view of the expression of all proteins under the three conditions on the Kidney Injury Array.

bioRxiv preprint doi: https://doi.org/10.1101/2025.08.08.669286; this version posted August 9, 2025. The copyright holder for this preprint (which was not certified by peer review) is the author/funder. All rights reserved. No reuse allowed without permission.



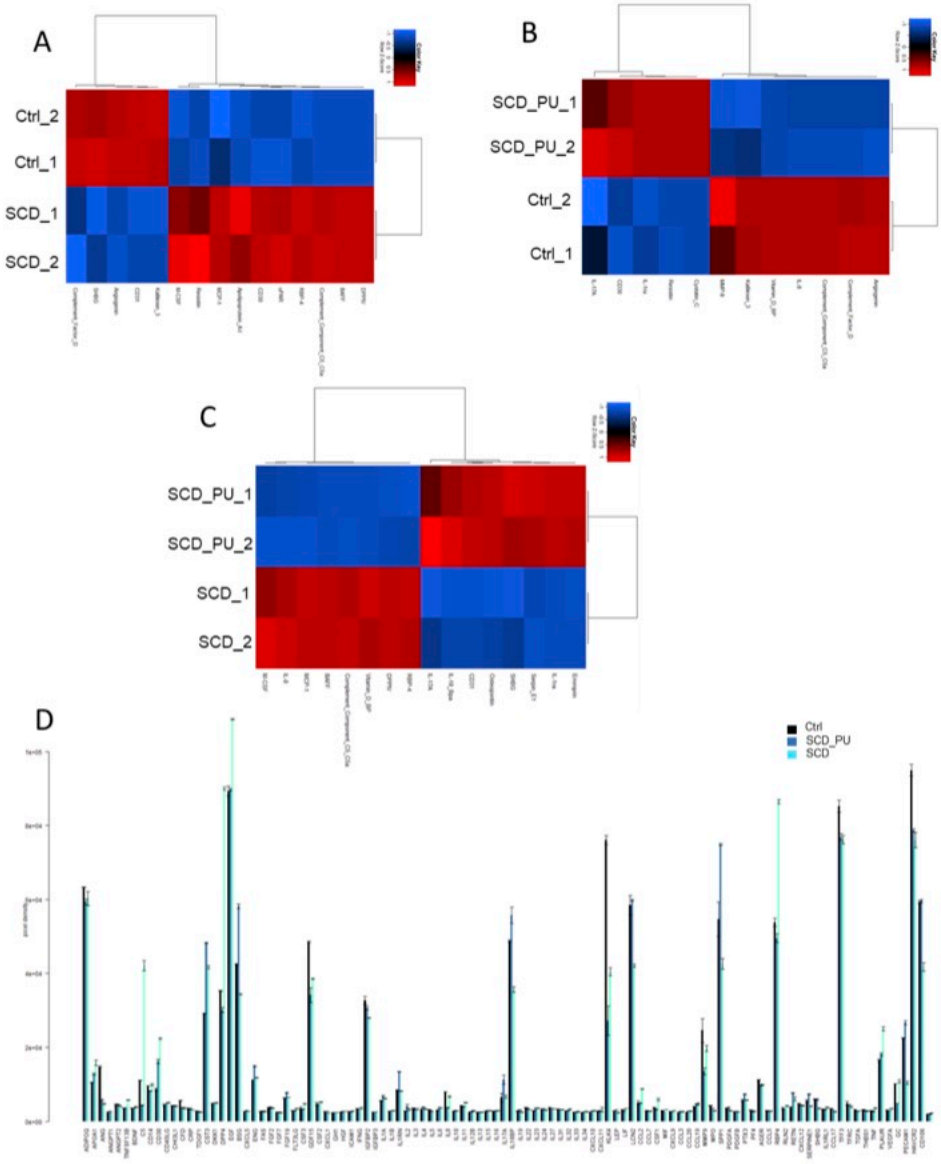
bioRxiv preprint doi: https://doi.org/10.1101/2025.08.08.669286; this version posted August 9, 2025. The copyright holder for this preprint (which was not certified by peer review) is the author/funder. All rights reserved. No reuse allowed without permission.

Figure 1: Pooled urine samples of SCD with and without Proteinuria (PU) have distinct kidney protein signatures. Pooled urine samples of SCD with and without Proteinuria were analyzed on the Human Kidney Biomarker Array. (A) The cluster dendrogram shows separate clusters of SCD with PU (SCD_PU), SCD without PU (SCD) and healthy control (Ctrl). (B) The heatmap shows expression of differentially expressed proteins between SCD and Ctrl. (C) The heatmap shows expression of differentially expressed proteins between SCD_PU and Ctrl. (D) The heatmap shows expression of differentially expressed proteins between SCD_PU and SCD. Resistin, IL1RA, RAGE, TFF3 and uPA (PLAU) are up-regulated in SCD_PU while DPPIV, FABP1, Angiotensinogen, PSA (KLK3), MMP9, Adiponectin, ANPEP and Clusterin are down-regulated. (E) The bar chart of ELISA measurements confirms higher expression of Clusterin in SCD than in control but lower expression in SCD_PU than in control. (F) The bar plot shows the absolute expression of all proteins on the Human Kidney Biomarker Array.

Comparison of kidney injury markers between SCD with and without Proteinuria

Furthermore, we set out to compare expression of cytokines between SCD_PU, SCD and healthy control. Again, we pooled urine samples of SCD_PU, SCD and control and analyzed them - this time on a Human Cytokine XL array. The heatmaps in Figure 2A and B show expression of differentially expressed proteins between SCD and ctrl and between SCD_PU and ctrl. The heatmap in Figure 2C shows expression of differentially expressed proteins between SCD_PU and SCD. Emmprin, IL1RA, SerpinE1, SHBG, Osteopontin, CD31, IL-18-Bpa and IL-17A are up-regulated in SCD_PU while RBP4, DPPIV, Vitamin-D-BP, Complement-Component-C5-C5a, BAFF, MCP-1, IL-8 and M-CSF are down-regulated. The bar plot in Figure 2D provides an overview of the absolute expression of all proteins on the Human XL cytokine Array for the three conditions Ctrl, SCD_PU and SCD.

bioRxiv preprint doi: https://doi.org/10.1101/2025.08.08.669286; this version posted August 9, 2025. The copyright holder for this preprint (which was not certified by peer review) is the author/funder. All rights reserved. No reuse allowed without permission.

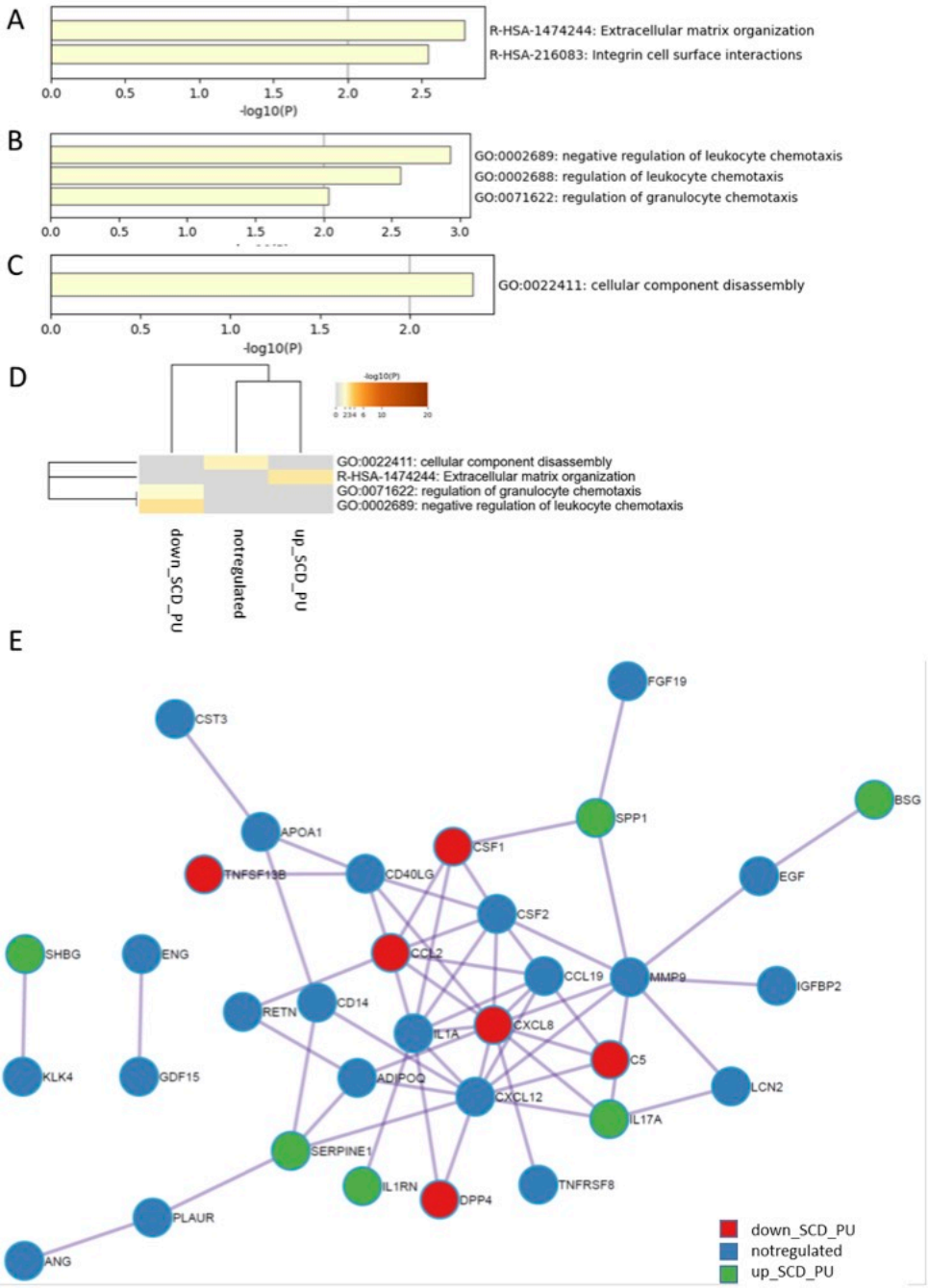


bioRxiv preprint doi: https://doi.org/10.1101/2025.08.08.669286; this version posted August 9, 2025. The copyright holder for this preprint (which was not certified by peer review) is the author/funder. All rights reserved. No reuse allowed without permission.

Figure 2: Pooled urine samples of SCD with and without Proteinuria (PU) have distinct cytokine signatures. Pooled urine samples of SCD with and without Proteinuria were analyzed on a Human XL cytokine array. (A) The heatmap shows expression of differentially expressed proteins between SCD and ctrl. (B) The heatmap shows expression of differentially expressed proteins between SCD_PU and Ctrl. (C) The heatmap shows expression of differentially expressed proteins between SCD_PU and SCD. Emmprin, IL1RA, SerpinE1, SHBG, Osteopontin, CD31, IL-18-Bpa and IL-17A are up-regulated in SCD_PU while RBP4, DPPIV, Vitamin-D-BP, Complement-Component-C5-C5a, BAFF, MCP-1, IL-8 and M-CSF are down-regulated. (D) The bar plot shows the absolute expression of all proteins on the Human XL cytokine Array.

In order to assign functional annotations associated with the development of proteinuria in SCD we performed a Metascape analysis of up-, down- and not-regulated cytokines by comparing SCD_PU vs SCD (Figure 3). Figure 3A depicts the Reactome pathways “Extracellular matrix organization” and “Integrin cell surface interactions” over-represented in cytokines up-regulated in SCD_PU . Figure 3B lists the Gene Ontologies “negative regulation of leukocyte chemotaxis”, “regulation of leukocyte chemotaxis” and “regulation of granulocyte chemotaxis” over-represented in cytokines down-regulated in SCD_PU. The gene ontology “cellular component disassembly” was over-represented in not-regulated cytokines but expressed in both conditions (Figure 3C). Figure 3D shows a heatmap and Figure 3E a protein interaction network resulting from the Metascape analysis of up-, down- and not-regulated cytokines.

bioRxiv preprint doi: https://doi.org/10.1101/2025.08.08.669286; this version posted August 9, 2025. The copyright holder for this preprint (which was not certified by peer review) is the author/funder. All rights reserved. No reuse allowed without permission.



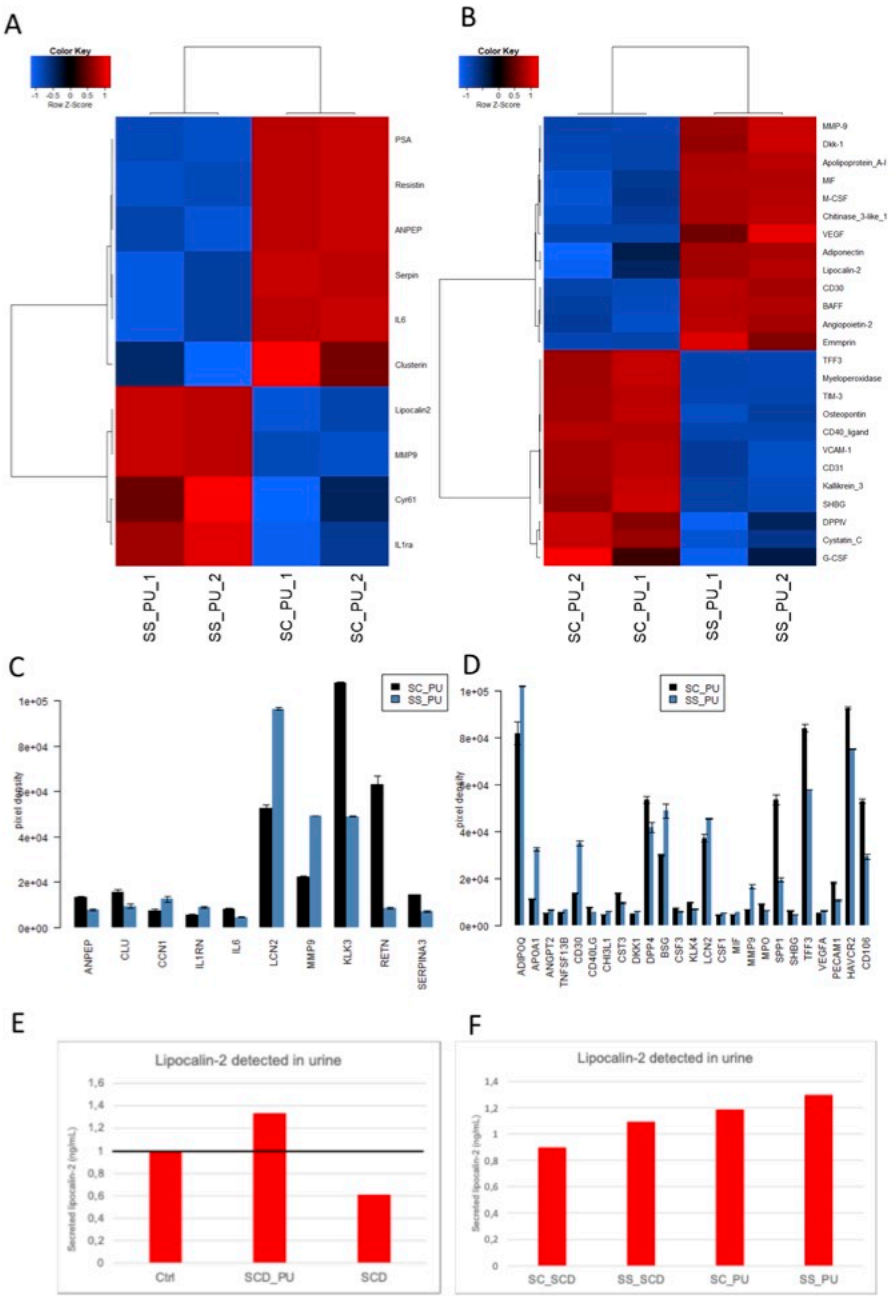
bioRxiv preprint doi: https://doi.org/10.1101/2025.08.08.669286; this version posted August 9, 2025. The copyright holder for this preprint (which was not certified by peer review) is the author/funder. All rights reserved. No reuse allowed without permission.

Figure 3: SCD_PU vs SCD Metascape analysis. Up-, down- and not-regulated cytokines when comparing SCD_PU vs. SCD were subjected to metascape analysis. (A) Reactome pathways "Extracellular matrix organization" and "Integrin cell surface interactions" were over-represented in cytokines up-regulated in SCD_PU. (B) Gene ontologies "negative regulation of leukocyte chemotaxis", "regulation of leukocyte chemotaxis" and "regulation of granulocyte chemotaxis" were over-represented in cytokines down-regulated in SCD_PU. (C) The gene ontology "cellular component disassembly" was over-represented in cytokines not-regulated but expressed in both conditions.(D) shows a heatmap and (E) a protein interaction network resulting from the combined Metascape analysis of up-, down- and not-regulated cytokines.

Comparison of Proteinuria in genotypes SS and SC

Pooled urine samples of genotypes SS and SC from SCD patients with and without Proteinuria were analyzed on Human XL cytokine and kidney biomarker arrays **(**Figure 4). The heatmaps in Figure 4A and B show expression of differentially expressed kidney injury marker proteins (Figure 4A) and cytokines (Figure 4B) between SCD_PU patients with the genotypes SS and SC. The bar plots in Figure 4C and D show expression of differentially expressed kidney injury marker proteins (Figure 4C) and cytokines (Figure 4D) between SCD_PU patients with the genotypes SS and SC. The kidney injury markers Lipocalin-2 (LCN2 / NGAL), MMP9, CCN1 and IL1RN (IL1RA) are up-regulated in SS_PU while ANPEP, CLU (Clusterin), IL6, KLK3, RETN and SERPINA3 are down-regulated in SS_PU (Figure 4C). Amongst the up-regulated cytokines in SS_PU (Figure 4D), LCN2 and MMP9 levels were also upregulated in the kidney injury analyses. (E) Up-regulation of the established kidney injury marker LCN2 (NGAL) between SS_PU and SC_PU (C) was confirmed by ELISA measurements in SCD_PU vs SCD (Figure 4E) and between SS_PU and SC_PU (Figure 4F).

bioRxiv preprint doi: https://doi.org/10.1101/2025.08.08.669286; this version posted August 9, 2025. The copyright holder for this preprint (which was not certified by peer review) is the author/funder. All rights reserved. No reuse allowed without permission.



bioRxiv preprint doi: https://doi.org/10.1101/2025.08.08.669286; this version posted August 9, 2025. The copyright holder for this preprint (which was not certified by peer review) is the author/funder. All rights reserved. No reuse allowed without permission.

Figure 4: Comparison of Proteinuria in genotypes SS and SC on Human cytokine XL and kidney arrays . Pooled urine samples of genotypes SS and SC from SCD patients with and without Proteinuria were analyzed on the Human XL cytokine and kidney biomarker arrays. (A) The heatmap shows expression of differentially expressed kidney injury marker proteins between SCD_PU patients with the genotypes SS and SC. (B The heatmap shows expression of differentially expressed cytokines between SCD_PU patients with the genotypes SS and SC. (C) The bar plot shows expression of differentially expressed kidney injury marker proteins between SCD_PU patients with the genotypes SS and SC. Lipocalin-2 (LCN2 / NGAL), MMP9, CCN1 and IL1RN (IL1RA) are up-regulated in SS_PU while ANPEP, CLU (Clusterin), IL6, KLK3, RETN and SERPINA3 are down-regulated in SS_PU. (D) The bar plot shows expression of differentially expressed cytokines between SCD_PU patients with the genotypes SS and SC. Amongst the cytokines up-regulated in SS_PU, the increased levels of LCN2 and MMP9 were also confirmed in the kidney biomarker array. (E) Up-regulation of the established kidney injury marker LCN2 (NGAL) between SS_PU and SC_PU (C) was confirmed by ELISA in SCD_PU vs SCD and between SS_PU and SC_PU (F).

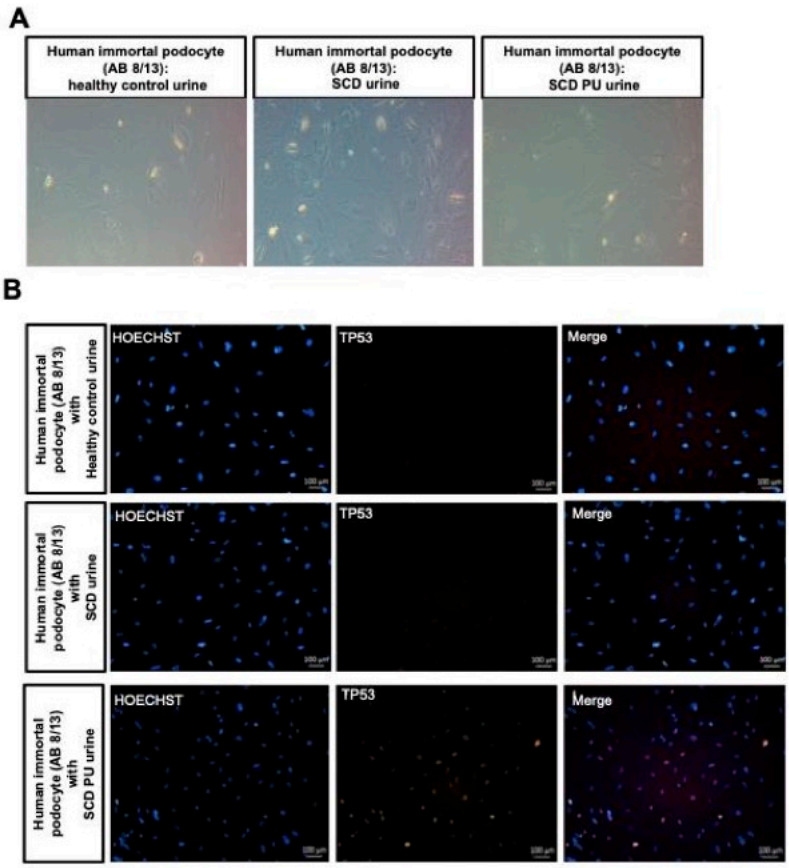
The effects of urine-secreted cytokines from SCD, SCD_PU and healthy individuals on human podocytes.

For this investigation, human immortalized podocytes (AB8/13) were cultured for 14 days in advanced RPMI medium supplemented with 30 µM retinoic acid (RA) on collagen type I-coated plates. The cells were then exposed for an additional five days with pooled urine samples from healthy controls, SCD and SCD_PU patients Following the treatment, light microscopy revealed no morphological changes in podocytes exposed to urine from all groups (Figure 5A). The podocyte specific marker Podocin (NPHS2) served as a positive control demonstrating successful podocyte differentiation whilst Phalloidin served to show the morphology of the cytoskeleton (Figure 5B). Immunofluorescence staining showed increased TP53 protein expression in podocytes treated with SCD_PU urine, thus implying activation of cell cycle

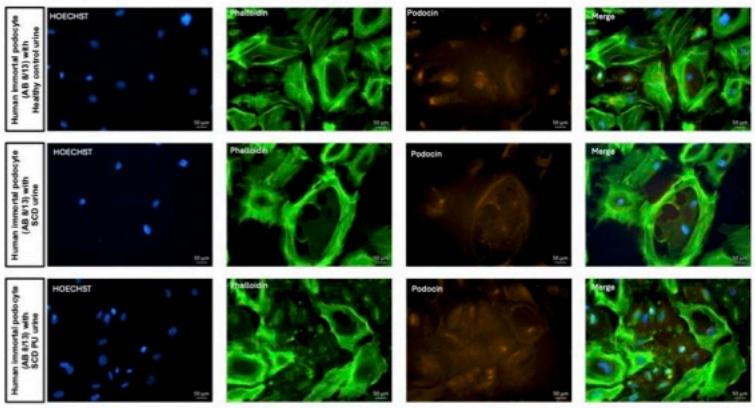
bioRxiv preprint doi: https://doi.org/10.1101/2025.08.08.669286; this version posted August 9, 2025. The copyright holder for this preprint (which was not certified by peer review) is the author/funder. All rights reserved. No reuse allowed without permission.

arrest due to stress responses (Figure 5B). Quantitative real-time PCR analysis demonstrated a downregulation in the expression of the podocyte-specific markers Nephrin (NPHS1) and upregulation of CD2-associated protein (CD2AP). Both mRNA and protein levels of TP53 were upregulated (Figure 5C). Furthermore, transcripts of kidney injury markers- Cystatin C (CysC) and Neutrophil gelatinase-associated lipocalin (NGAL), and pro-inflammatory markers- Tumor necrosis factor alpha (TNF-α), Transforming growth factor beta (TGF-β), Vascular endothelial growth factor (VEGF), Interleukin 6 (IL-6) and Interleukin (IL-8) were significantly elevated in podocytes treated with SCD_PU urine, thus indicating enhanced cellular stress and injury. Clusterin (CLU) and Dipeptidyl peptidase-4 inhibitor (DPP4) levels were downregulated in both SCD and SCD_PU compared to the healthy control (Figure 5C).

bioRxiv preprint doi: https://doi.org/10.1101/2025.08.08.669286; this version posted August 9, 2025. The copyright holder for this preprint (which was not certified by peer review) is the author/funder. All rights reserved. No reuse allowed without permission.

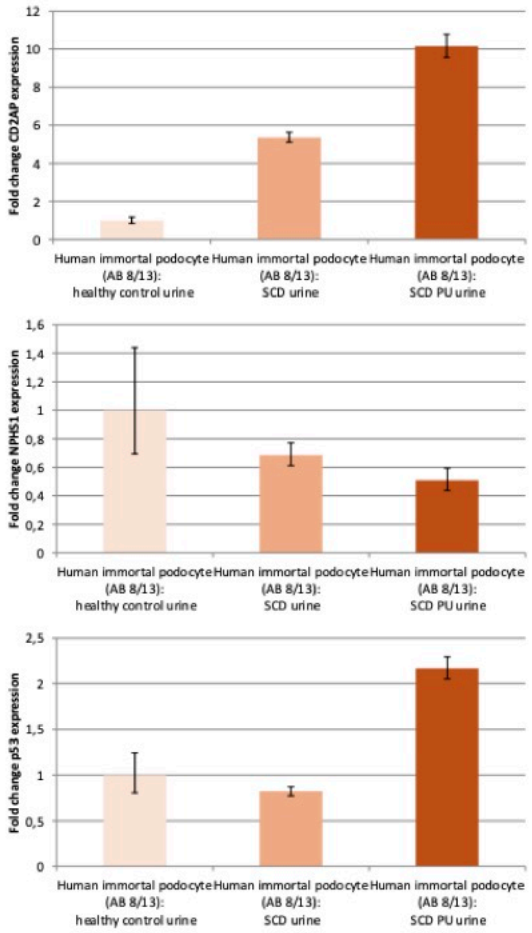


bioRxiv preprint doi: https://doi.org/10.1101/2025.08.08.669286; this version posted August 9, 2025. The copyright holder for this preprint (which was not certified by peer review) is the author/funder. All rights reserved. No reuse allowed without permission.

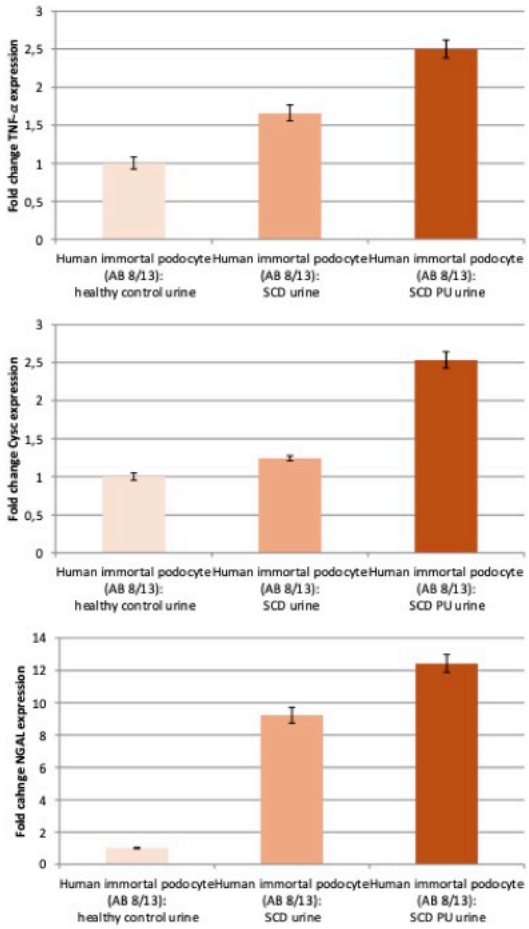


bioRxiv preprint doi: https://doi.org/10.1101/2025.08.08.669286; this version posted August 9, 2025. The copyright holder for this preprint (which was not certified by peer review) is the author/funder. All rights reserved. No reuse allowed without permission.

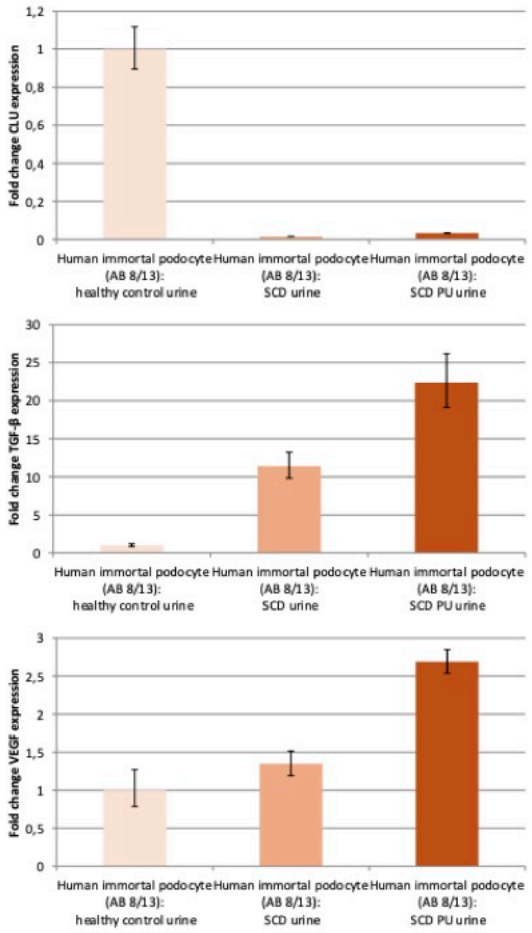
C



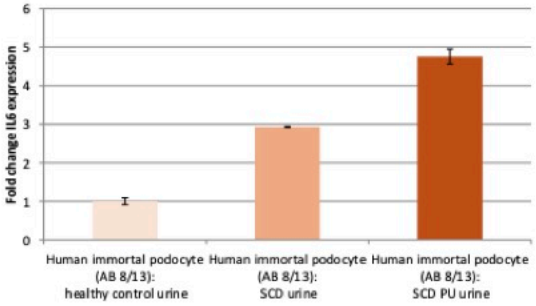
bioRxiv preprint doi: https://doi.org/10.1101/2025.08.08.669286; this version posted August 9, 2025. The copyright holder for this preprint (which was not certified by peer review) is the author/funder. All rights reserved. No reuse allowed without permission.

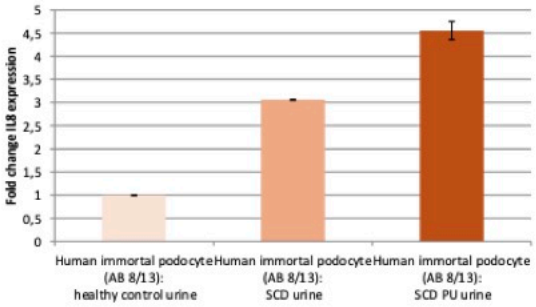


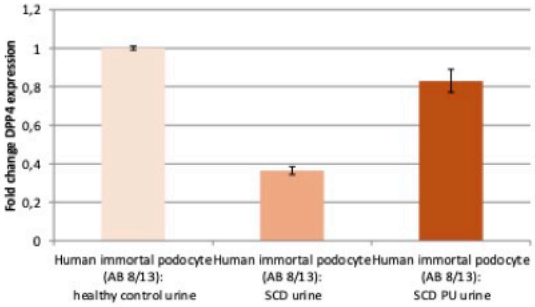
bioRxiv preprint doi: https://doi.org/10.1101/2025.08.08.669286; this version posted August 9, 2025. The copyright holder for this preprint (which was not certified by peer review) is the author/funder. All rights reserved. No reuse allowed without permission.



bioRxiv preprint doi: https://doi.org/10.1101/2025.08.08.669286; this version posted August 9, 2025. The copyright holder for this preprint (which was not certified by peer review) is the author/funder. All rights reserved. No reuse allowed without permission.







bioRxiv preprint doi: https://doi.org/10.1101/2025.08.08.669286; this version posted August 9, 2025. The copyright holder for this preprint (which was not certified by peer review) is the author/funder. All rights reserved. No reuse allowed without permission.

Figure 5: Upregulated expression of TP53, pro-inflammatory and kidney injury-associated markers in podocytes exposed to urine from SCD and SCD_PU patients.

Human immortalized podocytes (AB8/13) were cultured at 37 °C for 14 days in Advanced RPMI medium supplemented with 30 µM retinoic acid (RA) on collagen type I-coated plates. The cells were then treated for five days with urine samples from healthy controls, SCD amd SCD_PU patients. (A) Representative light microscopy images of podocytes after five days of urine exposure. (B) TP53, NPHS2 and Phalloidin protein expression visualized by immunofluorescence staining. (C) Quantitative real-time PCR analysis of mRNA expression levels for podocyte markers (NPHS1, CD2AP), the regulator of cellular stress (TP53), and kidney injury- associated genes (CysC, NGAL and CLU) and pro-inflammatory associated genes (TNF-α, TGF-β, VEGF, IL6, IL8 and DPP4).

Discussion

In previous studies we used urine samples to identify cytokines and kidney injury- associated biomarkers in patients diagnosed with Acute Kidney injury and Chronic kidney disease [31], [30] .

In this study we investigated the similarities and differences between SCD_PU with proteinuria, SCD without proteinuria and healthy individuals with respect to the secretion of cytokines and kidney injury-associated proteins in pooled urine samples. Table 2 provides an overview of the resulting proteins.

Resistin, IL1RA, RAGE, TFF3 and uPA (PLAU) are up-regulated in SCD_PU vs SCD while DPPIV, FABP1, Angiotensinogen, PSA (KLK3), MMP9, Adiponectin, ANPEP and Clusterin are down-regulated.

bioRxiv preprint doi: https://doi.org/10.1101/2025.08.08.669286; this version posted August 9, 2025. The copyright holder for this preprint (which was not certified by peer review) is the author/funder. All rights reserved. No reuse allowed without permission.

Clusterin which we identified to be secreted at a lower level in SCD_PU than in SCD patients has been reported as biomarker for microalbinuria in a consecutive cohort study of 146 type 2 diabetes mellitus (T2DM) patients [42] and additionally attenuates renal fibrosis in rodent models [41] . Numerous studies have described an association between elevated Resistin and Proteinuria [43], [44], thus arguing that the level of Resistin is rather connected to inflammation and glomerular filtration impairment than to Insulin Resistance. The reported increased levels of Resistin corroborates our finding of up-regulated levels of Resistin in SCD_PU.

IL-1Ra is a receptor antagonist of the inflammation-mediator IL-1, and the balance between IL-1 and IL-1Ra plays an important role in several diseases including renal diseases [45]. IL-1 is involved in inflammation-associated development of diseases which can be reversed by the antagonist IL-1Ra– this has been exploited in therapies based on recombinant IL-1Ra (anakinra) [46] . Human immune cells can secrete IL-1Ra to compensate for IL-1-mediated inflammation. Thus, IL-1Ra can also be a marker of diseases. This has been shown in rat studies of glomerulonephritis with anti-glomerular basement membrane (GBM) antibodies showing production of IL-1 and IL-1Ra within the rat kidney [47]. Descamps-Latscha described elevated levels of IL-1Ra in patients at various stages of chronic renal failure and the correlation of IL-l Ra with the soluble TNFA-receptor,- TNF-sR55 [48].

The receptor of advanced glycation end product (RAGE) was up-regulated in SCD_PU. Increased levels of RAGE has been shown to induce oxidative stress in diabetic kidney disease and ageing kidney via NAPDH (nicotinamide adenine dinucleotide phosphate) oxidase [49], [50], [51]. In their review, Duni et al. described models of podocyte injury induced by increased levels of reactive oxygen species (ROS) which led to ultrastructural changes in podocytes, defective anchorage due to alteration in the adhesion molecule- a3b1-integrin [49].

Interestingly, Reactome pathway analyses revealed “Integrin cell surface interactions” as over-represented amongst the proteins up-regulated between SCD_PU and SCD. Integrins bind podocyte foot processes to the glomerular basement membrane (GBM) and their impairment leads to detachment of foot processes from the GBM and glomerular filtration problems [52],

bioRxiv preprint doi: https://doi.org/10.1101/2025.08.08.669286; this version posted August 9, 2025. The copyright holder for this preprint (which was not certified by peer review) is the author/funder. All rights reserved. No reuse allowed without permission.

[53], [54], [55] . By examining the details of the Integrin pathway, we identified PECAM1, SPP1 and BSG among the SCD_PU up-regulated proteins. PECAM1 has been described to directly interact with Integrin αvβ3 to mediate adhesion of leukocytes to the endothelium [56],[57]. Increased levels of PECAM1 is considered a marker for endothelial cells and also for their hyperplasia [58] is in line with SCD hyperplasia associated with hyperfiltration [17] Up-regulated levels of uPA in SCD_PU samples might be further evidence supporting the report that uPA receptor activates integrin αvβ3 in podocytes [59]. Sheinman in his review, described hyperfiltration as a contributing factor that induces endothelial hyperplasia and ultimately glomerular fibrosis [60].

Levels of TFF3 was up-regulated in SCD_PU samples and interestingly increased levels have been associated with CKD [61]. For patients with Type II diabetes which can arise from SCD and mediated by effects on pancreas [62] . It has been hypothesized that the increase in blood glucose and insulin and decrease in short-chain fatty acids may lead to the elevation of serum TFF3 [60] .

Urokinase-type plasminogen activator (uPA/PLAU),which is up-regulated in SCD_PU, correlates with disease progression in experimental models of CKD [63]. The level of Its receptor uPAR, decreases in podocyte injury and foot process effacement via activation of α5β3 integrin as reported in a mouse model of lipopolysaccharide (LPS)-induced nephropathy [64], [59].

Comparing the genotypes SS and SC, we identified kidney injury markers Lipocalin-2 (the gene *LCN2* coding the protein NGAL), MMP9, CCN1 and IL1RN (IL1RA) as up-regulated in SS_PU and ANPEP, CLU (Clusterin), IL6, KLK3, RETN and SERPINA3 down-regulated in SS_PU. Furthermore, we could confirm the up-regulation of LCN2 / NGAL in ELISA-based assays. Marouf et al. proposed LCN2/NGAL as a biomarker for nephropathy in sickle cell disease by studying patients with the SS genotype and the HbS/ß0-thalassemia genotype [65] which is also classified as severe and is more prevalent in the Eastern Mediterranean and India [4]. The authors [65] found a correlation of NGAL with microalbuminuria and a better

bioRxiv preprint doi: https://doi.org/10.1101/2025.08.08.669286; this version posted August 9, 2025. The copyright holder for this preprint (which was not certified by peer review) is the author/funder. All rights reserved. No reuse allowed without permission.

performance of urinary NGAL than serum NGAL for the prediction of vaso-occlusive crisis (VOC) with an Area under the Receiver Operating Characteristic curve for plasma NGAL of 0.69 and for urine NGAL of 0.86. In our experiments, we also observed higher levels of LCN2 in the SC genotype with proteinuria than without in the ELISA assays and additionally higher LCN2 ($p=3.42x10^{-5}$, FDR= 0,0003, ratio=1.42 below our threshold of 1.5) when comparing SCD_PU vs. SCD. NGAL is a transmembrane protein transporting lipophilic substances [65] and has been established as a predictive marker of acute kidney injury [66], [67] and also found to be elevated in SCD during VOC [68]. NGAL is freely filtered through the glomerulus and is re-absorbed by healthy proximal tubular cells and not diseased or injured cells. Lack of re-absorption leading to increased NGAL levels in the urine of patients with kidney injury [66], [65]. By binding to MMP9 (matrix metalloproteinase-9), NGAL inhibits the degradation of MMP9 thus enabling its proteolytic activity and both proteins are correlated with albuminuria in type 1 diabetes patients [69]. Muramatsu and colleagues reported that CCN1 (Cyr61) which is up-regulated in SS_PU, was rapidly induced in rodent proximal tubules and detected in the urine after renal ischemic reperfusion injury [70]. The authors found Cyr61 in the outer rat medulla after ischemic events, in line with medullary VOC in SCD.

In our fluorescence staining and RT-PCR experiments we revealed increased p53 levels in podocytes supplemented with urine from SCD_PU patients. In addition, elevated levels of pro-inflammatory associated mRNAs such as TGFβ in podocytes treated with urine from SCD-PU patients led us to the hypothesis depicted in the scheme in Figure 6: SCD patients with severe inflammation leading to nephropathy is manifested by elevated levels of TGFβ, p53 and also inflammation-associated cytokines RETN, IL1RA, RAGE, TFF3 and PLAU. TGFβ has already been proposed as a urinary marker of renal dysfunction in sickle cell disease [71]. Overstreet et al. proposed that TGFβ contributes to renal injury and fibrosis and that TGFβ activates p53 by phosphorylation which together with SMAD3 transcription factors induce fibrosis in several renal cell types [72] . p53 protein responds to diverse cellular stresses to regulate expression of target genes, thereby inducing cell cycle arrest, apoptosis, senescence and changes in metabolism. Podocyte injury and death has been shown in the mouse by silencing p53 and its

bioRxiv preprint doi: https://doi.org/10.1101/2025.08.08.669286; this version posted August 9, 2025. The copyright holder for this preprint (which was not certified by peer review) is the author/funder. All rights reserved. No reuse allowed without permission.

inhibitor MDM2 [73]. Further biological processes involved in renal injury include e-organization of the extra-cellular matrix and Integrin cell surface interactions. Kidney injury is manifested by increased levels of LCN2 (NGAL) and decreased levels of CLU. Both our urine SCD, SCD_PU patient and healthy urine analyses coupled with independent analysis of the effect of secreted proteins on human podocytes confirmed the involvement of VEGF (Vascular Endothelial Growth Factor) in the progression of CKD and fibrosis. Interestingly numerous clinical trials are currently exploring the role of VEGF in kidney diseases by using VEGF inhibitors to reduce proteinuria and slow disease progression in conditions like diabetic nephropathy. There is also research into using mesenchymal stem cells over expressing VEGF to promote renal recovery and improve outcomes in chronic kidney disease [74], [75] .

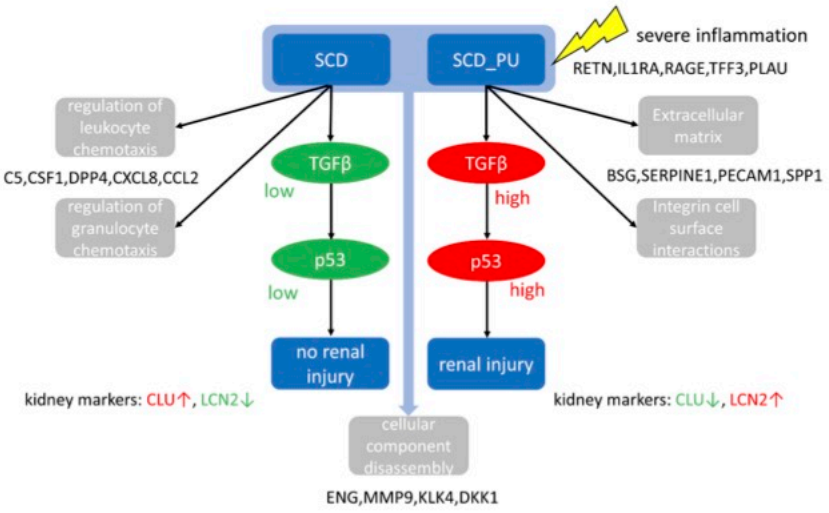


Figure 6: proposed model of how the TGFβ-p53 axis induce renal injury in sickle cell patients. In our cell culture model, we uncovered increased levels of TGFβ and p53 in podocytes supplemented with urine from SCD patients with proteinuria. We therefore hypothesize that SCD patients with more severe inflammation which is manifested by higher levels of TGFβ and other pro-inflammation-associated cytokines RETN, IL1RA, RAGE, TFF3

bioRxiv preprint doi: https://doi.org/10.1101/2025.08.08.669286; this version posted August 9, 2025. The copyright holder for this preprint (which was not certified by peer review) is the author/funder. All rights reserved. No reuse allowed without permission.

and PLAU develop nephropathy mediated by p53. Additional biological processes involved in this include organization of the extra-cellular matrix and Integrin cell surface interactions. Kidney injury can be further characterized by high levels of LCN2 (NGAL) and low levels of CLU.

In conclusion, our study revealed distinct urinary kidney injury and cytokine protein profiles between SCD patients without and SCD_PU patients with proteinuria compared to healthy individuals. These profiles also enabled distinguishing SS and SC genotypes. We validated up-regulation of NGAL (encoded by the gene LCN2) in SCD_PU (also in both genotypes SS and SC) and down-regulation of Clusterin with ELISA assays. Follow-up analysis reconstructed a network of urinary secreted proteins in SCD and up-, down or not-regulated in the SCD_PU condition. Proteins up-regulated in SCD_PU were associated with the pathway- "integrin cell surface interactions" which might imply that disrupting the association between hyperfiltration, linking of and integrins to the glomerular basement membrane ultimately leads to glomerular fibrosis.

We finally proposed model of how the TGFβ and p53 axis induce renal injury in sickle cell patients with severe inflammation.

Author contributions

J.A. and V.B. conceived the study. VB, YD-A, M L, designed and conducted the clinical study, supervised the recruitment and collection of the patient samples.

JA and TK-A stratified patient urine samples.

AIP, CL, RM and CT carried out the experiments and analysed the data. WW provided bioinformatics support. WW, AIP and CT wrote the manuscript.

JA supervised the work, co-wrote the manuscript, edited and gave the final approval.

bioRxiv preprint doi: https://doi.org/10.1101/2025.08.08.669286; this version posted August 9, 2025. The copyright holder for this preprint (which was not certified by peer review) is the author/funder. All rights reserved. No reuse allowed without permission.

Competing interests

The authors declare no competing interests.

Acknowledgments

James Adjaye acknowledges financial support from the Medical faculty of the Heinrich-Heine University, Duesseldorf.

Vincent Boima acknowledges support from the University of Ghana Medical School and all participants who consented to participate in this study.

Data availability

The datasets generated during the current study are provided as supplementary data.

References

1. Elendu C, Amaechi DC, Alakwe-Ojimba CE, Elendu TC, Elendu RC, Ayabazu CP, et al. Understanding Sickle cell disease: Causes, symptoms, and treatment options. Medicine (Baltimore). 2023;102:e35237. https://doi.org/10.1097/MD.0000000000035237.

2. Thein SL. The molecular basis of β-thalassemia. Cold Spring Harb Perspect Med. 2013;3:a011700. https://doi.org/10.1101/cshperspect.a011700.

3. Bunn HF. Pathogenesis and treatment of sickle cell disease. N Engl J Med. 1997;337:762–9. https://doi.org/10.1056/NEJM199709113371107.

4. Rees DC, Williams TN, Gladwin MT. Sickle-cell disease. Lancet. 2010;376:2018–31. https://doi.org/10.1016/S0140-6736(10)61029-X.

5. Kato GJ, Gladwin MT, Steinberg MH. Deconstructing sickle cell disease: reappraisal of the role of hemolysis in the development of clinical subphenotypes. Blood Rev. 2007;21:37–47. https://doi.org/10.1016/j.blre.2006.07.001.

6. Platt OS, Brambilla DJ, Rosse WF, Milner PF, Castro O, Steinberg MH, et al. Mortality in sickle cell disease. Life expectancy and risk factors for early death. N Engl J Med. 1994;330:1639–44. https://doi.org/10.1056/NEJM199406093302303.

bioRxiv preprint doi: https://doi.org/10.1101/2025.08.08.669286; this version posted August 9, 2025. The copyright holder for this preprint (which was not certified by peer review) is the author/funder. All rights reserved. No reuse allowed without permission.

7. Weatherall D, Hofman K, Rodgers G, Ruffin J, Hrynkow S. A case for developing North-South partnerships for research in sickle cell disease. Blood. 2005;105:921–3. https://doi.org/10.1182/blood-2004-06-2404.

8. Azevedo-Silva F. Lipids and Sickle Cell Disease. International Journal of Cardiovascular Sciences. 2022;35:780–3. https://doi.org/10.36660/ijcs.20220169.

9. Saraf SL, Molokie RE, Nouraie M, Sable CA, Luchtman-Jones L, Ensing GJ, et al. Differences in the clinical and genotypic presentation of sickle cell disease around the world. Paediatr Respir Rev. 2014;15:4–12. https://doi.org/10.1016/j.prrv.2013.11.003.

10. Kato GJ, Piel FB, Reid CD, Gaston MH, Ohene-Frempong K, Krishnamurti L, et al. Sickle cell disease. Nat Rev Dis Primers. 2018;4:18010. https://doi.org/10.1038/nrdp.2018.10.

11. Aeddula NR, Bardhan M, Baradhi KM. Sickle Cell Nephropathy. In: StatPearls. Treasure Island (FL): StatPearls Publishing; 2025.

12. Derebail VK, Nachman PH, Key NS, Ansede H, Falk RJ, Kshirsagar AV. High prevalence of sickle cell trait in African Americans with ESRD. J Am Soc Nephrol. 2010;21:413–7. https://doi.org/10.1681/ASN.2009070705.

13. Yium J, Gabow P, Johnson A, Kimberling W, Martinez-Maldonado M. Autosomal dominant polycystic kidney disease in blacks: clinical course and effects of sickle-cell hemoglobin. J Am Soc Nephrol. 1994;4:1670–4. https://doi.org/10.1681/ASN.V491670.

14. Sesso R, Almeida MA, Figueiredo MS, Bordin JO. Renal dysfunction in patients with sickle cell anemia or sickle cell trait. Braz J Med Biol Res. 1998;31:1257–62. https://doi.org/10.1590/s0100-879x1998001000004.

15. Ajayi AA, Kolawole BA. Sickle cell trait and gender influence type 2 diabetic complications in African patients. Eur J Intern Med. 2004;15:312–5. https://doi.org/10.1016/j.ejim.2004.06.003.

16. Amarapurkar P, Roberts L, Navarrete J, El Rassi F. Sickle Cell Disease and Kidney. Advances in Chronic Kidney Disease. 2022;29:141-148.e1. https://doi.org/10.1053/j.ackd.2022.03.004.

17. Ataga KI, Derebail VK, Archer DR. The glomerulopathy of sickle cell disease. American J Hematol. 2014;89:907–14. https://doi.org/10.1002/ajh.23762.

18. Allon M, Lawson L, Eckman JR, Delaney V, Bourke E. Effects of nonsteroidal antiinflammatory drugs on renal function in sickle cell anemia. Kidney Int. 1988;34:500–6. https://doi.org/10.1038/ki.1988.209.

19. Tanaka T, Maruyama S, Chishima N, Akiyama H, Shimamoto K, Inokuchi S, et al. Population characteristics and diagnosis rate of chronic kidney disease by eGFR and proteinuria in Japanese clinical practice: an observational database study. Sci Rep. 2024;14:5172. https://doi.org/10.1038/s41598-024-55827-7.

20. O'Connor NR, Corcoran AM. End-stage renal disease: symptom management and advance care planning. Am Fam Physician. 2012;85:705–10.

21. Artom M, Moss-Morris R, Caskey F, Chilcot J. Fatigue in advanced kidney disease. Kidney Int. 2014;86:497–505. https://doi.org/10.1038/ki.2014.86.

bioRxiv preprint doi: https://doi.org/10.1101/2025.08.08.669286; this version posted August 9, 2025. The copyright holder for this preprint (which was not certified by peer review) is the author/funder. All rights reserved. No reuse allowed without permission.

22. Cravedi P, Remuzzi G. Pathophysiology of proteinuria and its value as an outcome measure in chronic kidney disease. Br J Clin Pharmacol. 2013;76:516–23. https://doi.org/10.1111/bcp.12104.

23. Haynes J, Haynes R. Proteinuria. BMJ. 2006;332:284. https://doi.org/10.1136/bmj.332.7536.284.

24. Nielsen R, Christensen EI. Proteinuria and events beyond the slit. Pediatr Nephrol. 2010;25:813–22. https://doi.org/10.1007/s00467-009-1381-9.

25. Haider MZ, Aslam A. Proteinuria. In: StatPearls. Treasure Island (FL): StatPearls Publishing; 2025.

26. Lim D, Lee D-Y, Cho SH, Kim OZ, Cho SW, An SK, et al. Diagnostic accuracy of urine dipstick for proteinuria in older outpatients. Kidney Res Clin Pract. 2014;33:199–203. https://doi.org/10.1016/j.krcp.2014.10.003.

27. Tomonaga Y, Risch L, Szucs TD, Ambühl PM. The prevalence of chronic kidney disease in a primary care setting: a Swiss cross-sectional study. PLoS One. 2013;8:e67848. https://doi.org/10.1371/journal.pone.0067848.

28. Kaze FF, Kengne A-P, Atanga LC, Monny Lobe M, Menanga AP, Halle M-P, et al. Kidney function, urinalysis abnormalities and correlates in equatorial Africans with sickle cell disease. Clin Kidney J. 2013;6:15–20. https://doi.org/10.1093/ckj/sfs100.

29. Schwartz GJ, Muñoz A, Schneider MF, Mak RH, Kaskel F, Warady BA, et al. New equations to estimate GFR in children with CKD. J Am Soc Nephrol. 2009;20:629–37. https://doi.org/10.1681/ASN.2008030287.

30. Erichsen L, Thimm C, Wruck W, Kaierle D, Schless M, Huthmann L, et al. Secreted Cytokines within the Urine of AKI Patients Modulate TP53 and SIRT1 Levels in a Human Podocyte Cell Model. IJMS. 2023;24:8228. https://doi.org/10.3390/ijms24098228.

31. Wruck W, Boima V, Erichsen L, Thimm C, Koranteng T, Kwakyi E, et al. Urine-Based Detection of Biomarkers Indicative of Chronic Kidney Disease in a Patient Cohort from Ghana. JPM. 2022;13:38. https://doi.org/10.3390/jpm13010038.

32. Schneider CA, Rasband WS, Eliceiri KW. NIH Image to ImageJ: 25 years of image analysis. Nat Methods. 2012;9:671–5. https://doi.org/10.1038/nmeth.2089.

33. Gentleman RC, Carey VJ, Bates DM, Bolstad B, Dettling M, Dudoit S, et al. Bioconductor: open software development for computational biology and bioinformatics. Genome Biol. 2004;5:R80. https://doi.org/10.1186/gb-2004-5-10-r80.

34. Du P, Kibbe WA, Lin SM. lumi: a pipeline for processing Illumina microarray. Bioinformatics. 2008;24:1547–8. https://doi.org/10.1093/bioinformatics/btn224.

35. Smyth GK. Linear Models and Empirical Bayes Methods for Assessing Differential Expression in Microarray Experiments. Statistical Applications in Genetics and Molecular Biology. 2004;3. https://doi.org/10.2202/1544-6115.1027.

36. Warnes GR, Bolker B, Bonebakker L, Gentleman R, Liaw WHA, Lumley T, et al. gplots: Various R Programming Tools for Plotting Data. 2015.

37. Saleem MA, O'Hare MJ, Reiser J, Coward RJ, Inward CD, Farren T, et al. A Conditionally Immortalized Human Podocyte Cell Line Demonstrating Nephrin and Podocin Expression.

bioRxiv preprint doi: https://doi.org/10.1101/2025.08.08.669286; this version posted August 9, 2025. The copyright holder for this preprint (which was not certified by peer review) is the author/funder. All rights reserved. No reuse allowed without permission.

Journal of the American Society of Nephrology. 2002;13:630–8. https://doi.org/10.1681/ASN.V133630.

38. Erichsen L, Thimm C, Bohndorf M, Rahman MS, Wruck W, Adjaye J. Activation of the Renin–Angiotensin System Disrupts the Cytoskeletal Architecture of Human Urine-Derived Podocytes. Cells. 2022;11:1095. https://doi.org/10.3390/cells11071095.

39. Thimm C, Erichsen L, Wruck W, Adjaye J. Unveiling Angiotensin II and Losartan-Induced Gene Regulatory Networks Using Human Urine-Derived Podocytes. IJMS. 2023;24:10551. https://doi.org/10.3390/ijms241310551.

40. Miller RG, Brown BW. Beyond ANOVA: basics of applied statistics. 1st ed. London ; New York: Chapman & Hall; 1997.

41. Jung G-S, Kim M-K, Jung Y-A, Kim H-S, Park I-S, Min B-H, et al. Clusterin attenuates the development of renal fibrosis. J Am Soc Nephrol. 2012;23:73–85. https://doi.org/10.1681/ASN.2011010048.

42. Zeng X-F, Lu D-X, Li J-M, Tan Y, Li Z, Zhou L, et al. Performance of urinary neutrophil gelatinase-associated lipocalin, clusterin, and cystatin C in predicting diabetic kidney disease and diabetic microalbuminuria: a consecutive cohort study. BMC Nephrol. 2017;18:233. https://doi.org/10.1186/s12882-017-0620-8.

43. Ellington AA, Malik AR, Klee GG, Turner ST, Rule AD, Mosley TH, et al. Association of Plasma Resistin With Glomerular Filtration Rate and Albuminuria in Hypertensive Adults. Hypertension. 2007;50:708–14. https://doi.org/10.1161/HYPERTENSIONAHA.107.095257.

44. Axelsson J, Bergsten A, Qureshi AR, Heimbürger O, Bárány P, Lönnqvist F, et al. Elevated resistin levels in chronic kidney disease are associated with decreased glomerular filtration rate and inflammation, but not with insulin resistance. Kidney Int. 2006;69:596–604. https://doi.org/10.1038/sj.ki.5000089.

45. Arend WP. The balance between IL-1 and IL-1Ra in disease. Cytokine Growth Factor Rev. 2002;13:323–40. https://doi.org/10.1016/s1359-6101(02)00020-5.

46. Afsar B, Covic A, Ortiz A, Afsar RE, Kanbay M. The Future of IL-1 Targeting in Kidney Disease. Drugs. 2018;78:1073–83. https://doi.org/10.1007/s40265-018-0942-2.

47. Tam FW, Smith J, Cashman SJ, Wang Y, Thompson EM, Rees AJ. Glomerular expression of interleukin-1 receptor antagonist and interleukin-1 beta genes in antibody-mediated glomerulonephritis. Am J Pathol. 1994;145:126–36.

48. Descamps-Latscha B, Herbelin A, Nguyen AT, Roux-Lombard P, Zingraff J, Moynot A, et al. Balance between IL-1 beta, TNF-alpha, and their specific inhibitors in chronic renal failure and maintenance dialysis. Relationships with activation markers of T cells, B cells, and monocytes. The Journal of Immunology. 1995;154:882–92. https://doi.org/10.4049/jimmunol.154.2.882.

49. Duni A, Liakopoulos V, Roumeliotis S, Peschos D, Dounousi E. Oxidative Stress in the Pathogenesis and Evolution of Chronic Kidney Disease: Untangling Ariadne's Thread. IJMS. 2019;20:3711. https://doi.org/10.3390/ijms20153711.

50. Wu X-Q, Zhang D-D, Wang Y-N, Tan Y-Q, Yu X-Y, Zhao Y-Y. AGE/RAGE in diabetic kidney disease and ageing kidney. Free Radical Biology and Medicine. 2021;171:260–71. https://doi.org/10.1016/j.freeradbiomed.2021.05.025.

bioRxiv preprint doi: https://doi.org/10.1101/2025.08.08.669286; this version posted August 9, 2025. The copyright holder for this preprint (which was not certified by peer review) is the author/funder. All rights reserved. No reuse allowed without permission.

51. Zhou LL, Hou FF, Wang GB, Yang F, Xie D, Wang YP, et al. Accumulation of advanced oxidation protein products induces podocyte apoptosis and deletion through NADPH-dependent mechanisms. Kidney Int. 2009;76:1148–60. https://doi.org/10.1038/ki.2009.322.

52. Scott RP, Quaggin SE. The cell biology of renal filtration. Journal of Cell Biology. 2015;209:199–210. https://doi.org/10.1083/jcb.201410017.

53. Pozzi A, Jarad G, Moeckel GW, Coffa S, Zhang X, Gewin L, et al. β1 integrin expression by podocytes is required to maintain glomerular structural integrity. Developmental Biology. 2008;316:288–301. https://doi.org/10.1016/j.ydbio.2008.01.022.

54. Kreidberg JA, Donovan MJ, Goldstein SL, Rennke H, Shepherd K, Jones RC, et al. Alpha 3 beta 1 integrin has a crucial role in kidney and lung organogenesis. Development. 1996;122:3537–47. https://doi.org/10.1242/dev.122.11.3537.

55. El-Aouni C, Herbach N, Blattner SM, Henger A, Rastaldi MP, Jarad G, et al. Podocyte-Specific Deletion of Integrin-Linked Kinase Results in Severe Glomerular Basement Membrane Alterations and Progressive Glomerulosclerosis. Journal of the American Society of Nephrology. 2006;17:1334–44. https://doi.org/10.1681/ASN.2005090921.

56. Piali L, Hammel P, Uherek C, Bachmann F, Gisler RH, Dunon D, et al. CD31/PECAM-1 is a ligand for alpha v beta 3 integrin involved in adhesion of leukocytes to endothelium. J Cell Biol. 1995;130:451–60. https://doi.org/10.1083/jcb.130.2.451.

57. Buckley CD, Doyonnas R, Newton JP, Blystone SD, Brown EJ, Watt SM, et al. Identification of αvβ3 as a heterotypic ligand for CD31/PECAM-1. Journal of Cell Science. 1996;109:437–45. https://doi.org/10.1242/jcs.109.2.437.

58. Khan S, Lakhe-Reddy S, McCarty JH, Sorenson CM, Sheibani N, Reichardt LF, et al. Mesangial Cell Integrin αvβ8 Provides Glomerular Endothelial Cell Cytoprotection by Sequestering TGF-β and Regulating PECAM-1. The American Journal of Pathology. 2011;178:609–20. https://doi.org/10.1016/j.ajpath.2010.10.031.

59. Wei C, Möller CC, Altintas MM, Li J, Schwarz K, Zacchigna S, et al. Modification of kidney barrier function by the urokinase receptor. Nat Med. 2008;14:55–63. https://doi.org/10.1038/nm1696.

60. Scheinman JI. Sickle cell disease and the kidney. Nat Rev Nephrol. 2009;5:78–88. https://doi.org/10.1038/ncpneph1008.

61. Du T, Luo H, Qin H, Wang F, Wang Q, Xiang Y, et al. Circulating Serum Trefoil Factor 3 (TFF3) Is Dramatically Increased in Chronic Kidney Disease. PLoS ONE. 2013;8:e80271. https://doi.org/10.1371/journal.pone.0080271.

62. Obeagu EI, Obeagu GU. Management of diabetes mellitus patients with sickle cell anemia: Challenges and therapeutic approaches. Medicine (Baltimore). 2024;103:e37941. https://doi.org/10.1097/MD.0000000000037941.

63. Zhang G, Eddy AA. Urokinase and its receptors in chronic kidney disease. Front Biosci. 2008;13:5462–78. https://doi.org/10.2741/3093.

64. Ahn S-Y, Chin HJ. Urokinase-type plasminogen activator receptor in IgA nephropathy. Korean J Intern Med. 2014;29:166–9. https://doi.org/10.3904/kjim.2014.29.2.166.

65. Marouf R, Adekile AD, El-Muzaini H, Abdulla R, Mojiminiyi OA. Neutrophil gelatinase–associated lipocalin as a biomarker of nephropathy in sickle cell disease. Ann Hematol. 2021;100:1401–9. https://doi.org/10.1007/s00277-021-04500-4.

bioRxiv preprint doi: https://doi.org/10.1101/2025.08.08.669286; this version posted August 9, 2025. The copyright holder for this preprint (which was not certified by peer review) is the author/funder. All rights reserved. No reuse allowed without permission.

66. Devarajan P. Review: Neutrophil gelatinase-associated lipocalin: A troponin-like biomarker for human acute kidney injury. Nephrology. 2010;15:419–28. https://doi.org/10.1111/j.1440-1797.2010.01317.x.

67. Mishra J, Ma Q, Prada A, Mitsnefes M, Zahedi K, Yang J, et al. Identification of Neutrophil Gelatinase-Associated Lipocalin as a Novel Early Urinary Biomarker for Ischemic Renal Injury. Journal of the American Society of Nephrology. 2003;14:2534–43. https://doi.org/10.1097/01.ASN.0000088027.54400.C6.

68. Audard V, Moutereau S, Vandemelebrouck G, Habibi A, Khellaf M, Grimbert P, et al. First evidence of subclinical renal tubular injury during sickle-cell crisis. Orphanet J Rare Dis. 2014;9:67. https://doi.org/10.1186/1750-1172-9-67.

69. Thrailkill KM, Moreau CS, Cockrell GE, Jo C-H, Bunn RC, Morales-Pozzo AE, et al. Disease and gender-specific dysregulation of NGAL and MMP-9 in type 1 diabetes mellitus. Endocr. 2010;37:336–43. https://doi.org/10.1007/s12020-010-9308-6.

70. Muramatsu Y, Tsujie M, Kohda Y, Pham B, Perantoni AO, Zhao H, et al. Early detection of cysteine rich protein 61 (CYR61, CCN1) in urine following renal ischemic reperfusion injury. Kidney Int. 2002;62:1601–10. https://doi.org/10.1046/j.1523-1755.2002.00633.x.

71. Mohtat D, Thomas R, Du Z, Boakye Y, Moulton T, Driscoll C, et al. Urinary transforming growth factor beta-1 as a marker of renal dysfunction in sickle cell disease. Pediatr Nephrol. 2011;26:275–80. https://doi.org/10.1007/s00467-010-1677-9.

72. Overstreet JM, Gifford CC, Tang J, Higgins PJ, Samarakoon R. Emerging role of tumor suppressor p53 in acute and chronic kidney diseases. Cell Mol Life Sci. 2022;79. https://doi.org/10.1007/s00018-022-04505-w.

73. Thomasova D, Bruns HA, Kretschmer V, Ebrahim M, Romoli S, Liapis H, et al. Murine Double Minute-2 Prevents p53-Overactivation-Related Cell Death (Podoptosis) of Podocytes. J Am Soc Nephrol. 2015;26:1513–23. https://doi.org/10.1681/ASN.2014040345.

74. Yuan L, Wu M-J, Sun H-Y, Xiong J, Zhang Y, Liu C-Y, et al. VEGF-modified human embryonic mesenchymal stem cell implantation enhances protection against cisplatin-induced acute kidney injury. Am J Physiol Renal Physiol. 2011;300:F207-218. https://doi.org/10.1152/ajprenal.00073.2010.

75. Tögel F, Zhang P, Hu Z, Westenfelder C. VEGF is a mediator of the renoprotective effects of multipotent marrow stromal cells in acute kidney injury. J Cell Mol Med. 2009;13:2109–14. https://doi.org/10.1111/j.1582-4934.2008.00641.x.

bioRxiv preprint doi: https://doi.org/10.1101/2025.08.08.669286; this version posted August 9, 2025. The copyright holder for this preprint (which was not certified by peer review) is the author/funder. All rights reserved. No reuse allowed without permission.

Tables

Table 1: Clinical features of patients whose urine samples were pooled into the SCD_PU, SCD and control groups

AGE	GENDER	Genotype	Std dipstick	Hb	Wbc	Platelet	S-Cr	GFR(CKC)		S- Alb.	U-Albu.	U-Cr	U-Al/Cr
						SCD_PU							
27	M	SS	Positive	6,8	14,9	518	31	>89		36	809,61	5,88	137,69
21	M	SC	Positive	10,4	13,3	258	72	>89		36	33,25	13,69	2,43
21	F	SS	Positive	9,9	8,2	538	64	>89		40	947,21	9,58	98,87
29	F	SS	Positive	9,5	7,9	490	28	>89		36	176,33	6,29	28,03
28	F	SS	Positive	6,9	9,9	461	38	>89		47	314	0,49	640,82
31	F	SC	Positive	9,9	11,5	460	65	>89		43	333,15	8,69	38,34
19?	M	SC	Positive	9,5	16,3	655	61	>89		36	246,74	18,14	13,6
26	F	SS	Positive	6,7	6,2	358							
28?	F	SS	Positive	6,5	12,6	616	71	>89		42	885,78	16,63	53,26
						SCD							
18	M	SC	Negative	8,7	8,4	480	64	>89		44	36,97	7,09	5,21
45	F	SS	Negative	8	9,1	257	46	>89		44	20,15	8,49	2,37
48/49	F	SS	Negative	9,5	6,1	88	60	>89		48	5,86	9,8	0,6
18	M	SC	Negative	10,4	14,4	412	55	>89		43	17,52	4,16	4,21
42	F	SC	Negative	11,8	7,5	272	103		72	40	3,5	6,91	0,51
37	F	SS	Negative	11,2	7,07	242	55	>89		45	3,88	8,32	0,47
43	F	SS	Negative	10,2	5,64	305	30	>89		46	5,56	5,39	1,03
23?	F	SS	Negative	6,8	8,2	386	37	>89		46	53,98	19,56	2,76
29	F	SS	Negative	8	7,2	436	53	>89		44	33,81	11,05	3,06
						control							
32	M	AA	Negative	14,2	4,3	276	120		69	42	0,97	10,62	0,09
21	M	AC	Negative	14,8	7,5	223	55	>89		46	2,84	9,94	0,29
31	F	AC	Negative	13,4	5,7	272	60	>89		41	5,23	19,75	0,26
34	F	AA	Negative	13	6,2	86	58	>89		44	4,24	12,54	0,34
31	M	AA	Negative	15,2	3,9	251	78	>89		47	4,29	16,48	0,26
39	M	AA	Negative	14,6	5,1	189	75	>89		41	4,6	10,33	0,45
43	M	AA	Negative	13,8	4,7	237	71	>89		42	68,52	14,56	4,71
38	M	AA	Negative	14,1	3,9	149	71	>89		45	13,15	15,37	0,86
30	M	AA	Negative	14,3	6,2	259	82	>89		40	43,5	14,94	2,91
27	F	AA	Negative	12,8	9,2	209	53	>89		43	4,88	12,21	0,4

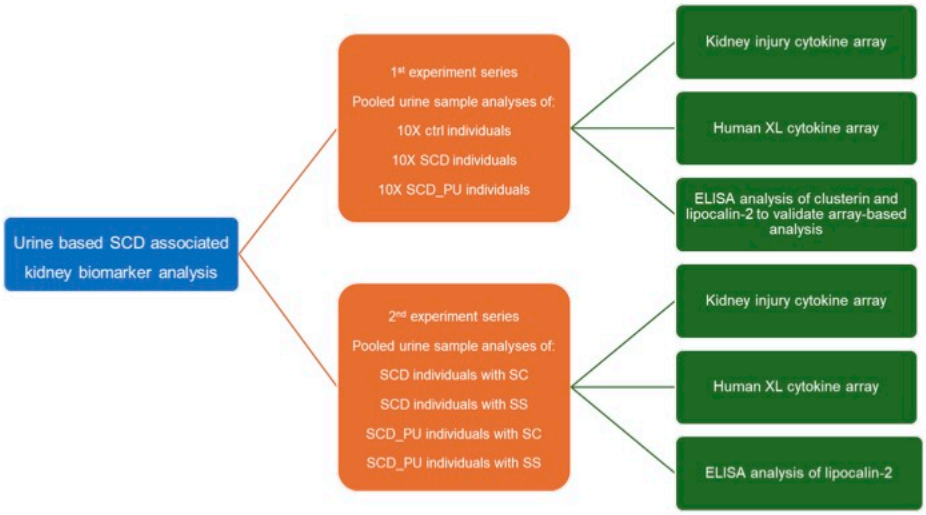
bioRxiv preprint doi: https://doi.org/10.1101/2025.08.08.669286; this version posted August 9, 2025. The copyright holder for this preprint (which was not certified by peer review) is the author/funder. All rights reserved. No reuse allowed without permission.

Table 2: Up- and down-regulated proteins between SCD_PU, SCD and control and SS_PU and SC_PU

protein	SCD_PU_vs_SCD	SCD_PU_vs_ctrl	SCD_vs_ctrl	SS_PU_vs_SC_PU	array
ADIPOQ	down		up		kidney
ANPEP	down		up	down	
AG	down				
CLU	down		up	down	
DPP4	down	down	up		
FABP1	down		up		
MMP9	down				
KLK3	down		down	down	
CCL2		down	down		
PLAU	up	down	down		
VEGF		down	down		
RETN	up	up	down	down	
IL1RN	up	up			
AGER	up				
TFF3	up				
CXCL16			up		
IL6				down	
SERPINA3				down	
TNFSF13B	down		up	up	human_XL
C5	down	down	up		
DPP4	down		up	down	
IL8	down	down			
CCL2	down		up		
CSF1	down		up	up	
RBP4	down		up		
GC	down	down			
ANG		down	down		
CFD		down			
KLK4		down	down	down	
MMP9		down		up	
CFD			down		
SHBG	up		down	down	
PECAM1	up		down	down	
BSG	up				
IL1RN	up	up			
IL17A	up	up			
IL18BP	up				
SPP1	up			down	
SERPINE1	up				
CD30		up			
CST3		up		down	
RETN		up	up		
APOA1			up	up	
CD30			up	up	
CD40LG				down	
CSF3				down	
MPO				down	
TFF3				down	
HAVCR2				down	
CD106				down	
ADIPOQ				up	
ANGPT2				up	
CHI3L1				up	
DKK1				up	
BSG				up	
LCN2				up	
MIF				up	
VEGFA				up	

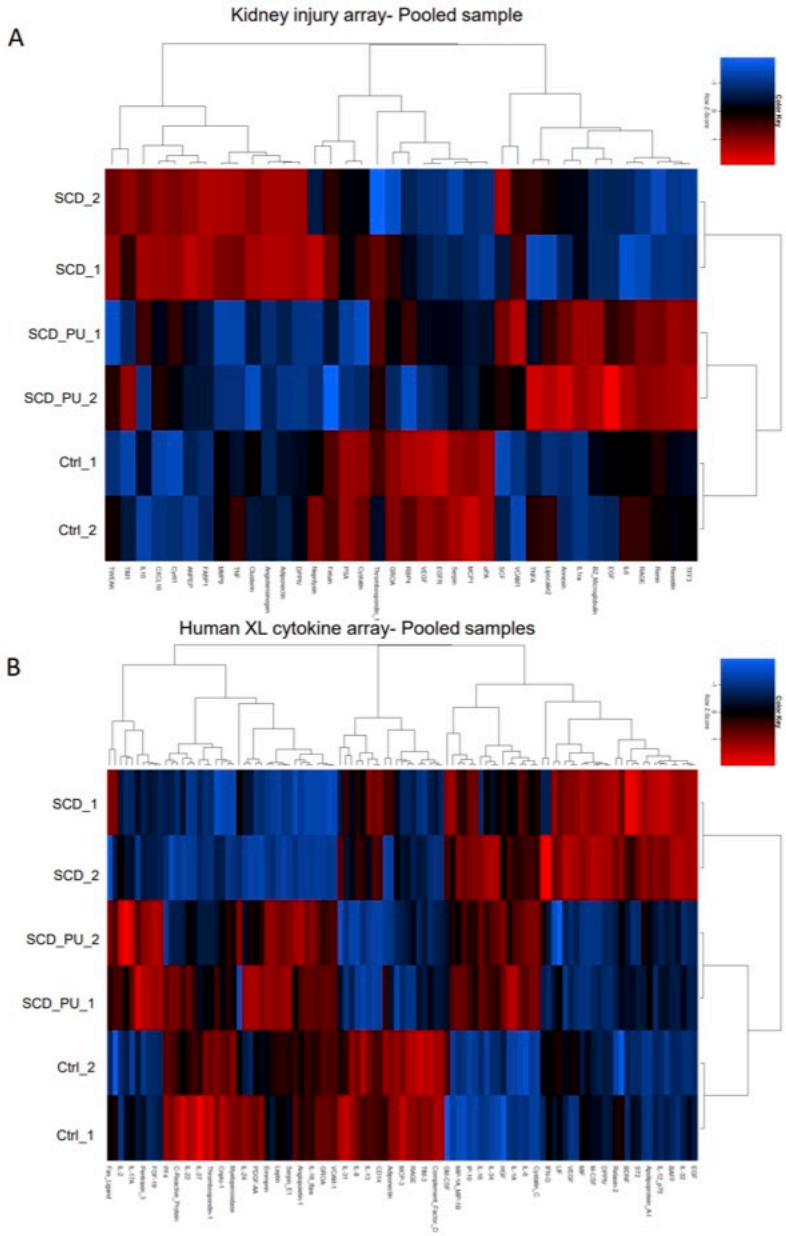
bioRxiv preprint doi: https://doi.org/10.1101/2025.08.08.669286; this version posted August 9, 2025. The copyright holder for this preprint (which was not certified by peer review) is the author/funder. All rights reserved. No reuse allowed without permission.

Supplementary Information



Supplementary Figure 1: Flow chart of experiment series of cytokine measurements in urine samples from SCD patients with and without proteinuria and with SC and SS genotypes.

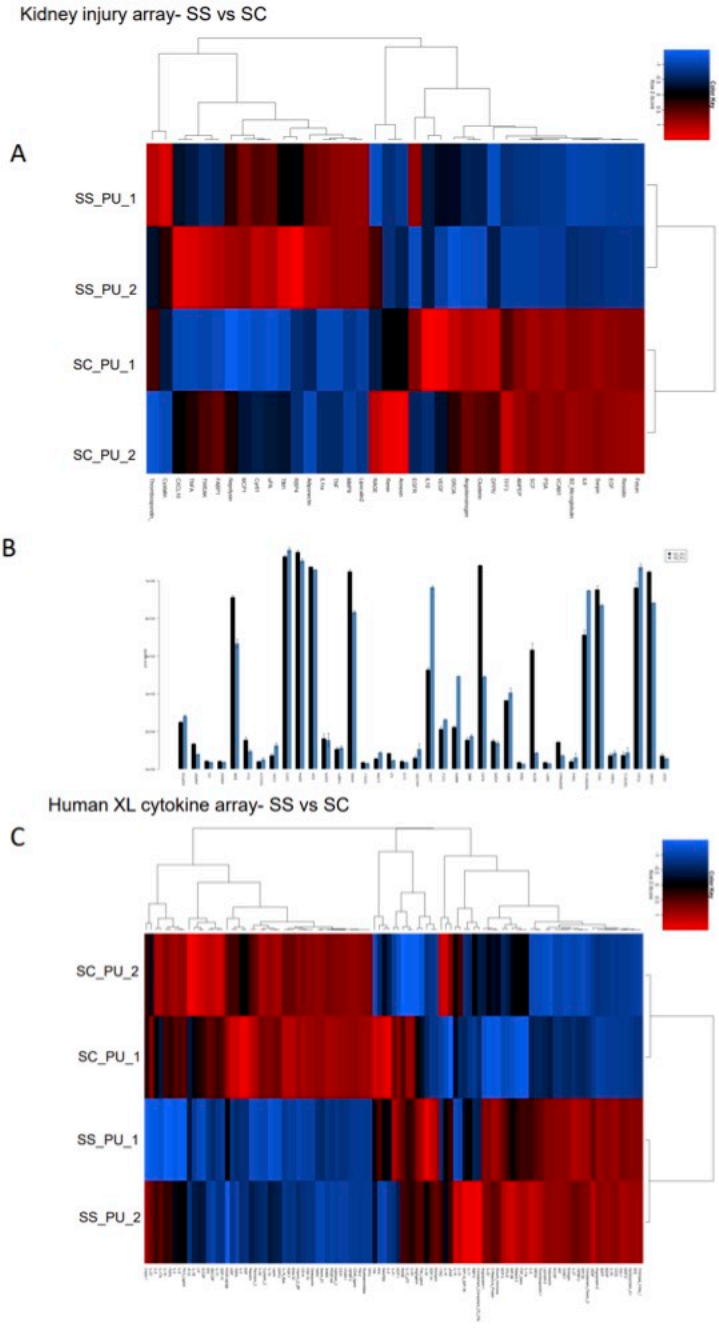
bioRxiv preprint doi: https://doi.org/10.1101/2025.08.08.669286; this version posted August 9, 2025. The copyright holder for this preprint (which was not certified by peer review) is the author/funder. All rights reserved. No reuse allowed without permission.



bioRxiv preprint doi: https://doi.org/10.1101/2025.08.08.669286; this version posted August 9, 2025. The copyright holder for this preprint (which was not certified by peer review) is the author/funder. All rights reserved. No reuse allowed without permission.

Supplementary Figure 2: Comparison of protein expression in SCD with and without proteinuria and healthy control. (A) Kidney injury array- Pooled sample. (B) Human XL cytokine array- Pooled samples.

bioRxiv preprint doi: https://doi.org/10.1101/2025.08.08.669286; this version posted August 9, 2025. The copyright holder for this preprint (which was not certified by peer review) is the author/funder. All rights reserved. No reuse allowed without permission.



bioRxiv preprint doi: https://doi.org/10.1101/2025.08.08.669286; this version posted August 9, 2025. The copyright holder for this preprint (which was not certified by peer review) is the author/funder. All rights reserved. No reuse allowed without permission.

Supplementary Figure 3 (linked to main fig 1+2): Comparison of protein in genotypes SS and SC. (A) Heatmap depicting expression of proteins on the Kidney injury array- SS vs SC. (B). Bar chart depicting expression of proteins on the Kidney injury array- SS vs SC. (C) Heatmap depicting expression of proteins on the Human XL cytokine array- SS vs SC.

Supplementary Figure 4 (figS4.pdf, linked to main fig 1, 2 and 4): Scanned cytokine arrays of experiments in this study:(A) Pooled urine samples of SCD_PU, SCD and Ctrl on kidney protein array. (B) Pooled urine samples of SCD_PU, SCD and Ctrl on Human XL cytokine array. (C) Pooled urine samples of genotypes SS and SC on kidney protein array. (D) Pooled urine samples of genotypes SS and SC on Human XL cytokine array.

Supplementary Tables

Supplementary Table 1 (table S1.xlsx): Antibodies and primers.

Supplementary Table 2 (tableS2_kmembrane_SCD_PU_SCD_ctrl.xlsx): mean values and statistical test results of (a) SCD_PU vs. control, (b) SCD vs. control and (c) SCD_PU vs. SCD on kidney injury marker array.

Supplementary Table 3 (tableS3_humanXL_SCD_PU_SCD_ctrl.xlsx): mean values and statistical test results of (a) SCD_PU vs. control, (b) SCD vs. control and (c) SCD_PU vs. SCD on human XL cytokine array. Corresponding metascape enrichment results are in sheets (d-f)

Supplementary Table 4 (tableS4_SS_PU_vs_SC_PU.xlsx): mean values and statistical test results of genotype SS and SC comparisons (a) SS_PU vs. SC_PU on kidney injury marker array, (b) SS_PU vs. SC_PU on human XL cytokine array.

3.11 Human Urine-derived SIX2-positive renal progenitor cells improve kidney injury in an IRI mouse model

Claus Kordes, Lucas-Sebastian Spitzhorn, Martina Bohndorf, Audrey Ncube, **Chantelle Thimm**, Lars Erichsen, Wasco Wruck, James Adjaye

BioRxiv, 2025

Abstract

Cells with the characteristics of renal progenitor cells are shed in urine. The aim of this study was to investigate whether these SIX2-positive urine-derived renal progenitor cells (UdRPC) have therapeutic potential in treating or managing acute to chronic kidney injuries. Human UdRPC were obtained from a woman aged 35 years, expanded, and characterized in vitro and finally transplanted unilaterally under the renal capsule of mouse kidneys that had undergone ischemia reperfusion injury (IRI). Analyses of blood serum from the mice revealed that the transplanted human UdRPC transiently influenced the secretome of the animals by triggering the release of inflammatory and angiogenic factors. Of obvious therapeutic relevance, however, was the finding that the transplanted cells suppressed renal fibrosis resulting from IRI. The expression of genes linked to inflammation and chronic kidney disease was also reduced in mouse kidneys in the presence of UdRPC. Ultimately, the human UdRPC were able to alleviate the severity of the injury through the amelioration of fibrosis but were unable to restore complete kidney function within 21 days. Nevertheless, the findings of this study demonstrate a significant influence of transplanted UdRPC on kidney fibrosis after acute to chronic injury presumably via an altered secretome.

Author contribution of C.T. included 10%:

I was responsible for establishing and maintaining the cell culture system, which included the cultivation of UdRPCs as well as the differentiation into podocytes and tubular cells. In addition, I performed immunofluorescence staining and analyzed the samples using the Proteome Profiler Human Kidney Biomarker Kit and the Proteome Profiler Human Cytokine Array Kit.

Status: Pre-print available in the open access pre-print BioRxiv (Under revision in Stem Cell Research and Therapy).

DOI: https://doi.org/10.1101/2025.07.02.662781

This article is an open access article distributed under the terms and conditions of the Creative Commons Attribution (CC BY) 4.0 license, which permits unrestricted use, distribution, and reproduction in any medium, provided the original work is properly cited.

bioRxiv preprint doi: https://doi.org/10.1101/2025.07.02.662781; this version posted July 3, 2025. The copyright holder for this preprint (which was not certified by peer review) is the author/funder, who has granted bioRxiv a license to display the preprint in perpetuity. It is made available under aCC-BY 4.0 International license.

Human Urine-derived SIX2-positive renal progenitor cells improve kidney injury in an IRI mouse model

Claus Kordes[1#], Lucas-Sebastian Spitzhorn[1#], Martina Bohndorf[1], Audrey Ncube[1], Chantelle Thimm[1], Lars Erichsen[1], Wasco Wruck[1], James Adjaye [1, 2*]

[1] Institute of Stem Cell Research and Regenerative Medicine, Medical Faculty and University Hospital Düsseldorf, Heinrich-Heine University Düsseldorf, 40225 Düsseldorf, Germany

[2] University College London (UCL) –EGA Institute for Women's Health, Zayed Centre for Research into Rare Diseases in Children (ZCR), London WC1N 1DZ, UK

[#] Shared first authorship.

* Correspondence: James.Adjaye@med.uni-duesseldorf.de

Claus.Kordes@hhu.de

Running head

Urine-derived progenitor cells improve kidney injury

bioRxiv preprint doi: https://doi.org/10.1101/2025.07.02.662781; this version posted July 3, 2025. The copyright holder for this preprint (which was not certified by peer review) is the author/funder, who has granted bioRxiv a license to display the preprint in perpetuity. It is made available under aCC-BY 4.0 International license.

ABSTRACT

Cells with the characteristics of renal progenitor cells are shed in urine. The aim of this study was to investigate whether these SIX2-positive urine-derived renal progenitor cells (UdRPC) have therapeutic potential in treating or managing acute to chronic kidney injuries. Human UdRPC were obtained from a woman aged 35 years, expanded, and characterized *in vitro* and finally transplanted unilaterally under the renal capsule of mouse kidneys that had undergone ischemia reperfusion injury (IRI). Analyses of blood serum from the mice revealed that the transplanted human UdRPC transiently influenced the secretome of the animals by triggering the release of inflammatory and angiogenic factors. Of obvious therapeutic relevance, however, was the finding that the transplanted cells suppressed renal fibrosis resulting from IRI. The expression of genes linked to inflammation and chronic kidney disease was also reduced in mouse kidneys in the presence of UdRPC. Ultimately, the human UdRPC were able to alleviate the severity of the injury through the amelioration of fibrosis but were unable to restore complete kidney function within 21 days. Nevertheless, the findings of this study demonstrate a significant influence of transplanted UdRPC on kidney fibrosis after acute to chronic injury presumably via an altered secretome.

Key words

urine progenitor cells; ischemia reperfusion injury; kidney fibrosis

bioRxiv preprint doi: https://doi.org/10.1101/2025.07.02.662781; this version posted July 3, 2025. The copyright holder for this preprint (which was not certified by peer review) is the author/funder, who has granted bioRxiv a license to display the preprint in perpetuity. It is made available under aCC-BY 4.0 International license.

INTRODUCTION

Acute kidney injury (AKI) is triggered by ischemia, hypoxia, or nephrotoxicity which initiate inflammatory processes that can lead to a chronic progression of the disease and renal fibrosis [1,2,3]. Chronic kidney disease (CKD) is further initiated independently from AKI by diabetes or hypertension but can also be caused by the natural ageing processes [4,5]. The prevalence of CKD is increasing worldwide, and it has been estimated to represent the seventh leading cause of death worldwide [6]. In Europe, CKD affects one in 10 people and is therefore a serious problem for the healthcare system [4]. Over the years, reports have described urine as a promising source for stem cells in clinical use [7]. Urine has been shown to harbor urine-derived renal progenitor cells (UdRPC). UdRPC express key kidney transcription factors such as SIX2 [8,9]. Furthermore, their identity as kidney progenitor cells which can differentiate into podocytes has been reported [10]. Their capacity to differentiate into renal tubule cells can be assumed because the UdRPC express SIX2. This transcription factor regulates self-renewal of bipotent nephron progenitor cells during kidney organogenesis [11]. Apart from their kidney specific features, UdRPC expanded *in vitro* on plastic exhibit properties of mesenchymal stem cells such as a trilineage differentiation into adipocytes, osteocytes, and chondrocytes as well as secretion of immunomodulatory cytokines and angiogenic growth factors [9]. First attempts have been made by several groups to estimate the therapeutic value of transplanted urine stem cells using rodent models of AKI and CKD with beneficial effects on kidney function and regression of renal fibrosis [12,13,14,15,16]. However, mechanisms initiated by SIX2-expressing kidney progenitor cells that contribute to the alleviation of renal fibrosis remain largely unknown.

To explore this, AKI was performed in the present study by transient, unilateral clipping of the renal pedicle to initiate ischemia reperfusion injury (IRI) in mice. IRI interrupts blood circulation of the kidneys resulting in endothelial cell damage, tubular cell injury, and inflammation which can trigger fibrosis [17]. Depending on the duration of the ischemic status, the consequences of AKI can vary between mild as well as severe forms with progression into CKD as has been shown for the well-established model organism mouse [18,19]. Unilateral transient clipping of the renal pedicle of mice for

bioRxiv preprint doi: https://doi.org/10.1101/2025.07.02.662781; this version posted July 3, 2025. The copyright holder for this preprint (which was not certified by peer review) is the author/funder, who has granted bioRxiv a license to display the preprint in perpetuity. It is made available under aCC-BY 4.0 International license.

45 min as performed in the present study induced AKI to CKD accompanied by renal fibrosis and impaired kidney function. Injection of human UdRPC under the capsule of IRI-injured kidneys, however, was unable to completely restore kidney function but prevented the progression of renal fibrosis as reported in this study.

RESULTS

Characterization and transplantation of UdRPC

Isolated human UdRPC showing a spindle-shaped cell morphology expressed CD133 and the kidney progenitor markers SIX homeobox 2 (SIX2) and Cbp/p300 interacting transactivator with Glu/Asp rich carboxy-terminal domain 1 (CITED) (Fig. 1A). Flow cytometry analysis revealed that UdRPC express the well-established kidney progenitor cell surface proteins CD24 (99%), CD106 (58%), and CD133 (99%) (Fig. 1B). UdRPC could be differentiated into both podocytes expressing NPHS1 adhesion molecule (NPHS1/nephrin), α-actinin 4, synaptopodin (SYNPO), and NPHS2 stomatin family member (NPHS1/podocin) (Fig. 1C) as well as tubular cells expressing Na^+/K^+-ATPase, CLCNKB (chloride voltage-gated channel Kb), SOX17 (SRY-box transcription factor 17), and ZO-1 (zonular occludens-1) (Fig. 1D). Approximately $1x10^6$ UdRPC in 20 µl PBS were injected under the capsule of the left kidney of sham operated mice (group 1), while the vehicle PBS was injected in the same way into the contralateral kidney (Fig. 2A). The left kidney of group 2 and 3 underwent IRI and animals of the IRI group 2 received PBS injections in both kidneys, while mice of the IRI group 3 received $1x10^6$ UdRPC into the clipped left kidney and only PBS was injected into their contralateral kidney (Fig. 2A).

As indicated by the experimental timeline (Fig. 2B), blood samples were taken and the body weights were monitored prior to surgical intervention at day 0 as well as after surgery at day 1, 7, 14, and 21. The body weight of mice remained unchanged during the course of the experiment which implies that the surgery had no significant influence on the health status of the mice (Fig. 2C; supplemental Table S2). After 21 days, the animals were sacrificed, and the kidney wet weight was determined. IRI triggered a significant weight loss in the left kidney of mice in groups 2 and 3 in comparison to the

bioRxiv preprint doi: https://doi.org/10.1101/2025.07.02.662781; this version posted July 3, 2025. The copyright holder for this preprint (which was not certified by peer review) is the author/funder, who has granted bioRxiv a license to display the preprint in perpetuity. It is made available under aCC-BY 4.0 International license.

contralateral kidneys (control I) and the left sham treated controls (control II) (Fig. 2D). No significant differences were observed in the kidney wet weight between the group 2 (IRI) and 3 (IRI/UdRPC) (Fig. 2D).

Renal function after IRI

The concentration of blood urea nitrogen (BUN) in the serum of mice was increased in both IRI groups (group 2: 13 mmol/L; group 3: 10 mmol/L) on day 1 after surgery but only the BUN levels of the IRI group 2 reached significance when compared to the sham treatment (group 1: 8 mmol/L) (Fig. 3A). A significant increase in BUN levels was also observed for the IRI group 2 on day 7 post-surgery when compared to the sham control (group 1), whereas BUN levels of the group 3 (IRI/UdRPC) were elevated but not significantly different from the sham control throughout the entire experiment (Fig. 3A), suggesting better recovery of the kidneys after AKI in the presence of UdRPC. A similar pattern emerged for the creatinine levels in the blood serum. Serum creatinine increased in both IRI groups up to approximately 30 µmol/L on day 1 post-surgery compared to baseline (day 0) and the sham control (day 1), which showed a concentration of approximately 24 µmol/L (Fig. 3B). On day 7 post injury, creatinine levels of the IRI group 2 were still significantly increased, whereas in the IRI group 3 with transplanted UdRPC no significant differences compared to baseline and sham control was observed (Fig. 3B), thus indicating supportive effects of UdRPC on injured kidney tissue.

Proteome analyses

To gain insight into the underlying mechanisms of transplanted UdRPC on kidney function, the blood serum of the mice was analyzed prior to surgery (day 0) and on day 14 and 21 after AKI using proteome analyses that include kidney biomarkers (Fig. 3C-E). Proteins with an influence on vascular system were found to be increased in the blood serum of the IRI/UdRPC group 3, particularly on day 14 (Fig. 3D). The renin/angiotensin system capable of elevating blood pressure was more pronounced on this day

bioRxiv preprint doi: https://doi.org/10.1101/2025.07.02.662781; this version posted July 3, 2025. The copyright holder for this preprint (which was not certified by peer review) is the author/funder, who has granted bioRxiv a license to display the preprint in perpetuity. It is made available under aCC-BY 4.0 International license.

in the UdRPC transplantation group 3. Moreover, vascular endothelial growth factor A (VEGFA), trefoil factor 3 (TFF3), and urokinase (uPA) are factors that promote the survival and proliferation of vascular cells or facilitate thrombolysis, were more abundant in group 3. In addition, adipokines such as resistin, adiponectin, and serpine are known to exert effects on endothelial cells and their expression was found to be elevated in IRI/UdRPC group 3 at day 14 (Fig. 3D). On the other hand, an increased release of factors such as interleukine-6 (IL-6), C-C motif chemokine ligand 2 (CCL2/MCP1, monocyte chemoattractant protein 1) and tumor necrosis factor α (TNFα), which are associated with inflammatory processes and elevated in injured tissue, was found in the IRI/UdRPC transplant group (Fig. 3D). In contrast, the increased expression of the immunosuppressive factors interleukine-10 (IL-10) and interleukin-1 receptor antagonist (IL-1ra) as well as the extracellular matrix (ECM)-degrading matrix metalloproteinase 9 (MMP9) implies potential beneficial effects of UdRPC on injured kidneys (Fig. 3D). Unlike the situation on day 14, the serum proteome analysis on day 0 and 21 showed minor differences between the different experimental groups (Fig. 3C, E; supplemental Fig. S1A-C), suggesting that UdRPC transiently influenced receiving kidneys at an early stage after transplantation as already indicated by the serum BUN and creatinine analyses (Fig. 3A, B).

Cytokines released by the UdRPC into the culture medium were investigated by a proteome array covering 105 human cytokines to assess the origin of cytokines in the blood of mice on day 14 after transplantation of UdRPC (Fig. 4A-D; supplemental Fig. S2). Individual factors such as colony stimulating factor 2 (CSF2/GMCSF), growth and differentiation factor (GDF15), insulin-like growth factor binding proteins 2/3 (IGFBP2/3), and VEGFA emerged in particular due to their quantity (Fig. 4A). The cytokines released by cultured UdRPC were subjected to GO term analysis with regard to biological processes and cellular components. It was of interest that among the biological processes “tissue homeostasis” and “wound healing” were found (Fig. 4B; supplemental Table S4), which indicated a support of the injured kidney tissue by the detected cytokines. A comparison with the cytokines released in the blood serum on day 14 suggested that the factors found in the blood of the mice of the IRI/UdRPC group 3, such as IL-1ra, IL-10, MMP9, and TNFα, apparently originated from

bioRxiv preprint doi: https://doi.org/10.1101/2025.07.02.662781; this version posted July 3, 2025. The copyright holder for this preprint (which was not certified by peer review) is the author/funder, who has granted bioRxiv a license to display the preprint in perpetuity. It is made available under aCC-BY 4.0 International license.

mouse cells, as these were not clearly evident in the UdRPC culture medium (Fig. 4D). In contrast, receptor for advanced glycosylation end product-specific (RAGE) could be distinguished as a factor associated with IRI in mouse blood. It should be emphasized that VEGFA as part of the biological processes "tissue homeostasis" and "wound healing" (Fig. 4B) and the majority of the GO terms referring to cellular components (Fig. 4C; supplemental Table S4) was clearly prominent under all conditions (Fig. 4D).

Analyses of kidney fibrosis

Matrix degrading enzymes like MMP9 detected in blood serum proteome analysis prompted us to investigate the ECM deposition of the injured mouse kidneys by Sirius Red staining in response to transplanted UdRPC. The animals from both control groups (control I: contralateral kidney; control II: sham treatment with UdRPC) were combined to obtain a robust mean value as a reference value to analyze fibrosis. This was justified because the kidneys of the animals in both controls showed no differences in kidney weight or the molecular biology and histology analyses as described in the following. Quantification of the Sirius Red-stained areas revealed a significant increase of matrix protein deposition in mice of the IRI group 2 on day 21 and indicated kidney fibrosis (Fig. 5A, B). In contrast, the transplantation of UdRPC into the injured kidney prevented excessive ECM production (Fig. 5A, B). Furthermore, the expression of fibrosis-associated genes such as connective tissue growth factor (*Ctgf/Ccn2*) remained low despite AKI when UdRPC were transplanted (Fig. 5C). Reduced kidney fibrosis in the IRI group 3 with UdRPC was further manifested by the expression analysis of collagen genes. The expression of the *Col1α2* and *Col3α1* chains was significantly lower in the IRI/UdRPC group 3 than in the IRI group 2 (Fig. 5D, E) whereas the expression of the *Col4α1* chain and *Sox9* only showed a tendency towards reduction after transplantation of UdRPC (Fig. 5F, G). Significantly reduced expression was observed for the inflammation-associated genes *Ccl2* and intercellular adhesion molecule 1 (*Icam1*) (Fig. 5H, I) in the mouse kidneys after IRI and transplantation of UdRPC compared

bioRxiv preprint doi: https://doi.org/10.1101/2025.07.02.662781; this version posted July 3, 2025. The copyright holder for this preprint (which was not certified by peer review) is the author/funder, who has granted bioRxiv a license to display the preprint in perpetuity. It is made available under aCC-BY 4.0 International license.

to IRI group 2. This further indicated a lower inflammation of the injured kidney tissue in the presence of UdRPC.

Transplanted human UdRPC in mouse kidney

To detect the presence of human UdRPC in mouse kidneys, ISH of human-specific ALU repeats was performed. The transplanted UdRPC were predominantly found in the renal cortex at low cell numbers and mainly located between the tubules where the capillary system is located as shown for 3 mice that received UdRPC (Fig. 5J). According to our ISH analysis only a small number of UdRPC survived in the kidneys. It can be assumed that most of the human cells were presumably eliminated by the immune system during the 21-day period which provides an explanation for the transiently altered blood serum secretome on day 14 (Fig. 3D). However, the positive effect of transplanted UdRPC on prevention of kidney fibrosis persisted (Fig. 5B).

DISCUSSION

The aim of this study was to test if urine-derived SIX2-positive UdRPC can support injured kidney and thus establish and confirm their therapeutic value and application. Research by other groups has already indicated this [12,13,14,15,16]. The present study demonstrated that UdRPC have the ability to differentiate into podocytes and tubular cells, as expected for renal progenitor cells. Thus far, very few attempts were made to unravel the mechanisms underlying positive effects of transplanted urine progenitor cells on injured kidneys. For example, exosomal miRNA species such as miR-146-5p and IL-10 have already been associated with beneficial effects of urine stem cells [13,14]. However, it is more likely that there is a broad spectrum of factors released by urine progenitor cells influencing the recovery of injured kidney tissue.

In the present study, quantification of ECM proteins in renal tissue using Sirius Red staining revealed that the transplanted UdRPC significantly prevented the development of renal fibrosis as seen in the

bioRxiv preprint doi: https://doi.org/10.1101/2025.07.02.662781; this version posted July 3, 2025. The copyright holder for this preprint (which was not certified by peer review) is the author/funder, who has granted bioRxiv a license to display the preprint in perpetuity. It is made available under aCC-BY 4.0 International license.

IRI model without transplanted cells. A possible mechanistic approach to explain this was provided by secretome analyses in the present study. When the proteome of mouse serum and UdRPC culture supernatant were compared, IL-1ra and IL-10, MMP9, and TNFα were found to be increased only in the serum of mice of the IRI/UdRPC group 3. Presumably, this was a response of the mouse tissue to factors released by the transplanted UdRPC, as these proteins were not clearly detectably released by UdRPC into the culture medium. IL-1ra binds IL-1 and has an anti-inflammatory effect [20,21], as observed for IL-10. In line with this, a decrease in inflammation in mouse kidneys with IRI and transplanted UdRPC was indicated by a reduced expression of the genes *Ccl2* and *Icam1*.

VEGFA was among the factors produced by UdRPC that were also prominent in the blood serum of mice of the group 3 (IRI/UdRPC). While VEGFA is well known to stimulate angiogenesis and able to counteract ischemia, PDGFB secreted by endothelial cells attracts pericytes which maintain the vasculature [22,23,24]. According to our proteome analyses, PDGFB is also released from UdRPC into the cell culture medium and can therefore potentially influence the regenerative process. IGFBP2/3, VEGFA, and GDF15 were also among the factors released by UdRPC. Although IGFBP bind and transport insulin-like growth factors (IGF), IGFBP2/3 seem to promote angiogenesis, too [25,26]. GDF15, in turn, is apparently secreted by senescent endothelial cells presumably to facilitate blood vessel regrowth [27,28]. Hence, several factors released by UdRPC have an effect that promotes the vascular system. It is interesting to note that an increase in the density of the peritubular capillary system counteracts CKD and reduces kidney fibrosis [29]. CSF2 is another factor released by UdRPC. In mice with targeted deletion of CSF2 bleomycin-induced lung fibrosis is more severe than in wild type mice apparently by lowered prostaglandin E2 levels [30]. This can promote immune cell but also sympathetic nervous system activation which both contribute to fibrogenesis [31,32]. Thus, immunomodulatory and angiogenic mechanisms triggered by UdRPC can explain their anti-fibrotic effect reported herein. However, it remains to be investigated whether the transplanted UdRPC have actually led to a change in the vascular system. This requires further extensive analyses, which should include the aforementioned cytokines.

bioRxiv preprint doi: https://doi.org/10.1101/2025.07.02.662781; this version posted July 3, 2025. The copyright holder for this preprint (which was not certified by peer review) is the author/funder, who has granted bioRxiv a license to display the preprint in perpetuity. It is made available under aCC-BY 4.0 International license.

Limitations of the study

The sera of several animals had to be pooled in order to obtain sufficient sample material for the proteome analyses, as only small volumes of blood serum can be obtained from living mice. This means that individual variations between the animals in a group cannot be mapped. Furthermore, the low number of UdRPC still present in the mouse tissue between tubules after 21 days suggests that most of the human cells either did not engraft into the kidneys or were rejected by the immune system, as the immunocompetent animals of the C57Bl/6N strain did not receive immunosuppression. Moreover, the limitation of the observation period to 21 days did not enable investigation of potential beneficial long-term effects of UdRPC on mouse kidneys. It is also not clear whether the immunosuppressive IL-10 and IL-1ra as potential modulators of inflammatory processes counteracted the effect of other pro-inflammatory cytokines (e.g. TNFα and IL-6) or whether the elevated levels of IL-6 in blood serum even had a favorable effect on the regenerative process via the induction of increased endothelial cell proliferation by triggering VEGFA expression [33,34].

Conclusion

Despite these limitations, the present study has unveiled an anti-fibrotic effect of transplanted UdRPC in ischemia-induced acute to chronic renal injury in mice. Anti-inflammatory and angiogenic factors could have mediated the positive effects of UdRPC on the regenerative processes of the mouse kidneys. Further studies are required to identify individual factors in the secretome of UdRPC that can be used in the prevention or treatment of renal fibrosis in patients.

bioRxiv preprint doi: https://doi.org/10.1101/2025.07.02.662781; this version posted July 3, 2025. The copyright holder for this preprint (which was not certified by peer review) is the author/funder, who has granted bioRxiv a license to display the preprint in perpetuity. It is made available under aCC-BY 4.0 International license.

MATERIALS AND METHODS

Characterization of UdRPC

Human UdRPC (UF31) were isolated from the urine of a 35-year-old healthy female donor of African origin. Informed consent was obtained by the donor of the urine cells and ethical approval for their use in research was given by the ethical commission of the Heinrich Heine University. All methods were performed in accordance with the relevant guidelines and regulations. UdRPC were initially selected from urine by their adherent growth on plastic as proposed for MSCs. The proliferating UdRPC were expanded using culture medium composed of 50% Dulbecco's Modified Eagle Medium (high glucose) and 50% keratinocyte medium supplemented with 5% fetal bovine serum (FBS), 0.5% non-essential amino acids, 0.25% GlutaMAX, 0.5% penicillin/streptomycin, and basic fibroblast growth factor (5 ng/ml, Cat# 100-18B, PreproTech Germany, Hamburg, Germany) at 37°C and 5% oxygen. If not otherwise indicated, all components of the culture medium were purchased from Gibco (Carlsbad, CA, USA). UdRPC were fixed with 4% paraformaldehyde (PFA) and incubated with primary antibodies directed against SIX2 (#H00010736-M01, Abnova, Taipei City, Taiwan), CD133 (#C2514-90B, US Biological; PA2049, Boster Biological), Cbp/p300 interacting transactivator with Glu/Asp rich carboxy-terminal domain 1 (CITED1, #PA5-40585, Thermo Fisher Scientific) as well as corresponding secondary Cy3-, Alexa Fluor 555-, or Alexa Fluor 488-labelled antibodies (Thermo Fisher Scientific) and Hoechst 33258 dye (Merck, Darmstadt, Germany) using a standard protocol. The actin cytoskeleton (f-actin) was labelled by phalloidin-FITC (#P5282, Merck). UdRPC were also subjected to flow cytometry using the CyAn ADP (Beckman Coulter, Indianapolis, IA, USA) to specifically detect renal progenitor cell surface markers by using antibodies directed against CD24-FITC (#FCMAB188F, Merck), VCAM-1/CD106-PE (#FAB5649P, R&D Systems), and CD133-APC (#FAB11331A, R&D Systems).

Differentiation of UdRPC into podocytes and tubular cells

Podocytes differentiation was initiated after culturing UdRPC on rat collagen type I coated plates to a confluency of approximately 60-70% in advanced RPMI medium supplemented with 30 µM retinoic

bioRxiv preprint doi: https://doi.org/10.1101/2025.07.02.662781; this version posted July 3, 2025. The copyright holder for this preprint (which was not certified by peer review) is the author/funder, who has granted bioRxiv a license to display the preprint in perpetuity. It is made available under aCC-BY 4.0 International license.

acid for 14 days [10]. Expression of α-actinin 4 (#AB108198, Abcam, Cambridge, UK), podocin (NPHS2, #AB50339, Abcam), nephrin (NPHS1 adhesion molecule, #AB4626861, Thermo Fisher Scientific), synaptopodin (SYNPO, #A5-56997, Thermo Fisher Scientific) and the cytoskeletal marker phalloidin-Alexa Fluor 488 (#A12379, Thermo Fisher Scientific) was confirmed as described [10].

Tubular cell differentiation was initiated after culturing undifferentiated UdRPC on laminin-421-coated plates to a confluency of approximately 90% (laminin-421, #LN421-02, BioLamina, Sundbyberg, Sweden). The cells were induced to differentiate in renal epithelial cell growth medium (REGM) supplemented with 10 ng/ml bone morphogenetic protein 2 (BMP2) and 2.5 ng/ml BMP7 for seven days [35]. The tubular-associated markers zonular occludens-1 (ZO-1, #33-9100, Thermo Fisher Scientific), Na^+/K^+-ATPase (#ab76020, Abcam), chloride voltage-gated channel Kb (CLCNKB, #AB236733, Abcam), and SRY-box transcription factor 17 (SOX17, #AF1924, R&D) were confirmed by immunofluorescence.

UdRPC transplantation

The animal experiments were performed by Phenos GmbH (Hannover, Germany) according to our specifications. All procedures were approved by the local authorities for animal protection (Niedersächsisches Landesamt für Verbraucherschutz und Lebensmittelsicherheit; reference number 33.19-42502-04-22-00107) and were performed in accordance with the German animal welfare act and the ARRIVE guidelines. A total of 21 male C57Bl/6N mice (12-15 weeks old; Charles River, Sulzfeld, Germany) were used for the present study (supplemental Table S1, S2). The animals received a standard diet with free access to food and water in an enriched environment and were monitored daily. To ensure analgesia, Buprenorphine and Metamizole were administered subcutaneously prior to surgery. As a contralateral control (control I; n = 21), 20 µl phosphate buffered saline (PBS) were injected under the renal capsule of the right kidney of all animals used for the study. In the sham group (group 1; control II; n = 5), 20 µl of UdRPC suspension ($1x10^6$ cells) were injected under the renal capsule of the left kidney. In group 2 and 3 the left renal pedicle was clamped with a microaneurysm

bioRxiv preprint doi: https://doi.org/10.1101/2025.07.02.662781; this version posted July 3, 2025. The copyright holder for this preprint (which was not certified by peer review) is the author/funder, who has granted bioRxiv a license to display the preprint in perpetuity. It is made available under aCC-BY 4.0 International license.

clip for 45 min (IRI model). In group 2 (n = 8), 20 µl of the vehicle PBS were injected into the left kidney. The group 3 (n = 8) received also $1x10^6$ UdRPC in 20 µl PBS under the renal capsule of the clamped left kidney. Body weight was measured, and blood samples were taken prior to surgery (day 0) and on day 1, 7, 14, and 21. On day 21 the mice were euthanized in deep isoflurane anesthesia by blood sampling via the left ventricle. After terminal blood collection whole body perfusion was performed with ice cold PBS via the left ventricle which results in circulatory arrest. The fresh weight of the kidneys was subsequently determined.

Clinical chemistry and proteome analyses

For assessing renal function, s-creatinine and blood urea nitrogen (BUN) were measured in serum samples of mice on day 0, 1, 7, 14, and 21 using the Olympus analyzer (AU400) by the Phenos GmbH. Serum samples from mice were further analyzed on day 0, 14, and 21 using the Proteome Profiler Human Kidney Biomarker Array Kit (ARY019; R&D Systems, Minneapolis, MN, USA) according to the manufacturer's recommendations. Collected blood samples were pooled from distinct animals based on their experimental group assignment to obtain sufficient amounts of protein. The secretome of UdRPC UF31 was analyzed by the Proteome Profiler Human XL Cytokine Array Kit (ARY022B; R&D Systems) in cell culture medium as specified by the manufacturer. Image analysis including grid-finding and quantification was semi-automatically performed using the FIJI/ImageJ software [36], normalized via the mean of the reference spots in the R/Bioconductor [37] and assessed for gene expression via detection-p-values < 0.05 as described [38]. GO over-representation analysis was performed via the R package GOstats [39] using the total list of proteins of the Proteome Profiler Human XL Cytokine Array as background. For the Venn diagram comparison of proteins detected in the secretome of UdRPC UF31 and in animal blood samples only the overlap of cytokines between both array types ARY019 and ARY022B was considered.

bioRxiv preprint doi: https://doi.org/10.1101/2025.07.02.662781; this version posted July 3, 2025. The copyright holder for this preprint (which was not certified by peer review) is the author/funder, who has granted bioRxiv a license to display the preprint in perpetuity. It is made available under aCC-BY 4.0 International license.

Sirius Red staining

The amount of extracellular matrix protein (ECM) was quantified after Sirius Red staining of paraffin-embedded mouse kidney sections (10 µm). The Pico-Sirius Red Stain Kit (#SCY-PSR-1, Biozol Diagnostica GmbH, Echingen, Germany) was used according to the protocol provided by the manufacturer. Stained areas of the kidney sections were quantified using the CellSens Dimension software (version 1.16, Evident Europe GmbH, Hamburg, Germany).

Reverse transcriptase quantitative polymerase chain reaction (RT-qPCR)

TaqMan Reverse Transcription Reagents (#N8080234, Applied Biosystems) were used to synthesize cDNA from 1 µg total RNA per sample. For the PCR, 10 ng cDNA, 0.6 µM from each primer set (supplemental Table S3), and the Takyon No Rox SYBR Green MasterMix dTTP Blue (#UF-NSMT-B0701, Eurogentec, Seraing, Belgium) were mixed. The PCR products were amplified by applying a standard protocol. The CT values were analyzed by the 2(−ΔΔCt) method and normalized against the housekeeping gene hypoxanthine-guanine-phosphoribosyl transferase 1 (*Hprt1*).

In-situ hybridization of ALU repeats

To identify transplanted UdRPC, in-situ hybridization (ISH) of human-specific ALU repeat sequences was performed on paraffin-embedded mouse kidney sections after target retrieval through Tris-EDTA buffer (10 mM Tris base, 1 mM EDTA solution, 0.05% Tween 20, pH 9.0) treatment for 30 min at 85°C and blocking of peroxidase activity (Dual Enzyme block; #S2003, Dako-Agilent, Santa Clara, CA, USA). The tissue sections were permeabilized using proteinase K (10 µg/ml, #P2308, Merck) diluted in digestion buffer (2x saline sodium citrate buffer/SSC, 2.5% sodium dodecyl sulfate). The ZytoFast DNA (+) control probe with digoxigenin (#T-1053-100; ZytoVision GmbH, Bremerhaven, Germany) was directly layered onto each section, denatured at 75°C for 5 min, and hybridized at 37°C for 2 hours. DIGX rabbit anti-digoxigenin antibody (#ENZ-ABS303; Enzo Biochem Inc., Long Island, NY, USA), anti-rabbit antibody coupled with horseradish peroxidase/HRP (#K4010, Dako-Agilent), and 3,3'-

bioRxiv preprint doi: https://doi.org/10.1101/2025.07.02.662781; this version posted July 3, 2025. The copyright holder for this preprint (which was not certified by peer review) is the author/funder, who has granted bioRxiv a license to display the preprint in perpetuity. It is made available under aCC-BY 4.0 International license.

diaminobenzidine (SIGMAFAST DAB, #D4293, Merck) was applied to stain the bound probes. The cell nuclei were counterstained by diluted hematoxylin solution (#1.05175.0500, Merck).

Statistics

Statistical analyses were performed using GraphPad Prism software version 10.4.1 (GraphPad Software, San Diego, CA, USA). Statistical significance was tested by one way analysis of variance (ANOVA). Significant differences were indicated by asterisks. Results are presented in scatter plots and the arithmetic mean as well as standard error of mean (SEM) is indicated.

REFERENCES

1. Basile, D. P., Anderson, M. D. & Sutton, T. A. Pathophysiology of Acute Kidney Injury. *Comprehensive Physiology* **2**, 1303–1353 (2012).
2. Hoste, E. A. J. et al. Global epidemiology and outcomes of acute kidney injury. *Nature Reviews Nephrology* **14**, 607–625 (2018).
3. Kurzhagen, J. T., Dellepiane, S., Cantaluppi, V. & Rabb, H. AKI: an increasingly recognized risk factor for CKD development and progression. *Journal of Nephrology* **33**, 1171–1187 (2020).
4. Sundström, J. et al. Prevalence, outcomes, and cost of chronic kidney disease in a contemporary population of 2·4 million patients from 11 countries: The CaReMe CKD study. *Lancet* **20**, 100438 (2022).
5. Ortiz, A., Mattace-Raso, F., Soler, M. J. & Fouque, D. Ageing meets kidney disease. *Nephrology Dialysis Transplantation* **38**, 523–526 (2023).
6. Francis, A. et al. Chronic kidney disease and the global public health agenda: an international consensus. *Nature Reviews Nephrology* **20**, 473–458 (2024).
7. Yu, P. et al. Beyond waste: understanding urine's potential in precision medicine. *Trends in Biotechnology* **42**, 953–969 (2024).

bioRxiv preprint doi: https://doi.org/10.1101/2025.07.02.662781; this version posted July 3, 2025. The copyright holder for this preprint (which was not certified by peer review) is the author/funder, who has granted bioRxiv a license to display the preprint in perpetuity. It is made available under aCC-BY 4.0 International license.

8. Bohndorf, M. et al. Derivation and characterization of integration-free iPSC line ISRM-UM51 derived from SIX2-positive renal cells isolated from urine of an African male expressing the CYP2D6 *4/*17 variant which confers intermediate drug metabolizing activity. *Stem Cell Research* **25**, 18–21 (2017).
9. Rahman, M. S. et al. The FGF, TGFβ and WNT axis Modulate Self-renewal of Human SIX2+ Urine Derived Renal Progenitor Cells. *Scientific Reports* **10**, 739 (2020).
10. Erichsen, L. et al. Activation of the Renin–Angiotensin System Disrupts the Cytoskeletal Architecture of Human Urine-Derived Podocytes. *Cells* **11**, 1095 (2022).
11. Kobayashi, A. et al. Six2 Defines and Regulates a Multipotent Self-Renewing Nephron Progenitor Population throughout Mammalian Kidney Development. *Cell Stem Cell* **3**, 169–181 (2008).
12. Dong, X. et al. Beneficial effects of urine-derived stem cells on fibrosis and apoptosis of myocardial, glomerular and bladder cells. *Molecular and Cellular Endocrinology* **427**, 21–32 (2016).
13. Tian, S. F. et al. Human urine-derived stem cells contribute to the repair of ischemic Acute kidney injury in rats. *Molecular Medicine Reports* **16**, 5541–5548 (2017).
14. Li, X. et al. Human urine-derived stem cells protect against renal ischemia/reperfusion injury in a rat model via exosomal miR-146a-5p which targets IRAK1. *Theranostics* **10**, 9561–9578 (2020).
15. Zhang, C. et al. Reno-protection of urine-derived stem cells in a chronic kidney disease rat model induced by renal ischemia and nephrotoxicity. *International Journal of Biological Sciences* **16**, 435–446 (2020).
16. Gao, W. W. et al. Locally transplanted human urine-induced nephron progenitor cells contribute to renal repair in mice kidney with diabetic nephropathy. *Biochemical and Biophysical Research Communications* **629**, 128–134 (2022).
17. Bonventre, J. v. & Yang, L. Cellular pathophysiology of ischemic acute kidney injury. *Journal of Clinical Investigation* **121**, 4210–4221 (2011).

bioRxiv preprint doi: https://doi.org/10.1101/2025.07.02.662781; this version posted July 3, 2025. The copyright holder for this preprint (which was not certified by peer review) is the author/funder, who has granted bioRxiv a license to display the preprint in perpetuity. It is made available under aCC-BY 4.0 International license.

18. Hueper, K. et al. Acute Kidney Injury: Arterial Spin Labeling to Monitor Renal Perfusion Impairment in Mice—Comparison with Histopathologic Results and Renal Function. *Radiology* **270**, 117–124 (2014).
19. Thorenz, A. et al. IL-17A blockade or deficiency does not affect progressive renal fibrosis following renal ischaemia reperfusion injury in mice. *Journal of Pharmacy and Pharmacology* **69**, 1125–1135 (2017).
20. Colantuoni, M. et al. Constitutive IL-1RA production by modified immune cells protects against IL-1–mediated inflammatory disorders. *Science Translational Medicine* **15**, eade3856 (2023).
21. Saxton, R. A. et al. Structure-based decoupling of the pro- and anti-inflammatory functions of interleukin-10. *Science* **371**, eabc8433 (2021).
22. Suzuki, S. et al. Clinicopathological significance of platelet-derived growth factor (PDGF)-B and vascular endothelial growth factor-A expression, PDGF receptor-β phosphorylation, and microvessel density in gastric cancer. *BMC Cancer* **10**, 659 (2010).
23. Lin, Y. et al. Role of endothelial PDGFB in arterio-venous malformations pathogenesis. *Angiogenesis* **27**, 193–209 (2024).
24. Cressman, A. et al. Investigational New Drug-enabling studies to use genetically modified mesenchymal stromal cells in patients with critical limb ischemia. *Stem Cells Translational Medicine* **14**, szae094 (2025).
25. Slater, T., Haywood, N. J., Matthews, C., Cheema, H. & Wheatcroft, S. B. Insulin-like growth factor binding proteins and angiogenesis: from cancer to cardiovascular disease. *Cytokine and Growth Factor Reviews* **46**, 28–35 (2019).
26. Li, T. et al. IGFBP2: integrative hub of developmental and oncogenic signaling network. *Oncogene* **39**, 2243–2257 (2020).
27. Wang, S. et al. Growth differentiation factor 15 promotes blood vessel growth by stimulating cell cycle progression in repair of critical-sized calvarial defect. *Scientific Reports* **7**, 9027 (2017).

bioRxiv preprint doi: https://doi.org/10.1101/2025.07.02.662781; this version posted July 3, 2025. The copyright holder for this preprint (which was not certified by peer review) is the author/funder, who has granted bioRxiv a license to display the preprint in perpetuity. It is made available under aCC-BY 4.0 International license.

28. Ha, G. et al. GDF15 secreted by senescent endothelial cells improves vascular progenitor cell functions. *PLOS ONE* **14**, e0216602 (2019).

29. Ren, Z. et al. Contribution of alterations in peritubular capillary density and microcirculation to the progression of tubular injury and kidney fibrosis. *The Journal of Pathology* **266**, 95-108 (2025).

30. Moore, B. B. et al. GM-CSF Regulates Bleomycin-Induced Pulmonary Fibrosis Via a Prostaglandin-Dependent Mechanism. *The Journal of Immunology* **165**, 4032–4039 (2000).

31. Liu, L. et al. Sympathetic nerve promotes renal fibrosis by activating M2 macrophages through β2-AR-Gsa. *Clinical Immunology* **270**, 110397 (2025).

32. Hu, B. et al. Sensory nerves regulate mesenchymal stromal cell lineage commitment by tuning sympathetic tones. *Journal of Clinical Investigation* **130**, 3483–3498 (2020).

33. Cohen, T., Nahari, D., Cerem, L. W., Neufeld, G. & Levi, B.-Z. Interleukin 6 Induces the Expression of Vascular Endothelial Growth Factor. *Journal of Biological Chemistry* **271**, 736–741 (1996).

34. Wang, M.-J. et al. The double-edged effects of IL-6 in liver regeneration, aging, inflammation, and diseases. *Experimental Hematology & Oncology* **13**, 62 (2024).

35. Mboni-Johnston, I. M. et al. Sensitivity of Human Induced Pluripotent Stem Cells and Thereof Differentiated Kidney Proximal Tubular Cells towards Selected Nephrotoxins. *International Journal of Molecular Sciences* **25**, 81 (2023).

36. Schneider, C. A., Rasband, W. S. & Eliceiri, K. W. NIH Image to ImageJ: 25 years of image analysis. *Nature Methods* **9**, 671–675 (2012).

37. Gentleman, R. C. et al. Bioconductor: open software development for computational biology and bioinformatics. *Genome Biology* **5**, R80 (2004).

38. Wruck, W. et al. Urine-Based Detection of Biomarkers Indicative of Chronic Kidney Disease in a Patient Cohort from Ghana. *Journal of Personalized Medicine* **13**, 38 (2022).

39. Falcon, S. & Gentleman, R. Using GOstats to test gene lists for GO term association. *Bioinformatics* **23**, 257–258 (2007).

bioRxiv preprint doi: https://doi.org/10.1101/2025.07.02.662781; this version posted July 3, 2025. The copyright holder for this preprint (which was not certified by peer review) is the author/funder, who has granted bioRxiv a license to display the preprint in perpetuity. It is made available under aCC-BY 4.0 International license.

List of supplementary materials

Supplemental Figure S1: Proteins expressed on the Proteome Profiler Human Kidney Biomarker Array Kit (ARY019) are associated with inflammation and vascular processes.

Supplemental Figure S2: Membranes of the Proteome Profiler Human Kidney Biomarker Array Kit (ARY019) used for this study to analyze serum samples.

Supplemental Table S1: List of mice used for the experiments and labelling of tissue sections.

Supplemental Table S2: Body weight of mice before (day 0/d0) and after surgery.

Supplemental Table S3: Mouse primer sets for RT-qPCR.

Supplemental Table S4: GO term analysis of cytokines released by cultured UdRPC UF31.

Acknowledgements

The authors are grateful to the Phenos GmbH (Hannover, Germany) for performing the *in vivo* experiments.

Funding

J.A. acknowledges support from the medical faculty of Heinrich Heine University Düsseldorf and the federal ministry for economic affairs and climate action as well as the European Social Fund (EXIST Transfer of Research, grant number 03EFNNW217).

bioRxiv preprint doi: https://doi.org/10.1101/2025.07.02.662781; this version posted July 3, 2025. The copyright holder for this preprint (which was not certified by peer review) is the author/funder, who has granted bioRxiv a license to display the preprint in perpetuity. It is made available under aCC-BY 4.0 International license.

Author contributions

CK, LS, JA: wrote the manuscript; LS, AN, MB: isolated and maintained UdRPC; LS, AN, CT, JA: characterization of UdRPC; LS, AN: transplantation management; WW: carried out bioinformatics; CK: histological examination and microscopy; CK, MB: performed RT-PCR analyses; CT, LE: conducted secretome analyses. All authors approved the manuscript.

Competing interest

The authors declare that no competing financial interest exists.

Data and materials availability

The authors declare that all data supporting the findings of this study are available within the article and its supplementary material.

bioRxiv preprint doi: https://doi.org/10.1101/2025.07.02.662781; this version posted July 3, 2025. The copyright holder for this preprint (which was not certified by peer review) is the author/funder, who has granted bioRxiv a license to display the preprint in perpetuity. It is made available under aCC-BY 4.0 International license.

FIGURES AND FIGURE LEGENDS

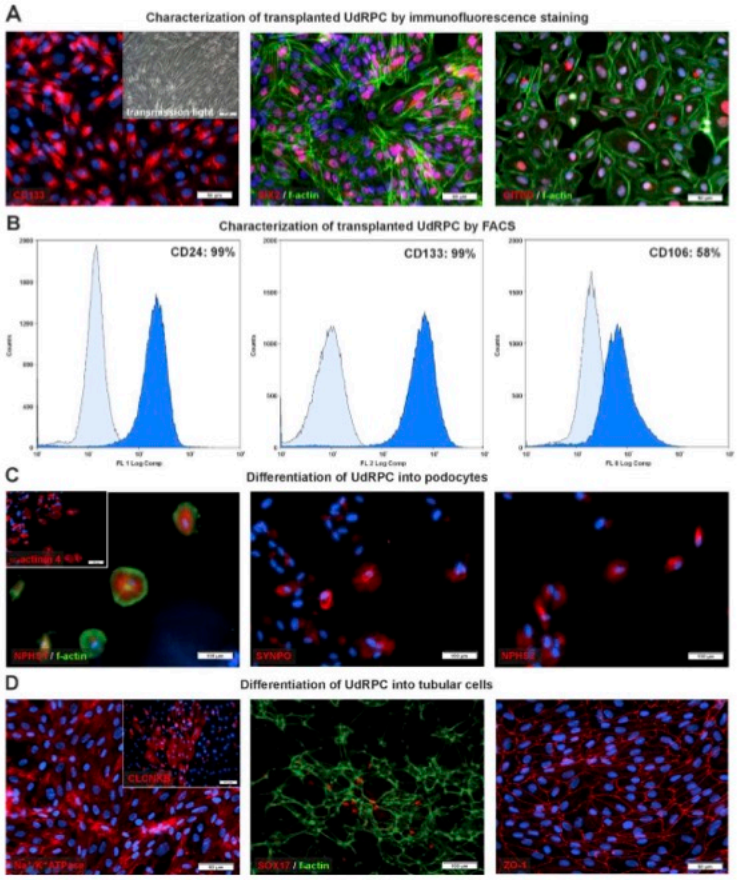


Figure 1: Characterization of UdRPC by immunofluorescence and flow cytometry. *(**A**) Transmission light microscopic image of UdRPC showing spindle-shaped cell morphology (insert). Immunofluorescence staining of UdRPC using antibodies against the kidney progenitor cell markers CD133, SIX2, and CITED (red). The cell nuclei were stained with Hoechst 33258 (blue) and the actin cytoskeleton was labelled by phalloidin (green). Scale bars represent 50 µm. (**B**) The renal progenitor cell markers CD24, CD106 (VCAM1), and CD133 were detectable as cell surface proteins on UdRPC by flow cytometry. Dark blue histograms indicate the fluorescence-labelled antibodies against CD24, CD106, or CD133, respectively, whereas light blue histograms represent antibody isotype controls. (**C**) Podocytes differentiated from UdRPC expressed characteristic podocyte markers NPHS1, α-actinin 4 (insert), SYNPO, and NPHS2 (red). The cytoskeletal marker phalloidin is shown in green. (**D**) UdRPC differentiated into tubular cells showed tubular-associated markers Na^+/K^+-ATPase, CLCNKB (insert), SOX17, and ZO-1 (red) at protein level, along with phalloidin. Scale bars indicate 50 and 100 µm.*

bioRxiv preprint doi: https://doi.org/10.1101/2025.07.02.662781; this version posted July 3, 2025. The copyright holder for this preprint (which was not certified by peer review) is the author/funder, who has granted bioRxiv a license to display the preprint in perpetuity. It is made available under aCC-BY 4.0 International license.

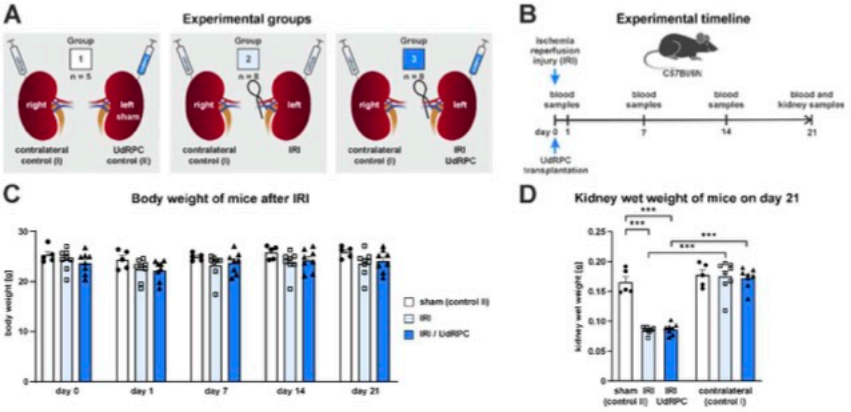


Figure 2: Experimental procedure and health status of mice as indicated by body and kidney weight. *(**A**). Group 1 was sham operated and received UdRPC injection into the left kidney. IRI-induced AKI was triggered by unilateral transient clipping of the left renal pedicle in group 2 and 3. The injured left kidney of the group 3 received an injection of UdRPC whereas only the vehicle PBS was injected into the left kidney of group 2. The contralateral (right) kidneys always received the vehicle in all groups. (**B**) Timeline of the experimental procedure. (**C**) Body weight of mice was determined prior to surgery (day 0) and on day 1, 7, 14, and 21. (**D**) Kidney wet weight on day 21. Data are indicated as mean ± SEM. Statistical significance was tested by one way ANOVA. Significant differences were ***p<0.001.*

bioRxiv preprint doi: https://doi.org/10.1101/2025.07.02.662781; this version posted July 3, 2025. The copyright holder for this preprint (which was not certified by peer review) is the author/funder, who has granted bioRxiv a license to display the preprint in perpetuity. It is made available under aCC-BY 4.0 International license.

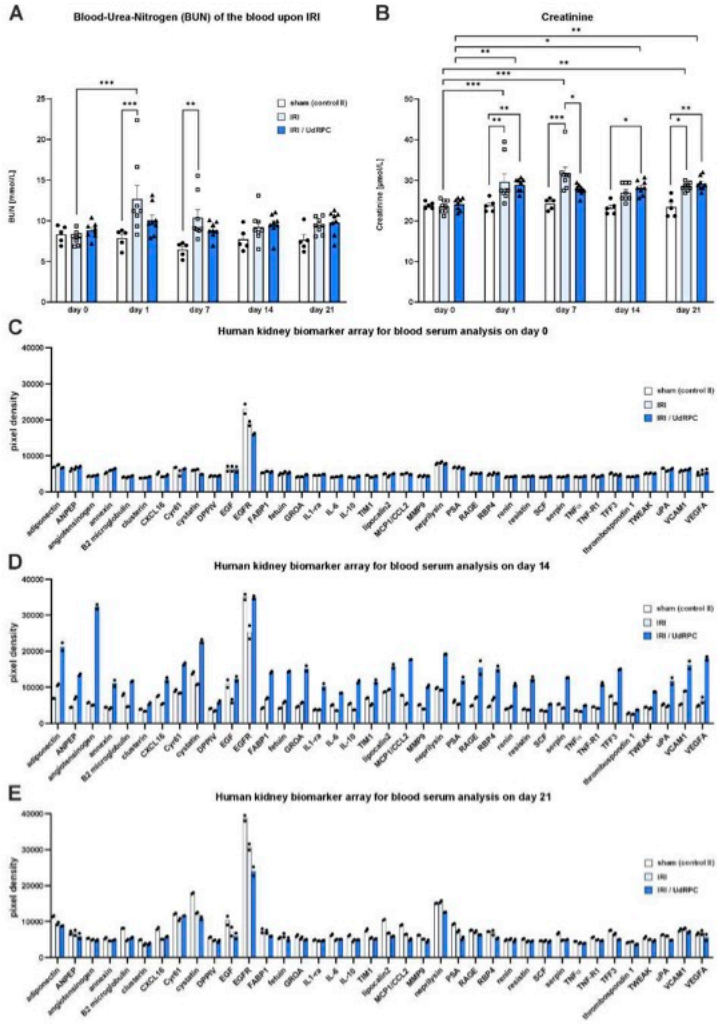


Figure 3: Blood serum analyses. *(**A**) Blood-urea-nitrogen (BUN) and (**B**) creatinine concentrations as indicators of kidney injury were measured in the blood serum prior to surgery (day 0) and on day 1, 7, 14, and 21. Data are shown as mean ± SEM (n = 5-8). Statistical significance was tested by one way ANOVA. Significant differences were *p<0.05, **p<0.01, ***p<0.001. (**C-E**) Proteome Profiler Human Kidney Biomarker Arrays have been used to monitor cytokines and growth factors associated with kidney diseases in the blood serum of mice at day 0, 14, and 21. The serum samples were pooled from different animals according to their experimental group assignment to receive sufficient protein amounts. The bars indicate mean values, and the dots represent individual values of double measurements.*

bioRxiv preprint doi: https://doi.org/10.1101/2025.07.02.662781; this version posted July 3, 2025. The copyright holder for this preprint (which was not certified by peer review) is the author/funder, who has granted bioRxiv a license to display the preprint in perpetuity. It is made available under aCC-BY 4.0 International license.

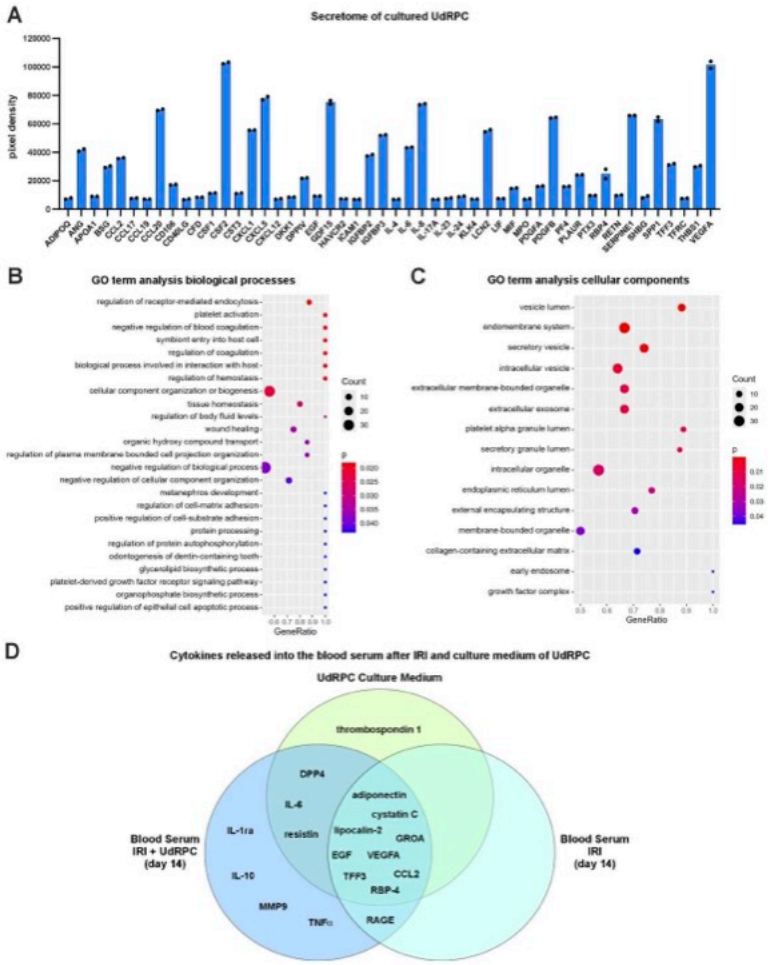


Figure 4: Secretome analysis of UdRPC. *(**A**) Cytokines released by UdRPC into the culture medium were analyzed by the Proteome Profiler Human XL Cytokine Array covering 105 cytokines. Only the expressed cytokines that have a detection-p-value below a threshold of 0.05 are shown. The bars indicate mean values, and the dots represent individual values of double measurements. GO over-representation analysis was performed to identify gene ontology (GO) terms of (**B**) biological processes and (**C**) cellular components associated with the cytokines released by UdRPC as indicated by the aforementioned proteome array. (**D**) Matching cytokines from the Proteome Profiler Human Kidney Biomarker Array Kit (ARY019), which was used to analyze the blood serum of the mice 14 days after IRI, and the Proteome Profiler Human XL Cytokine Array Kit (ARY022B), which was applied to identify the cytokines released by UdRPC into the culture medium, were compared in a Venn diagram. In addition to the UdRPC culture medium, the blood sera of mice after IRI were illustrated with and without transplanted UdRPC for day 14 after kidney injury.*

4 Discussion

Kidney diseases describe the condition of the kidney in which its function is restricted or even inoperable. Their mortality rate has risen in recent years. Globally, deaths attributed to kidney disease increased by 50% between 2000 and 2019[225].
Common kidney diseases are chronic and acute kidney failure, degenerative kidney diseases, various kidney inflammations, kidney stones, renal cell cancer and genetic kidney diseases such as familial cystic kidneys or rare inherited kidney diseases such as Bartter syndrome. However, since the human body is a complex and far-reaching system, kidney diseases are closely linked to other organs such as the heart or the brain. It is known that a damaged and non-functioning kidney stops the elimination of waste products from the blood and therefore an enormous amount of fluid collects in the blood vessels, causing e.g. high blood pressure[226]. The harmony and balance of the system and the cooperation of the organs is essential.

In the past, disease modelling of the kidney has been extremely difficult due to the challenge of obtaining cells derived from the kidney. Although relatively few kidney cells are shed under healthy compared to dysfunctional conditions[227,228] , we were able to isolate, cultivate and expand urine cells from healthy donors[16]. Previous studies of ours have described a protocol by which they have found urine to be a reliable, non-invasive, robust, and cost-effective source of kidney stem cells, as opposed to amniotic fluid or kidney biopsies[16,215,217,229]. Ethical perspective should also not be ignored regarding the positive properties of the use of urine.
Urine provides as a non-invasive source a variety of renal cells e.g. podocytes which is a promising means to study the biology of podocytes and renal disease.
Renal progenitor cells called UdRPCs are one cell type that can be isolated from urine and express self-renewal markers as well as typical mesenchymal markers such as SIX2, SSEA4, and vimentin, but not the essential pluripotency regulating transcription factors OCT4, SOX2 and NANOG. The expression of surface markers like CD106, CD24, and CD133 decisive for their renal origin. For instance, cells that express CD106 are only found in the renal capsule, while cells expressing CD24 and CD133 are found in both the renal capsule and the tubules[230]. SIX2-positive UdRPCs have the potential to differentiate into various renal cell types, including podocytes[231,232]. Podocytes are a specialized and highly differentiated epithelial cell type of the glomerulus. They are situated on the exterior of the glomerular capillaries and extend into the urinary space of Bowman's capsule. These cells feature a sizable cell body from which many foot processes extend and taper around the glomerular capillaries. Isolating of UdRPCs

facilitates the harvesting of the cells, as these podocytes are usually obtained from iPSC or harvested from the glomeruli[233].
However, primary UdRPCs proliferation capacity is also limited by the Hayflick phenomenon in vivo and the cell culture environment. As these cells are very rare and have a limited cultivation potential, their use in long-lasting experiments is limited. One way of circumventing this issue is the immortalization of those cells to unlock unlimited proliferation capacity by the cost possible of genomic alterations.

4.1 Generation and characterization of immortalized podocytes derived from human urine

Immortalization of cells refers to the process by which normal somatic cells acquire the ability to divide and proliferate indefinitely without undergoing age associated changes and/or senescence. This often occurs through genetic changes that affect cell cycle control or through the introduction of oncogenes that promote cell growth and division but also rendering the cells vulnerable to oncogenic transformation. As previous studies have shown, the division potential of primary cells is not only explicitly limited in the kidney[234,235]. The use of kidney-specific cell types is essential for the investigation and further training of kidney diseases. Podocytes are specialized cells located in the glomerulus of the kidney, where they play a crucial role in blood filtration. Since mature podocytes are terminally differentiated and unable to divide in vivo[236],establishing podocyte cell cultures presents a considerable challenge. One approach to cell moralization is the ectopic expression of the telomerase reverse transcriptase protein (TERT)[237,238]. This protein is inactive in most somatic cells, but when hTERT is exogenously expressed, cells are able to avoid replicative senescence. Studies have shown that overexpression of hTERT can efficiently extend the lifespan of immortalized cells and maintain a stable genotype and important phenotypic characteristics[239].

We also showed the successful immortalization of a human podocyte precursor cell line, UM51-PrePodo-hTERT, derived from UdRPCs isolated directly from the urine of a man of African descent[240]. UM51-PrePodo-hTERT was cultured for one year with over 100 passages and demonstrated high proliferative capacity. The immortalization of this cell line was achieved by overexpressing *hTERT*, which resulted in chromosomal aneuploidies and alterations in gene expression[241,242]. While UM51-PrePodo-hTERT exhibits a hypertriploid karyotype, the cells maintain contact inhibition and express and activate p53, suggesting that they have not

lost cell cycle checkpoints or undergone malignant transformation. Despite exhibiting characteristics typically associated with cancer cells, such as predominantly short telomeres and telomerase activity, which is observed in 85-90% of human cancers[243,244], these cells do not appear to have undergone oncogenic transformation.

In parallel, another nephron progenitor cell line was successfully immortalized by transfecting two plasmids containing the reprogramming factors OCT4, SOX2, NANOG, cMyc, KLF4 (OSKM) and the SV40 LT. Thereby we were able to achieve a human podocyte progenitor cell line UM30-OSN, where the primary cells were isolated directly from the urine of a 30-year-old male. UM30-OSN was cultured over one year within 100 passages with high proliferation capacity. The plasmids were successfully excreted over the passages. During cellular reprogramming is driven by epigenetic restructuring, reorganisation of chromatin state, erasure of somatic identity and finally, expression of the pluripotent gene regulatory network[245–247]. During cellular reprogramming, all age-related defects are restored when the cell identity is reset, so that adult somatic cells are reset to a young state and have, among other things, an increased telomere length[248,249]. In 2006, this process was made possible by Shinya Yamanaka, who analyzed 24 genes associated with embryonic stem cell identity and discovered four transcription factors to be sufficient to induce pluripotency - Oct4, Sox2, Klf4 and cMyc[185]. These four transcription factors induce pluripotency in any cell type. Partial reprogramming does not result in complete reprogramming, which means that the cell identity is not completely reset. During the reprogramming process into iPSC, cells undergo a "transgene-dependent period," during which the presence of transgenic factors is essential for reprogramming progression[250]. Once these transgenes are lost, the cells typically achieve a stable pluripotent state. The reprogramming process marks the time window during which cells activate endogenous pluripotency loci and transition to a state of transgene independence, accompanied by the mesenchymal-to-epithelial transition (MET)[250]. However, in the case of UM30-OSN cells, which lose the introduced plasmids at an earlier stage, this stable pluripotent phase is not reached. This suggests that the SV40 Large T antigen plays a critical role in the immortalization of these cells and may be essential for completing the reprogramming process.

Immortalizing cells by using the SV40 LT antigen, leads to inactivation of tumour suppressor genes[208] and induction of telomerase activity[208]. The conferral of unlimited cell division is likewise as the hTERT overexpression, associated with chromosomal alterations and genomic instabilities[241,242]. In the UM30-OSN, these are also present, whereby P53, P21, as well as

PCNA and KI67 expression and their activation and downregulation indicate intact cell cycle checkpoints. At the same time, they show no cancerous transformation, even though they share some characteristics such as shortened telomeres or increased telomerase activity[243,244].

Both cell lines were tested for their potential to differentiate into a kidney-associated cell types, such as podocytes[231,232,240]. This protocol has also been successfully and reproducible applied to urine-derived cells immortalized with hTERT from a 51-year-old African man (UM51 hTERT)[240] and via two plasmids including an SV40-T-antigen and OSKM from a 30-year-old man (UM30-OSN[251]. Nephron progenitor cells can be associated as renal progenitor cells, as they express in their undifferentiated stage the renal stem cell markers SIX2, CITED1, CD24, and CD106[16,252]. The markers CD133, CD24, and CD106 are of curial importance to indicate the progenitor direction of the cells. Cells localized in Bowman's capsule express $CD133^+$, $CD24^+$, and $CD106^+$, whereas $CD133^+$, $CD24^+$, and $CD106^-$ cells are the progenitors of proximal tubular cells[253]. Podocytes belong to Bowman's capsule, causing their progenitor cells to be CD24 and CD106 positive, completely differentiated podocytes upregulate the podocyte-specific genes *SYNPO*, *NPHS1* and *NPHS2* which are required for the formation of the slit membrane and foot processes[232]. Furthermore, there is an upregulation of the podocyte-specific marker *PODXL,* which regulates morphogenesis and differentiation of developing podocytes. This occurs through the dissolution of tight and adherens junctions and the subsequent formation of microvilli, foot processes and slit membranes, the key ultrastructural elements that enable glomerular filtration[254,255]. The generated podocytes not only exhibit the expression of the specific genes but also show the typical podocyte "fried egg" morphology. Both cell lines can be considered as a suitable cell model for podocyte differentiation and can be used to study numerous renal diseases. Nevertheless, it should be kept in mind that they have an aberrant karyotype and thus may have deviations in e.g. gene expression compared to the primary cells. Due to their high proliferation rate, they have far-reaching advantages, especially in screening. The use of immortalized urine-derived podocytes can be approached as an easily manageable cellular model, which opens a new dimension for the investigation of renal diseases, like podocyte damage, regulation of high blood pressure, CKD, AKI and renal tubular disorder.

4.2 Reduction of ANGII-induced cytoskeletal changes in human podocytes by angiotensin receptor blockade

Globally, approximately 9.4 million deaths annually are attributed to elevated blood pressure. The RAAS plays a critical role in regulating blood pressure as well as maintaining electrolyte and fluid balance in the body. ANG II, the primary effector of the RAAS, is central to the regulation of blood pressure and fluid balance. ANG II can activate two receptors AGTR1 and AGTR2. ANG II exerts its effects predominantly through AGTR1 and, to a lesser extent, AGTR2[256,257]. AGTR expression has been widely observed across various segments of the nephron, including the distal tubule, collecting duct, and renal vasculature[258–263]. Thereby, *AGTR1* is expressed 8 – 10-fold higher at the mRNA level than *AGTR2* in the human kidney[264]. In the kidney, elevated levels of circulating and intracellular ANG II have been implicated in a range of deleterious effects, including vasoconstriction, inflammation, fibrosis, and hypertrophy[265]. The persistent activation of AGTR1 by ANG II induces renal vasoconstriction, impairing sodium excretion due to reduced medullary blood flow[266]. This leads to podocyte damage and eventual loss, which compromises the structural integrity of the glomerular filtration barrier. Our study showed a ANG II-mediated cytoskeletal remodeling results in the deformation of podocytes, characterized by a transition from their typical fried-egg morphology to a rounded and contracted form[232,240]. This study confirmed the downregulation of podocyte-specific genes, including *NPHS1* and *SYNPO,* following 24-hour ANG II treatment, consistent with findings by Rüster and Wolf[267]. The detrimental effects of ANG II also include triggering a pro-fibrotic and inflammatory milieu, promoting podocyte dysfunction through cytoskeletal disarray and slit diaphragm disruption[268,269]. Moreover, ANG II's role in podocyte injury is closely linked to an upregulation of AGTR1 expression, further amplifying its pathological effects such as nephrosclerosis, endothelial dysfunction, and vascular hypertrophy[256]. By contrast, AGTR2 activation has been linked to beneficial effects, including vasodilation, tissue repair, and cell differentiation[256]. It remains unclear whether podocytes can adapt their phenotype and whether the observed morphological changes become chronic under prolonged ANG II stimulation.

Clinically, ARBs and ACEIs are widely used to treat various renal disorders. In the follow-up study, the use of losartan, an ARB, highlighted the importance of AGTR1 in ANG II-induced damage[231]. Losartan acts as an antihypertensive agent by blocking AGTR1 through a competitive and reversible binding, thereby counteracting ANG II effects. ANG II signaling via

AGTR2 has been linked to vasodilation, development, cell differentiation, tissue repair, and apoptosis[256]. We demonstrated that losartan effectively mitigates ANG II-induced cytoskeletal changes, preserving podocyte architecture and restoring nephrin and synaptopodin expression. Interestingly, a receptor switch from AGTR1 to AGTR2 was observed upon losartan treatment, suggesting that ANG II might preferentially bind to AGTR2 when AGTR1 is blocked. This receptor switch appears to facilitate the re-differentiation of podocytes and the re-expression of podocyte-specific genes. Beyond that, we suggest that ANG II has sex- and age-dependent effects, with variability in response observed among cell models. The results indicate that ANG II and losartan have varying effects depending on the sex and age of the cells studied. This variability suggests a high degree of individuality in the selected cell models, potentially making them more representative of in vivo conditions or revealing inherent differences among them. For instance, a study involving female mice reported a significant correlation between hypertension and AGTR1 expression. Genetic variants that enhance AGTR1 expression were found to influence blood pressure and gene expression, whereas no such correlation was observed in male mice[270]. The findings underscore the importance of considering sex-specific differences in experimental and clinical outcomes.

These studies presented by our lab not only show the importance of different cell modelling approaches but also the essential connection between the organs and their consequences. The study described above successfully elucidated critical links between the RAAS and the AGTR signaling pathways, providing valuable insights into the mechanisms underlying the function of angiotensin type II receptors. These findings hold significance for advancing nephrotoxicity research and for understanding the mechanisms and signalling cascades involved in various kidney diseases. It may provide far-reaching insights for possible therapeutic approaches to be used in the future.

4.3 Secreted urinary cytokines in AKI and CKD patients as diagnostic and prognostic tools for kidney diseases

Acute kidney injury and chronic kidney disease are among the most common and significant kidney diseases worldwide. Both conditions are not only clinical challenges but are also closely related pathophysiological conditions. AKI can significantly increase the risk of developing CKD, while CKD patients are at higher risk of acute deterioration of their kidney function [68]. The global impact of these diseases is enormous. It is estimated that around 13 million people

worldwide are affected by AKI each year, 85% of whom live in low- and middle-income countries. In addition, more than 10% of the world's population suffers from CKD, with rising incidence rates due to an aging population and an increase in chronic diseases such as diabetes and hypertension[271,272].

The importance of research into AKI and CKD lies primarily in the need to understand the mechanisms that lead to the progression from AKI to CKD. This includes the investigation of inflammatory processes, fibrosis formation, and epigenetic changes that can cause long-term damage after AKI[273]. Findings from such studies could contribute to the development of new therapeutic approaches to prevent the transition from AKI to CKD. However, as acute kidney injury can also occur without signs or symptoms[274] , the identification of cytokines is beneficial as a tool for early diagnosis. Since the increase in plasma levels of pro-inflammatory cytokines predicts mortality in patients with AKI[275]. Therefore, the secretome of urine from an AKI patient cohort was analyzed using a commercially available renal biomarker cytokine assay. In addition, we analyzed the effect of patient and healthy urine on human podocytes. Nowadays, it can be concluded that biological processes can produce variations depending on gender and age. As we only had access to a limited sample pool for this study, we tried to exclude individual variations by pooling the samples. Sex-specific analyses were performed to avoid variations due to the influence of sex hormones such as testosterone and oestradiol on the modulation of SIRT1 expression[276–278].

In our study, we identified Adiponectin (ADIPOQ), Epidermal Growth Factor (EGF), and SERPIN3A as potential early biomarkers that could detect AKI as early as 24 hours after surgery. ADIPOQ is of special interest since it has been described to directly regulate the expression of three of the identified cytokines that were upregulated 72 hours after surgery, namely C-X-C Motif Chemokine Ligand 1 (CXCL1), Vascular Endothelial Growth Factor (VEGF), and Renin (REN). Adiponectin exerts its effect via multiple pathways, leading to the suppression of endothelial inflammatory signaling and inhibition of apoptosis in tubular epithelial cells[279]. Inhibition of the renin-angiotensin system has been reported to significantly elevate adiponectin levels[280]. We hypothesize that the upregulation of secreted renin observed in AKI urine samples 72 hours post-surgery may be responsible for the downregulation of secreted adiponectin. In contrast, the early upregulation of adiponectin appears to activate angiogenesis-related genes, such as *CXCL1* and *VEGF*, signaling the initiation of nephron repair processes[281–283]. VEGF has been recognized as a critical mediator in both early and late phases of renal protection following AKI, particularly in the context of stem cell-based

therapies[284]. Furthermore, EGF was found to be upregulated 24h post-surgery and its known for its pivotal role in tissue repair and regeneration[285]. Experimental models of AKI have demonstrated that exogenous administration of EGF can enhance tubular regeneration and reduce fibrosis, improving renal function outcomes. Moreover, endogenous EGF levels are often reduced during AKI, suggesting a potential therapeutic window for intervention[286]. Moreover, studies have shown that EGF can modulate the immune response by attenuating the release of pro-inflammatory cytokines and reducing oxidative damage, further supporting its protective role in AKI[287].

In the context of biomarker discovery, urinary EGF levels have been investigated as a potential diagnostic and prognostic indicator for AKI[97]. Lower urinary EGF concentrations are often associated with more severe injury and poorer recovery, highlighting its potential utility in clinical settings[288].

The *EGFR* promoter is known to harbor p53-responsive elements, linking its activity to p53-mediated pathways[289]. Renal fibrosis, a key complication in kidney disease, has been associated with the activation of EGFR and p53[290]. Supporting this, the FDA-approved test "NephroCheck®" predicts moderate to severe AKI risk within 24 hours. It measures tissue inhibitor of metalloproteinase 2 (TIMP-2) and insulin-like growth factor binding protein 7 (IGFBP7), biomarkers secreted by renal tubular cells under stress[291]. These factors induce G1-phase cell-cycle arrest by activating p27 via TIMP-2 and p53/p21 via IGFBP7, emphasizing the role of TP53 in AKI's clinical progression[292,293]. A study by Montero et al. further correlated VEGF and p53 expression, highlighting their potential as independent prognostic factors[294]. Our findings demonstrate that secreted EGFR and VEGF can elevate *TP53* mRNA and protein levels in immortalized podocytes, though further verification is needed[295]. Pierzchalski et al. also noted that p53 can induce apoptosis through the RAAS[296], a pathway we have shown to detrimentally affect podocyte morphology and function in our previous research[231,232,240]. Thus, we propose that EGFR and VEGF secretion primarily drives angiogenesis, p53 activation, and RAS stimulation, which could explain the transition from AKI to CKD.

Interestingly, our study of CKD patients from Ghana revealed decreased secretion of EGFR and VEGF in CKD progression[97]. This suggests that EGFR and VEGF may act as initiators in AKI and diminish during CKD progression. VEGF, in particular, has shown potential in facilitating renal recovery after AKI, although the mechanisms remain unclear[297]. Post-AKI

kidney tissue often exhibits impaired endothelial proliferation and mesenchymal transition, leading to vascular attrition and CKD advancement[273].

The combination of the identified cytokines represents a promising strategy to accurately diagnose the development of AKI within 24 to 72 hours after surgery. Our results show that the cytokines present in high concentrations in the urine of AKI patients can trigger repair processes in the damaged nephron. These processes activate TP53 and SIRT1, among others, to maintain a balance between cell proliferation, angiogenesis, and cell cycle arrest.

Finally, the current, AKI and CKD diagnosis relies on urea and creatinine clearance, which only detects nephron damage after filtration impairment. A cytokine-based diagnostic approach could offer earlier detection, as evidenced by our finding of ADIPOQ accumulation in urine 24 hours post-surgery in AKI patients. Early detection of such cytokines could enable timely interventions to prevent filtration barrier breakdown, potentially yielding significant patient benefits. Moreover, cytokine-based tests are non-invasive, cost-effective, and easily conducted using urine samples and flow-cell detection devices, presenting a promising alternative for AKI and CKD monitoring. However, further studies are needed to validate these findings and their clinical applicability. The use of urine-derived stem cells shows the far-reaching potential in research of kidney diseases.

4.4 JAK1/JAK2-Inhibition reduces IFN–γ–induced APOL1 expression and fibrotic markers in human podocytes

APOL1 play a privotal role in podocyte injury and the development of CKD over the JAK/STAT signaling pathway. JAK1-mediated signaling has been identified as a key driver of inflammatory and fibrotic processes, both of which are recognized as major contributors to CKD progression[133]. Within this context, APOL1 risk variants are of particular clinical importance, as they exert a toxic gain-of-function effect in podocytes, leading to in cellular damage and nephron loss[117,137,138,221]. Numerous studies have demonstrated that APOL1 expression is upregulated by pro-inflammatory cytokines such as IFN-γ, a process that is directly mediated through the JAK-STAT signaling cascade[112,114,136,140–144]. This highlights targeted modulation of this pathway as a promising therapeutic strategy, as preclinical studies have shown[112,118,136,145]. The avaible functional studies of APOL1 have important limitations.

Much of the mechanistic understanding of APOL1 biology stems from overexpression models in mice or HEK293 cells expressing the G0, G1, or G2 variants[112,126,136,137,221–224]. While these systems have provided crucial insights into pathogenic mechanisms, they fail to fully recapitulate the unique physiology of human podocytes and the native regulatory context of APOL1. Future studies should therefore prioritize human podocyte-based systems to enhance the translational relevance of preclinical findings and to more effectively assess targeted therapeutic strategies.

Based on this, in this study, UdRPCs from a West African donor (UM30-OSN) were immortalized and used to investigate the effect of APOL1 expression and renal injury markers using IFN-γ and the JAK1/JAK2 inhibitor baricitinib in podocytes[251].

IFN-γ stimulation for 24 h resulting in increased phosphorylation of STAT1, activation of APOL1, upregulation of pro-inflammatory and fibrotic markers such as, IL-6, TGF-β, Vimentin, Fibronectin, and morphological changes indicative of cell stress.

Morphologically, IFN-γ stimulation resulted in an increase in rounded, detached cells compared to the untreated control, as observed by light microscopy. This cytoskeletal change has also already been demonstrated by the use of ANGII[231,232,240]. This suggests that not only the RAAS play a crucial role in podocyte injury and the development of CKD, but also the JAK/STAT signalling pathway.

In addition to the morphological changes, there was a significant increase in APOL1 expression and consequently also an increase in pro-inflammatory and fibrotic markers such as, IL-6, TGF-β, vimentin, fibronectin. As is already known, inflammation and fibrosis are crucial for the progression of kidney disease and show the dependence of APOL1 risk variants and the progression of kidney disease. Due to the West African origin coupled to the APOL1 risk variants, a permanent activation of the JAK/STAT signalling pathway marked by phosphorylation of STAT1 followed by increased APOL1 expression seems to lead to an increase in inflammation and fibrosis associated markers. These observations are conistent with previous studies in overexpressing models, such as HEK293 cells, demonstrating that APOL1 risk variants can trigger cytotoxic responses under pro-inflammatory conditions[112,114,136,140–144].

Our results support the notion that APOL1 risk variants confer a toxic gain-of-function effect in human podocytes. In individuals of West African ancestry, constitutive or cytokine-induced JAK/STAT activation appears to drive sustained APOL1 expression, leading to an inflammatory and profibrotic microenvironment. These processes are well-recognized

mediators of CKD progression and underscore the clinical relevance of targeting the JAK/STAT/APOL1 axis.

Importantly, co-treatment with Baricitinib effectively mitigated IFN-γ-induced morphological and molecular alterations in human urine-derived podocytes. Baricitinib significantly preserved podocyte morphology, reduced the number of detached cells, and normalized the APOL1 and downstream inflammatory and fibrotic markers. This protective effect is consistent with observations in human kidney biopsies and podocyte models, where Baricitinib has been shown to reduce APOL1-driven cytotoxicity under pro-inflammatory conditions[145]. The translational significance of these findings is further supported by the Phase 2 JUSTICE trial, which evaluated Baricitinib in patients with high-risk APOL1 genotypes and reported reductions in proteinuria, highlighting the therapeutic potential of JAK inhibition in APOL1-associated nephropathies[146].

In conclusion, our study provides a valuable additional model for investigating kidney-associated diseases such as APOL1 high-risk variants and mechanistic evidence linking IFN-γ–induced JAK/STAT activation to APOL1-mediated podocyte injury and identifies Baricitinib as a promising candidate for therapeutic intervention. By interrupting the cycle of inflammation and fibrosis, JAK1/2 inhibition may represent a targeted strategy to slow CKD progression in individuals carrying APOL1 risk variants.

4.5 Understanding the effects of RAAS overactivation in the aging process using sodium-wasting models

Every person encounters the progressive biological process of aging, recognized as a major risk factor for widespread chronic diseases. Aging is driven among others by factors such as oxidative stress, cellular senescence, and the accumulation of ROS. The RAAS plays a central role in regulating blood pressure, which can be disrupted by electrolyte imbalances. During RAAS activation, ANG II binds to the AGTR1, stimulating intracellular NADPH oxidase. This process generates superoxide anions, promotes the uncoupling of endothelial nitric oxide (NO) synthase, reduces NO availability, and increases ROS production. The oxidative stress and DNA damage induced by ANG II are tightly regulated. In individuals with sodium-wasting conditions such as BS, inflammatory processes are downregulated, resulting in lower levels of oxidative stress and ROS.

In 1962, Bartter et al. identified the so-called Bartter syndrome[157]. BS is a rare hereditary renal tubular disorder characterized by impaired salt reabsorption in the thick ascending limb (TAL) of the loop of Henle. This condition leads to a variety of electrolyte imbalances, including hypokalemia, hypochloremia, salt wasting, metabolic alkalosis, and hyperaldosteronism, all occurring without elevated blood pressure. Additionally, hyperplasia of the juxtaglomerular apparatus (JGA) is commonly observed[157,160,162,163]. BS is a polygenic disorder caused by homozygous or compound heterozygous mutations in one of several genes, including *SLC12A1*, *KCNJ1*, *CLCNKB*, *BSND*, or *CASR*[169,298].

In regards to the previous studies, Bartter syndrome has an interesting angle, by looking at hypertension and aging-related processes, as revised in Thimm et. al.[169]. The RAAS involves several systematic processes to regulate blood pressure. Dysregulation in blood pressure can be caused by electrolyte imbalance.

Salt intake is a critical factor influencing hypertension and plays a significant role in determining sensitivity to hypertensive responses. Salt-sensitive individuals exhibit stronger hypertensive reactions compared to patients with BS[299,300]. Magnesium deficiency, commonly associated with conditions like BS, further highlights the interplay of these syndrome with electrolyte imbalances. The binding of ANGII to AGTR1 triggers ROS production, leading to cellular senescence, mitochondrial dysfunction, hypertrophy, inflammation, and renal fibrosis[301–303] However, BS patients, despite consuming high-salt supplements, such as potassium chloride, sodium, or/and magnesium, do not typically exhibit these hypertensive outcomes[304,305]. These patients demonstrate downregulation of inflammatory processes, reduced oxidative stress, and lower ROS production. Possible explanations include decreased messenger release via AGTR1[306], reduced Ca^{2+} release and PKC activation[306], or elevated SIRT1 expression[307]. Moreover, SIRT1 is a critical regulator of aging and its activity decreases in age. Interestingly, BS patients tend to have higher SIRT1 activity compared to healthy individuals of the same age. This elevated SIRT1 expression in BS patients may reflect a protective trend toward improved health and resistance to aging-related stressors.

There is a bidirectional relationship between aging and hypertension, in which age-related vascular changes promote the development of hypertension and hypertension in turn accelerates aging. For its part, high blood pressure acts as an accelerator of aging processes, by promoting vascular and cellular damage. Chronically elevated blood pressure increases the mechanical load on the vascular walls and intensifies oxidative stress mechanisms and inflammatory processes[308]. With increasing age, structural and functional changes occur in the vascular system,, such as arterial stiffening, reduced elasticity, endothelial dysfunction, and

increased intimal thickening, which contributes to the development of hypertension[309]. A central role is played by arterial stiffness, which is caused by the loss of elasticity in large arteries such as the aorta. This loss is primarily due to the degeneration of elastic fibers, the accumulation of collagen and the fragmentation of elastic lamellae[310]. At the cellular level, hypertension also influences telomere length. Studies show that patients with hypertension have shorter telomeres, which is a marker for accelerated biological aging[311].

Another feature of vascular aging is endothelial dysfunction, which is characterized by a reduced bioavailability of NO. NO is a key mediator of vascular relaxation, and its reduction leads to increased vascular tension and ultimately to an increase in blood pressure[312]. A better understanding of these interactions is crucial to optimize prevention and treatment strategies and improve quality of life in old age.

For studying the etiology of Bartter syndrome at the molecular level an iPSC of an 18-year-old Bartter syndrome type 3 (BS3) patient within a homozygous whole gene deletion of CLCNKB genotype was generated and characterized[313]. At present, there is no iPSC cell line from BS3 patients available. Only cell lines derived from patients with gene mutations of the sodium-potassium-chloride cotransporter gene (SLC12A1) or also known as Bartter syndrome type 1 (BS1)[314] or from another sodium deficiency-associated disease called Gitelman syndrome (GS)[315,316].

Given the limited data, further studies are needed to validate, the link between immune deficiencies in salt-wasting tubulopathies, such as BS, and the protective effects against certain aging-related conditions. Analyzing signaling pathways influenced by salt loss could uncover novel connections between BS and resistance to aging-related effects. For this purpose, healthy iPSC cell lines[317] as well as BS patient iPSC[313,314] can be differentiated into various kidney-associated cell lines, such as tubular cells, and the molecular differences can be analyzed. In contrast to GS, Bartter syndrome is characterized by a more severe congenital kidney damage phenotype that often manifests earlier, usually within the first year of life[159]. iPSCs revolutionize the way we approach biological research and medical treatments by combining the ethical benefits of a non-embryonic source with the functional capabilities of pluripotent cells[318–321]. Their adaptability, patient specificity, and potential for broad applications make them a cornerstone of modern regenerative medicine and disease research. The simple and inexpensive procurement of stem cells from urine, which can be easily reprogrammed into iPSCs, appears to have widespread potential in regenerative medicine.

4.6 Urine-derived renal progenitor cells as a therapeutic approach in an IRI mouse model

The significant potential of deriving stem cells from urine was further substantiated in a subsequent study, which explored the therapeutic application of SIX2-positive UdRPCs in the context of acute and chronic kidney injury[322].

Previous studies conducted only limited experiments to elucidate the mechanisms underlying the beneficial effects of transplanted urine-derived stem cells on the regeneration of injured kidneys.

In this study, we demonstrate that SIX2-positive UdRPCs from a 31-year-old female donor exert therapeutic effects in a murine model of ischemia–reperfusion injury (IRI), a widely used model for both acute and progressive kidney damage[252,323]. UdRPC administration significantly attenuated renal fibrosis, as evidenced by reduced extracellular matrix deposition and decreased expression of profibrotic markers such as CTGF, COL1A2, and COL3A1. These findings are consistent with previous work showing that renal progenitor cells can inhibit TGF-β–driven fibrotic pathways and preserve tubular integrity[252]. In addition to their antifibrotic effects, UdRPCs demonstrated immunomodulatory properties. The downregulation of CCL2 and ICAM1, key mediators of monocyte recruitment and leukocyte adhesion, respectively, suggests that UdRPCs suppress inflammatory signaling pathways known to exacerbate CKD progression[324,325]. This aligns with recent studies reporting that progenitor cells exert anti-inflammatory effects via paracrine signaling and exosome release[323].

Interestingly, UdRPCs also appeared to transiently modulate the systemic secretome, potentially by releasing anti-inflammatory and vasoactive mediators. Similar effects have been reported for other stem and progenitor cell types, which can influence vascular tone and immune responses through secretion of bioactive factors such as IL-10, VEGF, and HGF[326–329].

However, despite these protective effects, UdRPC treatment did not fully restore renal function within the 21-day observation period. This limitation has been observed in other progenitor-based therapies and may reflect the need for prolonged cell survival, repeated dosing, or co-treatment with supportive agents to achieve long-term functional recovery[330]. An important aspect of our model is the xenogeneic transplantation of human-derived UdRPCs into immunocompetent mice without immunosuppression. Although no overt immune rejection was observed, the long-term survival and engraftment of UdRPCs remain unclear. Future studies should investigate the immunogenicity and fate of transplanted cells in more detail[331].

Although in this the aspect the R^3 principle-Reduce, Refine, Replace should be be taken into consideration and could be a main aspect in the incomplete regeneration process of the mice kidney.

All in all, our findings support the therapeutic relevance of SIX2-positive UdRPCs for kidney injury. Their dual antifibrotic and anti-inflammatory effects, likely mediated through paracrine mechanisms, highlight their potential as a novel, non-invasive cell source for regenerative nephrology.

5 Conclusion

Urine and urine-derived nephron progenitor cells represent an innovative and non-invasive resource for regenerative medicine[97,169,231,232,240,251,295,313,322,332,333]. Their simple extraction from urine samples, along with their ability to differentiate into various cell types such as bone, muscle, nerve, and fat, opens new avenues in personalized medical applications. With their strong proliferative capacity, genetic stability, and low immunogenicity, UdRPCs emerge as a promising option for diverse cell-based therapies

This research successfully established immortalized UdRPC lines and highlighted their specific potential for addressing kidney diseases. The cost-effective and accessible procurement of these stem cells, combined with their ability to be reprogrammed into iPSCs, underscores their versatility in regenerative applications. Additionally, the use of immortalized urine-derived podocytes presents a practical cellular model for exploring renal diseases, providing a valuable tool for nephrotoxicity studies and understanding signaling pathways in kidney disorders. This knowledge lays the groundwork for innovative therapeutic strategies and offers promising insights into future treatments.

The remarkable potential of urine-derived cells enables comprehensive investigation into a wide spectrum of kidney-associated diseases. This study not only provides in-depth insights into conditions such as AKI, CKD, Bartter syndromes, APOL1-mediated kidney disease, sickle cell disease, hypertension, and the molecular parallels between the kidney and brain, but also establishes a conceptual and methodological framework for future experimental research. Moreover, it has been demonstrated that these cells are not limited to two-dimensional culture systems. Further studies successfully utilized in three-dimensional models[334–336]. This underscores their prospective utility in advancing biomedical research across various domains, with particular relevance to nephrology.
Figure 6 represents all my findings in a schematic figure.

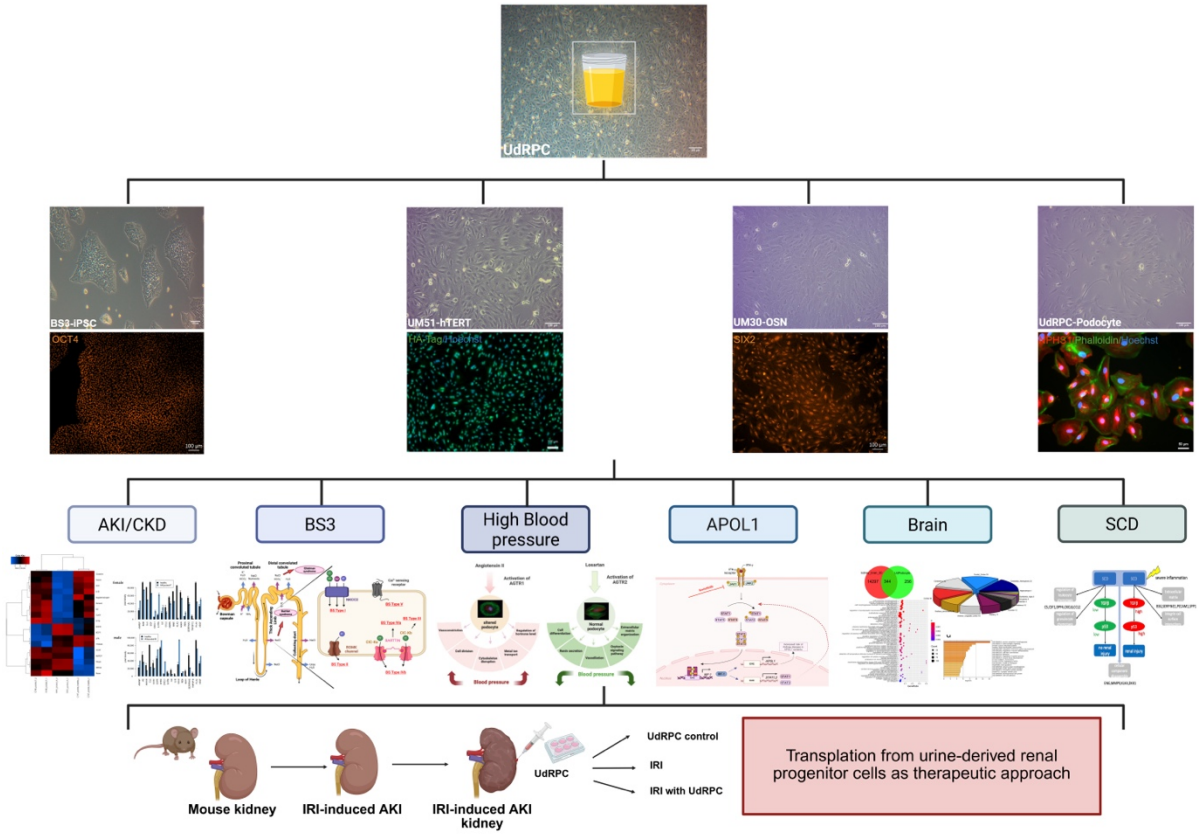


Figure 6: Therapeutic potential of urine-derived renal progenitor cells (UdRPCs).

The top center represent a light microscope picture of UdRPCs isolated from human urine. The second row shows the different cell types, which were generated in the following thesis with representive markers. On the left side is a light microscope picture of the Bartter syndrome type 3 induced pluripotent stem cell (BS3 iPSC) pictures showing by immunofluorescence staining the expression of the pluripotent marker OCT4. Next to the BS iPSC are the UM51 hTERT cell lines showing expression of HA-tag and Hoechst. The second immortal cell line UM30-OSN expressing the nephron progenitor marker SIX2 (orange). On the right side the UdRPCs were differentiatet into podocytes expressing podocyte specific markers Nephrin and a cytoskeleton marker Phalloidin. The miiddle row represents the various disease models explored using UdRPCs in this thesis including: Acute kidney injury (AKI), Chronic kidney disease (CKD), High Blood pressure, Apolipoprotein L1 (APOL1), Similarities between brain and kidney and Sickle cell disease (SCD). The bottom row show a schematic of cell transplantation as a therapeutic approach. UdRPCs are injected into a mouse model with IRI-induced AKI to assess regenerative effects. UdRPCs present a versatile and promising cell source for disease modeling and regenerative therapies, particularly for kidney-related and systemic diseases. Created in https://BioRender.com[169].

6 References

1. Schmidt, R. F., Lang, F. & Heckmann, M. *Physiologie des Menschen*. (Springer, 2017).

2. Molina, D. K. & DiMaio, V. J. M. Normal Organ Weights in Men: Part II—The Brain, Lungs, Liver, Spleen, and Kidneys. *Am. J. Forensic Med. Pathol.* **33**, 368–372 (2012).
3. Molina, D. K. & DiMaio, V. J. M. Normal Organ Weights in Women: Part II—The Brain, Lungs, Liver, Spleen, and Kidneys. *Am. J. Forensic Med. Pathol.* **36**, 182–187 (2015).
4. Rosenbaum, D., Korngold, E. & Teele, R. Sonographic assessment of renal length in normal children. *Am. J. Roentgenol.* **142**, 467–469 (1984).
5. Su, H.-A. *et al.* Reference ranges for ultrasonographic renal dimensions as functions of age and body indices: A retrospective observational study in Taiwan. *PLOS ONE* **14**, e0224785 (2019).
6. Oxburgh, L. Kidney Nephron Determination. *Annu. Rev. Cell Dev. Biol.* **34**, 427–450 (2018).
7. Adapted from"Kidney Anatomy" by BioRender.com. *BioRender* https://app.biorender.com/biorender-templates (2024).
8. Meng, P., Zhu, M., Ling, X. & Zhou, L. Wnt signaling in kidney: the initiator or terminator? *J. Mol. Med.* **98**, 1511–1523 (2020).
9. Saxén, L. & Sariola, H. Early organogenesis of the kidney. *Pediatr Nephrol.* **1**, 385–92 (1987).
10. Xu, P. X. *et al.* Eya1-deficient mice lack ears and kidneys and show abnormal apoptosis of organ primordia. *Nat Genet.* **23**, 113–7 (1999).
11. Wellik, D. M., Hawkes, P. J. & Capecchi, M. R. Hox11 paralogous genes are essential for metanephric kidney induction. *Genes Dev.* **16**, 1423–32 (2002).
12. James, R. G., Kamei, C. N., Wang, Q., Jiang, R. & Schultheiss, T. M. Odd-skipped related 1 is required for development of the metanephric kidney and regulates formation and differentiation of kidney precursor cells. *Development.* **133**, 2995–3004 (2006).
13. Torres, M., Gómez-Pardo, E., Dressler, G. R. & Gruss, P. Pax-2 controls multiple steps of urogenital development. *Development.* **121**, 4057–65 (1995).
14. Basta, J. M., Robbins, L., Kiefer, S. M., Dorsett, D. & Rauchman, M. Sall1 balances self-renewal and differentiation of renal progenitor cells. *Development.* **141**, 1047–1058 (2014).
15. Kobayashi, A. *et al.* Six2 defines and regulates a multipotent self-renewing nephron progenitor population throughout mammalian kidney development. *Cell Stem Cell.* **3**, 169–81 (2008).
16. Rahman, M. S. *et al.* The FGF, TGFβ and WNT axis Modulate Self-renewal of Human SIX2 + Urine Derived Renal Progenitor Cells. *Scientific Reports* **10**, 739 (2020).
17. Constantini, F. & Kopan, R. Patterning a complex organ: branching morphogenesis and nephron segmentation in kidney development. *Dev Cell .* **18**, 698–712 (2010).
18. Schumacher, A. *et al.* Defining the variety of cell types in developing and adult human kidneys by single-cell RNA sequencing. *npj regenerative medicine* **6**, 1–11 (2021).
19. Smith, H. W. The fate of sodium and water in the renal tubules H W SMITH. *Bull N Y Acad Med .* **35**, 293–316 (1959).

20. Hoenig, M. P. & Zeidel, M. L. Homeostasis, the milieu intérieur, and the wisdom of the nephron. *Clin J Am Soc Nephrol.* **9**, 1272–81 (2014).
21. Huber, T. B. Molekulare Pathogenese Der Proteinurie. (Thieme, 2008).
22. Reiser, J., Kriz, W., Kretzler, M. & Mundel, P. The Glomerular Slit Diaphragm Is a Modified Adherens Junction. *J Am Soc Nephrol* 1–8 (2000).
23. Schnabel, E., Anderson, J. M. & Farquhar, M. The Tight Junction Protein ZO-1 Is Concentrated Along Slit Diaphragms of the Glomerular Epithelium. *The Journal of Cell Biology* 1255–1263 (1990).
24. Donoviel, D. *et al.* Proteinuria and perinatal lethality in mice lacking NEPH1, a novel protein with homology to NEPHRIN. *Molecular and Cellular Biology* **21**, 4829–36 (2001).
25. Inoue, T. *et al.* FAT is a component of glomerular slit diaphragms. *Kidney international* 1003–1012 (2001) doi:https://doi.org/10.1046/j.1523-1755.2001.0590031003.x.
26. Ha, T.-S. Roles of adaptor proteins in podocyte injury. *WJN* 1–10 (2013) doi:10.5527/wjn.v2.i1.1.
27. Boute, N. *et al.* NPHS2, encoding the glomerular protein podocin, is mutated in autosomal recessive steroid-resistant nephrotic syndrome. *Nature Genetics* 349–354 (2000).
28. Li, C., Ruotsalainen, V., Tryggvason, K., Shaw, A. & Miner, J. CD2AP is expressed with nephrin in developing podocytes and is found widley in mature kidney and elsewhere. *The American Journal of Physiology - Renal Physiology* 785–792 (2000) doi:091.036.155.088.
29. Schwarz, K. *et al.* Podocin, a raft-associated component of the glomerular slit diaphragm, interacts with CD2AP and nephrin. *JCI* 1621–1629 (2001).
30. Martin, C. & Jones, N. Nephrin Signaling in the Podocyte: An Updated View of Signal Regulation at the Slit Diaphragm and Beyond. *frontiers in Endocrinology* (2018) doi:10.3389/fendo.2018.00302.
31. Critchley, D. R. Focal adhesions- the cytoskeletal connection. *Cell Biology* 133–139 (2000) doi:0955-0647/00.
32. Sjöblom, B., Salmazo, A. & Djinovic-Carugo, K. a-Actinin structure and regulation. *Cell.Mol.Life Sci.* 2688–2701 (2008) doi:10.1007/s00018-008-8080-8.
33. Shankland, S., Pippin, J., Reiser, J. & Mundel, P. Podocytes in cultue: past, present, and future. *Kidney international* 26–36 (2007).
34. Debruin, E. *et al.* Podocalyxin Regulates Murine Lung Vascular Permeability by Altering Endothelial Cell Adhesion. *PLoS One* (2014).
35. Mundel, P. *et al.* Synaptopodin: An Actin-associated Protein in Telencephalic Dendrites and Renal Podocytes. *J. Cell Biol.* **139**, 193–204 (1997).
36. Mottl, A. Glomerular Disease. National Institute of Diabetes and Digestive and Kidney Diseases (2024).
37. Hall, J. E. Guyton and Hall Textbook of Medical Physiology E-Book: Guyton and Hall Textbook of Medical Physiology E-Book. (Elsevier - Health Sciences Division, Chantilly, 2015).
38. Gasparo, M. & Unger, T. International Union of Pharmacology. XXIII. The angiotensin II receptors. *Pharmacological Reviews* (2000).

39. Siragy, H. M., Howell, N. L., Virginia Ragsdale, N. & Carey, R. M. Renal Interstitial Fluid Angiotensin Modulation by Anesthesia, Epinephrine, Sodium Depletion, and Renin Inhibition. *Hypertension* **25**, 1021–1024 (1995).
40. Hollenberg, N. K., Fisher, N. D. L. & Price, D. Pathways for Angiotensin II Generation in Intact Human Tissue Evidence From Comparative Pharmacological Interruption of the Renin System. *ahajournals* (1998).
41. Schmieder, R. E., Hilgers, K. F., Schlaich, M. P. & Schmidt, B. M. Renin-angiotensin system and cardiovascular risk. *The Lancet* **369**, 1208–1219 (2007).
42. Bader, M. *et al.* Tissue renin-angiotensin systems: new insights from experimental animal models in hypertension research. *J Mol Med* 76–102 (2001) doi:10.1007/s001090100210.
43. Siragy, H. M. AT1 and AT2 Receptor in the Kidney: Role in Health and Disease. *Seminars in Nephrology* **24**, 93–100 (2004).
44. Zhuo, J., Maric, C., Harris, P. J., Alcorn, D. & Mendelsohn, F. Localization and Functional Properties of Angiotensin II AT1 Receptors in the Kidney: Focus on Renomedullary Interstitial Cells. *Hypertension Research* **20**, 233–250 (1997).
45. Ames, M., Atkins, C. & Pitt, B. The renin-angiotensin-aldosterone system and its suppression. *J Vet Intern Med.* 363–382 (2018) doi:10.1111/jvim.15454.
46. Clauser, E. *et al.* Angiotensin II receptors: protein and gene structures, expression and potential pathological involvements. *European Journal of Endocrinology* 403–411 (1996) doi:https://doi.org/10.1530/eje.0.1340403.
47. Dinh, D. T., Fraumann, A., Johnston, C. & Fabiani, M. Angiotensin receptors: distribution, signalling and function. *Clinical Science* 481–92 (2001).
48. GUO, D.-F., SUN, Y. L., HAMET, P. & Inagami, T. The angiotensin II type 1 receptor and receptor-associated proteins. *Cell research* 165–180 (2001).
49. Arima, S. & Ito, S. Angiotensin II type 2 receptors in the kidney: evidence for endothelial-cell-mediated renal vasodilatation. *Nephrology Dialysis Transplantation* 448–451 (2000).
50. Hoffmann, S., Podlich, D., Hähnel, B., Kriz, W. & Gretz, N. Angiotensin II Type 1 Receptor Overexpression in Podocytes Induces Glomerulosclerosis in Transgenic Rats. *J Am Soc Nephrol* 1475–1487 (2004) doi:10.1097/01.ASN.0000127988.42710.A7.
51. Currie, G. & Delles, C. Proteinuria and its relation to cardiovascular disease. *Int J Nephrol Renovasc Dis.* **7**, 13–24 (2014).
52. Macconi, D. *et al.* Permselective Dysfunction of Podocyte-Podocyte Contact upon Angiotensin II Unravels the Molecular Target for Renoprotective Intervention. *American Journal of Pathology* 1073–1085 (2006) doi:10.2353/ajpath.2006.050701.
53. Suzuki, K. *et al.* Angiotensin II Type 1 and Type 2 Receptors Play Opposite Roles in Regulating the Barrier Function of Kidney Glomerular Capillary Wall. *The American Journal of Pathology* 1841–1853 (2007) doi:10.2353/ajpath.2007.060484.
54. Remuzzi, G., Benigni, A. & Remuzzi, A. Mechanisms of progression and regression of renal lesions of chronic nephropathies and diabetes. *JCI* 288–296 (2006) doi:https://doi.org/10.1172/JCI27699.

55. Ferrario, C. Role of Angiotensin II in Cardiovascular Disease — Therapeutic Implications of More Than a Century of Research. *JRAAS* 3–145 (2006).
56. Hernàndez-Hernàndez, R. *et al.* Angiotensin II receptor antagonists role in arterial hypertension. *Journal of Human Hypertension* 93–99 (2002).
57. Atlas, S. The Renin-Angiotensin Aldosterone System: Pathophysiological Role and Pharmacologic Inhibition. *J Manag Care Pharm.* 9–20 (2007).
58. Chi-Xianggeng *et al.* Losartan treating podocyte injury induced by Ang II via downregulation of TRPC6 in podocytes. *Journal of the Renin-ANgiotensin-Aldosterone System* 1118–1124 (2015) doi:10.1177/1470320315573682.
59. Mehta, R. L. *et al.* International Society of Nephrology's 0by25 initiative for acute kidney injury (zero preventable deaths by 2025): a human rights case for nephrology. *The Lancet* **385**, 2616–2643 (2015).
60. Coca, S. G., Singanamala, S. & Parikh, C. R. Chronic kidney disease after acute kidney injury: a systematic review and meta-analysis. *Kidney Int.* **81**, 442–448 (2012).
61. Sohaney, R. *et al.* In-Hospital and 1-Year Mortality Trends in a National Cohort of US Veterans with Acute Kidney Injury. *Clin. J. Am. Soc. Nephrol.* **17**, 184–193 (2022).
62. Silver, S. A. *et al.* Causes of Death after a Hospitalization with AKI. *J. Am. Soc. Nephrol.* **29**, 1001–1010 (2018).
63. Abebe, A., Kumela, K., Belay, M., Kebede, B. & Wobie, Y. Mortality and predictors of acute kidney injury in adults: a hospital-based prospective observational study. *Sci. Rep.* **11**, 15672 (2021).
64. Susantitaphong, P. *et al.* World Incidence of AKI: A Meta-Analysis. *Clin. J. Am. Soc. Nephrol.* **8**, 1482–1493 (2013).
65. Radi, Z. A. Immunopathogenesis of Acute Kidney Injury. *Toxicol. Pathol.* **46**, 930–943 (2018).
66. Makris, K. & Spanou, L. Acute Kidney Injury: Definition, Pathophysiology and Clinical Phenotypes. *Clin Biochem Rev* . **37**, 85–98 (2016).
67. Scope of Work KDIGO Clinical Practice Guideline for Acute Kidney Injury (AKI) and Acute Kidney Disease (AKD) Update 2023. *KDIGO* https://kdigo.org/wp-content/uploads/2023/10/KDIGO-AKI-Guideline_Scope-of-Work_25Oct2023_Final.pdf.
68. Chawla, L. S., Eggers, P. W., Star, R. A. & Kimmel, P. L. Acute Kidney Injury and Chronic Kidney Disease as Interconnected Syndromes. *N. Engl. J. Med.* **371**, 58–66 (2014).
69. Mehta, R. L. *et al.* Recognition and management of acute kidney injury in the International Society of Nephrology 0by25 Global Snapshot: a multinational cross-sectional study. *The Lancet* **387**, 2017–2025 (2016).
70. Finlay, S. *et al.* Identification of risk factors associated with acute kidney injury in patients admitted to acute medical units. *Clin. Med.* **13**, 233–238 (2013).
71. Jiang, Y.-J. *et al.* Risk factors, clinical features and outcome of new-onset acute kidney injury among critically ill patients: a database analysis based on prospective cohort study. *BMC Nephrol.* **22**, 289 (2021).
72. Shozushima, T. Presepsin (sCD14-ST) as a new diagnostic biomarker of sepsis: development of diagnostic tools using the whole blood. *Crit. Care* **15**, P3, cc10372 (2011).

73. Sise, M. E., Barasch, J., Devarajan, P. & Nickolas, T. L. Elevated urine neutrophil gelatinase-associated lipocalin can diagnose acute kidney injury in patients with chronic kidney diseases. *Kidney Int.* **75**, 115–116 (2009).
74. Zhang, D. *et al.* Tubular p53 Regulates Multiple Genes to Mediate AKI. *J. Am. Soc. Nephrol.* **25**, 2278–2289 (2014).
75. Megyesi, J., Udvarhelyi, N., Safirstein, R. L. & Price, P. M. The p53-independent activation of transcription of p21 WAF1/CIP1/SDI1 after acute renal failure. *Am. J. Physiol.-Ren. Physiol.* **271**, F1211–F1216 (1996).
76. Pabla, N., Huang, S., Mi, Q.-S., Daniel, R. & Dong, Z. ATR-Chk2 Signaling in p53 Activation and DNA Damage Response during Cisplatin-induced Apoptosis. *J. Biol. Chem.* **283**, 6572–6583 (2008).
77. Pabla, N., Ma, Z., McIlhatton, M. A., Fishel, R. & Dong, Z. hMSH2 Recruits ATR to DNA Damage Sites for Activation during DNA Damage-induced Apoptosis. *J. Biol. Chem.* **286**, 10411–10418 (2011).
78. Jiang, M. & Dong, Z. Regulation and Pathological Role of p53 in Cisplatin Nephrotoxicity. *J. Pharmacol. Exp. Ther.* **327**, 300–307 (2008).
79. Kellum, J. A. *et al.* Acute kidney injury. *Nat. Rev. Dis. Primer* **7**, 52 (2021).
80. Agarwal, A. *et al.* Cellular and Molecular Mechanisms of AKI. *J. Am. Soc. Nephrol.* **27**, 1288–1299 (2016).
81. Kovesdy, C. P. Epidemiology of chronic kidney disease: an update 2022. *Kidney International Supplements* **12**, 7–11 (2022).
82. Bello, A. K. *et al.* An update on the global disparities in kidney disease burden and care across world countries and regions. *Lancet Glob. Health* **12**, e382–e395 (2024).
83. Jankowski, J., Floege, J., Fliser, D., Böhm, M. & Marx, N. Cardiovascular Disease in Chronic Kidney Disease: Pathophysiological Insights and Therapeutic Options. *Circulation* **143**, 1157–1172 (2021).
84. National Kidney Foundation. K/DOQI clinical practice guidelines for chronic kidney disease: evaluation, classification, and stratification. *Am. J. Kidney Dis. Off. J. Natl. Kidney Found.* **39**, S1-266 (2002).
85. Levey, A. S. *et al.* Definition and classification of chronic kidney disease: A position statement from Kidney Disease: Improving Global Outcomes (KDIGO). *Kidney Int.* **67**, 2089–2100 (2005).
86. Levey, A. S. & Coresh, J. Chronic kidney disease. *The Lancet* **379**, 165–180 (2012).
87. Levey, A. S. *et al.* National Kidney Foundation Practice Guidelines for Chronic Kidney Disease: Evaluation, Classification, and Stratification. *Ann. Intern. Med.* **139**, 137 (2003).
88. Stevens, P. E. *et al.* KDIGO 2024 Clinical Practice Guideline for the Evaluation and Management of Chronic Kidney Disease. *Kidney Int.* **105**, S117–S314 (2024).
89. Torino, C., Dounousi, E., Abd ElHafeez, S. & Prohic, N. Editorial: Molecular Mechanisms in Chronic Kidney Disease. *Front. Cell Dev. Biol.* **9**, 712834 (2021).
90. Duni, A., Liakopoulos, V., Roumeliotis, S., Peschos, D. & Dounousi, E. Oxidative Stress in the Pathogenesis and Evolution of Chronic Kidney Disease: Untangling Ariadne's Thread. *Int. J. Mol. Sci.* **20**, 3711 (2019).
91. Niwa, T. Indoxyl Sulfate Is a Nephro-Vascular Toxin. *J. Ren. Nutr.* **20**, S2–S6 (2010).

92. Mertowska, P., Mertowski, S., Smarz-Widelska, I. & Grywalska, E. Biological Role, Mechanism of Action and the Importance of Interleukins in Kidney Diseases. *Int. J. Mol. Sci.* **23**, 647 (2022).
93. Barreto, D. V. *et al.* Plasma interleukin-6 is independently associated with mortality in both hemodialysis and pre-dialysis patients with chronic kidney disease. *Kidney Int.* **77**, 550–556 (2010).
94. Mantovani, A., Dinarello, C. A., Molgora, M. & Garlanda, C. Interleukin-1 and Related Cytokines in the Regulation of Inflammation and Immunity. *Immunity* **50**, 778–795 (2019).
95. Romanova, Y. *et al.* Proteomic Analysis of Human Serum from Patients with Chronic Kidney Disease. *Biomolecules* **10**, 257 (2020).
96. Wei, C.-C. *et al.* Interleukin-20 targets renal cells and is associated with chronic kidney disease. *Biochem. Biophys. Res. Commun.* **374**, 448–453 (2008).
97. Wruck, W. *et al.* Urine-Based Detection of Biomarkers Indicative of Chronic Kidney Disease in a Patient Cohort from Ghana. *J. Pers. Med.* **13**, 38 (2022).
98. Yuan, Q., Tang, B. & Zhang, C. Signaling pathways of chronic kidney diseases, implications for therapeutics. *Signal Transduct. Target. Ther.* **7**, 182 (2022).
99. O'Toole, J. F., Bruggeman, L. A., Madhavan, S. & Sedor, J. R. The Cell Biology of APOL1. *Semin. Nephrol.* **37**, 538–545 (2017).
100. Nichols, B. *et al.* Innate immunity pathways regulate the nephropathy gene Apolipoprotein L1. *Kidney Int.* **87**, 332–342 (2015).
101. Madhavan, S. M. *et al.* APOL1 Localization in Normal Kidney and Nondiabetic Kidney Disease. *J. Am. Soc. Nephrol.* **22**, 2119–2128 (2011).
102. Matsha, T. E., Kengne, A. P., Masconi, K. L., Yako, Y. Y. & Erasmus, R. T. APOL1 genetic variants, chronic kidney diseases and hypertension in mixed ancestry South Africans. *BMC Genet.* **16**, 69 (2015).
103. Genovese, G. *et al.* Association of trypanolytic ApoL1 variants with kidney disease in African Americans. *Science* **329**, 841–845 (2010).
104. Cooper, A. *et al.* APOL1 renal risk variants have contrasting resistance and susceptibility associations with African trypanosomiasis. *eLife* **6**, e25461 (2017).
105. Limou, S., Nelson, G. W., Kopp, J. B. & Winkler, C. A. APOL1 Kidney Risk Alleles: Population Genetics and Disease Associations. *Adv. Chronic Kidney Dis.* **21**, 426–433 (2014).
106. Kopp, J. B. *et al.* APOL1 Genetic Variants in Focal Segmental Glomerulosclerosis and HIV-Associated Nephropathy. *J. Am. Soc. Nephrol.* **22**, 2129–2137 (2011).
107. Foster, M. C. *et al.* APOL1 variants associate with increased risk of CKD among African Americans. *J. Am. Soc. Nephrol. JASN* **24**, 1484–1491 (2013).
108. Kopp, J. B. *et al.* Clinical Features and Histology of Apolipoprotein L1-Associated Nephropathy in the FSGS Clinical Trial. *J. Am. Soc. Nephrol.* **26**, 1443–1448 (2015).
109. Gbadegesin, R. A. *et al. APOL1* Bi- and Monoallelic Variants and Chronic Kidney Disease in West Africans. *N. Engl. J. Med.* **392**, 228–238 (2025).
110. Tzur, S. *et al.* Missense mutations in the APOL1 gene are highly associated with end stage kidney disease risk previously attributed to the MYH9 gene. *Hum. Genet.* **128**, 345–350 (2010).

111. Blessing, N. A. *et al.* Lack of APOL1 in proximal tubules of normal human kidneys and proteinuric APOL1 transgenic mouse kidneys. *PLOS ONE* **16**, e0253197 (2021).
112. Olabisi, O. A. *et al.* APOL1 kidney disease risk variants cause cytotoxicity by depleting cellular potassium and inducing stress-activated protein kinases. *Proc. Natl. Acad. Sci.* **113**, 830–837 (2016).
113. Beckerman, P. *et al.* Transgenic expression of human APOL1 risk variants in podocytes induces kidney disease in mice. *Nat. Med.* **23**, 429–438 (2017).
114. Lan, X. *et al.* APOL1 risk variants enhance podocyte necrosis through compromising lysosomal membrane permeability. *Am. J. Physiol.-Ren. Physiol.* **307**, F326–F336 (2014).
115. Wen, H. *et al.* APOL1 risk variants cause podocytes injury through enhancing endoplasmic reticulum stress. *Biosci. Rep.* **38**, BSR20171713 (2018).
116. Fu, Y. *et al.* APOL1-G1 in Nephrocytes Induces Hypertrophy and Accelerates Cell Death. *J. Am. Soc. Nephrol.* **28**, 1106–1116 (2017).
117. Wakashin, H. *et al.* APOL1 renal risk variants exacerbate podocyte injury by increasing inflammatory stress. *BMC Nephrol.* **21**, 371 (2020).
118. Vasquez-Rios, G., De Cos, M. & Campbell, K. N. Novel Therapies in APOL1-Mediated Kidney Disease: From Molecular Pathways to Therapeutic Options. *Kidney Int. Rep.* **8**, 2226–2234 (2023).
119. Lee, S.-Y., Kim, S. I. & Choi, M. E. Therapeutic targets for treating fibrotic kidney diseases. *Transl. Res.* **165**, 512–530 (2015).
120. Miguel, V., Shaw, I. W. & Kramann, R. Metabolism at the crossroads of inflammation and fibrosis in chronic kidney disease. *Nat. Rev. Nephrol.* **21**, 39–56 (2025).
121. Humphreys, B. D. Mechanisms of Renal Fibrosis. *Annu. Rev. Physiol.* **80**, 309–326 (2018).
122. Kuppe, C. *et al.* Decoding myofibroblast origins in human kidney fibrosis. *Nature* **589**, 281–286 (2021).
123. Liu, Y. Cellular and molecular mechanisms of renal fibrosis. *Nat. Rev. Nephrol.* **7**, 684–696 (2011).
124. Huang, S. *et al.* Jagged1/Notch2 controls kidney fibrosis via Tfam-mediated metabolic reprogramming. *PLOS Biol.* **16**, e2005233 (2018).
125. Sampson, M. G. *et al.* Integrative Genomics Identifies Novel Associations with APOL1 Risk Genotypes in Black NEPTUNE Subjects. *J. Am. Soc. Nephrol.* **27**, 814–823 (2016).
126. Yang, Y.-W. *et al.* Antisense oligonucleotides ameliorate kidney dysfunction in podocyte-specific APOL1 risk variant mice. *Mol. Ther.* **30**, 2491–2504 (2022).
127. Wu, J. *et al.* The key role of NLRP3 and STING in APOL1-associated podocytopathy. *J. Clin. Invest.* **131**, (2021).
128. Freedman, B. I. & Moxey-Mims, M. The APOL1 Long-Term Kidney Transplantation Outcomes Network—APOLLO. *Clin. J. Am. Soc. Nephrol.* **13**, 940–942 (2018).
129. Doshi, M. D. *et al.* APOL1 Genotype and Renal Function of Black Living Donors. *J. Am. Soc. Nephrol. JASN* **29**, 1309–1316 (2018).
130. Cohen, D. M., Mittalhenkle, A., Scott, D. L., Young, C. J. & Norman, D. J. African American Living-Kidney Donors Should Be Screened for APOL1 Risk Alleles. *Transplantation* **92**, 722–725 (2011).

131. Newell, K. A. *et al.* Integrating APOL1 Gene Variants Into Renal Transplantation: Considerations Arising From the American Society of Transplantation Expert Conference. *Am. J. Transplant.* **17**, 901–911 (2017).
132. Villarino, A. V., Kanno, Y. & O'Shea, J. J. Mechanisms and consequences of Jak-STAT signaling in the immune system. *Nat. Immunol.* **18**, 374–384 (2017).
133. Brosius, F. C. & He, J. C. JAK inhibition and progressive kidney disease. *Curr. Opin. Nephrol. Hypertens.* **24**, 88–95 (2015).
134. Kulling, P. M. *et al.* Dysregulation of the IFN-γ-STAT1 signaling pathway in a cell line model of large granular lymphocyte leukemia. *PLOS ONE* **13**, e0193429 (2018).
135. Majoros, A. *et al.* Canonical and Non-Canonical Aspects of JAK–STAT Signaling: Lessons from Interferons for Cytokine Responses. *Front. Immunol.* **8**, (2017).
136. Juliar, B. A. *et al.* Interferon-γ induces combined pyroptotic angiopathy and APOL1 expression in human kidney disease. *Cell Rep.* **43**, 114310 (2024).
137. Datta, S. *et al.* Kidney Disease-Associated APOL1 Variants Have Dose-Dependent, Dominant Toxic Gain-of-Function. *J. Am. Soc. Nephrol. JASN* **31**, 2083–2096 (2020).
138. Ge, M. *et al.* APOL1 risk variants affect podocyte lipid homeostasis and energy production in focal segmental glomerulosclerosis. *Hum. Mol. Genet.* **30**, 182–197 (2021).
139. Kumar, V. & Singhal, P. C. APOL1 and kidney cell function. *Am. J. Physiol. Renal Physiol.* **317**, F463–F477 (2019).
140. Pollak, M. R. & Friedman, D. J. APOL1 and APOL1-Associated Kidney Disease: A Common Disease, an Unusual Disease Gene – Proceedings of the Henry Shavelle Professorship. *Glomerular Dis.* 75–87 (2023) doi:10.1159/000529227.
141. Limou, S., Dummer, P. D., Nelson, G. W., Kopp, J. B. & Winkler, C. A. APOL1 toxin, innate immunity, and kidney injury. *Kidney Int.* **88**, 28–34 (2015).
142. Sana, T., Janatpour, M., Sathe, M., Mcevoy, L. & Mcclanahan, T. Microarray analysis of primary endothelial cells challenged with different inflammatory and immune cytokines. *Cytokine* S1043466605000104 (2005) doi:10.1016/j.cyto.2004.11.003.
143. Zhaorigetu, S. *et al.* ApoL1, a BH3-only lipid-binding protein, induces autophagic cell death. *Autophagy* **4**, 1079–1082 (2008).
144. Taylor, H. E., Khatua, A. K. & Popik, W. The Innate Immune Factor Apolipoprotein L1 Restricts HIV-1 Infection. *J. Virol.* **88**, 592–603 (2014).
145. Nystrom, S. E. *et al.* JAK inhibitor blocks COVID-19 cytokine–induced JAK/STAT/APOL1 signaling in glomerular cells and podocytopathy in human kidney organoids. *JCI Insight* **7**, (2022).
146. Olabisi, O. A. *et al.* Design and Rationale of the Phase 2 Baricitinib Study in Apolipoprotein L1–Mediated Kidney Disease (JUSTICE). *Kidney Int. Rep.* **9**, 2677–2684 (2024).
147. Al-Salama, Z. T. & Scott, L. J. Baricitinib: A Review in Rheumatoid Arthritis. *Drugs* **78**, 761–772 (2018).
148. Rossi, M. *et al.* JAK Inhibitors in Atopic Dermatitis: Does Weight Matter? A Real-World, Nationwide Retrospective Study: IL-AD (Italian Landscape Atopic Dermatitis). *Dermatol. Ther.* (2025) doi:10.1007/s13555-025-01477-0.

149. Vignoli, C. A. *et al.* Baricitinib for the treatment of severe alopecia areata: results from a 52-week multicenter retrospective real-world study. *J. Dermatol. Treat.* **36**, 2444494 (2025).
150. Hassanien, M., Moshrif, A. & Hetta, H. OP0053 EFFICACY AND SAFETY OF BARICITINIB IN PATIENTS WITH ACTIVE LUPUS NEPHRITIS: A DOUBLE-BLIND, RANDOMIZED, PLACEBO-CONTROLLED PHASE 3 TRIAL. *Ann. Rheum. Dis.* **82**, 34–35 (2023).
151. Swaminathan, R. Magnesium Metabolism and its Disorders. *Clin Biochem Rev .* **24**, 47–66 (2003).
152. Ryan, M. F. The Role of Magnesium in Clinical Biochemistry: An Overview. *Ann. Clin. Biochem. Int. J. Lab. Med.* **28**, 19–26 (1991).
153. Elin, R. J. Magnesium: The Fifth but Forgotten Electrolyte. *Am. J. Clin. Pathol.* **102**, 616–622 (1994).
154. Dietary Reference Intakes for Calcium, Phosphorus, Magnesium, Vitamin D, and Fluoride. 5776 (National Academies Press, Washington, D.C., 1997). doi:10.17226/5776.
155. Agus, Z. S. Hypomagnesemia. *J Am Soc Nephrol .* **10**, 1616–22 (1999).
156. Gitelman, H. J., Graham, J. B. & Welt, L. G. A new familial disorder characterized by hypokalemia and hypomagnesemia. *Trans Assoc Am Physicians .* **79**, 221–35 (1966).
157. Bartter, F. C., Pronove, P., Gill, J. R. & Maccardle, R. C. Hyperplasia of the juxtaglomerular complex with hyperaldosteronism and hypokalemic alkalosis. A new syndrome. *Am J Med .* **33**, 811–28 (1962).
158. Gröber, U. Magnesium and Drugs. *Int. J. Mol. Sci.* **20**, 2094 (2019).
159. Konrad, M. *et al.* Mutations in the chloride channel gene CLCNKB as a cause of classic Bartter syndrome. *J Am Soc Nephrol .* **11**, 1449–1459 (2000).
160. Lee, B. H. *et al.* Genetic basis of Bartter syndrome in Korea. *ndt* **27**, 1516–1521 (2012).
161. Kurtz, I. Molecular pathogenesis of Bartter's and Gitelman's syndromes. *Kidney Int .* **54**, 1396–410 (1998).
162. da Silva Cunha, T. & Pfefermann Heilberg, I. Bartter syndrome: causes, diagnosis, and treatment. *Int J Nephrol Renovasc Dis.* **11**, 291–301 (2018).
163. Bokhari, S. R. A., Zulfiqar, H. & Mansur, A. *Bartter Syndrome*. (StatPearls Publishing LLC., 2023).
164. Verberckmoes, R., van Damme, B., Clement, J., Amery, A. & Michielsen, P. Bartter's syndrome with hyperplasia of renomedullary cells: successful treatment with indomethacin. *Kidney Int .* **9**, 302–7 (1976).
165. Nascimento, C. L. P., Garcia, C. L., Schvartsman, B. G. S. & Vaisbich, M. H. Treatment of Bartter syndrome. Unsolved issue. *J Pediatr (Rio J) .* **90**, 512–7 (2014).
166. Nuñez-Gonzale, L., Carrera, N. & Garcia-Gonzale, M. A. Molecular Basis, Diagnostic Challenges and Therapeutic Approaches of Bartter and Gitelman Syndromes: A Primer for Clinicians. *Int. J. Mol. Sci.* **22**, 11414 (2021).
167. Morales, J. M. *et al.* Long-term enalapril therapy in Bartter's syndrome. *Nephron .* **48**, 327 (1988).
168. Hené, R. J. *et al.* Correction of Hypokalemia in Bartter's Syndrome by Enalapril. *Am J Kidney Dis .* **9**, 200–5 (1987).

169. Thimm, C. & Adjaye, J. Untangling the Uncertain Role of Overactivation of the Renin–Angiotensin–Aldosterone System with the Aging Process Based on Sodium Wasting Human Models. *Int. J. Mol. Sci.* **25**, 9332 (2024).
170. Lòpez-Otìn, C., Blasco, M. A., Partridge, L., Serrano, M. & Kroemer, G. The Hallmarks of Aging. *Cell.* **153**, 1194–1217 (2013).
171. Kirkwood, T. B. L. Understanding the Odd Science of Aging. *Cell* **120**, 437–447 (2005).
172. López-Otìn, C., Blasco, M. A., Patridge, L., Serrano, M. & Kroemer, G. Hallmarks of aging: An expanding universe. *Cell* **186**, 243–278 (2023).
173. Hayflick, L. & Moorehead, P. S. The serial cultivation of human diploid cell strains. *Experimental Cell Research* 585–621 (1961) doi:10.1016/0014-4827(61)90192-6.
174. Allsopp, R. C. & Harley, C. B. Evidence for a critical telomere length in senescent human fibroblasts. *Experimental Cell Research* **219**, (1995).
175. Gladyshev, V. N. The Free Radical Theory of Aging Is Dead. Long Live the Damage Theory! *Antioxid. Redox Signal.* **20**, 727–731 (2014).
176. Chen, C., Zhou, M., Ge, Y. & Wang, X. SIRT1 and aging related signaling pathways. *Mech. Ageing Dev.* **187**, 111215 (2020).
177. Kim, E.-J. & Um, S.-J. SIRT1: roles in aging and cancer. *BMB Rep.* **41**, 751–756 (2008).
178. Jeong, J. *et al.* SIRT1 promotes DNA repair activity and deacetylation of Ku70. *Exp. Mol. Med.* **39**, 8–13 (2007).
179. Solomon, J. M. *et al.* Inhibition of SIRT1 catalytic activity increases p53 acetylation but does not alter cell survival following DNA damage. *Mol. Cell. Biol.* **26**, 28–38 (2006).
180. Erichsen, L. & Adjaye, J. Crosstalk between age accumulated DNA-damage and the SIRT1-AKT-GSK3ß axis in urine derived renal progenitor cells. *Aging* **14**, 8179–8204 (2022).
181. Darvishzadeh Mahani, F., Khaksari, M. & Raji-amirhasani, A. Renoprotective effects of estrogen on acute kidney injury: the role of SIRT1. *Int. Urol. Nephrol.* **53**, 2299–2310 (2021).
182. Khawar, M., Sohail, A. & Li, W. SIRT1: A Key Player in Male Reproduction. *Life* **12**, 318 (2022).
183. Karolczak, K. & Watala, C. Estradiol as the Trigger of Sirtuin-1-Dependent Cell Signaling with a Potential Utility in Anti-Aging Therapies. *Int. J. Mol. Sci.* **24**, 13753 (2023).
184. Tsuchiya, T., Takei, A., Tsujikado, K. & Inukai, T. Effects of androgens and estrogens on sirtuin 1 gene expression in human aortic endothelial cells. *Saudi Med. J.* **41**, 361–368 (2020).
185. Yamanaka, S. & Takahashi, K. Induction of Pluripotent Stem Cells from Mouse Embryonic and Adult Fibrolast Culture by Defined Factors. *Cell* **126**, 663–676 (2006).
186. Kohli, R. M. & Zhang, Y. TET enzymes, TDG and the dynamics of DNA demethylation. *Nature* **502**, 472–479 (2013).
187. Apostolou, E. & Hochedlinger, K. Chromatin dynamics during cellular reprogramming. *Nature* **502**, 462–471 (2013).
188. Ebrahimi, B. Reprogramming barriers and enhancers: strategies to enhance the efficiency and kinetics of induced pluripotency. *Cell Regen.* **4**, 4:10 (2015).
189. Lin, T. *et al.* A chemical platform for improved induction of human iPSCs. *Nat. Methods* **6**, 805–808 (2009).

190. Folmes, C. D. L. *et al.* Somatic Oxidative Bioenergetics Transitions into Pluripotency-Dependent Glycolysis to Facilitate Nuclear Reprogramming. *Cell Metab.* **14**, 264–271 (2011).
191. Takahashi, K. *et al.* Induction of Pluripotent Stem Cells from Adult Human Fibroblasts by Defined Factors. *Cell* **131**, 861–872 (2007).
192. Thomson, J. A. *et al.* Embryonic Stem Cell Lines Derived from Human Blastocysts. *Science* **282**, 1145–1147 (1998).
193. Malik, N. & Rao, M. S. A Review of the Methods for Human iPSC Derivation. in *Pluripotent Stem Cells* (eds. Lakshmipathy, U. & Vemuri, M. C.) vol. 997 23–33 (Humana Press, Totowa, NJ, 2013).
194. Blackburn, E. H. & Gall, J. G. A tandemly repeated sequence at the termini of the extrachromosomal ribosomal RNA genes in Tetrahymena. *Journal of Molecular Biology* **120**, 33–53 (1978).
195. Bodnar, A. *et al.* Extension of Life-Span by Introduction of Telomerase into Normal Human Cells. *SCIENCE* **279**, 349–352 (1998).
196. Quellette, M. & Lee, K. Telomerase: diagnostics, cancer therapeutics and tissue engineering. *Drug Discovery Today* 1231–1237 (2001) doi:10.1016/s1359-6446(01)02052-9.
197. Watson, J. D. Origin of concatemeric t7dna. *Nature New Biology* **239**, 197–201 (1972).
198. Harley, C., Futcher, A. B. & Greider, C. W. Telomeres shorten during ageing of human fibroblasts. *Nature* 458–460 (1990).
199. Nakayama, J. *et al.* Telomerase activation byhtrt in human normal fibroblasts and hepatocellular carcinomas. *Nature Genetics* **18**, 65–68 (1998).
200. Morin, G. B. The human telomere terminal transferase enzyme is a ribonucleoprotein that synthesizes ttagg repeats. *Cell* **59**, 521–9 (1989).
201. Wong, M. S., Wright, W. E. & Shay, J. W. Alternative splicing regulation of telomerase: a new paradigm? *Trends in genetics* **30**, 430–8 (2014).
202. Zhao, Y., Wang, S., Popova, E. Y., Grigoryev, S. A. & Zhu, J. Rearrangement of upstream sequences of the hTERT gene during cellular immortalization. *Genes. Chromosomes Cancer* **48**, 963–974 (2009).
203. Yao, Y. & Dai, W. Genomic Instability and Cancer. *J. Carcinog. Mutagen.* **5**, 1000165 (2014).
204. Liberti, M. V. & Locasale, J. W. The Warburg Effect: How Does it Benefit Cancer Cells? *Trends Biochem. Sci.* **41**, 211–218 (2016).
205. Wright, W. E., Pereira-Smith, O. M. & Shay, J. W. Reversible Cellular Senescence: Implications for Immortalization of Normal Human Diploid Fibroblasts. *Mol. Cell. Biol.* **9**, 3088–3092 (1989).
206. Radna, R. L. *et al.* Growth of immortal simian virus 40 tsA-transformed human fibroblasts is temperature dependent. *Mol. Cell. Biol.* **9**, 3093–3096 (1989).
207. Neufeld, D. S., Ripley, S., Henderson, A. & Ozer, H. L. Immortalization of human fibroblasts transformed by origin-defective simian virus 40. *Mol. Cell. Biol.* **7**, 2794–2802 (1987).
208. Jha, K. K., Banga, S., Palejwala, V. & Ozer, H. L. SV40-Mediated Immortalization. *Exp. Cell Res.* **245**, 1–7 (1998).

209. Bartek, J., Bartkova, J. & Lukas, J. The Retinoblastoma Protein Pathway in Cell Cycle Control and Cancer. *Exp. Cell Res.* **237**, 1–6 (1997).
210. Wiman, K. p53: Emergency Brake and Target for Cancer Therapy. *Exp. Cell Res.* **237**, 14–18 (1997).
211. Weinberg, R. A. The retinoblastoma protein and cell cycle control. *Cell* **81**, 323–330 (1995).
212. Schafer, K. A. The Cell Cycle: A Review. *Vet. Pathol.* **35**, 461–478 (1998).
213. Hubbard, K. & Ozer, H. L. Mechanism of immortalization. *Age* **22**, 65–69 (1999).
214. Petreski, T., Varda, L., Gradišnik, L., Maver, U. & Bevc, S. Renal Proximal Tubular Epithelial Cells: From Harvesting to Use in Studies. *Nephron* **147**, 650–654 (2023).
215. Arcolino, F. O. *et al.* Human Urine as a Noninvasive Source of Kidney Cells. *Stem Cells International* (2014).
216. Yu, D. *et al.* Urinary Podocyte Loss Is a More Specific Marker of Ongoing Glomerular Damage than Proteinuria. *American Society of Nephrology* 1733–1741 (2005) doi:10.1681/ASN.2005020159.
217. Lazzeri, E. *et al.* Human Urine-Derived renal progenitors for personalized Modeling of Genetic Kidney Disorders. *Journal of the American Society of Nephrology* 1961–1974 (2015).
218. Rosenberg, A. Z. & Kopp, J. B. Focal Segmental Glomerulosclerosis. *Clin. J. Am. Soc. Nephrol.* **12**, 502–517 (2017).
219. Sagoo, M. K. & Gnudi, L. Diabetic Nephropathy: An Overview. in *Diabetic Nephropathy* (eds. Gnudi, L. & Long, D. A.) vol. 2067 3–7 (Springer US, New York, NY, 2020).
220. Robert Koch-Institut. Hypertonie. *Robert Koch Institut* https://www.rki.de/DE/Content/Gesundheitsmonitoring/Themen/Chronische_Erkrankungen/Hypertonie/Hypertonie_node.html (2015).
221. McCarthy, G. M. *et al.* Recessive, gain-of-function toxicity in an APOL1 BAC transgenic mouse model mirrors human APOL1 kidney disease. *Dis. Model. Mech.* **14**, dmm048952 (2021).
222. Vandorpe, D. H. *et al.* Apolipoprotein L1 (APOL1) cation current in HEK-293 cells and in human podocytes. *Pflugers Arch.* **475**, 323–341 (2023).
223. Zimmerman, B. *et al.* Small molecule APOL1 inhibitors as a precision medicine approach for APOL1-mediated kidney disease. *Nat. Commun.* **16**, 167 (2025).
224. Granado, D. *et al.* Intracellular APOL1 Risk Variants Cause Cytotoxicity Accompanied by Energy Depletion. *J. Am. Soc. Nephrol. JASN* **28**, 3227–3238 (2017).
225. Francis, A. *et al.* Chronic kidney disease and the global public health agenda: an international consensus. *Nat. Rev. Nephrol.* **20**, 473–485 (2024).
226. Carey, R. M., Wright, J. T., Taler, S. J. & Whelton, P. K. Guideline-Driven Management of Hypertension: An Evidence-Based Update. *Circ. Res.* **128**, 827–846 (2021).
227. Ingelfinger, J. R. Nephrogenic Adenomas as Renal Tubular Outposts. *N. Engl. J. Med.* **347**, 684–686 (2002).
228. Mulder, J. *et al.* Generation of infant- and pediatric-derived urinary induced pluripotent stem cells competent to form kidney organoids. *Pediatr. Res.* **87**, 647–655 (2020).

229. Rahman, M. S. *et al.* The presence of human mesenchymal stem cells of renal origin in amniotic fluid increases with gestational time. *Stem Cell Res. Ther.* **9**, 113 (2018).
230. Lasagni, L., Lazzeri, E., Peired, A. & Romagnani, P. Evidence for Renal Progenitors in the Human Kidney. in *Kidney Development, Disease, Repair and Regeneration* 395–406 (Elsevier, 2016). doi:10.1016/B978-0-12-800102-8.00029-1.
231. Thimm, C., Erichsen, L., Wruck, W. & Adjaye, J. Unveiling Angiotensin II and Losartan-Induced Gene Regulatory Networks Using Human Urine-Derived Podocytes. *Int J Mol Sci.* **24**, 10551 (2023).
232. Erichsen, L. *et al.* Activation of the Renin–Angiotensin System Disrupts the Cytoskeletal Architecture of Human Urine-Derived Podocytes. *Cells* **11**, 1095 (2022).
233. Qian, T. *et al.* Directed Differentiation of Human Pluripotent Stem Cells to Podocytes under Defined Conditions. *Scientific Reports* **9**, (2019).
234. Stewart, S. A. & Weinberg, R. A. Senescence: does it all happen at the ends? *Oncogene* **21**, 627–630 (2002).
235. Hayflick, L. The limited in vitro lifetime of human diploid cell strains. *Exp. Cell Res.* **37**, 614–636 (1965).
236. Greka, A. & Mundel, P. Cell Biology and Pathology of Podocytes. *Annu. Rev. Physiol.* **74**, 299–323 (2012).
237. Lundberg, A. S., Hahn, W. C., Gupta, P. & Weinberg, R. A. Genes involved in senescence and immortalization. *Curr. Opin. Cell Biol.* **12**, 705–709 (2000).
238. Fridman, A. L. & Tainsky, M. A. Critical pathways in cellular senescence and immortalization revealed by gene expression profiling. *Oncogene* **27**, 5975–5987 (2008).
239. Ouellette, M. M. The establishment of telomerase-immortalized cell lines representing human chromosome instability syndromes. *Hum. Mol. Genet.* **9**, 403–411 (2000).
240. Erichsen, L. *et al.* Derivation of the immortalized cell line-UM51-PrePodo-hTERT and its responsiveness to Angiotensin II and activation of RAAS. *Cells* **12**, (2023).
241. Twine, N. A. *et al.* Molecular Phenotyping of Telomerized Human Bone Marrow Skeletal Stem Cells Reveals a Genetic Program of Enhanced Proliferation and Maintenance of Differentiation Responses. *JBMR Plus* **2**, 257–267 (2018).
242. Lindvall, C. *et al.* Molecular characterization of human telomerase reverse transcriptase-immortalized human fibroblasts by gene expression profiling: activation of the epiregulin gene. *Cancer Research* **63**, 1743–7 (2003).
243. Shay, J. W. & Bacchetti, S. A survey of telomerase activity in human cancer. *Eur. J. Cancer* **33**, 787–791 (1997).
244. Kim, N. W. *et al.* Specific Association of Human Telomerase Activity with Immortal Cells and Cancer. *Science* **266**, 2011–2015 (1994).
245. Koche, R. P. *et al.* Reprogramming Factor Expression Initiates Widespread Targeted Chromatin Remodeling. *Cell Stem Cell* **8**, 96–105 (2011).
246. Morgan, H. D., Santos, F., Green, K., Dean, W. & Reik, W. Epigenetic reprogramming in mammals. *Hum. Mol. Genet.* **14**, R47–R58 (2005).
247. Polo, J. M. *et al.* A Molecular Roadmap of Reprogramming Somatic Cells into iPS Cells. *Cell* **151**, 1617–1632 (2012).

248. Lanza, R. P. *et al.* Extension of Cell Life-Span and Telomere Length in Animals Cloned from Senescent Somatic Cells. *Science* **288**, 665–669 (2000).
249. Sinclair, K. D. *et al.* Healthy ageing of cloned sheep. *Nat. Commun.* **7**, 12359 (2016).
250. Hochedlinger, K. & Jaenisch, R. Induced Pluripotency and Epigenetic Reprogramming. *Cold Spring Harb. Perspect. Biol.* **7**, a019448 (2015).
251. Thimm, C., Mack, R., Adjei-Aruna, O., Wruck, W. & Adjaye, J. Modelling APOL1-mediated kidney inflammation and fibrosis using a partially reprogrammed urine derived SIX2-positive renal progenitor cell line. Preprint at https://doi.org/10.1101/2025.07.28.667124 (2025).
252. Angelotti, M. L. *et al.* Characterization of Renal Progenitors Committed Toward Tubular Lineage and Their Regenerative Potential in Renal Tubular Injury. *STEM CELLS* **30**, 1714–1725 (2012).
253. Huling, J. & Yoo, J. J. Comparing adult renal stem cell identification, characterization and applications. *Journal of Biomedical Science* **24**, 1–11 (2017).
254. Doyonnas, R. *et al.* Anuria, Omphalocele, and Perinatal Lethality in Mice Lacking the Cd34-Related Protein Podocalyxin. *J Exp Med.* 13–28 (2001) doi:10.1084/jem.194.1.13.
255. Kim, Y. K. *et al.* Gene-Edited Human Kidney Organoids Reveal Mechanisms of Disease in Podocyte Development. *STEM CELLS* 2366–2378 (2017).
256. Kaschina, E. & Unger, T. Angiotensin AT1/AT2 Receptors: Regulation, Signaling and Function. *Blood Pressure* **12**, 70–88 (2003).
257. Crowley, S. D. *et al.* Angiotensin II causes hypertension and cardiac hypertrophy through its receptors in the kidney. *Proceedings of the National Academy of Sciences of the United States of America* 47 (2006) doi:10.1073/pnas.0605545103.
258. Tojo, A., Tisher, C. C. & Madsen, K. M. Angiotensin II regulates H(+)-ATPase activity in rat cortical collecting duct. *American Journal of Physiology* **267**, F1045-51 (1994).
259. Barreto-Chaves, M. L. & Mello-Aires, M. Effect of luminal angiotensin II and ANP on early and late cortical distal tubule HCO3- reabsorption. *American Journal of Physiology* **271**, F977–F984 (1996).
260. Wang, T. & Giebisch, G. Effects of angiotensin II on electrolyte transport in the early and late distal tubule in rat kidney. *American Journal of Physiology* **271**, F143-9 (1996).
261. Kwon, T.-H. *et al.* Regulation of sodium transporters in the thick ascending limb of rat kidney: response to angiotensin II. *American Journal of Physiology* **285**, F152-65 (2003).
262. Rocque, B. L. *et al.* Deficiency of the Planar Cell Polarity Protein Vangl2 in Podocytes Affects Glomerular Morphogenesis and Increases Susceptibility to Injury. *Journal of the American Society of Nephrology* **26**, 576–586 (2015).
263. Xie, K. *et al.* Yes-associated protein regulates podocyte cell cycle re-entry and dedifferentiation in adriamycin-induced nephropathy. *Cell Death & Disease* **10**, 915 (2019).
264. Sobczuk, P., Szcylik, C., Porta, C. & Czarnecka, A. M. Renin angiotensin system deregulation as renal cancer risk factor. *Oncology Letters* **14**, 5059–5068 (2017).
265. Stegbauer, J. & Coffman, T. M. New insights into angiotensin receptor actions: from blood pressure to aging. *Current Opinion in Nephrology and Hypertension* **20**, 84–8 (2011).
266. Reiser, J. & Mundel, P. Dual effects of RAS blockade on blood pressure and podocyte function. *Current Hypertension Reports* **9**, 408–8 (2007).

267. Rüster, C. & Wolf, G. Renin-angiotensin-aldosterone system and progression of renal disease. *Journal of American Society of Nephrology* **17**, 2985–91 (2006).
268. Liu, Y. *et al.* IQGAP1 regulates actin cytoskeleton organization in podocytes through interaction with nephrin. *Cell Signal* **27**, 867–77 (2015).
269. Yang, Q. *et al.* Angiotensin II down-regulates nephrin–Akt signaling and induces podocyte injury: roleof c-Abl. *Molecular Biology of the Cell* **27**, 197–208 (2016).
270. Le, T. H. *et al.* Physiological Impact of Increased Expression of the At1 Angiotensin Receptor. *Hypertension* **42**, 507–514 (2003).
271. Jha, V. *et al.* Chronic kidney disease: global dimension and perspectives. *The Lancet* **382**, 260–272 (2013).
272. Hill, N. R. *et al.* Global Prevalence of Chronic Kidney Disease – A Systematic Review and Meta-Analysis. *PLOS ONE* **11**, e0158765 (2016).
273. Basile, D. P., Anderson, M. D. & Sutton, T. A. Pathophysiology of Acute Kidney Injury. in *Comprehensive Physiology* (ed. Prakash, Y. S.) 1303–1353 (Wiley, 2012). doi:10.1002/cphy.c110041.
274. Ronco, C., Bellomo, R. & Kellum, J. A. Acute kidney injury. *The Lancet* **394**, 1949–1964 (2019).
275. Simmons, E. M. *et al.* Plasma cytokine levels predict mortality in patients with acute renal failure. *Kidney Int.* **65**, 1357–1365 (2004).
276. Bendale, D. S. *et al.* 17-β Oestradiol prevents cardiovascular dysfunction in post-menopausal metabolic syndrome by affecting SIRT1/AMPK/H3 acetylation. *Br. J. Pharmacol.* **170**, 779–795 (2013).
277. Ota, H. *et al.* Testosterone Deficiency Accelerates Neuronal and Vascular Aging of SAMP8 Mice: Protective Role of eNOS and SIRT1. *PLoS ONE* **7**, e29598 (2012).
278. Yu, X., Zheng, J., Cai, T., Wang, Z. & Zhu, G. Testosterone antagonizes paraquat-induced cardiomyocyte senescence via the mIGF-1/SIRT1 signaling pathway. *Braz. J. Med. Biol. Res.* **53**, e9849 (2020).
279. Chen, H.-H., Lin, Y.-C., Chen, T.-W. & Lin, H. Roles of Adiponectin in Acute Kidney Injury. *J. Exp. Clin. Med.* **4**, 145–148 (2012).
280. Furuhashi, M. *et al.* Blockade of the Renin-Angiotensin System Increases Adiponectin Concentrations in Patients With Essential Hypertension. *Hypertension* **42**, 76–81 (2003).
281. Cai, L. *et al.* Adiponectin induces CXCL1 secretion from cancer cells and promotes tumor angiogenesis by inducing stromal fibroblast senescence. *Mol. Carcinog.* **55**, 1796–1806 (2016).
282. Ma, C. *et al.* CXCL1 stimulates decidual angiogenesis via the VEGF-A pathway during the first trimester of pregnancy. *Mol. Cell. Biochem.* **476**, 2989–2998 (2021).
283. Wei, Z.-W. *et al.* CXCL1 promotes tumor growth through VEGF pathway activation and is associated with inferior survival in gastric cancer. *Cancer Lett.* **359**, 335–343 (2015).
284. Tögel, F., Zhang, P., Hu, Z. & Westenfelder, C. VEGF is a mediator of the renoprotective effects of multipotent marrow stromal cells in acute kidney injury. *J. Cell. Mol. Med.* **13**, 2109–2114 (2009).
285. Cao, S. *et al.* Epidermal growth factor receptor activation is essential for kidney fibrosis development. *Nat. Commun.* **14**, 7357 (2023).

286. Klein, J., Bascands, J.-L., Buffin-Meyer, B. & Schanstra, J. P. Epidermal growth factor and kidney disease: a long-lasting story. *Kidney Int.* **89**, 985–987 (2016).
287. Lee, C.-C. *et al.* Incidence and outcomes of acute kidney injury in extremely-low-birth-weight infants. *PLOS ONE* **12**, e0187764 (2017).
288. Ostermann, M. *et al.* Controversies in acute kidney injury: conclusions from a Kidney Disease: Improving Global Outcomes (KDIGO) Conference. *Kidney Int.* **98**, 294–309 (2020).
289. Sheikh, M. S., Carrier, F., Johnson, A. C., Ogdon, S. E. & Jr, A. J. F. Identification of an additional p53-responsive site in the human epidermal growth factor receptor gene promotor. *Oncogene* **15**, 1095–1101 (1997).
290. Samarakoon, R. *et al.* Induction of renal fibrotic genes by TGF-β1 requires EGFR activation, p53 and reactive oxygen species. *Cell. Signal.* **25**, 2198–2209 (2013).
291. Vijayan, A. *et al.* Clinical Use of the Urine Biomarker [TIMP-2] × [IGFBP7] for Acute Kidney Injury Risk Assessment. *Am. J. Kidney Dis.* **68**, 19–28 (2016).
292. Wang, W. *et al.* Changes in inflammatory biomarkers after renal revascularization in atherosclerotic renal artery stenosis. *Nephrol. Dial. Transplant.* **31**, 1437–1443 (2016).
293. Kashani, K. *et al.* Discovery and validation of cell cycle arrest biomarkers in human acute kidney injury. *Crit. Care* **17**, R25 (2013).
294. Montero, E., Abreu, C. & Tonino, P. Relationship between VEGF and p53 expression and tumor cell proliferation in human gastrointestinal carcinomas. *J. Cancer Res. Clin. Oncol.* **134**, 193–201 (2007).
295. Erichsen, L. *et al.* Secreted Cytokines within the Urine of AKI Patients Modulate TP53 and SIRT1 Levels in a Human Podocyte Cell Model. *Int. J. Mol. Sci.* **24**, 8228 (2023).
296. Pierzchalski, P. *et al.* p53 Induces Myocyte Apoptosis via the Activation of the Renin–Angiotensin System. *Exp. Cell Res.* **234**, 57–65 (1997).
297. Engel, J. E., Williams, E., Williams, M. L., Bidwell, G. L. & Chade, A. R. Targeted VEGF (Vascular Endothelial Growth Factor) Therapy Induces Long-Term Renal Recovery in Chronic Kidney Disease via Macrophage Polarization. *Hypertension* **74**, 1113–1123 (2019).
298. Fulchiero, R. & Seo-Mayer, P. Bartter Syndrome and Gitelman Syndrome. *Pediatr. Clin. North Am.* **66**, 121–134 (2019).
299. Morimoto, A. *et al.* Sodium sensitivity and cardiovascular events in patients with essential hypertension. *Lancet .* **350**, 1734–7 (1997).
300. Weinberger, M. H., Fineberg, N. S., Fineberg, S. E. & Weinberger, M. Salt sensitivity, pulse pressure, and death in normal and hypertensive humans. *Hypertension .* **37**, 429–32 (2001).
301. Gilliam-Davis, S. *et al.* Long-term AT1 receptor blockade improves metabolic function and provides renoprotection in Fischer-344 rats. *Am J Physiol Heart Circ Physiol .* **293**, H1327-33 (2007).
302. Herbert, K. E. *et al.* Angiotensin II-mediated oxidative DNA damage accelerates cellular senescence in cultured human vascular smooth muscle cells via telomere-dependent and independent pathways. *Circ Res .* **102**, 201–8 (2008).
303. Rajagopalan, S. *et al.* Angiotensin II-mediated hypertension in the rat increases vascular superoxide production via membrane NADH/NADPH oxidase activation. Contribution to alterations of vasomotor tone. *J Clin Invest.* **97**, 1916–1923 (1996).

304. Sartori, M. *et al.* Autonomic nervous system function in chronic hypotension associated with Bartter and Gitelman syndromes. *Am J Kidney Dis.* **49**, 330–5.
305. Harris, P. J. & Young, J. A. Dose-dependent stimulation and inhibition of proximal tubular sodium reabsorption by angiotensin II in the rat kidney. *Pflugers Arch .* **367**, 295–7 (1977).
306. Calò, L. A., Davis, P. A. & Rossi, G. P. Understanding the mechanisms of angiotensin II signaling involved in hypertension and its long-term sequelae: insights from Bartter's and Gitelman's syndromes, human models of endogenous angiotensin II signaling antagonism. *J Hypertens.* **32**, 2109–19 (2014).
307. Davis, P. A. *et al.* SIRT1, heme oxygenase-1 and NO-mediated vasodilation in a human model of endogenous angiotensin II type 1 receptor antagonism: implications for hypertension. *Hypertension Research* **36**, 873–878 (2013).
308. Intengan, H. D. & Schiffrin, E. L. Vascular Remodeling in Hypertension: Roles of Apoptosis, Inflammation, and Fibrosis. *Hypertension* **38**, 581–587 (2001).
309. Xu, X. *et al.* Age-related Impairment of Vascular Structure and Functions. *Aging Dis.* **8**, 590 (2017).
310. Laurent, S., Boutouyrie, P. & Lacolley, P. Structural and Genetic Bases of Arterial Stiffness. *Hypertension* **45**, 1050–1055 (2005).
311. Benetos, A. *et al.* Telomere Length as an Indicator of Biological Aging: The Gender Effect and Relation With Pulse Pressure and Pulse Wave Velocity. *Hypertension* **37**, 381–385 (2001).
312. Seals, D. R., Jablonski, K. L. & Donato, A. J. Aging and vascular endothelial function in humans. *Clin. Sci.* **120**, 357–375 (2011).
313. Thimm, C. *et al.* Generation of a Bartter syndrome type 3 patient-derived induced pluripotent stem cell line ISRM-BS3-UM18-iPSC (HHUUKDi014-A). *Stem Cell Res.* **87**, 103760 (2025).
314. Ji, W. *et al.* Generation of an induced pluripotent stem cell line from a Bartter syndrome patient with the homozygote mutation p.A244D (c.731C>A) in SLC12A1 gene. *Stem Cell Res.* **52**, 102228 (2021).
315. Guo, X. *et al.* Generation of a human induced pluripotent stem cell line (WMUi021-A) from a Gitelman syndrome patient carrying a SLC12A3 gene mutation (c.179C > T). *Stem Cell Research* **53**, (2021).
316. Lim, S. W. *et al.* Generation of a human induced pluripotent stem cell line (CMCi002-A) from a patient with Gitelman's syndrome. *Stem Cell Research* **49**, (2020).
317. Bohndorf, M. *et al.* Derivation and characterization of integration-free iPSC line ISRM-UM51 derived from SIX2-positive renal cells isolated from urine of an African male expressing the CYP2D6 *4/*17 variant which confers intermediate drug metabolizing activity. *Stem Cell Res.* **25**, 18–21 (2017).
318. Konagaya, S., Ando, T., Yamauchi, T., Suemori, H. & Iwata, H. Long-term maintenance of human induced pluripotent stem cells by automated cell culture system. *Sci. Rep.* **5**, 16647 (2015).

319. Bragança, J., Lopes, J. A., Mendes-Silva, L. & Santos, J. M. A. Induced pluripotent stem cells, a giant leap for mankind therapeutic applications. *World J. Stem Cells* **11**, 421–430 (2019).
320. Shi, Y., Inoue, H., Wu, J. C. & Yamanaka, S. Induced pluripotent stem cell technology: a decade of progress. *Nat. Rev. Drug Discov.* **16**, 115–130 (2017).
321. Moradi, S. *et al.* Research and therapy with induced pluripotent stem cells (iPSCs): social, legal, and ethical considerations. *Stem Cell Res. Ther.* **10**, 341 (2019).
322. Kordes, C. *et al.* Human Urine-derived SIX2-positive renal progenitor cells improve kidney injury in an IRI mouse model. Preprint at https://doi.org/10.1101/2025.07.02.662781 (2025).
323. Bruno, S. *et al.* Mesenchymal Stem Cell-Derived Microvesicles Protect Against Acute Tubular Injury. *J. Am. Soc. Nephrol.* **20**, 1053–1067 (2009).
324. Anders, H.-J. & Ryu, M. Renal microenvironments and macrophage phenotypes determine progression or resolution of renal inflammation and fibrosis. *Kidney Int.* **80**, 915–925 (2011).
325. Lin, S.-L. *et al.* Macrophage Wnt7b is critical for kidney repair and regeneration. *Proc. Natl. Acad. Sci.* **107**, 4194–4199 (2010).
326. English, K. Mechanisms of mesenchymal stromal cell immunomodulation. *Immunol. Cell Biol.* **91**, 19–26 (2013).
327. Kinnaird, T. *et al.* Marrow-Derived Stromal Cells Express Genes Encoding a Broad Spectrum of Arteriogenic Cytokines and Promote In Vitro and In Vivo Arteriogenesis Through Paracrine Mechanisms. *Circ. Res.* **94**, 678–685 (2004).
328. Nakamura, T. & Mizuno, S. The discovery of Hepatocyte Growth Factor (HGF) and its significance for cell biology, life sciences and clinical medicine. *Proc. Jpn. Acad. Ser. B* **86**, 588–610 (2010).
329. Lai, R. C., Yeo, R. W. Y. & Lim, S. K. Mesenchymal stem cell exosomes. *Semin. Cell Dev. Biol.* **40**, 82–88 (2015).
330. Tögel, F. & Westenfelder, C. Adult bone marrow–derived stem cells for organ regeneration and repair. *Dev. Dyn.* **236**, 3321–3331 (2007).
331. Phinney, D. G. & Pittenger, M. F. Concise Review: MSC-Derived Exosomes for Cell-Free Therapy. *Stem Cells* **35**, 851–858 (2017).
332. Wruck, W., Thimm, C. & Adjaye, J. Evidence for conserved gene expression and biological processes operative in human podocytes and adult brain. Preprint at https://doi.org/10.1101/2025.03.17.643629 (2025).
333. Wruck, W. *et al.* Urinary proteins from Sickle Cell patients induce inflammation and kidney injury via the TGFβ-p53 axis in a podocyte cell culture model. Preprint at https://doi.org/10.1101/2025.08.08.669286 (2025).
334. Nguyen, L., Wruck, W., Erichsen, L., Graffmann, N. & Adjaye, J. The Nephrotoxin Puromycin Aminonucleoside Induces Injury in Kidney Organoids Differentiated from Induced Pluripotent Stem Cells. *Cells* **11**, 635 (2022).
335. Ding, H. *et al.* 3D Spheroids of Human Primary Urine-Derived Stem Cells in the Assessment of Drug-Induced Mitochondrial Toxicity. *Pharmaceutics* **14**, 1042 (2022).

336. Guo, H. *et al.* 3-D Human Renal Tubular Organoids Generated from Urine-Derived Stem Cells for Nephrotoxicity Screening. *ACS Biomater. Sci. Eng.* **6**, 6701–6709 (2020).

7 Appendix

7.1 Poster presentations

Lars Erichsen, Wasco Wruck, Lea Doris Friedel Kloss, **Chantelle Thimm,** Martina Bohndorf, Kira Schichel and James Adjaye.Derivation of the Immortalized Cell Line UM51-PrePodo-hTERT and Its Responsiveness to Angiotensin II and Activation of the RAAS Pathway. 2022 IMB conference: Epigenetics of Aging: Responses to Adversity across Scales, Mainz.

Wasco Wruck, **Chantelle Thimm** and James Adjaye. Evidence for conserved gene expression and biological processes operative in human podocytes and adult brain. 2025 15th International podocyte conference and ISGD meeting, Hamburg.

8 Declaration of independence

I declare that I have written the enclosed thesis completely by myself, and have not used sources or means without declaration in the text. Any thoughts from others or literal quotations are clearly marked. The thesis was not used in the same or in a similar version to achieve an academic grading or is being published elsewhere.

Ort, Datum

Chantelle Thimm